The role of dendritic cells in response to cytokine gene adjuvants

Katie Matthews

PhD
The University of Edinburgh
2005

THE UNIVERSITY OF EDINBURGH

ABSTRACT OF THESIS

(Regulation 3.5.13)

Name of Candidate: Katie Matthews

Address :

Postal Code:

Degree: PhD *Date* 01/01/05

Title of Thesis: The role of dendritic cells in response to cytokine gene adjuvants

No. of words in the main text of Thesis: 65,000

DNA vaccination is a novel means of expressing antigens *in vivo* for the generation of humoral and cell-mediated immune responses. DNA vaccines elicit protective immunity in mice; however, DNA vaccination in outbred species requires optimisation. Dendritic cells (DC) are unique in that they are the only cells capable of stimulating naïve T cells, the major requirement of successful vaccination. Lack of efficacy of DNA vaccines may be due to inefficient targeting of DC. One strategy to improve DNA vaccines is to use cytokine gene adjuvants to recruit DC, such as GM-CSF and IL-3.

The aim of the work carried out in this thesis was to investigate the effects of GM-CSF and IL-3 after gene-gun vaccination. Initial studies focused on the histological effects of GM-CSF and IL-3 in ovine skin. GM-CSF induced a linear increase in IL-1β transcripts from 1–24 hours concomitant with pronounced neutrophilic infiltration and micro-abscess formation by 24 hours. Maximal GM-CSF and IL-3 mRNA expression was evident at approximately 4 hours, whereas IL-1β and TNF-α transcripts remained highly elevated up to 96 hours. Infiltration of DC, coordinately with a rise in MHC class II DRα expression in perivascular regions, was observed 72–96 hours after GM-CSF administration. Recruitment of eosinophils and neutrophils was evident 24–48 hours after administration of IL-3, whereas infiltates of B cells and DC were observed at 24 and 72 hours, respectively.

Subsequent work characterised DC draining skin before and after GM-CSF administration by means of cannulation of the pseudoafferent lymphatics. Two sub-populations of afferent lymph DC (ALDC) were isolated based on differential expression of SIRPα as described in both cattle and rats. Ovine $SIRP\alpha^+$ ALDC constitutively express high levels of IL-1β, IL-18 and IL-10 mRNA. Conversely, $SIRP\alpha^-$ ALDC do not express IL-10 but express high levels of IL-12p40. $SIRP\alpha^+$ ALDC may contain Langerhans' cells since both ATPase and langerin were detected. Both subpopulations express Toll like receptor 3 (TLR3) and TLR9, whereas $SIRP\alpha^+$ ALDC uniquely express TLR4 (+/– CD14). Gene-gun vaccination with pGM-CSF resulted in increased cytokine transcripts in both ALDC subpopulations and an upregulation of surface MHC class IIα, CD1b, CD40, CD86 and CD11c. These studies have extended the knowledge of GM-CSF and IL-3 as adjuvants and highlight the use of the cannulation model to further decipher the immune mechanisms of adjuvants. This work has demonstrated that GM-CSF not only recruits DC into skin but also activates DC, possibly as a result of increased expression of "danger signals" including IL-1β and TNF-α.

Acknowledgements

I would like to thank Professor John Hopkins and Dr Bob Dalziel for supervising this work and the BBSRC for funding the project and my trip to the Keystone Symposia in Colorado. I am very grateful to Dr Anton Gossner for his constant support, advice and guidance. Thanks also to both Shonna and Andrew Sanderson for help with flow cytometry and cell sorting experiments; Neil McIntyre, Brian Kelly, Andrew Dawson and Sharon Moss for carrying out tissue sectioning and advising on immunohistochemistry; Susan Rhind for examining tissue sections; Professor Gordon Harkiss and Dr Craig Watkins for help and advice with DNA vaccination; Ian Bennett for sequencing; everybody at the Marshall Building, Roslin, for looking after the animals and helping out with experiments. Also thanks to Iain Finlayson for sorting text and figures. Everybody in the department contributed to making my time enjoyable. I am indebted to all in the Herpes Virus Group as well as Kirsty Newman, Claire Cotterill, Clemence Hindley, Clive McKimmie, Katrina Thom, Dale Finlayson and Niall Finlayson for being so supportive, especially during the difficult times!

None of this work would have been possible without the love and support of Iain, my mum and dad, my sister and my friends.

Declaration

I declare that the composition of this thesis and the work presented herein are my own except where specifically stated.

Katie Matthews 2005

Contents

List of figures

List of tables

Abbreviations

1°	primary
2-ME	2-mercaptoethanol
AF	ascitic fluid
ALC	afferent lymph cell
ALDC	afferent lymph dendritic cell
ALVC	afferent lymph veiled cells
AM	alveolar macrophage
APC	antigen presenting cell
ATP	adenosine triphosphate
BHK	baby hamster kidney
bio	biotinylated
bov	bovine
BSA	bovine serum albumin
CCR	chemotactic cytokine receptor
CD	cluster of differentiation
CD40L	CD40 ligand
cDNA	complementary DNA
cm	centimetre
CMV	cytomegalovirus
ConA	concanavalin A
CpG	(unmethylated) cytidine - phosphate – guanosine
Ct	crossover threshold
CTL	cytotoxic T lymphocyte
Cv	coefficient of variability
DC	dendritic cell
DEC-205	CD205
dH_20	distilled water
DLN	draining lymph node

DMEM	Dulbecco's modified eagles medium
DMSO	dimethyl sulfoxide
DNA	deoxyribonucleic acid
dNTP	deoxynucleoside triphosphate
ds	double stranded
dsDNA	double stranded DNA
E. coli	Escherichia coli
EBVC	Easter Bush Veterinary Centre
EDTA	ethylenediaminetetraacetic acid
ELISA	enzyme-linked immunosorbent assay
EMBL	European Molecular Biology Laboratory
FACS	fluorescence activated cell sorting
FCS	foetal calf serum
FITC	fluorescein isothiocyanate
Flt-3L	foetal liver tyrosine kinase 3 ligand
FSC	forward scatter
g	gravitational (force)
GAPDH	glyceraldehyde-3-phosphate dehydrogenase
GFP	green fluorescent protein
GM-CSF	granulocyte macrophage colony stimulating factor
H&E	haematoxylin and eosin
HBSS	Hank's balanced salt solution
HIV	human immunodeficiency virus
HLA	human leukocyte antigens
HRP	horse radish peroxidase
Hsps	heat shock proteins
HSV	herpes simplex virus-1
HSV-TK	HSV thymidine kinase
hu	human
IAH	Institute of Animal Health

ICAM	intracellular adhesion molecule
IE	immediate early
IEC	intraepithelial cell
IFN	interferon
Ig	immunoglobulin
IL	interleukin
IL-1R	interleukin-1 receptor
IPTG	isopropyl-β-D-thyogalactopyranoside
kb	kilobase
kDa	kilo Dalton
LB	Luria Burtani
LC	Langerhans' cell
L-glu	L-glutamine
LPS	lipopolysaccharide
m	murine
mAb	monoclonal antibody
MART	melanoma antigen
MCS	multiple cloning site
MHC	major histocompatibility complex
min	minimum
MIP	monocyte inflammatory protein
ml	millilitres
MLN	mesenteric lymph node
MLR	mixed leukocyte reaction
MMLV	Mouse Moloney Leukaemia Virus
MoDC	monocyte-derived DC
mRNA	messenger RNA
MyD	myeloid differentiation
MΦ	macrophage
NF	non-functional

NF-κB	nuclear factor-κB
NGS	normal goat serum
NK	natural killer
NMS	normal mouse serum
NSE	non-specific esterase
OD	optical density
ov	ovine
OVA	ovalbumin
p/v	post vaccination
PAGE	polyacrylamide gel electrophoresis
PBMC	peripheral blood mononuclear cell
PBS	phosphate buffered saline
PBST	PBS-tween
PCR	polymerase chain reaction
pDC	plasmacytoid DC
pEGFP-N1	(plasmid) enhanced green fluorescent protein
pen/strep	penicillin/streptomycin
pGM-CSF	(plasmid) granulocyte-macrophage colony stimulating factor
pGM-CSF	plasmid GM-CSF
pIL-3	plasmid IL-3
PMN	polymorphonuclear cell
PMT	photomultiplier tube
por	porcine
PRR	pattern recognition receptor
pre-DC	DC precursor
PVDF	polyvinylidene fluoride
PVP	polyvinylpyrrolidone
r	rat

RANTES	regulated on activation, normal T expressed and secreted
RNA	ribonucleic acid
rpm	revolutions per minute
RPMI	Roswell Park Memorial Institute
RT	reverse transcriptase
rt	room temperature
SAP	shrimp alkaline phosphatase
SA-PE	streptavidin-phycoerythrin
SDS	sodium dodecyl sulphate
SDS-PAGE	SDS-polyacrylamide gel electrophoresis
SIRPα	signal regulatory protein–α
sPBS	sterile PBS
SS	saturated supernatant
SSC	side scatter
SSk	sheep skin
ssRNA	single-stranded RNA
T4	T4 bacteriophage
Taq	Thermus aquaticus strain YT1
TB	tuberculosis
TBS	tris buffered saline
TCR	T cell receptor
Th	T helper
TLR	toll-like receptor
TNF	tumour necrosis factor
U	units (of enzyme)
UTP	uridine triphosphate
w/v	weight per volume
WC	workshop cluster

X-Gal	5-bromo-4-chloro-3-indolyl-β-D-galactopyranoside
ZSF	zinc salts fixative

1 Introduction

1.1 DNA Vaccination

1.1.1 A brief history of DNA vaccines

Vaccination is undoubtedly one of the major triumphs of medicine and is the most commonly employed immunological intervention. Current effective vaccines protect hosts primarily via neutralising antibodies. There are however many infections for which there are no effective vaccines and which continue to challenge immunologists. Vaccines that do not work satisfactorily and do not induce long-term protection include vaccinations against most parasitic infections, tuberculosis (TB), leprosy and a plethora of viruses including human immunodeficiency virus (HIV), dengue, herpes and papilloma viruses. These infections have in common that neutralising antibodies alone are not sufficient to eliminate or control the infection (reviewed in Zinkernagel, 2003). Efficient control of these infectious agents requires T cell-mediated effector mechanisms in addition to protective antibodies, since these infections are essentially inaccessible to antibodies once intracellular infection is established. In addition, many of these infections persist in tissues where antibodies cannot permeate, for instance in epithelial tissue (papilloma virus) or in granulomas (Mycobacteria).

DNA vaccination was first proposed in a report by Wolff and colleagues in 1990, which demonstrated that purified plasmid DNA was stably expressed following intramuscular injection in mice (Wolff et al., 1990). Tang and colleagues (Tang et al., 1992) subsequently demonstrated that expression of plasmid DNA induced a humoral immune response that was specific for the encoded antigen. Two independent reports generated much excitement in the vaccine field in 1993; mice were protected from a lethal challenge of influenza A virus following intramuscular vaccination with plasmids encoding either haemaglutinin (Fynan et al., 1993) or nucleoprotein (Ulmer et al., 1993). Of paramount interest was the demonstration of an induction of nucleoprotein-specific cytotoxic $CD8^+$ T cells (CTL), which conferred protection from a heterologous strain of influenza virus.

DNA vaccines have since been demonstrated to be an effective means of inducing protective cell-mediated immune responses and humoral immune responses in many animal models of infectious disease (Table 1.1) and some neoplasms (reviewed in Gurunathan et al., 2000). Substantial interest into DNA vaccines has been generated and research has rapidly progressed from the laboratories to clinical trials for several human diseases, ranging from HIV (Mwau et al., 2004), Human Papilloma Virus (HPV) (Klencke et al., 2002) and malaria

(Wang et al., 1998; Wang et al., 2001), to prostate (Mincheff et al., 2000) and colorectal cancer (Conry et al., 2002).

1.1.2 Principles of DNA vaccination

DNA vaccines are composed of backbone plasmid DNA into which a gene encoding a protective antigen is inserted. Expression of the gene is under the control of a viral eukaryotic promoter (usually the immediate early gene of cytomegalovirus (CMV)), followed by an mRNA termination/polyadenylation sequence, thus enabling expression of the gene in mammalian cells. In addition, the plasmid contains an antibiotic resistance gene to aid *in vitro* manipulation and selection. Since the first few publications, a range of methods have been employed to deliver plasmids (reviewed in Donnelly et al., 2003); however, plasmid DNA is traditionally injected either intramuscularly or intradermally. Alternatively, plasmid DNA is coated onto microscopic gold particles and bombarded into tissue using a gene-gun pressurised with helium or CO_2 resulting in efficient transfection of host cells (Williams et al., 1991). This method proved to be by far the most efficient method of DNA immunisation in one study, where administration of only 0.4μg of DNA vaccine in mice resulted in 95% survival after challenge with a lethal dose of influenza virus (Fynan et al, 1993). It is of interest to note that the route of administration of DNA vaccines strongly influences the T helper 1 (Th1)-type or Th2-type immunity and is discussed in more detail in Section 1.2.4.

Regardless of the method employed to administer the plasmid DNA, transfection of cells ensues and the cell machinery then performs DNA transcription, translation of mRNA and production of the immunogenic polypeptide, which may then be processed via the transporters associated with antigen processing (TAP)-dependent, endogenous-processing pathway (major histocompatibility complex (MHC) class I presentation pathway), resulting in the presentation of MHC class I-peptide complexes on the cell surface, thereby enabling recognition by antigen-specific MHC class I-restricted CTL (Section 1.2). This essentially mimics the presentation of antigens during a natural intracellular infection. Alternatively, soluble or secreted antigen may be phagocytosed by antigen presenting cells (APC) and gain entry into the MHC class II exogenous pathway, thus enabling the induction of humoral immunity, where antigen-specific $CD4^+$ T helper (Th) cells promote immunoglobulin (Ig) secretion by primed B cells. Importantly, plasmid DNA encoding immunogenic antigens also results in the production of proteins with native post-translational modifications and conformation. Release of intact polypeptides by transfected cells into the extracellular milieu

may result in the production of immunologically relevant neutralising antibodies, since the Ig receptor of B cells directly recognises complex folded proteins.

1.1.3 Advantages of DNA vaccines

A major drawback of most current vaccine formulations is the apparent failure in the generation of $CD8^+$ T cell responses. Current vaccine formulations, including protein subunit and heat-killed vaccines, generate neutralising antibodies through adaptive humoral responses. Live, attenuated vaccines can induce robust cellular immune responses, but there is concern over the reversion to virulence or indeed causing disease in immunocompromised individuals. Genetic immunisation with DNA represents a novel vaccination strategy that overcomes several limitations imposed by conventional vaccines. Expression of plasmid DNA by the host cell machinery essentially mimics an intracellular infection and strong cell mediated immune responses (interferon (IFN)-γ-secreting T cells) are indeed well documented for a number of infectious agents in mice (Table 1.1). Importantly, DNA vaccines are also capable of inducing strong humoral immunity (IgG-secreting B cells). A recent report which involved intramuscular vaccination of mice with a plasmid encoding the spike glycoprotein of the severe acute respiratory syndrome (SARS) coronavirus illustrates this well (Yang et al., 2004). A spectrum of immune responses were elicited after DNA vaccination, including an expansion of virus-specific $CD4^+$ and $CD8^+$ T cells and antibody; however, donor immune T cells were unable to reduce pulmonary viral replication in recipient animals, whereas passive transfer of purified IgG from immunised mice provided immune protection comparable to that observed in DNA vaccinated animals. The mechanisms by which DNA vaccines induce immunity are described in detail in Section 1.2.

An added advantage of DNA vaccines is their intrinsic immunostimulatory capacity, owing to the presence of unmethylated cytidine-phosphate-guanosine (CpG) dinucleotides (Sato et al., 1996), a feature of prokaryotic DNA. CpG motifs can directly stimulate leukocytes to produce pro-inflammatory cytokines such as interleukin (IL)-6, IL-12 and IFN-γ (Hartmann et al., 1999; Klinman et al., 1996) via interaction with toll like receptor (TLR) 9 (TLR9) (Hemmi et al., 2000) (Section 1.4.4.2). CpG motifs could therefore be considered to be a built-in adjuvant, alerting the immune system to the presence of a potential pathogen. Genetic immunisation exhibits several other advantages over traditional vaccines. For instance, DNA vaccination is highly versatile; current molecular biology techniques enable easy manipulation of plasmid vectors to include virtually any gene or indeed several genes (termed bicistronic plasmids) under the control of the same or different promoters. In addition, DNA is relatively cheap to manufacture and can be produced at large scale in

bacteria. Furthermore, DNA is stable and resists extreme temperatures and could potentially be lyophilised prior to being distributed. This is of great significance since it would impact the requirement of cold chain storage and would thus facilitate storage, transport and distribution of vaccines in third world countries, where cold chain storage can be problematic.

Table 1.1 DNA vaccines induce protective immunity for a number of intracellular infectious agents in murine models of infectious disease.

infection	gene inserted into plasmid	route of administration	immune response induced	reference
influenza A	nucleoprotein	intramuscular	nucleoprotein-specific CTL	Ulmer et al (1993)
	haemaglutinin	intramuscular & intradermal (gene-gun)	IgG	Fynan et al (1993)
SARS corona virus	spike glycoprotein	intramuscular	protective antibody virus-specific $CD4^+$ and CTL	Yang et al. (2004)
rabies	glycoprotein	intramuscular	virus-specific T cells and neutralising antibody	Xiang et al (1995)
measles virus	nucleoprotein	intradermal	virus-specific CTL	Hsu et al (1998)
HIV	Gag	intramuscular	Gag-specific CTL	Wang et al (1994)
Mycobacterium tuberculosis	85A antigen (Ag85A)	intramuscular	induction of anti-Ag85A antibodies and robust cell-mediated immune responses	Montgomery et al (1997)
Chlamydia pneumoniae	heat shock protein 60 (Hsp-60)	intranasal	$CD4^+$ and $CD8^+$ T cell dependent High IFN-γ production	Svanholm et al (2000)
Leishmania major	P4 nuclease protein and Hsp70 of *L. amazonensis*	intramuscular in combination with subcutaneous injections	induction of high levels of IFN-γ, IL-10 and TNF-α	Campbell et al (2003)

1.2 Mechanisms of immunity following DNA vaccination

1.2.1 Role of tissue resident somatic cells

The mechanisms underlying DNA vaccination are complex and are yet to be fully elucidated. The introduced plasmid and encoded antigen(s) have been detected predominantly in resident keratinocytes and occasionally in fibroblasts after intradermal vaccination (Eisenbraun et al., 1993; Hengge et al., 1996; Raz et al., 1994; Williams et al, 1991) and in myocytes after intramuscular injection (Wolff et al, 1990; 1992b). Tissue-resident (somatic) cells take up naked DNA by an unidentified mechanism and this is followed by expression of the antigen encoded within the DNA plasmid vector. Monolayers of keratinocytes do not however take up naked DNA (Hengge et al, 1996), suggesting that these cells must be in an organised epidermis for DNA uptake to occur. The process of how naked uncomplexed DNA is internalised by cells is intriguing and still not understood. Uptake of DNA may involve either potocytosis by caveolae (Wolff et al., 1992a), or even the formation of semi-permanent membrane vesicles for uptake of extracellular molecules via a nonendocytic pathway (Dowty et al., 1995).

1.2.2 Role of bone-marrow derived APC

Although plasmid DNA immunisation provides an effective means of inducing CTL responses to an expressed antigen, the mechanism by which CTL precursors are activated was something of a mystery. Since resident somatic cells are the principal cell type transfected after intramuscular (myocytes) and intradermal (keratinocytes and fibroblasts) DNA vaccination, it is not surprising that strong CTL responses were initially believed to be induced by these cells. Somatic cells are however deemed unlikely to be directly responsible for the induction of immunity following DNA vaccination. Although fibroblasts (Pober et al., 1984) and myocytes (Karpati et al., 1988; Stan et al., 2001) are known to be facultative APC due to inducible expression of MHC class II, they are incapable of stimulating naïve T cells due to the lack of expression of costimulatory molecules (CD40, CD80 and CD86). Stimulation of naïve T cells requires that they receive (at least) 2 signals; signal 1 is delivered via the T cell receptor by peptides presented on MHC molecules, whereas signal 2 is delivered by costimulatory molecules to the CD28 receptor on the T cell. Resident somatic cells do not therefore account for the potent T cell responses generated by DNA vaccination.

Substantial evidence has accumulated to suggest that professional bone marrow-derived APC play a pivotal role in the induction of immunity following DNA vaccination. Evidence to support the role of APC has been demonstrated in transplantation studies involving bone marrow chimeric mice, where mice are lethally irradiated and reconstituted with the bone marrow of an MHC disparate donor. These studies have shown that the induction of a CTL response is restricted to the MHC haplotype of the bone marrow-derived APC and not restricted to the haplotype of transfected somatic cells, after both intramuscular (Corr et al., 1996; Doe et al., 1996; Ulmer et al., 1996) and gene-gun administration of plasmid DNA (Iwasaki et al., 1997).

The evidence that bone marrow-derived APC are indeed responsible for the induction of immunity after DNA vaccination, rather than resident somatic cells, encouraged researchers to look more closely into the role of a family of potent APC known as dendritic cells (DC). DC are unique in that they are the only APC capable of stimulating naïve T cells (Steinman, 1991), which is the major requirement of successful primary vaccination. DC are strategically positioned at all major portals of entry, notably forming networks underlying major body surfaces such as the skin, trachea and intestine (Table 1.2). A key feature of the lifecycle of DC is their ability to acquire antigens in peripheral tissues (as immature DC) and traffic from their tissue of residence, through afferent lymphatic vessels into lymphoid organs where they present processed peptides to recirculating T cells, clearly distinguishing DC from tissue resident somatic cells (reviewed in Banchereau and Steinman, 1998). DC are highly equipped to stimulate naïve T cells due to a high density of antigen presentation molecules (10–100 fold greater expression of MHC class I and class molecules than on other APC), costimulatory molecules (CD40, CD80, CD83, CD86) and accessory molecules (ICAM-1, ICAM-3 and LFA-3); experimentally only one DC is required to stimulate 100-3000 T cells (Stockwin et al., 2000). DC can therefore be regarded as sentinels of the immune system, poised ready for potential invading pathogens in the periphery and conveying information with cells of the adaptive immune system.

Table 1.2 Examples of DC *in vivo*. DC represent a trace population of cells in all tissues. Follicular DC are distinct from the other DC subsets listed, these cells are involved in the retention of immune complexes and have a unique role in the stimulation of B cells and maintenance of B cell memory.

DC subset	location
Langerhans' cell	epidermis, mucosal lining of trachea
interstitial DC	dermis, heart, lungs, liver and other organs
veiled DC	afferent lymph
interdigitating DC	T cell-rich areas of lymphoid tissue
thymic DC	thymus
follicular DC	follicles of lymph nodes and spleen

1.2.3 Role of dendritic cells following DNA vaccination

1.2.3.1 DNA vaccination targets dendritic cells

Delivery of DNA via intradermal injection and via the gene-gun targets the skin, a highly immunocompetent site, which harbours two populations of immature DC. One population consists of numerous and readily accessible Langerhans' cells (LC) which are scattered in the outermost layers (epidermis) of skin with densities of ~1000 cells/mm^2 in mice (Bergstresser et al., 1980). A second population of DC is the dermal DC population (a type of interstitial DC), which are quite distinct from LC (reviewed in Lappin et al., 1996). Unlike interstitial DC, LC are completely absent in muscle. Surgical ablation experiments suggest that there may be a different contribution of local tissue antigen expression, depending on how DNA vaccines are administered. Excision of an injected muscle bundle within minutes of DNA inoculation did not affect the magnitude or longevity of the humoral and CTL responses, possibly due to injected plasmid entering the lymphatic or circulatory systems. By contrast, excision of the epidermal site of the skin up to 24 hours after gene gun bombardment completely abrogated the antibody response in the majority of mice (Torres et al., 1997). Klinman and colleagues also demonstrated complete abrogation of an immune response in mice whose injection site (skin) was removed immediately after gene-gun immunisation (Klinman et al., 1998); however, low level primary IgG responses were induced if the skin was left in place for 5 hours. Interestingly, IFN-γ production in spleen cells was observed in naïve littermates grafted with transfected skin within 5 hours of vaccination, suggesting that primary immunity is induced by transfected migratory skin cells.

1.2.3.2 Dendritic cells generate immunity following DNA vaccination

Several groups have successfully demonstrated that DC induce immunity in mice after DNA vaccination. For instance, Bot and co-workers (Bot et al., 2000) removed skin from the ears of mice after intradermal vaccination with a plasmid encoding nucleoprotein of influenza virus (containing a dominant murine class I/K^d restricted epitope) and then employed a skin explant culture system to isolate migratory MHC class II^+ DC. Importantly, adoptive transfer of migratory MHC class II^+ epidermal DC into naïve animals induced remarkably potent priming of virus-specific CTL. Further convincing evidence that DC are pivotal in the induction of immunity after DNA vaccination came from experiments where lymph node DC from DNA vaccinated mice were adoptively transferred into syngeneic naïve mice and induced strong CTL activity (Bouloc et al., 1999). Porgador and colleagues elegantly demonstrated the role of DC in the induction of CTL responses following gene-gun bombardment (Porgador et al., 1998). This involved delivery of gold beads coated with a β-galactosidase (β-gal) encoding plasmid, followed by the isolation of different lymph node cell populations and incubation with $CD8^+$ T cells specific for a β-gal-derived determinant presented by K^b. DC expressing the DNA-encoded antigen were rare, yet depletion of DEC-205^+ DC eliminated up to 70% of the presentation activity, whereas depletion of macrophages and B cells had no effect. Although DC were well demonstrated to induce immunity after DNA vaccination, the mechanism(s) by which DC come into contact with the plasmid/encoded antigen remained unanswered. For instance, were directly transfected DC responsible for the induction of immunity after vaccination, or were T cells primed with DC which had taken up antigen released from transfected somatic cells?

1.2.3.3 Transfected DC induce immunity after DNA vaccination

There is convincing evidence that resident DC are directly transfected by plasmid DNA after vaccination. Plasmid DNA has been detected in DC isolated from lymph node and skin after intramuscular and intradermal vaccination (Casares et al., 1997). Fluorescently-labelled, skin-derived DC have not only been found to contain gold beads in the draining lymph node (DLN), but also to express green fluorescent protein (GFP), after gene-gun administration of plasmid encoding GFP (Condon et al., 1996). Furthermore, antigen-specific mRNA has been detected in migratory LC after gene-gun vaccination of human skin organ cultures; LC were then demonstrated to efficiently present a peptide derived from the melanoma antigen (MART-1) to MART-1-specific CTL (Larregina et al., 2001b). Priming of $CD4^+$ T cells by directly transfected DC has also been demonstrated *in vivo* (Akbari et al., 1999). Moreover, as few as 500 *in vitro* transfected DC are capable of inducing both strong humoral and cell-

mediated immune responses *in vivo* (Timares et al., 1998), suggesting that direct transfection of DC is largely responsible for the generation of immunity after DNA vaccination.

1.2.3.4 Dendritic cells gain access to antigen from non-bone-marrow derived cells (cross-priming)

Although it has been demonstrated that a small number of DC are directly transfected following DNA vaccination, an alternative mechanism whereby DC gain access to antigen is by uptake of secreted protein synthesised by transfected skin or muscle cells. DC have indeed been shown to acquire antigen from transfected myoblasts and cross-present this antigen to antigen-specific $CD4^+$ T cells (Casares et al, 1997). In addition, DC have a unique ability to channel exogenous antigen into the MHC class I presentation pathway. This property is termed "cross-priming" and enables DC to present exogenous antigen on both MHC class II and class I molecules (Brossart and Bevan, 1997; Shen et al., 1997). Two routes for the exogenous MHC class I pathway have been described, a TAP-independent pathway in which Ag is hydrolysed in endosomes, and a phagosome-to-cytosol pathway, that is TAP dependent (reviewed in Banchereau et al., 2000). Cross-priming may occur by direct transfer of MHC class I-associated peptide on the surface of transfected somatic cells to DC, or secreted antigen may be taken up by DC by micropinocytosis. Alternatively, chaperone: peptide complexes may be taken up by a receptor-mediated mechanism (Kumaraguru et al., 2000), or DC may acquire antigen by phagocytosis of apoptotic cells via $\alpha v\beta 5$ and CD36 and cross present the antigen to $CD8^+$ T cells (Albert et al., 1998). Transfected somatic cells could therefore be regarded as antigen-producing "factories", secreting antigen into the extracellular milieu or releasing the antigen upon dying. And importantly, DC are well equipped to stimulate both $CD4^+$ and $CD8^+$ T cells, which is imperative since CTL responses to both intramuscular and intradermal DNA vaccination are highly dependent upon the generation of $CD4^+$ T cell help via a class II MHC-dependent pathway (Maecker et al., 1998).

The unique ability of DC to channel exogenous antigen into the MHC-I presentation pathway explains how transplantation of stably transfected myoblasts into chimeric mice induces a protective antibody and CTL response that is restricted to the haplotype of the recipient mice bone marrow cells (Ulmer et al, 1996). However, cross-priming was not found to make a substantial contribution to $CD8^+$ T cell priming in Porgador's study (Porgador et al, 1998), where instead a predominant role of directly transfected DC in antigen presentation to $CD8^+$ T cells was highlighted, since removal of directly transfected lymph node DC from mice reduced presentation by 60–70% 24 hours after gene-gun

bombardment with a plasmid-encoding human CD4 and β-gal. The relative contribution of secreted and non-secreted antigen in the induction of T cell priming after DNA vaccination has been investigated by Rush and colleagues (Rush et al., 2002), where fluorescently labelled ovalbumin (OVA)-specific TCR transgenic T cells were adoptively transferred into mice, followed by vaccination with DNA vectors encoding cell-associated or soluble secreted OVA. DNA vectors encoding cell-associated OVA resulted in greater $CD8^+$ T cell division, whereas vectors encoding soluble secreted OVA (targeted to the classical secretory pathway) enhanced division of $CD4^+$ T cells and to a lesser extent, $CD8^+$ T cells, suggesting that although secreted antigen can access the MHC class I-processing pathway (by cross-priming), it is less efficiently presented to $CD8^+$ T cells than cell-associated forms.

Plasmid DNA is rapidly disseminated throughout the body via blood (Nichols et al., 1995) and lymph (Mena et al., 2001; Watkins et al., 1999), and can even reach remote areas such as lymph nodes (Akbari et al, 1999) where plasmid DNA could be taken up and expressed by resident lymph node DC. It is also possible that migratory DC internalise plasmid DNA during transit. Collection of lymph following intradermal vaccination with a construct encoding GFP revealed that plasmid DNA was present in lymph fluid within one hour of injection (Watkins et al, 1999) and approximately 1% of afferent lymph DC (ALDC) contained GFP protein, with fluorescence peaking 2–4 hours after-vaccination; however, PCR analysis of the afferent lymph cell (ALC) pellets failed to demonstrate the presence of the GFP plasmid. Alternatively, DC migrating from the periphery could transfer their captured antigens to other DC in the lymph node for presentation to T cells. Such transfer could occur by phagocytosis of the antigen-loaded DC (Inaba et al., 1998) or by the release of antigen-bearing vesicles (exosomes) derived from DC lysosomal compartment (Thery et al., 1999).

1.2.4 The method of delivery of DNA affects the type of immune response induced

The method employed to deliver plasmid DNA has long been known to affect the type of immune response induced. This has made it difficult to compare the immunogenicity of various vaccines where different routes of administration have been employed. DNA vaccine efficacy is strongly influenced by the route of vaccination in mice and there is evidence that this may also be the case in large outbred animals. Production of IgG2a is a hallmark of Th1-type immunity, reflecting IFN-γ enhanced Ig isotype switching to IgG2a, whereas Th2 responses favour the generation of the IgG1 subclass (Stevens et al., 1988). Studies in mice have shown that DNA vaccines injected intramuscularly elicit strong CTL responses and

humoral responses characterised by serum IgG2a (indicating a predominant Th1 response). Conversely, gene-gun-mediated DNA immunization is often characterised by lower CTL activity and predominant IgG1 (Th2-type response) (Feltquate et al., 1997). Furthermore, injection of DNA into the skin induces higher CTL activity than when DNA is administered by gene-gun vaccination (Bouloc et al, 1999).

Differences in the Th response after DNA vaccination have been partly attributed to the amount of DNA used in the delivery system. Gene-gun vaccination uses small amounts of DNA (typically 0.5–2μg/shot), whereas intramuscular injection generally requires more plasmid (~10μg) and so it has been speculated that a Th1-biased immune response is promoted following intramuscular injection, since more CpG motifs would be available to stimulate innate immune cells including DC to produce Th1 polarising cytokines. In agreement with this, Th2 immunity to hepatitis B surface antigen primed by gene-gun mediated DNA vaccination can be shifted towards Th1-type immunity by codelivery of CpG motif-containing oligodeoxynucleotides (Zhou et al., 2003). The intramuscular route was indeed reported to be more effective than gene-gun or intradermal DNA vaccination in sheep and resulted in better protection of animals following challenge with live *Corynebacterium pseudotuberculosis* (De Rose et al., 2002). This was suggested to be due to a more pronounced Th1 response characterised by elevated IgG2 responses.

The induction of strong CTL responses after intramuscular injection may also be due to the relatively inefficient cellular uptake of DNA by myocytes. Based on reporter gene expression, DNA plasmid injection into mouse muscle produces only picogram amounts of protein in muscle cells (Wolff et al, 1990). Importantly, the level of antigen expression can have important consequences in terms of activating $CD4^+$ and $CD8^+$ T cells. Recent data indicate that $CD8^+$ and $CD4^+$ T cells are fundamentally different in their requirements for activation and clonal expansion (Foulds et al., 2002). In contrast to humoral responses, only a very small amount of antigen, when presented in the context of a DC, is sufficient to prime and sustain strong CTL responses and is not influenced by the duration of antigen presentation. In contrast, $CD4^+$ cells require repeated antigen exposure and increased amounts of antigen for the survival of proliferating cells.

1.3 Optimisation of DNA vaccines

1.3.1 General introduction

DNA vaccination is in many cases hampered by poor efficacy in species other than mice; clinical trials in humans have so far been largely disappointing (reviewed in Donnelly et al, 2003). A recurring observation in clinical studies reported in the literature so far is that antibody responses induced by DNA vaccination are relatively low compared with those induced by direct injection of proteins with adjuvants. Whilst CTL are required to control and eliminate an infection once it has become established, neutralising antibodies are necessary in order to prevent establishment of the infection (reviewed in Zinkernagel, 2003). It has been proposed that although plasmid DNA may persist for some time (Williams et al, 1991), the levels of antigen produced may be insufficient to induce adequate antibody production (Foulds et al, 2002). Results of the first human trial of a malaria vaccine showed no antibody response in any volunteer despite the induction of CTL responses in the majority of vaccinees (Wang et al, 1998). Interestingly, Whitton and colleagues, have designed a DNA vaccine which induced a CTL response, but did not induce antibodies and argue that this is due to a lack of release of intact protein (Whitton et al., 1999). Furthermore, DNA vaccines designed to express a correctly folded immunogen can induce a highly specific antibody response (Benvenuti and Burrone, 2001). Increasing antigen expression and designing plasmids which ensure some of the immunogen is released intact and correctly folded, may hold the key to enhanced antibody responses generated by DNA vaccines.

The evaluation of DNA vaccines in outbred animals has been particularly challenging due to the high cost, the absence of well-characterised populations and the limited number of immunological reagents. Few studies have focused on veterinary species and while results obtained in laboratory animals can be extrapolated to veterinary species, this is not always relevant. Indeed experiments in large out-bred animals suggest that DNA vaccines are not nearly as immunogenic as they are in rodents (reviewed in Babiuk et al., 2003). Drew and colleagues have directly compared the immunogenicity of DNA vaccines encoding *Taenia ovis* host-protective antigens in both mice and sheep (Drew et al., 2000). DNA vaccines were immunogenic in mice and generated significant titres of antigen-specific antibody after intramuscular injection, whereas vaccination of sheep generated significantly lower titres of specific antibody. It has been suggested that the transfection efficiency of myocytes is lower in larger animals than in mice, resulting in low antigen expression (Han et al., 2000). Promisingly, *in vivo* electroporation has been successfully utilised to enhance transfection of ovine myocytes and resulted in enhanced humoral immunity, possibly due to an increased release of intact protein (Scheerlinck et al., 2004).

Despite considerable effort expended in improving DNA vaccine delivery, only minute amounts of antigen are available for immune induction following DNA vaccination in large animals, particularly with regard to gene-gun vaccination. Experiments conducted by Braun and colleagues (Braun et al., 1999), demonstrated that mice can be readily immunised with the gene-gun; yet in cattle, a secondary immunisation was required for seroconversion, even after receiving 10-100 times as much plasmid. Booster vaccinations are commonly employed by researchers and yet still cannot guarantee protection. For instance, only partial protection against foot-and-mouth disease virus challenge has been demonstrated after gene-gun vaccination of swine, even with administration of booster vaccines (Benvenisti et al., 2001). Furthermore, vaccination of large animals generally requires milligram doses of DNA, which is unfavourable from both safety and economic viewpoints.

1.3.2 Strategies employed to enhance efficacy of DNA vaccines

It has been speculated that the lack of efficacy of DNA vaccines may be due to the fact that the delivery conditions do not efficiently target resident DC, resulting in inadequate access of antigens to these cells. In addition, insufficient activation of DC (Section 1.4) or possibly even ineffective targeting of a particular DC subset may account for the lack in efficacy of DNA vaccines. Evidently there is a requirement to further optimise DNA vaccines before this technology can be applied to humans and livestock. One method is to employ a "prime-boosting" strategy. The basic prime-boost strategy involves priming the immune system to a target antigen delivered by one vector (plasmid DNA) and then selectively boosting this immunity to a protective level by re-administration of the antigen in the context of a second and distinct vector (reviewed in Woodland, 2004), such as live-attenuated or killed vaccines. Heterologous prime-boost strategies gaining most interest use DNA vaccine priming followed by boosting with a recombinant vaccinia virus.

Researchers have also focused on modifying plasmid vectors to enhance protein expression, for instance by including introns in the gene (Rush et al, 2002) or by targeting antigen to MHC class II- or I-processing pathways (Gurunathan et al, 2000). Methods to improve DNA uptake have also been investigated and include administration of cationic lipids and even the application of electric currents after intramuscular injection of DNA (reviewed in Donnelly et al, 2003). Other methods include inducing apoptosis in transfected cells and promoting phagocytosis of transfected cells (Gurunathan et al, 2000). Enhancement of the immune response to DNA vaccines has been achieved by co-administration of immunomodulatory genes including cytokines (Section 1.3.3), chemokines (including RANTES and MIP-1α),

costimulatory molecules (CD80, CD86 and CD40), heat-shock proteins (Hsps) such as Hsp 70, and the complement protein C3d (reviewed in Sasaki et al., 2003).

1.3.3 Cytokines as molecular adjuvants

Strategies involving the combination of DNA immunisation and molecular adjuvants are under intense investigation. The magnitude and direction (humoral or cellular) of the immune response can be manipulated upon administration of DNA vaccines containing cytokine genes as molecular adjuvants. For instance, inclusion of genes encoding the Th1-polarising cytokines IL-12, IFN-γ (Chow et al., 1998; Kim et al., 1998) and IL-18 (Kim et al., 2001) as molecular adjuvants have been shown to skew the immune response towards the Th1 phenotype and to induce potent CTL responses following DNA vaccination. In contrast, co-injection of the IL-4 gene enhances development of antigen specific Th2 cells and increases production of IgG1, whereas Th1 differentiation and IgG2a production are suppressed (Chow et al, 1998; Kim et al, 1998). Another method to enhance the immune response is to employ genetic cytokine adjuvants to recruit DC to the site of inoculation. Granulocyte-Macrophage Colony-Stimulating Factor (GM-CSF) and IL-3 are both potent cytokines known to cause the growth and differentiation of immature haematopoietic cells and have been implicated in the development of DC.

1.3.3.1 GM-CSF and IL-3 biology

GM-CSF and IL-3 are haematopoietic cytokines that share several common features. Both cytokines stimulate the proliferation, differentiation, and activation of haematopoietic cells in the bone marrow (reviewed in Martinez-Moczygemba and Huston, 2003). Part of the overlap in function of these cytokines can be explained by their use of a common signalling component in their receptors. Receptors for GM-CSF and IL-3 consist of two subunits, where an α subunit is specific for each cytokine and a β unit is common to both cytokines (reviewed in Bagley et al., 1997). IL-3 is expressed predominantly by activated T cells, mast cells, and natural killer (NK) cells. The expression of IL-3 in mice and humans is co-regulated with that of GM-CSF in both T cells and NK cells; however, IL-3 expression is not readily detected in macrophages, fibroblasts or endothelial cells, all of which express GM-CSF (McInnes et al., 1993).

1.3.3.2 GM-CSF and IL-3 are used to propagate DC *in vitro*

DC are found in virtually all tissues and DC precursors (pre-DC) circulate in the blood and seed tissues. Large-scale preparation of DC is however hampered by their low frequency in blood (DC constitute only 1–2% of circulating leukocytes) and their relative scarcity in tissues. Furthermore, the isolation of DC from tissues is difficult and requires extensive purification procedures including enzymatic digestion of the collagenase matrix (Steinman et al., 1974). Alternatively, human DC can either be generated from the $CD34^+$ progenitor pool contained in cord blood (Caux et al., 1996a) and in peripheral blood (Romani et al., 1994). In addition, DC can be propagated *in vitro* using $CD14^+$ blood monocytes (Zhou and Tedder, 1996). Murine DC can be propagated from either mouse bone marrow or blood according to methods established by Inaba and co-workers (Inaba et al., 1992a; Inaba et al., 1992b). *In vitro* culture systems generate large numbers of DC and have enabled researchers to study these rare and enigmatic cells.

DC of lymphoid and myeloid origin were originally proposed in both mice and in humans, although the precise origin of these subsets *in vivo* is not clear as both common myeloid and lymphoid progenitors can give rise to both "myeloid" ($CD8\alpha^-$) and "lymphoid" ($CD8\alpha^+$) DC in mice (Manz et al., 2001; Traver et al., 2000). GM-CSF is used extensively for the *in vitro* generation of myeloid DC ("DC1") from human monocytes (Sallusto and Lanzavecchia, 1994) and from pluripotent progenitors (Caux et al., 1992b; Santiago-Schwarz et al., 1992). GM-CSF is also used to generate myeloid DC from mouse bone marrow (Inaba et al, 1992a) and blood (Inaba et al, 1992b) and is essential for the viability and function of cultured murine epidermal LC (Witmer-Pack et al., 1987). Both murine thymic pre-DC (Saunders et al., 1996) and human plasmacytoid DC (pDC), also referred to in the literature as "DC2" (and proposed to be of lymphoid origin) (Grouard et al., 1997; Kohrgruber et al., 1999; Olweus et al., 1997) show a dependence on IL-3 rather than GM-CSF for survival and development into mature DC. In addition, foetal liver tyrosine kinase 3 ligand (Flt-3L), a stromal cell product, is used to propagate murine plasmacytoid-type DC (Gilliet et al., 2002).

In terms of DC development *in vivo*, it may be an oversimplification to assume that one type of DC relies exclusively on one cytokine and not on another. It is likely that GM-CSF and IL-3 (and other growth factors such as Flt-3L) have overlapping functions *in vivo*. Although GM-CSF is an important cytokine for the generation of myeloid-related DC *in vitro*, examination of mice deficient in GM-CSF or in GM-CSF receptor (GM-CSFR(β)) indicates that DC development in lymphoid tissues is not dramatically affected (Vremec et al., 1997). Furthermore, myeloid DC can be propagated from bone marrow cells obtained from GM-CSFR knockout mice, if supplied with Flt-3L and IL-6 (Hikino et al., 2000). Such flexibility in the DC system is further demonstrated by the finding that LC (proposed to be of myeloid

origin) can be propagated from cord blood $CD34^+$ haematopoietic progenitor cells with IL-3 in conjunction with TNF-α (Caux et al., 1996b) or TGF-β (Mollah et al., 2003). IL-3 in combination with IL-4 has also been used to generate human myeloid "DC1" which preferentially induce a Th2 response (Ebner et al., 2002). Conversely, human "lymphoid" DC can be generated from early human thymic T-precursors supplied with a GM-CSF based cytokine mix (Kelly et al., 2001).

1.3.3.3 Administration of GM-CSF and IL-3 *in vivo*: expansion of DC

Both GM-CSF and IL-3 increase the recycling and maturation of haematopoietic progenitors in the bone marrow. For this reason GM-CSF (and to a lesser extent IL-3) are well documented as immunotherapeutic agents clinically exploited to augment regimens for cancer therapy and bone marrow transplantation (reviewed in Armitage, 1998). For instance, GM-CSF is well documented to increase antibody-dependent cell-mediated cytotoxicity towards tumour cells and this is believed to be due to enhancement of the generation and function of DC. GM-CSF has pleiotropic effects *in vivo*, including upregulation of MHC class II antigen expression on macrophages and DC, induction of inflammation at the inoculation site and mobilisation and maturation of DC. Indeed GM-CSF is often exploited specifically to expand DC in humans, for instance, to mobilise DC in breast cancer patients undergoing autologous stem cell transplantation (Avigan et al., 1999) and also to generate autologous tumour DC vaccines *in vitro* (Nestle et al., 1998).

Although flexibility has been demonstrated with regard to the type of DC propagated *in vitro* with different cocktails of cytokines (Section 1.3.3.2), it cannot be disputed that GM-CSF favours the outgrowth of myeloid DC *in vitro*. Not surprisingly, expansion of myeloid DC has also been documented after *in vivo* administration of recombinant GM-CSF. Systemic administration of GM-CSF and IL-4 preferentially expands and matures myeloid pre-DC1 into DC1 (human leukocyte antigen (HLA)-$DR^+/CD11c^+$) in patients with advanced metastatic cancer (Kiertscher et al., 2003). DC were found to express higher levels of HLA-DR, CD11c and CD80 than pre-treatment cells and Mixed Leukocyte Reaction (MLR) activity was comparable to that of monocyte-derived DC (MoDC) generated *in vitro* from the patients' pre-treatment blood using GM-CSF and IL-4. Administration of recombinant GM-CSF in humans has also been reported to expand $S100^+$, Factor $XIIIa^+$ myeloid DC after intradermal injection into melanoma skin metastases (Nasi et al., 1999) and to significantly increase $S100^+$ DC in tumour DLN in breast cancer patients (Pinedo et al., 2003). There are few reports on the administration of recombinant GM-CSF in outbred species other than

humans, although a significant increase in dermal MHC class II^+ $CD1^-$ DC was observed in skin after intradermal injection of recombinant GM-CSF in sheep (Haig et al., 1995a).

Studies in mice have also revealed the ability of GM-CSF to augment the immune response. For instance, injection of irradiated tumour cells genetically engineered to secrete murine GM-CSF stimulated potent and long-lasting anti-tumour immunity, requiring both $CD4^+$ and $CD8^+$ T cells (Dranoff et al., 1993). A later study demonstrated that injection of tumour cells co-transduced with GM-CSF and CD40 resulted in a marked infiltration of DC into tumours with enhanced capacity to take up and present endogenous tumour-associated antigens and prime tumour-specific $CD8^+$ T cells (Chiodoni et al., 1999). Expansion of splenic DC with enhanced allostimulatory capacity in MLR (Hanada et al., 1996) and enhanced uptake and processing of particulate antigen (Storozynsky et al., 1999) has also been described after injection of mice with tumour cells transfected with GM-CSF. Expansion of splenic DC with enhanced antigen uptake and presentation was also reported after injection of tumour cells transfected with IL-3 (Storozynsky et al, 1999), although a proportion of the DC infiltrate had some macrophage-like characteristics, including expression of Mac-1. Indeed, IL-3 has been well demonstrated to enhance presentation of particulate antigen presentation by APC and to prime tumour-specific CTL (Lord et al., 1998; Yeh et al., 1998).

Preferential expansion of the myeloid subset ($CD11c^+$ $CD11b^{bright}$) and not lymphoid-related DC ($CD11c^+$ $CD11b^{dull/-}$) in mouse spleen has been documented following subcutaneous administration of a polyethylene glycol-modified form of recombinant GM-CSF (Daro et al., 2000; Pulendran et al., 1999) and unmodified recombinant GM-CSF (O'Keeffe et al., 2002; Parajuli et al., 1999). In addition, expanded DC isolated from GM-CSF-treated mice captured and processed antigen more efficiently than DC from Flt-3L-treated mice but were equally efficient at stimulating allogeneic and antigen-specific T cell proliferation *in vitro* (Daro et al, 2000). Preferential expansion of myeloid $CD11c^+$ DEC 205^- DC was also reported following adenoviral-mediated GM-CSF over-expression in the liver (Pillarisetty et al., 2003). Interestingly, GM-CSF does not appear to skew the cytokine profiles of DC, but instead may augment cytokine production. This is illustrated by the finding that the preferentially expanded myeloid DC subset in mice (which was originally described as "Th2 inducing"; section 1.4.4.2) contain more abundant IL-10 transcripts after administration of recombinant GM-CSF; whereas IL-12p40 mRNA expression is increased in the isolated $CD8\alpha^+$ lymphoid DC subset (which has a capacity to express high levels of IL-12p70; section 1.4.4.2) (Parajuli et al., 2001). Furthermore, GM-CSF expanded myeloid DC induced antigen-specific $CD4^+$ transgenic T cells to secrete large amounts of the Th2 cytokines IL-4 and IL-10 when restimulated *in vitro* (Pulendran et al, 1999). Myeloid DC also induced Th1-associated cytokines (IFN-γ and IL-2) in antigen-specific $CD4^+$ transgenic T cells in mice

primed with OVA-peptide pulsed DC; however, GM-CSF treatment significantly increased IgG1 titres and failed to stimulate IgG2a in one strain of mouse. It was proposed that the Th2 cytokines mitigated the effects of IFN-γ, thus favouring an IgG1 response.

1.3.3.4 GM-CSF as a molecular adjuvant

GM-CSF has received considerable interest as a molecular adjuvant, whilst IL-3 has not as yet been investigated. Much interest has focused on the use of GM-CSF to overcome poorly immunogenic antigens, such as those associated with intracellular infection and cancer. Furthermore, GM-CSF is well documented to augment the primary antibody response (reviewed in Warren and Weiner, 2000). While the mechanism for the adjuvant effects of GM-CSF has not been completely elucidated, it seems likely that the ability of GM-CSF to attract immature DC into the tissues following inoculation enhances the ability of the coadministered DNA vaccine to be presented by DC. Infiltration of $CD11c^+$ (myeloid) immature DC at the inoculation site of GM-CSF DNA injection has been postulated as a mechanism by which immune responses are enhanced in mice after both intramuscular (Haddad et al., 2000; Ou-Yang et al., 2002) and intradermal vaccination (Bowne et al., 1999).

Plasmid GM-CSF (pGM-CSF) was first shown to enhance both B cell and Th cell activity after coadministration with plasmid DNA encoding the glycoprotein of rabies virus (Xiang and Ertl, 1995). It was suggested that a significant increase in levels of neutralising antibody conferred protection following challenge with virus. pGM-CSF administration has subsequently been shown to augment antigen-specific antibody responses to hepatitis C virus core protein (Geissler et al., 1997; Ou-Yang et al, 2002), HIV (Kim and Weiner, 1997), herpes simplex virus type-2 (Sin et al., 1998; Sin et al., 1999) and Plasmodium yoelii (Wang et al, 1998). There are however some discrepancies in the predominant isotype induced by GM-CSF, since induction of antigen-specific IgG1 antibodies (a hallmark of Th2-type immunity) have been documented (Burger et al., 2001; Harrison et al., 2002; Kim and Weiner, 1997; Liu et al., 1998a; Sin et al, 1998), whereas others have demonstrated the induction of IgG2a antibodies (Sakai et al., 1999; Sun et al., 2002), a hallmark of Th1-type immunity. The balance of activation and expansion of DC subsets by GM-CSF plasmid DNA injection might be one of the factors implicated in different Th responses.

pGM-CSF enhances CTL responses to a number of infections, including hepatitis C (Geissler et al, 1997; Ou-Yang et al, 2002), and the envelope gene of HIV (Moore et al., 2002). CTL activity was significantly increased in mice co-injected with pGM-CSF and a β-gal plasmid (Burger et al, 2001); although interestingly an IgG1 response was induced. Most

CTL responses require Th1 polarising cytokines (IL-2 and IFN-γ) for their induction; however, CTL can be primed by DC in the absence of $CD4^+$ T cells (Schlecht et al., 2001). Some evidence suggests that the adjuvant effect of GM-CSF might also be related to enhanced phagocytosis or pinocytic uptake of antigen by DC (Lutz et al., 1996). Increased antigen uptake in conjunction with increased MHC and costimulatory molecule expression may result in a more effective $CD8^+$ T cell priming capacity. Furthermore, Sin and colleagues (Sin et al, 1998) demonstrated that although GM-CSF coinjection induced a dramatic increase in IgG1 levels as compared to IgG2a levels, Th cell proliferation and secretion of Th1-polarising cytokines were significantly increased, thus an overall increase in either isotype should be interpreted with some degree of caution. Others have reported some enhancement of CTL activity by GM-CSF, which was less potent than other plasmid-encoded cytokines such as IL-2 (Geissler et al, 1997), IL-12 or IFN-γ (Chow et al, 1998). Conversely, others found that GM-CSF has little effect on induction of CTL activity when used as a plasmid adjuvant (Kim et al, 1998). The differences in the findings among these studies are significant and may reflect differences in expression vectors, assays employed and the antigen(s) of choice.

The induction of a predominantly humoral or cellular immune response may also be an inherent property of the antigen after DNA vaccination. This is illustrated by work conducted by Moore and colleagues (Moore et al, 2002) where in the absence of GM-CSF, a strong CTL response was elicited in response to plasmid encoding the envelope gene of HIV, whereas a strong humoral immune response was elicited to the nef gene. The predominance of a cellular or humoral response was not reversed by GM-CSF in this study; instead GM-CSF enhanced the already biased immune response, such that env-specific IFN-γ producing $CD4^+$ Th1 cells and a strong CTL response were induced.

Bicistronic plasmids contain two genes under the control of the same or separate promoters. Bicistronic plasmids expressing GM-CSF and an antigen have been shown to further augment immunity. Co-administration of a GM-CSF plasmid and a plasmid encoding gp120 of HIV led to a marginal increase in gp120-specific $CD4^+$ T cell response (Barouch et al., 2002); however, immunization with a bicistronic plasmid led to a dramatic augmentation of $CD4^+$ T cell responses. Bicistronic plasmids are more effective at inducing immunity to melanoma (Sun et al, 2002); hepatitis C (Lee et al., 1998), and *Mycobacterium tuberculosis* (Kamath et al., 1999). These data suggest that by linking antigen and GM-CSF expression closely *in vivo*, a more conductive microenvironment is provided for the uptake and presentation of antigen by DC. The optimal induction of immune responses through APC may require close proximity of the antigen and appropriate signals that allow for maturation and migration of antigen loaded APC, as demonstrated by the fact that priming of a distant

injection site with pGM-CSF 5 days prior to exposure to plasmid encoding β-gal antigen did not enhance the IgG response to β-gal, whereas injection at the same site enhanced antibody production (Burger et al, 2001). It is puzzling why the timing of administration of pGM-CSF can influence the Th response (Kusakabe et al., 2000). Injection of pGM-CSF 3 days before vaccination with a HIV-antigen encoding plasmid induced a Th2 response in mice. Conversely, injection of pGM-CSF 3 days after DNA vaccination induced a Th1 response.

There are limited studies where pGM-CSF has been employed as a molecular adjuvant in outbred species. In marked contrast to the enhanced serological responses observed in mice after DNA vaccination with pGM-CSF, Nobiron and co-workers found no evidence of increased antibody titres in cattle vaccinated with constructs expressing the E2 envelope glycoprotein of bovine viral diarrhoea virus plus pGM-CSF, than in animals vaccinated with the E2-encoding plasmid alone (Nobiron et al., 2003). Similarly, pGM-CSF did not significantly affect the neutralizing antibody levels to dengue virus type 1 in *Aotus* monkeys; however, pGM-CSF administration in combination with immunostimulatory sequences and the DNA vaccine afforded 100% protection to animals challenged 6 months after vaccination (Raviprakash et al., 2003). Co-delivery of pGM-CSF in conjunction with a protein boost significantly enhanced the antibody response to EG95 of *Echinococcus granulosus* in sheep (Scheerlinck et al., 2001). The mechanisms involved in the induction of immunity after pGM-CSF administration are however, poorly defined and require further attention if pGM-CSF is to be fully exploited in DNA vaccination.

1.3.3.5 GM-CSF is a potent inducer of inflammation

GM-CSF is not only a potent growth factor for DC, but it is also a major inducer of inflammation and localised inflammation at the injection site has been well documented (Warren and Weiner, 2000). Conventional adjuvants such as Freund's adjuvant (widely used to augment antibody responses in experimental animals), cause marked inflammation at the site of inoculation and act by inducing DC maturation, resulting in an upregulation of MHC and costimulatory molecules, a release of cytokines and an upregulation of chemokine receptor CCR7 (Medzhitov and Janeway, Jr., 1999). Adjuvants could therefore be interpreted to "trick" DC into responding as though an active infection is taking place, therefore promoting DC migration and maturation to the DLN and interaction with naïve T cells. DC are highly flexible cells and it is now becoming apparent that the environment in which an immature DC first encounters antigen will shape the way in which that DC functions. To understand the implications of GM-CSF as an adjuvant, this necessitates a closer

examination of the role of DC as immunological sentinels and how inflammatory signals in the periphery affect the biology of DC and ultimately the instruction of T cells.

1.4 Dendritic cells and inflammation

1.4.1 *In vitro*-generated DC require inflammatory stimuli to become mature DC

In most culture systems DC exist in two functionally and phenotypically distinct states, immature and mature (reviewed in Mellman and Steinman, 2001). Immature cells are adept at endocytosis and express relatively low levels of surface MHC class I and II products and costimulatory products (CD80 and CD86). Abundant MHC class II molecules are synthesised, but they are mainly sequestered intracellularly in late endocytic compartments. Immature DC are remarkable fluid phase endocytic cells; to date they are the only cells found to perform fluid phase macropinocytosis constitutively (Sallusto et al., 1995). Thus, immature DC in culture are active in antigen uptake but do not present antigen efficiently to T cells.

The addition of exogenous factors, for example, proinflammatory cytokines such as TNF-α and IL-1β, or microbial products such as lipopolysaccharide (LPS), (a feature of Gram negative bacteria); CpG motifs, or dsRNA (RNA viruses) can convert these cells into a mature phenotype, characterised by high surface expression of MHC and costimulatory molecules and a reduced capacity for antigen uptake but now with an exceptional capacity for T cell stimulation (reviewed in Stockwin et al, 2000). This transition (often referred to as "activation") is accompanied by a dramatic cytoplasmic reorganisation highlighted by a redistribution of MHC class II from intracellular compartments to the plasma membrane. The cells extend long dendritic cell processes (membrane folds) that increase opportunities for T cell capture and interaction.

1.4.2 *Ex-vivo* isolated Langerhans' cells become activated by inflammatory stimuli

Defined maturational stages of DC have also been described in DC isolated from tissues; early studies demonstrated that when DC were isolated from lymphoid tissue, a terminally differentiated population of DC was obtained, characterised by high surface expression of MHC class II, but low rates of MHC biosynthesis (reviewed in Watts, 1997). As a result, these DC stimulated T cells that could recognise the existing surface MHC-peptide complexes, but they were poor at capturing and presenting newly offered antigens. Conversely, analyses of DC isolated from peripheral tissues and studied immediately *ex vivo* suggested that DC exist as immature cells that can be roused by various stimuli. For instance, freshly isolated epidermal LC are phagocytic and endocytic (Reis e Sousa et al., 1993) and can acquire and process protein antigens, but are poor at presenting antigen to responsive T lymphocytes (Romani et al., 1989). After culture, they become weakly endocytic and lose the ability to process native antigens, but develop potent immunostimulatory capacity (Schuler and Steinman, 1985).

Skin explant models are useful tools which have helped to define the migratory pathways of cutaneous DC. Briefly, skin patches are explanted and LC are challenged with an antigen or some form of stimulus and migration of DC into the tissue culture medium is observed. Following culture with inflammatory mediators such as LPS, TNF-α or IL-1β (reviewed in Banchereau et al, 2000), LC downregulate E-cadherin expression and loosen their connections with surrounding keratinocytes (Tang et al., 1993), invade the lymphatic vessels in the dermis and end up in the culture medium (Lukas et al., 1996). Migrated LC are of a mature phenotype, as illustrated by their potent ability in MLR due to high surface expression of MHC class II and costimulatory molecules. Thus, *in vitro* cultured murine epidermal LC more closely resemble terminally differentiated cells isolated from lymphoid tissues, capable of forming clusters with resting T cells, whereas fresh LC are of an immature phenotype (Schuler and Steinman, 1985).

1.4.3 *In vivo* exposure of skin to inflammatory mediators causes DC migration and maturation

Cumberbatch and co-workers have conducted several *in vivo* studies in which they have demonstrated that intradermal injection of recombinant TNF-α, (Cumberbatch and Kimber, 1992), IL-1β (Cumberbatch et al., 1997a; Cumberbatch et al., 1997b; Cumberbatch et al., 1997c) and IL-18 (Cumberbatch et al., 2001) reduce the number of LC in murine epidermis

and increase the number of DC in DLN. Subcutaneous application of LPS to mice also results in a loss of LC in the epidermis; emigrating DC become visible in lymph vessels and accumulate in T cell rich areas of lymphoid organs draining the site of exposure (Roake et al., 1995). CpG motifs (Ban et al., 2000) and heat shock proteins (Binder et al., 2000) have also been demonstrated to promote LC maturation and migration. There is even evidence that inflammatory cytokines cause LC migration in humans; intradermal administration of TNF-α resulted in a dose-dependent reduction in the frequency of $CD1a^+$ $HLA\text{-}DR^+$ epidermal LC (Cumberbatch et al., 1999).

1.4.4 DC are activated by "danger signals"

Inflammatory signals have therefore been well documented to cause profound changes in DC function, namely to cause DC maturation and *en masse* migration to the DLN. DC are capable of detecting a plethora of microbial and inflammatory stimuli and such DC-activating stimuli have been termed "danger signals". Danger signals were proposed as part of a model of immunity that suggests that the immune system responds to danger, rather than to those that are simply foreign (Matzinger, 1994). Danger signals consist of molecules or molecular structures, released or produced by cells undergoing stress or abnormal cell death and induce APC to become activated, upregulate costimulatory molecules and thus to initiate immune responses.

DC are remarkably plastic cells and their subsequent response appears to depend on the nature of the stimulus. Such plasticity is demonstrated by studies that have been conducted using murine DC (Gallucci et al., 1999) and human DC (Sauter et al., 2000) where cells, killed by acute necrotic death activated resting DC, whereas cells dying by physiological apoptotic death did not. Matzinger and colleagues (Matzinger, 1994) have argued that since apoptotic bodies are normally seen to be a natural part of cell death they are not normally seen as "danger signals". Although "resting" DC are indeed capable of engulfing apoptotic bodies and presenting them, this does not result in activation. Conversely, necrotic cells are often a feature of infection, where cell death is uncontrolled and results in the release of Hsps, which can maturate DC (Basu et al., 2000). In this way, Matzinger has proposed that only pathological death stimulates the immune system; physiological apoptotic death, which happens continuously in the body is neutral and may indeed be anti-inflammatory (Fadok et al., 1998). Danger signals can be divided into two large subclasses according to their source; endogenous signals are products of the host organism and exogenous signals are products or components of pathogens.

1.4.4.1 Endogenous danger signals

The activation of DC in response to infection can occur either indirectly or directly by inflammatory mediators (Table 1.3). Importantly, IL-1β and TNF-α are regarded as primal danger signals induced in keratinocytes by inflammatory stimuli (Zepter et al., 1997). In mice, IL-1β is produced almost exclusively by epidermal LC (Heufler et al., 1992; Schreiber et al., 1992). Furthermore, a substantial proportion of murine LC express IL-1R1, the signal-transducing receptor for IL-1 (Cumberbatch et al., 1998) and are therefore poised ready to detect this cytokine and amplify the immune response by acting as a positive feedback signal. In addition, activated cells of the immune system express TNF-α and IL-1β, thus amplifying the immune response further. A study conducted by Perales et al., (Perales et al., 2002) demonstrated that pGM-CSF administration induced high levels of TNF-α, IL-1β, IL-6, RANTES, MIP-1α and MCP-1 in skin, later followed by expression of precursor Th1 cytokines, IL-12 and IL-18, concomitant with IFN-γ production. Local production of GM-CSF protein also resulted in the early recruitment of polymorphonuclear cells (PMN) and later recruitment of mononuclear cells, including DC. GM-CSF is thus a potent inducer of "danger" which is likely to have profound effects on DC biology.

IFNs are also examples of endogenous danger signals. Virtually all cells can produce type-1 IFNs upon viral infection. Indeed Matzinger and colleagues have argued that alarm signals produced by virally infected tissues are sufficient to activate DC. Importantly, apoptotic bodies produced as a consequence of viral infection have been demonstrated to activate immature DC in the presence of IFN-α (Matzinger, 1994). Keratinocytes exposed to a mimic of viral double-stranded RNA produce cytokines (type I IFNs, TNF-α and IL-18) that induce DC to produce Th1-polarising cytokines. CD40L has also been proposed to be an endogenous danger signal and is commonly employed to maturate DC *in vitro* (Caux et al., 1994) and LC migration is stimulated following systemic treatment with an anti-CD40 monoclonal antibody (mAb) (Jolles et al., 2002). CD40L is upregulated on activated T cells and this requires previous activation of DC; however, CD40L is also expressed by activated platelets (Henn et al., 1998). Under normal conditions, platelets and tissue-resident DC do not come in contact with each other, but in injured and bleeding tissue, the platelet-expressed CD40L may serve as an early source of DC stimulation (Gallucci and Matzinger, 2001).

Table 1.3 Examples of endogenous danger signals which activate DC and other innate immune cells. (ATP, adenosine triphosphate; UTP, uridine triphosphate.)

endogenous danger signal	source	reference
uric acid crystals	necrotic cells	Schnurr et al (2000); Shi et al (2003)
ATP and UTP		
IL-1β, TNF-α,	distressed/infected cells	Sallusto et al (1995)
CD40L	T cell signals	Caux et al (1994); Henn et al (1998)
	activated platelets	
Hsps	necrotic cells	Asea et al (2000); Singh-Jasuja et al (2000)
metalloproteinase-9	matrix-proteolytic enzyme	Kobayashi et al (1999)
Type 1 IFN (IFN-α/β)	virally infected cells	

1.4.4.2 Exogenous danger signals: PAMP-dependent DC activation

DC are also activated directly by conserved molecular signatures of potential pathogens, the so-called pathogen-associated molecular patterns (PAMP). Cells of the innate immune system, including DC, possess pattern-recognition receptors (PRR) that recognise PAMP from viruses, bacteria, fungi and protozoa (Table 1.4). Direct contact with many pathogens leads to the maturation of DC, which is characterised by an increase in antigen presentation, upregulation of costimulatory molecules, and subsequent stimulation of naïve T cells in lymphoid organs (Banchereau and Steinman, 1998). C-type lectins constitute a major class of PRR and activation of DC may occur following their engagement with carbohydrate structures on pathogens. Dectin-1 acts as a PRR for β-glucan and could play an important role in DC activation by yeasts (Brown et al., 2003). DC-specific ICAM-3-grabbing nonintegrin (DC-SIGN/CD209) is another example of a C-type lectin and importantly recent studies demonstrate that DC-SIGN is a universal pathogen receptor that recognises gp120 of HIV, Ebola, cytomegalovirus, *Mycobacteria*, *Helicobacter pylori*, *Leishmania mexicana* and *Schistosoma mansoni* (reviewed in Geijtenbeek and van Kooyk, 2003); however, some pathogens have exploited binding to this receptor to further dissemination (HIV) or inhibit the immunostimulatory function of DC (*M. tuberculosis*). Some C-type lectins may act as endocytic receptors as has been discovered with DEC-205, concentrating potential pathogens for antigen presentation and recognition by PRR (Engering et al., 2002).

Recognition of pathogens is largely dependent on TLR

TLR were only discovered recently, yet they are undoubtedly the best-studied PPR. Although LPS, peptidoglycan, unmethylated DNA and other microbial products were long known to be the primary targets of innate immune recognition, researchers puzzled as to how each molecule triggered a response. It is now known that the TLR are the principle signalling molecules through which mammals sense infection. Each TLR recognises a restricted subset of molecules produced by microbes. Cells of the innate immune system may express any of 10 distinct TLR thereby allowing recognition of, and reaction to, a broad range of PAMP. More recently, TLR 11–13 have been isolated in mice, although little is known as yet with regard to the microbial ligands involved (O'Neill, 2004).

The responsiveness to a given PAMP has been linked to the expression of a particular TLR (reviewed in Athman and Philpott, 2004). For instance, the recognition of RNA viruses involves TLR3, which recognises dsRNA that is present either as part of viral genomic structures (for example, reovirus) or is generated during viral replication (Alexopoulou et al., 2001). More recently TLR7 has been shown to recognise single-stranded (ss) RNA viruses in

Table 1.4 Examples of exogenous danger signals. DC-SIGN* is a C-type lectin which may function as PRR and alert DC to the presence of a pathogen; however, this molecule has also been exploited as a means of pathogen dissemination in HIV and *M. tuberculosis* pathogenesis (Geijtenbeek and van Kooyk, 2003).

exogenous danger signal	source	receptors	reference
peptidoglycan	Gram positive bacteria	TLR2	Ozinsky et al (2000); Yoshimura et al (1999)
zymosan	fungal walls	TLR2	Ozinsky et al (2000); Sato et al (2003)
lipopeptide	bacteria	TLR2	Ozinsky et al (2000)
dsRNA	RNA viruses	protein kinase R (PKR) TLR3	Alexopoulou et al (2001); Diebold et al (2003)
LPS	Gram negative bacteria	TLR4	Chow et al (1999); Hoshino et al (1999); Poltorak et al (1998); Takeuchi et al (1999)
ss RNA viruses	influenza vesicular stomatitis virus (VSV)	TLR7	Diebold et al (2004); Heil et al (2004); Lund et al (2004)
ssRNA		TLR7 (murine) TLR8 (human)	Diebold et al (2004); Heil et al (2004)
unmethylated CpG DNA	Prokaryotic DNA	TLR9	Ahmad-Nejad et al (2002); Hemmi et al (2000)
surface glycans	*M. tuberculosis*	DC-SIGN*	Appelmelk et al (2003); Maeda et al (2003); Tailleux et al (2003)
gp120	HIV	DC-SIGN*	Geijtenbeek et al (2000)
$NiCl_2$ $MnCl_2$ sodium lauryl sulphate	skin sensitizers	unknown	Cumberbatch et al (1993)

mice (Diebold et al., 2004; Heil et al., 2004; Lund et al., 2004) whereas TLR8 has been implicated in recognition of ss RNA oligonucleotides in humans (Heil et al, 2004). Importantly, ss RNA species are only recognized as "danger signals" if they are present in the endosomal compartment. TLR9 recognises CpG motifs present in viral, fungal and bacterial DNA (Table 1.4). Initially, TLR2 was reported to have a role in sensing LPS (Kirschning et al., 1998; Yang et al., 1998). This later turned out to be due to a peptidoglycan contaminant in the LPS used; TLR2 is now known to be implicated in the recognition of bacterial peptidoglycan (Yoshimura et al., 1999). Beutler's group later identified TLR4 as the receptor of LPS (Poltorak et al., 1998), since mice with mutations in the TLR4 gene were resistant to the effects of LPS. Others have made similar findings (Chow et al., 1999; Qureshi et al., 1999). LPS is now known to be recognised by a receptor complex composed of TLR4, CD14 and MD-2 (reviewed in Miyake, 2004).

Most microbial ligands for TLR have similar effects on DC; engagement of TLR results in recruitment of an adaptor protein (MyD88) to the receptor complex and this activates intracellular signalling via the Toll-IL-1 receptor pathway, resulting in activation of nuclear factor-κB (NF-κB) (Medzhitov et al., 1998), although a MyD88-independent signalling pathway that mediates NF-κB activation is suggested following ligation of TLR4 with LPS (Akira et al., 2000). Engagement of TLR results in DC activation and helps to induce differentiation into professional APC, by increasing surface expression of MHC-peptide complexes and co-stimulatory molecules CD80 and CD86, as well as the production of proinflammatory cytokines including TNF-α, IL-6 and IL-12 (reviewed in Takeda et al., 2003) all of which have a profound effect on T cell priming and differentiation.

Engagement of PPR affects cytokine production by DC and subsequent Th differentiation

DC are not only responsible for priming and sustaining the expansion of naïve T cells, but also to direct T cell effector differentiation. DC determine the type of immune response that is initiated, primarily by affecting the cytokine environment in which the T cells respond. Immune responses dominated by $CD4^+$ T cells producing IFN-γ and B cells secreting IgG2a antibody are termed Th1 responses; those dominated by $CD4^+$ T cells producing IL-4 and IL-10 and B cells secreting IgG1 are termed Th2 responses. At the individual T cell level, considerable heterogeneity of cytokine profiles can be seen with T cell clones, raising the possibility that the Th1 and Th2 phenotypes may represent two polar extremes of all possible single cell phenotypes (Kelso, 1995). In general, the production of IL-12 by DC has been shown to bias naïve T cells towards a Th1 type (IFN-γ-producing) response (Heufler et al., 1996; Macatonia et al., 1995; Seder et al., 1993). Conversely, the absence of IL-12 and

presence of IL-6 and IL-10 have been implicated in skewing naïve T cells toward Th2-type (IL-4-producing) responses (Liu et al., 1998b; Rincon et al., 1997).

DC subsets were originally suggested to be pre-programmed to direct the differentiation of $CD4^+$ T cells into either IFN-γ-producing Th1 cells or IL-4-producing Th2 cells. Evidence for this hypothesis came from studies of DC derived from humans and mice which identified a number of different sub-populations that varied in their ability to stimulate T cells and influence the bias of the T cell response (Liu et al., 2001). Based on *in vitro* studies with human blood DC, the DC1 and DC2 dichotomy was proposed to describe the capacity of MoDC ("DC1") to produce high levels of IL-12 after activation and to preferentially induce the generation of Th1 cells, whereas pDC ("DC2") were found to have a strong capacity to generate Th2 cells (Rissoan et al., 1999). In the mouse, the best studied DC subpopulations are found in the $CD11c^{bright}$ fraction of spleen and comprise at least three subsets defined on the basis of CD4 and CD8α expression: $CD8\alpha^+$ $CD4^-$ "lymphoid" DC and "myeloid" DC ($CD8\alpha^-$ $CD4^+$ and $CD8\alpha^-$ $CD4^-$ DC) (Vremec et al., 2000). Moser and colleagues reported that immunisation of mice with antigen-pulsed $CD8\alpha^+$ DC led to Th1 priming, whereas immunisation with $CD8\alpha^-$ DC induced a Th2 response (Maldonado-Lopez et al., 1999; Maldonado-Lopez et al., 2001). In parallel studies, Pulendran showed that both $CD8\alpha^+$ and $CD8\alpha^-$ DC populations induced Th1 development (Pulendran et al, 1999), but that only the $CD8\alpha^-$ (myeloid) subset promoted Th2 differentiation. This led to the proposal that DC represented lineage-committed cells, where each population has a precommitted role *in vivo*.

More recent experiments have now led to an alternative hypothesis about DC, which demonstrate that the induction of a distinct Th phenotype by DC ultimately depends on the "environmental education" of DC in the periphery and may not therefore be dependent on the type of DC. DC are remarkably plastic cells capable of responding to a plethora of pathogens and pathogen by-products by engagement with their PPR and tailoring their cytokine profile accordingly. For instance, following ligation of TLR7 with a TLR7 agonist, murine myeloid DC ($CD8\alpha^-$ $CD11c^+$ $CD11b^+$) express high levels of IL-12 and TNF-α (Doxsee et al., 2003). Indeed, both murine lymphoid and myeloid DC have the ability to produce either IL-12p70 or IL-10 depending on the nature of the stimulus. Both subsets can direct increased Th1 development in response to stimuli known to elicit IL-12 production (including purified protein from *M. tuberculosis*) and both subsets can suppress Th1 development and allow Th2 cells to expand upon-exposure to IL-10-inducing microbial agents (heat-killed yeast or zymosan particles) (Manickasingham et al., 2003). Furthermore, Boonstra and co-workers have shown that mouse myeloid and pDC cultured from bone marrow precursors and *ex vivo* splenic DC subsets can induce the development of both Th1 and Th2 effector cells depending on the dose of antigen; high antigen doses induced Th1

development whereas low antigen doses induced Th2 cell development, regardless of the DC subset (Boonstra et al., 2003). Such flexibility has also been demonstrated in the human system, where human pDC ("DC2") activated by influenza virus and CD40L are capable of driving potent Th1 polarisation (Fonteneau et al., 2003). Viral infection can also switch non-pDC into high IFN producers (Diebold et al., 2003). Therefore, although certain DC subsets may be intrinsically more prone to induce Th1 or Th2 differentiation, this property can be either strengthened or overridden by PRR signals from microbes (perhaps due to the chemistry of the antigen). The response of DC may also depend on the local cytokine milieu in which the immature DC resides, the dose of the pathogen and other such environmental cues.

Huang and colleagues (Huang et al., 2001) have further illustrated the plasticity of DC in their ability to respond to infection and direct adaptive immunity by measuring gene expression profiles of human myeloid DC after exposure to a range of microorganisms and molecular components. A core response was elicited, including a rapid decline in expression of genes associated with phagocytosis and pathogen recognition, a transient increase in the expression of cytokines and chemokines, followed by induction of antigen processing and presentation genes. Pathogen-specific programs of gene expression were also observed. *E. coli* exposure resulted in rapid upregulation of most innate immune genes and at later time points, genes that regulate adaptive immune responses, including T cell-stimulating genes and a subset of chemokines that attract naïve Th2 Th cells. The adaptive response to influenza included upregulation of IFN-α/β and IFN-inducible chemokines genes, which may induce migration of naïve Th1 cells. Such plasticity has even been demonstrated with the same pathogen; studies with the fungus *Candida albicans* showed that myeloid DC stimulated a protective Th1 response following ingestion of yeasts, whereas ingestion of hyphae induced a non-protective Th2 response (d'Ostiani et al., 2000), demonstrating that the diverse functions of DC in immune regulation are dictated by the instructions they received during innate immune responses to different pathogens.

DC are therefore equipped with the capacity to sense diverse pathogens and elicit tailored, pathogen-specific immune responses through ligation of conserved receptors, ultimately affecting cytokine expression and the subsequent bias in the T cells responses that they induce. Different stimuli are likely to trigger qualitatively different states of maturation, suggesting that DC "decode" environmental signals via TLR or other receptors, allowing the development of mature DC capable of polarising T cell responses, or inducing tolerance (in the absence of "danger"). DC are therefore responsible for ensuring that the specificity of the innate immune system, which distinguishes between many classes of potential pathogens, is translated into an equally specific class of adaptive immune response. Inflammation induced

by PAMP is sufficient to activate DC; however, Reis e Sousa argues that direct PRR triggering, but not indirect activation, allows DC to differentiate between classes of pathogen and that the main function of DC-exposed PPR may not be to activate a DC to become immunogenic APC, but rather to convey information about the nature of the insult, thus to allow DC to direct an appropriate class of immune response (Reis e Sousa, 2004).

TLR expression by DC subsets

What has also become apparent from recent studies is that different DC subsets can express distinct TLR repertoires, suggesting that DC may have an inherent ability to recognise different pathogens. A major dichotomy in TLR expression has been observed in human blood DC subtypes, where myeloid DC and myeloid pre-DC (monocytes) express all TLR investigated with the exception of TLR7 and TLR9, which are preferentially expressed by both pDC and plasmacytoid pre-DC (Jarrossay et al., 2001). In accordance with their TLR expression, these DC/pre-DC subsets were found to respond to their respective ligands. For instance, only pDC and their precursors responded to CpG-oligodeoxynucleotides, whereas only monocytes and myeloid DC responded to the TLR2 and TLR4 ligands, peptidoglycan and LPS. In the murine system, pDC, like their human counterparts, express high levels of TLR9 but selectively lack TLR3 and TLR4 (Boonstra et al, 2003). In addition, both cultured and *ex vivo*-derived splenic pDC enhance $CD4^+$ T cell proliferation and induce Th1 cell development when activated with CpG, but not with LPS. However, it should be noted that in mice TLR9 expression is not restricted to pDC, since it is also expressed by non-plasmacytoid spleen DC, which respond to CpG-containing oligonucleotides by producing IL-12 (Edwards et al., 2003).

It is possible that DC are equipped with specialised functions *in vivo*. Of the number of DC subtypes identified in recent years, the pDC is characterised for its potent ability to secrete high levels of type I IFNs in response to viruses in both humans (Siegal et al., 1999) and in mice (Brawand et al., 2002) and thus an innate antiviral role has been proposed. Although non-pDC in mice can be induced to secrete IFNs, pDC are the major producers of IFNα/β in response to most viruses. Furthermore, expression of IFNs by murine pDC has been shown to regulate multiple DC responses, limiting viral replication and IL-12 production in other DC (Dalod et al., 2003). Recently, pDC have been shown to recognise the CpG–rich dsDNA genome of the herpes simplex virus type 1 and type 2 via the TLR9/MyD88 pathway (Krug et al., 2004; Lund et al., 2003). Furthermore, murine pDC have been found to recognise ssRNA viruses (vesicular stomatitis virus and influenza virus) through TLR7, resulting in upregulation of costimulatory molecules and production of IFN-α (Lund et al, 2004),

whereas TLR8 has been implicated in the recognition of ss viruses by human pDC and production of IFN-α (Heil et al, 2004).

Selective expression of TLR9 and DNA vaccine efficacy

As has already been highlighted (Section 1.3.1), DNA vaccination is less successful in outbred species than in murine models of infectious disease and thus understanding the immunology of DNA vaccination is imperative. One possible contributing factor as to why DNA vaccines are more effective in mice may be due to different expression patterns of TLR9. Both TLR2 (Kawai et al., 2002) and TLR4 (Song et al., 2002) are expressed by murine resident keratinocytes, whereas TLR9 is not constitutively expressed in skin; however, Liu and colleagues (Liu et al., 2003) have demonstrated that the physical trauma of intradermal vaccination induces TLR9 expression to levels comparable with that of plasmid-injected skin. Although TLR9 expressing cells were not clearly identified, the authors suggest that TLR9 expression was the result of infiltration by blood leukocytes that express TLR9, rather than *de novo* synthesis by resident skin cells. Thus physical damage alone to the skin results in infiltration of TLR9 expressing cells, which may then be responsive to the injected DNA at the site of injection. It is possible, although not yet proven, that differences in vaccine efficacy could be partly attributed to differences in TLR9 expression by DC subsets. It is interesting to speculate that TLR9 expression in several murine DC subsets, including LC (Mitsui et al., 2004), but its unique expression in human blood pDC, may help to explain the apparent lack of efficacy of DNA vaccines in humans. Spies and colleagues have, however, negated a dominant role of CpG-DNA/TLR9 interactions in long-term vaccination protocols (Spies et al., 2003), since priming and expansion of OVA-specific CTL were reported to be equal in wildtype and TLR9 knockout ($TLR9^{-/-}$) and $MyD88^{-/-}$ mice after vaccination with a plasmid containing a transcription unit for OVA.

Selective expression of TLR by DC subsets may however imply that there is some degree of inflexibility in the DC system, where some DC are uniquely sensitive to some pathogens but perhaps not to others. Experiments by Manickasingham and colleagues (Manickasingham et al, 2003) demonstrate that whilst murine splenic DC subsets can be skewed into polarising either Th1 or Th2 immune responses *ex vivo* following exposure to different pathogens, subtle differences between the populations were evident. In particular, priming with $CD8\alpha^+$ DC generally increased the frequency of Th1 cells developing under neutral conditions while both subsets of $CD8\alpha^-$ DC tended to promote Th2 differentiation. The authors concluded that although not very pronounced, these biases agree overall with the results by Maldonado-Lopez (Maldonado-Lopez et al, 1999; Maldonado-Lopez et al, 2001) and Pulendran

(Pulendran et al, 1999), where murine DC subsets propagated *in vitro* and transferred into mice directed the development of distinct Th populations *in vivo*.

1.5 Accessing migratory DC

1.5.1 Danger signals are not mandatory for DC migration

The current and popularly cited lifecycle of DC has immature DC strategically placed encountering antigen in the periphery (antigen capturing mode) and upon exposure to various inflammatory stimuli (danger signals), DC become activated, resulting in their migration and maturation *en route* to the DLN, whereupon stimulation of T cells takes place (Banchereau and Steinman, 1998). While valuable in general terms, this view is too simple for describing the real DC system *in vivo*. Whilst it is evident that inflammatory and microbial stimuli activate DC and can result in *en masse* migration to DLN, such signals are not mandatory for migration. A paper by Geissmann and colleagues (Geissmann et al., 1999) challenged DC researchers to re-examine the widely accepted idea that migration of LC in response to inflammatory stimuli is coupled to and follows their maturation. Lymph nodes from patients with dermatopatic lymphadenopathy[1] contained LC with characteristic LC markers (CD1a and langerin) but none showed expression of the maturation markers CD83 and CD86. In addition, the group showed that cultures of LC (derived from monocytes co cultured in IL-4, GM-CSF and TGF-β) did not become $CD83^+$ even when exposed to TNF-α or *E. coli,* although these inflammatory stimuli were sufficient to induce expression of CCR7 and migratory responses to CCR7 chemotactic ligands, indicating that LC migration and maturation can be independently regulated.

1.5.1.1 Access to genuine migratory dendritic cells by cannulation of the afferent lymphatics

Highly informative animal models with regard to the study of the phenotype of migratory lymph DC are those in which afferent lymph is sampled from cannulating lymphatic ducts after the ablation of lymph nodes. Peripheral afferent lymph is known to contain a small number (1–10%) of cells with veiled or dendritic morphology. Cannulation of the afferent lymphatics provides direct access to *ex vivo* DC migrating from tissue to the regional lymph node in which they act. This has been carried out in several animal species, including sheep

[1] A pathological disorder marked by excessive accumulation of nonproliferative LC in lymph nodes that drain a chronically inflamed site.

(Hall, 1967) and cattle (Emery et al., 1987), where afferent lymph draining the skin is collected, and also in rats (Pugh et al., 1983), where intestinal lymph is obtained. It has long been known from such models that DC migrate constitutively from peripheral tissues in the absence of any overt antigenic or inflammatory stimuli (Pugh et al, 1983; Smith et al., 1970).

Furthermore, it is not possible to study all aspects of DC biology by investigating cells derived and maintained *in vitro* and it has been suggested that *in vitro*-derived DC might be deficient in some important immunological functions and that they might not accurately represent the DC population(s) naturally developed and maintained *in vivo* (Morse et al., 2002). A study conducted by MacPherson and co-workers illustrates this well; rat bone-marrow-derived DC (BMDC) expressed some, but not all markers expressed by splenic DC and lymph-derived DC. BMDC also functionally differed from *ex vivo*-derived DC as APC, as they were only relatively weak stimulators of an allogeneic MLR in comparison to splenic and lymph-derived DC (Powell et al., 2003).

DC are highly flexible cells and isolation of DC from tissues is likely to modify their phenotype and function. The isolation of DC from tissues is difficult and requires extensive purification procedures. For instance, the isolation of epidermal LC requires mechanical disruption and enzymatic treatment. Disruption of the epidermis has been reported to induce DC maturation (Inaba et al., 1986; Schuler and Steinman, 1985). Perhaps the greatest advantage of investigating the function of ALDC is that they have not been subjected to enzymatic treatment, or extensive periods of culture, which could modify these highly plastic cells. Cannulation of the afferent lymphatics therefore provides access to DC, which resemble more closely DC *in vivo*.

Constitutive migration of DC from peripheral tissues to DLN has been proposed to maintain tolerance to self- or harmless foreign antigens, although the factors which control such steady-state migration are yet to be elucidated. DC in the steady-state flux have indeed been found to capture antigens against which immunity is normally avoided, including environmental proteins found in the respiratory tract and digestive tracts (Vermaelen et al., 2001), as well as self-antigens derived from tissues exhibiting constitutive cell turnover (Huang et al., 2000). Conceivably, the capture of proteins in the steady-state (in the absence of microbial or endogenous danger signals) allows DC to maintain tolerance to self and normal environmental constituents, so they are of a mature enough phenotype to present the self-antigen on their cell surface, but do not have sufficiently high costimulatory molecule expression, thus inducing tolerance (due to absence of signal 2). The finding that DC of an immature phenotype are present in lymphoid tissues supports this (Wilson et al., 2003).

To further complicate matters, DC directly isolated ex *vivo* from afferent lymph draining the skin or intestine are highly heterogeneous and are of different maturational stages. Whilst ALDC stimulate proliferative responses in allogeneic $CD4^+$ and $CD8^+$ T cells *in vitro* (Howard et al., 1996) and prime $CD4^+$ T cells *in vivo* (McKeever et al., 1992), consistent with the idea that migratory DC are mature, the notion that all migratory DC have lost characteristics normally "restricted" to immature DC is in fact wrong. For instance, ALDC are indeed capable of endocytosis as demonstrated by the observation that ovine ALDC can acquire soluble protein antigen *in vivo* or *in vitro* and present the material directly to autologous T cells in an antigen-specific manner (Bujdoso et al., 1989). Furthermore, antigen uptake occurs rapidly in the presence of specific antibodies, suggesting that ALDC may concentrate antigen on their surface efficiently via FcR (Harkiss et al., 1990) and this has been shown to augment antigen presentation and $CD4^+$ T cell proliferation in *in vitro* secondary responses (Coughlan et al., 1996).

It cannot be denied that inflammatory stimuli induce DC maturation and migration and result in an accumulation of DC in the DLN; however, these factors are not solely responsible for the migration of DC. Cannulation models enable researchers to assess real changes to DC following administration of a stimulus. For instance, after systemic administration of LPS, the flux of intestinal DC emigration from the gut via lymph increases 8–15 fold (MacPherson et al., 1995). Importantly, the relative proportion of the less mature DC population does not change after LPS treatment, suggesting that the migration-enhancing effects of LPS may not entirely stem from its maturation-inducing properties. *In vivo* antigenic stimulation in primed animals has been shown to have profound effects on the quantitative expression of MHC class II, similar to the relative increase induced by exogenous stimuli on mouse epidermal LC (Schuler and Steinman, 1985). In addition, the capacity of ALDC to enhance *in vitro* lymphocyte proliferation correlates directly with increased MHC class II expression, but not with CD1 expression (Hopkins et al., 1989).

Origin of ALDC

Afferent lymph veiled cells (ALVC) and lymph node DC have been isolated with antigen on their cell surface following skin painting with dinitrofluorobenzene (DNFB) (Lens et al., 1983) and fluorescein isothiocyanate (FITC) (Macatonia et al., 1987), demonstrating that ALDC are involved in the transport of antigens to the lymph node by migration through the afferent lymphatics to the paracortical areas of the lymph node, where they develop into interdigitating DC and present antigen to naïve T cells. The origin of ALDC and their relationship to other DC, such as epidermal LC, has however been a subject of active investigation (Bujdoso et al, 1989; Gliddon et al., 2004; Knight, 1984). Evidence from these

studies suggests that ALDC contain cells (or subpopulations) which have originated from LC and/or dermal DC. Cells with Birbeck granules (a unique feature of epidermal LC) have been found in afferent lymph and T-cell areas of lymph nodes following skin sensitisation (Silberberg-Sinakin et al., 1976).

ALDC and MyD-1 (SIRPα) expression

ALDC can be further characterised based on the differential expression of the myeloid restricted molecule, MyD-1 (CD172). Perhaps the studies carried out with murine and human DC will reveal similar findings. MyD-1 was initially described in the bovine system where it was shown to be expressed on bovine monocytes, macrophages, granulocytes and a subset of ALVC (Brooke et al., 1998; McKeever et al., 1991). MyD-1 is also expressed on a subpopulation of rat (Liu et al., 1998c), and ovine ALDC (Bailey, 2003) and on human myeloid cells (Seiffert et al., 1999). MyD-1 is a type 1 glycoprotein belonging to the Ig superfamily comprising 3 extracellular Ig-like domains with several glycosylation sites, a transmembrane region consisting of a single hydrophobic stretch of 22 amino acids, and at least 4 possible tyrosine phosphorylation sites including one or more putative immunoreceptor tyrosine-based inhibition motifs (ITIMS) within the cytoplasmic tail (Brooke et al, 1998). MyD-1 is a member of the signal regulatory protein (SIRP) family (Vely and Vivier, 1997) and will now be referred to in the text as SIRPα. SIRPs are a family of transmembrane glycoproteins that are involved in the negative regulation of receptor tyrosine kinase signalling pathways (Ostman and Bohmer, 2001).

Studies in which COS-7 cells were transfected with the cDNA encoding the SIRPα molecule showed that this molecule mediated binding of $CD4^+$ T cells (Brooke et al, 1998). The ligand for SIRPα is now known to be the integrin-associated protein, CD47 (Vernon-Wilson et al., 2000). CD47 is a widely distributed molecule expressed on a variety of haematopoietic cells including monocytes and T cells (Mawby et al., 1994), although it is expressed at significantly higher levels on T cells (Latour et al., 2001). Importantly, soluble CD47 mAb exerts inhibitory functions in allogeneic MLR (Reinhold et al., 1997; Waclavicek et al., 1997). Early experiments demonstrated that ligation of the SIRPα molecule with mAb inhibited antigen-specific T cell responses. For instance, the proliferation of resting memory bovine $CD4^+$ T cells to OVA-pulsed monocytes *in vitro* was significantly reduced in the presence of mAb to SIRPα (Brooke et al, 1998). SIRPα mAb have also been demonstrated to strongly inhibit T cell proliferation in both MLR and anti-CD3 assays (Patel et al., 2002).

More recently, ligation of SIRPα on human APC was found to induce suppression of PAMP-induced TNF-α secretion by DC by ~50%, suggestive of a possible role of SIRPα in the regulation of the innate immune system (Smith et al., 2003). Importantly, inhibition of TNF-

α production by DC resulted in the inhibition of subsequent T cell activation induced by either CD3 or allogeneic APC. Furthermore, anti-SIRPα treatment resulted in tyrosine phosphorylation of SIRPα and inhibition of the PI-3-kinase signalling pathway, resulting in cellular retention of TNF-α. These data strongly suggest that SIRPα may act to suppress aberrant induction of TNF-α and inflammation. These data are also in agreement with those described by Latour and colleagues (Latour et al, 2001), where CD47-Fc potently suppressed TNF-α release by MoDC stimulated by *Staphylococcus aureus*. The latter study also highlighted the ability of CD47 and its receptor SIRPα to deliver a bidirectional negative signal to both T cells and DC, since not only was a decrease in IL-12 production by DC observed, but also an inhibition of IL-12 responsiveness in CD3 activated PBMC.

Rat ALDC

Two functionally different DC populations have been isolated from rat intestinal lymph, distinguished by the differential expression of SIRPα, the target of the OX41 mAb (Adams et al., 1998), and CD4 (Liu et al, 1998c). Both populations ($SIRP\alpha^+/OX41^+$ $CD4^+$ DC and $SIRP\alpha^-/OX41^-$ $CD4^-$ DC) express similar levels of MHC class II, ICAM-1, CD11b, CD11c and OX62; however, $OX41^-$ DC stain more strongly for both CD80 and invariant chain. The $OX41^+$ population (which comprise 50–60% of ALDC) display short, fine pseudopodia and stain weakly for non-specific esterase (NSE). Conversely, $OX41^-$ DC possess long pseudopodia and stain strongly for NSE and also contain many cytoplasmic inclusions. Furthermore, these phenotypic differences are still evident after overnight culture. Surprisingly, $OX41^+$ ALDC are more potent APC than $OX41^-$ ALDC exemplified by a more robust activity in MLR, for sensitised T cells *in vitro* and naive T cells *in vivo*. Furthermore, $OX41^+$ ALDC continue to process and present antigen *in vitro,* whereas $OX41^-$ ALDC cannot present native antigen. It is interesting to speculate about these populations, do they represent distinct DC lineages or are they the result of differentiation modulated by different micro environmental stimuli?

A later study conducted revealed that the cytoplasmic inclusions described earlier in $OX41^-$ ALDC contain apoptotic DNA (Huang et al, 2000). Two approaches were undertaken to show that this population also contained intestinal intraepithelial cell (IEC) remnants. Firstly, $OX41^-/CD4^-$ ALDC were positive for IEC-restricted cytokeratins. The second approach identified the origin of NSE (of which more than 80% of intestinal ALDC stain positive) and demonstrated that IECs and $OX41^-$ ALDC contained NSE variants with identical mobilities, suggesting that NSE reactivity in $OX41^-$ ALDC derives from endocytosed apoptotic IEC. Furthermore, NSE^+ DC were identified in T cell areas of mesenteric lymph node (MLN). These data elegantly show that $OX41^-$ DC constitutively endocytose and transport fragments

of apoptotic gut epithelial cells to the T cell area of mesenteric lymph nodes. It has therefore been suggested that this pathway of self-antigen transport could be involved in the maintenance of peripheral self-tolerance (Huang and MacPherson, 2001).

Two phenotypically distinct subsets of DC with different T cell stimulatory activities have been also been isolated in rat spleen based on SIRPα expression (Voisine et al., 2002). In contrast to data obtained from ALDC, freshly isolated splenic SIRPα$^+$ DC were of an intermediate maturity (moderate expression of CD80) whereas SIRPα$^-$ DC were immature, although DC could be matured by overnight culture. Furthermore, unlike lymph-derived SIRPα$^+$ DC, splenic SIRPα$^+$ DC induced only slightly higher proliferation of allogeneic naïve CD4$^+$ T cells than splenic SIRPα$^-$ DC. SIRPα$^-$ DC were comparatively poor at inducing allogeneic naïve CD8$^+$ T cell proliferation and IFN-γ secretion (even after overnight culture) unless an additional maturational stimulus such as CD40L was administered. In addition, freshly isolated SIRPα$^-$ DC produced large amounts of the proinflammatory cytokines IL-12 and TNF-α and promoted differentiation of IFN-γ-secreting CD4$^+$ T cells. SIRPα$^+$ DC also induced differentiation of Th1 cells despite a low production of IL-12, suggesting an IL-12-independent Th1-priming capacity; yet only SIRPα$^+$ DC induced allogeneic CD4$^+$ T cells to produce the Th2 cytokine IL-13. Based on the high IL-12 production, the low capacity to stimulate CD8$^+$ T cells, the large size, spontaneous maturation and poor viability *in vitro*, the authors propose that rat splenic SIRPα$^-$CD4$^-$ DC are the equivalent of murine splenic CD8$^+$ ("lymphoid") DC.

Bovine ALDC

Two major populations have been defined on the basis of expression of a number of antigens in bovine afferent lymph (Howard et al., 1997; Howard and Hope, 2000); the major population (approximately 80% of DC in afferent lymph) expresses SIRPα. The smaller and more homogeneous SIRPα$^-$ population expresses an antigen recognised by the mAb CC81, high levels of CD11a and the bovine WC10 antigen (that has now been identified as CD26). The SIRPα$^+$ population lacks expression of CD26 and the antigen recognised by the mAb CC81 present on the minor population.

Howard and colleagues have investigated the way in which the SIRPα$^+$ and SIRPα$^-$ ALDC populations interact with T cells *in vitro* (Howard et al, 1997). Although both DC populations were capable of taking up the soluble protein antigen OVA and stimulating memory T cells from OVA-immune cattle, SIRPα$^+$ DC were more effective than SIRPα$^-$ DC at presenting inactivated respiratory syncytial virus (RSV) antigen to T cells from RSV-immune cattle. The SIRPα$^-$ population was also relatively ineffective at stimulating CD8$^+$ T cells in an allogeneic model, as was reported with rat splenic SIRPα$^-$ DC (Liu et al, 1998c).

A similar disparity in the stimulation of $CD8^+$ lymphocyte proliferation has also been reported for subsets of murine splenic DC (Kronin et al., 1996). Interestingly, differences in the induction of $CD8^+$ T cells by bovine ALDC was not due to differences in surface expression of costimulatory molecules (CD80, CD86 and CD40), but rather due to a difference in IL-1α synthesis; supernatant from $SIRP\alpha^+$ ALDC significantly enhanced $SIRP\alpha^-$ ALDC to stimulate the proliferation of allogeneic $CD8^+$ T cells and this stimulatory capacity was blocked upon addition of an anti-IL-1α mAb (Hope et al., 2001).

Further investigation revealed differences in the expression of cytokine transcripts by bovine $SIRP\alpha^+$ and $SIRP\alpha^-$ ALDC that may have significant effects on the T cell response (Stephens et al., 2003). A quantitative approach was adopted in order to measure cytokine transcripts from freshly sorted DC. Notably, the $SIRP\alpha^-$ population contained more numerous transcripts of IL-12p40, whereas transcripts for IL-1α, IL-1β, IL-6 and IL-10 were more numerous in the $SIRP\alpha^+$ ALDC population. In general, $SIRP\alpha^+$ DC expressed 2–3 fold more IL-1β and IL-6 transcripts than $SIRP\alpha^-$ DC sorted from the same afferent lymph sample. The authors propose that high levels of expression of IL-12 in the $SIRP\alpha^-$ DC (and expression of CD26) would promote a strong Th1 biased immune response; however, low levels of IL-1α would result in a poor induction of $CD8^+$ T cell immune responses. Conversely, presentation by the $SIRP\alpha^+$ population would be expected to promote a more intense $CD8^+$ T cell response, but the lower levels of IL-12 and higher levels of IL-10 in this population may result in an immune response that has less of a Th1 bias. In mice the presence of IL-6 and IL-10 during T cell stimulation has been linked to the generation of Th2 immune responses (Liu et al, 1998b; Rincon et al, 1997), whereas in cattle and humans, IL-10 has a down-regulatory effect, reducing the proliferation of both Th1- and Th2-type clones (Brown and Estes, 1997; Del Prete et al., 1993). It has therefore been proposed that IL-10 production may imply an anti-inflammatory role for this subpopulation of ALDC or indeed for a subset of cells within it.

The model in which human myeloid pre-DC1 mature into DC1 secreting high levels of IL-12, while "lymphoid" pre-DC2 mature into cells secreting low levels of IL-12 would suggest that $SIRP\alpha^-$ DC are the equivalent of myeloid DC1, whereas $SIRP\alpha^+$ DC are related to the "lymphoid" DC2 subset. This does not appear to be the case as the Myd-1/SIRPα antigen is "myeloid" restricted. It is interesting to note that surface expression of CD8 has been observed on $SIRP\alpha^-$ALDC in both cattle and sheep (Bailey, 2003), although it appears equally unlikely that this subpopulation is the equivalent of the lymphoid ($CD8\alpha^+$) DC subset found in mice, since $SIRP\alpha^-$ ALDC also express myeloid-restricted antigens. It is possible that CD8 expression is a consequence of adsorption of this molecule from neighbouring cells rather than endogenous expression of CD8.

1.6 Aims of the project

1.6.1 Characterisation of immunohistological events following administration of pGM-CSF and pIL-3

GM-CSF is an attractive molecular adjuvant, since this cytokine not only recruits DC, but also acts as a danger signal by causing inflammation at the inoculation site and such inflammatory signals likely modulate DC function and phenotype. Whilst GM-CSF has attracted considerable attention as a molecular adjuvant, the mechanisms by which GM-CSF exerts its effects are still to be fully elucidated; in particular there is little information with regard to the kinetics of expression of proinflammatory mediators which activate DC. IL-3 has not as yet been investigated as a molecular adjuvant and since IL-3 has been implicated in DC development and is chemotactic for a variety of cells (including eosinophils and neutrophils), the resulting inflammatory response may have profound affects upon DC phenotype and function. Plasmid DNA itself has important adjuvant effects by ligation with TLR9 expresssed by DC and other cells of the immune system. Understanding which signs are both necessary and sufficient to convert DC into the immunostimulatory APC that prime appropriate effector T cells will hold the key to improved strategies for vaccination (Reis e Sousa, 2004).

There is a surprising paucity of published material that describes the immunohistological characteristics following gene-gun vaccination with pGM-CSF. Better characterisation of the inflammatory events after administration of cytokine gene adjuvants may help to better understand the mechanisms involved in DNA vaccination. The aim of the first part of the project was therefore to determine the effects in ovine skin after gene-gun bombardment with pGM-CSF or pIL-3 and to compare the inflammatory events with a control plasmid. An investigation into the cell types recruited to the site of DNA vaccination was required, with particular interest with regard to the time-frame in which DC infiltrate the skin. In order to determine the kinetics of plasmid expression and the expression of proinflammatory cytokines in the skin, including TNF-α, IL-1β and IL-18, a quantitative RT-PCR method was developed.

1.6.2 Characterisation of ovine ALDC in the steady-state

Ovine ALDC have been partially characterised based on expression of SIRPα (Bailey, 2003); however little is known about the cytokine expression of these subsets in the steady-state flow. Further characterisation of ALDC subsets is required in order to accurately assess any changes in cytokine expression after cytokine gene administration. Expression of Th1-polarising cytokines (IL-12p40 and IL-18), a Th2-polarising cytokine (IL-10) and proinflammatory cytokines (TNF-α and IL-1β) required investigation (by quantitative RT-PCR). In addition, no information is as yet available with regard to expression of TLR by ALDC in any species and an investigation into these receptors may further our understanding of the inherent functions of $SIRP\alpha^+$ and $SIRP\alpha^-$ ALDC subsets *in vivo*. The origin of $SIRP\alpha^+$ and $SIRP\alpha^-$ ALDC and how they equate to human and murine DC is still under debate, although evidence suggests that $SIRP\alpha^+$ ALDC contain cells derived from epidermal LC (Gliddon et al, 2004). Further analysis of each population is imperative to address this further, including an investigation into the expression of langerin and CD1a transcripts (LC-specific transcripts) in addition to morphological and ultrastructural analysis.

1.6.3 Characterisation of ALDC after cytokine gene administration

The second part of the project involved investigation of the effects of pGM-CSF on DC trafficking from the skin to the DLN via the afferent lymphatics. Cannulation of the afferent lymphatics of sheep provides a unique method to investigate DC in their closest possible form and therefore may help to understand the immune mechanisms underlying the effects of GM-CSF as a molecular adjuvant. It was hypothesised that pGM-CSF would act upon pre-DC recruited from the blood and/or resident immature DC in the skin (epidermal LC and/or dermal DC) after gene-gun bombardment and this may be reflected by an increase in DC numbers in the lymph when compared to those collected prior to DNA vaccination. Furthermore, upregulation of proinflammatory cytokines in the skin is hypothesised to cause DC maturation. Therefore, analysis of antigen presentation molecules (CD1 and MHC class II), costimulatory molecules (CD80, CD86 and CD40), accessory molecules (CD2 and LFA-3) and the β-integrin CD11c was carried out, since an increase in surface expression of these molecules is indicative of DC maturation and enhanced T cell stimulatory capacity. In addition, expression of a range of genes involved in T helper cell polarisation was investigated in purified ALDC populations by quantitative real-time RT-PCR and compared to expression profiles of DC obtained during the steady-state flux. These experiments were designed to decipher if pGM-CSF has the potential to influence the type and the magnitude of the immune response generated to a particular antigen.

2 Materials and Methods

Unless otherwise stated all chemicals were of analytical grade where available and supplied by BDH or Sigma-Aldrich. Life Technologies supplied plastic ware for tissue culture purposes.

The companies supplying the reagents used in this work are referred to in the text.

The compositions of all solutions can be found in Appendix I.

All company addresses are listed in Appendix II.

2.1 Cell culture

2.1.1 Recovery of cells from liquid nitrogen

Cells were recovered from liquid nitrogen by thawing in a 37°C water bath. Pre-warmed wash medium (outlined below) was slowly added to equilibrate the osmotic pressure. The cells were then centrifuged at 400 × g for 7 minutes in a bench centrifuge. This was followed by resuspension of the cell pellet in 5ml of tissue culture medium. Cells were seeded into 25cm^2 culture flasks.

2.1.2 Culturing cells

All cells were cultured in a humidified 5% CO_2 incubator (Heraeus) at 37°C and fed every 2–3 days with tissue culture medium (outlined below).

2.1.2.1 Sheep skin fibroblasts

A primary culture of sheep skin (SSk) fibroblasts was derived from a tissue biopsy (Laurence Dickson, Department of Veterinary Pathology, University of Edinburgh). SSk fibroblasts were cultured in Dulbecco's Modified Eagles Medium (DMEM, produced in-house) and supplemented with a 2mM final concentration of L-glutamine (L-glu), 100 units/ml (U/ml) of penicillin/streptomycin (pen/strep) and 5% v/v foetal calf serum (FCS) in 75cm^2 flasks.

2.1.2.2 Baby hamster kidney cells

Baby hamster kidney cells (BHK-21) (Macpherson and Stoker, 1962) were maintained in Glasgow's Modified Eagle's medium supplemented with 10% v/v tryptose phosphate broth (Life Technologies, Paisley) and 10% v/v new born calf serum, L-glu (2mM), pen/strep (100 U/ml).

2.1.2.3 Hybridoma cell lines

B hybridoma monoclonal cell lines were maintained in RPMI-1640, 20% v/v FCS, 2mM L-glu (2mM) and sodium pyruvate (1mM). Hybridoma cells grew as non-adherent aggregates and were passaged every 2–3 days. Once the cells were established in culture, FCS content in the culture medium was reduced by half with each passage and replaced with Ultradoma PF serum free medium (BioWhittaker).

2.1.3 *In vitro* stimulation of peripheral blood mononuclear cells

Blood was collected by jugular venipuncture into heparinised containers (5U/ml). The mononuclear fraction was isolated by overlaying the blood onto an equal volume of Ficoll-Hypaque (density 1.077, Sigma), followed by centrifugation at 1600 × g for 30 minutes at room temperature (rt). No brake was applied on deceleration. The mononuclear layer was collected from the interface and washed twice in prewarmed Hank's balanced salt solution (HBSS) at 300 × g for 5 minutes at rt.

Peripheral blood mononuclear cells (PBMC) were resuspended at 2×10^6 cells/ml in RPMI 1640 (Life Technologies) supplemented with 10% FCS, 2-mercaptoethanol (2-ME), L-glu (2mM), pen/strep (100 U/ml). A 75cm^2 flask was then seeded with 8ml of cell suspension. LPS derived from *Salmonella typhimurium* (Sigma) was added to the cell suspension at a final concentration of 1μg/ml and cells were stimulated for 24–48 hours at 37°C. Alternatively, concanavalin A (Con A, Sigma) was added to the cell suspension at a final concentration of 10μg/ml and cells were stimulated for 24–48 hours.

2.1.4 Counting cells

A 10µl volume of cell suspension was mixed with 10µl of 0.5% (weight/volume (w/v)) trypan blue in phosphate buffered saline (PBS, Appendix I). A 10µl aliquot of the mixture was placed on a haemocytometer (Weber Improved Neubauer, Merck). Cells were counted using a light microscope (Leitz). The cells that excluded the dye (viable cells) were counted.

2.1.5 Freezing cells

Approximately 10^7 cells were centrifuged at 400 × g for 7 minutes in a bench centrifuge, followed by two washes with wash medium at 400 × g for 7 minutes. The cells were then resuspended in 1 ml of freezing medium (90% FCS, 10% dimethylsulfoxide (DMSO)) in a cryotube (Nunc, Life Technologies), which was placed overnight at –70°C. The cells were then transferred to a liquid nitrogen tank (Jencons).

2.2 Immunochemistry

2.2.1 Monoclonal antibodies

The monoclonal antibodies (mAb) used in this thesis are listed in Table 2.1 and Table 2.2. This illustrates their isotype, specificity and source for both immunolabelling (Table 2.1) and flow cytometric analysis (Table 2.2). mAb were obtained from in-house stocks (John Hopkins, University of Edinburgh), with the exception of IL-A24 and WC6 (European Collection of Cell Cultures); IL-A156, IL-A159 and IL-A190 (kind gifts from Dr. Jan Naessens, International Livestock Research Institute, Nairobi) and CC20 (Moredun Research Institute, Scotland). mAb specificity was confirmed by flow cytometric analysis and reactivity with PBMC or ALC.

Table 2.1 mAb used in immuno(histo)chemistry. A panel of mAb was used in the detection of cells in paraffin wax embedded tissues (lymph node and skin biopsies) and on frozen sections (cryostats) and on cytospins of cell preparations. (CD, cluster of differentiation; WC-1, workshop cluster 1; IAH, Institute of Animal Health; Ig LC, Ig light chain; AF, ascitic fluid; SS, saturated supernatant; ov, ovine; bov, bovine.)

mAb	antigen	reactivity	reference
VPM 54 SS	MHC class II DRα	DC, macrophages, B cells, activated T cells	Dutia et al (1995)
IAH-CC20 AF	CD1b	DC	Howard et al (1993)
IAH-CC14 AF	CD1b	DC	MacHugh et al (1988)
SBU-T6 SS	CD1	DC/B cells	MacKay et al (1988b)
VPM 5 SS	CD1	DC	Budjoso et al (1989)
OM1	CD11c	DC, macrophages, B cells	Gupta et al (1993)
IL-A53 SS	WC6	DC	Dutia et al (1993b)
IL-A24 SS	SIRPα	$SIRP\alpha^+$ DC & monocytes	Brooke et al (1998); Ellis et al (1988)
VPM 67 SS	CD14	monocytes & macrophages	Hopkins and Gupta (1996)
VPM 65 SS	CD14	monocytes & macrophages	Gupta et al (1996)
VPM 30 SS	28 kD	ovine pan B cell (hi) activated T cells (lo)	Naessens and Howard (1991)
VPM 8	Ig LC	B cells	Yirrell et al (1991)
73B SS	$CD45^{RA}$	B cells, T cell subset,	Dutia et al (1993c)
IAH CC15 SS	WC-1	γδ T cells	Clevers et al (1990)
SBU-T8 SS	CD8	CD8 T cells	Maddox et al (1985)
SBU-T4 SS	CD4	CD4 T cells	Maddox et al (1985)
36F SS	CD2	αβ T cells	MacKay et al (1988a)

Table 2.2 mAb used in two-colour flow cytometry. Isotype and original references are listed. Some mAb recognise antigens that have no established CD homologue but have been given workshop cluster (WC) numbers at the International Ruminant Leukocyte Workshops (Howard et al., 1991; Parsons et al., 1993). SIRPα is the ruminant homologue of human signal regulatory protein–α (Brooke et al, 1998). (m, murine; r, rat; bio, biotinylated mAb.)

mAb	specificity	isotype	reference
SW73.2 SW73.2-bio	MHC class II DRβ & DQβ	rIgG2a	Hopkins et al (1986)
VPM 54	MHC class II DRα	IgG1	Dutia et al (1995)
IL-A24 IL-A24-bio	SIRPα	mIgG1	Ellis et al (1988); Brooke et al (1998)
IL-A53 IL-A53-bio	WC6	mIgG2a	Dutia et al (1993b)
CC14-bio	CD1b	mIgG	MacHugh et al (1988)
IL-A159	CD80	mIgG	J. Naessens (personal communication)
IL-A190	CD86	mIgG	J. Naessens (personal communication)
IL-A156	CD40	mIgG	J. Naessens (personal communication)
VPM 5	CD1b	mIgM	Bujdoso et al (1989)
OM1	CD11c	mIgG1	Gupta et al (1993)
IAH-CC6	CD2	mIgG2a	MacKay et al (1988a)

2.2.1.1 Purification of Ig from ascitic fluid and saturated supernatant

Ig from ascitic fluid (AF) or hybridoma supernatant (SS) was purified by ammonium sulphate precipitation according to the method of Hudson and Hay (Hudson and Hay, 1989). Briefly, Ig was precipitated with ammonium sulphate (pH 6–7) at 50% saturation (w/v) for 30 minutes (AF) or 20 minutes (saturated supernatants (SS)) at rt. The preparations were centrifuged at 10,000 × g for 20 minutes. The precipitate was washed twice with 50% saturated ammonium sulphate, re-dissolved in PBS and extensively dialysed into PBS for 12 hours at 4°C. The protein concentration was determined by spectrophotometry OD_{280}, where an absorbance reading of 1.35 is equivalent to 1mg/ml protein. mAb were stored at –20°C in the presence of 0.01% sodium azide.

When new mAb preparations were used, Ig content was analysed by fractionating the proteins by polyacrylamide gel electrophoresis (PAGE) and visualised by Coomassie Blue staining (Section 2.2.5.2) or Immunoblotting (Section 2.2.5.3).

2.2.1.2 Biotinylation of monoclonal antibodies

Igs were either extensively dialysed in 0.1 M $NaHCO_3$ (pH 8.3), or a buffer exchange into 0.1 M $NaHCO_3$ was carried out using a Sephadex G 25 (PD-10) column (Amersham). The concentration of Ig was adjusted to 1 mg/ml by dilution in 0.1M $NaHCO_3$ prior to biotinylation. Biotinylation was carried out by incubating Ig for 5 hours with biotin (biotin-amido caproate N-hydroxysuccinimide ester) in DMSO (2.5 mg/ml) at a biotin to protein ration of 75µg: 1 mg. Biotinylated (bio) Ig was then extensively dialysed against PBS, 0.01% sodium azide, pH 7.2 for 12 hours at 4°C before a final 3 hour dialysis against PBS-azide containing 20% glycerol. Biotinylated mAb were stored at –80°C.

2.2.2 Preparation for immunohistochemistry

2.2.2.1 Paraffin wax embedded tissue

Prefemoral lymph nodes were removed from Suffolk sheep during routine cannulation surgery to obtain a source of material on which mAb could be applied to test for reactivity against a variety of cell types. The tissue was placed on a petri dish and lymphoid tissue was dissected from the surrounding fibrous connective tissue with a sterile scalpel. Lymph nodes were fixed in zinc salts fixative (ZSF; Appendix I) for 6–8 hours at rt and then trimmed and fixed in fresh ZSF for 24–72 hours (Gonzalez et al., 2001).

Skin samples from shaved skin were removed using a disposable biopsy-punch (6mm × 5mm; Stiefler) immediately at post-mortem. Connective tissue and hair was trimmed. Biopsies were then fixed in either (i) ZSF (as described above), or (ii) 4% paraformaldehyde (in PBS, 0.22µm filtered, pH 7.2) for 24–48 hours at 4°C.

Following fixation, tissues were trimmed and subjected to an automated process through increasing concentrations of ethanol, isopropanol and xylene, prior to embedding in low temperature paraffin wax. Biopsies were sectioned at 5µm, mounted on treated glass slides (Superfrost Plus, Menzel–Glaser, Germany) and allowed to dry overnight at 37°C. Neil McIntyre, Andrew Dawson and Sharon Moss at Easter Bush Veterinary Centre (EBVC), Midlothian, Scotland, processed and sectioned all tissues and stained skin sections with haematoxylin and eosin (H & E).

2.2.2.2 Frozen tissue

Skin biopsies were snap-frozen at –70°C in a mixture of dry ice and isopentane and stored at –80°C until sectioned.

2.2.2.3 Cytospins

Cytospins of single cell suspensions from lymph were prepared by spinning 100µl of cell suspension (1×10^6 cells/ml) onto pre-chilled silane-prep™ microscope slides (Sigma) at 300 revolutions per minute (rpm) for 3 minutes using a Cytopsin-2 (Shandon). Cytospins were fixed in ice-cold acetone for 5 minutes, air-dried and then stored at –20°C until stained. Cytospins were also prepared from purified ALDC populations (approximately 25,000–100,000 cells/ml) and either fixed in acetone (for subsequent immunostaining) or air-dried (ATPase staining) prior to storage at –20°C. Cytospins were stained with Gurr® Giemsa's stain solution (improved R66, BDH) for 15 minutes. After staining, cytospins were washed in tap water, rinsed briefly in dH_20 and dried. ATPase staining was carried out with Neil McIntyre (EBVC).

2.2.3 Immunohistochemistry

2.2.3.1 Immunostaining of paraffin-wax embedded tissue

Immunohistochemical labelling was carried out using a Dako Envision Horseradish Peroxidase (HRP) kit, based on a published method (Gonzalez et al, 2001). Slides were dewaxed by immersion in Clearene (Surgipath) for 15 minutes and gradually hydrated through graded alcohols. Slides were then washed twice in distilled water (dH_20) and immersed in Tris Buffered Saline (TBS; Appendix I). Two initial blocking steps were carried out:

(i) Endogenous peroxidase activity was quenched with a peroxidase block (supplied in the kit) for 5 minutes at rt

(ii) Non-specific tissue antigens were "blocked" by incubating the sections with 25% normal goat serum (NGS) for 30 minutes at rt in a humidity chamber.

Sections were incubated with mAb (Table 2.1) overnight at 4°C in a humidity chamber after which they were rinsed once and then washed three times in TBS containing 0.1% Tween-20 (TBST) with gentle agitation. The secondary antibody (HRP-conjugated goat anti-mouse antibody) was applied for 30 minutes at rt and sections were washed 3 times in TBST. Conjugate binding was detected by adding the substrate chromagen (3,3'-diaminobenzadine;

DAB (Sigma)) and colour was allowed to develop for 7–8 minutes. Finally, tissue sections were rinsed in dH_20 and counter-stained with haematoxylin, rinsed in tap water, dehydrated and mounted.

TBST was used to wash the tissue sections between each stage of the labelling procedure and TBS was used to prepare NGS and antibody dilutions. Omission of the primary antibody was used to provide a negative control.

2.2.3.2 Antigen retrieval

After blocking of endogenous peroxidase, PFA-fixed tissues were subjected to trypsin treatment (trypsin tablets, Sigma) for 15–30 minutes at 37°C. Slides were washed twice in TBST and then blocked for 30 minutes in 25% NGS. Staining was then carried out as already described.

2.2.3.3 Immunochemical labelling of cytospins and cryostats

Cryostats and cytospins were allowed to reach rt, air dried for 5–10 minutes, rehydrated in PBS and washed in TBS. After rehydration, a hydrophobic barrier was drawn around sections using a Pap-pen (Zymed Laboratories Inc.) and slides were again air dried for 3 minutes. Blocking of endogenous peroxidase and non-specific antigens and the staining procedure was carried out as described in Section 2.2.3.1 with the exception that incubation with primary antibody was carried out for 1 hour at rt. Haematoxylin was used as a counterstain.

2.2.3.4 Double Immunochemical labelling of cytospins

Detection of primary antibody was carried out as described in Section 2.2.3.1. After incubation with DAB substrate, slides were rinsed twice in dH_20 and then once in TBST, blocked for 30 minutes in 25% NGS and then incubated with a second mAb for 1 hour. Slides were washed three times in TBST and a secondary biotinylated antibody (ABC kit, Vector Laboratories) was then applied for 30 minutes. Slides were washed and ABC-AP reagent was added to sections and incubated for 30 minutes. Slides were washed again and Vector Blue alkaline phosphatase was added and colour was allowed to develop for up to 20 minutes.

2.2.3.5 Immunofluorescent staining of transfected cells

Transfected SSk fibroblasts or BHK cells were harvested 16 hours post-transfection (Section 2.3.8.1) by rinsing the cells with sterile PBS (sPBS) followed by rinsing in 500µl versene EDTA solution (BioWhittaker™) until cells detached. Cells were transferred into 1.5ml Eppendorf tubes, washed twice in sPBS and then resuspended in 20µl sPBS. Cells were spotted onto a multiwell slide (BDH), air-dried and fixed in ice-cold methanol/acetone for 30 seconds. Prior to immunostaining, cells were permeabilised by immersion in 0.1% Triton-X. Non-specific binding was prevented by incubating slides in blocking solution (25% NGS in sPBS) for 10 minutes at rt. Primary antibody (2H11; 1:200 in blocking solution) was then added to the cells and incubated for 1 hour at rt. Primary antibody was removed by washing slides three times in PBS. Secondary antibody (TRITC-conjugated goat anti-mouse IgG) was added and incubated for 1 hour. Cells were washed in PBS, slides were mounted with anti-fade mounting solution (Dako) and visualised by fluorescent microscopy.

2.2.4 Flow cytometry

2.2.4.1 Cell preparation

Pseudoafferent lymph was obtained from chronic cannulation of the prefemoral efferent and pseudoafferent lymphatics (Hall, 1967; Hopkins et al., 1986). Lymph was collected into sterile plastic bottles containing 400U of heparin, 1000U penicillin, 1mg streptomycin. In experiments evaluating cytokine expression of DC, all buffers were supplemented with actinomycin D (final concentration 1µg/ml, Sigma) in order to prevent *de novo* transcription. Collections were performed at 24-hour intervals to record lymph volume and cell counts. Animals were allowed at least six days post-operative recovery and the lymph was assessed for erythrocyte and PMN contamination by flow cytometric light scatter profiles.

2.2.4.2 Single colour flow-cytometry

ALC were collected by centrifugation at 300 × g for 5 minutes at 4°C. Cells were washed twice in ice-cold FACS buffer (PBS, 2% bovine serum albumin (BSA), 0.05% sodium azide, pH 7.2) and then resuspended in blocking buffer (FACS buffer containing 10% NGS) at a concentration of 1×10^7 cells/ml for 30 minutes on ice. Cells were dispensed into FACS tubes (50µl/tube) and incubated for 15 minutes at 4°C with 25µl of primary mAb (biotinylated or non-biotinylated mAb; (Table 2.2) diluted appropriately in FACS blocking buffer. Unbound antibody was removed by washing twice with 2.5ml ice-cold FACS buffer. Biotinylated primary mAb were detected following incubation with 3.5µl streptavidin-

phycoerythrin (SA-PE, Sigma) in the dark for 15 minutes at 4°C. Non-biotinylated mAb were detected following incubation in the dark for 15 minutes with 25µl of FITC conjugated anti-mouse Ig (Sigma) diluted 1:1000 in FACS buffer. Cells were washed twice in FACS buffer and re-suspended in 2% paraformaldehyde prior to analysis.

Normal mouse serum (NMS; 1:500) was used as a negative control to assess non-specific binding. Biotinylated NMS (1:100) was used to assess background staining where biotinylated mAb were used.

2.2.4.3 Two-colour flow-cytometry

For double staining (using antibodies of the same isotype), cells were first incubated with the mAb to be labelled with FITC. Cells were washed and incubated with FITC-antiglobulin conjugate. After washing, cells were incubated with the second biotinylated antibody (Table 2.2) for 15 minutes at 4°C and washed twice. The second biotinylated mAb was detected with SA-PE in the dark for 15 minutes. Cells were washed and prepared for flow cytometric analysis as above.

2.2.4.4 Flow cytometer settings

The immunofluorescence studies described were carried out using the Becton Dickinson (BD) FACScan flow cytometer and data were analysed using the Cell Quest software. Data were obtained by analysis of 5000–10,000 cells (events) from each sample. Different cell populations were distinguished by gating using appropriate linear photomultiplier tube (PMT) voltage amplifications for forward scatter (FSC) and side scatter (SSC) parameters. FSC and SSC parameters define cell size and complexity respectively. ALDC have high FSC and SSC (Figure 2.1). Fluorescence measurements were made on homogenous populations of cells by setting gates on dot plots. For two-colour flow cytometry analysis, compensation settings were determined to overcome the spectral overlap from FITC and SA-PE fluorochromes. The appropriate %FL1-FL2 and %FL2-FL1 PMT voltage compensation was used. Cells were single stained for MHC class II with mAb VPM 54 (DRα) (detected with anti-Ig-FITC) or SW73.2 (DRβ DQβ) biotin conjugate (detected with SA-PE). Compensation thresholds for FL1 and FL2 were adjusted so that fluorescent cells were in line with quadrants set with negative controls and parallel to the axis (Figure 2.2).

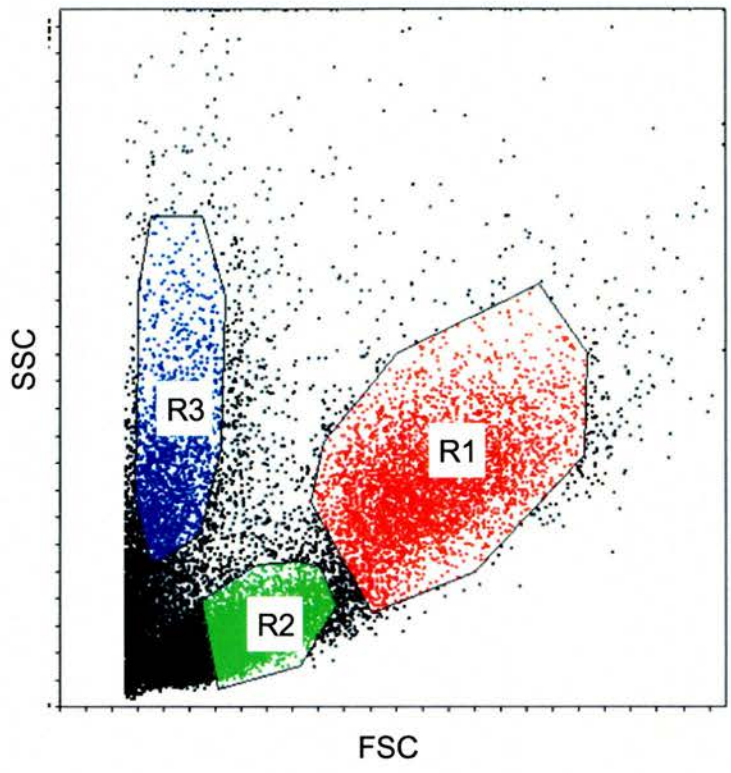

Figure 2.1 Gate criteria used in flow cytometry. Cell populations were defined by light scatter properties and gates were positioned around homogeneous populations of cells. ALDC were defined by high FSC and high SSC (R1). Lymphocytes were defined by low to medium FSC and low SSC (R2). PMN were defined by low FSC and high SSC (R3).

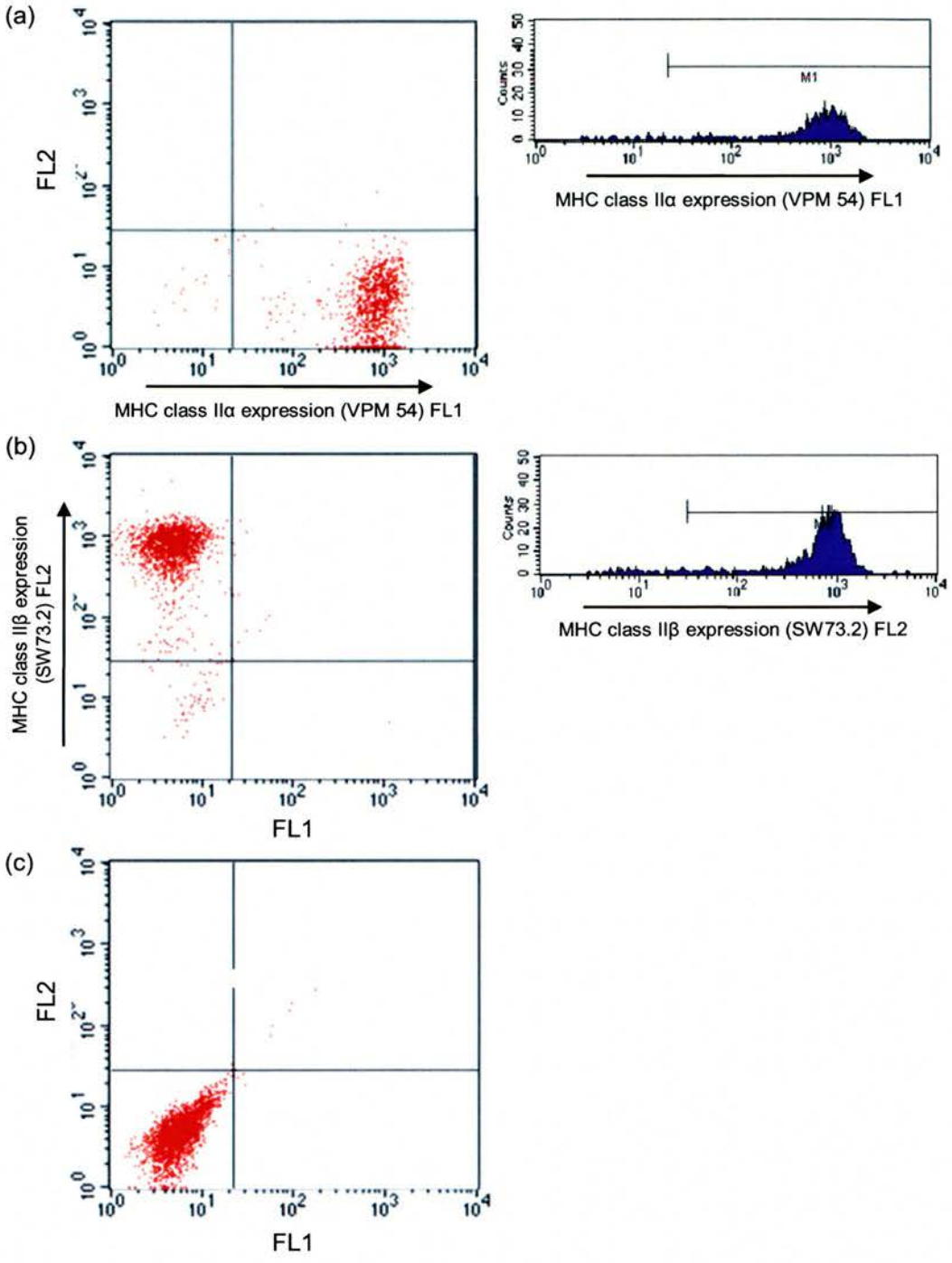

Figure 2.2 Compensation settings for two-colour flow cytometry. ALC were resuspended at 1×10^7 cells/ml and then single-stained with either (a) VPM 54 supernatant (anti-MHC class II DRα) or (b) biotinylated SW73.2 (anti-MHC class II DRβ DQβ) diluted 1:1500. Compensation settings were finely adjusted until single stained cells were contained in either FL1 (VPM 54) or FL2 (SW73.2) quadrants and aligned with the centre of the unstained cell population (c).

2.2.4.5 Titration of mAb

mAb used in flow cytometry experiments were titrated on ALC to establish optimal working concentrations. The optimal dilution of the primary antibody was that which gave strongest specific fluorescence and lowest background staining of the negative population. A normal histogram distribution was considered to be mAb-binding saturation (Figure 2.3c).

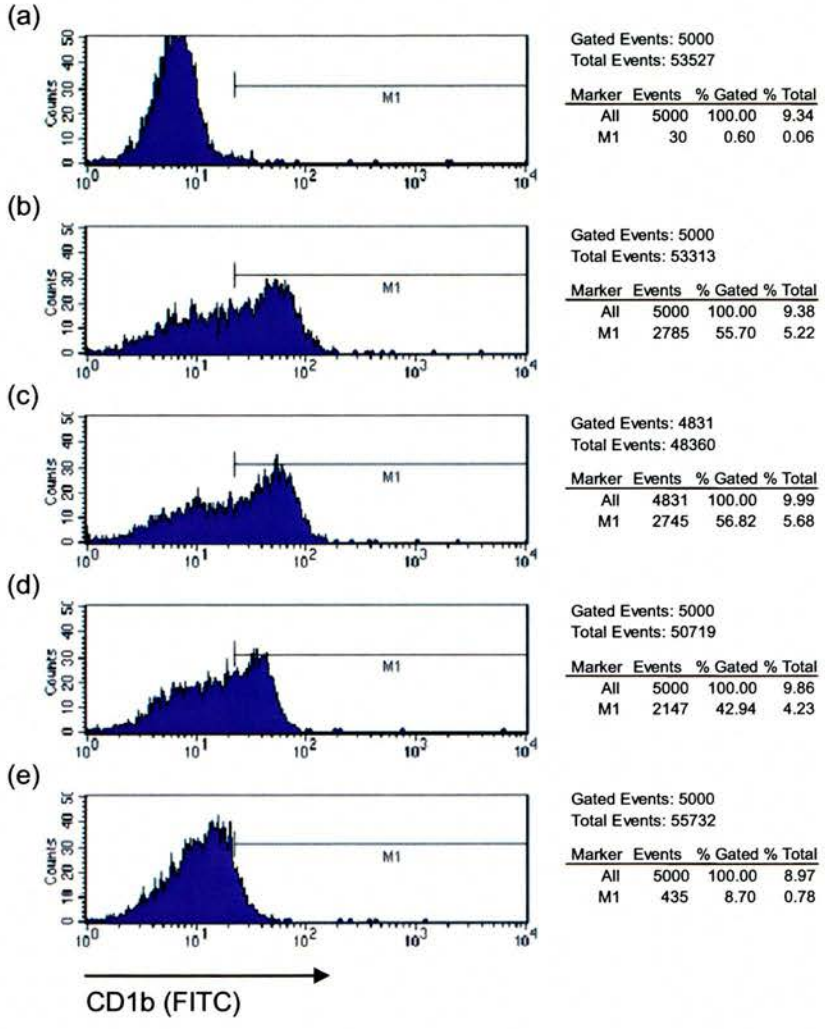

Figure 2.3 Titration of anti-CD1b mAb (VPM 5) on ALC. ALC were resuspended at 1 × 10^7 cells/ml and stained with (a) negative control (NMS) diluted 1:100 in FACS buffer. Note that < 1% of (background) staining is evident. VPM 5 diluted (b) 1:75, (c) 1:100, (d) 1:250 and (e) 1:500. 5000 events were counted in the DC (R1) gate (Figure 2.1). A normal histogram distribution is evident in (c).

2.2.4.6 Enrichment of ALDC for cell sorting

ALDC were enriched by centrifugation through OptiPrep™ (Axis-shield) based on a published method for isolating blood monocytes (Graziani-Bowering et al., 1997). The OptiPrep™ solution was allowed to reach rt and mixed well prior to use.

ALC were collected by centrifugation at 300 × g for 5 minutes at 4°C. The cells were then washed and resuspended in 0.22μm filtered Buffer B (sPBS, 1mM EDTA, 0.5% BSA) at 2 × 10^7 cells/ml. The method is summarised in Figure 2.4. To a 2.5ml volume of cell suspension, 1ml of OptiPrep™ was added and gently mixed. Using a sterile pastette, the lymph–OptiPrep™ mixture was carefully overlaid with 4ml of a 1.078 g/ml lymphocyte-specific density layer (OptiPrep™ was diluted in sPBS containing 1mM EDTA). This layer was overlaid with 10 ml of a 1.068 g/ml solution, which was then overlaid with 1ml sPBS. Care was taken to prevent mixing of layers. The lymph/OptiPrep™ mixture was centrifuged at 600 × g for 25 minutes at rt with a swing-out rotor; no brake was applied on deceleration. Cells were collected from the interphase of the 1.068g/ml layer and sPBS (fraction 1) and were washed with 5ml of sPBS and centrifuged at 200 × g for 5 minutes at rt. The supernatant was removed and the cells were washed again in 20ml ice-cold FACS buffer at 300 × g for 5 minutes at 4°C. Cells were then resuspended in either (i) blocking buffer (for subsequent staining for cell sorting) or (ii) sPBS for cytospin preparations. DC were enriched to 48–75%, as determined by flow cytometry (Figure 2.5) and immunostaining (Figure 2.6).

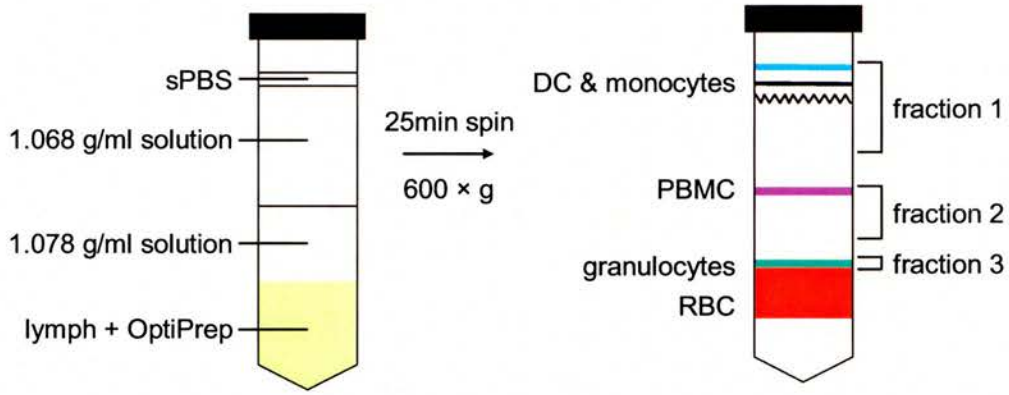

Figure 2.4 Schematic representation of the DC isolation procedure from afferent lymph using OptiPrep™. The diagram illustrates the set-up of the lymph/OptiPrep™ mixture and the various density layers and the banding patterns of the cells following a 25 minute spin at 600 × g. Adapted from (Graziani-Bowering et al, 1997).

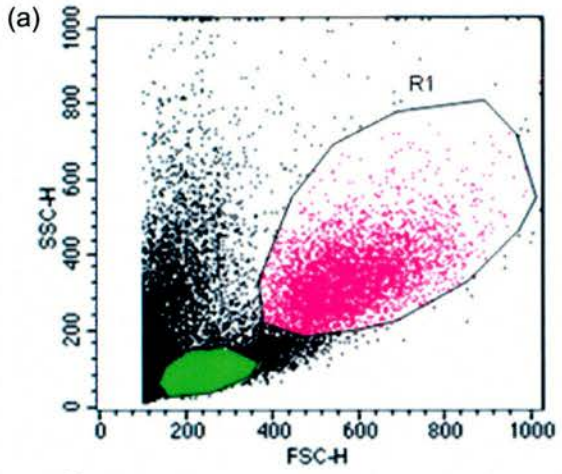

Gated Events: 55110
Total Events: 55110

Region	Events	% Gated	% Total
R1	4674	8.48	8.48
R2	40976	74.35	74.35

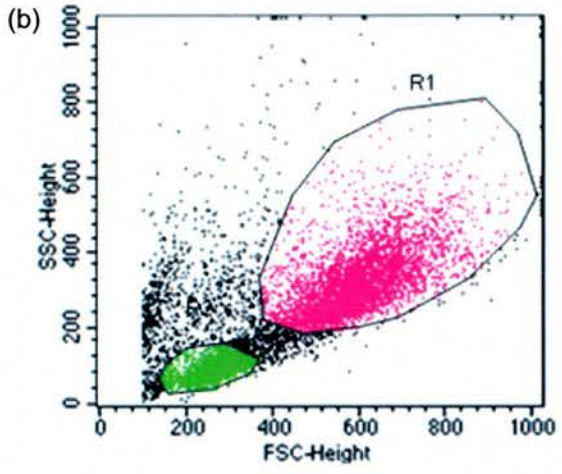

Gated Events: 10477
Total Events: 10477

Region	Events	% Gated	% Total
R1	5000	47.72	47.72
R2	3753	35.82	35.82

Figure 2.5 Enrichment of DC from afferent lymph. DC were enriched by centrifugation with Optiprep™ (Section 2.2.4.6, Figure 2.4). Unfractionated lymph and the enriched DC-fraction were washed twice in FACS buffer and resuspended at 5×10^6 cells/ml. Cells were fixed in 2% paraformaldehyde and flow cytometry analysis was carried out. DC comprise approximately 9% in unfractionated lymph (a), and are enriched to approximately 48% following centrifugation in OptiPrep™ (b).

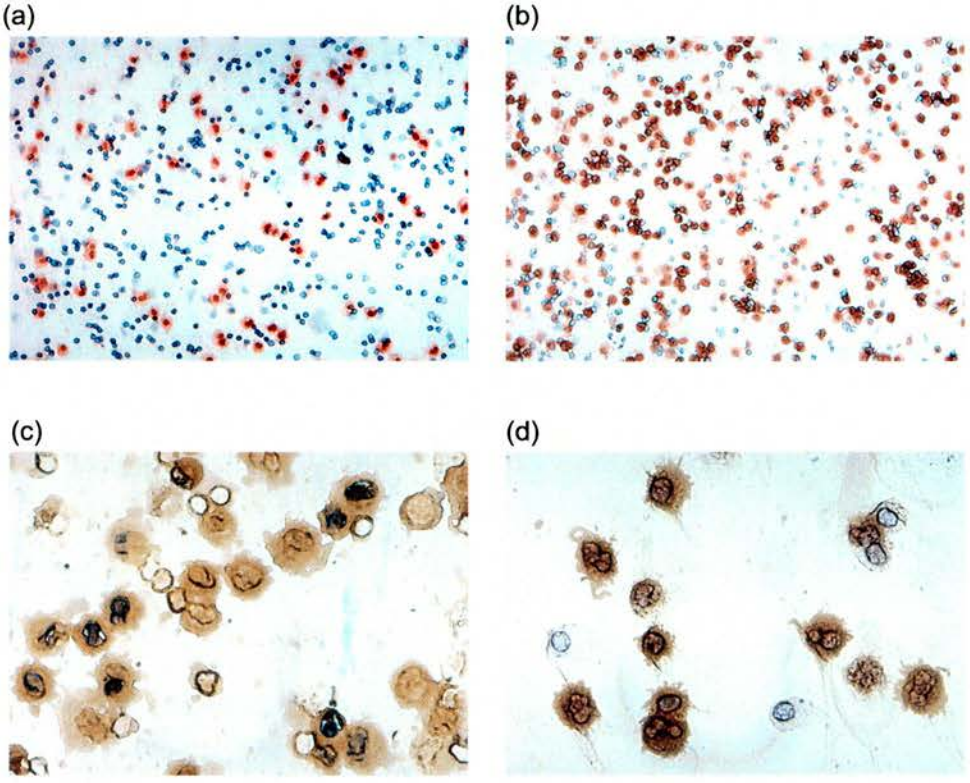

Figure 2.6 Immunoperoxidase stained cytospins of unfractionated lymph and DC-enriched fractions. (a) Unfractionated lymph immunolabelled with SBU-T6 (pan anti-CD1) and counterstained with haematoxylin (original magnification, ×80); (b) DC-enriched fraction (fraction 1) immunolabelled with SBU-T6 (original magnification, ×80); (c) double immunolabelled DC (fraction 1) stained with VPM 54 (MHC class II DRα, brown cells) and SBU-T6 (blue cells) (original magnification, ×250); (d) DC-enriched fraction (fraction 1) stained with SBU-T6 (original magnification, ×250).

2.2.4.7 Immunolabelling of ALDC for cell sorting

Two subpopulations of ALDC were easily distinguished based on expression of SIRPα (mAb IL-A24) and MHC class II expression (mAb SW73.2) (Figure 2.7a), whereas populations were not as easily defined after staining with IL-A24 and biotinylated CC14 (anti-CD1b; Figure 2.7b) or after staining with IL-A24 and a biotinylated WC6 (anti-DEC 205; Figure 2.7c). IL-A24 and biotinylated SW73.2 were therefore used for all subsequent cell sorting experiments.

Immunolabelling prior to cell sorting was carried out essentially as described for immunolabelling of ALC. Briefly, the enriched DC-fraction (following centrifugation with OptiPrep™) was washed in sPBS and resuspended in FACS blocking buffer. Cells were counted and dispensed into FACS tubes ($2 \times 10^6 - 8 \times 10^6$ cells/tube). Cells were centrifuged at 300 × g for 5 minutes at 4°C and resuspended in a total volume of 500µl blocking buffer (containing actinomycin-D) for 30 minutes on ice. Sequential staining was then carried out

using 250µl of each of the antibodies diluted appropriately in FACS buffer. Undiluted tissue culture IL-A24 supernatant (anti-SIRPα) and biotinylated SW73.2 (anti-MHC class II β, diluted 1:1500) were used to stain cells (Figure 2.7a). Half of the recommended volume of SA-PE was used to detect the biotinylated mAb. After each stage, cells were washed twice in 3.75ml ice-cold FACS buffer. Cells were stored in FACS buffer containing actinomycin-D until cell sorting was carried out.

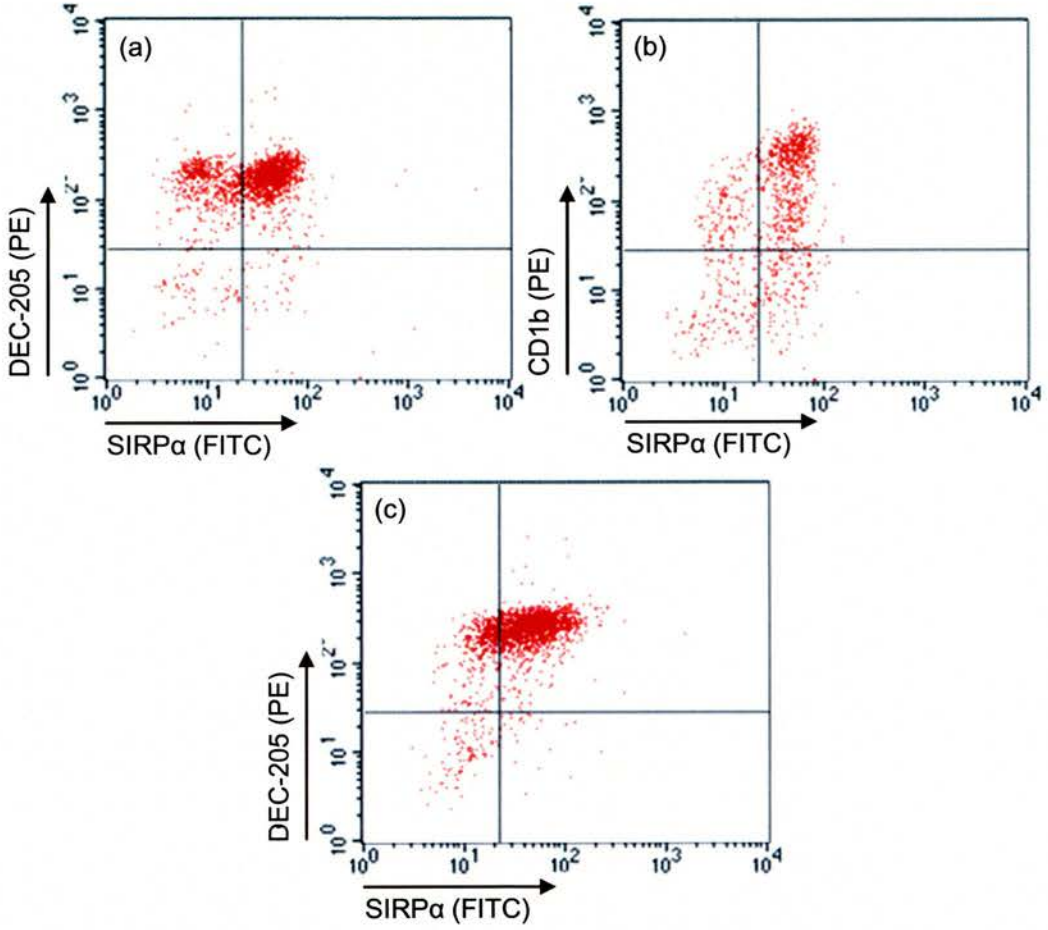

Figure 2.7 Double immunolabelling of ALDC. Enriched DC were immunolabelled with mAb IL-A24 (anti-SIRPα) followed by (a) biotinylated SW73.2 (anti-MHC class IIβ), (b) biotinylated CC14 (anti-CD1b) and (c) biotinylated WC6 (anti-DEC-205).

2.2.4.8 Fluorescence activated cell sorter settings

DC populations were purified using fluorescent activated cell sorting (FACS) (FACSvantage, Becton Dickinson). PMT voltage settings for FSC and SSC parameters, and compensations defining fluorochrome light emittance were determined for each experiment, as described in Section 2.2.4.4. Samples were analysed and sorted using a sheath pressure of 9 psi, analysing approximately 20,000 cells per second (2 cells were analysed per drop). The flow rate of cells analysed was similar in each experiment. This enables the software to discern individual cells for analysis and sorting. At higher flow rates, or where cell resolution was not achievable, cells were 'aborted'. The abort rate was consistently 5–10% of cells analysed. Samples that were sorted at abort rates higher than 10% were discarded.

2.2.4.9 Electron microscopy of FACS–sorted DC

FACS–sorted DC were centrifuged at 10,000 × g for 3 minutes and the supernatant carefully removed. Cells were washed once in sPBS and centrifuged as above. Approximately 1ml of 3% glutaraldehyde (in 0.1M cacodylate buffer) was added to the pellet and cells were fixed for 2–3 hours at 4°C with occasional agitation. Cells were again centrifuged and 1ml of fixative was slowly added to the pellet. Care was taken so as not to disturb the cell pellet and cells were stored overnight at 4°C in fixative. Further processing of samples was carried out by Steve Mitchell (Division of Veterinary Biomedical Sciences, University of Edinburgh). This involved post-fixing the cells in osmium tetroxide in 0.2M cacodylate buffer, followed by several washes. Cells were than gradually dehydrated in ethanol, propylene oxide and epoxy resin and finally embedded in resin until sectioned.

2.2.5 Detection of protein

2.2.5.1 Sodium dodecyl sulphate (SDS)-PAGE

Proteins were fractionated by SDS-PAGE. Samples were boiled for 5 minutes in an equal volume of double strength sample buffer (Appendix I), then vortexed for 30 seconds and centrifuged at 10,000 × g for 3 minutes at rt. The samples were separated by electrophoresis under reducing conditions using a 12% acrylamide resolving gel and a 4% acrylamide stacking gel (Appendix I) at a constant 140V for approximately 80 minutes until the dye front reached the bottom of the gel. This was performed at rt in a gel electrophoresis tank (Biorad) containing running buffer (Appendix I). Following electrophoresis, the gel was either stained in Coomassie blue or prepared for Western Blotting. Biorad low range molecular weight markers (range 20.5–111 kDa) were run on each gel.

2.2.5.2 Coomassie blue staining

Gels were stained for 30 minutes in Coomassie blue (0.1% Coomassie Brilliant Blue R-250 in 10% methanol, 10% acetic acid), then rinsed briefly in tap water and transferred to Coomassie blue destain (20% methanol and 10% acetic acid) and left overnight or until bands were clearly visible.

2.2.5.3 Detection of purified mAb by Western blotting

Following SDS-PAGE separation, the proteins were transferred to a polyvinylidene fluoride (PVDF) membrane (Roche) using a semi-dry electroblotter (Trans-Blot SD, Biorad). Transfer was performed in transfer buffer (Appendix I) for 1 hour at a constant current of 120mA. Following transfer, non-specific sites on the membrane were blocked in a solution of 0.2% Tween-20 (Sigma) and 5% w/v dried milk (Cadbury's Marvel) in PBS overnight at rt. Blots were washed 5 times over 30 minutes in wash buffer (PBS, 0.1% Tween-20) and then incubated with 1:1000 dilution of HRP-conjugated rabbit anti-mouse antibody (Dako) followed by washing. Conjugate binding was detected by adding the substrate chromagen (3,3'-diaminobenzadine; DAB) (Sigma) and colour was allowed to develop for 7–8 minutes.

2.2.5.4 Detection of IL-3 by Western blotting

This was carried out as essentially as already described with the exception of the following. After blocking, the membrane was cut into several strips. Each strip was then incubated with a primary anti-IL-3 antibody diluted in wash buffer (1:200 dilutions of the following AF: 2H11 H6 clone 2; 2H11, 3F7 D4, 2H11 and neat hybridoma supernatant, 5A6/F9) for 2 hours and washed as above. Detection of bound antibody was carried out by incubating blots for 1 hour at rt in a 1:1000 dilution of HRP-conjugated rabbit anti-mouse antibody (Dako).

ECL was also used to provide increased sensitivity in development of membranes probed with anti-IL-3 antibodies (as recommended by the manufacturer). All steps were carried out as described above with the exception of washes being carried out in a solution of PBS, 0.5% Tween-20 (PBST) for 45 minutes.

2.2.5.5 Detection of GM-CSF by sandwich ELISA

This was carried out according to a published method (Entrican et al., 1996). Recombinant GM-CSF and anti-GM-CSF mAb were obtained from Dr Gary Entrican (Moredun Research Institute, Scotland). Flat-bottomed 96 well ELISA plates (Immulon, Dynex) were coated

with 50µl per well of 8D8 affinity mAb at a concentration of 1µg/ml in 0.1M carbonate buffer (pH 9.6; Appendix I) and incubated at 4°C overnight. Plates were washed twice with PBST and then blocked for 30 minutes rt with 100µl per well PBST containing 3% BSA and 0.05% Tween-20. The plates were then washed twice with PBST. GM-CSF standards and tissue culture supernatants were prepared by dilution in 3%BSA/PBS/Tween-20. 50µl of the GM-CSF standards and the test samples (supernatants from transfected cells) were loaded.

The plates were incubated for 1–1.5 hours at rt and then washed six times with PBST. 50µl of the affinity purified monoclonal 3C2-peroxidase conjugate (diluted 1:500 in PBST) was loaded into each well and then incubated for 1 hour at rt and washed six times in PBST. 50µl/well TMB Microwell Peroxidase substrate (Sigma) was added to each well and colour was allowed to develop for approximately 10 minutes. The reaction was stopped by adding 50µl/well 0.1M Hydrochloric acid. The optical density (OD) was measured using a Dynex ELISA reader equipped with a 450nm filter. Blank wells contained all reagents with the exception of sample/GM-CSF standard; supernatant was added to these wells.

2.3 Molecular biology section

2.3.1 Handling of RNA and DNA and molecular biological techniques

Many of the methods used in handling DNA or RNA were based on methods given in "Molecular Cloning: A Laboratory manual" (Sambrook et al., 1989). All restriction enzymes and buffers were obtained from New England Biolabs (NEB).

2.3.2 Measurement of DNA/RNA concentration

The amount of DNA or RNA present in the sample is directly proportional to the amount of UV radiation absorbed by the sample. The concentration of nucleic acid was determined by spectrophotometry (GeneQuant II, Amersham Pharmacia Biotech). Absorbance was measured at wavelengths of 260 and 280nm.

DNA concentration = Absorption at 260nm (A^{260}) × 50 × dilution factor,

RNA concentration = Absorption at 260nm (A^{260}) × 40 × dilution factor,

where an A^{260} of 1.0 is equivalent to 50mg/ml of DNA and 40mg/ml of RNA. The purity of DNA was calculated as a ratio of OD_{260}/OD_{280}. A value greater than 1.8 (DNA) and 1.9 (RNA) indicates that the sample is free of protein contamination.

2.3.3 RNA isolation

Precautions were taken to preserve the integrity of RNA transcripts throughout the following procedures. Particular emphasis was placed on avoiding contamination with ribonucleases (RNases). Bench surfaces and pipettes were thoroughly cleaned with 70% ethanol, followed by removal of RNases with RNaseZAP® (Sigma) in combination with molecular grade water (Sigma). Sterile disposable plastic ware was used and gloves were changed frequently. Molecular grade water was used for all elution steps and preparation of wash solutions. Molecular grade ethanol was used for all wash steps.

2.3.3.1 Isolation of total RNA from tissue

Total RNA was isolated from skin biopsies and spleen samples using the RNeasy® Mini kit (Qiagen®), which allows the purification of up to 100µg RNA from animal cells and tissues. Immediately post-mortem, biopsies were removed using a sterile biopsy-punch and then placed into 1ml RNA*later*™ (Sigma). Tissue was stored in RNA*later*™ overnight at 4°C and then removed from RNA*later*™ into fresh 1.5ml Eppendorf tubes and stored at –80°C until RNA extraction was performed.

Homogenisation of tissues

Skin biopsies and spleen samples were removed from –80°C storage and allowed to reach rt. Each biopsy was placed onto a sterile Petri dish and finely chopped into small pieces using two sterile scalpels. The shreds of tissue (no more than 30mg) were then carefully placed into a clean 1.5ml Eppendorf tube, to which 350µl of lysis buffer (supplied with the kit) was added. Lysis buffer contained the RNase inhibitor 2-ME. The tissue was homogenised using a motorised pestle and mortar until the sample was uniformly homogenised. Following homogenisation in lysis buffer, 550µl of nuclease-free water was added followed by 10µl proteinase K (20mg/ml; Sigma). The contents were thoroughly mixed and incubated for 15 minutes at 55°C in a hot-block. Genomic DNA was sheared by complete homogenisation

with a 20-gauge needle (0.9mm diameter). To avoid contamination between samples, separate pestles were used for each biopsy. Pestles were autoclaved and soaked in RNaseZAP® (Sigma) and nuclease-free water overnight prior to use.

RNA extraction from tissue

Briefly, homogenates were centrifuged at 10,000 × g for 3 minutes at rt. The supernatants were dispensed into Qiagen® mini spin columns and all steps thereafter were carried out as outlined in the manufacturer's instructions. All samples were treated with DNase (Qiagen® DNase kit) on the spin column membranes.

2.3.3.2 Removal of plasmid DNA from skin biopsy RNA samples

Further treatment of RNA samples extracted from DNA vaccinated skin sites was required in order to remove remaining plasmid DNA not completely removed by the on-membrane DNase step (Qiagen® kit). Complete removal of plasmid DNA was essential prior to quantitative RT-PCR analysis of gene expression in skin (Section 2.6.2). Further removal of plasmid DNA in RNA samples was carried out in solution with DNase and restriction enzymes.

Removal of plasmid DNA from RNA

To remove plasmid DNA containing the GM-CSF insert, 10µl reactions were prepared as follows. To a 0.6ml Eppendorf tube, 6µl of RNA (0.5–7µg total RNA), 1µl 10 × BSA (NEB), 1µl RQ1 buffer (Promega), 1µl (1 U) of RQ1 DNase and 1µl (20 U) Pst-1 were added and gently mixed. Removal of plasmid containing the IL-3 insert was carried out as described above, with the exception that (i) 7µl of RNA was treated in each reaction (ii) BSA was omitted and (iii) 1µl Hinf-1 (10 U) was used instead of Pst-1.

Approximately 10µg of total RNA was treated in this manner for each individual biopsy; multiple reactions were prepared for each sample. All treatments were incubated at 37°C for 1.5 hours. Tubes were gently mixed halfway through the incubation. Following treatment of RNA to remove plasmid DNA, tubes were briefly centrifuged to collect the contents. DNase was inactivated by addition of 1µl RQ1 Stop Solution (Promega). DNase was further inactivated by heating at 65°C for 10 minutes. Tubes were then immediately place on ice for 5 minutes and the contents collected by centrifugation. RNA samples from the same biopsy were pooled and volumes adjusted to a total volume of 100µl in nuclease-free water.

RNA clean-up

To remove any reagents which may interfere with downstream applications, DNase/restriction enzyme treated RNA samples were purified using the Qiagen® RNA mini spin columns as described by the manufacturer's instructions ("RNA clean-up procedure"). RNA was eluted in 30µl of nuclease-free water.

2.3.3.3 RNA isolation from cells in suspension

Total RNA was isolated from cells in suspension using the SV Total RNA kit (Promega). No more than 5×10^6 cells were used for each extraction.

Harvesting of cells

In vitro stimulated PBMC. Following 24–48 hour *in vitro* stimulation, non-adherent PBMC and culture medium were removed from the flask(s). Cells were collected by centrifugation at 300 × g for 5 minutes at 4°C. Cells were then washed twice in sPBS to remove FCS. Adherent cells were rinsed in sPBS followed by the addition of 0.5ml of pre-warmed trypsin (in-house) until cells detached. PBMC were washed as above and combined with the adherent-cell fraction and stored on ice until lysis was carried out.

Transfected fibroblasts. Approximately 48 hours after transfection, fibroblasts were harvested by trypsin treatment, washed twice in sPBS and stored on ice until extraction was performed.

FACS–sorted ALDC. ALDC populations purified by FACS were transported on ice and were temporarily stored in FACS buffer containing actinomycin D (1µg/ml final concentration). Cells were collected by centrifugation at 300 × g for 5 minutes at 4°C and washed once in 2ml ice-cold sPBS.

Cell lysis and RNA extraction

Cells were counted prior to RNA extraction (with the exception of FACS–sorted ALDC). Prior to cell lysis, cells were collected by centrifugation at 300 × g. Supernatants were carefully aspirated and any residual liquid was allowed to drain onto tissue paper. 175µl of SV RNA lysis buffer (Promega) was added to the cell pellets and mixed by vigorous vortexing. Genomic DNA was sheared by homogenisation through a 20-gauge needle. Total RNA was isolated using the SV Total RNA kit as described by the manufacturer. All samples were subjected to DNase treatment on the membrane (supplied with the kit).

2.3.3.4 Concentration of RNA

RNA was concentrated under vacuum with a Savant DNA 110 Speed Vac Concentrator System. Eppendorf lids were pierced several times using a sterile needle. The rotor was thoroughly cleaned with ethanol and RNaseZAP® prior to use. RNA samples were concentrated by spinning at ambient temperature under vacuum until the correct volume was obtained for reverse transcription.

2.3.4 First strand cDNA synthesis using reverse transcriptase

RNA was reverse transcribed using an oligo dT primer to give a heterogeneous population of cDNA templates, which were subsequently used as the starting template for RT-PCR. The presence of undegraded genomic material was tested for each RNA sample. Briefly, 1µg of RNA[2] was diluted in nuclease-free water to give a final volume of 13µl. 500ng of Oligo-$(dT)_{15}$ (Promega) was added to the RNA and incubated at 70°C for 5 minutes, followed by cooling on ice to allow annealing of the primer. Contents were collected by brief centrifugation and 10µl of the reaction mix (Table 2.3) was added to each tube.

The reactions were gently mixed and 1µl (50U) of MMLV-RT (Promega) added. To test for the presence of undegraded genomic DNA, 1µl of nuclease-free water was added instead of the RT enzyme. Reactions were then incubated for 10 minutes at 40°C, followed by 50 minutes at 42°C. The cDNA was heated for 15 minutes at 70°C to inactivate the RT enzyme.

Table 2.3 RT master reaction mix. 10µl of the mix was added to the RNA/Oligo dT prior to the addition of the RT enzyme.

reagent	company	volume
5 × M-MLV (H-) reaction buffer	Promega	5 µl
RNase block ribonuclease inhibitor (40U/µl)	Invitrogen	0.5 µl
100 mM dNTPs	Biogene	1.25 µl
Nuclease-free water	Sigma	3.25 µl

[2] When available. RNA yields from purified ALDC populations after a 24-hour collection of lymph were low (average yield 0.5µg RNA from SIRPα$^+$ ALDC; range 0.2µg-2.5µg).

2.3.5 Reverse transcriptase polymerase reaction (RT)-PCR

RT-PCR was carried out essentially as described by (Sambrook et al, 1989). GAPDH (glyceraldehyde-3-phosphate dehydrogenase) RT-PCR was performed on all samples to confirm the presence of amplifiable cDNA on each occasion. Each RNA sample was tested for the presence of undegraded genomic material (–RT reactions). For every run, appropriate positive and negative controls were included. Sterile dH_20 was always included as a control for DNA contamination.

2.3.5.1 Safe PCR Practice

Care was taken throughout the preparation of PCR reactions to avoid contamination of samples with amplified products, or unwanted DNA. Gloves were worn and changed regularly, and sterile tubes and aerosol resistant tips were used throughout the procedure. All PCR reagents were aliquoted and stored in smaller volumes.

2.3.5.2 Primer design for conventional RT-PCR

The primer pairs for all genes were designed from gene sequences deposited in GenBank (Table 2.4) and designed using Netprimer3[3]. Primers were checked for secondary structures using Premier Biosoft[4]. Parameters for the design of primers for quantitative real-time RT-PCR are listed in Table 2.10.

[3] http://www-genome.wi.mit.edu/cgi-bin/primer/primer3_www.cgi
[4] http://www.premierbiosoft.com/netprimer/index.html

Table 2.4 GenBank accession numbers of sequences used to design primers. (*, human and murine sequences were aligned and primers were designed from homologous regions; †, primer details for these genes are listed in Table 2.11 and Table 2.12.)

gene	GenBank accession number	species
GAPDH	AF022183	ovine
GM-CSF	X53561	ovine
	X55991	
IL-3	Z18897	ovine
TLR3	AY124007	bovine
TLR4	AB056444	bovine
TLR9	AJ509825	bovine
CD1a	M27735	human
langerin*	NM_015717	human
	AJ302711	mouse
CCR7	AB116555	porcine
IL-12p40†	AF004024	ovine
	AF209435	
IL-18†	AJ401033	ovine
IL-10†	U11421	ovine
TNF-α†	X56756 &	ovine
	X55152	
IL-1β†	X56972	ovine

2.3.5.3 Reaction mixture

Amplification was carried out in a final volume of 50µl for the RT-PCR using 2µl of cDNA synthesised from 1µg of total RNA from the RT reaction. Briefly, the reaction mixture was prepared by combining the following reagents to a total volume of 50µl in thin-walled PCR tubes. Each reaction mixture consisted of 2µl template (cDNA or 10ng plasmid DNA); 1 × (Promega) PCR buffer (50mM KCl, 10mM Tris-HCl (pH 9.0), 1.5mM $MgCl_2$), 20pmol of each oligonucleotide primer (Sigma–Genosys); 200µM each dNTP (Biogene) and 2.5 U Taq (*Thermus aquaticus* strain YT1) DNA polymerase. The reaction conditions for each primer pair were optimised (Table 2.5)

Table 2.5 Primers used for conventional RT-PCR. (R: reverse primer, F: forward primer, ov: ovine, bov: bovine, hu: human; por: porcine, *: Langerin primers were designed from homologous regions of aligned human and murine cDNA sequences)

gene	primer sequence (5'→3')	product size	annealing temp (°C)	cycles
ovGAPDH	F: AAG GCA GAG AAC GGG AAG R: AGT GAT GGC GTG GAC AGT	366bp	55	25
ovGAPDH	F: GGT GAT GCT GGT GCT GAG TA R: TCA TAA GTC CCT CCA CGA TG	265bp	57	25
ovGM-CSF	F: GTC CTC AAG AGG ATG R: GTC AAG GAG CCC GTG	300bp	57	30
ovIL-3	F: CAA GAC AGA ATC CGC CCT GC R: AGG AGC CTT CTG GAC TCG GA	192bp	57	30
bovTLR3	F: ATA GGG ATT GGG TCT GGA A R: TTT CTG CTC CTT CTG ATG CT	139bp	58	40
bovTLR4	F: GTT TCA AGG GTT GCT GTT CT R: TGT TTC AGA GTG GAA TGC TG	151bp	58	40
bovTLR9	F: TGC TGT CCT ACA ACC ACA TT R: GCG GAA CCA ATC TTT CTC TA	239bp	55	40
huCD1a	F: TGC TGT TTT TGC TAC TTC CA R: TTC CTG AGA CCT TTC CAG AG	384bp	53	40
langerin*	F: GTC GTG TGG ACA ACA TCA G R: GGC ACT ATA CCA GGT CTT TG	400bp	53	40
porCCR7	F: ACA TCC TCT TCC TCC TGA CC R: GAA AGC CCA CCA CCA TCT	387bp	55	40

2.3.5.4 Amplification

PCR amplification was carried out in a Hybaid Sprint Thermocycler. The oligonucleotide primer pairs used for conventional RT-PCR are shown in Table 2.5. Optimisation of the cycle number and annealing temperature for each primer pair was carried out. All RT-PCR programs followed a similar thermal cycling profile, as described below:

An automatic "hot-start" was employed for PCR, to prevent mispriming and amplification of non-specific products. The DNA template was initially denatured at 94°C for 3 minutes prior to the addition of Taq polymerase. The reaction mixture was then cycled as follows:

(i) 1 cycle of denaturation at 94°C for 1 minute

(ii) 1 cycle of annealing at *°C (Table 2.5) for 1 minute

(iii) 1 cycle of extension at 72°C for 1 minute

(iv) *cycles (Table 2.5) of denaturation (1 minute), annealing (1 minute) and extension (1 minute) with 15-second increments per cycle

(v) 1 cycle of final extension at 72°C for 10 minutes.

2.3.5.5 Agarose gel electrophoresis

Preparation of agarose gels

The range of efficient separation of DNA in agarose gels of different concentrations is shown in Table 2.6. The appropriate amount of Biogene® agarose (Table 2.6) was dissolved in 1 × Tris acetate buffer (TAE, Appendix I) and heated in the microwave until the agarose was completely dissolved. 1μg/ml of Ethidium Bromide (Promega) was added to the gel solution to visualise the DNA. The molten gel was poured into the appropriate casting tray and allowed to set.

Table 2.6 Percentage of agarose for optimal resolution of DNA.

agarose (%)	efficient range of separation of linear DNA molecules
0.7	0.8–10 kb
0.9	0.5–7 kb
1.2	0.4–6 kb
1.5	0.2–3 kb

Running agarose gels

The cast gel was submerged in 1 × TAE. Samples were mixed with 6 × loading buffer (Promega) and loaded into the wells. For DNA fragments between 100bp-1kb, 100bp or 1kb (Promega) DNA ladders were used. For DNA fragments >1 kb, EcoR1/HindIII digested lambda DNA markers (Promega) were used. 1μg of markers were run on each gel. Electrophoresis was carried out at 70mA until sufficient separation of the DNA was achieved. The DNA was visualised and photographed using a UV Gel Documentation System. (Ultra Violet Products).

2.3.6 Quantitative real-time RT-PCR

The strategy employed for quantitative real-time RT-PCR and optimisation of this technique is discussed in Section 2.5.

Quantitative real-time RT-PCR was performed according to the instructions outlined in the LightCycler®-FastStart DNA Master SYBR Green I instruction manual (Roche). Capillaries were pre-chilled prior to loading with samples. Cycling was performed in 20µl reaction volumes containing 2µl template, 13.4µl nuclease-free water, 1µM of each of the (internal) oligonucleotide primers, 2µl of LightCycler®-FastStart Master SYBR Green I (containing Taq polymerase with reaction buffer, dNTP mix, SYBR Green dye and 1mM $MgCl_2$) and 2.4µl[5] of additional $MgCl_2$ (4mM final concentration of $MgCl_2$). The capillaries were then centrifuged for 30 seconds and loaded into the LightCycler®.

The cycling conditions are summarised in Table 2.7. Briefly, a hotstart was performed at 94°C for 10 minutes to activate Taq polymerase enzyme. Annealing temperatures for all primer pairs was 57°C and reactions were carried out for 30–40 cycles followed by melting curve analysis.

Table 2.7 Cycling conditions, optimised according to guidelines in the Roche handbook. All primers were designed with an annealing temperature of 57°C.

segment	target temp (°C)	hold time (sec)	slope (C°/sec)	cycles	acquisition mode
(denaturation)				1	
1	95	600	20		none
(amplification)				40	
1	95	5	20		none
2	57	10	7.999		none
3	72	30	12		single
(melting curve)				1	
1	95	5	20		none
2	62	15	20		none
3	95	0	0.1		continuous
(cooling)				1	
1	40	30	20		none

[5] $MgCl_2$ was titrated and 4mM was the optimum concentration for all primers tested.

2.3.7 DNA Extraction and cloning methods

2.3.7.1 Purification of DNA

DNA from PCR reactions, which was subsequently to be cloned, was purified by excising the relevant band from the gel and subjecting it to a commercially available purification kit (QIAquick Gel Extraction Kit, Qiagen®). The solutions and protocol were supplied with the kit.

Alternatively PCR products and restriction enzyme digests were directly purified using Qiagen® spin columns (Qiagen® PCR Purification kit) according to the manufacturer's instructions.

2.3.7.2 Cloning of PCR products

Cloning of PCR products was carried out using a commercially available kit, pGEM®-T Easy Vector Systems (Promega), which utilises the nontemplate-dependent activity of Taq polymerase which adds a single deoxyadenosine ('A') to the 3' ends of PCR products. The supplied, linearised vectors have a single 3' deoxythymidine ('T') residue, which allows the PCR inserts to ligate efficiently with the vector.

The pGEM®-T Easy vectors contain a multiple cloning region with the α-peptide coding region of the enzyme β-galactosidase fused to the *lacZ* gene. Insertional inactivation of the α-peptide allows recombinant clones to be directly identified by colour screening on IPTG-X-Gal plates.

2.3.7.3 Ligation reactions

25–50ng of vector pGEM®-T Easy was ligated to the insert in the range of 3:1 to 10:1 (insert: vector). For subcloning of cytokine-gene constructs, 70-100ng of vector pEGFP-N1 vector was ligated to the insert at 1:1, 1:3 and 3:1 molar ratios. Reactions were carried out in a 10µl reaction containing vector and insert, 5 µl 2 × rapid ligation buffer (Promega) and 3 U of T4 DNA ligase (Promega) and incubated at 4°C for 16 hours. Appropriate controls were included to assess ligase, transformation efficiency and religation of the vector.

2.3.7.4 Transformation of competent cells

2µl of the ligation reaction was added to 50µl of JM109 or DH5α (Promega) "High Efficiency" competent cells and incubated on ice for 20 minutes. The cells were heat-

shocked for 45 seconds at 42°C and then placed back on ice for a further 2 minutes. 950µl of SOC medium (Appendix I) was added to the cells and incubated at 37°C for 1.5 hours in a shaking incubator. pGEM®-T Easy transformed cells (100µl) were plated onto 1.5% agar in Luria Bertoni (LB) medium (Appendix I) containing ampicillin (50µg/ml), 200µM IPTG and 0.004% X-Gal in DMF. The plates were incubated at 37°C overnight and then placed at 4°C to allow colour development. Single white colonies were transferred into 10ml LB medium supplemented with (10µg/ml) ampicillin and shaken at 37°C for 16 hours. pEGFP-N1 transformed cells were spread onto plates containing kanamycin (50µg/ml), and incubated at 37°C overnight. Single colonies were transferred to 10ml LB medium supplemented with kanamycin (50µg/ml).

2.3.7.5 Preparation of plasmid DNA

Preparation of plasmid DNA was performed according to published methods (Birnboim and Doly, 1979; Ish-Horowicz and Burke, 1981). Briefly, 1.5ml overnight cultures were pelleted at 12,000 × g for 2 minutes and resuspended in 50mM glucose, 25mM Tris-Cl (pH 8.0), 10mM EDTA (pH 8.0). Cells were then lysed in 0.2M NaOH, 1% SDS for 5 minutes at 4°C. Precipitation of bacterial DNA was carried out by addition of 5M potassium acetate, incubation on ice for 10 minutes, followed by high-speed centrifugation for 3 minutes. The supernatant was then phenol/chloroform extracted, precipitated with isopropanol, washed in ethanol and resuspended in 50µl Tris-EDTA (TE) buffer (Appendix I). Ribonuclease (RNase) was then added to a final concentration of 40µg/ml to remove contaminating RNA (Sigma).

Plasmid DNA for sequencing was isolated using Qiagen® spin columns (mini kit) according to the manufacturer's instructions. In order to remove contaminating LPS, the Endofree Maxi kit (Qiagen®) was used to purify plasmid DNA used for *in vivo* experiments and *in vitro* transfection work.

2.3.7.6 Endonuclease restriction digest

DNA restrictions were carried out for 2–4 hours at 37°C using commercially (NEB) available restriction endonucleases. 3–10 U of enzyme were used to digest 2–4µg of DNA in a 20µl volume of the recommended buffer. Restriction endonuclease buffers were supplied at 10 × concentration. pGEM®-T Easy clones were screened for the presence of inserts by restriction digest with EcoR1. For enzymes with incompatible buffer requirements, sequential digests were carried out (cloning of pEGFP-N1 constructs). Following digestion,

inserts were analysed by running 10µl of the restriction digest on an agarose gel alongside uncut plasmid.

2.3.7.7 SAP treatment

Following digests of pEGFP-N1 vector DNA, the 5' end of the linearised plasmid was dephosphorylated to help prevent religation by addition of 1 U of shrimp alkaline phosphatase (SAP) (Roche) and the manufacturer's buffer for 15 minutes at 37°C. Inactivation of SAP was achieved by heat inactivation at 70°C for 20 minutes.

2.3.7.8 Blunt-ending

DNA fragments for blunt ended-cloning were prepared using the Klenow fragment of *E.coli* DNA Polymerase I (Roche) to "fill in" recessed 3' ends. Following restriction endonuclease digest, DNA fragments were incubated at 20°C for 20 minutes with 33µM of each dNTP (Biogene) and a further 1µl of 10 × BamH1 buffer (NEB) and 2U of Klenow in a total volume of 30µl.

Mungbean nuclease (Promega) was also used to generate blunt-ends with fragments containing 5' overhangs. Buffers containing 100-400 mM NaCl (inhibit Mungbean nuclease activity) were firstly removed using the High Pure PCR Purification kit (Roche). 10µg DNA (in Tris-Cl, pH 8.0), 60 U of Mungbean nuclease, 0.001% Triton X-100 in 1 × reaction buffer were then incubated in a total volume of 50µl for 37°C for 10 minutes. Mungbean nuclease was inactivated by adding 10µl of Tris-Cl (pH 8.0, Appendix I).

2.3.7.9 Sub-cloning of cytokine genes & preparation of gene gun cartridges

The pEGFP-N1 plasmid encoding a red shifted variant of GFP under the control of a cytomegalous virus (CMV) immediate early (IE) promoter was obtained from Clontech (Figure 2.8). The Multiple Cloning Site (MCS) is between the immediate early (IE) promoter of CMV and the EGFP coding sequences. The vector backbone contains an SV-40 early promoter, a neomycin resistance cassette and polyadenylation signals from the herpes simplex virus-1 thymidine kinase (HSV TK) gene.

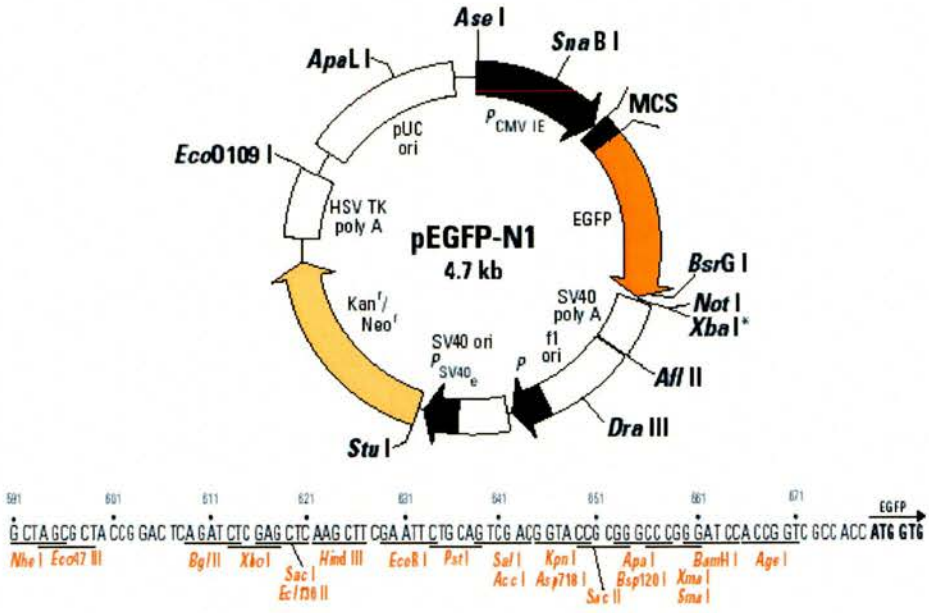

Figure 2.8 Restriction Map and Multiple Cloning Site (MCS) of the 4.7kb pEGFP-N1 plasmid (Clontech).

Cloning of GM-CSF into pEGFP-N1

GM-CSF was sub-cloned into the Sma1 site of PBS +/– phagemid vector (Bluescribe) by Dr Colin McInnes (Moredun Research Institute, Roslin, Midlothian). GM-CSF was excised from the Bluescribe vector as a 520bp HindIII-HindIII fragment and subsequently blunt-ended with Mungbean nuclease (Promega), followed by restriction enzyme digest with BamH1. pEGFP-N1 was linearised with Not1 and blunt-ended with Mungbean nuclease. BamH1 digest was then carried out in order to remove the GFP gene. GM-CSF[6] was sub-cloned into the BamH1 and blunt-ended Not1 site of pEGFP-N1. A control non-functional version of GM-CSF (NF-GM-CSF) was generated as follows. GM-CSF was excised from the Bluescribe vector as a 550bp BamH1-EcoR1 fragment (Figure 2.9) and cloned into the 3'-5' orientation of the vector by cloning into the EcoR1-BamH1 sites of pEGFP-N1.

[6] Sub-cloning of functional GM-CSF into pEGFP-N1 was carried out by Dr Anton Gossner (Department of Veterinary Pathology, University of Edinburgh).

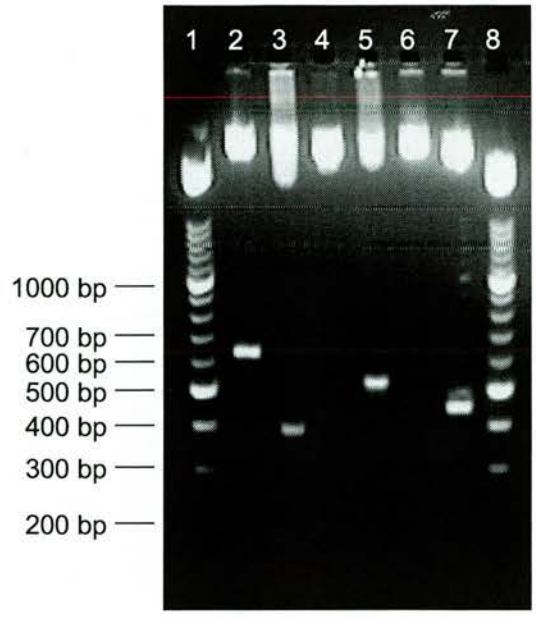

Figure 2.9 Analysis of plasmid constructs by restriction endonuclease digest. Each plasmid was incubated with restriction enzymes for 2–4 hours at 37°C. DNA was then subjected to gel electrophoresis and visualised by UV.

Lane 1 100bp ladder
Lane 2 BamH1 and Sac1 digest of pIL-3
Lane 3 EcoR1 and Nhe1 digests of pIL-3
Lane 4 EcoR1 and Nhe1 digests of NF-IL-3
Lane 5 BamH1 and EcoR1 digest of NF-GM-CSF
Lane 6 Nhe1 and Xmn1 digest of NF-GM-CSF
Lane 7 Nhe1 and Xmn1 digest of pGM-CSF
Lane 8 100bp ladder

Cloning of IL-3 into pEGFP-N1

IL-3 was sub-cloned into the Sma1 site of PBS +/– phagemid vector (Bluescribe) by Dr Colin McInnes. IL-3 was removed from the Bluescribe vector by sequential digest with BamH1 and Sac1 restriction enzymes and the 650bp fragment was cloned into the Sac1-BamH1 site of pEGFP-N1 (Figure 2.9). A non-functional version of IL-3 (NF-IL-3) was constructed as follows. IL-3 was excised from pEGFP-N1 by sequential digest with BamH1 and Sac1. Following restriction endonuclease digest, 3' recessed ends were filled in by Klenow enzyme, followed by Kpn1 digest. IL-3 was cloned into pEGFP-N1 following linearization of pEGFP-N1 with HindIII, treatment with Klenow enzyme and Kpn1 digest.

Removal of GFP gene from pEGFP-N1 constructs

The GFP gene was removed from the plasmids by restriction digest with BamH1 and Not1 followed by gel extraction of the remaining backbone plasmid DNA and treatment with Klenow enzyme to "fill-in" recessed ends.

Preparation of plasmid DNA coated gold beads

Plasmid DNA for all *in vivo* experiments was isolated from transformed *E.coli* using the EndoFree® Plasmid Mega kit (Qiagen®) in order to remove contaminating immunostimulatory endotoxin from plasmid preparations. The kit enables the purification of up to 2.5mg endotoxin-free ultrapure plasmid DNA. Endotoxin-free plasticware and glassware were always used after the removal of endotoxin. Plasmid DNA was analysed by UV spectrophotometry to assess the purity of plasmid DNA. Restriction enzyme digest was carried out to confirm the presence and orientation of cytokine genes and was subsequently sequenced by Mr. Ian Bennett.

DNA coated gold beads were prepared by firstly mixing 100µl 0.05M spermidine with 20mg 1.0µm gold beads (Biorad). 100µg of purified plasmid DNA was added to the mix and precipitated onto the gold beads by the drop-wise addition of 100µl 1M $CaCl_2$, whilst slowly vortexing the mixture. The beads were washed 5–6 times in 1ml 100% ethanol (centrifuging at 1800 × g for 15 seconds in-between washes) and then resuspended in 2.4ml ethanol containing 0.05mg/ml polyvinylpyrrolidone (PVP). The DNA-coated beads were then bound to the inner surface of gold-coat tubing as recommended by the manufacturer.

2.3.8 *In vitro* transfection

2.3.8.1 Electroporation

Cells were maintained as described in Section 2.1. Cells were "split" the day before transfection (1:2 SSk fibroblasts and 1:10 BHK cells) and were in log-phase of growth at the time of transfection. Tissue culture medium was removed and the cells were rinsed in sPBS and then harvested by adding 0.25ml of pre-warmed trypsin (in-house) to a T75 flask and cells were observed until they started to detach. Cells were washed once in DMEM by centrifugation at 300 × g for 5 minutes and resuspended at 2.5 × 10^6 cells/ml in DMEM. 800µl cell suspensions (2 × 10^6 cells) were then incubated with 10µg of each plasmid construct or mock transfected (no plasmid) for 2 minutes on ice. Cell suspensions were transferred into sterile electroporation cuvettes (Equibrio). Transfections were performed using an Easyjet electroporator using the following parameters: 280mV, 1050µF, and 99mΩ. Cell suspensions were immediately transferred into 10ml medium. 10ml of each cell suspension was then added to 2 wells of a 6-well plate and incubated for 48 hours at 37°C. The culture medium was replenished after overnight culture.

Following an incubation of 48 hours, supernatants were removed and concentrated using Amicon spin columns (Millipore) according to the manufacturer's instructions. Trypsin was

used to remove adherent cells. Cells were washed in sPBS, counted and RNA extraction was performed (Section 2.3.3.3).

2.3.8.2 Transfection of ovine fibroblasts by gene-gun

The efficacy of the plasmid-coated gold particles was evaluated by firing gold particles into SSk cells. A Helios (Biorad), helium powered gene gun was used to fire the gold particles into a 6-well plate containing near confluent SSk cells according to the manufacturer's protocol. Briefly, the medium was firstly removed and the cells were washed with sPBS. Each well received one of the plasmid-containing cartridges at 15psi. Fresh DMEM (10% FCS) was replaced into each of the wells and the cells were incubated at 37°C, 5% CO_2. After 48 hours cells were harvested for RNA extraction (2.3.3.3).

2.3.9 DNA sequencing of double-stranded DNA templates

Cloned DNA was sequenced using the LICOR 4000L automated sequencer (MWG Biotech), and the Sequitherm Excel™ II kit (Cambio). Primers were purchased from MWG Biotech (sequences shown below). Sequencing was kindly performed by Mr. Ian Bennet (Department of Veterinary Pathology, University of Edinburgh).

Sequencing primer	Sequence (5'–3')
pGEM®-T Easy	M13 primer
pEGFP-C1[7]	ATGGGCGTGGATAGCGGTTTGACTC

2.4 Gene-gun vaccination of sheep

Prior to DNA vaccination, the skin on the flanks of sheep was prepared by firstly clipping the wool, followed by cleaning the skin with Hibitane scrub and warm water and shaving any remaining wool. The skin was then washed in absolute ethanol and vaccine sites were drawn on the skin with a marker pen. On each day of vaccination, skin was cleaned again with Hibitane scrub and closely shaved. For biopsy experiments, three replicates (0.5–1.0μg plasmid DNA/shot) of each cytokine construct or non-fuctional control plasmid were administered by gene-gun at a pressure of 500psi (optimal pressure for delivery of gold particles to the epidermal-dermal junction). 5mm × 6mm biopsies were removed by punch-

[7] Also used to sequence inserts sub-cloned into pEGFP-N1 (position 390 for both plasmids)

biopsy immediately at post-mortem (Stiefler). Table 2.8 lists the details of each biopsy experiment carried out.

DNA vaccination of cannulated sheep was carried out essentially as described with the exception that 5 replicates of plasmid DNA were administered to the skin in the drainage area of the cannula. Lymph was collected every 24 hours and lymph volumes were carefully recorded. To prevent *de novo* cytokine expression, actinomycin-D was added to bottles prior to lymph collection (Section 2.2.4.1).

Table 2.8 *In vivo* experiments carried out where various plasmid constructs were administered to the flank of sheep over a time-course and biopsies removed at post-mortem. Note that in the preliminary biopsy experiment (A), pEGFP-N1 served as a control and that the IL-3 construct still contained the GFP gene. A–E refers to the order that the experiments were carried out.

biopsy experiment	plasmid constructs	time-points (hours p/v)	sheep ID
A	pGM-CSF pIL-3 + GFP pEGFP-N1	24, 48 (sheep 2 only), 72 (sheep 1 only), 96, 120, 144, 166	1, 2
B	pGM-CSF pIL-3 pNF-GM-CSF pNF-IL-3	1, 2, 4, 6, 24	3
E	pGM-CSF pIL-3 pNF-GM-CSF pNF-IL-3	1, 2, 4, 6, 24	4
C	pGM-CSF pIL-3 pNF-GM-CSF pNF-IL-3	16, 24, 48, 72, 96	5
D	pGM-CSF pIL-3 pNF-GM-CSF pNF-IL-3	24, 48, 72, 96	6

2.5 Development of a quantitative RT-PCR method

2.5.1 Introduction to quantitative RT-PCR

The analysis of cytokine profiles is crucial in the characterisation of immune responses and in the identification of functional properties of immune cell subpopulations. Tissue biopsy samples are often too small to allow the detection of cytokine protein and quantitative systems for the detection of ruminant cytokine proteins are still being developed. The detection of mRNA by RT-PCR analysis is a useful and sensitive method often employed to investigate the cytokine milieu in inflammatory lesions. Traditional RT-PCR methods rely on end-point analysis and are at best semi-quantitative. Quantitative RT-PCR is a novel method that enables simple and rapid measurement of fluorescent PCR product accumulation during the log-linear reaction phase. The fluorescence generated is proportional to the amount of product present. The cycle number at which the level of fluorescence rises above a background threshold value is inversely proportional to the log of the initial number of template copies (Higuchi et al., 1993).

The use of hybridisation probes in quantitative RT-PCR is now well established. Probes require both synthesis and optimisation of a specific probe for each gene of interest and this can be expensive. An alternative method to monitor DNA amplification employs the high affinity double-stranded DNA (dsDNA) binding dye SYBR Green I. SYBR Green has negligible fluorescence in the absence of dsDNA but has large fluorescence enhancement upon binding to dsDNA. The major advantage of this technique is that SYBR Green can be used with any primer pair, provided that no products other than the specific one of interest are amplified.

Aim

To develop and optimise a method for quantitative RT-PCR for a universally expressed housekeeping gene, GAPDH and several cytokine genes (GM-CSF, IL-3, IL-1β, IL-10, IL-12, IL-18 and TNF-α) using the DNA-binding fluorescent dye SYBR green.

2.5.2 Strategy

2.5.2.1 Overview of quantitative real-time RT-PCR strategy

Briefly, two sets of primers were designed from available ovine and bovine (IL-18) cytokine cDNA sequences in order to perform nested PCR. RNA was extracted from *in vitro* stimulated PBMC (Section 2.1.3) and reverse transcribed. Conventional RT-PCR was then carried out using the external primers to generate primary (1°) PCR products for each of the genes of interest. 1° PCR products were purified and serial dilutions were prepared. Internal primers and SYBR green were then used to amplify serial dilutions of 1° PCR product to create a standard curve on the LightCycler®. Once standard curves had been generated, quantitative RT-PCR was carried out on cDNA samples to amplify target species. In addition, one or more of the diluted 1° PCR products (standards) were included and acted as reference point(s) on the imported standard curve.

2.5.2.2 Generation of standards by conventional RT-PCR

A source of material was required to provide standards of each cytokine in order to generate standard curves. IL-12p40 and IL-18 could not be detected in freshly isolated PBMC (results not shown). PBMC were therefore stimulated using either LPS from *S. typhimurium* or Con A (Section 2.1.3). LPS induces IL-18 mRNA expression after binding CD14 (and TLR4) on human blood monocytes *in vitro* (Manigold et al., 2000). Con A is a lectin and a well known T cell mitogen and stimulation of PBMC with Con A results in detectable expression of several cytokines, including IL-12p40 and IL-12p35 (De Rose et al., 2000). After PBMC stimulation, RNA was extracted and reverse transcribed. External primers (Section 2.5.5) were tested on cDNA obtained from either LPS or Con A-stimulated PBMC. Both IL-12p40 and IL-18 primers generated gene fragments after either form of stimulation (results not shown). GM-CSF, IL-3, IL-10, TNF-α and IL-1β were amplified from cDNA derived from Con A stimulated PBMC. 20µl of each 1° PCR product was then fractionated by agarose gel electrophoresis and confirmed to be the correct size. The remaining 30µl was then purified by PCR-clean-up reaction (Qiagen® PCR Purification kit). Serial 1:10 dilutions were prepared in nuclease-free water and aliquots were stored at –20°C.

Prior to quantitative PCR, internal primers were tested for specificity by conventional nested PCR. 2µl of each of the 1:100 and 1:1000 dilutions of each 1° PCR product were amplified for 30 cycles at 37°C. Following secondary amplification, 20µl of each sample was fractionated by agarose gel electrophoresis. The remaining 30µl of PCR reaction was

purified (Qiagen® spin column) and cloned into pGEM®-T Easy (Section 2.3.7.2) and sequenced (Appendix III).

2.5.2.3 Generation of a standard curve with 1° PCR products

Serial 1:10 dilutions of 1° PCR products (diluted in nuclease-free water) were used to construct standard curves on the LightCycler®. Quantitative RT-PCR was performed (Section 2.3.6) using specific internal primers (Table 2.11). 2µl of each of the standards (1° PCR products; 10^{-3}–10^{-10}) were run in duplicate on the LightCycler® alongside a negative control (nuclease-free water). The cycling conditions are summarised in Table 2.7. An example of an amplification plot, a standard curve and a melting curve is shown in Figure 2.10. Standard curves were automatically constructed by the LightCycler® software (second derivative method, Section 2.5.3), where the error can be reduced by manual deletion of standards. Standard curves were generated for each of the cytokine genes and also for the housekeeping gene GAPDH.

Melting curve analysis was carried out for every LightCycler® experiment carried out in order to assess the extent of primer-dimerisation and that specific product had accumulated in the target samples. This is essential, since SYBR Green binds non-specifically to all dsDNA species. Melting curve analysis was performed after the amplification stage of the program and involved raising the temperature successively through 1°C steps and comparing the melting temperature of specific product (diluted standards) with the melting temperature of each sample and a no-template control. Primer-dimers are easily distinguished from specific product since they melt at a lower temperature due to their small size (approximately 25bp). Specific products show one sharp and fully overlapping melting peak indicating the specificity of primers designed from partial sequences (Figure 2.10c). In addition, products were analysed by gel electrophoresis to confirm that the amplicon of the correct size was obtained (results not shown).

2.5.2.4 Quantification of cytokine transcripts by real-time RT-PCR

RNA was extracted from skin biopsies and purified DC populations and reverse transcribed (sections 2.3.3 and 2.3.4). Conventional GAPDH RT-PCR was first performed to confirm that amplifiable material was present and that genomic DNA had been degraded. cDNA samples were diluted 1:100 in nuclease-free water and 2µl of diluted cDNA was subjected to quantification, alongside at least one standard (diluted 1° PCR product) for the gene of interest. For quantification, a standard curve was then imported at the end of a sample run.

Standard(s) included on that particular run served as reference points on the standard curve and the LightCycler® software calculated crossover threshold (Ct) values for each of the cDNA samples. Quantitative analysis of cytokine cDNA was performed in comparison to the universally expressed housekeeping gene GAPDH and allowed for corrections of variations in different numbers of cells in the starting material; differences in the efficiencies of RNA extraction, and in the reverse transcription procedure.

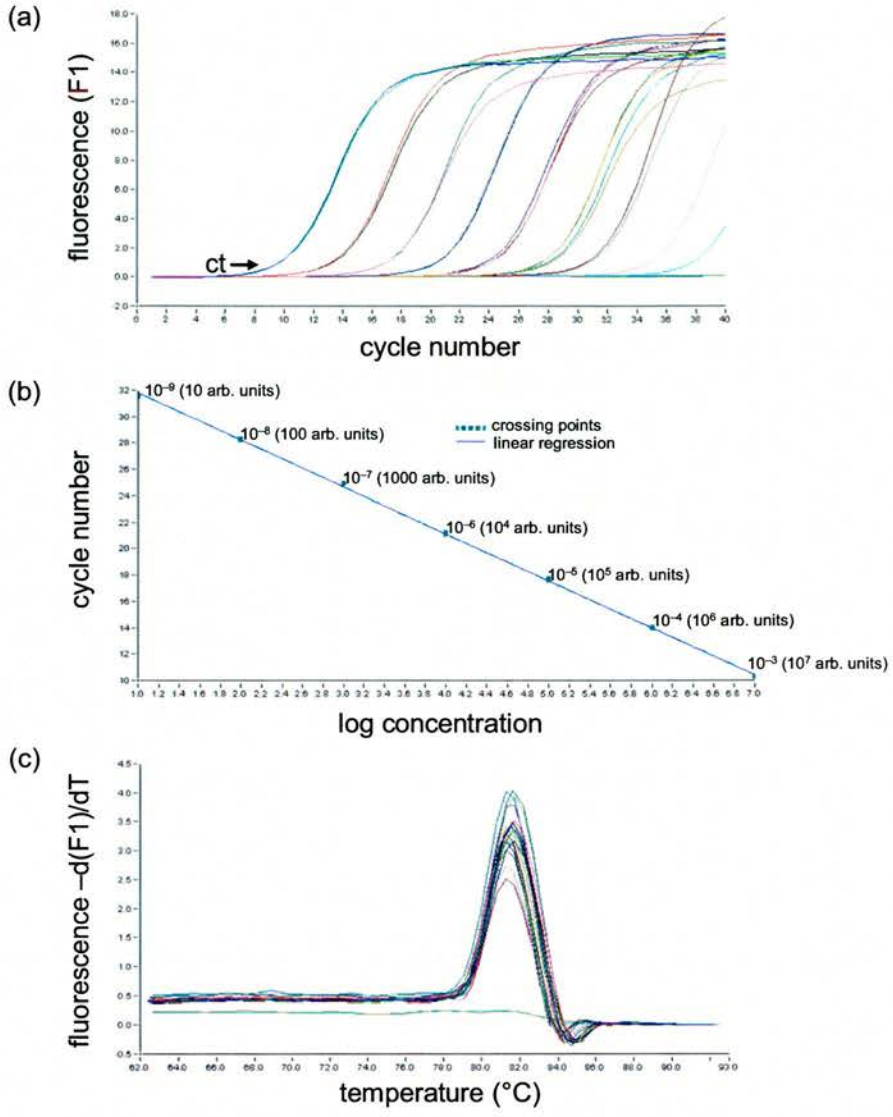

Figure 2.10 Generation of a standard curve using 1° PCR products. (a) PCR amplification of IL-18 1° PCR standards over eight orders of magnitude (diluted 10^{-3}–10^{-10}) as a graph of cycle number versus fluorescence intensity (cDNA samples (diluted 1:10 and 1:100) derived from stimulated PBMC were also included); (b) standard curve as a graph of *log concentration versus cycle number obtained by second derivative maximum method. Note that *log concentration refers to the log of arbitrary (arb.) units assigned to each standard in the dilution series; (c) melting curve analysis of products where –d (F1)/dT refers to the rate of change of fluorescence. Note that the amplicons generated from the dilution series of 1° PCR products melt at the same temperature (approximately 81°C.), whereas no product or primer-dimer is evident in the no-template control (flat green line).

2.5.3 Data analysis

Data analysis was performed by the LightCyler® software (version 3.5). Two methods of quantification are available.

(i) fit points
(ii) second derivative maximum

The fit-points method requires manual adjustment of the noise band or crossing line to exclude non-informative background fluorescence data from quantitative analysis, whereas the second derivative maximum method is automated. The second derivative maximum method was chosen for all data analysis as this method gives rise to a lower coefficient of variability (Cv) value and is thus more reliable for gene quantification. Furthermore, unlike the fit points method, this method is not subjected to input variations of bias. The standard curve was generated by the LightCycler® software based on the values of crossing points (Ct values) and the log value of the standard concentration. The relative values for target abundance in each experimental sample were then extrapolated from the standard curve.

Standard curves were imported into all amplification programs where only one or two standards could be included due to the large number of samples to be analysed (a maximum of 32 capillaries can be analysed on the LightCyler®). When possible, several standards were included with cDNA samples so that standard curves could be generated for that particular run. The experimental setup of this technique is summarised in Figure 2.11.

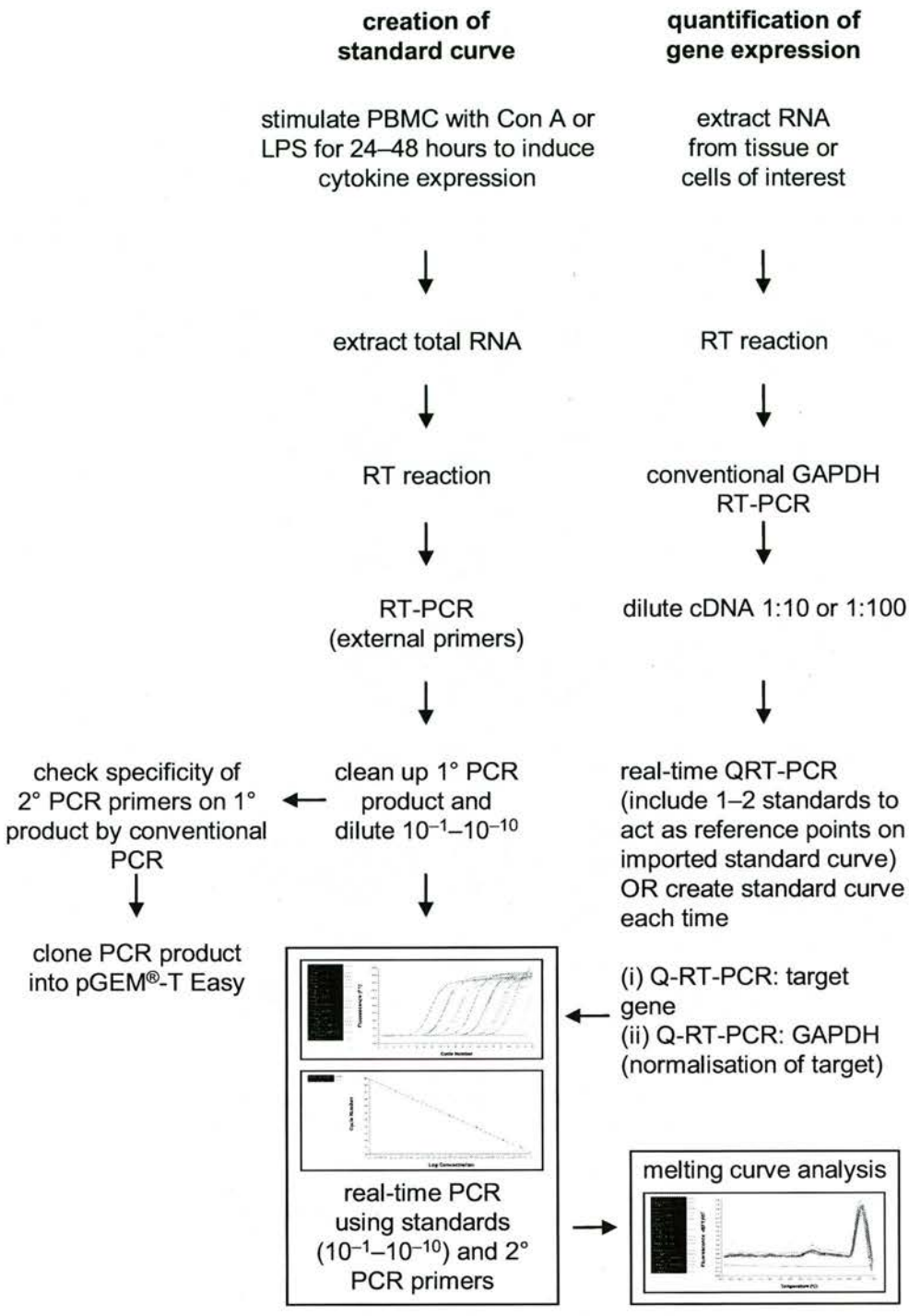

Figure 2.11 Overview of quantitative RT-PCR method using diluted 1° PCR products generated from *in vitro* stimulated PBMC as standards.

2.5.4 Normalisation of data

Variations in the starting material were normalised by calculating a normalisation coefficient. The concentration of GAPDH (arbitrary units) was calculated for each cDNA sample by importing the GAPDH standard curve after each run was completed. The mean value (excluding the Ct values of the included standard(s)), was then calculated from all cDNA samples analysed on that run. To obtain a normalisation coefficient, the following equation was applied:

normalisation coefficient = GAPDH Ct value of sample / mean Ct

Gene expression of the target gene (after importation of the standard curve for that gene) was then normalised against GAPDH (see example in Table 2.9) by applying the following equation:

expression of target gene = Ct value of sample / normalisation coefficient

Table 2.9 Normalisation of gene expression with the housekeeping gene GAPDH

sample	GAPDH concentration	normalisation coefficient	GM-CSF concentration	normalised GM-CSF concentration
1	2	0.53	4	7.6
2	4	1.1	8	7.3
3	8	2.1	10	4.8
4	4	1.05	2	1.9
5	1	0.26	12	46.2

2.5.5 Primer Design

A database search for ovine mRNA sequences was performed (Table 2.4). PCR primers were designed by both Oligo 6 (Cambio) and Netprimer3. The parameters used to design primers for use on the LightCycler® are summarised in Table 2.10. Stringent parameters were used for primer design since SYBR green binds to all double stranded species. Specificity of primer sequences was confirmed by the Fasta3-Nucleic acid-EMBL database program[8]. Primers were also analysed for hairpin structures, palindromes and primer-dimerisation with

[8] http://www.ebi.ac.uk/fasta33/

the following programs (i) Premier Biosoft and (ii) Primer-finder software with 10T Oligo Analyser[9].

Table 2.10 Parameters chosen for the design of internal primers for use in quantitative RT-PCR (min, minimum; max, maximum; opt, optimum).

parameter	design
GC content	min: 40%, opt: 50%, max: 60%
primer Tm	min: 55°C, opt: 57°C, max: 60°C
primer size	min: 18, opt: 20, max: 22
max self complementarity	3.00
min 3' self complementarity	2.00
amplicon size	min: 250 opt: 300 max: 400

All (internal) primers intended for use in quantitative RT-PCR were designed with an annealing temperature of 57°C. Roche recommend that PCR products generated on the LightCycler® do not exceed more than 900bp and are not smaller than 100bp (Roche real-time PCR course, 2002); thus amplicon sizes were designed to be approximately 190–300bp. Internal primer sequences and amplicon size are listed in Table 2.11. The parameters for the design of external primers were generally not as stringent as the parameters used in the design of internal primers, since they were only intended to generate material (1° PCR product) to act as reference standards on the LightCycler® (Table 2.12).

[9] http://eatworms.swmed.edu/~tim/primerfinder/

Table 2.11 Internal Primers used for quantitative real-time RT-PCR. All internal primers were designed with an annealing temperature of 57°C. 40 rounds of amplification were carried out for most LightCycler® assays. 25–30 cycles were first employed to determine the specificity of the primers by conventional PCR using 1° PCR products.

gene	primer sequence 5' → 3'	product size
GAPDH	F: GGT GAT GCT GGT GCT GAG TA	265bp
	R: TCA TAA GTC CCT CCA CGA TG	
GM-CSF	F: GAT GGA TGA AAC AGT AGA AGT CG	261bp
	R: CAG CAG TCA AAG GGA ATG AT	
IL-3*	F: CAA GAC AGA ATC CGC CCT GC	192bp
	R: AGG AGC CTT CTG GAC TCG GA	
IL-12p40	F: TCA GAC CAG AGC AGT GAG GT	243bp
	R: GCA GGT GAA GTG TCC AGA AT	
IL-18	F: GAG CAC AGG CAT AAA GAT GG	241bp
	R: TGA ACA GTC AGA ATC AGG CAT A	
IL-10	F: CTG TTG ACC CAG TCT CTG CT	250bp
	R: ACC GCC TTG CTC TTG TTT	
TNF-α	F: GAA TAC CTG GAC TAT GCC GA	238bp
	R: CCT CAC TTC CCT ACA TCC CT	
IL-1β	F: CCT TGG GTA TCA GGG ACA A	317bp
	R: TGC GTA TGG CTT TCT TTA GG	

* Note that another set of primers was designed for ovine IL-3 (shown below) and successfully amplified specific IL-3 product where cDNA generated from stimulated PBMC was used. Problems were however encountered with this set of primers where cDNA samples generated from pIL-3 vaccinated biopsies were used, since the part of the sequence where the reverse primer binds is not present in the pIL-3 construct.

F: TGA AGT CTG AAG CCC AGT TC

R: ATT CCC AAG TCC CCA TCT TA

Table 2.12 External primers used for conventional RT-PCR. Primers were used for the first-round of amplification of ovine GAPDH, GM-CSF, IL-3, IL-10, IL-12, IL-18, TNF-α and IL-1β to generate standards for use on the LightCycler®. *IL-3 external primers were also used as internal primers due to problems encountered with the original primers.

gene	primer sequence 5' → 3'	product size	annealing temp (°C)	cycles
GAPDH	F: AAG GCA GAG AAC GGG AAG R: AGT GAT GGC GTG GAC AGT	366bp	55	25
GM-CSF	F: GCT TCT CCT GGG CAC TGT R: GCC TGC TTC ACT TCT GGA C	425bp	55	30
IL-3*	F: CAA GAC AGA ATC CGC CCT GC R: AGG AGC CTT CTG GAC TCG GA	192bp	57	30
IL-12p40	F: CTG GTT TTC CCT GGT TTT G R: CTG CTG CTT TTG ACA CTG AA	452bp	54	40
IL-18	F: TCA GAT CAC GTT TCC TCT CC R: GAT GGT TAC AGC CAG ACC TC	348bp	55	40
IL-10	F: TAC CCA CTT CCC AGC CAG R: CGT TGT CAT GTA GGA TTC TAT GTA G	432bp	58	30
TNF-α	F: CAC TGA CGG GCT TTA CCT C R: TCC TTG GTG ATG GTT GGT	548bp	58	40
IL-1β	F: CAA AAA TCC CTG GTG CTG R: CTG TGT TCT TCC CTT CCC TT	518bp	55	30

2.6 Optimisation of method for quantification of GM-CSF and IL-3 transcripts after DNA vaccination

2.6.1 Introduction

Quantitative real-time RT-PCR was required in order to quantify the kinetics of expression of GM-CSF and IL-3 mRNA in skin after DNA vaccination with plasmid constructs containing these cytokines. Each construct was administered by gene-gun vaccination to the skin on the flank of sheep. Each skin sample was removed at post-mortem using a sterile biopsy punch and bisected. RNA was extracted from one half of each biopsy and reverse transcribed.

2.6.2 Standard DNase treatment incompletely removes plasmid DNA

cDNA samples obtained from pGM-CSF vaccinated skin were initially analysed by quantitative real-time RT-PCR alongside control (–RT) samples. It was evident that plasmid DNA was not completely degraded by DNase digestion, since specific product was detected in the control –RT samples by melting curve analysis (Figure 2.12). Quantitative PCR is a highly sensitive method and can detect even low levels of undegraded plasmid DNA and thus it was necessary that further treatment was carried out on all RNA samples in order to accurately assess the kinetics of GM-CSF and IL-3 mRNA expression in skin. Initial unsuccessful attempts to degrade contaminating plasmid DNA involved extended incubation with DNase and doubling the volume of DNase added to the spin column membranes; plasmid DNA was however still present following such treatment (results not shown).

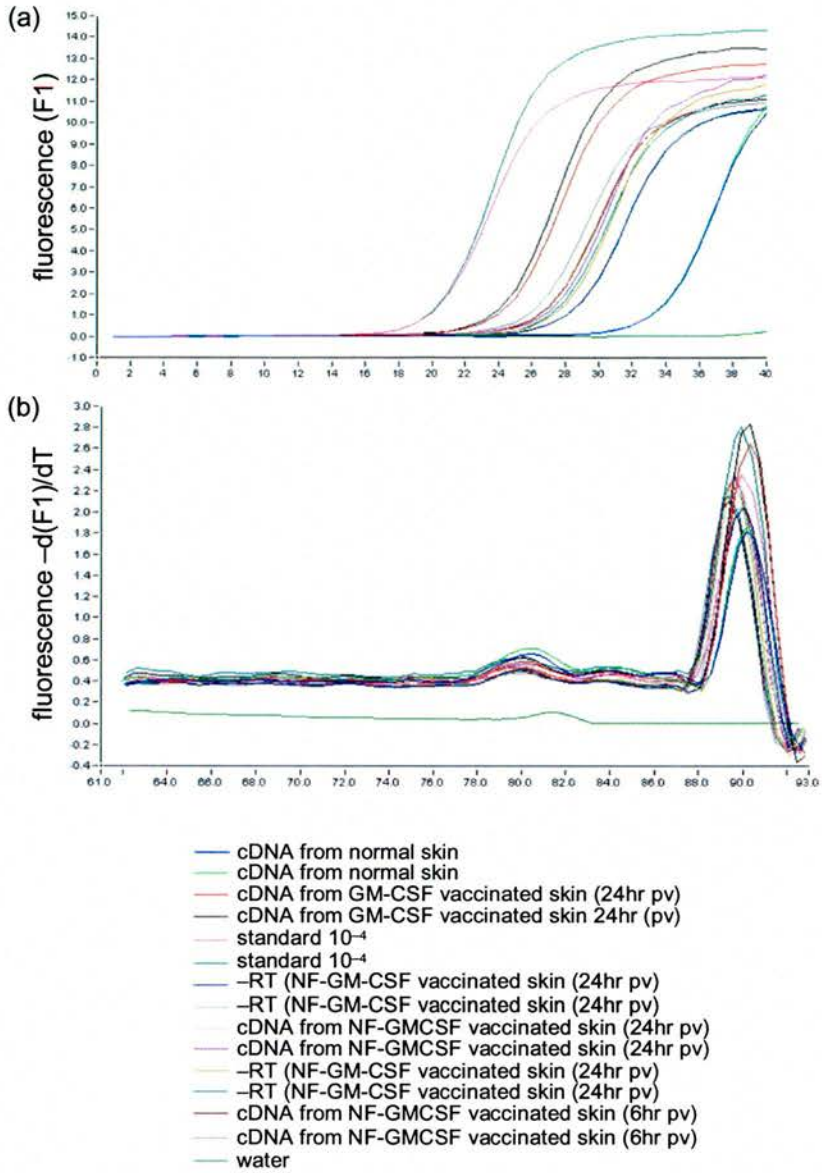

Figure 2.12 Plasmid DNA is incompletely removed with conventional DNase treatment. RNA was extracted from biopsies vaccinated with pGM-CSF or NF-GM-CSF and reverse transcribed. (a) cDNA samples were analysed by quantitative RT-PCR. Control (–RT) samples containing 1µg RNA were included in order to assess the presence of undegraded plasmid DNA; (b) specific product was detected in –RT samples which had been confirmed by GAPDH RT-PCR not to contain genomic DNA. Plasmid DNA was thus present in samples tested. Specific product was observed in cDNA samples obtained from normal skin (endogenous GM-CSF expression), whereas no transcripts were present in the no-template control.

2.6.3 Removal of plasmid DNA in RNA samples by restriction enzyme and DNase treatment

2.6.3.1 Introduction

Since DNase incubation on the spin column membranes was unsuccessful in eliminating plasmid DNA, alternative methods were required. It is possible that DNase was not gaining sufficient access to plasmid DNA on the spin column membrane and treatment of RNA samples in solution with DNase is necessary for complete degradation of plasmid DNA. Additionally, a restriction enzyme which cuts the GM-CSF (or IL-3) insert would theoretically prevent PCR amplification of these fragments and such linearisation of plasmid DNA may further aid removal of plasmid by DNase. Removal of plasmid DNA was therefore attempted with DNase alone and also in combination with a restriction enzyme.

The restriction enzymes Pst-1 and Hinf-1 were chosen from pGM-CSF and pIL-3 sequences; Pst-1 cuts the GM-CSF insert 3 times whereas Hinf-1 cuts the IL-3 insert 5 times. Prior to treatment of RNA containing pGM-CSF or pIL-3, it was necessary to assess the buffer requirements of both restriction enzymes and DNase, since all enzymes are supplied with their own buffers and may have stringent buffer requirements. Reaction mixes containing 2µg pGM-CSF or pIL-3 were prepared and incubated for 1 hour at 37°C. Pst-1 and Hinf-1 were active in the DNase supplied buffer and DNase was active in either of the buffers supplied with the restriction enzymes (Figure 2.13). Undigested plasmid is not shown on this gel image, however in previous experiments undigested plasmid was verified to contain only plasmid and no other DNA fragments. In the reactions containing pGM-CSF, a fragment of <250bp is evident (expected size is 175bp), the other smaller fragments (expected sizes of 24bp and 32bp) cannot be observed. In the reactions containing pIL-3, at least 9 DNA fragments are evident. Hinf-1 cuts the pEGFP-N1 backbone 13 times and some of these fragments can be observed. For example, fragments corresponding to 1000bp (expected size 1010bp) and 800bp (expected sizes 804 and 782bp) can clearly be observed, whereas the smaller fragments (~130bp and less) could be generated from either the backbone or the IL-3 insert. From this experiment, it appeared that plasmid DNA could indeed be degraded with DNase in combination with either enzyme and that DNase was not affected by the addition of BSA (required for optimal Pst-1 activity).

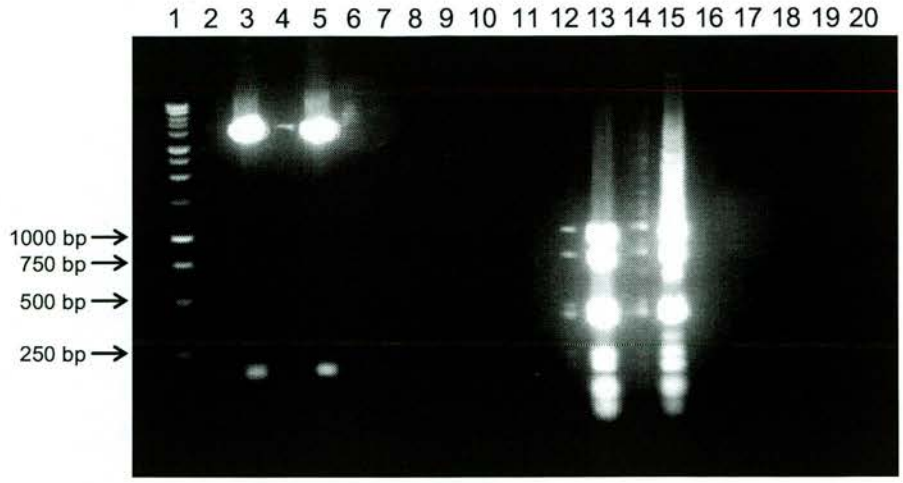

Figure 2.13 Compatibility of buffer requirements for the enzymes Pst-1, Hinf-1 and DNase. Reaction mixes were prepared containing either plasmid and incubated for 1 hour at 37°C. Restriction enzymes are sufficiently active in either of the supplied NEB buffers or the DNase buffer (RQ1, Promega). DNase completely degrades pGM-CSF and pIL-3 when incubated in the supplied RQ1 buffer and also in both NEB buffers, with or without BSA supplementation. Undigested plasmids are not shown on this gel image.

Lane 1, 1kb ladder;
(to test for degradation of pGM-CSF)
Lane 3, Pst-1 in supplied buffer (NEB) & BSA supplementation
Lane 5, Pst-1 in DNase buffer (RQ1)
Lane 7, DNase in Pst-1 supplied buffer (NEB)
Lane 9, DNase in RQ1 buffer
Lane 10, DNase in RQ1 buffer + BSA supplementation
Lane 11, DNase in RQ1 buffer + Pst-1 + BSA
(to test for degradation of pIL-3)
Lane 13, Hinf-1 in supplied buffer (NEB)
Lane 15, Hinf-1 in DNase buffer (RQ1)
Lane 17, DNase in Hinf-1 buffer (NEB)
Lane 19, DNase in RQ1 buffer
Lane 20, DNase in RQ1 buffer + Hinf-1

2.6.3.2 pGM-CSF spiking experiment

To avoid wasting precious RNA samples obtained from biopsy experiments, a spiking experiment was designed in order to identify the optimum way of eliminating plasmid DNA (Figure 2.14). Briefly, following homogenisation of a (non-vaccinated) skin sample, 1μg of plasmid DNA (pGM-CSF) was added to the homogenate. 1μg of plasmid DNA was chosen as this is approximately equivalent to the amount of DNA administered with one shot using the Helios gene-gun (range 0.5–2.0μg DNA).

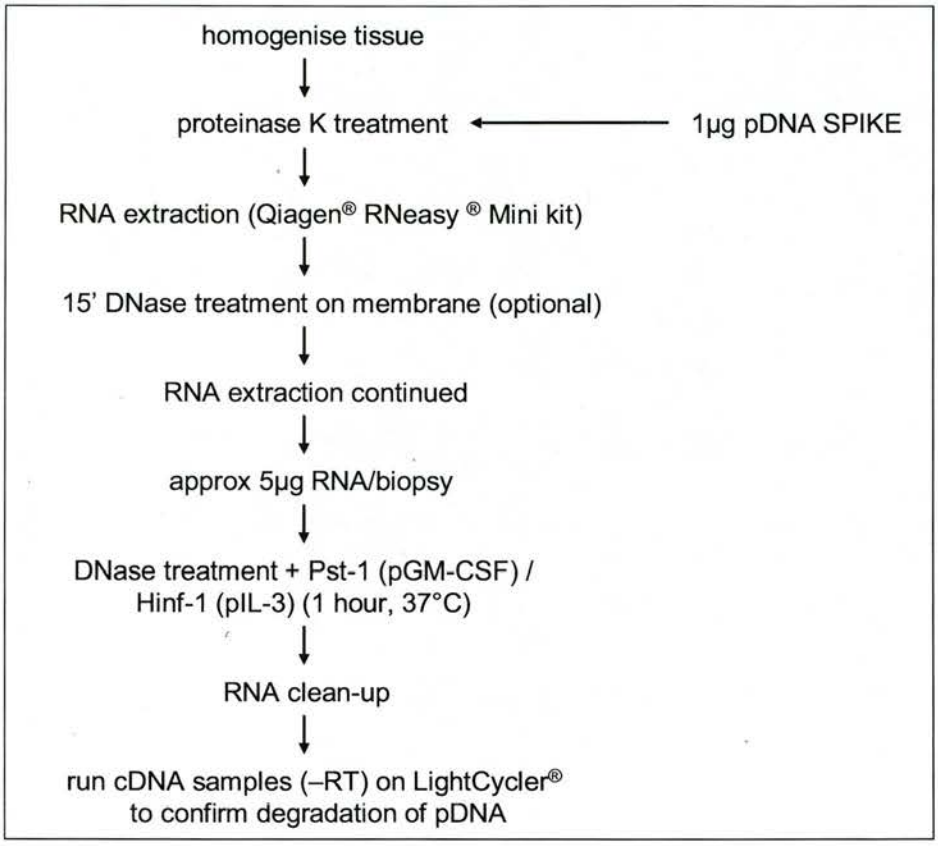

Figure 2.14 Schematic representation of the plasmid spiking experiment. This was carried out to investigate what methods were required to remove residual plasmid DNA remaining from the initial DNA vaccination procedure.

Spiked RNA samples were then treated with DNase alone and with DNase in combination with Pst-1 for 1 hour at 37°C (Section 2.3.3.2). Following treatment, RNA samples were purified and 1μg of each sample was then reverse transcribed or control (–RT) reactions were prepared (to ascertain the extent of plasmid DNA degradation). cDNA and control (–RT) samples were then analysed by quantitative RT-PCR. Although DNase in solution removes the majority of plasmid DNA, DNase in combination with Pst-1 restriction enzyme

was the most effective treatment and all spiked plasmid DNA containing the GM-CSF insert was removed in this manner (Figure 2.15).

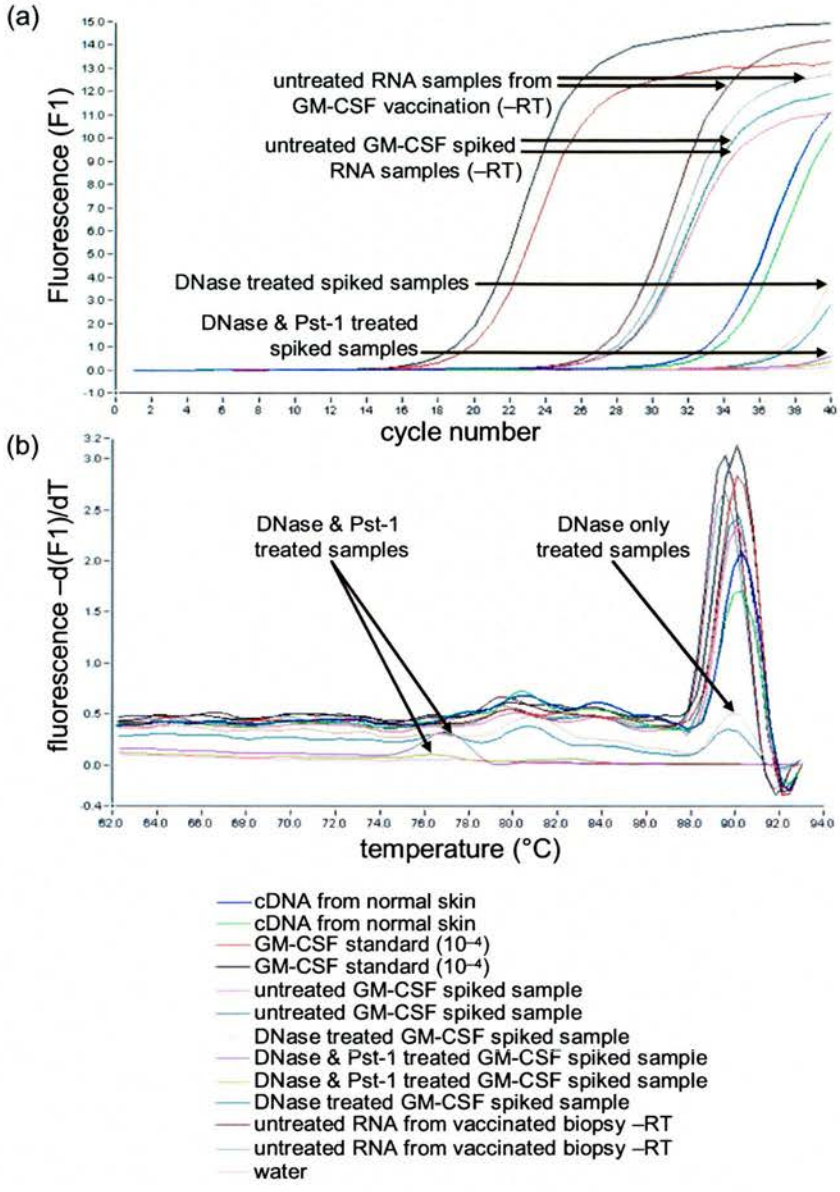

Figure 2.15 Pst-1 in combination with DNase removes pGM-CSF in spiked RNA samples. (a) Amplification of untreated RNA (–RT) samples after gene-gun vaccination with pGM-CSF and in normal skin homogenates spiked with pGM-CSF results in accumulation of product by approximately 27 cycles, whereas substantially less product is present in samples treated with DNase (~35 cycles) or DNase in combination with Pst-1 (~39 cycles). (b) Although DNase treatment in solution substantially reduces plasmid DNA, trace copies of plasmid are still present as illustrated in the melting curve analysis, where specific product melts at the same temperature as specific product (GM-CSF standards and spiked samples), whereas no specific product can be observed in the DNase/Pst-1 treated samples.

A further experiment was carried out to assess if DNase on the membrane was actually required. RNA was extracted from spiked skin homogenates, which were either treated with DNase on the spin column membranes for 15 minutes, or processed without this step. DNase treatment on the membrane followed by further removal of plasmid by DNase and restriction enzyme treatment in solution appeared to be the most effective method of ensuring complete removal of plasmid DNA (Figure 2.16).

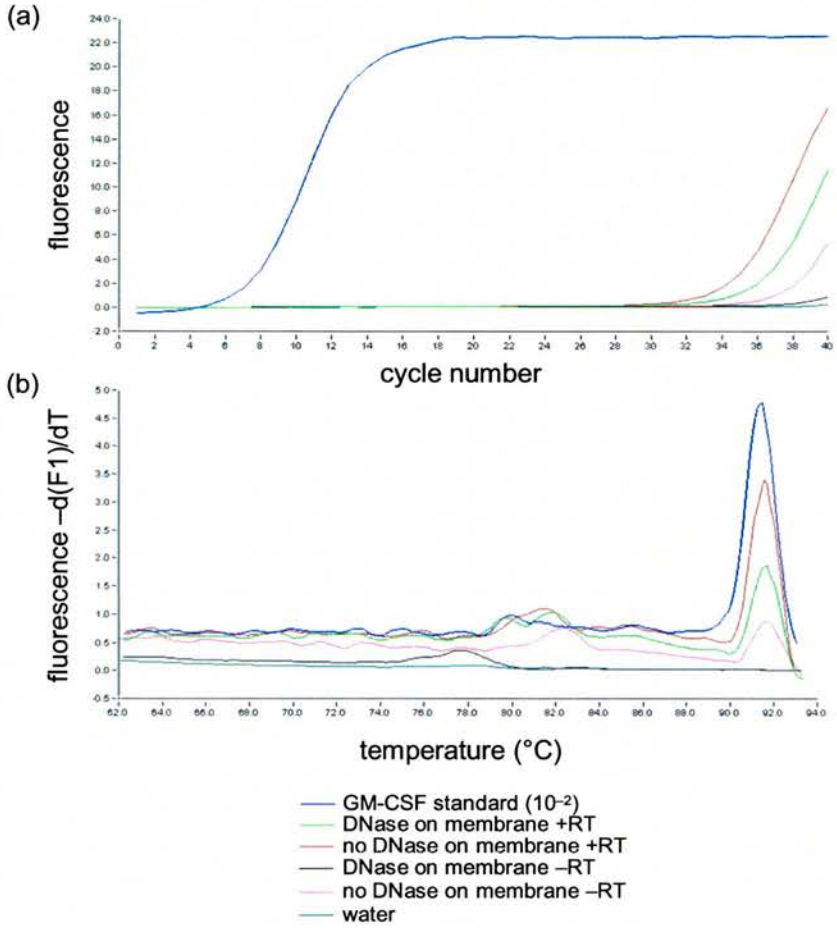

Figure 2.16 DNase treatment on membranes followed by DNase and Pst-1 treatment in solution is required for complete degradation of plasmid DNA. Homogenates from normal skin were spiked with pGM-CSF and RNA was extracted. Spiked samples were either subjected to on membrane DNase treatment, or this step was omitted from the procedure. (a) Amplification of pGM-CSF in samples treated with and without the additional DNase treatment; (b) melting curve analysis shows that specific product is still observed in the sample where the DNase step was omitted. No Specific product is observed in the sample treated with both DNase on the membrane followed by Pst-1 and DNase treatment in solution (–RT). GM-CSF transcripts are evident in the +RT sample and are due to endogenous expression of GM-CSF in skin (normal skin homogenate was spiked with pGM-CSF).

2.6.3.3 Overview of the procedure for the removal of plasmid DNA from pGM-CSF vaccinated biopsy samples

RNA was extracted from biopsy samples using the Qiagen® spin columns which included the on-membrane DNase step. Plasmid DNA was further removed from each RNA sample by incubation in solution with DNase and Pst-1 enzymes for 1–1.5 hours at 37°C (as multiple 10µl total volumes/sample). RNA was then purified and reverse transcribed. Conventional GAPDH RT-PCR was performed in order to assess that there was amplifiable material after such extensive treatment of the RNA and that all genomic DNA had been degraded sufficiently (an example is shown in Figure 2.17). –RT samples (diluted 1:10 in nuclease-free water) were then analysed on the LightCycler® to assess that plasmid DNA had been completely removed. For instance, in Figure 2.18a, detectable product is evident after approximately 32–44 cycles of amplification in 3 out of 16 cDNA samples. However, only 2 out of 16 cDNA samples still contain pGM-CSF, as shown by the melting curve (b) where 2 samples melt at the same temperature as the GM-CSF standard. Products were also subjected to agarose gel electrophoresis to confirm the results obtained from the melting curve analysis (c). An overview of the strategy employed to remove pGM-CSF (and pIL-3) is illustrated in Figure 2.19.

If –RT samples contained specific product, samples were then subjected to further enzymatic treatment to remove residual plasmid DNA. If the RNA yield was low from the first round of treatment, the original RNA sample was treated instead, or residual RNA from the first round of treatment was pooled with the original sample and aliquots of the mix were then used for treatments. RNA was again reverse transcribed and GAPDH conventional RT-PCR carried out. –RT samples were run onto LightCyler® and assessed for presence of plasmid DNA. Importantly, cDNA samples were only analysed by quantitative RT-PCR once all RNA samples had been validated to be free of residual plasmid DNA.

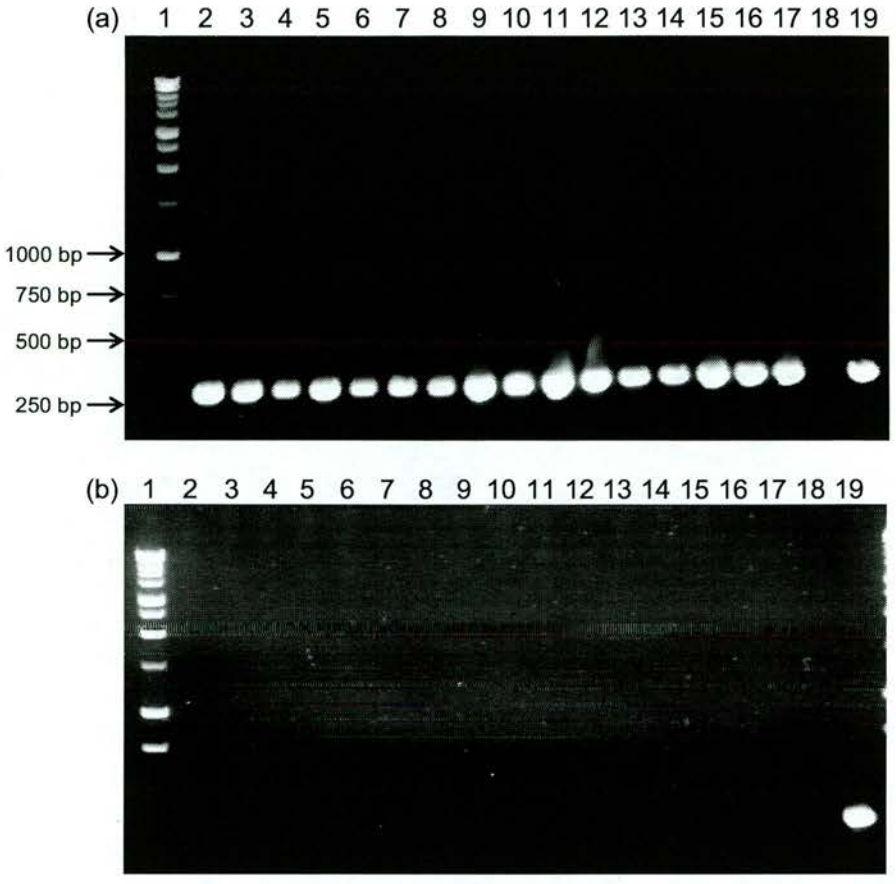

Figure 2.17 Extensive DNase/Pst-1 treatment of RNA samples obtained from pGM-CSF vaccinated skin does not cause degradation of RNA. Conventional GAPDH RT-PCR was carried out on each of the DNase/Pst-1 treated RNA samples where RT enzyme was either added (a) or omitted (b) prior to quantitative RT-PCR. (16 samples from biopsy experiment C are shown). Lane 1, 1kb ladder, lanes 2–17, samples obtained from pGM-CSF vaccinated skin; lane 18, water; lane 19, positive control (1:1000 diluted plasmid containing GM-CSF insert). After extensive treatment of RNA to remove plasmid DNA, transcripts are still present as indicated by a >250bp fragment (expected size, 265bp, Table 2.5) with GAPDH–specific primers.

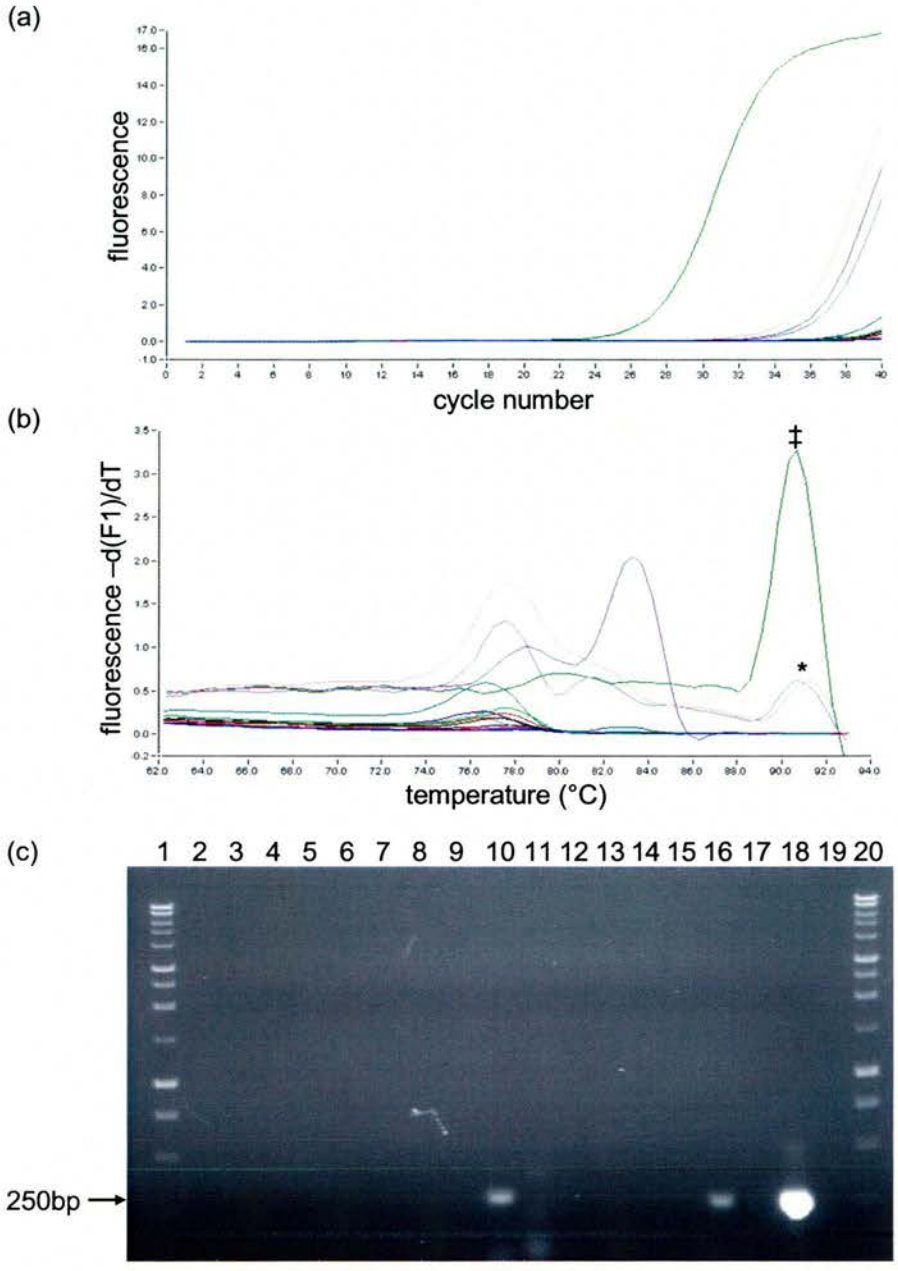

Figure 2.18 Validation of –RT samples to be free of residual plasmid DNA. DNase and Pst-1 treated samples from biopsy experiment C (Table 2.8) were reverse transcribed and quantitative RT-PCR using GM-CSF specific primers were used to amplify target species. (a) Detectable product is evident after approximately 32–44 cycles of amplification in 3 out of 16 –RT samples. (b) Only 2 out of 16 –RT samples still contain pGM-CSF where 2 samples (*) melt at the same temperature as the GM-CSF standard (‡) and (c) where LightCycler® products were subjected to electrophoresis and specific product (~250bp) is present in lanes 10 and 16. Lanes 1 and 20, 1kb ladder; lanes 2–17, –RT samples from pGM-CSF vaccinated biopsies; lane 18, standard (GM-CSF positive control) lane 19, no template control (negative control).

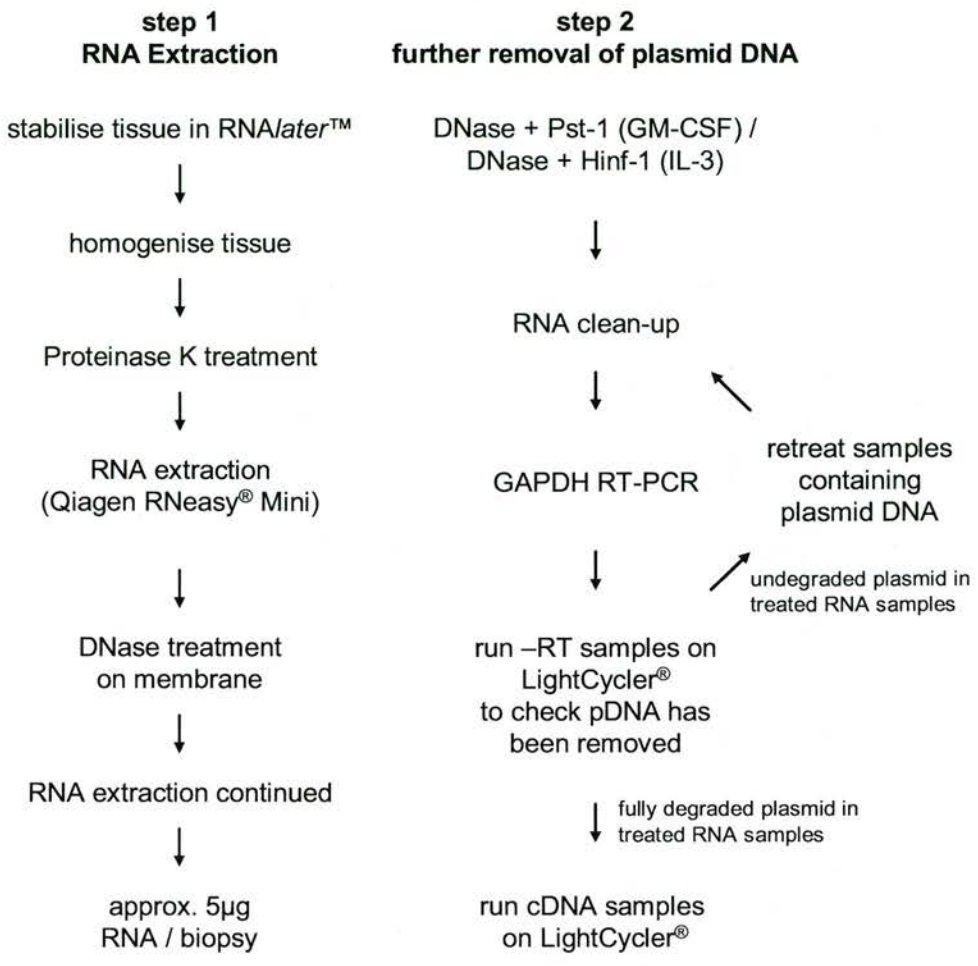

Figure 2.19 Strategy for preparation of biopsy RNA samples for quantitative real-time RT-PCR.

2.6.3.4 Removal of pIL-3

Homogenates from normal skin were spiked with 2µg pIL-3 and RNA was extracted. RNA samples were then treated in solution with DNase and Hinf-1 for 1 hour at 37°C. In addition, RNA extracted from pIL-3 vaccinated skin biopsies was treated to remove plasmid DNA. All RNA samples were purified and reverse transcribed. cDNA and control samples were then analysed by quantitative RT-PCR. Hinf-1and DNase treatment substantially reduced the amount of pIL-3 in the spiked sample (Figure 2.20). A slightly longer incubation time is required to remove 2µg pIL-3. In the DNase/Hinf-1 treated samples from pIL-3 vaccinated skin biopsies, trace amounts of plasmid were present in one sample, whereas complete removal of plasmid DNA was achieved in the other sample. Hinf-1 and DNase therefore provides an effective means of removing pIL-3.

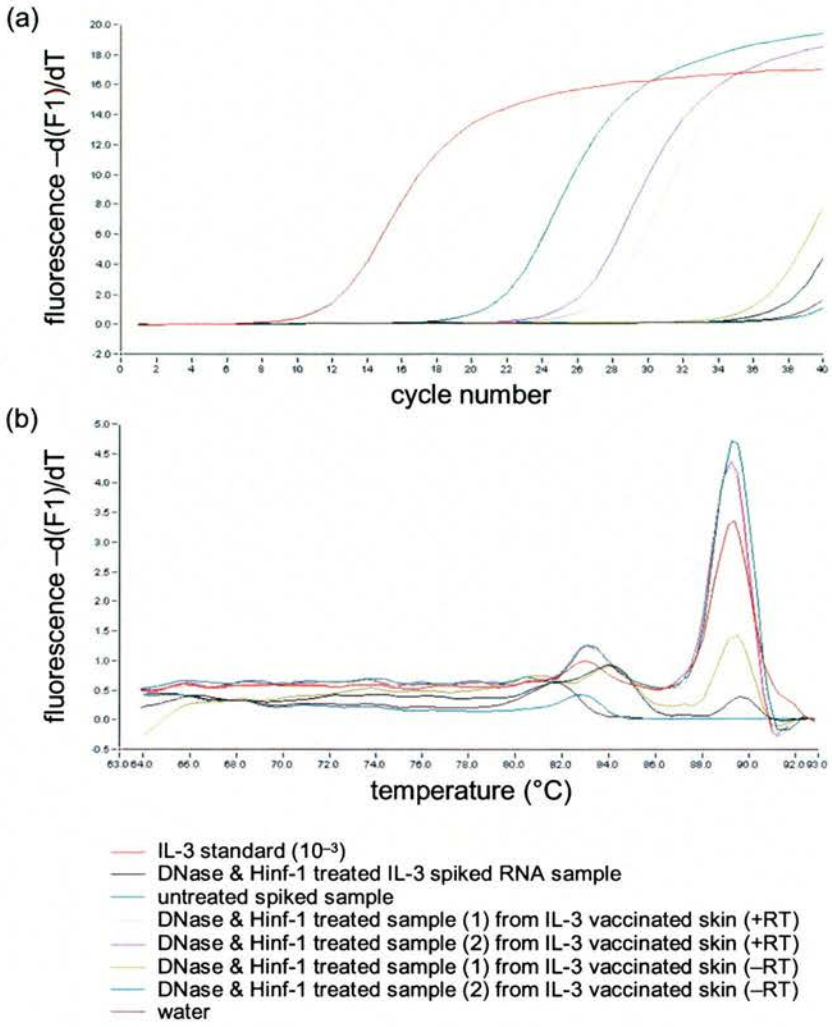

Figure 2.20 DNase in combination with Hinf-1 efficiently removes pIL-3. Plasmid DNA containing IL-3 insert was subjected to treatment with DNase in combination with the restriction enzyme Hinf-1 and was efficiently degraded. cDNA and –RT samples were amplified for 40 cycles on the LightCycler™ (a) and melting curve analysis performed (b).

2.7 Statistical analysis

Statistical analyses were performed using the GraphPad Prism package. For comparison of gene expression in different skin samples vaccinated at the same time (control plasmid vs. cytokine construct), the unpaired Student t-test was employed, whereas the two-tailed Student t-test was used to compare gene expression over the time-course of each experiment. The two-tailed Student t-test was also used to analyse gene expression in ALDC obtained from the same lymph sample and samples obtained from different animals. Where indicated in the text, the Wilcoxon Signed Rank test was also used as an extra sensitivity analysis to analyse data obtained from different animals (lymph experiments only). A p value of < 0.05 was considered statistically significant for all statistical analyses.

3 Immunopathology of gene gun delivered pGM-CSF and pIL-3

3.1 Introduction

The efficacy of DNA vaccines in humans and livestock is generally poor (reviewed in Babiuk et al., 1999). Several administrations of plasmid DNA, or strategies such as "prime-boosting", are generally required for seroconversion (Woodland, 2004). The reason for this apparent lack of efficacy in outbred species, when compared to the success of DNA vaccination in murine models of infectious disease, is not yet known. It is known that DC play a pivotal role in the induction of immunity after DNA vaccination; both directly transfected DC and DC that have taken up antigen from other cells induce immunity after DNA vaccination in mice (as outlined in Chapter 1). It has been suggested that DNA vaccines are not targeted efficiently to resident DC within the skin or muscle after delivery in larger species. In these species DNA vaccination requires optimisation and various methods are currently under intense investigation (Sasaki et al, 2003).

One method to enhance the immunogenicity of DNA vaccines is to use genetic cytokine adjuvants that expand and maturate DC at the site of inoculation. GM-CSF and IL-3 are both cytokines known to cause the growth and differentiation of immature haematopoietic cells and to some extent have overlapping roles in the development of DC *in vitro* and possibly *in vivo*. The use of IL-3 as a vaccine adjuvant has not as yet been reported and merits investigation of its adjuvant properties. Conversely, GM-CSF has been actively researched as a molecular adjuvant and shown to significantly enhance both humoral and cell-mediated immune responses, due to the recruitment of DC to the site of plasmid administration (Scheerlinck et al, 2001); although the exact mechanisms by which GM-CSF elicits such effects *in vivo* require further clarification. In particular, the ability of GM-CSF to act as a "danger signal" and induce proinflammatory cytokine expression in the skin requires further investigation, since the tissue microenvironment can influence the phenotype and functional responses of DC and thus the overall bias of the immune response.

There is a paucity of published material that describes the histological characteristics of skin after gene-gun administration of cytokine genes in outbred species (Mwangi et al., 2002). Better characterisation of the inflammatory events after administration of molecular adjuvants may help to improve DNA vaccine technology in large animals. The research described in this chapter involves characterisation of the effects of pGM-CSF and pIL-3 in ovine skin after gene-gun administration and comparison of inflammatory events with

control plasmid(s). It was of particular interest to this study to determine if DC infiltrated ovine skin after pGM-CSF and pIL-3 administration. It was hypothesised that GM-CSF and IL-3 would act upon pre-DC recruited from the blood after DNA vaccination with these constructs, and/or resident epidermal LC and dermal DC.

At present, there is also limited information with regard to the kinetics of mRNA expression of plasmid constructs after gene-gun vaccination. Armengol (Armengol et al., 2004) showed that plasmid DNA can persist for up to 2 years after intramuscular injection in mice with protein being expressed indefinitely. Conversely, it has been reported that expression of protein is lost by one week after gene-gun vaccination, consistent with the sloughing of the epidermal target site (Boyle and Robinson, 2000; Braun et al, 1999). It is crucial to our understanding of molecular adjuvants that the kinetics of expression of plasmid-encoded genes and other cytokines (TNF-α, IL-1β and IL-18), which have been implicated in both the activation and the migration of DC, are investigated. Analysis of the expression of proinflammatory mediators after pGM-CSF or pIL-3 administration may provide useful insight into the adjuvant potential of cytokine gene adjuvants, since DC activated in an inflammatory environment containing high levels of "danger signals" could be anticipated to present antigen in a non-tolerogenic fashion due to upregulation of costimulatory molecules (CD80 and CD86). In addition, an understanding of the kinetics of cytokine gene expression and the induction of proinflammatory genes may help to understand the time-frame during which activation of DC takes place.

In addition, cellular responses are induced as a consequence of the physical insult of the gold particles alone and such damage results in the release of pro-inflammatory cytokines; IL-1β and TNF-α are inducible products of keratinocytes in response to injury (Luger et al., 1996). These proinflammatory cytokines act upon the local blood vessels in the skin, increasing their permeability and allowing innate immune cells to enter the skin in response to inflammatory cytokines. Secretion of immunomodulatory factors in response to gene-gun delivery and indeed DNA itself (due to CpG motifs) may act in concert with the GM-CSF/IL-3 and could have significant qualitative and quantitative effects on the immune response generated. Quantitative real-time RT-PCR was therefore employed in this study as a tool to compare the dynamics of pro-inflammatory cytokine expression after administration of each construct.

3.2 Aims

(i) To characterise the histopathology of gene gun delivered plasmid DNA

(ii) To characterise the immunopathology of gene gun delivered pGM-CSF and pIL-3

(iii) To determine the kinetics of expression of plasmid DNA and inflammatory cytokines (TNF-α, IL-1β and IL-18) in the skin after vaccination

3.3 Cloning and *in vitro* expression of GM-CSF and IL-3

3.3.1 Cloning of cytokine genes

GM-CSF and IL-3 were individually cloned into the multiple cloning site of pEGFP-N1 vector (Figure 2.8). Non-functional GM-CSF (NF-GM-CSF) and IL-3 (NF-IL-3) were also cloned into pEGFP-N1 by insertion into the 3'–5' orientation of the vector, in order to determine that the biological effects elicited *in vivo* after gene-gun bombardment were indeed due to the biological activity of each cytokine. Analysis of constructs was carried out by restriction endonuclease digest (Figure 2.9) after sub-cloning into pEGFP-N1. In addition, all clones were sequenced and verified to contain cytokine genes in the correct orientation. It was necessary to clone NF constructs as it is now well established that regions of stimulatory sequences within prokaryotic DNA (CpG motifs) activate DC via TLR9 (Hemmi et al, 2000) and thus it is vital that the backbone DNA is identical to enable comparison of inflammatory events following vaccination with plasmids containing different cytokine genes. pEGFP-N1 was chosen as a suitable vector as it contains the immediate/early promoter from cytomegalovirus (CMV), which results in high expression levels *in vivo* (Galvin et al., 2000).

3.3.2 *In vitro* expression of GM-CSF and IL-3 mRNA in SSk fibroblasts.

It was necessary to determine if GM-CSF and IL-3 were expressed by ovine skin fibroblasts following *in vitro* transfection with pGM-CSF and pIL-3. Fibroblasts were transfected with 10–20μg of each plasmid by electroporation (Section 2.3.8.1). Cells were harvested approximately 48 hours after transfection and RNA was extracted. GAPDH RT-PCR was then carried out to ascertain that all genomic material was degraded by the DNase step included in the RNA extraction procedure and that amplifiable material was present in each

sample. Amplifiable material was present in each of the samples and genomic DNA was fully degraded (Figure 3.1).

cDNA samples obtained from GM-CSF, NF-GM-CSF and mock transfected fibroblasts were then amplified with GM-CSF specific primers. GM-CSF mRNA was detected in fibroblasts which had been transfected with pEGFP-N1 containing GM-CSF, but not fibroblasts which had been mock transfected or transfected with the plasmid containing the NF version of the gene (Figure 3.2). In addition, cDNA samples obtained from IL-3, NF-IL-3 and mock transfected fibroblasts were amplified with IL-3 specific primers. IL-3 mRNA was detected in fibroblasts which had been transfected with pEGFP-N1 containing IL-3, but not in fibroblasts which had been mock transfected or transfected with NF-IL-3 (Figure 3.3).

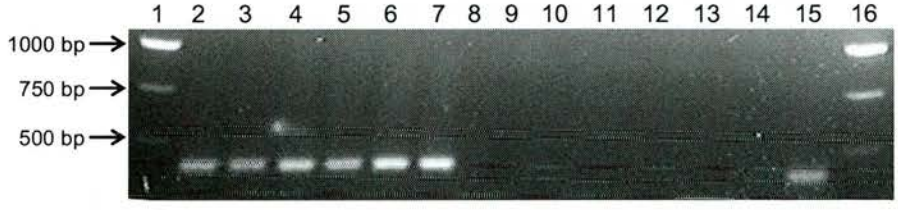

Figure 3.1 GAPDH RT-PCR performed with cDNA samples obtained after *in vitro* transfection of ovine fibroblasts. 1µg of total RNA was reverse transcribed. cDNA samples were then amplified with GAPDH-specific primers (Table 2.5) for 30 cycles at 55°C. ~366bp fragments are evident from each cDNA sample. Control (–RT) reactions were also prepared from each RNA sample to assess genomic contamination (lanes 8–13), no bands can be observed.

Lane 1 kb Molecular weight marker
Lane 2 pGM-CSF transfected fibroblasts (+RT)
Lane 3 NF-GM-CSF transfected fibroblasts (+RT)
Lane 4 pIL-3 transfected fibroblasts (+RT)
Lane 5 NF-IL-3 transfected fibroblasts (+RT)
Lane 6 mock transfected fibroblasts (+RT)
Lane 7 mock transfected fibroblasts (+RT)
Lane 8 pGM-CSF transfected fibroblasts (–RT)
Lane 9 NF-GM-CSF transfected fibroblasts (–RT)
Lane 10 pIL-3 transfected fibroblasts (–RT)
Lane 11 NF-IL-3 transfected fibroblasts (–RT)
Lane 12 mock transfected fibroblasts (–RT)
Lane 13 mock transfected fibroblasts (–RT)
Lane 14 negative control (molecular grade water)
Lane 15 positive control (1:1000 dilution of plasmid DNA containing GAPDH insert)
Lane 16 1kb Molecular weight marker

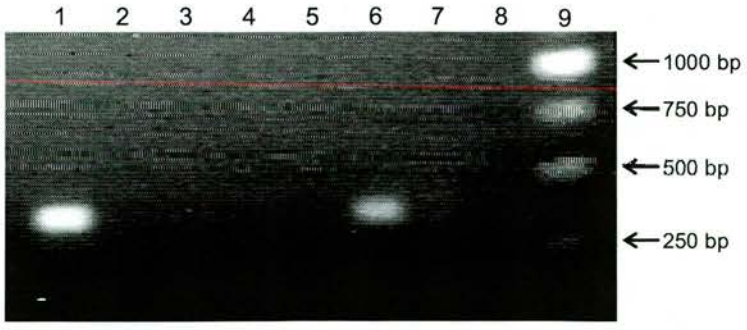

Figure 3.2 PCR–amplified GM-CSF cDNA from pGM-CSF, NF-GM-CSF and mock transfected fibroblasts. RNA was extracted from cells 48 hours after transfection and reverse transcribed. PCR amplification was carried out for 30 cycles. GM-CSF transcripts can only be detected in pGM-CSF transfected fibroblasts (~300bp product is evident).

Lane 1 positive control (1:1000 dilution of 1° PCR product)
Lane 2 NF-transfected (–RT)
Lane 3 mock (–RT)
Lane 4 pGM-CSF transfected (–RT)
Lane 5 NF-transfected (+RT)
Lane 6 pGM-CSF transfected (+RT)
Lane 7 mock transfected (–RT)
Lane 8 negative control (nuclease-free water)
Lane 9 1kb Molecular weight marker

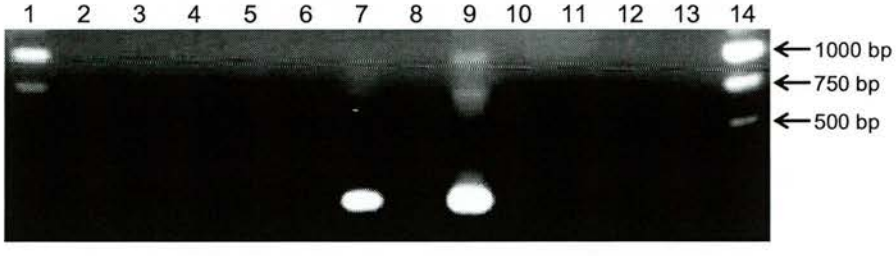

Figure 3.3 PCR–amplified IL-3 cDNA from pIL-3, NF-IL-3 and mock transfected fibroblasts. RNA was extracted from fibroblasts 48 hours after transfection and reverse transcribed. PCR amplification was carried out for 30 cycles. IL-3 mRNA is only detected in pIL-3 transfected fibroblasts (<250bp product is evident, expected size of amplicon is 192bp).

Lane 1 1kb ladder
Lane 2 mock (–RT)
Lane 3 NF-IL-3 (–RT)
Lane 4 pIL-3 (–RT)
Lane 5 mock (+RT)
Lane 6 NF-IL-3 (+RT)
Lane 7 pIL-3 transfected (+RT)
Lane 9 positive control (diluted pIL-3 1:5000)
Lane 11 negative control (nuclease-free water)
Lane 14 1kb ladder

3.3.3 Detection of recombinant GM-CSF by ELISA

Supernatants and cell pellets were collected 48 hours post-transfection and subjected to SDS-PAGE followed by staining with Coomassie Blue in order to detect recombinant GM-CSF (and IL-3). No bands at the expected molecular weight (15–25 kDa) were observed (data not shown) and more sensitive detection systems were therefore required. Supernatants from cells transfected with GM-CSF and NF-GM-CSF constructs were concentrated under vacuum (approximately 4 ×) and tested for the presence of recombinant GM-CSF by ELISA (Entrican et al, 1996) with reagents supplied by Moredun Research Institute. Using this more sensitive assay, it was evident that transfection of fibroblasts with pGM-CSF resulted in both expression and secretion of recombinant GM-CSF into the extracellular milieu (Table 3.1). The concentration of GM-CSF in the supernatant of fibroblasts transfected with pGM-CSF was approximately 400 pg/ml (calculated from a standard curve generated from known standards of recombinant GM-CSF) (Figure 3.4). The concentration of GM-CSF in mock transfected cells and cells transfected with NF-GM-CSF could not be quantified as the absorbance readings were below the level of quantification of the assay.

Table 3.1 Mean absorbance values of supernatants analysed by GM-CSF ELISA. Supernatants were collected 48 hours after transfection of fibroblasts with pGM-CSF, NF-GM-CSF or mock transfected (no DNA). A standard curve was constructed with diluted recombinant GM-CSF (supplied by Moredun Research Institute).

mock	NF-GM-CSF	GM-CSF
0.0270	0.01600	0.11400

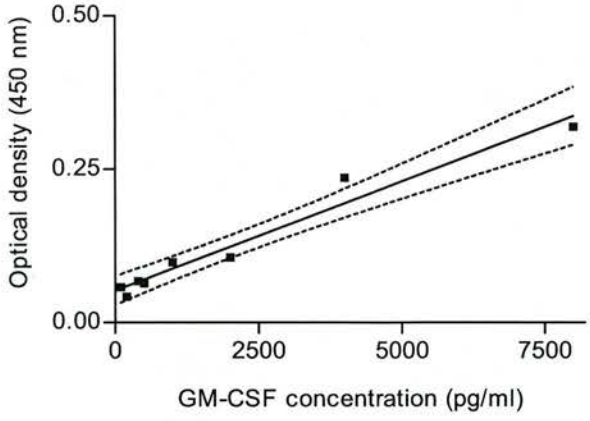

Figure 3.4 Representative standard curve for GM-CSF ELISA. Recombinant GM-CSF was diluted in assay buffer. Recombinant GM-CSF was kindly supplied by Dr. G. Entrican (Moredun Research Insitute). The solid line is the line of best-fit and dashed lines represent 95% confidence intervals.

3.3.4 Detection of recombinant IL-3

3.3.4.1 Western Blotting

Western Blotting was used to detect recombinant IL-3 using a panel of murine anti-IL-3 mAb and recombinant IL-3 derived from transfected Chinese Hamster Ovary (CHO) cell supernatant from Moredun Research Institute. IL-3 was not detected in supernatants obtained from transfected fibroblasts as assessed by Western blots developed with the substrate chromagen DAB (Figure 3.5). In addition, no bands were observed in lanes where supernatant from transfected CHO cell supernatant ("positive control") was loaded (lanes 3, 4, 6 and 7), although no information was available with regard to the outcome of the transfection experiment (for example, results obtained from RT-PCR/Western blotting). In lanes 2 and 10, recombinant IL-3 mAb were loaded into the acrylamide gel to confirm that antibody was indeed present in the supplied aliquots and to validate that the SDS-PAGE and transfer procedures were carried out satisfactorily; both heavy chains (~50 kDa) and light chains (~25 kDa) of IgG are clearly visible.

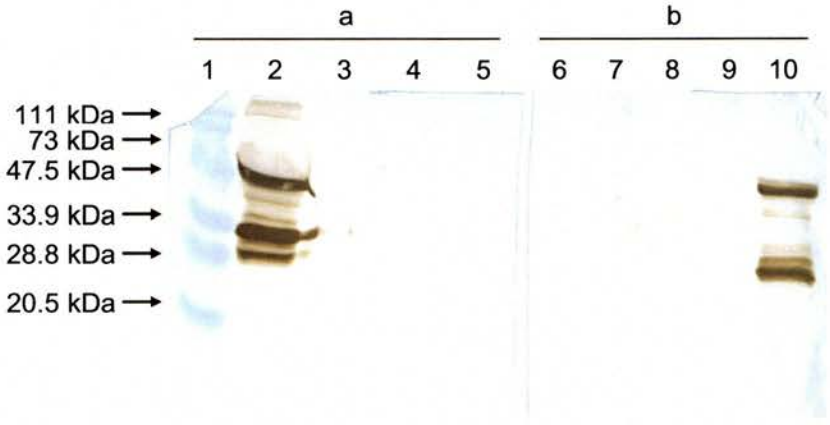

Figure 3.5 Western blot of recombinant IL-3. Blots were incubated for 2 hours at rt with either (a) mAb 3F7 (diluted 1: 200) or (b) mAb 2H11 (diluted 1:200).

Lane 1 Biorad low-range molecular marker
Lanes 2 & 10 10µl anti-IL-3 mAb 3F7 and 2H11 (1:200)
Lanes 3 and 4, 6 and 7 recombinant IL-3 (diluted 1:2, supplied by Dr G. Entrican)
Lanes 5 & 8 supernatant from pIL-3 transfected fibroblasts (diluted 1:2)

In order to enhance the sensitivity of the detection system, enhanced chemo luminescence (ECL) reagents (Amersham) were employed; however, it was still not possible to detect recombinant IL-3 from either transfected cell line, even when additional anti-IL-3 mAb were tested for reactivity (data not shown).

3.3.4.2 Detection of IL-3 by immunofluorescent staining

After several unsuccessful attempts to detect recombinant IL-3 by Western blotting, an alternative method was performed using immunofluorescent staining to detect intracellular recombinant IL-3. Cells were harvested approximately 16 hours post-transfection and fixed in ice-cold acetone and methanol and spotted onto a multiwell slide. After extensive blocking of non-specific antigens, staining was carried out with a panel of IL-3 mAb (Section 2.2.3.5) followed by TRITC-conjugated goat anti-murine IgG. Recombinant IL-3 was only detected by 2H11 mAb in cells transfected with pIL-3 (Figure 3.6) and not in mock transfected fibroblasts. Attempts to repeat this experiment (and to include the NF-control transfected cells) were however unsuccessful.

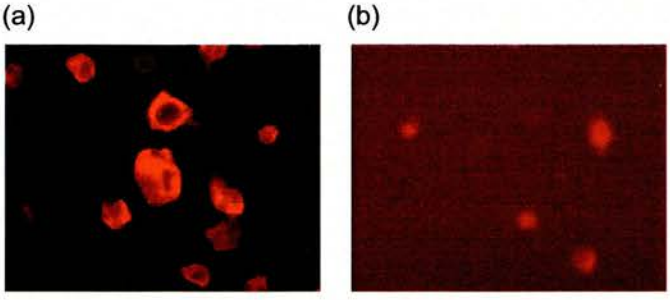

Figure 3.6 Immunofluorescent staining of pIL-3-transfected fibroblasts. Fibroblasts were either (a) transfected with pIL-3 or (b) mock transfected (no DNA). 16 hours after transfection, cells were fixed, blocked and stained with a panel of mAb raised against ovine IL-3. (a) shows possible staining of cytoplasmic protein with mAb 2H11 in pIL-3 transfected cells. (b) image has been lightened to show background (non-specific) staining

3.4 Gene-gun administration of cytokine gene adjuvants *in vivo* over 7 days

The first part of the project addressed the histological events after gene-gun bombardment with pGM-CSF, pIL-3 and pEGFP-N1. The aim of this experiment was to crudely ascertain the *in vivo* effects of GM-CSF and IL-3 in ovine skin in comparison to a control plasmid (pEGFP-N1). In particular, it was necessary to determine if indeed DC were recruited to the skin and therefore be equipped to plan future experiments which included the appropriate time-points. A previous study in murine muscle demonstrated maximal infiltration of DC approximately 7 days after intramuscular administration of pGM-CSF (Bowne et al, 1999). In addition, Haig and colleagues (1995) reported maximal infiltration of DC 5 days into ovine skin after administration of recombinant GM-CSF in combination with TNF-α. The preliminary biopsy experiment was therefore carried out over 7 days so as to provide ample

opportunity to identify if indeed DC were recruited to the skin after gene-gun vaccination with pGM-CSF (and pIL-3).

An overview of the preliminary biopsy experiment ("biopsy experiment A") is shown in Figure 3.7. Briefly, pIL-3, pGM-CSF and pEGFP-N1 were administered in triplicate by gene-gun into the skin of two clinically normal sheep at daily intervals for seven days. NF-GM-CSF and NF-IL-3 were not available at this point in the study and pEGFP-N1 therefore served as an appropriate control. Plasmid DNA coated particles were targeted towards the epidermal/dermal junction using a previously optimised technique (Watkins et al, 1999). At this point in the study the IL-3 construct also contained the gene encoding GFP. Neither sheep had previous contact with GFP, nor had been used for any DNA vaccination work. Skin samples were removed immediately at post-mortem by punch biopsy (day 7 of the experiment) and were fixed in zinc acetate fixative, processed and stained with H & E or used for immunohistochemistry.

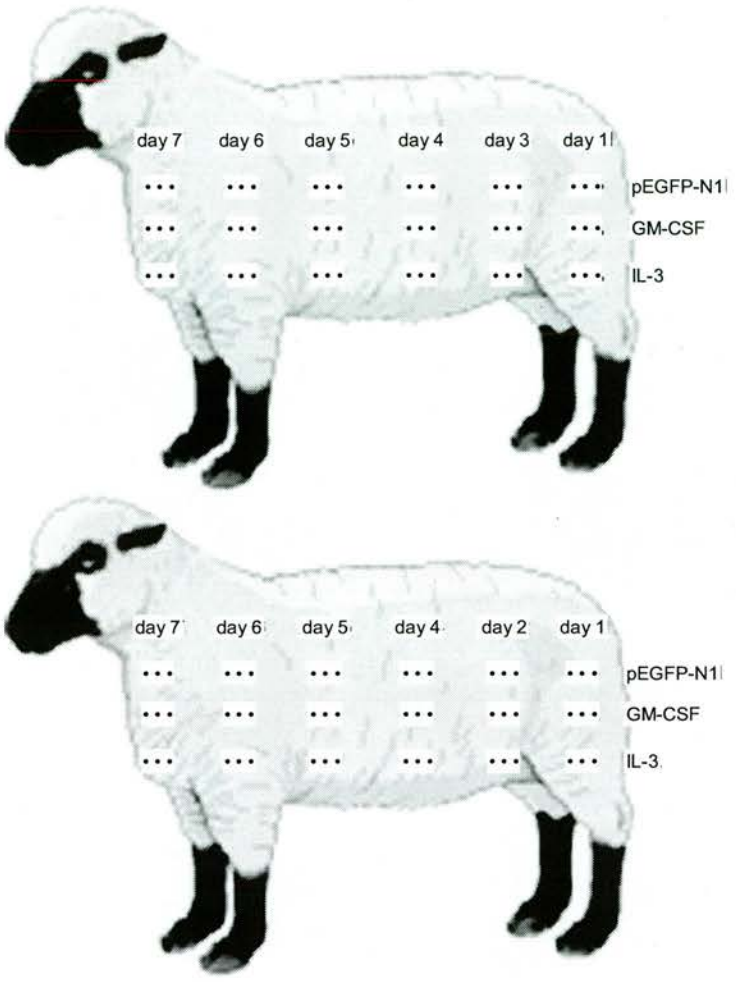

Figure 3.7 Overview of biopsy experiment A. Two sheep were each vaccinated with pIL-3, pGM-CSF and pEGFP-N1 over seven days. Skin was prepared by clipping and shaving the flank of each animal, followed by washing the area with HIBI scrub and 100% ethanol (Section 2.4). Triplicate shots of each plasmid were delivered. At post-mortem, samples were removed by punch biopsy and immediately placed into ZSF for subsequent H & E staining and for immunohistochemistry. Note that the day 2 time-point was omitted from sheep 1 (top) whereas the day 3 time-point was omitted from sheep 2 (bottom).

3.4.1 Effects of pGM-CSF administration in skin over 7 days

Whilst the overall magnitude of the inflammatory reaction was grossly similar after gene-gun administration of cytokine genes in both animals, some differences were apparent. Presentation of representative data for both animals at each of the time-points investigated is therefore problematic. In addition, time-points of days 3 and 2 post-vaccination (p/v) were only available for animals 1 and 2, respectively (Figure 3.7). Representative images for each animal are shown and the main findings are summarised in Table 3.2 (animal 1) and Table 3.3 (animal 2). Figure 3.8 is representative of H & E stained sections obtained from normal (non-vaccinated) skin from each of the two animals used in the study. An epidermal layer of 4–6 cells is evident and relatively few leukocytes are located within the dermis.

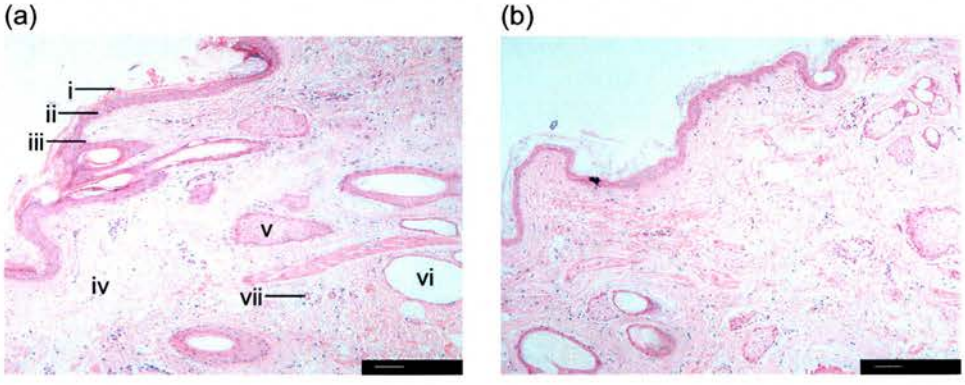

Figure 3.8 H & E stained sections from normal (non-vaccinated) skin from sheep 1 (a) and sheep 2 (b). (Scale bar = 250μm.)

(i) outer keratin layer
(ii) epidermis
(iii) epidermal: dermal junction
(iv) dermis
(v) sebaceous glands
(vi) wool follicle
(vii) capillary

3.4.1.1 Histological analysis of pGM-CSF vaccinated skin

It was evident that gene-gun administration of pEGFP-N1 induced an inflammatory response in both animals (Figure 3.9 and Figure 3.10). This may be a result of physical damage from the vaccination procedure in combination with the introduction of stimulatory CpG motifs into the skin; the relative contribution of each of these stimuli was not investigated in this study. In both animals, the inflammatory response induced after administration of pEGFP-N1 was characterised by an increase in dermal cellularity by 24 hours, and by 48 hours an epidermal neutrophilic pustule had formed. The dermal infiltrate after administration of pEGFP-N1 was generally mixed in composition; neutrophils, eosinophils, lymphocytes, macrophages and monocytes were observed throughout the time-course of the experiment, with the exception of 4 days p/v in both animals, where the infiltrate was composed largely of mononuclear cells.

It was evident that the magnitude of the reaction induced after gene-gun delivery of pGM-CSF was substantially more severe than observed with pEGFP-N1 (Figure 3.9 and Figure 3.10). An acute inflammatory reaction had taken place in both animals by 24 hours, characterised by an influx of neutrophils, resulting in the formation of a large epidermal pustule ("microabscess"/"crust"). Massive exocytosis was still evident 24 hours after pGM-CSF administration and focal disruption of the epidermal–dermal junction due to cell trafficking was evident in all sections examined. The extent of the epidermal and dermal reaction was however slightly more pronounced in sheep 1 than in sheep 2, 24 hours p/v. An inflammatory reaction was also evident underneath the basal membrane (superficial dermal reaction), which was mixed in composition; approximately 50% of the infiltrate was composed of eosinophils and some monocytes and macrophages were also observed. Little inflammation was apparent deeper within the dermis at this time-point, although cells could be observed in and around the blood vessels suggestive of active recruitment of cells to the site. Whereas much of the inflammatory reaction appeared to have taken place 48 hours after pEGFP-N1 administration, as indicated by minimal exocytosis and the presence of a confluent pustule, exocytosis was still pronounced 48 hours after pGM-CSF administration.

The severity of the reaction elicited by pGM-CSF did not increase over the time-course of the experiment but instead appeared to resolve, as shown by the degeneration of the microabscess approximately 4–5 days p/v. The peak inflammatory reaction therefore appeared to have taken place within the first 24 hours after gene-gun delivery of pGM-CSF. Interestingly, early time-points (24–48 hours) were largely characterised by the recruitment of PMN (neutrophils and eosinophils), whereas mononuclear cells were the predominant infiltrating cells at later time-points; the infiltrate was composed of >90% mononuclear cells

3 days p/v in sheep 1 (Table 3.2) and 4 days p/v in sheep 2 (Table 3.3), consistent with a slightly more delayed reaction in this animal. Between 5–6 days after pGM-CSF administration, healing of the skin was apparent as the crust began to resolve and epidermal thickening (acanthosis) was evident. By 6–7 days after gene-gun delivery of pGM-CSF, many of the pustules had sloughed off, and the epidermal layer was renewed, although slightly increased numbers of leukocytes were still present in the dermis at this time.

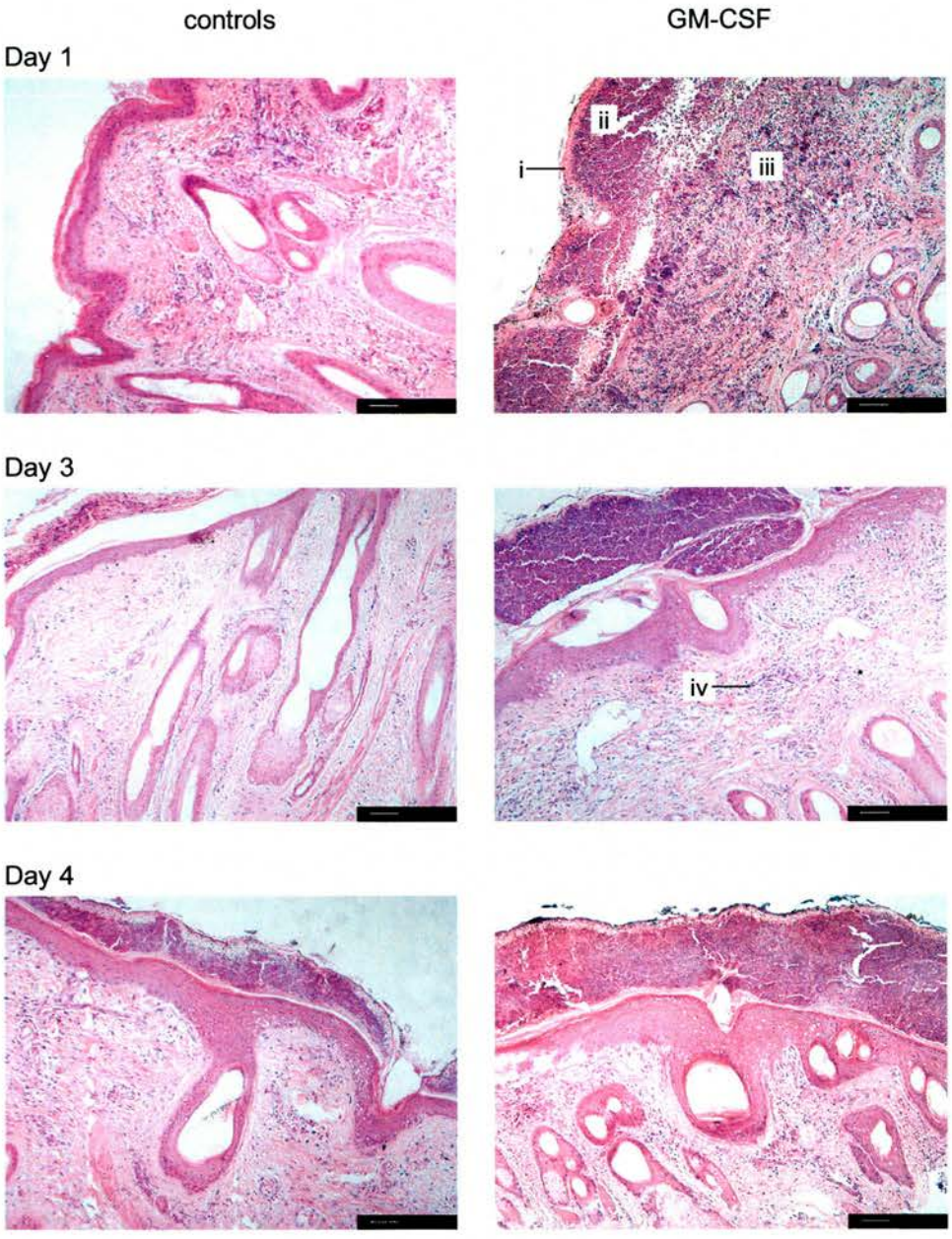

Figure 3.9 Comparison of the inflammatory events induced in the skin after gene-gun administration of pGM-CSF and pEGFP-N1 (sheep 1). Skin biopsies were removed immediately at post-mortem, fixed in ZSF and stained with H & E. Representative images from each of the time-points are shown. (Scale bar = 250μm.)

(i) gold bullets in outer epidermal layer
(ii) pustule (composed predominantly of neutrophils)
(iii) dermal infiltrate (predominantly eosinophils)
(iv) mononuclear infiltrate
(v) acanthosis (epidermal thickening)

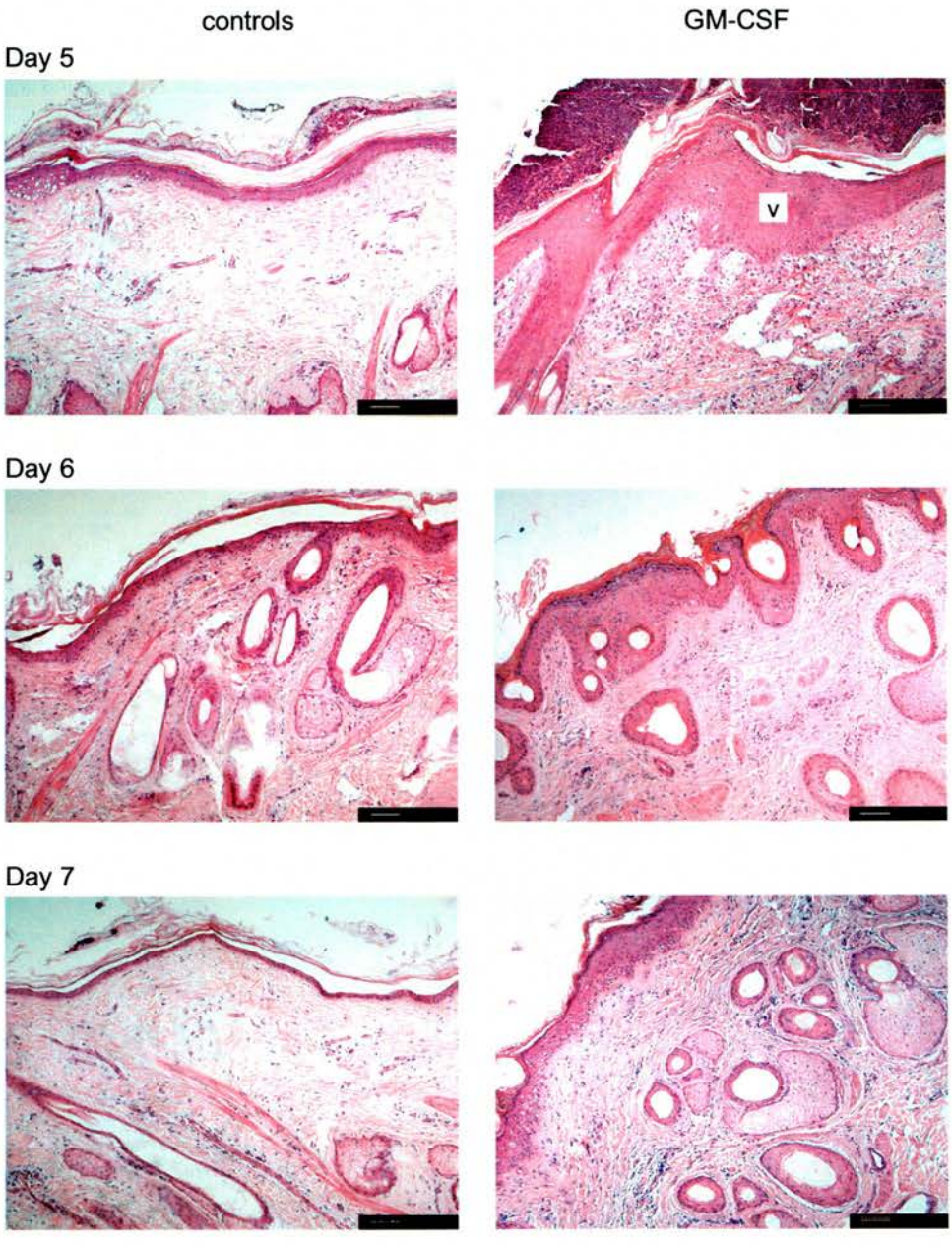

Figure 3.9 (cont.)

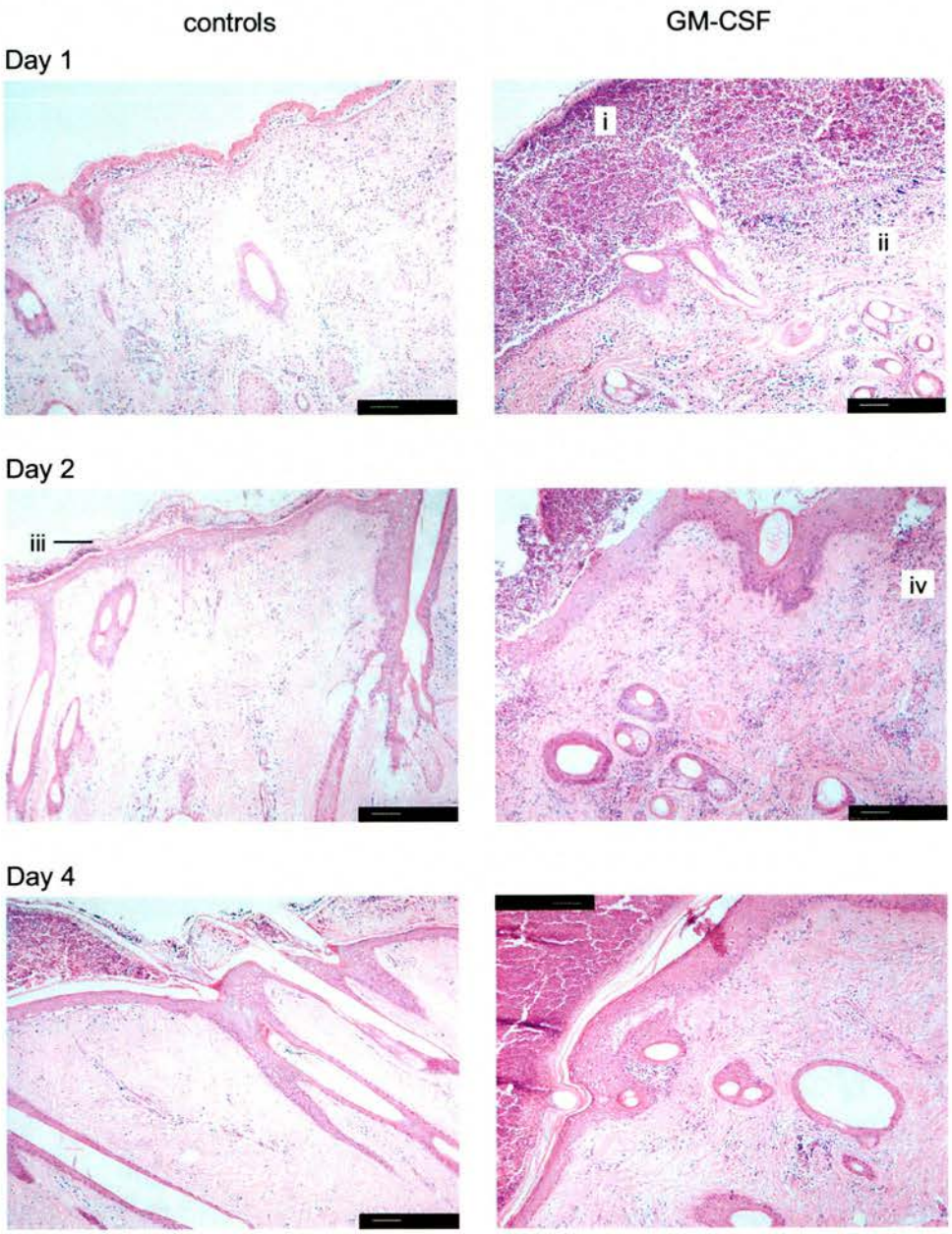

Figure 3.10 Comparison of the inflammatory events induced in the skin after gene-gun administration of pGM-CSF and pEGFP-N1 (sheep 2). Skin biopsies were removed immediately at post-mortem, fixed in ZSF and stained with H & E. Representative images from each of the time-points are shown. (Scale bar = 250μm.)

(i) pustule
(ii) dermal infiltrate
(iii) confluent pustule
(iv) cells trafficking to epidermis (exocytosis)
(v) epidermal thickening

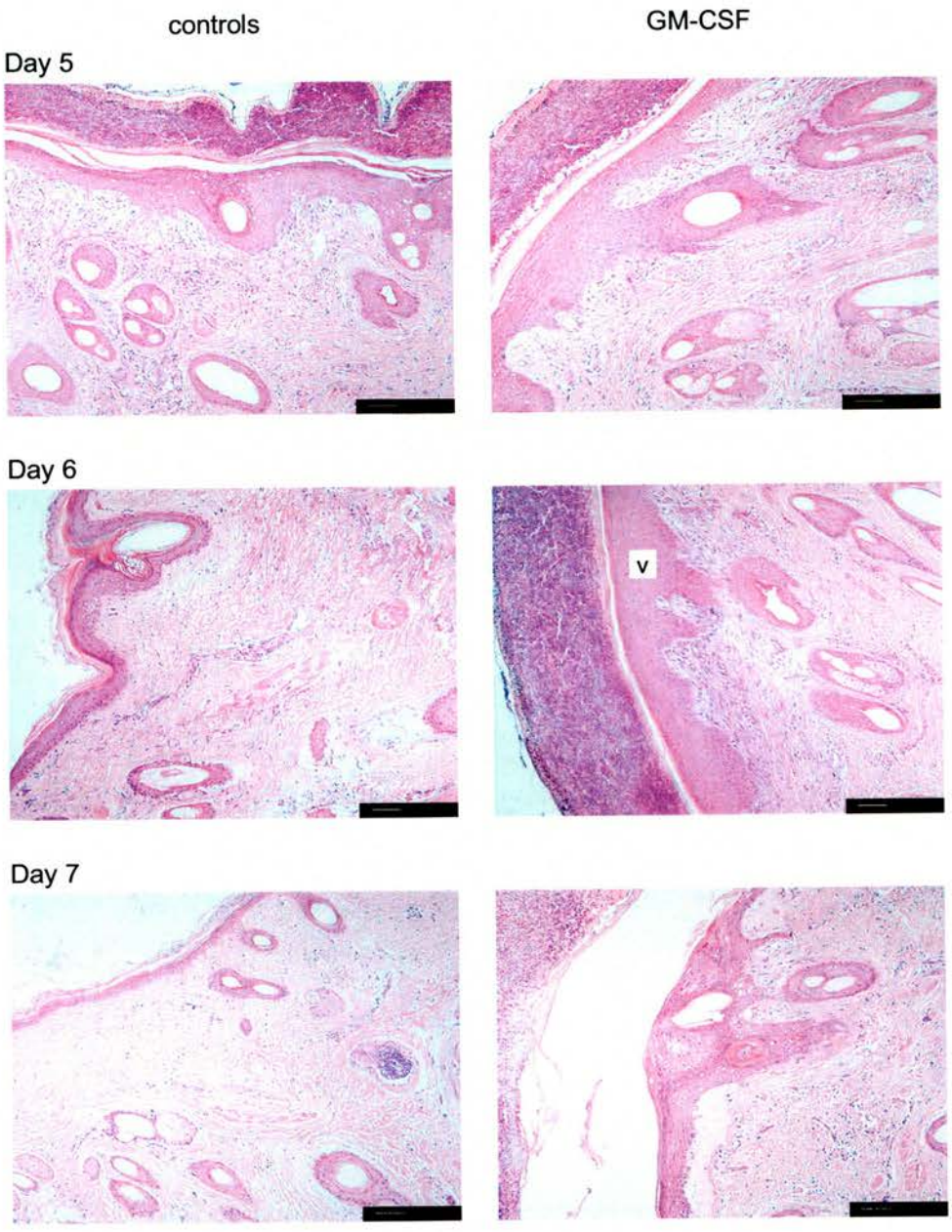

Figure 3.10 (cont.)

3.4.1.2 Immunohistological analysis of pGM-CSF vaccinated skin

In order to further investigate the histopathological changes after gene-gun administration of the plasmid constructs, mAb reactive with various immune cell populations were required. In order to obtain a panel of mAb for subsequent staining of ovine skin biopsies, lymph nodes were removed from sheep during routine cannulation surgery and fixed in ZSF. Gonzalez and colleagues (Gonzalez et al, 2001) have successfully identified a number of antibodies capable of staining ovine immune cells in lymph nodes previously fixed in ZSF. This method confers several advantages over conventional aldehyde-based fixatives; not only is the morphology of the cells maintained, but also antigen-retrieval steps are not required. A panel of approximately 20 mAb (shown to be reactive by flow cytometry) was tested on lymph node sections based on this method.

Whilst many of the mAb successfully identified cell populations within lymph node sections (results not shown), staining of resident cell populations within the skin was more problematic. In mammalian skin there are two major populations of DC, which differ in their anatomical localisation, phenotype and function. LC are located in the epidermis, whereas dermal DC are generally associated with dermal structures including blood vessels, hair follicles and sweat glands. Both populations express high levels of MHC class II with most cells also expressing the CD1 antigen (Townsend et al., 1997). mAb reactive with ovine CD1b (IAH-CC20 and IAH-CC14) and pan-CD1 (clone SBU-T6) identified DC when applied to paraffin wax-embedded lymph node sections; however, mAb did not successfully stain epidermal LC or dermal DC, even after extended incubation periods. Various antigen retrieval methods were attempted using normal skin sections fixed in paraformaldehyde with little success (results not shown). For this reason, identification of DC relied on MHC class II staining in combination with morphological assessment.

Immunoperoxidase staining of MHC class II^+ cells

Due to the problems encountered with identifying ovine LC and dermal DC by immunohistochemistry using a range of anti-CD1 mAb, VPM 54 (anti MHC class II DRα) was applied to skin sections in order to identify if indeed DC infiltrated the skin after gene-gun administration of pGM-CSF or pEGFP-N1; however, MHC class II is not only constitutively expressed on DC but on all professional APC (monocytes, macrophages and B cells) (Puri et al., 1987). In addition, its expression can be induced in activated T cells in sheep (Dutia et al., 1993a). Observations must therefore be interpreted with some degree of caution. In addition, only qualitative observations were made; no quantitative analysis of immunostained sections was carried out in this study.

Staining with mAb VPM 54 revealed a slight increase in MHC class II^+ cells in the skin 24 hours after administration of both pGM-CSF and pEGFP-N1 in sheep 1 (Figure 3.11). In contrast, a more pronounced accumulation of MHC class II^+ cells was evident 24 hours in pGM-CSF vaccinated biopsies than in control-vaccinated biopsies in sheep 2 (Figure 3.12); foci of MHC class II^+ cells were evident both at epidermal sites and also deep within the dermis and surrounding blood vessels, suggestive of active recruitment rather than proliferation of resident cells in this animal. Such observations are indeed consistent with the H & E stained sections evaluated by Dr Susan Rhind, where monocytes and macrophages were observed in and around the blood vessels in this animal 24 hours after pGM-CSF administration (Table 3.3), consistent with the observation that cells are being recruited to the site. A modest increase in MHC class II^+ cells in the dermis was also observed in pEGFP-N1 vaccinated skin of this animal; however, this was not as pronounced an increase as elicited after pGM-CSF administration and indeed the majority (>80%) of the dermal infiltrate was comprised of eosinophils.

Foci of MHC class II^+ cells within the dermis were evident in both the control and pGM-CSF vaccinated skin approximately 2 days after gene-gun bombardment in sheep 2; however at this time-point, no marked difference was apparent between pEGFP-N1 or pGM-CSF vaccinated skin. The most striking observation in this animal (sheep 2), occurred 4 days after pGM-CSF administration; at this time-point large foci of MHC class II^+ cells were evident particularly in and around blood vessels and deep within the dermis. This increase in MHC class II^+ cells was also in accord with the findings from the H & E stained skin sections (Table 3.3), where more than 90% of cells within the dermis were described as mononuclear. High magnification images of MHC class II^+ infiltrates are shown in Figure 3.12b. Upon closer examination, cells with the morphological appearance of DC can be observed; dendrites, an indented nucleus and high MHC class II expression are evident. This dramatic increase in MHC class II^+ cells was not observed in pEGFP-N1 vaccinated skin sites.

Perhaps consistent with a more acute inflammatory reaction in sheep 1 was an infiltration of MHC class II^+ DC 3 days after administration of pGM-CSF in this animal (as compared with an infiltration of DC 4 days after administration, as observed with sheep 2). Infiltrates were evident both within the epidermis and the superficial dermis. Such intense foci of DC were not observed 4 days after administration in this animal, although more MHC class II^+ cells were present than in the control pEGFP-N1 vaccinated site. Such discrepancies between the two animals are again in agreement with the earlier observations made from the H & E stained sections, where although the overall reaction in both sheep was of a similar magnitude, the cellular kinetics in sheep 2 were slightly delayed. In both animals, comparatively more MHC class II^+ cells were evident in pGM-CSF vaccinated skin biopsies

than in control pEGFP-N1 vaccinated skin 5–6 days p/v; however, infiltration was less pronounced than observed 3–4 days p/v. By 7 days p/v, numbers of MHC class II^+ cells were comparable to those observed in normal skin after vaccination with either plasmid.

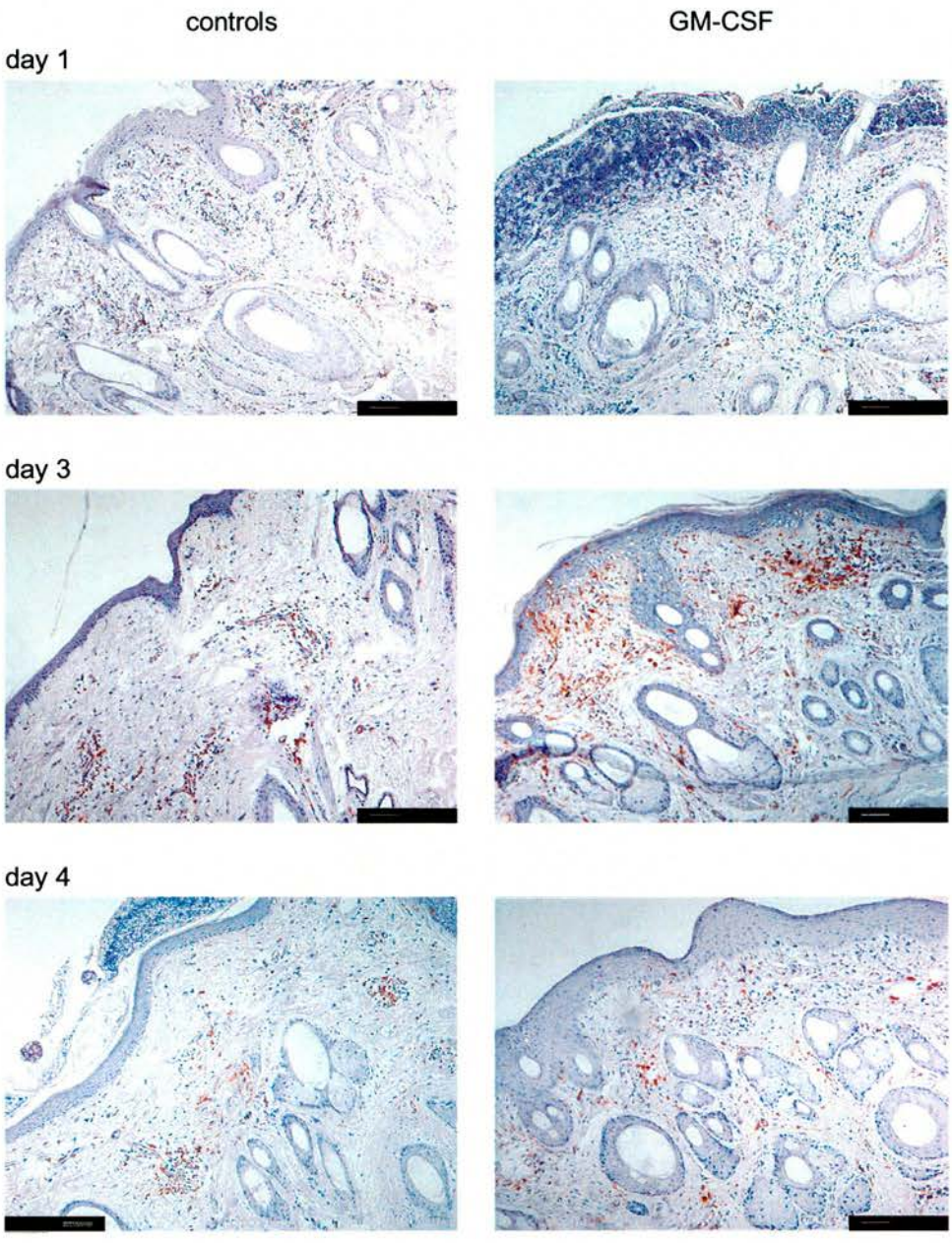

Figure 3.11 pGM-CSF enhances DC recruitment to the skin (sheep 1). Immunolabelling of skin sections with mAb VPM 54 (anti-MHC class II DRα) after gene-gun bombardment with pGM-CSF (right panels) and pEGFP-N1 (left panels). Sections were counterstained with haematoxylin. An increase in epidermal MHC class II DR^+ cells with the morphological appearance of DC is evident 3 days after delivery of pGM-CSF in this animal. (Scale bar = 250μm.)

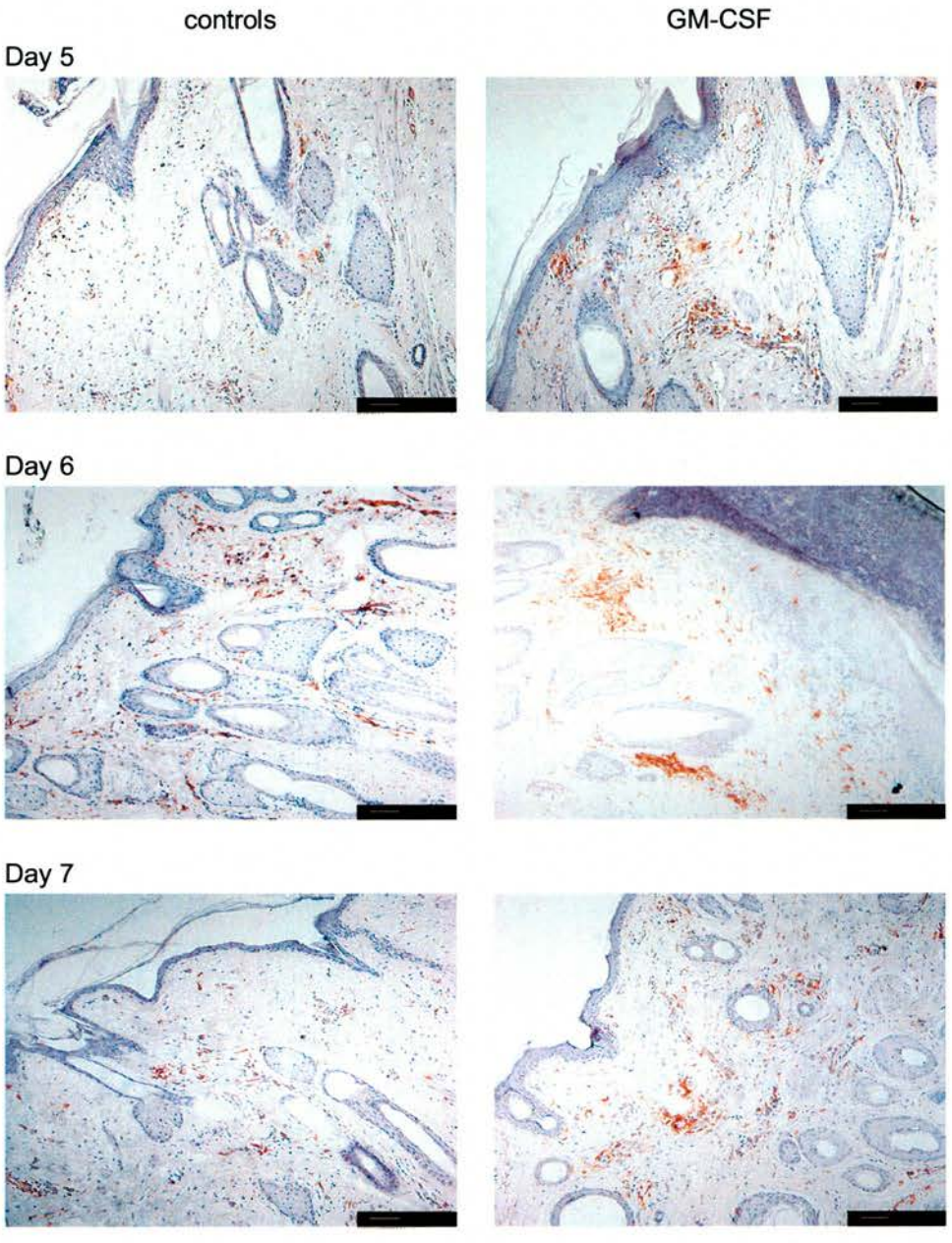

Figure 3.11 (cont.)

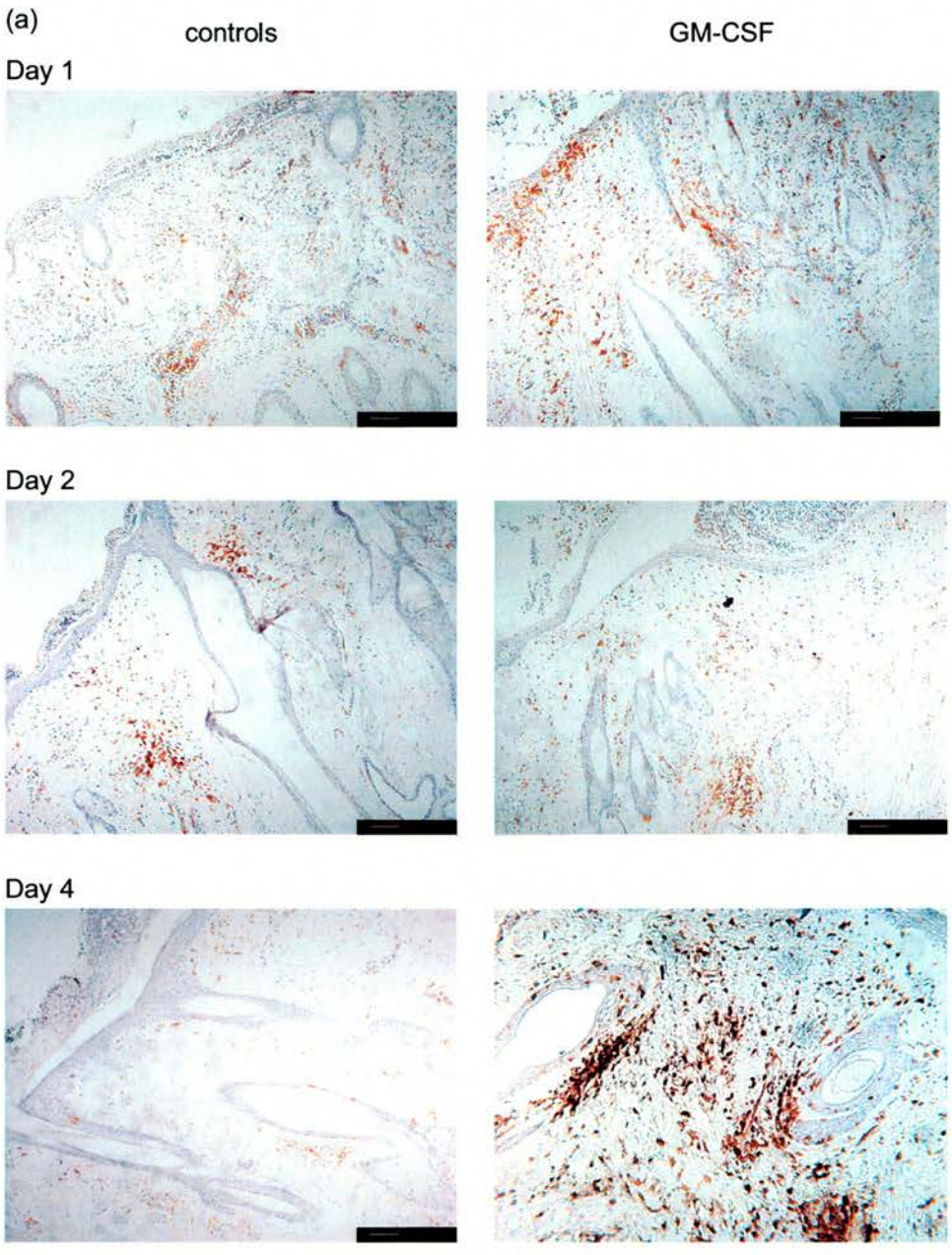

Figure 3.12 Recruitment of DC into skin 4 days after DNA vaccination with pGM-CSF (sheep 2). Immunolabelling of skin sections was carried out with mAb VPM 54 (anti-MHC class II DRα) after gene-gun bombardment with pGM-CSF (part (a), right panels) and pEGFP-N1 (part (a), left panels). Sections were counterstained with haematoxylin. Note that low power views (original magnification, ×80) have been used for all of the sections with the exception of day 4 after DNA vaccination with pGM-CSF (original magnification, ×250). Note the infiltration of dermal DC 4 days after pGM-CSF administration in this animal. (b) High magnification images reveal MHC class II^+ cells with a dendritic morphology (4 days p/v).

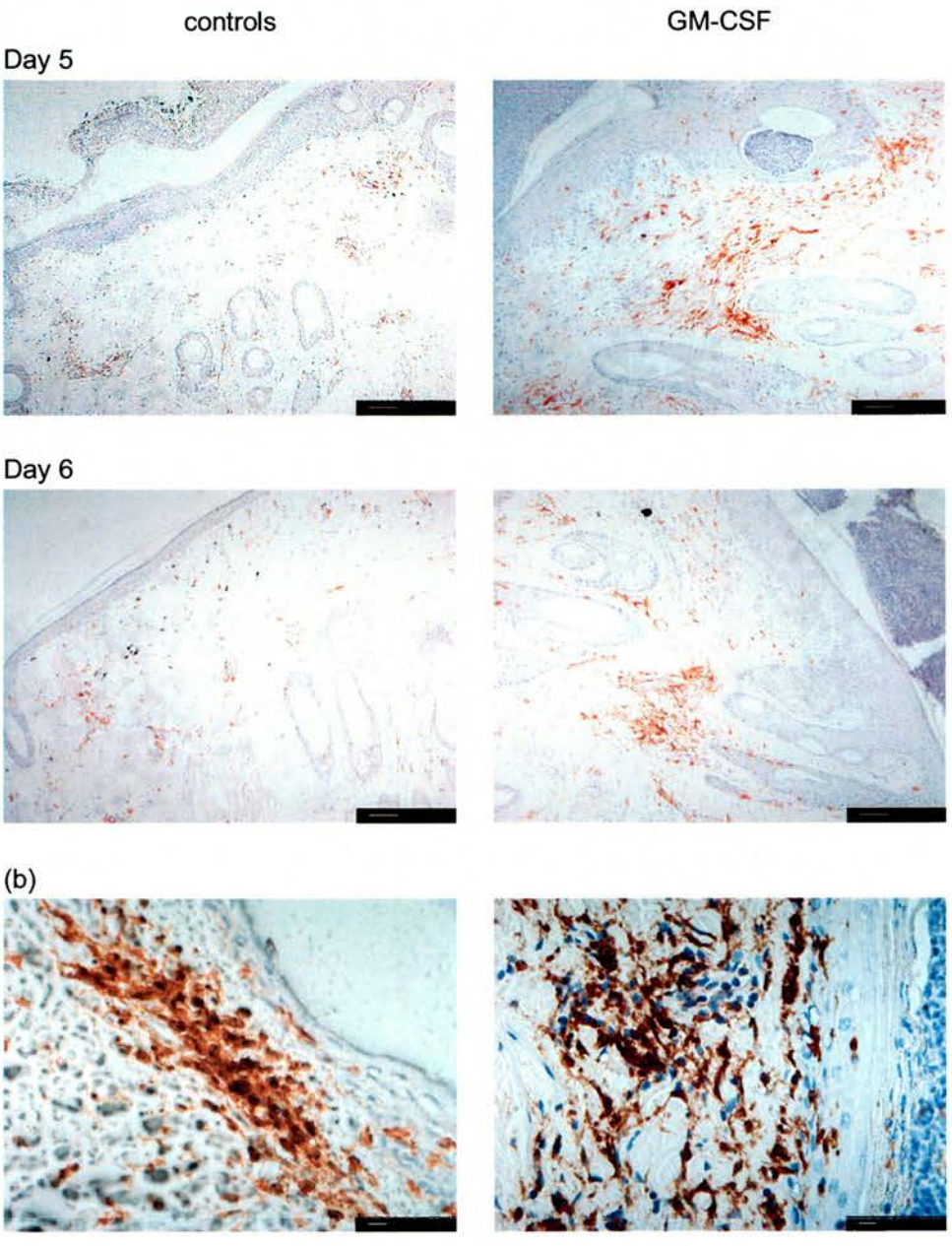

Figure 3.12 (cont.)

Immunoperoxidase staining of CD45RA$^+$ lymphocytes

CD45RA is a surface marker of ovine B cells and a T cell subset (Mackay et al., 1990). In a previous study with pGM-CSF, an infiltration of lymphocytes was observed several days after both intramuscular and intradermal delivery (Perales et al, 2002). Immunostaining with a mAb that recognises CD45RA (mAb 73B (Dutia et al., 1993c)) revealed a slight increase in the number of CD45RA$^+$ lymphocytes in the skin approximately 24 hours after gene-gun administration of both pGM-CSF and pEGFP-N1 constructs (Figure 3.13). A further increase in CD45RA$^+$ lymphocytes was evident 3–4 days after gene-gun delivery of pGM-CSF (data are shown for sheep 1 only); however serial sections stained with mAb 73B and VPM 54 revealed that MHC class II$^+$ infiltrates were not CD45RA$^+$ lymphocytes since MHC class II$^+$ infiltrates were localised within and in close proximity to the epidermis (Figure 3.11), whereas CD45RA$^+$ lymphocytes were present deeper within the dermis (Figure 3.13). Since there are very few naïve (CD45RA$^+$) T cells in afferent lymph (Mackay et al, 1990), these cells are likely to be B cells.

MHC class II$^+$ infiltrates may contain macrophages as well as DC. Unfortunately, attempts to stain for monocytes and macrophages with mAb specific for ovine CD14 and CD11b (and therefore enable discrimination of monocytes and macrophages from DC) were unsuccessful. It was interesting to observe that foci of CD45RA$^+$ lymphocytes were present 5–6 days after pGM-CSF administration, but not after bombardment with the pEGFP-N1 in any of the skin biopsies evaluated. Serial sections immunolabelled with mAb 73B and VPM 54 (anti MHC class II DRα) revealed a similar pattern of staining at later time-points (5–6 days after DNA vaccination with pGM-CSF), where CD45RA$^+$ MHC class II$^+$ cells (possibly B cells) were located deep within the dermis.

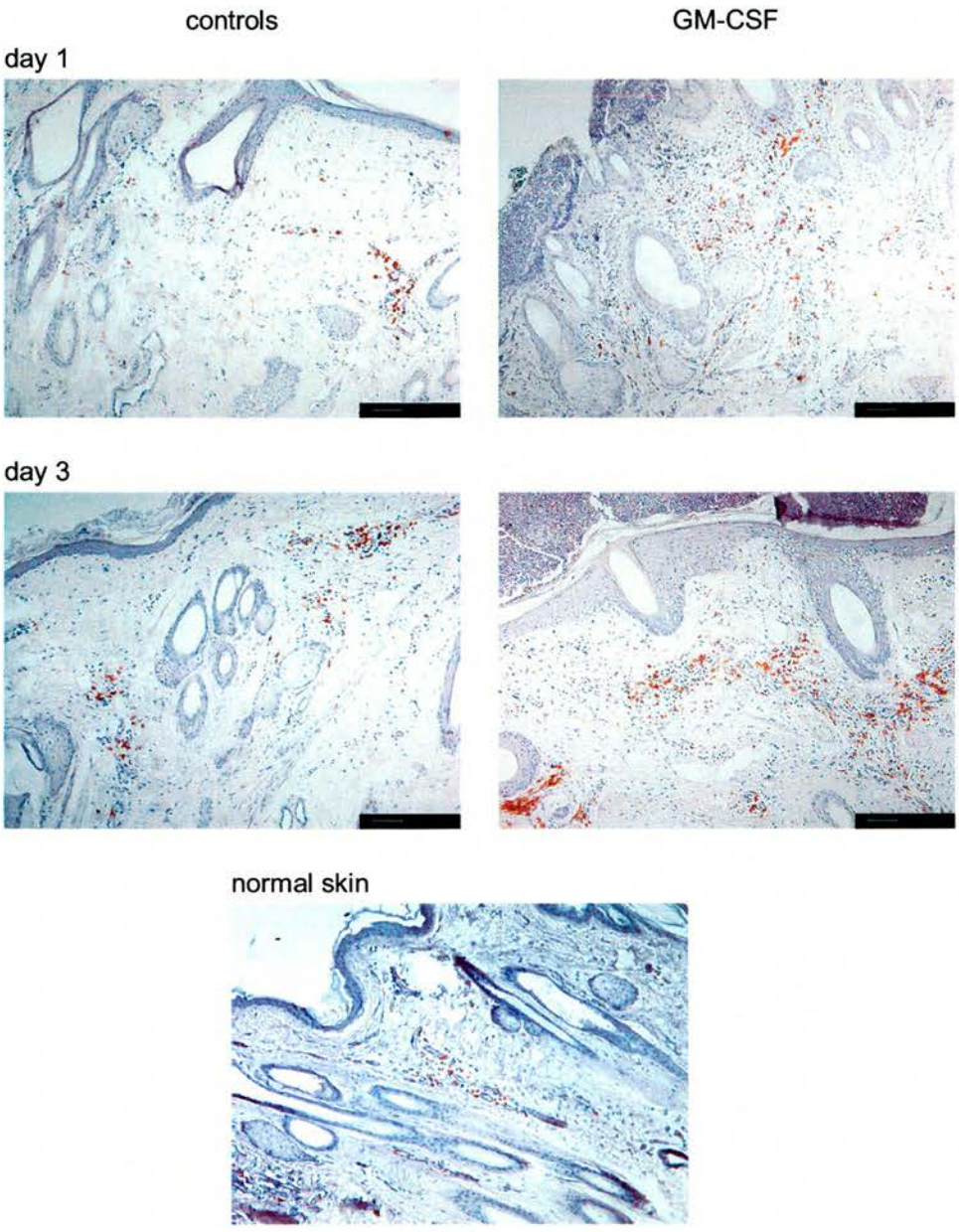

Figure 3.13 Infiltration of CD45RA$^+$ cells after pGM-CSF administration (sheep 1). Ovine skin sections were immunolabelled with mAb 73B (anti CD45RA) after gene-gun bombardment with pGM-CSF (right-hand side panels) and pEGFP-N1 (left panels). Sections were counterstained with haematoxylin. An infiltration of CD45RA$^+$ lymphocytes is evident in the dermis 3 days after pGM-CSF delivery (whereas MHC class II$^+$ cells were located near to the epidermis in this animal; Figure 3.11). Infiltration of CD45RA$^+$ lymphocytes is also evident 5–6 days after pGM-CSF delivery. (Scale bar = 250μm.)

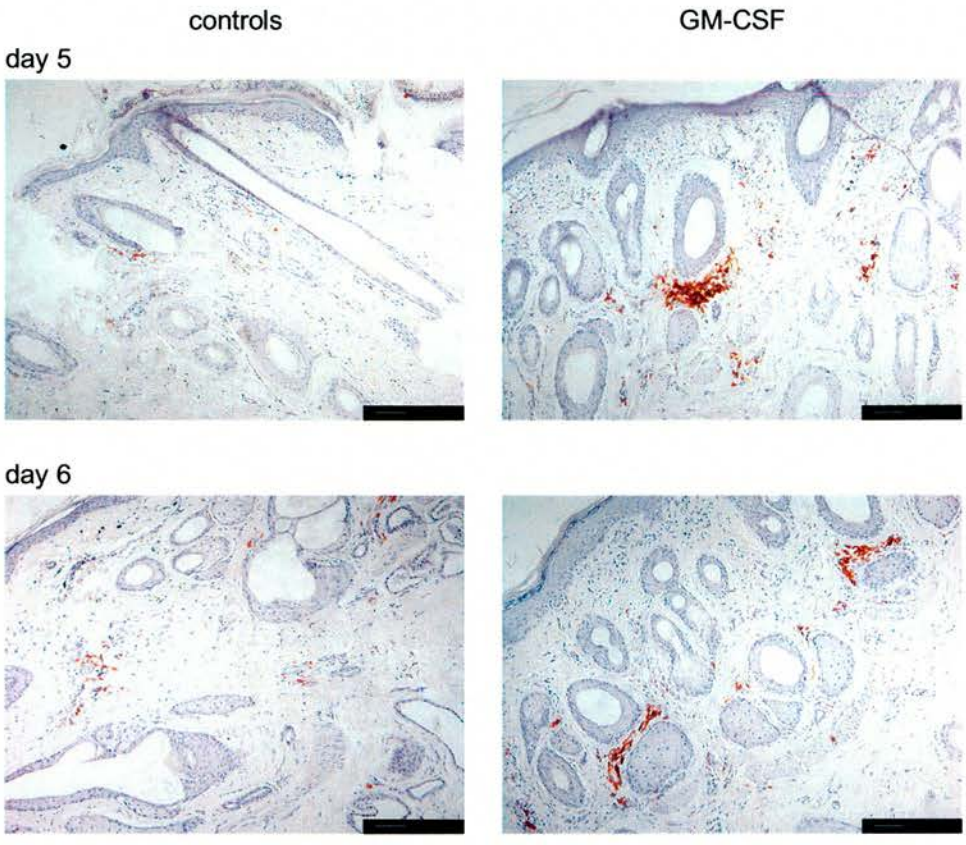

Figure 3.13 (cont.)

Immunoperoxidase staining of γδ T cells

Ruminant γδ T cells are concentrated at epithelial surfaces (Mackay and Hein, 1989) and share many common features with mice and human γδ T cells, although the latter species contain relatively few $\gamma\delta^+$ T cells in the epithelium. Human γδ T cells have been reported to induce DC maturation (Ismaili et al., 2002) and thus an increase in γδ cell numbers could have implications in terms of DC activation. In mice, epidermal $\gamma\delta^+$ T cells found in murine skin have been proposed to be related to resident DC in the skin (Bergstresser et al., 1983; Tschachler et al., 1983) and γδ DC are known to present antigen (Welsh and Kripke, 1990). Indeed, ovine γδ DC isolated from lymph have ultrastructural features characteristic of DC (Dandie et al., 2001).

A mAb specific for sheep WC1 that reacts with all γδ T cells (IAH-CC15) identified numerous cells in normal (non-vaccinated) skin sections (Figure 3.14). An increase in the number of γδ T cells in skin relative to those identified in normal skin was evident after gene-gun bombardment with both pGM-CSF and pEGFP-N1 constructs 24 hours in both animals (Figure 3.14 and Figure 3.15). Two days after plasmid administration (sheep 2 only), the number of γδ T cells had declined in the control vaccinated skin, but remained slightly elevated in the pGM-CSF vaccinated skin biopsies, whereas by 3–4 days p/v numbers of γδ T cells appeared comparable to those observed in normal skin. Of interest was an infiltration of γδ T cells 5 days after pGM-CSF in sheep 1 (Figure 3.14), particularly around wool follicles and this was also observed, but to a lesser extent in pEGFP-N1 vaccinated skin biopsies, where γδ T cells were also observed in and near to the epidermis. Six days after pGM-CSF and pEGFP-N1 administration (Figure 3.15), a slight increase in γδ T cells was identified in the skin of sheep 2, again consistent with the more delayed cellular kinetics in this animal. By day 7, the relative numbers of γδ T cells in skin vaccinated with either plasmid appeared similar to those identified in normal skin, although γδ T cells were more commonly observed in the epidermis of gene-gun vaccinated sections. In addition, some γδ T cells had a dendritic (branched) appearance upon closer magnification.

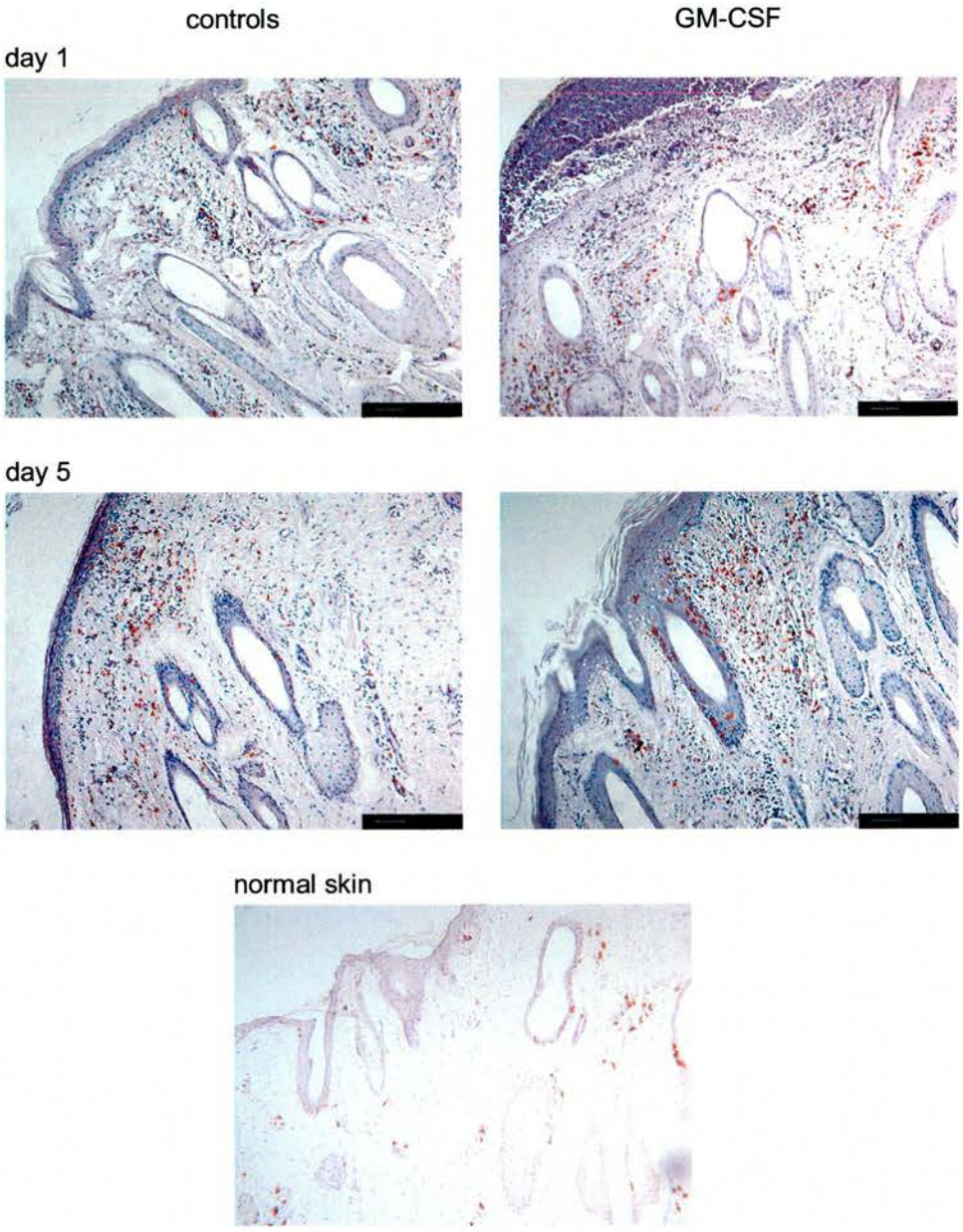

Figure 3.14 Infiltration of γδ T cells in skin after gene-gun vaccination (sheep 1). Immunolabelling of WC-1 epitopes was carried out with mAb IAH-CC15 (anti-γδ T cells) after gene-gun bombardment of the skin with pGM-CSF (right panels) and pEGFP-N1 (left panels). A representative image of normal skin from both animals stained with mAb IAH-CC15 is shown. Counterstained with haematoxylin. (Scale bar = 250μm.)

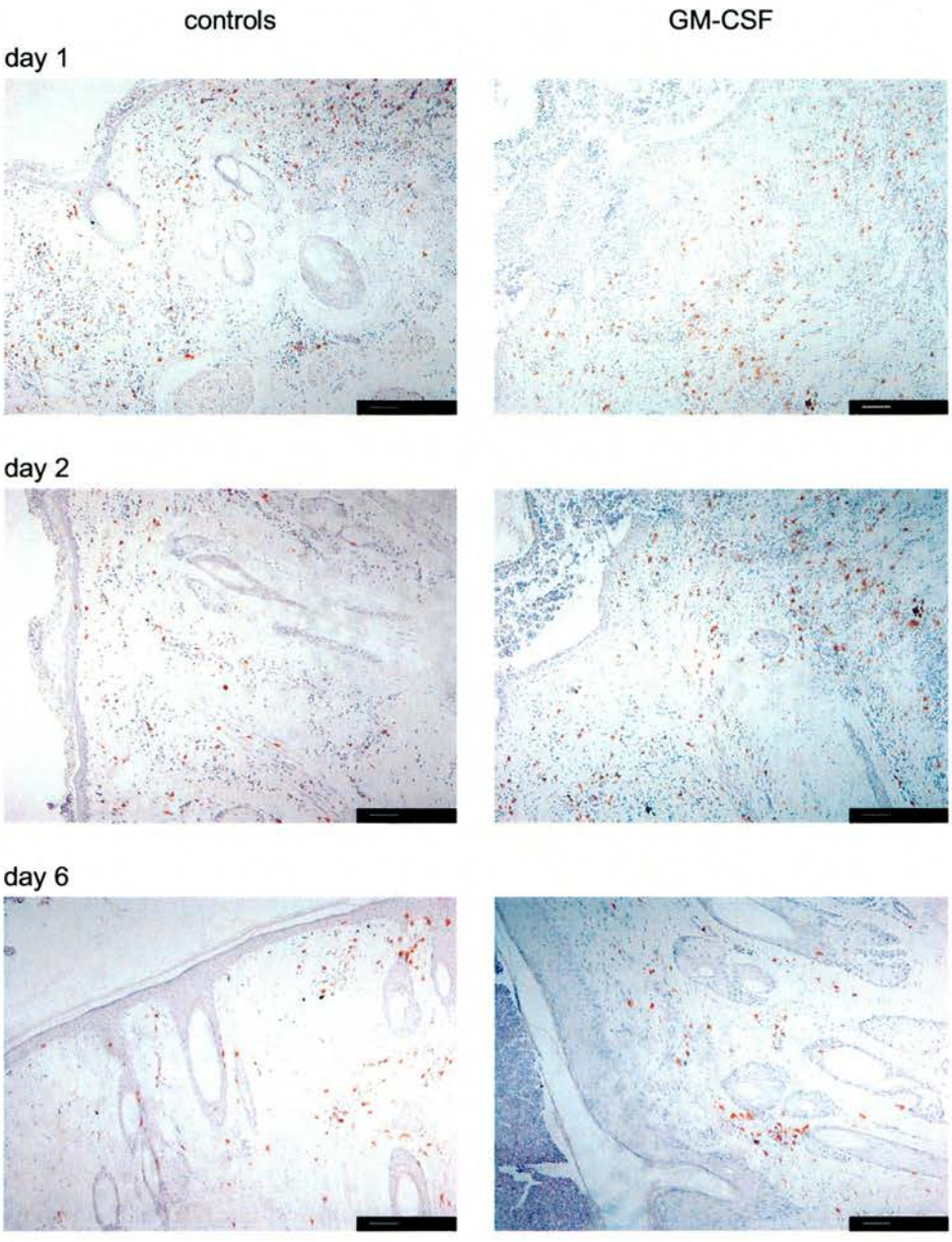

Figure 3.15 Infiltration of γδ T cells in skin after gene-gun vaccination (sheep 2). Immunolabelling of WC-1 epitopes with mAb IAH-CC15 (anti- γδ T cells) after gene-gun bombardment of the skin with pGM-CSF and pEGFP-N1. Slides were counterstained with haematoxylin. (Scale bar = 250μm.)

3.4.2 Effects of pIL-3 administration in skin over 7 days

3.4.2.1 Histological analysis of pIL-3 vaccinated skin

Representative images are shown for each animal after gene-gun bombardment with pIL-3 and pEGFP-N1 (Figure 3.16 and Figure 3.17). The extent of the inflammatory reaction after gene-gun delivery of pIL-3 was greater than observed with pEGFP-N1; however, the magnitude of the reaction was less severe in association with pIL-3 than with pGM-CSF. In addition, there appeared to be less consistent alterations in association with pIL-3, although the process of active exocytosis appeared to last longer than that observed after pGM-CSF administration. Again, a more pronounced reaction was observed in sheep 1 by 24 hours. As can be observed in Figure 3.16, pronounced exocytosis is evident and epidermal pustules (neutrophil exudates) had already formed by 24 hours in this animal, whereas pustules were still developing in sheep 2 up to 48 hours after pIL-3 administration (Figure 3.17). Indeed massive exocytosis and disruption of the epidermis was evident 2 days after gene-gun administration of pIL-3 in this animal. The early inflammatory response (24 hours) after gene-gun bombardment of the skin with pIL-3 was composed predominantly of eosinophils in both animals, although it should be noted that eosinophils were also the major cell type infiltrating the skin after DNA vaccination with pEGFP-N1 in sheep 2. At later time-points the inflammatory reaction was mixed, with the exception of day 5 in sheep 1, where many eosinophils were observed, particularly around vessels deep within the dermis.

Epidermal thickening was evident as early as 3 days after pIL-3 administration in sheep 1 and by 5 days in sheep 2. By 6–7 days after gene-gun bombardment, pustules had started to resolve and slough off in both animals and the keratin layer was returning to normal, as illustrated by the underlying "basketweave" of keratin. Minimal inflammation was evident 6–7 days after pIL-3 administration.

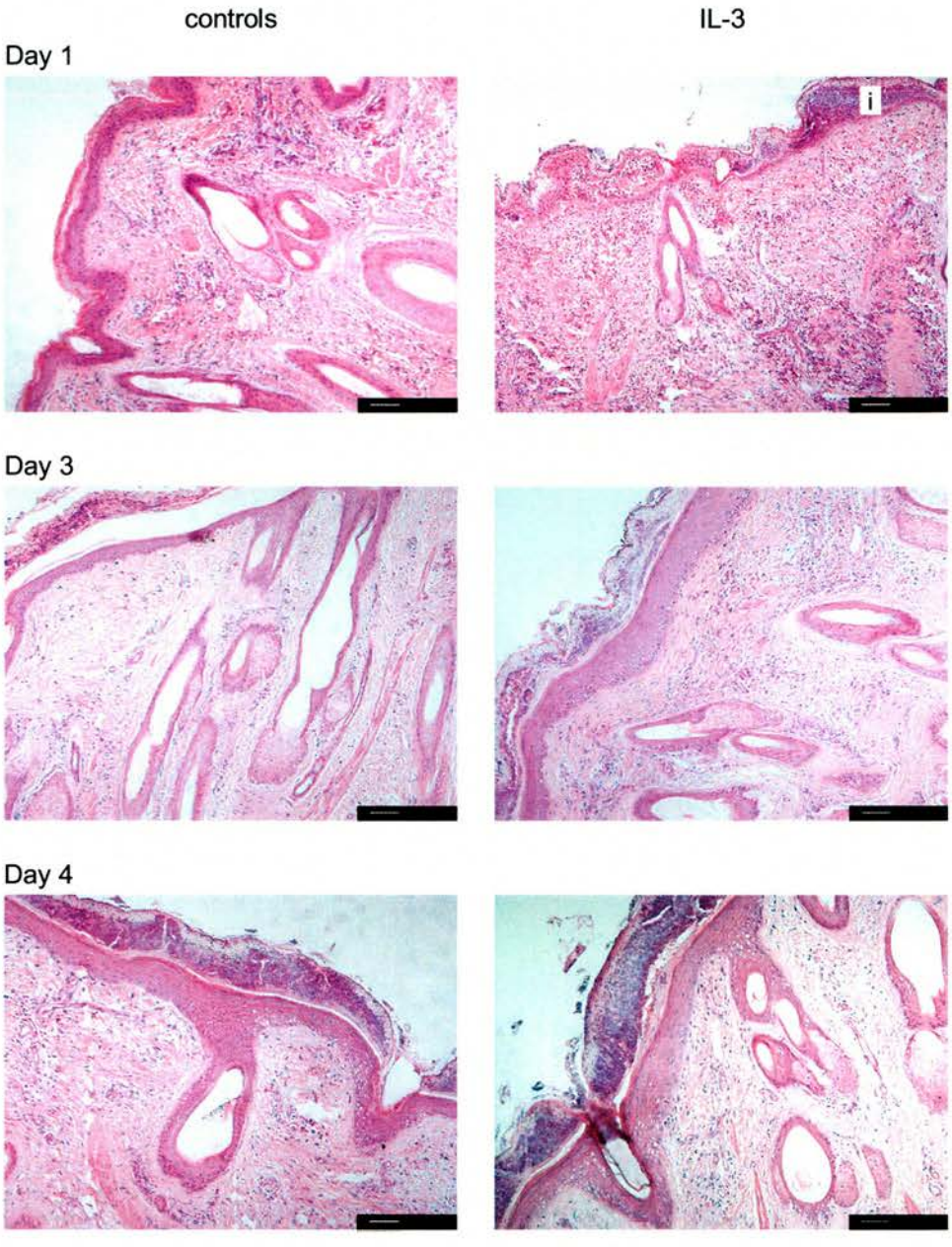

Figure 3.16 Comparison of the inflammatory events induced in the skin after gene-gun administration of pIL-3 and pEGFP-N1 (sheep 1). Skin biopsies were removed immediately at post-mortem, fixed in ZSF and stained with H & E. Representative images from each of the time-points are shown. (Scale bar = 250μm.)

(i) pustule formation by 24 hours
(ii) reforming keratin layer ("basket weave")

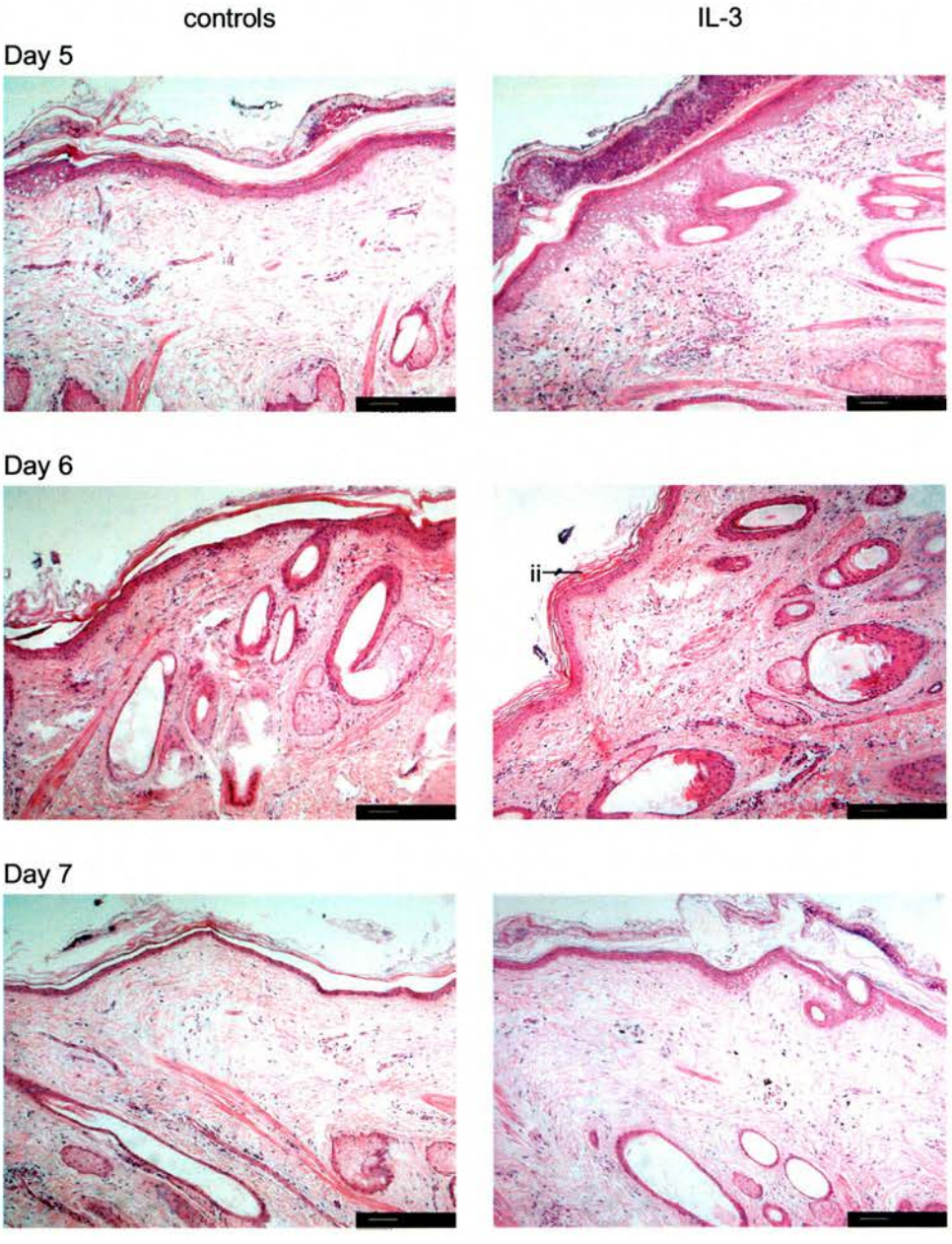

Figure 3.16 (cont.)

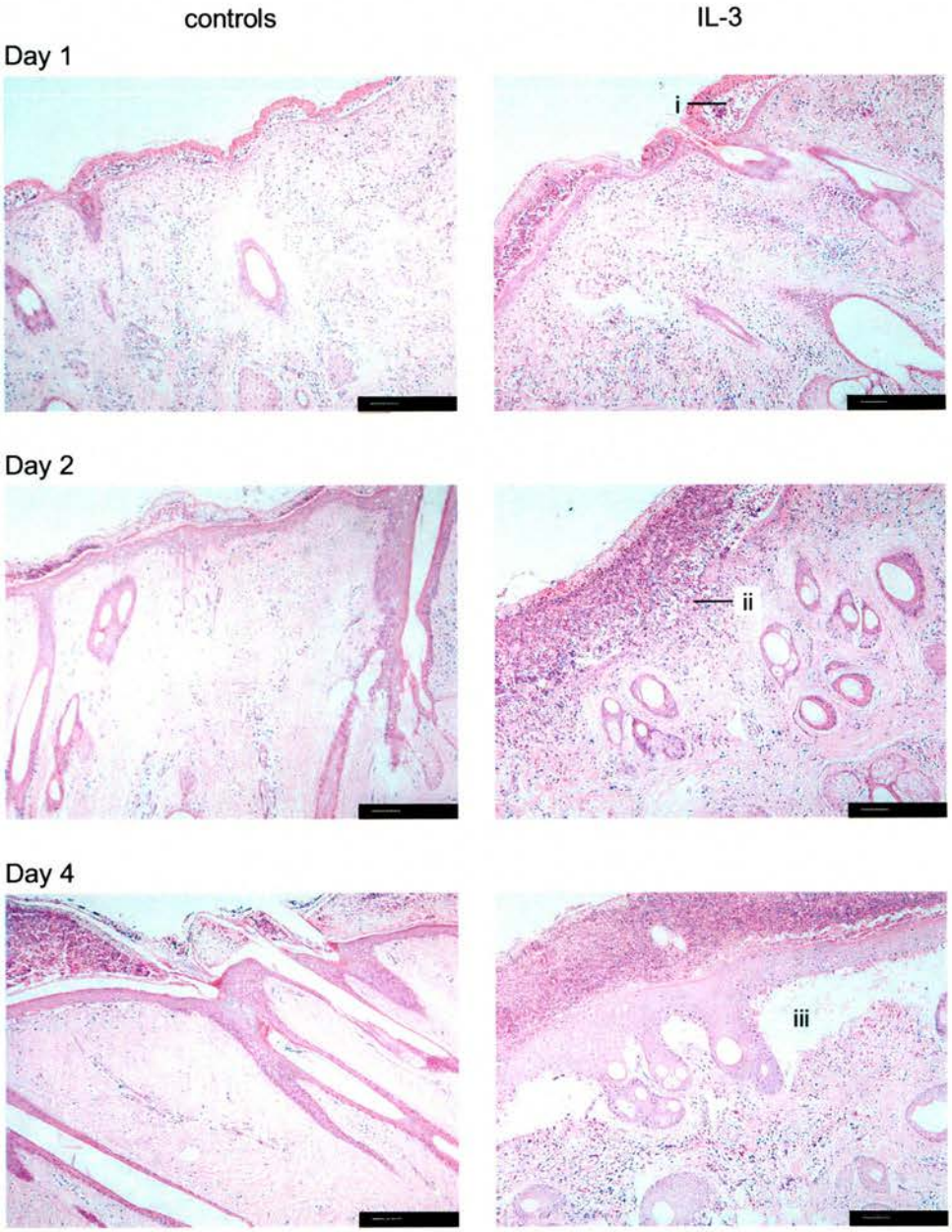

Figure 3.17 Comparison of the inflammatory events induced in the skin after gene-gun administration of pIL-3 and pEGFP-N1 (sheep 2). Skin biopsies were removed immediately at post mortem, fixed in ZSF and stained with H & E. Representative images from each of the time-points are shown. (Scale bar = 250µm.)

(i) developing pustule
(ii) pronounced exocytosis
(iii) dermal oedema
(iv) epidermal thickening
(v) aggregates of gold beads
(vi) "basket weave" of keratin (healing epidermis)

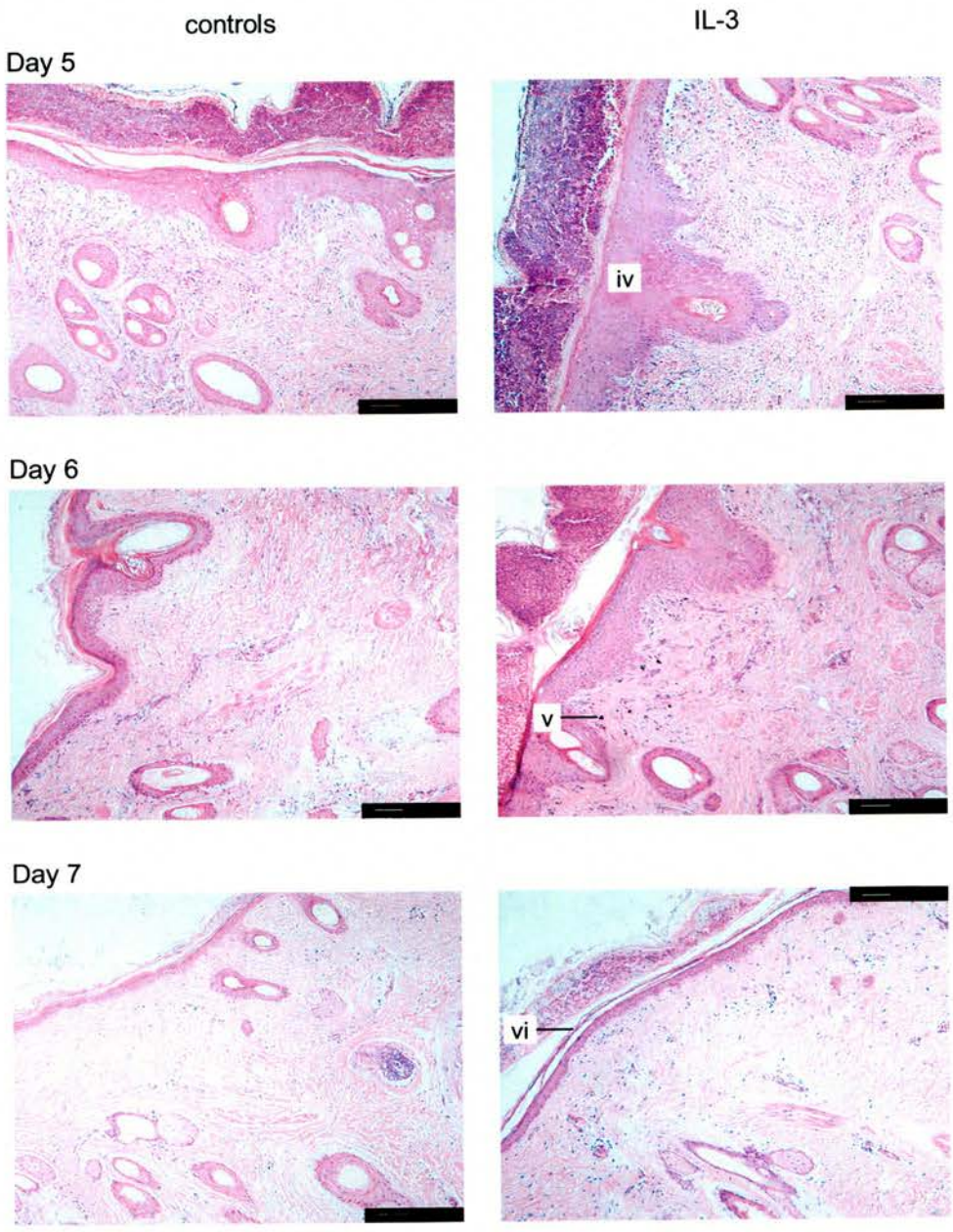

Figure 3.17 (cont.)

Table 3.2 Overview of the inflammatory reaction after gene-gun vaccination with pGM-CSF, pIL-3 and pEGFP-N1 (sheep 1). Note that the plasmid containing IL-3 still contained the GFP gene at this stage. (MΦ, macrophages; L, lymphocytes; eos, eosinophils; monos, mononuclear cells; +, mild; ++, moderate; +++, severe; ++++, extremely severe (beyond "normal" levels).)

days p/v	construct	location	cell type	severity (dermal)	epidermis	other comments
1	pEGFP-N1	mid adnexae	mixed	++	intraepidermal / subcorneal pustules	
	pGM-CSF	mid adnexae and deep perivascular	mixed, ~50% eos.	++++	massive crust. sub and intracorneal	massive exocytosis and effacing of d/e junction
	pIL-3	from mid adnexae	>80% eos. Some monos, MΦ, L	+++	subcorneal / intra epidermal pustules. pronounced exocytosis	
3	pEGFP-N1	from mid adnexae	mixed	+	intracorneal pustules	
	pGM-CSF	from mid adnexae	>90% mono	++/+++	massive crust/ intracorneal pustule – confluent, focal epidermal damage	dermal oedema
	pIL-3	from mid adnexae	20–30% eos. mixed	+++	pustules, mainly intracorneal. Foci intraepidermal inflammation / oedema	oedema-dermal / epidermal
4	pEGFP-N1	superficial, mostly perivascular	mixed, mostly mono	+/++	confluent intracorneal pustule. Acanthosis	oedema
	pGM-CSF	perivascular, mild	mixed	+	remarkably little dermal inflammation given epidermal reaction	massive thick crust. minimal exocytosis
	pIL-3	superficial	mixed	++		

Table 3.2 (Cont.)

5	pEGFP-N1	mid to superficial. perivascular	mixed	++	intracorneal pustule, acanthosis	oedema
	pGM-CSF	mid to superficial	>80% monos. mixed	++/+++	massive pustule, acanthosis marked	oedema fibroblasts
	pIL-3	mid to superficial. deep perivascular	mixed. many eos. around deep vessels	++/++++	confluent intra corneal pustule	oedema, focus of necrosis and epidermal disruption
6	pEGFP-N1	mid to superficial	mixed	+	intracorneal pustule, mild	
	pGM-CSF		mixed. mostly monos.	+	massive detached crust, acanthosis	
	pIL-3	perivascular (minimal)	mixed	+	keratin layer returning to normal	generally minimal change
7	pEGFP-N1	mid to superficial mainly perivascular (mild)	mixed	+	hyperkeratosis	
	pGM-CSF	mid to superficial	mixed	+	crust detached, some residual acanthosis / hyperkeratosis	
	pIL-3	mid to superficial mainly perivascular (mild)	mixed	–/+	minimal inflammation, mild hyperkeratosis	oedema, "depleted" dermis

Table 3.3 Overview of the inflammatory reaction following vaccination with pGM-CSF, pIL-3 and pEGFP-N1 (sheep 2). Note that the plasmid containing IL-3 still contained the GFP gene at this stage. (MΦ, macrophages; L, lymphocytes; eos, eosinophils; monos, mononuclear cells; +,mild; ++, moderate; +++, severe; ++++, extremely severe (beyond "normal" levels).)

days p/v	construct	location	cell type	severity (dermal)	epidermis	other comments
1	pEGFP-N1	deep adnexal to superficial	mixed	++	developing pustules, exocytosis	
	pGM-CSF	mainly mid to superficial	mixed, 30–50% eos.	+++/++++	developing pustules, massive exocytosis	focal disruption of epidermis and d/e junction. monos & MΦs in and around blood vessels
	pIL-3	deep adnexal to superficial	>70% eos	++/+++	developing pustules, exocytosis	
2	pEGFP-N1	mainly superficial and perivascular	mixed	+	confluent pustule, minimal exocytosis	
	pGM-CSF	deep adnexal to superficial, mainly perivascular	mixed ~50% eos.	++	massive pustule, trafficking/ exocytosis still in progress	
	pIL-3	mainly superficial	mixed	+/++	large pustule/crust developing, massive exocytosis and disruption of epidermis	

Table 3.3 (cont.)

4	pEGFP-N1	mainly superficial and perivascular	mainly mononuclear	+	massive crust, separating, minimal exocytosis	
	pGM-CSF	from mid adnexae	>90% mononuclear	++/+++	massive crust/intracorneal pustule, epidermal damage	dermal oedema
	pIL-3	mid adnexal to superficial	mainly mononuclear	++/+++	massive crust, minimal active trafficking	superficial oedema to d/e separation
5	pEGFP-N1	mainly superficial	mixed	++	large crust and acanthosis. d/e separation and oedema	
	pGM-CSF	mainly superficial and perivascular	mixed	++	massive crust. epidermal thickening. dermal/epidermal separation	
	pIL-3		mixed	++	massive crust. epidermal thickening. dermal/epidermal separation	
6	pEGFP-N1	minimal. superficial and perivascular	mixed	–/+		
	pGM-CSF	minimal. superficial and perivascular	mixed mostly monos.	–/+	massive crust. epidermal thickening. fibroblast activity superficial dermis	
	pIL-3	minimal	mixed	–/+	massive crust. epidermal thickening	

Table 3.3 (cont.)

7	pEGFP-N1	minimal perivascular			largely unremarkable
	pGM-CSF	superficial, mainly perivascular	mainly chronic	+/++	massive crust mild superficial oedema
	pIL-3	minimal. Superficial and perivascular	mixed	–/+	crust resolving. underlying "basketweave" keratin

3.4.2.2 Immunohistological analysis of pIL-3 vaccinated skin

Immunoperoxidase staining of MHC class II^+ cells

pIL-3 vaccinated skin biopsies were immunolabelled with mAb VPM 54 (anti-MHC class II DRα) and representative images from both animals are shown in Figure 3.18 (sheep 1) and Figure 3.19 (sheep 2). The initial immunohistological changes caused by pIL-3 vaccination were subtle. The numbers of MHC class II^+ cells were slightly elevated 24 hours after pIL-3 administration when compared to pEGFP-N1 vaccinated skin in sheep 1 (Figure 3.18), whereas no difference was apparent in pIL-3 and pEGFP-N1 vaccinated skin sites in sheep 2 (Figure 3.19). By 2 days, slightly more MHC class II^+ cells had infiltrated pIL-3 vaccinated skin; immunolabelled cells were small, round and mononuclear (possibly monocytes/B cells), but this did not differ markedly from the control (pEGFP-N1) vaccinated skin sections. No difference in the number of MHC class II^+ cells was apparent 3–4 days after administration of either pIL-3 or pEGFP-N1. Some infiltrates of MHC class II^+ cells were however evident in the dermis (sheep 2) and near to the epidermis (sheep 1) 6–7 days after pIL-3 administration and importantly, some cells had a dendritic appearance.

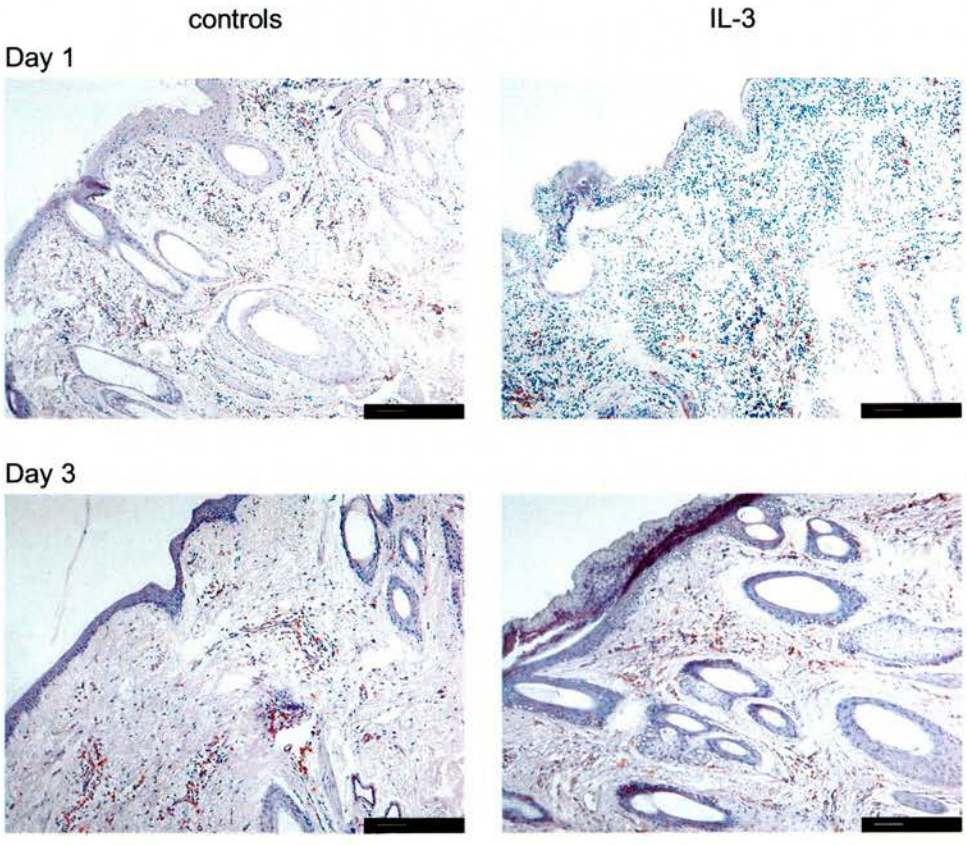

Figure 3.18 Identification of MHC class II^+ cells in skin vaccinated with pIL-3 and pEGFP-N1 (sheep 1). Skin sections were immunolabelled with mAb VPM 54 (MHC class II DRα) after gene-gun bombardment with pIL-3 (right-hand side panels) and pEGFP-N1 (left panels). Sections were counterstained with haematoxylin. (Scale bar = 250μm.)

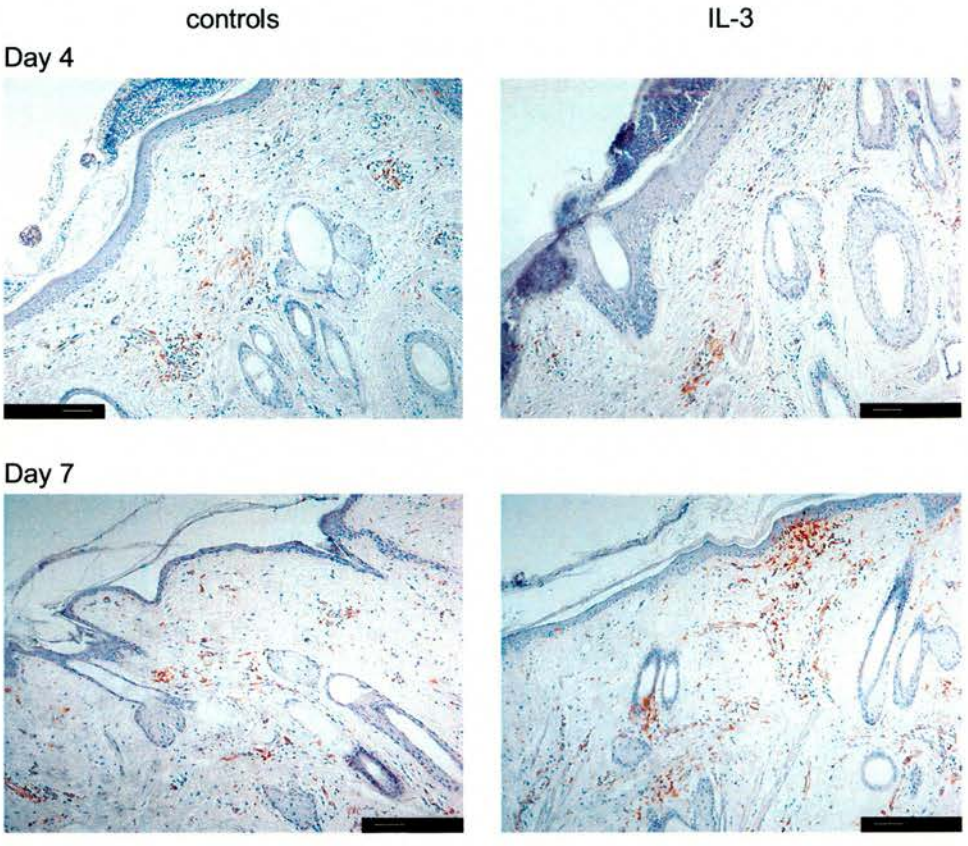

Figure 3.18 (cont.)

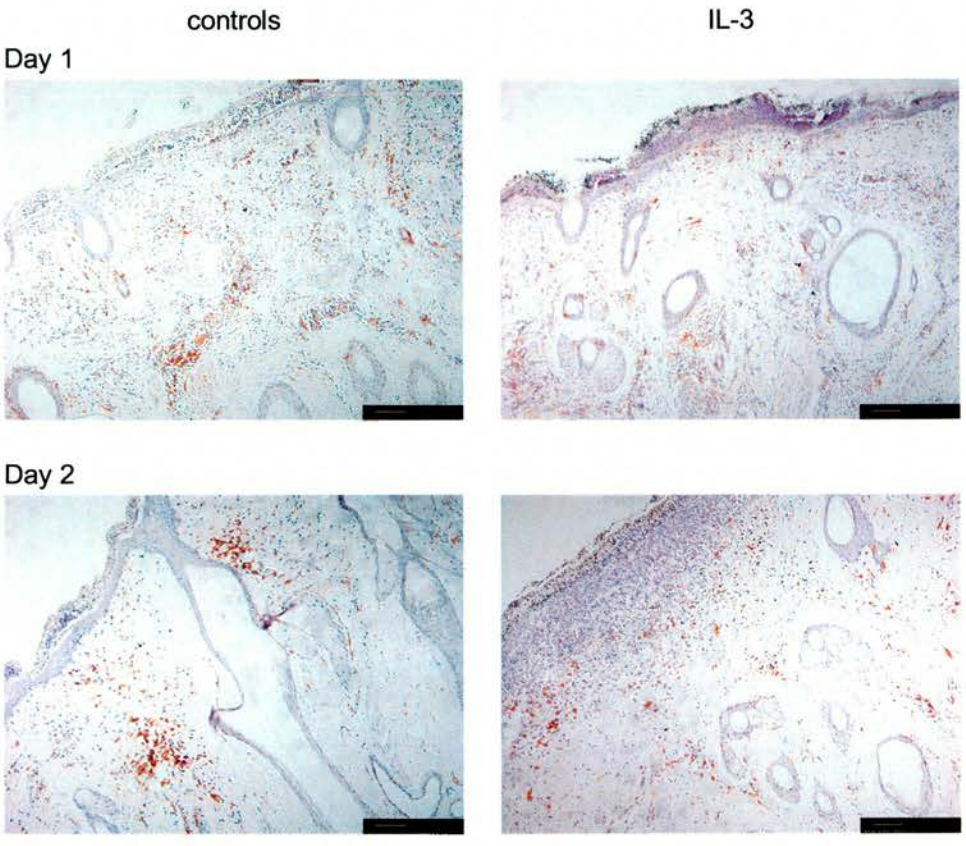

Figure 3.19 Identification of MHC class II^+ cells in skin vaccinated with pIL-3 and pEGFP-N1 (sheep 2). Skin sections were immunolabelled with mAb VPM 54 (MHC class II DRα) after gene-gun bombardment with pIL-3 (right panels) and pEGFP-N1 (left panels). Sections were counterstained with haematoxylin. (Scale bar = 250μm.)

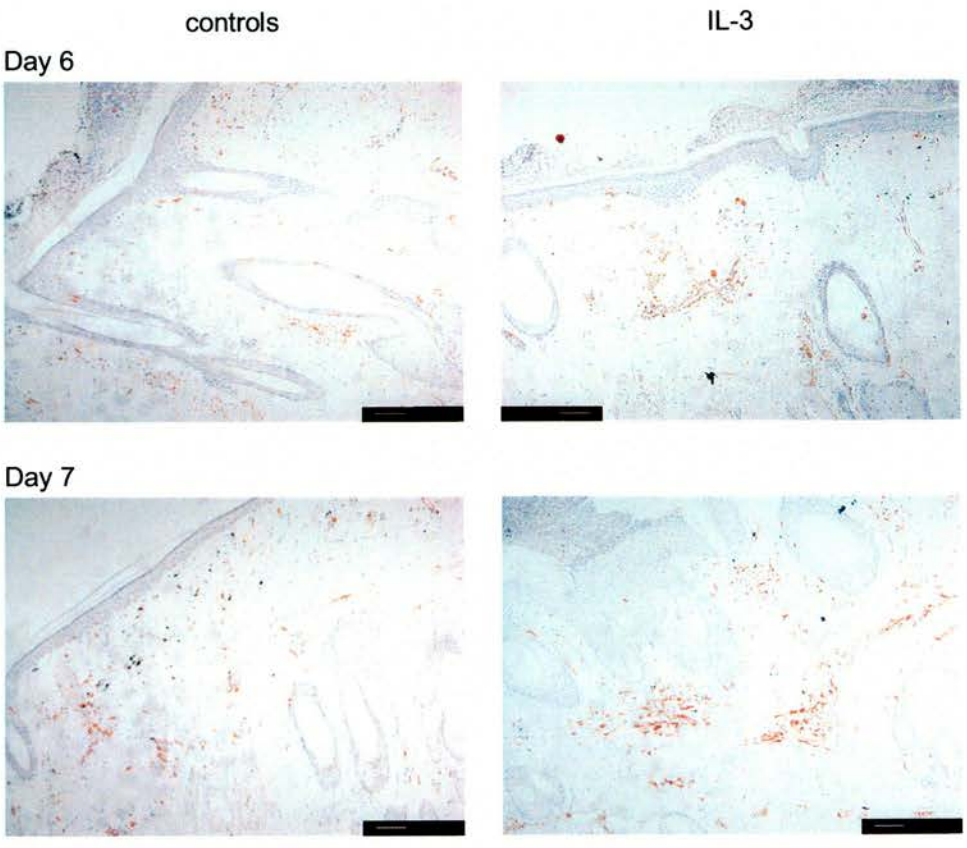

Figure 3.19 (cont.)

Immunoperoxidase staining of CD45RA$^+$ cells

Generally more CD45RA$^+$ lymphocytes were present in skin 24 hours after pIL-3 administration than observed in control-vaccinated skin (Figure 3.20a,b). Importantly, serial sections stained with VPM 54 and 73B mAb showed a similar pattern of staining; MHC class II$^+$ CD45RA$^+$ cells (possibly B cells) were generally present deep within the dermis. In addition, slightly more CD45RA$^+$ lymphocytes were present in the control-vaccinated skin than in non-vaccinated skin, indicating that an influx of CD45RA$^+$ lymphocytes is a result of the damage elicited to the skin during the gene-gunning procedure and/or administration of prokaryotic DNA. From 3–6 days, similar numbers of CD45RA$^+$ cells were apparent in pIL-3 vaccinated skin sections, although numbers were slightly elevated when compared to those in normal (non-vaccinated) skin sections (data not shown).

Immunoperoxidase staining of γδ T cells

Trafficking of γδ T cells into the skin was evident in both animals with both pIL-3 and pEGFP-N1 at the 24 hour time-point (Figure 3.20c,d). A modest increase in the numbers of γδ T cells was also evident in pIL-3 vaccinated skin biopsies approximately 5 days after gene-gun delivery when sections were compared with both pEGFP-N1 vaccinated biopsies and normal skin sections (data not shown). By day 7, the prevalence of γδ T cells in skin vaccinated with either plasmid appeared similar to those observed in normal skin.

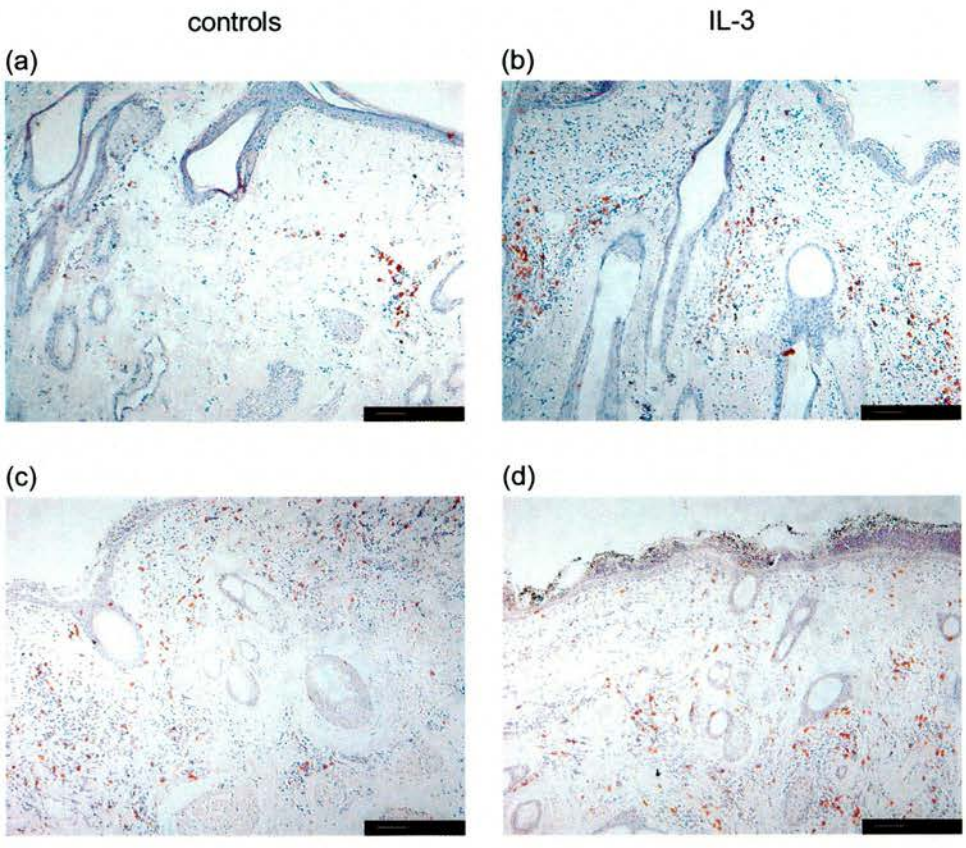

Figure 3.20 Immunolabelling of CD45RA$^+$ leukocytes and γδ T cells in skin after DNA vaccination with pIL-3 and pEGFP-N1. (a, b) Immunolabelling of CD45RA epitopes with mAb 73B (sheep 1); (c, d) immunolabelling of WC-1 epitopes with mAb CC15 24 hours after gene-gun delivery of pEGFP-N1 and pIL-3 (sheep 2). (Scale bar = 250μm.)

3.4.3 Summary of findings from biopsy experiment A

- pGM-CSF caused mass inflammation by 24 hours as shown by extensive pustule formation and dermal: epidermal effacing
- The early time-points (24–48 hours) revealed an infiltration of largely PMN after pGM-CSF administration, whereas mononuclear cells were the predominant cell type recruited at later time-points
- The most striking observation was the appearance of MHC class II^+ cells with the morphology of DC 72–96 hour after DNA vaccination with pGM-CSF
- Less consistent alterations to the skin were apparent after pIL-3 administration. pIL-3 caused less pathology than pGM-CSF, although the process of active exocytosis appeared to last longer
- Biopsies removed 24 hours after pIL-3 administration contained predominantly eosinophils (approximately 70–80% of the infiltrate). In addition, small mononuclear MHC class II $DR\alpha^+$ $CD45RA^+$ cells were present 24 hours p/v
- With the possible exception of later timepoints (6–7 days p/v), a pronounced infiltration of MHC class II^+ cells with the morphological appearance of DC was not observed after pIL-3 administration

3.5 Gene-gun administration of cytokine gene adjuvants over 24 hours

The results from biopsy experiment A (Section 3.4) necessitated a closer investigation into the histological events that take place within the first 24 hours, particularly since the peak inflammatory reaction appeared to have already taken place by 24 hours with pGM-CSF; earlier time-points were thus required to dissect the inflammatory events in more detail. It was also evident that the magnitude of the inflammatory reaction was greater with pGM-CSF than with pIL-3. At this point in the study, pIL-3 also contained the GFP gene and it was speculated that the fusion protein may have had more limited effects *in vivo*. The GFP gene was therefore removed from the IL-3 construct for future experiments. It was also imperative to include the NF cytokine constructs to ensure that the results from biopsy experiment A were indeed due to the biological activities of each cytokine and not due to any stimulatory sequences (CpG motifs) within each cytokine gene. NF-GM-CSF and NF-IL-3 (herein referred to as NF-controls) were employed for all subsequent experiments. Further experiments were needed to confirm the findings of biopsy experiment A and to correlate the histological findings with the kinetics of plasmid gene expression and expression of proinflammatory cytokines (IL-1β, TNF-α and IL-18).

This part of the study investigated the course of local inflammation in ovine skin 1–24 hours after DNA vaccination with pGM-CSF, pIL-3 and NF-controls. Two clinically healthy sheep were vaccinated over 24 hours (biopsy experiments B and E) as illustrated in Figure 3.21. Details of biopsy experiments are listed in Chapter 2 (Table 2.8). For these experiments (and those that followed), the GFP gene was removed from the IL-3 construct, which was sequenced to confirm that no alterations to the IL-3 gene had occurred. *In vitro* mRNA expression was again validated by RT-PCR (data not shown). For consistency, the GFP gene was also removed from both NF-controls. Each plasmid construct was administered in triplicate at each time-point. Immediately at post-mortem one half of each biopsy was fixed (either in ZSF or paraformaldehyde) for immunohistochemistry and H & E staining, and the other half of tissue was placed into RNA*later*™ for subsequent RNA extraction.

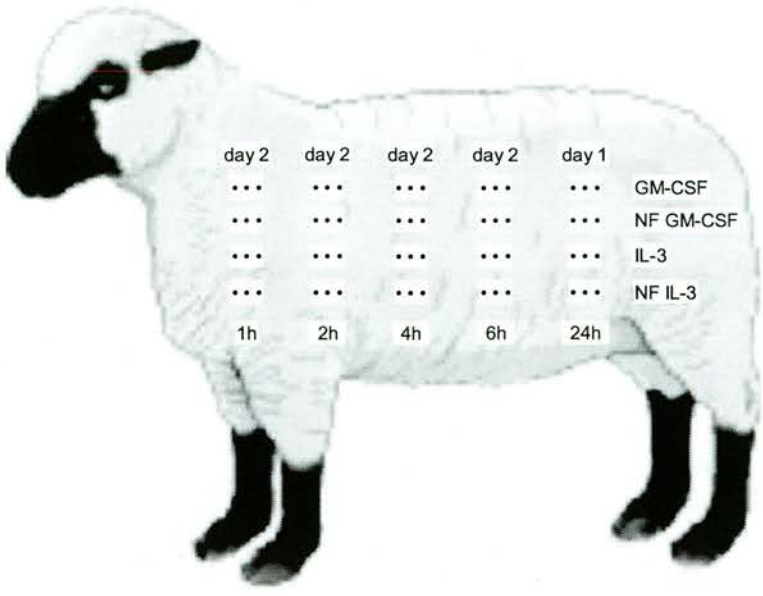

Figure 3.21 A representative example of a biopsy experiment carried out over 24 hours (biopsy experiments B and E, Table 2.8). In this experiment, two animals were vaccinated three times with each of the four plasmid constructs (pGM-CSF, pIL-3 and the NF-controls) by gene-gun administration over 24 hours (outlined in chapter 2). Sheep were sacrificed and biopsies were immediately removed and bisected. Biopsies used for RNA extraction and subsequent quantitative RT-PCR analysis were immediately placed into RNA*later*™.

3.5.1 Effects of pGM-CSF in skin 1–24 hours after administration

3.5.1.1 Skin histopathology after gene-gun vaccination with pGM-CSF

A histological examination of tissue sections was performed at intervals after gene-gun delivery of both pGM-CSF and the NF-control. The NF-control vaccinated biopsies revealed a slight increase in dermal cellularity at all time points investigated when compared to normal non-vaccinated skin biopsies (Figure 3.22); an increase in cellularity was evident as early as 1 hour after plasmid administration, where neutrophils were the predominant infiltrate. Neutrophils continued to be recruited over the time-course and accumulated in the dermis after DNA vaccination with the NF-control plasmid. There was however no pustule formation nor effacing of the dermal: epidermal junction 24 hours after gene-gun bombardment.

In accord with biopsy experiment A, gene-gun vaccination with pGM-CSF caused a severe inflammatory reaction by 24 hours, again characterised by pustule formation and epidermal–dermal junction separation due to *en masse* neutrophilic trafficking (Figure 3.22). Histopathologically, the first change in the skin after pGM-CSF delivery was the presence of marginating PMN within the dermal blood vessels, as was observed after delivery of the NF control. The infiltration of PMN was however substantially more pronounced after pGM-

CSF administration than after administration of the NF control; increased numbers were evident as early as 2 hours, but invariably by 4 hours and PMN tended to accumulate under the keratin layer. At this time, the epidermal layer was still recognisable, although changes in some of the epidermal cells were apparent. Between 4 and 6 hours p/v, large numbers of neutrophils continued to migrate to the site, and the development of a microabscess was apparent as PMN continued to accumulate under the keratin layer. By 24 hours the epidermal layer was not readily recognisable, due to a universal florid epidermal reaction involving PMN. As observed in biopsy experiment A, a mixed dermal reaction was also apparent by approximately 24 hours, composed of eosinophils and neutrophils and also some mononuclear cells.

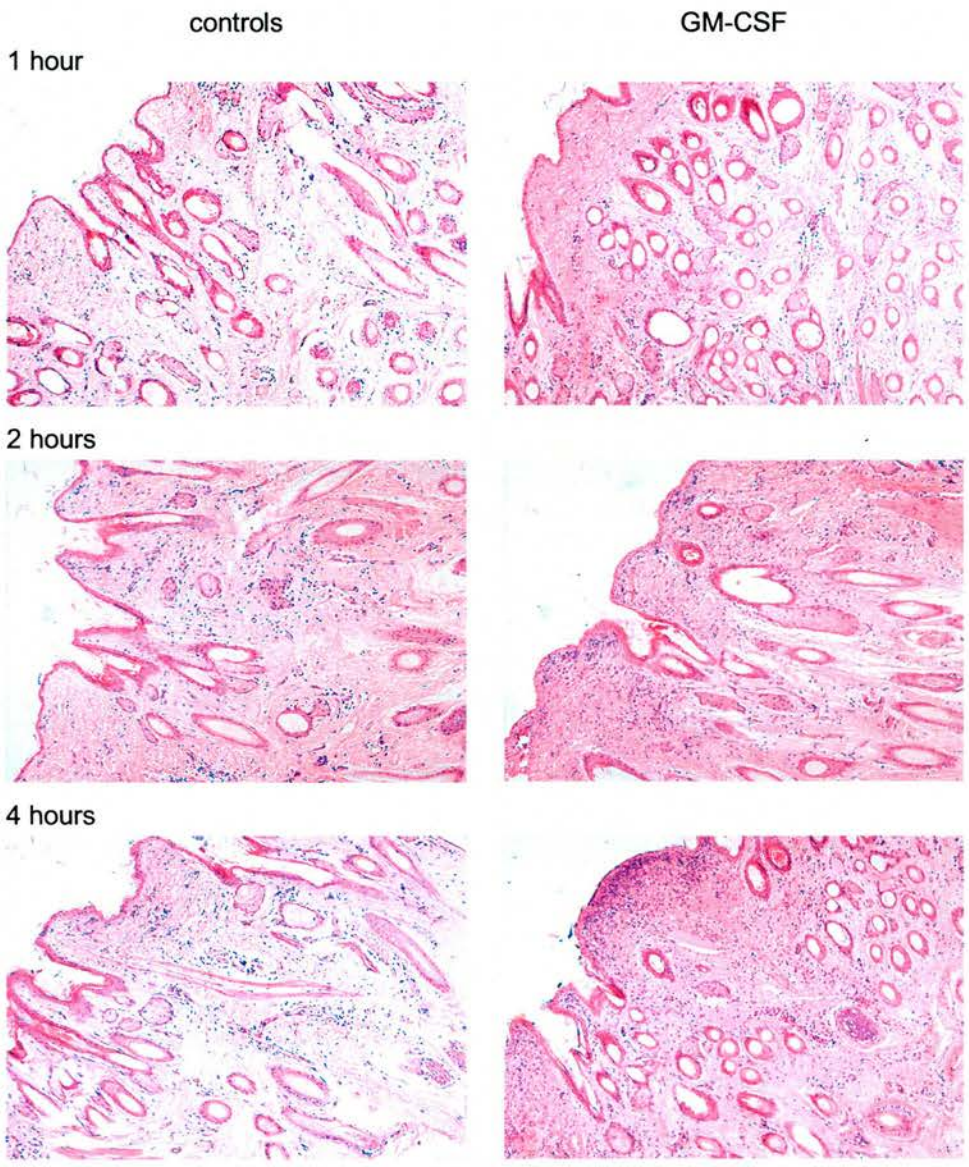

Figure 3.22 Comparison of the inflammatory events induced in the skin from 1–24 hours after gene-gun administration of pGM-CSF and the NF-control. Skin biopsies were removed immediately at post mortem, fixed in ZSF and stained with H & E. Representative images from each of the time-points are shown. After pGM-CSF delivery, many neutrophils have accumulated under the keratin layer and pustule formation is evident by approximately 4 hours. (Original magnification, ×80.)

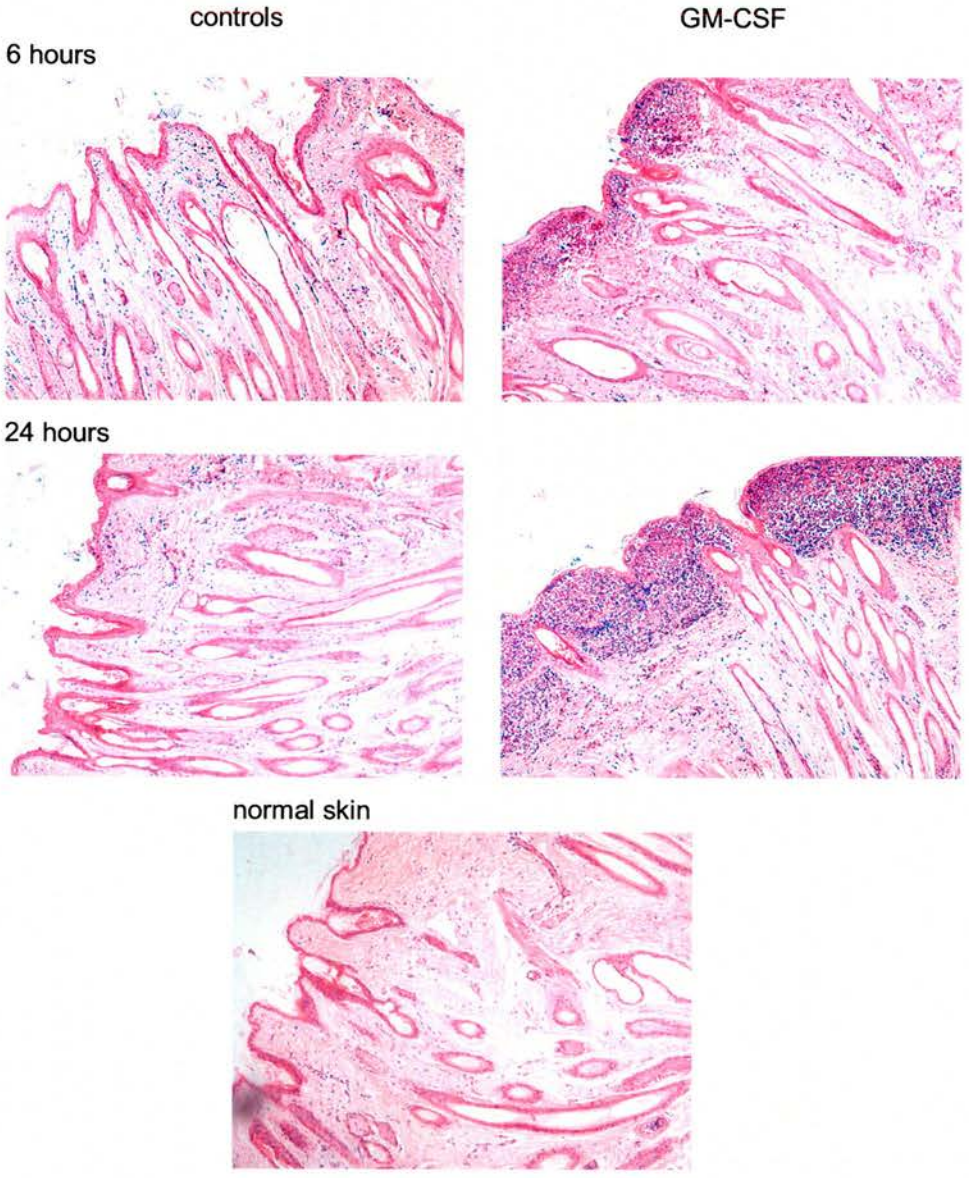

Figure 3.22 (cont.)

3.5.1.2 Immunohistological analysis of pGM-CSF vaccinated skin

The biopsies were bisected and stained with mAb in order to attempt to identify cell populations recruited to the skin over the time-course.

Immunoperoxidase staining of MHC class II$^+$ cells

Immunoperoxidase staining was carried with mAb VPM 54 (anti MHC class II DRα) on skin sections removed from pGM-CSF and NF-control sites and compared with normal (non-vaccinated skin) Representative images from each time-point are shown (Figure 3.23). Qualitative assessment of the sections obtained from NF-control vaccinated skin indicated a slight increase in the number of DR$^+$ cells when compared to normal skin at 6 and 24 hours p/v, whereas numbers of DR$^+$ cells were slightly elevated at all time-points (1–24 hours) after pGM-CSF administration. In addition, staining of endothelial cells and cells within the dermis (near to blood vessels) was evident as early as 1 hour after pGM-CSF administration. By 2–4 hours, DR$^+$ cells were identified amongst the infiltrating PMN population which had accumulated near to the epidermis and in the superficial dermis. At 6 hours, little difference was observed after administration of either of the plasmids; however, by 24 hours, a more pronounced infiltration of DR$^+$ cells was apparent in pGM-CSF vaccinated skin than in NF-control vaccinated skin.

Immunoperoxidase staining of CD45RA$^+$ lymphocytes and γδ T cells

Staining with mAb 73B was carried out in order to identify CD45RA$^+$ lymphocytes in skin before and after DNA vaccination with pGM-CSF and the NF-control. At 1, 2 and 4 hours after administration of either plasmid, no changes in the number of CD45RA$^+$ cells were evident when sections were compared to normal skin. At 6 and 24 hours p/v, a slight increase in CD45RA$^+$ lymphocytes was observed after administration of both pGM-CSF and NF-control. No changes in the number of γδ T cells (data not shown) were evident in any of the skin sections screened. Immunostaining with anti-CD4 and CD8 mAb showed that skin contains very few CD4$^+$/CD8$^+$ T cells and, as with γδ T cells there were no changes p/v.

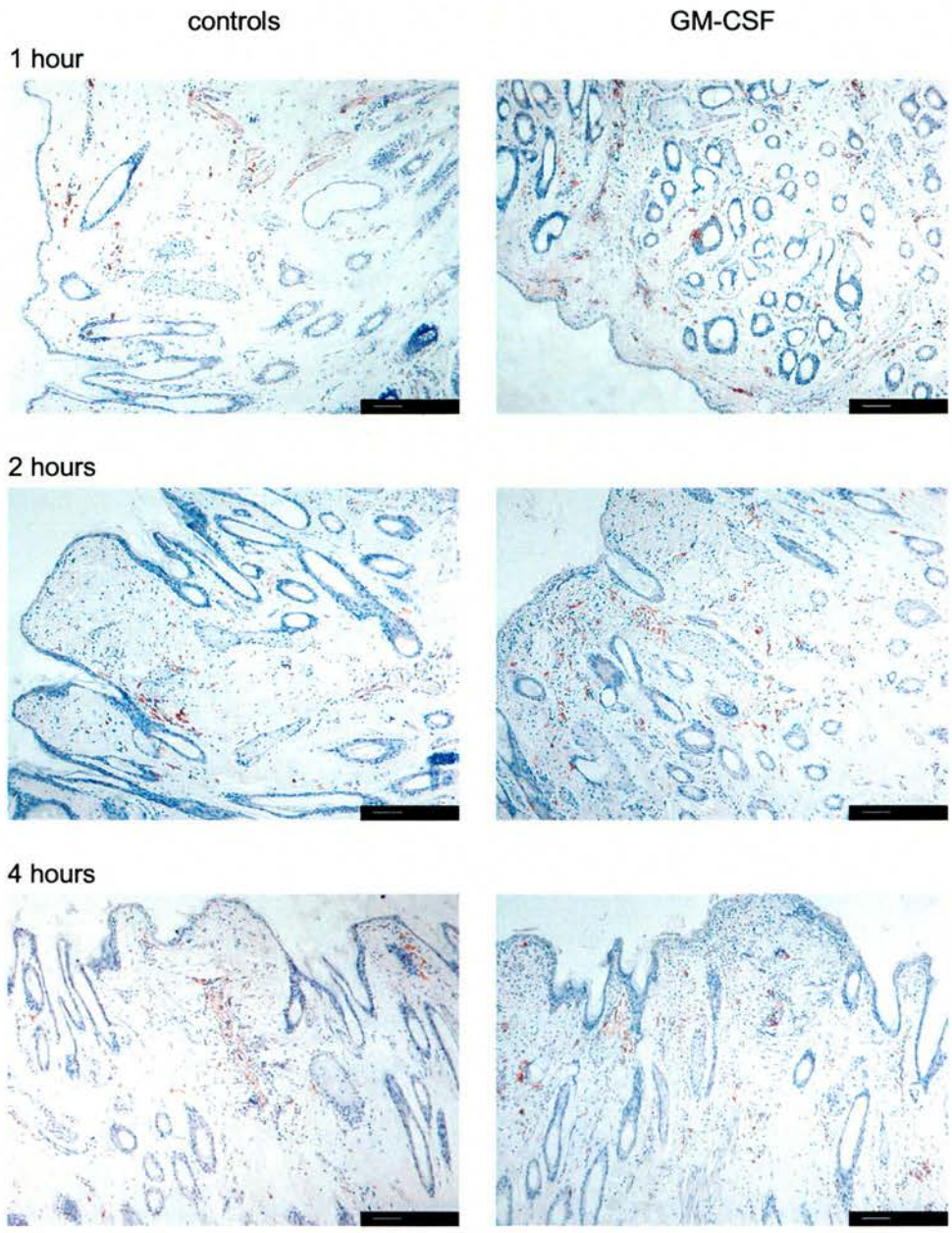

Figure 3.23 Immunolabelling of MHC class II^+ cells in skin 1–24 hours after gene-gun administration of pGM-CSF and the NF-control. Skin sections were immunoperoxidase labelled with mAb VPM 54 (MHC class II DRα). Representative images are shown after administration of pGM-CSF (right panels) and the NF-control (left panels). Sections were counterstained with haematoxylin. (Scale bar = 250μm.)

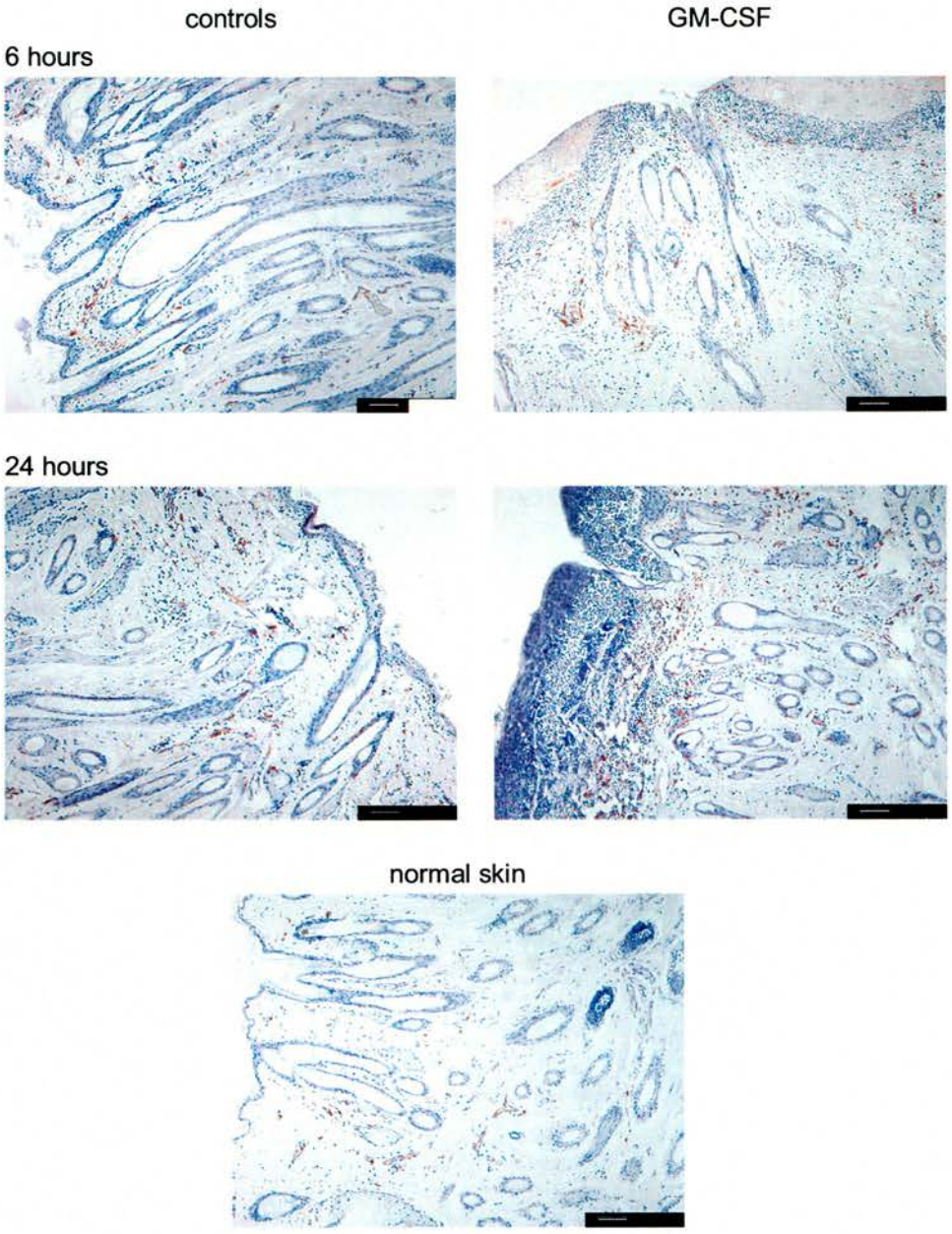

Figure 3.23 (cont.)

3.5.1.3 Cytokine mRNA expression in skin after gene-gun delivery of pGM-CSF

Quantitative RT-PCR was used to measure the kinetics of GM-CSF mRNA expression in skin 1–24 hours p/v. Since proinflammatory cytokines are well documented to be involved in the maturation of DC and in the migration of DC (as outlined in the Introduction), IL-1β, TNF-α and IL-18 mRNA transcripts were also quantified. Each plasmid construct was administered by gene-gun vaccination three times to the skin on the flank of two sheep over 24 hours. Immediately at post-mortem each biopsy was removed using a sterile biopsy punch and bisected. Half of each biopsy was placed into RNA*later*™ (to stabilise RNA species). Biopsies were stored at –80°C until RNA extraction was performed. Occasionally gold dust was not observed after gene-gun delivery; such "miss-fires" were noted at the time of the experiment and RNA was not extracted from these biopsies.

GM-CSF mRNA expression

It was evident that plasmid DNA from the original vaccination procedure was not completely degraded by the DNase step included in the RNA extraction procedure (Section 2.6). It was imperative that a method was developed that ensured that residual plasmid DNA was removed in order to accurately assess the kinetics of GM-CSF (and IL-3) mRNA expression. A method to degrade plasmid DNA was developed and optimised using RNA spiked with pGM-CSF and pIL-3. This involved retreating RNA samples in solution with DNase in combination with Pst-1 or Hinf-1 in order to degrade plasmids containing either pGM-CSF or pIL-3 respectively (Section 2.6). Prior to the evaluation of cDNA samples by quantitative RT-PCR, control (–RT) samples were first amplified with GM-CSF or IL-3 specific primers on the LightCycler®. Specific product was confirmed by melting curve analysis in combination with gel electrophoresis. If specific product was detected in any of the control (–RT) samples the cDNA was not used for analysis. Instead, further treatment of the RNA was carried out, or, if insufficient material was available, treatment of the original RNA sample was again performed. In either case, specific product was verified to be absent in the control (–RT) samples by amplification of these samples on the LightCycler® with GM-CSF or IL-3 primers.

Due to problems with eliminating residual plasmid DNA contained within the RNA samples early on in the study (biopsy experiments B (and C)), triplicate cDNA samples for each time-point were not initially available. Due to low yields of RNA after complete removal of contaminating plasmid DNA, RNA samples from sheep 3 (biopsy experiment B) were initially pooled. Figure 3.24 is representative of data obtained from cDNA samples analysed

on three separate occasions on the LightCycler® with GM-CSF specific primers and illustrates the reproducibility of the experiment.

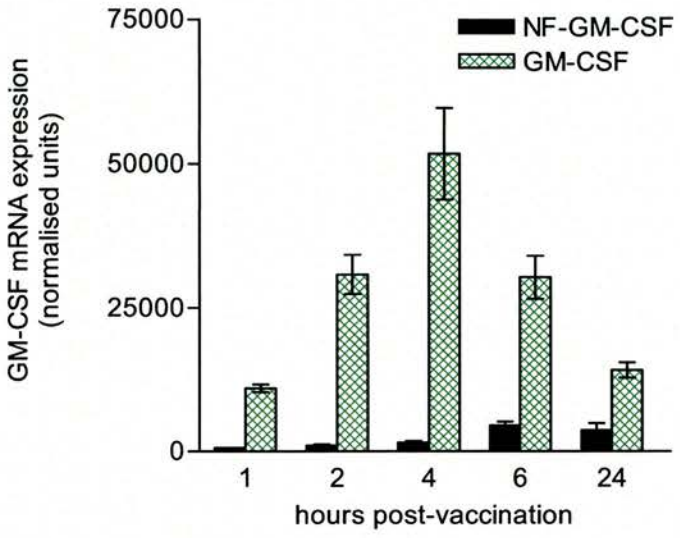

Figure 3.24 GM-CSF mRNA expression in skin 1–24 hours after gene-gun delivery of pGM-CSF and the NF-control. Representative of three independent LightCycler® experiments where cDNA samples from each time-point (from sheep 3, biopsy experiment B) were pooled. GM-CSF mRNA expression was normalised for the expression of GAPDH mRNA. Data are presented as mean ± SEM. pGM-CSF induced significantly more GM-CSF mRNA than the NF-control over 24 hours ($p < 0.02$, unpaired Student t-test).

When suitable methods to eradicate plasmid DNA were employed, more cDNA samples became available from biopsy experiment B as illustrated in Figure 3.25a. Figure 3.25b illustrates expression of GM-CSF mRNA in sheep 4 (biopsy experiment E), where triplicate biological samples were available for each of the time-points (1–24 hours) and analysed alongside cDNA derived from normal skin.

GM-CSF mRNA was detected in normal skin in both animals and is represented as a solid line on Figure 3.25a. Endogenous expression of GM-CSF mRNA was only just within the limit of quantification of the assay in sheep 4; (0.65 normalised units) and is not represented on Figure 3.25b. In both animals, an increase in GM-CSF mRNA was evident after gene-gun bombardment with the NF-control and expression peaked approximately 6 hours p/v; a 16 fold increase in GM-CSF mRNA was observed in sheep 3. In contrast, administration of pGM-CSF resulted in a more pronounced linear increase in GM-CSF mRNA in both animals, peaking at approximately 4 hours. Relative to levels induced by administration of the NF control, a 22 fold increase in GM-CSF mRNA was observed in sheep 3 and a 12-fold increase was observed in sheep 4 at this time-point. From 4–24 hours p/v, GM-CSF mRNA expression then declined in an almost linear fashion. Expression of GM-CSF transcripts was significantly higher in pGM-CSF vaccinated skin compared to skin which had been vaccinated with the NF-control over the entire time-course in sheep 3 ($p < 0.002$) and a statistically significant difference was also evident 4 hours p/v in sheep 4 ($p < 0.04$).

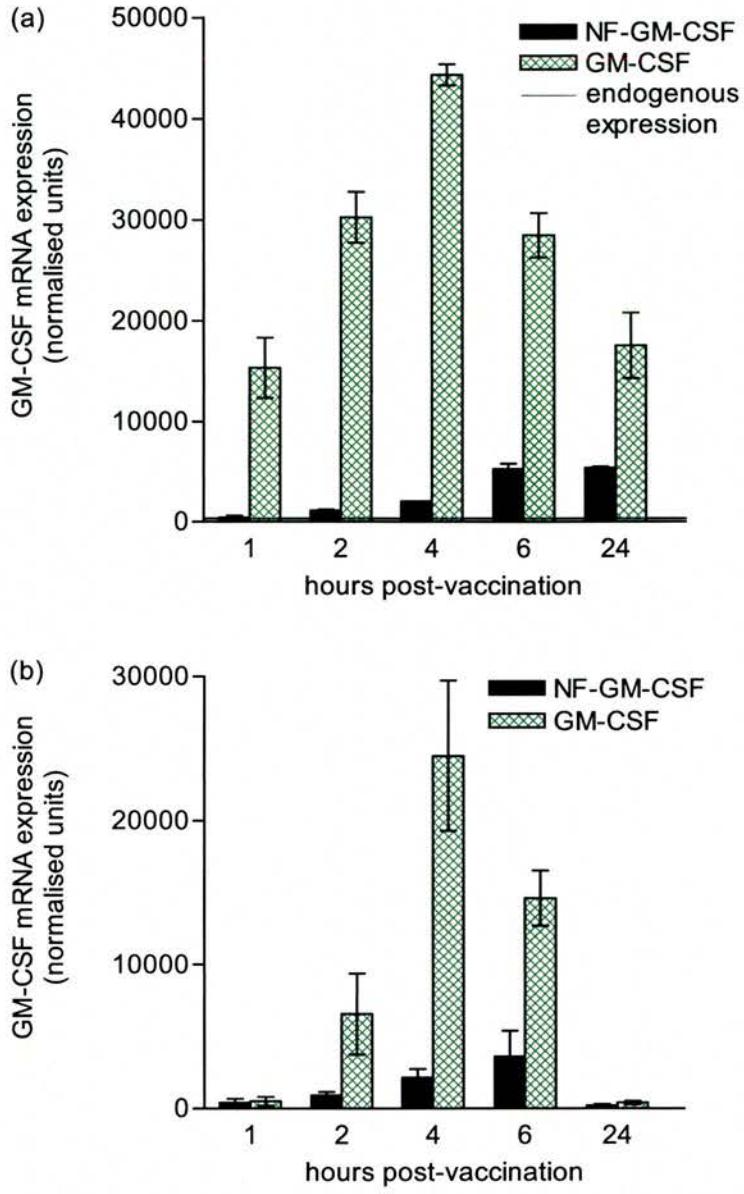

Figure 3.25 GM-CSF mRNA expression in skin 1–24 hours after gene-gun delivery of pGM-CSF and the NF-control. (a) Sheep 3 (biopsy experiment B; n = 2–3 biopsy samples for each time-point); (b) sheep 4 (biopsy experiment E; n = 3 biopsy samples for each time-point). Data are presented as mean ± SEM. Endogenous GM-CSF expression is represented as a solid line in (a). Endogenous GM-CSF mRNA expression was also detected in normal skin in sheep 4 (0.65 normalised units) and cannot be represented on this figure.

IL-1β mRNA expression

IL-1β mRNA was detected in normal skin in both animals and is represented as a solid line in Figure 3.26a (sheep 3). Administration of the NF-control and pGM-CSF induced a similar (approximately 2-fold) increase in IL-1β mRNA expression 1 hour after gene-gun delivery in this animal. Endogenous IL-1β mRNA expression in skin isolated from sheep 4 was only just within the limit of detection of the assay and is not represented on Figure 3.26b; however, a marked increase was also evident one hour after gene-gun administration of either plasmid in this animal (Figure 3.26c). Expression of IL-1β mRNA peaked 4 hours after administration of the NF-control in both animals.

In marked contrast, gene-gun bombardment of skin with pGM-CSF caused a much more pronounced increase in IL-1β mRNA. Expression of IL-1β mRNA followed a similar trend in both animals, where levels of IL-1β increased in an almost linear fashion over the first 24 hours after pGM-CSF administration. By 24 hours, a 200 fold increase in IL-1β mRNA was evident in sheep 3 (relative to IL-1β transcripts in NF-control vaccinated skin) and a 350 fold increase was evident in sheep 4. Moreover, where levels of IL-1β mRNA are compared after administration of either pGM-CSF or the NF-control in sheep 3, the difference is statistically significant over the entire time-course ($p < 0.02$, unpaired Student t-test). A statistically significant increase in IL-1β levels is also apparent 24 hours p/v in sheep 4 ($p < 0.002$, paired Student t-test).

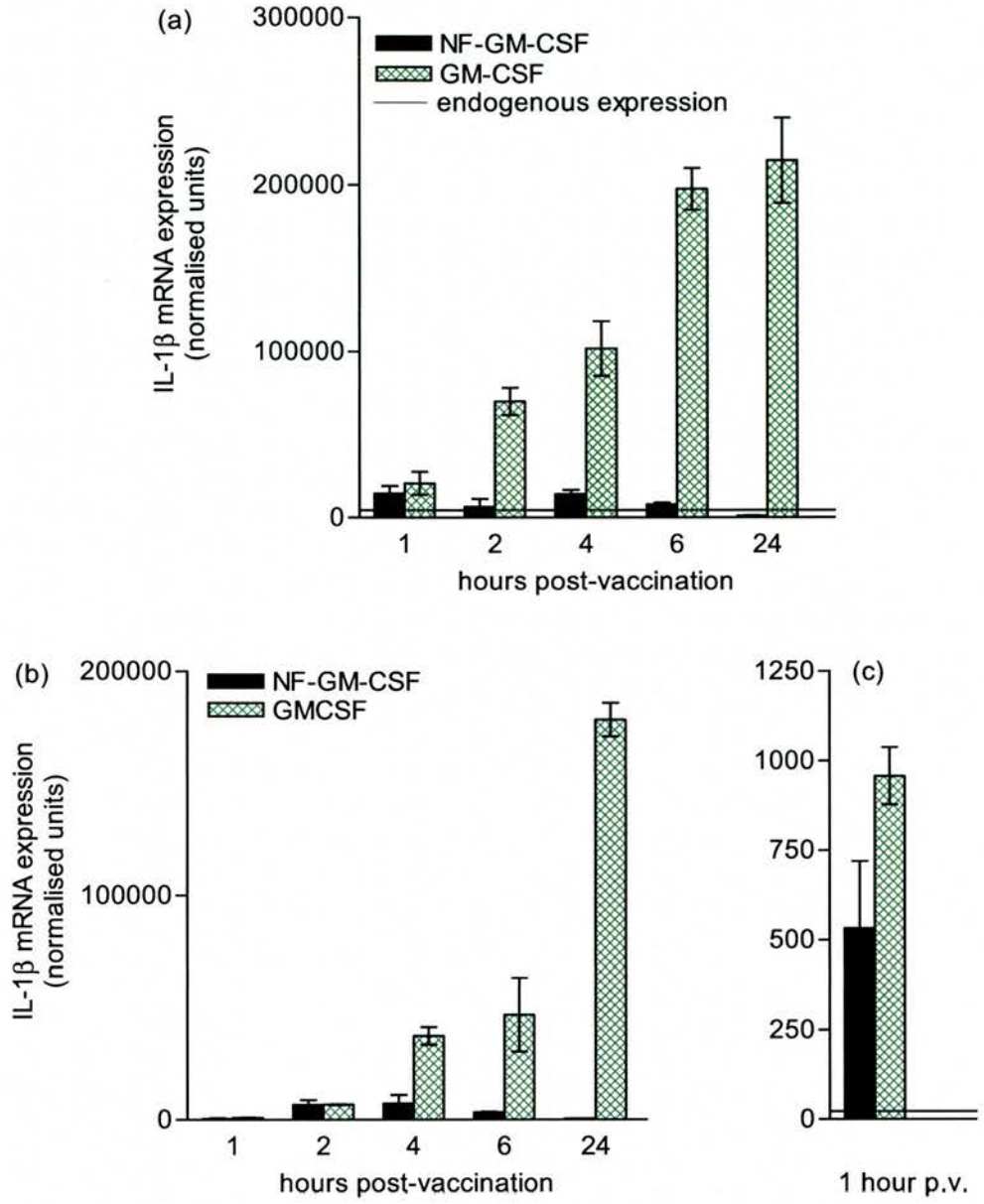

Figure 3.26 IL-1β mRNA expression in pGM-CSF and NF-control vaccinated skin from 1–24 hours. (a) Sheep 3, biopsy experiment B (n = 2–3 biological replicates; $p < 0.02$, unpaired Student t-test); (b) sheep 4, biopsy experiment E; n = 3 biological samples; (c) induction of IL-1β expression 1 hour after DNA vaccination with both pGM-CSF and the NF-control in sheep 4. Endogenous expression is represented by solid lines; data are presented as mean ± SEM.

IL-18 mRNA expression

Expression of IL-18 mRNA was similar following gene-gun delivery of either plasmid in sheep 3 (biopsy experiment B) (Figure 3.27a); indeed no statistically significant difference was apparent in skin samples where pGM-CSF had been administered when compared to NF-control vaccinated skin ($p > 0.05$). Endogenous IL-18 expression was also analysed in this LightCycler® assay and perhaps surprisingly, higher levels of IL-18 mRNA were observed in normal skin (represented as a solid line in Figure 3.27a) than in skin vaccinated with either pGM-CSF or with the NF-control. Endogenous expression of IL-18 was reanalysed in another experiment alongside cDNA samples obtained from NF-control vaccinated skin removed one hour after gene-gun vaccination (Figure 3.27b); a 5 fold reduction in IL-18 mRNA expression was again observed in gene-gun vaccinated skin.

In agreement with the findings from biopsy experiment B, there was no statistically significant difference in IL-18 transcripts in pGM-CSF or NF-control vaccinated skin in sheep 4 ($p > 0.05$). A decrease in IL-18 mRNA was also apparent after delivery of both plasmids in this animal from 1–6 hours and a further reduction was evident 24 hours p/v when levels are compared to normal skin (Figure 3.27c). Quantitative RT-PCR was repeated using two cDNA samples (derived from two biopsies) one hour after DNA vaccination with the NF-control or pGM-CSF. Samples were analysed alongside cDNA obtained from normal skin ($n = 2$). A similar (approximately 2–fold) decrease in IL-18 mRNA was again evident after delivery of either plasmid (Figure 3.27d).

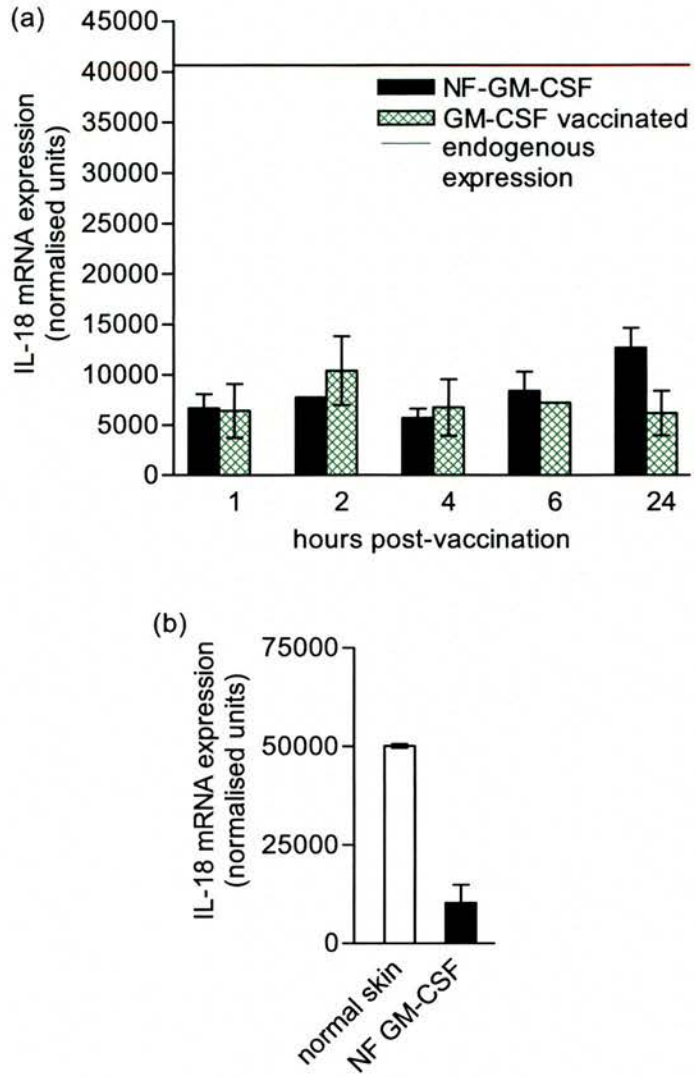

Figure 3.27 IL-18 mRNA expression in skin 1–24 hours after gene-gun vaccination with pGM-CSF and the NF-control. (a) Sheep 3 (biopsy experiment B, n = 2 biological samples); (b) sheep 3, expression of IL-18 in normal (non-vaccinated skin, n = 3) was analysed again alongside skin cDNA samples obtained 1 hour after administration of the NF-control. (c) Sheep 4 (biopsy experiment E, n = 3 biological samples); (d) sheep 4, analysis of IL-18 mRNA expression in normal skin and cDNA samples obtained from skin biopsies vaccinated with pGM-CSF and the NF-control (n = 2 biological samples). Endogenous expression is represented as a solid line; data are presented as mean ± SEM.

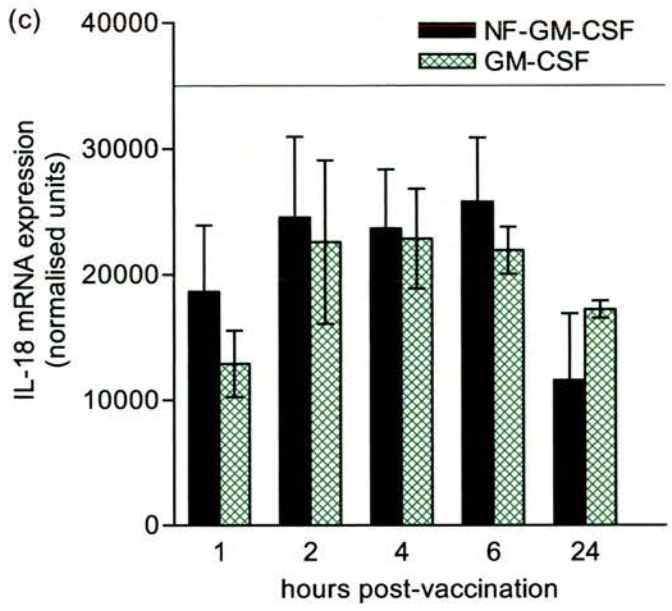

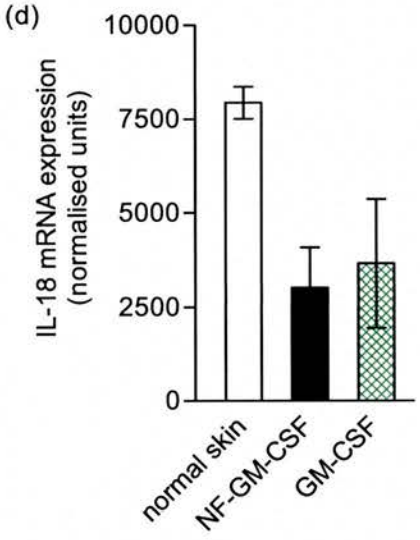

Figure 3.27 (cont.)

TNF-α mRNA expression

TNF-α mRNA expression was highly variable in the skin after gene-gun delivery of pGM-CSF and the NF-control. This was evident even in skin vaccinated with the same plasmid and harvested at the same time-points (Figure 3.28a,b). It was evident that gene-gun bombardment with the NF-control plasmid resulted in increased expression of TNF-α transcripts in the skin, which is illustrated in Figure 3.28b, where a 4–5 fold increase in TNF-α expression can be observed as early as 1 hour p/v (compared to endogenous TNF-α expression, which is illustrated as a solid line). From 1–6 hours p/v, TNF-α mRNA expression was variable and there was generally little difference between pGM-CSF or NF-control vaccinated skin in either animal. Conversely, by 24 hours, TNF-α transcripts were more abundant in pGM-CSF vaccinated skin than in NF-control vaccinated skin; a 2.5 fold difference was evident in sheep 3 and a 6–fold difference was evident in sheep 4.

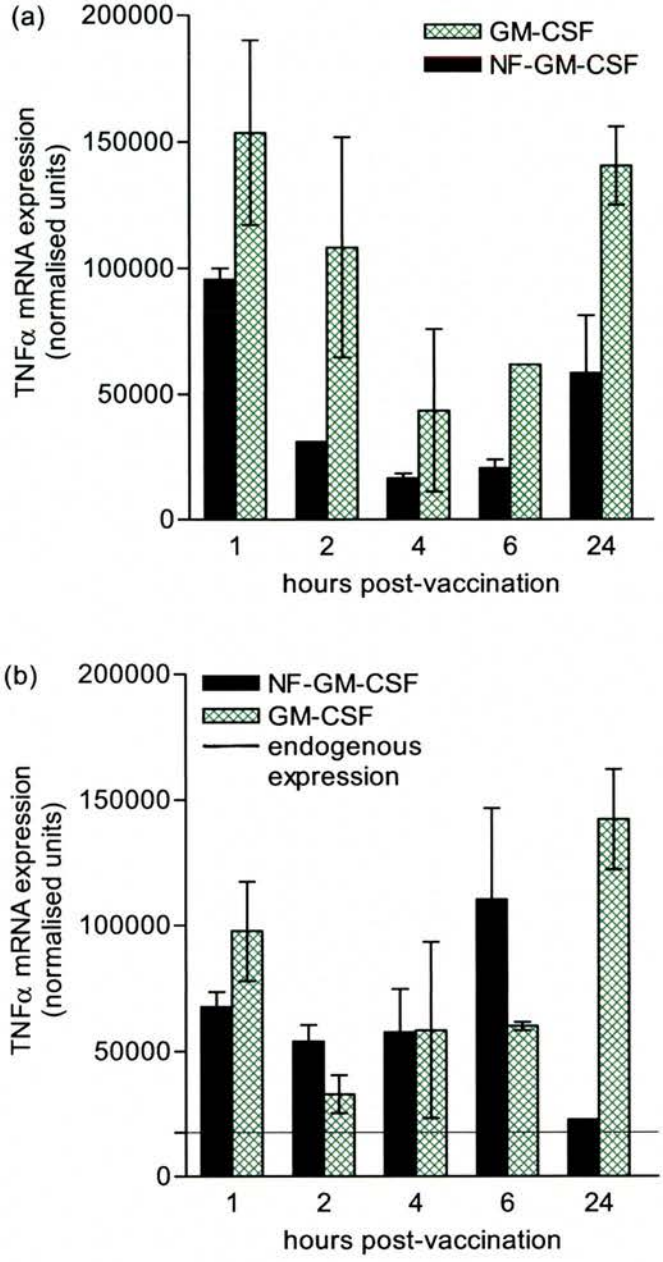

Figure 3.28 TNF-α mRNA expression in skin 1–24 hours after gene-gun administration of pGM-CSF and the NF-control. (a) Sheep 3 (biopsy experiment B); (b) sheep 4 (biopsy experiment E). Data are presented as mean ± SEM. Endogenous expression of TNF-α was not analysed in sheep 3.

IL-12p40 mRNA expression

LC-derived IL-12 plays a pivotal role in the initiation of contact hypersensitivity, a Th1 immune response in the skin. An increase in IL-12 protein was reported in a previous study after pGM-CSF administration in both murine skin and muscle (Perales et al, 2002). Due to the expense of quantitative RT-PCR using the LightCycler®, IL-12p40 mRNA expression was initially evaluated by conventional RT-PCR. Undiluted cDNA samples from each of the pGM-CSF vaccinated skin biopsies from sheep 4 (biopsy experiment E) were subjected to 40 cycles of amplification using an already optimised method with IL-12p40-specific primers. mRNAs encoding IL-12p40 were only detected in one out of the three pGM-CSF vaccinated biopsy samples from the 6 hour time-point and in one out of three samples obtained 24 hours p/v (Figure 3.29a), where an amplicon of approximately 250bp can be observed (expected size of amplicon is 243bp, Table 2.11). IL-12p40 mRNA expression was detected in normal skin and was subjected to further analysis by quantitative real-time RT-PCR (sheep 4, biopsy experiment E) (Section 3.6.1.3); however, no IL-12p40 transcripts were detected using this method where a 1:10 dilution of the cDNA was used.

IL-10 mRNA expression

Expression of the anti-inflammatory cytokine IL-10 was analysed by conventional RT-PCR essentially as described above. IL-10 transcripts were detected in all of the pGM-CSF vaccinated skin samples and also in normal skin obtained from the same animal (Figure 3.29b). No quantification of IL-10 was carried out using quantitative RT-PCR due to time constraints. Furthermore, although IL-10 transcripts were detected in normal skin by conventional RT-PCR, no specific product was detected on the LightCycler® after 40 cycles of amplification, where 1:10 dilutions of cDNA were used (Section 3.6.1.3). Undiluted cDNA samples require further analysis by quantitative RT-PCR.

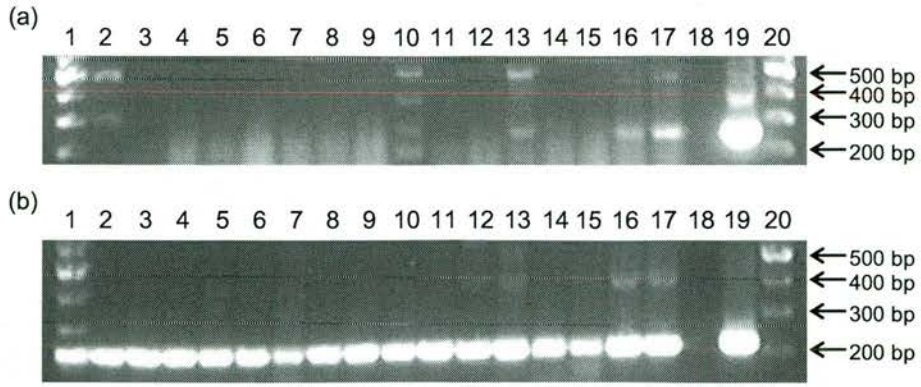

Figure 3.29 IL-12p40 (a) and IL-10 (b) mRNA expression in normal skin and in biopsies removed from pGM-CSF vaccinated skin sites. Amplification was carried out for 40 cycles. IL-12p40 mRNA expression is evident in normal (non-vaccinated) skin and also in one of the three skin samples removed 6 and 24 hours after administration of pGM-CSF. A ~250bp amplicon (expected size of amplicon is 243bp) can be observed in these samples. IL-10 mRNA expression is evident in all skin samples analysed.

Lanes 1 and 20, 100bp marker
Lanes 2–4, 1 hour p/v
Lanes 5–7, 2 hours p/v
Lanes 8–10, 4 hours p/v
Lanes 11–13, 6 hours p/v
Lanes 14–16, 24 hours p/v
Lane 17, normal skin
Lane 18, negative control (nuclease-free water)
Lane 19, positive control (1:1000 dilution of 1° PCR product)

3.5.1.4 Expression of TLR9 mRNA in normal skin and in plasmid DNA-vaccinated skin

A recent study reported that although TLR9 mRNA is not detected in normal murine skin, its expression can be induced by intradermal injection of either normal saline or CpG motifs (Liu et al, 2003). A similar experiment was carried out using cDNA obtained from skin biopsies removed from non-vaccinated skin sites and also using cDNA from pGM-CSF and NF-control vaccinated skin from biopsy experiment E (1–24 hours). Importantly, and in contrast to murine skin, TLR9 mRNA was detected in normal ovine skin from three different animals (Figure 3.30a). In all of the RT reactions, 1μg of total RNA was reverse transcribed. PCR amplification was carried out at 55°C for 40 cycles and all 50μl of each PCR reaction were loaded onto an agarose gel. TLR9 transcripts could only just be detected in some the vaccinated biopsies; biopsies obtained 4 hours after pGM-CSF delivery and 6 hours after delivery of the NF-control (Figure 3.30a,b); however, there did not appear to be any change in the relative intensity of any of the bands when visualised by UV when compared with normal skin samples, suggesting that CpG motifs/physical trauma does not cause TLR9 upregulation in sheep; however, this observation is merely qualitative and quantitative RT-PCR method should be employed to clarify this preliminary finding.

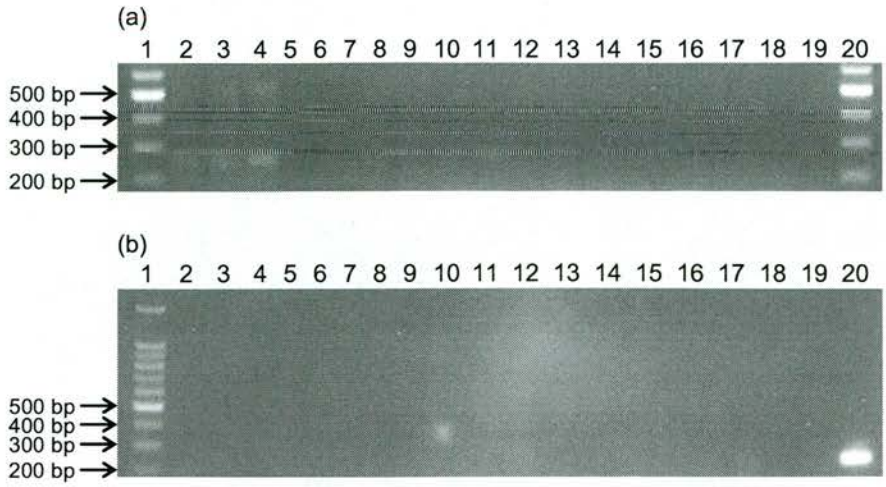

Figure 3.30 TLR9 mRNA expression in normal skin and after gene-gun delivery of pGM-CSF and the NF-control. 1µg of RNA was reverse transcribed from each skin biopsy. cDNA samples were amplified with ovine-specific TLR9 primers for 40 cycles and all 50µl of the PCR reaction were loaded onto an agarose gel (2%).

(a)
Lanes 1 & 20, 100bp marker
Lanes 2–4, normal skin obtained from biopsy experiments E, C and D
Lane 5 nuclease-free water
Lanes 7–9, 1 hour after NF-control
Lanes 10–12, 2 hours after NF-control
Lanes 13–15, 4 hours after NF-control
Lanes 16–18, 6 hours after NF-control
Lane 19, 24 hours after NF-control

(b)
Lane 1, 100bp marker
Lanes 2–3, 24 hours after NF-control
Lanes 5–7, 1 hour after pGM-CSF
Lanes 8–10, 2 hours after pGM-CSF
Lanes 11–13, 4 hours after pGM-CSF
Lanes 14–16, 6 hours after pGM-CSF
Lane 17-19 24 hours after pGM-CSF
Lane 20, positive control (combined cDNA obtained from ovine PBMC and spleen)

3.5.2 Effects of pIL-3 in skin 1–24 hours after administration

3.5.2.1 Skin histopathology after gene-gun vaccination with pIL-3

Microscopic evaluation revealed that gene-gun bombardment with pIL-3 caused severe pathological changes to the skin by 24 hours, whereas comparatively little inflammation was induced after gene-gun vaccination with the NF-control (Figure 3.31). Moreover, the kinetics of cellular infiltration were similar to that observed after gene-gun delivery of pGM-CSF, notably that at 1 hour after delivery of pIL-3 and the NF-control, little difference in cellularity was apparent, whereas at 2 hours significantly more PMN were evident in pIL-3 vaccinated skin sections, particularly associated with the epidermis. This accumulation of PMN in pIL-3 vaccinated sites was even more marked by 4 hours and continued to dramatically increase over the next couple of hours and by 24 hours pustule formation had occurred; effacing of the dermal: epidermal junction had taken place. In addition, an overlying epidermal oedema was evident 24 hours after pIL-3 administration in some of the sections screened. This was not observed in the previous experiment (biopsy experiment A). The dermal infiltrate was mixed and comprised predominantly of eosinophils after delivery of pIL-3. Mononuclear cells were also more prevalent within the dermis when sections were compared with normal and control-vaccinated skin sections, as was documented in the earlier biopsy experiment (A).

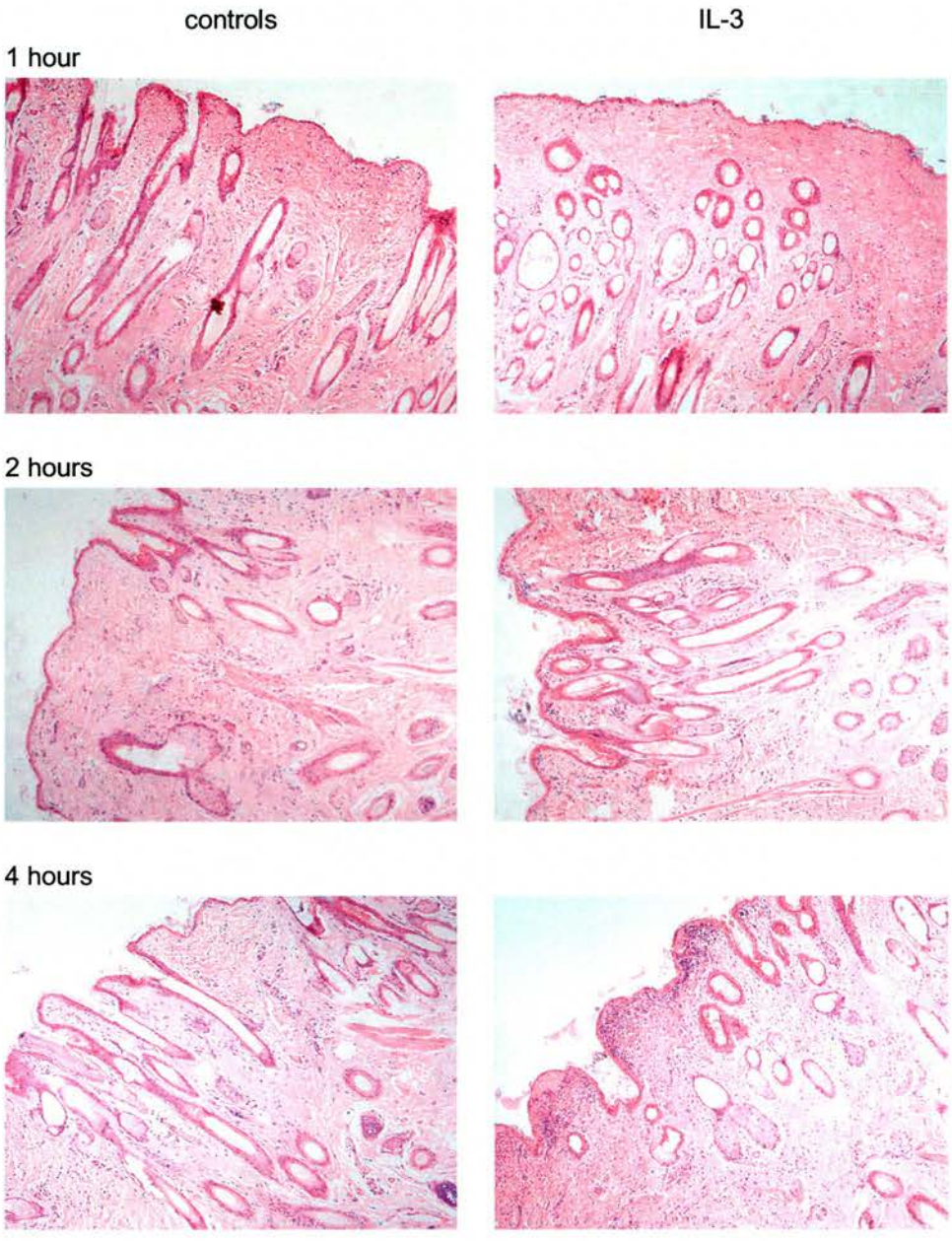

Figure 3.31 Comparison of the inflammatory events induced in the skin 1–24 hours after gene-gun administration of pIL-3 and the NF-control. Skin biopsies were removed immediately at post mortem, fixed in ZSF and stained with H & E. Representative images from each of the time-points are shown. (Original magnification, ×80.)

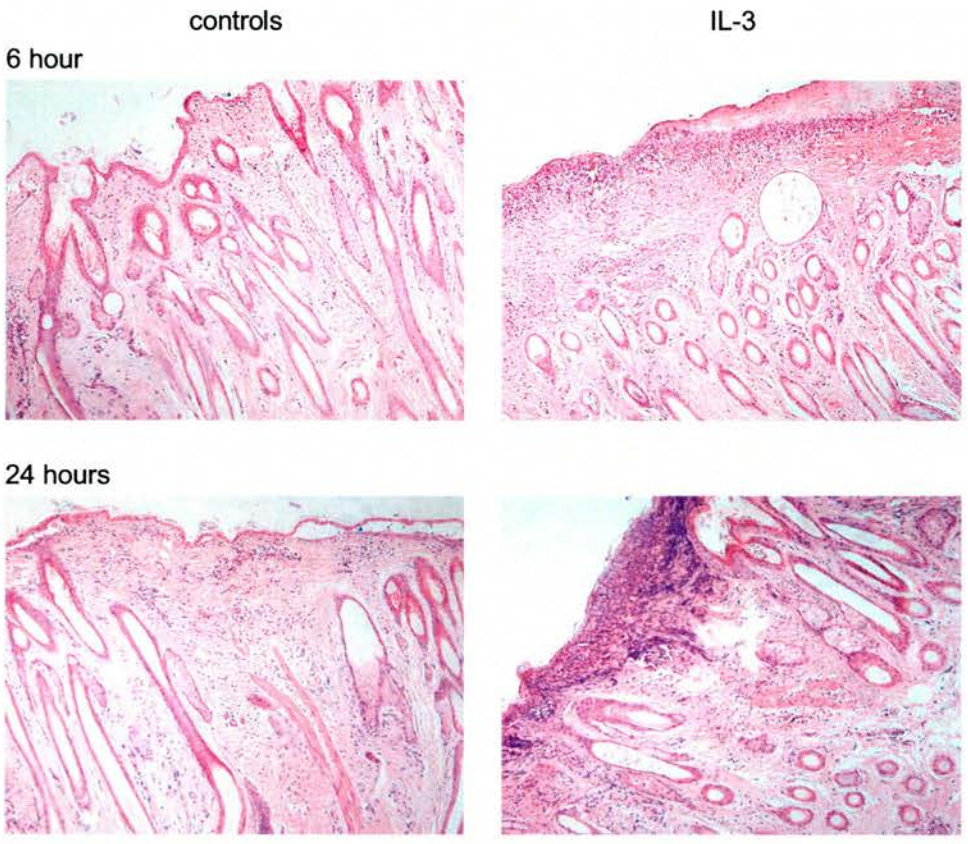

Figure 3.31 (cont.)

3.5.2.2 Immunohistological analysis of pIL-3 vaccinated skin

Skin sections were immunolabelled to identify cell populations recruited to skin 1–24 hours after pIL-3 administration. mAb VPM 54 (anti-MHC class II DRα) was applied to skin sections as previously described. There was little change in the prevalence of DR^+ cells within the skin 1–2 hours after gene-gun delivery of either pIL-3 or the NF-control (Figure 3.32), whereas from 4–24 hours, a slightly more pronounced infiltration was evident in pIL-3 vaccinated skin. DR^+ cells appeared to accumulate beneath the developing pustule.

Staining was also carried out with mAb 73B (anti-CD45RA). No difference in the number of $CD45RA^+$ cells was apparent 1–6 hours p/v in DNA vaccinated skin (pIL-3 and NF-control) when compared to normal skin (Figure 3.33); however, 24 hours after gene-gun delivery of the NF-control, a slight increase in $CD45RA^+$ lymphocytes was apparent and an even more marked infiltration was apparent after pIL-3 administration, particularly within the superficial dermis. In addition, immunoperoxidase staining was carried out with mAb IAH-CC15, which showed there was no change in γδ T cell numbers after gene-gun vaccination with either plasmid over the time-course (data not shown).

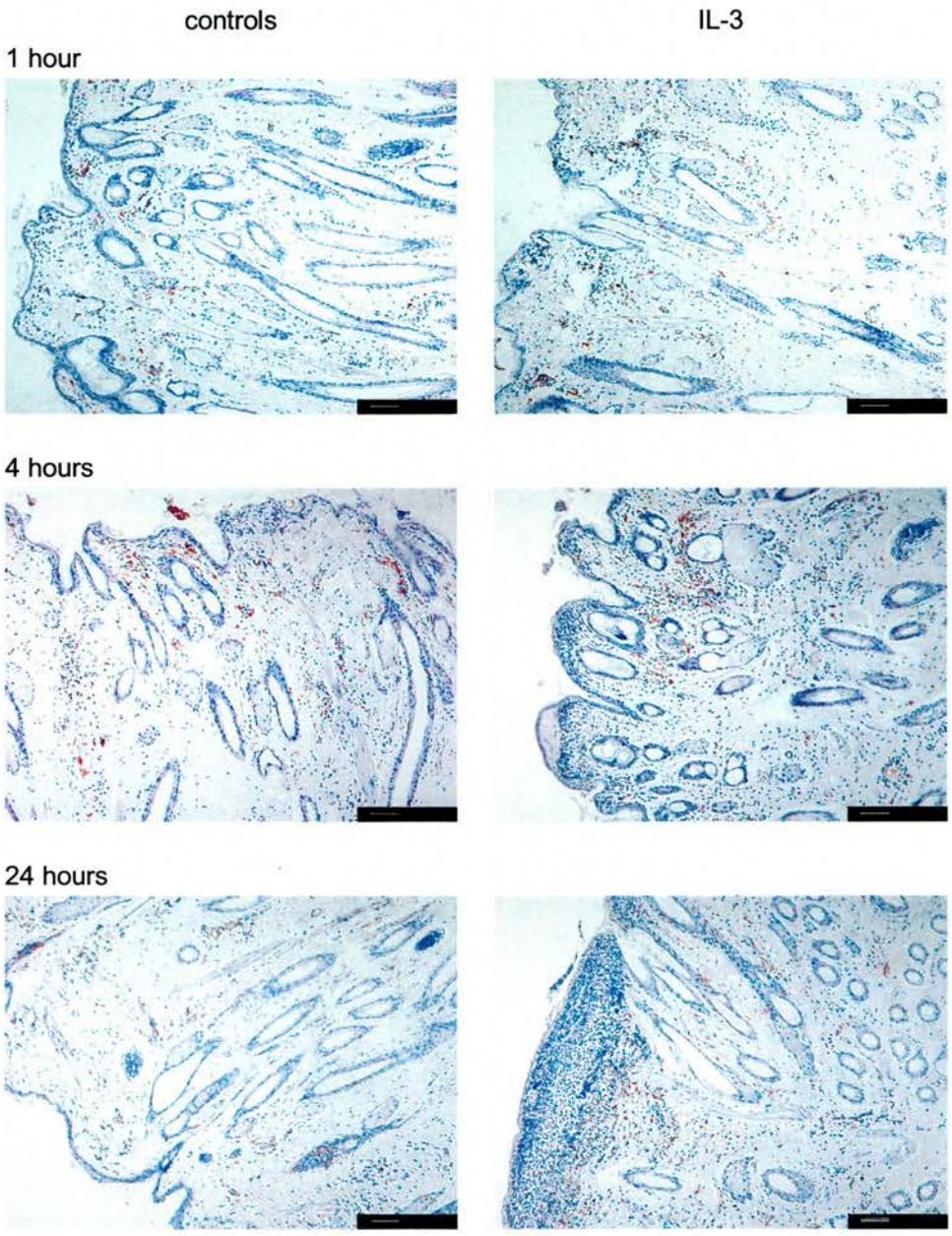

Figure 3.32 Infiltration of MHC class II^+ cells in skin 1–24 hours after gene-gun delivery of pIL-3. Sections were processed from skin vaccinated with pIL-3 (right-hand side panels) and the NF-control (left panels) and were immunolabelled with mAb VPM 54 (MHC class II DRα). Infiltrating DR^+ cells can be observed beneath the developing pustule 24 hours after pIL-3 administration. Sections were counterstained with haematoxylin. (Scale bar = 250μm.)

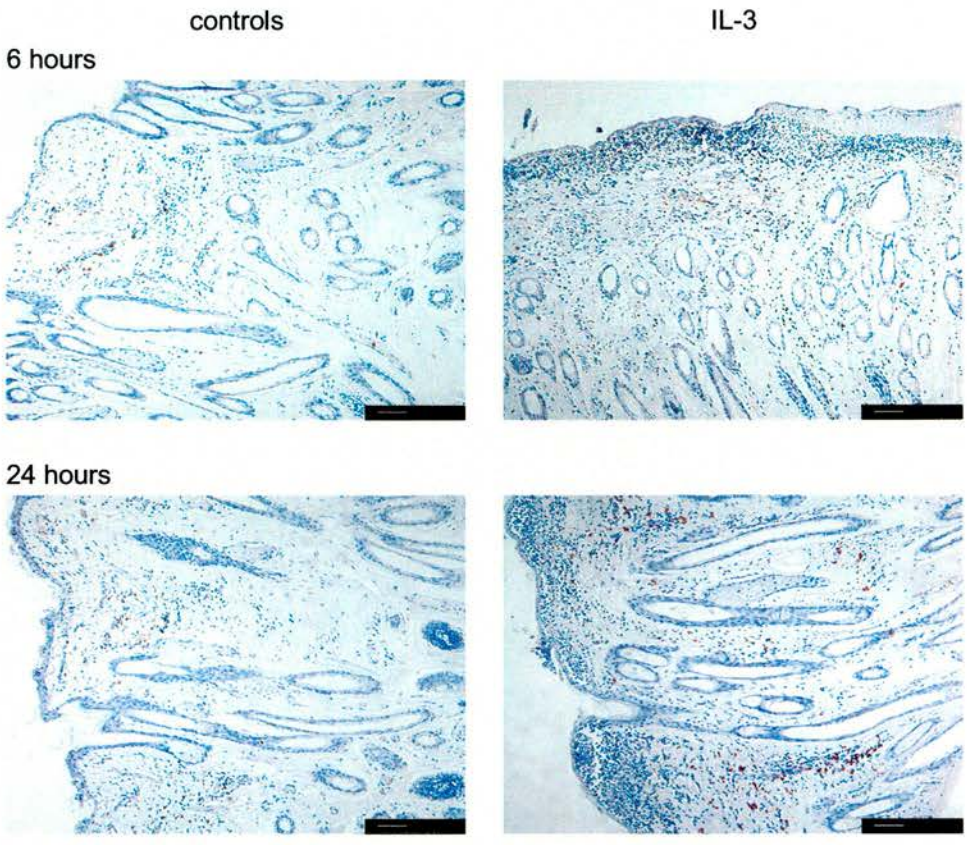

Figure 3.33 Immunolabelling of CD45RA$^+$ lymphocytes in pIL-3 and NF-control vaccinated skin 1–24 hours after gene-gun delivery. Skin biopsies were immunolabelled with mAb 73B (CD45RA). Representative images are shown from each time-point; pIL-3 (right-hand side panels) and the NF-control (left panels). Slight infiltration of CD45RA$^+$ cells is evident 24 hours after DNA vaccination with pIL-3. Sections were counterstained with haematoxylin. (Scale bar = 250μm.)

3.5.2.3 Cytokine mRNA expression in skin after gene-gun delivery of pIL-3

The kinetics of IL-3 mRNA expression and the expression of proinflammatory cytokines was investigated by quantitative RT-PCR. As discussed in Section 2.6, residual plasmid was a consistent problem after standard DNase treatment included in the protocol. RNA samples were therefore incubated again with DNase in combination with Hinf-1 in solution in order to degrade pIL-3. Prior to the evaluation of cDNA samples by quantitative real-time RT-PCR, control (–RT) samples were first amplified with IL-3 specific primers and validated to be free of residual pIL-3 (results not shown).

IL-3 mRNA expression

IL-3 mRNA was not detected in normal skin nor in samples obtained from control vaccinated skin (Figure 3.34), although this may be due to the lack of specificity of the primers, since extensive accumulation of non-specific product (melting temperature of 90°C compared to the specific IL-3 amplicon which melted at 88°C) was a consistent problem with this particular set of primers and occurred before 30 cycles of amplification. Due to the small size of the IL-3 insert, problems were encountered when designing primers since stringent parameters are required when the SYBR green method of quantification is employed.

IL-3 mRNA was detected in skin biopsies as early as 1 hour after gene-gun administration of pIL-3 in both animals (Figure 3.35). Levels of IL-3 mRNA increased in a linear fashion, peaking at 4 hours in sheep 3 and at 6 hours in sheep 4. From 4–24 hours, IL-3 mRNA declined in a linear fashion in sheep 3, whereas a more marked decrease was evident in sheep 4 after 6 hours.

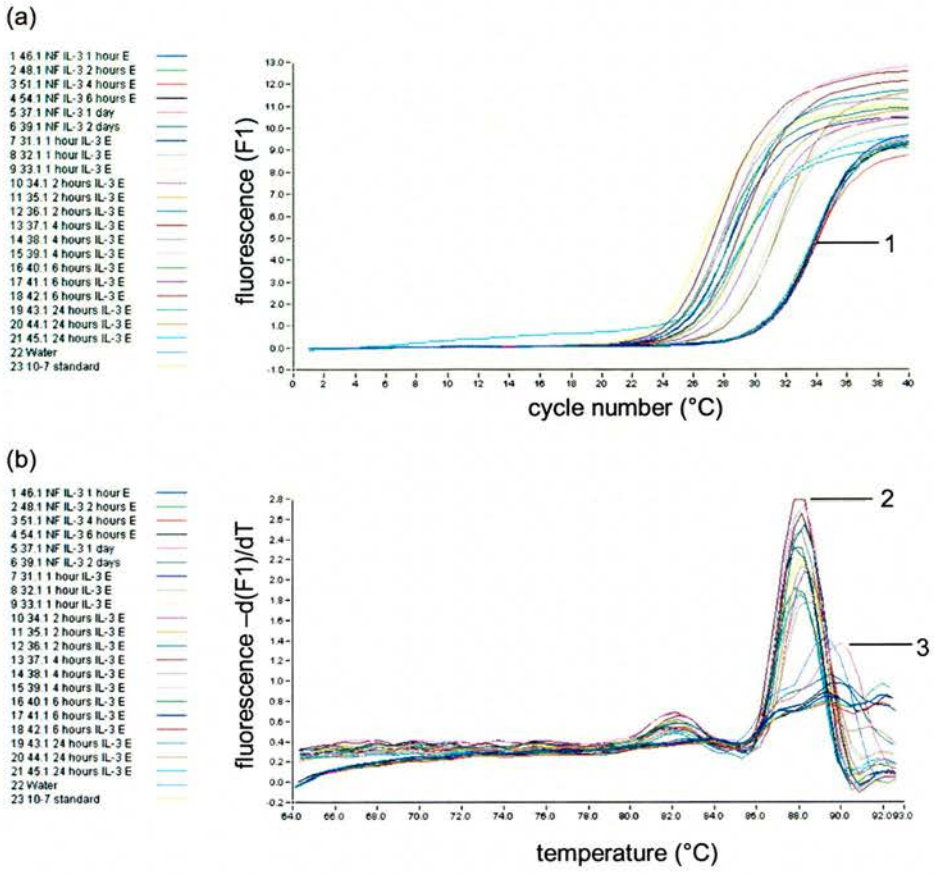

Figure 3.34 Specific IL-3 transcripts are detected in skin samples after gene-gun delivery of pIL-3 and not in normal skin or after delivery of the NF-control. Amplification of IL-3 transcripts in cDNA samples can be observed from approximately 22–26 cycles (a). An increase in fluorescence at approximately 30 cycles of amplification in both NF-control cDNA samples and the negative control (nuclease-free water) is evident (1). (b) Melting curve analysis shows specific product (2) is present in skin biopsies vaccinated with pIL-3 (melting at the same temperature (88°C) as the positive control sample). In contrast, (3) shows non-specific product (melting at 90°C) which has accumulated after 30 cycles of amplification with IL-3 primers in the negative control (water) and also in cDNA samples obtained from skin biopsies vaccinated with the NF-control.

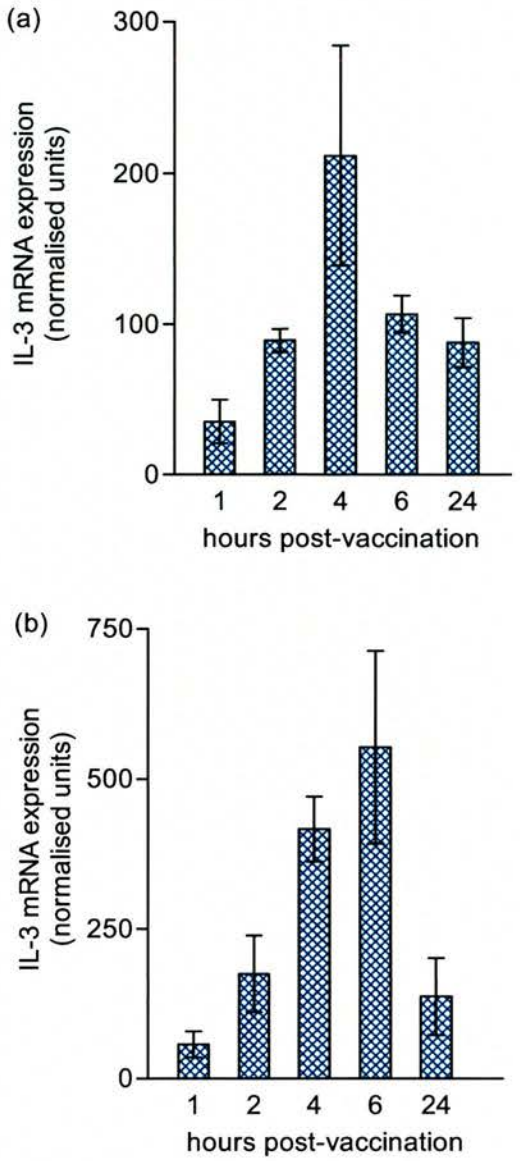

Figure 3.35 IL-3 mRNA expression in skin 1–24 hours after gene-gun vaccination with pIL-3. IL-3 mRNA in normal ovine skin or in NF control-vaccinated skin could not be quantified. (a) Sheep 3, biopsy experiment B; (b) sheep 4, biopsy experiment E. Data are presented as mean ± SEM and n = 3.

IL-1β mRNA expression

Endogenous expression of IL-1β mRNA was analysed alongside cDNA samples obtained from pIL-3 and NF-control vaccinated skin. An increase in IL-1β transcripts was observed in NF-control vaccinated skin and mRNA levels peaked at approximately 4 hours p/v in both animals (Figure 3.36). A more dramatic increase was apparent after gene-gun vaccination with pIL-3. It is of interest to note that in sheep 3, IL-1β mRNA expression mirrored the kinetics of IL-3 mRNA expression, again reaching maximal levels 4 hours p/v. A 6.5 fold increase in IL-1β mRNA (relative to levels induced after administration of the NF-control) was evident 4 hours p/v in sheep 3. Furthermore, this difference was statistically significant over the time-course of the experiment ($p < 0.02$). A similar trend was observed in sheep 4 where peak IL-1β mRNA expression was also observed 4 hours after pIL-3 administration; a 4 fold increase relative to expression in NF-control vaccinated skin was observed in this animal at this time-point ($p < 0.03$).

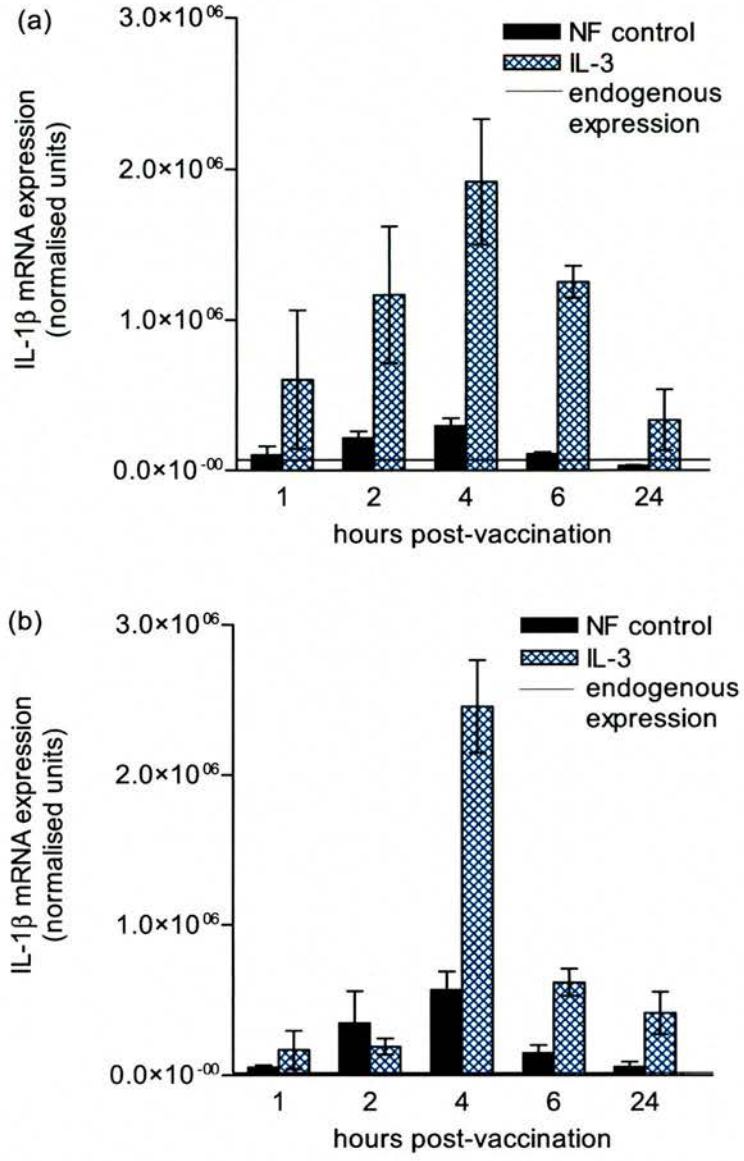

Figure 3.36 IL-1β mRNA expression in skin 1–24 hours after gene-gun administration of pIL-3 and the NF-control. (a) Sheep 3, (b) sheep 4. Data are presented as mean ± SEM.

IL-18 mRNA expression

Figure 3.37 shows expression of IL-18 mRNA before and after gene-gun delivery of pIL-3 and the NF-control in two animals over 24 hours. There was no significant difference in IL-18 mRNA expression in skin vaccinated with pIL-3 compared to skin vaccinated with the NF-control ($p > 0.05$), with the exception of the 24 hour time-point (sheep 3), where levels of IL-18 were approximately 3 fold higher in NF-control vaccinated skin than in pIL-3 vaccinated skin. In accord with earlier data obtained with normal skin and skin vaccinated with pGM-CSF or NF-control, IL-18 mRNA expression was approximately 5 fold higher in normal skin biopsies than in skin vaccinated with either of the plasmids in sheep 3 (Figure 3.37a) and approximately 3 fold higher in sheep 4 (Figure 3.37b). Since only two biopsies were removed from normal skin and this RNA was pooled prior to the RT reaction, no statistical analysis can be performed in order to compare this apparent reduction of IL-18 mRNA after gene-gun vaccination.

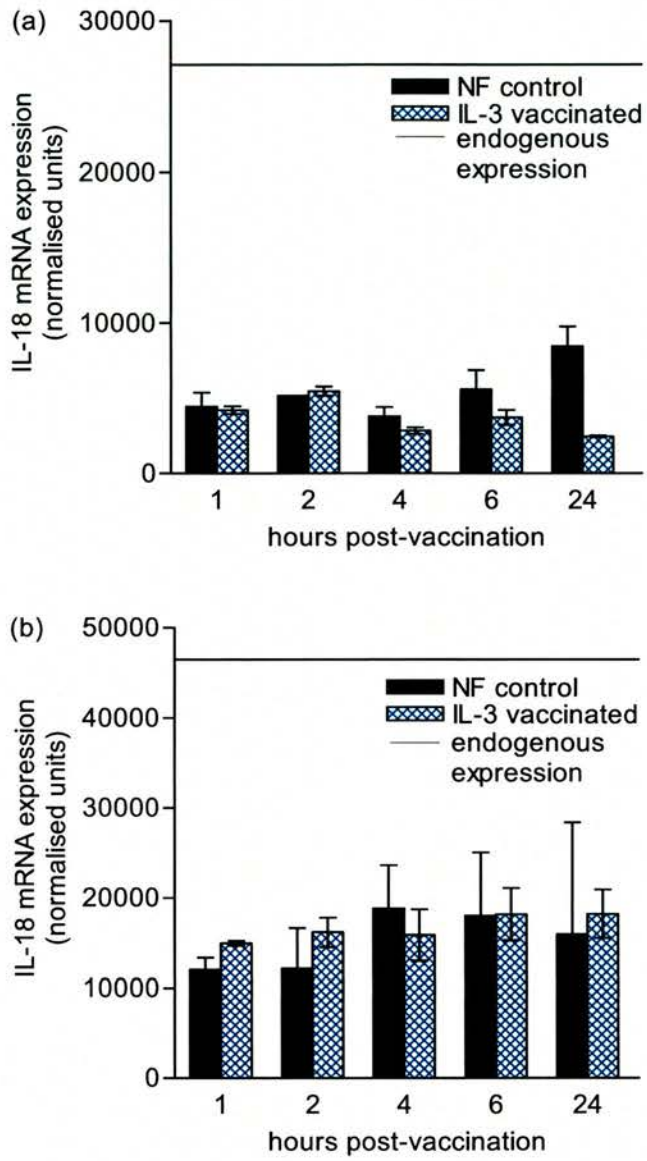

Figure 3.37 IL-18 mRNA expression in skin 1–24 hours after gene-gun delivery of pIL-3 and the NF-control in sheep 3 (a) and in sheep 4 (b). Endogenous expression of IL-18 is represented as a solid line. Data are presented as mean ± SEM.

TNF-α mRNA expression

TNF-α mRNA expression was highly variable in the skin of both animals over the time-course (1-24 hours) after administration of both pIL-3 and the NF-control. This variability was even apparent in biopsies where plasmids were administered at (approximately) the same time (Figure 3.38). Notably, administration of both plasmids resulted in increased TNF-α mRNA expression as early as one hour p/v (relative to transcripts quantified in normal skin). In general, there was little difference in abundance of TNF-α transcripts between NF-control or pIL-3 vaccinated skin samples over the time-course of the experiment ($p > 0.05$, sheep 3 and 4), with the exception of the 24 hour time-point after gene-gun delivery of pIL-3 in sheep 4, where a 3 fold increase in TNF-α mRNA expression was apparent.

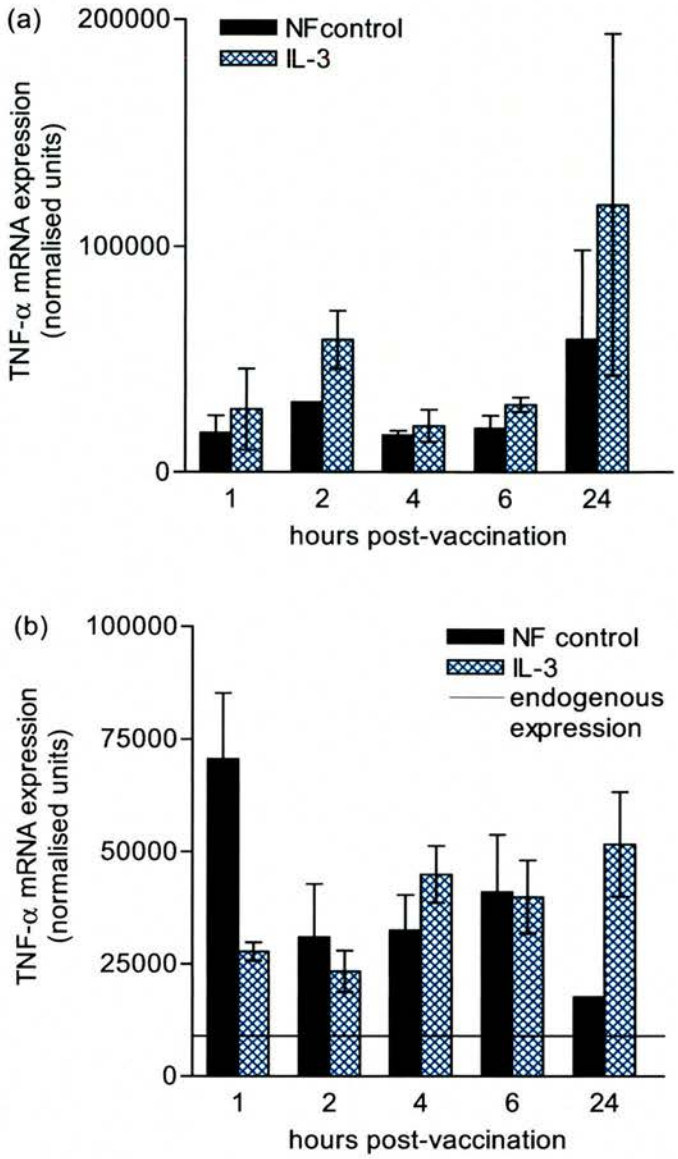

Figure 3.38 TNF-α mRNA expression in skin 1–24 hours after gene-gun vaccination with pIL-3 and the NF-control in sheep 3 (a) and in sheep 4 (b). Data are presented as mean ± SEM.

3.6 Gene-gun administration of cytokine gene adjuvants over 4 days

Biopsy experiment A identified a pronounced infiltration of MHC class II DR^+ cells with the morphology of DC 3–4 days after pGM-CSF administration. Notably this was not observed after administration of the control plasmid (pEGFP-N1). It was imperative to confirm the findings of biopsy experiment A and also to correlate the immunohistological findings with the expression of proinflammatory cytokines (IL-1β, TNF-α and IL-18). It was also necessary to investigate the effects of the NF-controls over a longer time period (>24 hours). In addition, no apparent infiltration of DC was observed after pIL-3 administration; although a slight increase in MHC class II^+ $CD45RA^+$ cells was observed 24 hours p/v. Further analysis was required to determine the *in vivo* effects of pIL-3 where the GFP gene had been removed from the construct, since expression of a fusion protein (as employed in biopsy experiment A) may have limited the *in vivo* effects of pIL-3.

Two sheep (animals 5 & 6) were prepared as described previously and vaccinated in triplicate over 4 days with pGM-CSF, pIL-3 and NF-controls (biopsy experiments C and D). The experiments are summarised in Figure 3.39. Note that the 16 hour time-point was omitted in the biopsy experiment D (sheep 6). Biopsies were removed immediately at post-mortem. Half of each biopsy was submerged into RNA*later*™ for subsequent quantitative RT-PCR analysis. The remaining biopsy fragments were fixed in either ZSF or PFA, paraffin-wax embedded and stained with H & E or used for subsequent immunohistochemistry.

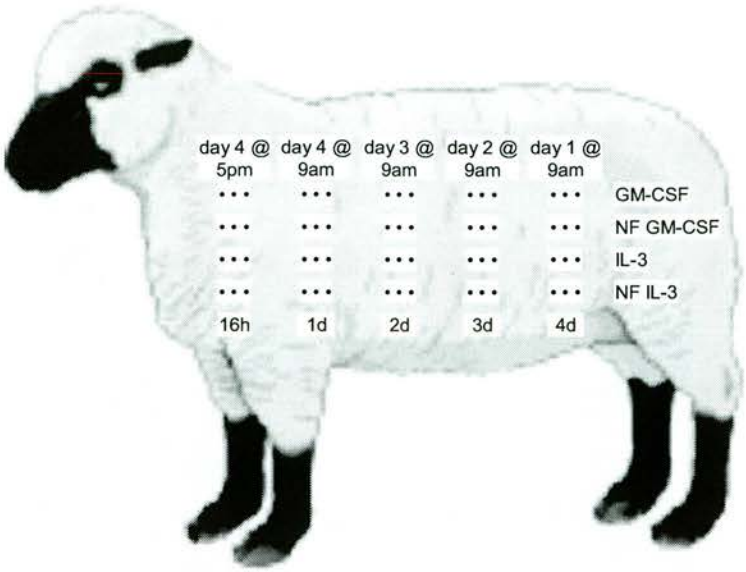

Figure 3.39 DNA vaccination over 4 days (biopsy experiments C and D) with pGM-CSF, pIL-3 and NF-controls. The 16-hour time-point was omitted in biopsy experiment D (sheep 6).

3.6.1 Effects of pGM-CSF in skin

3.6.1.1 Histological analysis of pGM-CSF vaccinated skin

Representative images from both sheep are shown in Figure 3.40. Importantly, comparatively little inflammation was induced after gene-gun administration of the NF-control plasmid over the time-course. Some minor changes to the epidermis were observed, but importantly (and in contrast with the previous experiments where pEGFP-N1 was used as a control), there was no pustule formation. Furthermore, the number of PMN did not increase over the 4 days; indeed little dermal infiltration was evident 2–4 days after gene-gun delivery of the NF-control plasmid.

In stark contrast with the effects of NF-control, but in keeping with biopsy experiments A, B and E, was the development of a severe inflammatory reaction in both animals 24 hours after delivery of pGM-CSF. Again, the peak reaction appeared to have taken place within the first 24 hours and is likely to have taken place from 16–24 hours in sheep 5 (biopsy experiment C). PMN (mostly neutrophils) again represented the predominant population from 16–24 hours, although a slight increase in mononuclear cells was observed by 24 hours. After the first 24 hours, thickening of the crust was evident and dermal-epidermal separation had taken place. The kinetics of the cellular response appeared almost identical in both animals. At 48–96 hours p/v there was a reduction in the level of infiltrating PMN and an increase in the numbers of mononuclear cells, with the marked presence of superficial oedema.

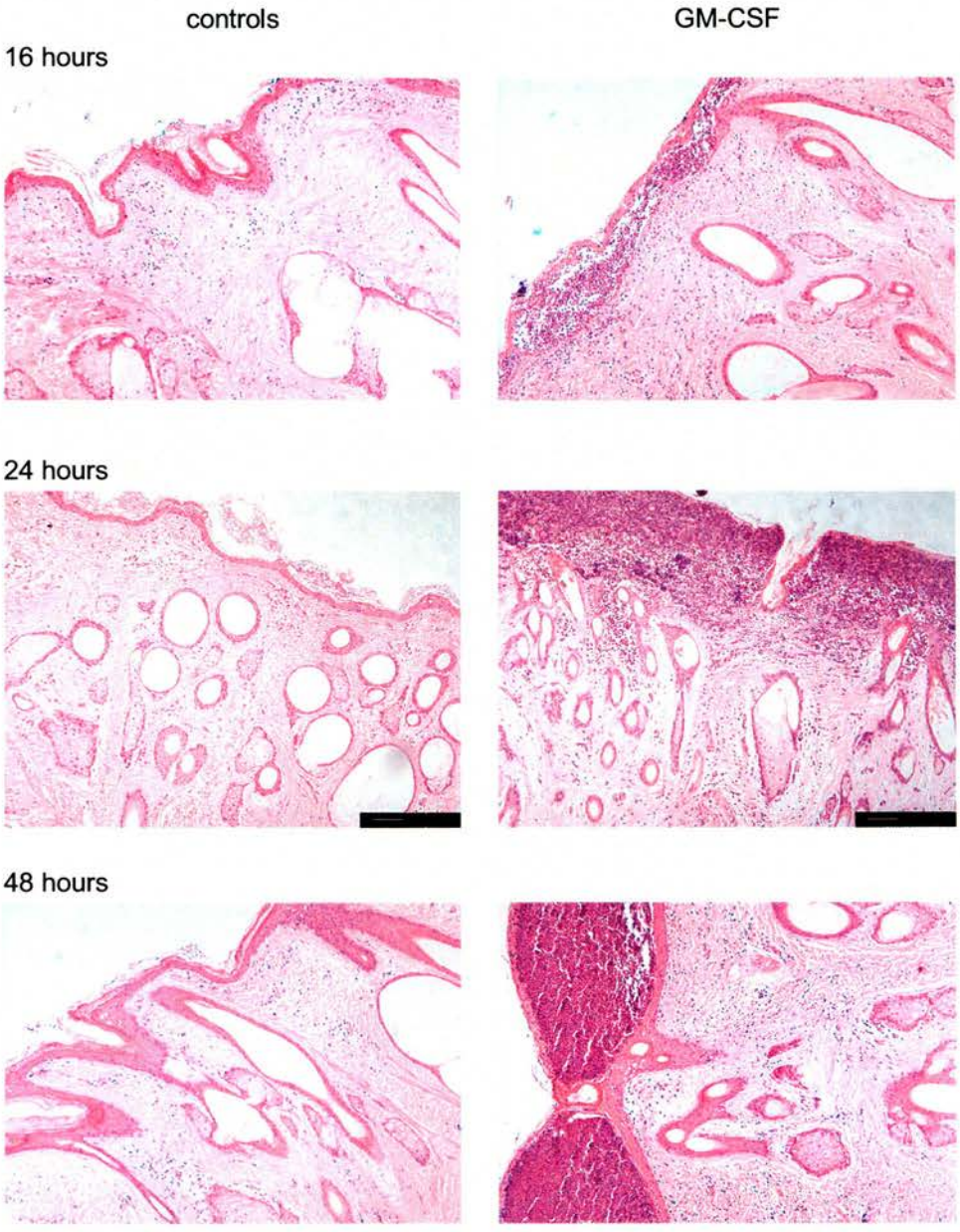

Figure 3.40 Comparison of the inflammatory events induced in the skin from 16–96 hours after gene-gun administration of pGM-CSF and the NF-control. Skin biopsies were removed immediately at post mortem, fixed in ZSF and stained with H & E. Representative images from each of the time-points are shown. (Original magnification, ×80.)

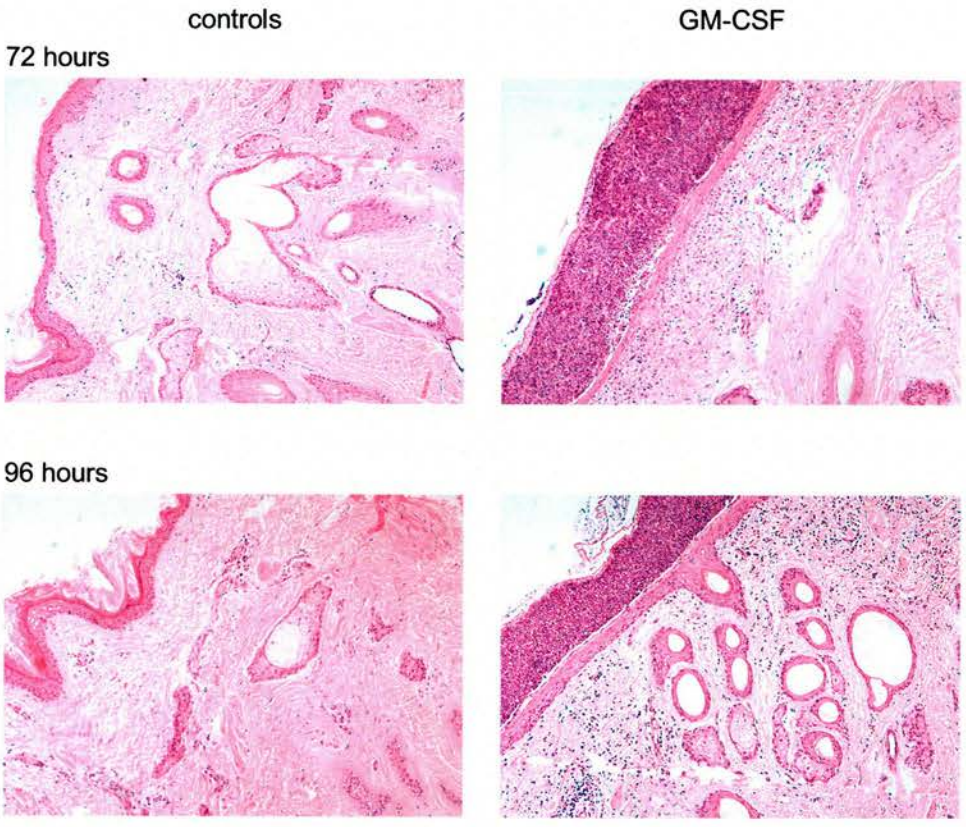

Figure 3.40 (cont.)

3.6.1.2 Immunohistological analysis of pGM-CSF vaccinated skin

Skin sections were immunolabelled to identify cell populations recruited to the skin up to 4 days after administration of pGM-CSF and the NF-control. Figure 3.41 shows representative images taken from biopsy experiments C and D. A slight increase in MHC class II^+ cells was observed after administration of the NF-control plasmid when compared to normal skin 16–48 hours after gene-gun bombardment; however, by 3–4 days p/v, numbers of MHC class II^+ cells were comparable to those observed in normal skin. In contrast, MHC class II DR^+ cells were more prevalent in pGM-CSF vaccinated skin than in NF-control skin at all time-points investigated and in both animals. Small MHC class II^+ mononuclear cells infiltrated the dermis and some staining was evident in the epidermal layer 16 hours p/v. Further infiltration of DR^+ cells was observed 3 days after delivery of pGM-CSF; cells were particularly prevalent under the pustule. The most striking observation in both animals, was the pronounced infiltration of MHC class II DR^+ cells with the morphological appearance of DC 4 days p/v.

Staining with anti-CD45RA (mAb 73B) revealed a modest increase in $CD45RA^+$ cells in biopsies removed from pGM-CSF vaccinated skin 16 hours after administration (Figure 3.42), whereas few $CD45RA^+$ positive cells were present in the NF-control vaccinated skin sites. At all of the other time-points investigated there did not appear to be any difference in $CD45RA^+$ cells after administration of pGM-CSF or NF-control; numbers were comparable to those observed in normal non-vaccinated skin, which suggests that the MHC class II^+ cells infiltrating the skin 4 days after pGM-CSF vaccination were not B cells (Mackay et al, 1990). Sections were also stained with IAH-CC15 and this revealed a slight increase in γδ T cells relative to normal skin, 24 hours after gene-gun vaccination with pGM-CSF. It was interesting to note that there appeared to be an infiltration of γδ T cells, particularly near to the epidermis 3 days after delivery of the NF construct and 4 days after delivery of pGM-CSF (Figure 3.43).

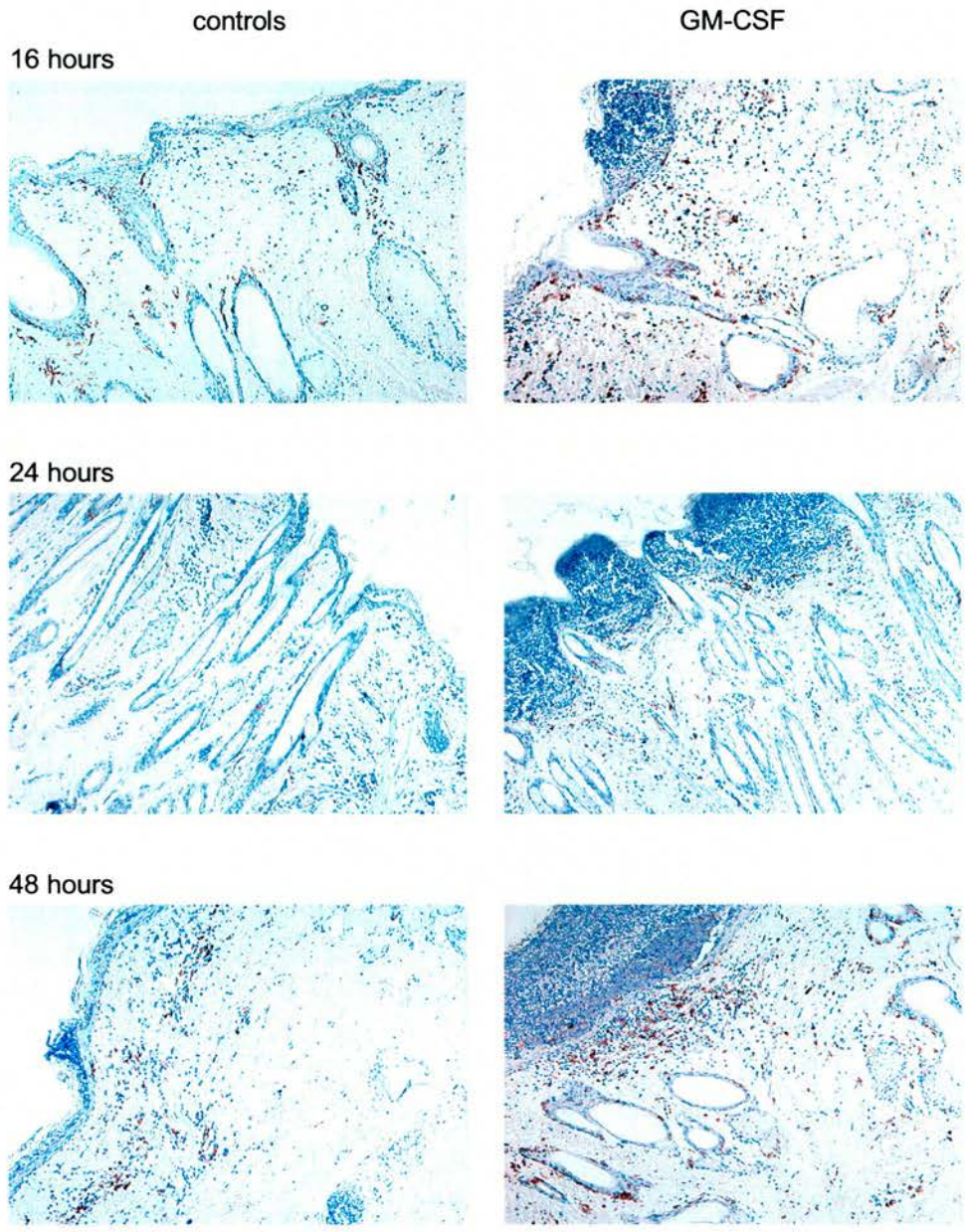

Figure 3.41 Infiltration of MHC class II$^+$ DC in skin 4 days after gene-gun delivery of pGM-CSF. Immunolabelling of skin biopsies was carried out with mAb VPM 54 (MHC class II DRα) obtained from sheep vaccinated from 16–96 hours with pGM-CSF (right-hand side panels) and the NF-control (left panels). Representative images are shown form both biopsy experiments (C and D), with the exception of the 16-hour time-point, where sections were only available from sheep 5. Sections were counterstained with haematoxylin. (Original magnification, ×80.)

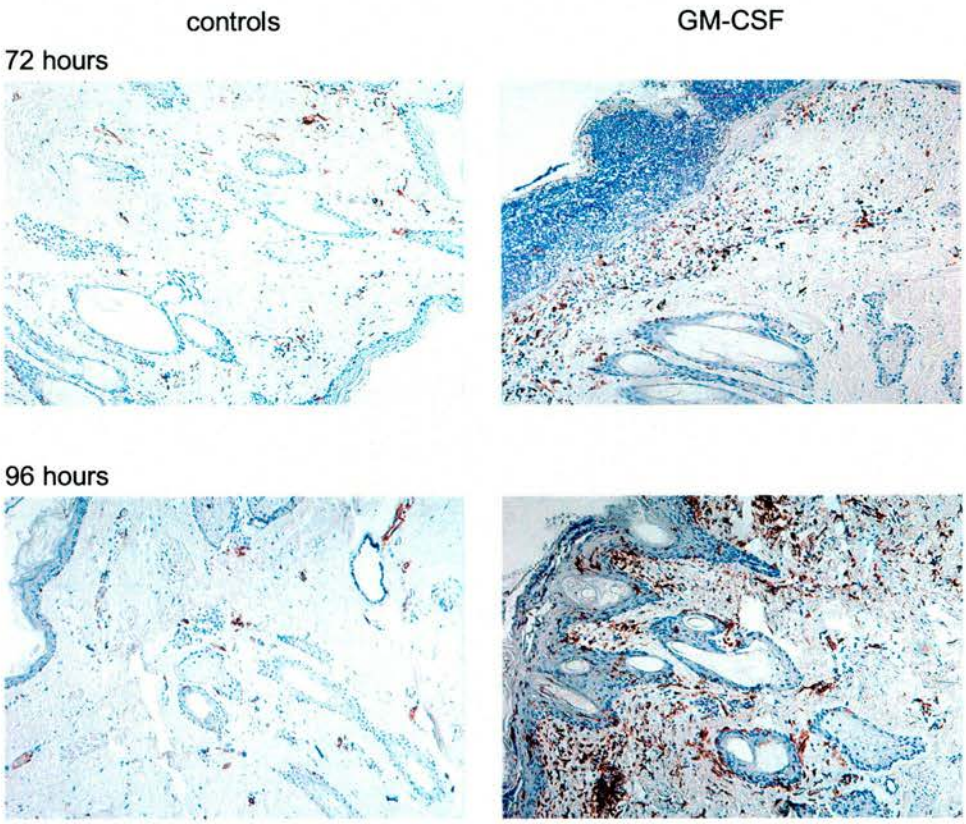

Figure 3.41 (cont.)

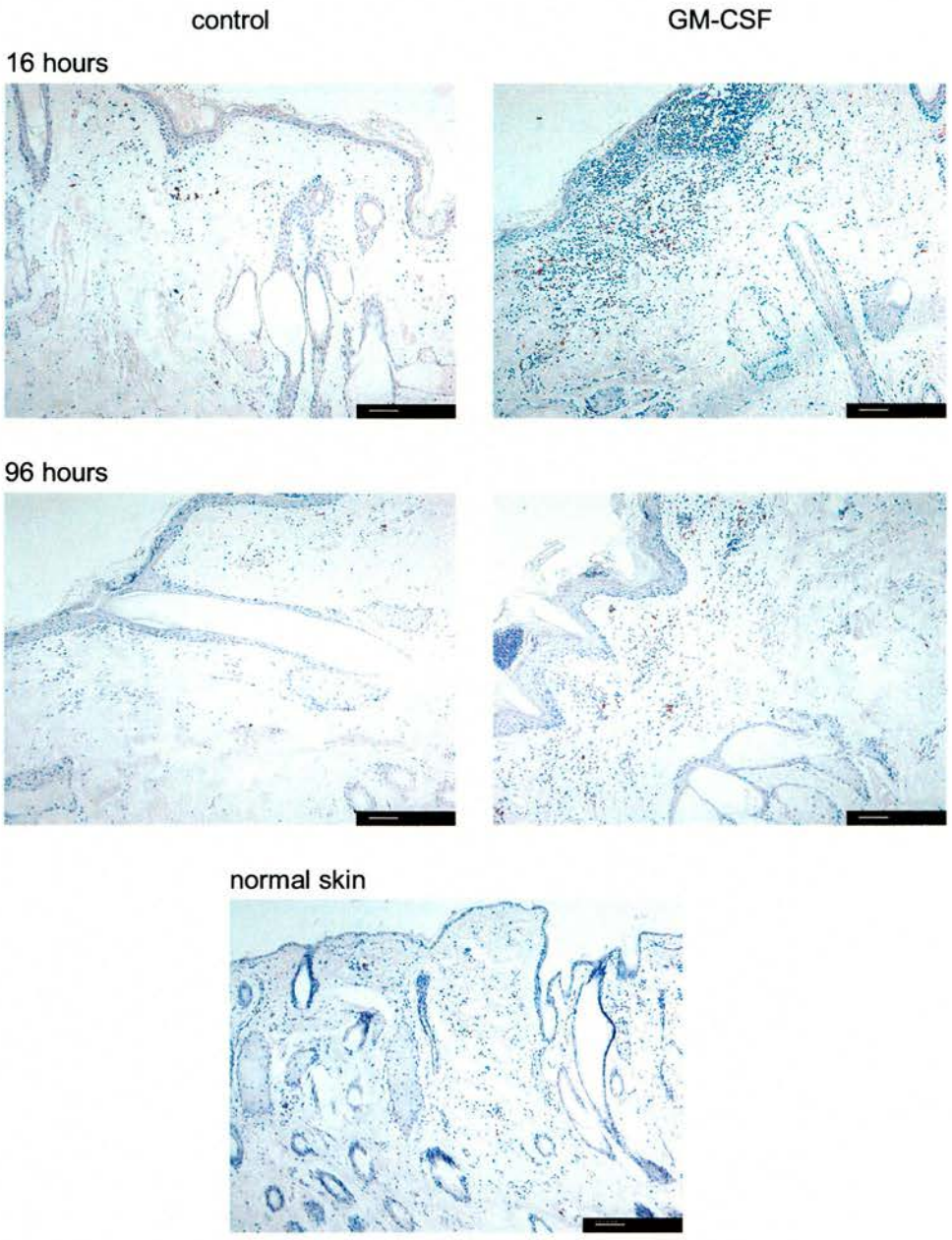

Figure 3.42 Immunohistochemical staining of $CD45RA^+$ lymphocytes 16 and 96 hours after gene-gun delivery of pGM-CSF and the NF-control. Note that 96 hours after pGM-CSF administration there are relatively few $CD45RA^+$ lymphocytes. Sections have been counterstained with haematoxylin. (Scale bar = 250μm.)

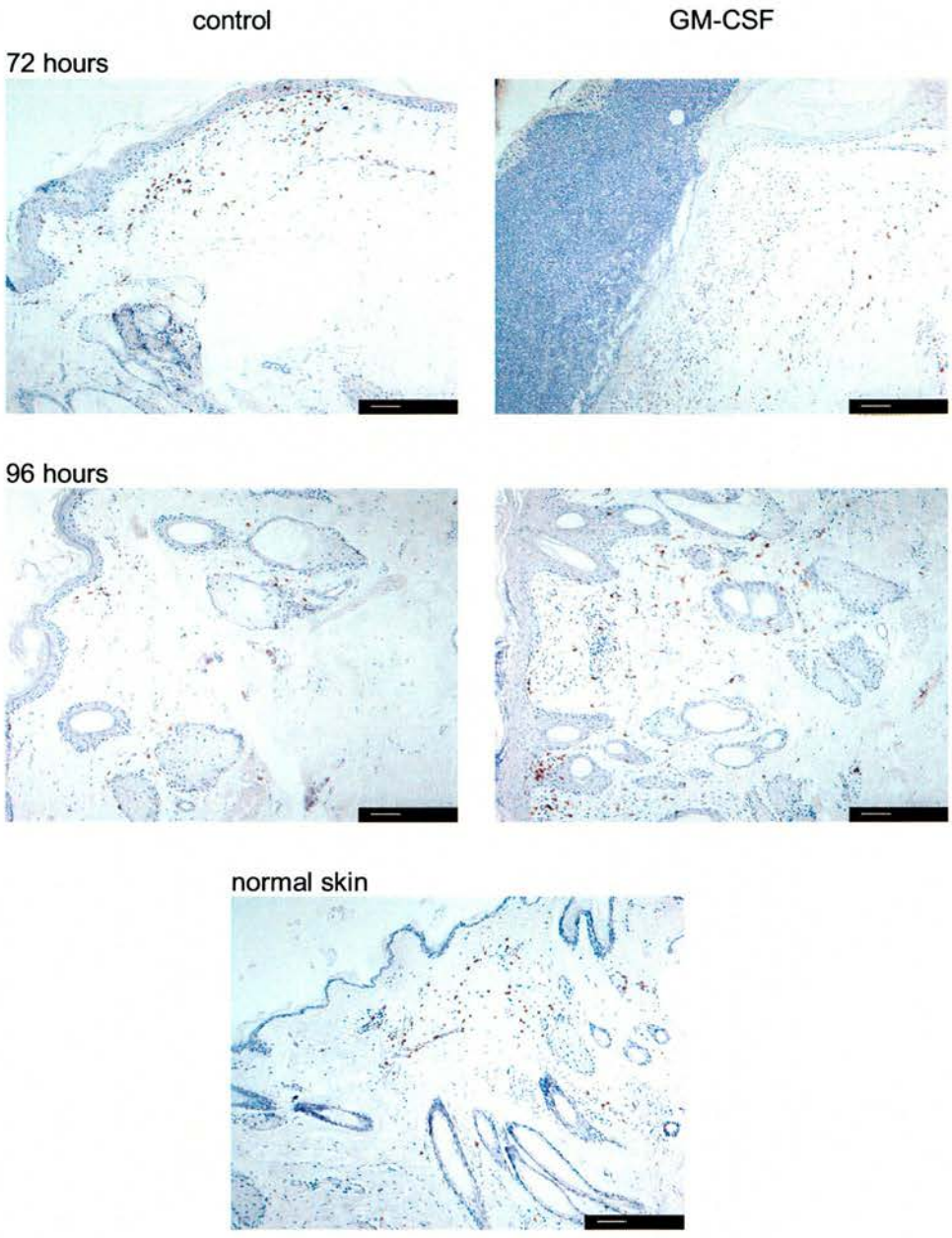

Figure 3.43 Immunohistochemical staining of γδ T cells in skin sections obtained 72 and 96 hours after gene-gun vaccination with pGM-CSF and the NF-control. Note the slight increase in γδ T cells 72 hours (NF-control) and 96 hours (pGM-CSF) after administration. (Scale bar = 250μm.)

3.6.1.3 Cytokine mRNA expression in skin after gene-gun delivery of pGM-CSF

Quantitative RT-PCR was next employed to investigate the kinetics of GM-CSF mRNA expression and the expression of proinflammatory cytokines in the skin up to 96 hours after gene-gun delivery of pGM-CSF (and the NF-control).

GM-CSF mRNA expression

In both animals, the level of GM-CSF transcripts declined in an almost linear fashion over the 4 days after administration of both pGM-CSF and the NF-control (Figure 3.44). GM-CSF mRNA was only just within the quantification limit of the assay 48–96 hours after delivery of the NF-control (sheep 5) and could not be accurately quantified in several cDNA samples in sheep 6 (at 72–96 hour time-points). In contrast, GM-CSF mRNA was still detectable up to 96 hours after administration of the functional version of the plasmid. No statistically significant difference in GM-CSF mRNA expression was however evident after administration of pGM-CSF when compared to the NF-control vaccinated skin (where mean values for each time-point have been calculated and compared; $p > 0.05$, sheep 5 and 6, unpaired Student t-test). In addition, although specific GM-CSF product was detected in normal skin from both animals by quantitative RT-PCR, levels were below the limit of quantification (Ct of the sample was lower than the minimum Ct on the standard curve; data not shown).

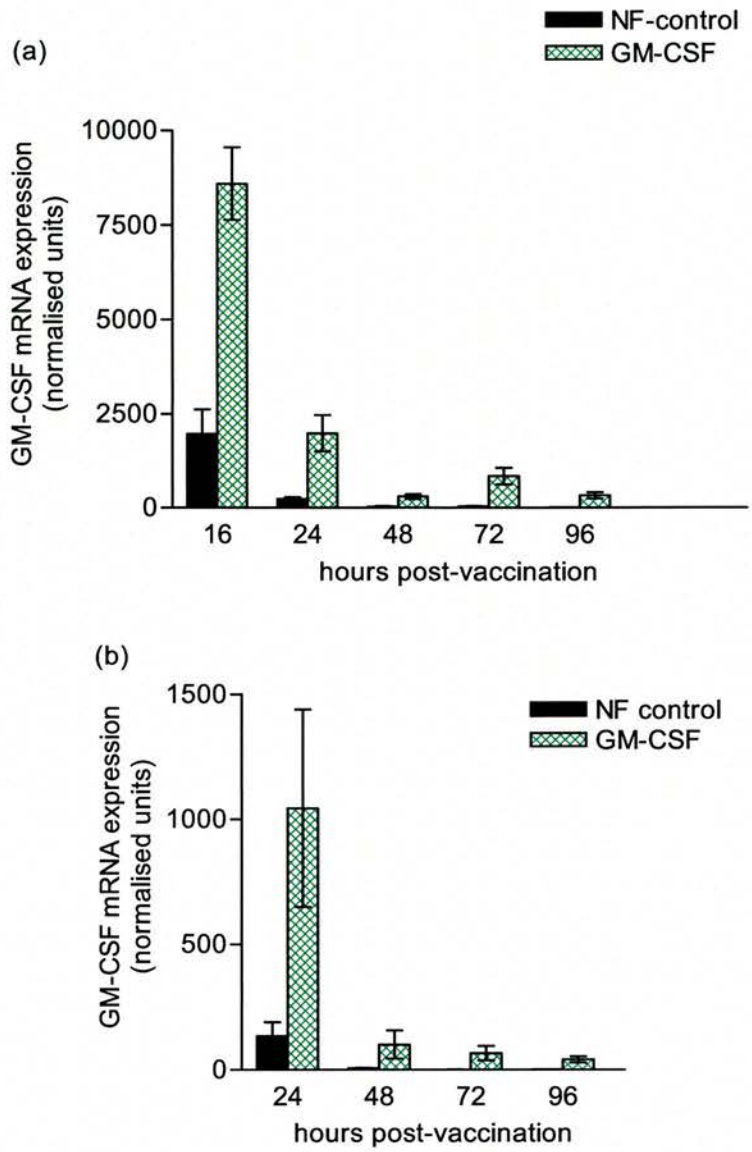

Figure 3.44 GM-CSF mRNA expression in skin over 96 hours after gene-gun administration of pGM-CSF and the NF-control. (a) Sheep 5 (biopsy experiment C), (b) sheep 6 (biopsy experiment D). Endogenous expression of GM-CSF mRNA could not be quantified in either LightCycler® experiment carried out, although specific product was detected (data not shown). GM-CSF mRNA was also below the level of quantification in several of the NF-control vaccinated skin biopsies (72–96 hours p/v) in sheep 6 (b). Data are presented as mean ± SEM.

IL-1β mRNA expression

IL-1β mRNA expression was highly elevated in skin up to 96 hours after gene-gun delivery of pGM-CSF (Figure 3.45a,b). Importantly, a statistically significant difference is apparent when mRNA levels of IL-1β are compared to those induced after NF-control delivery over the entire time-course of the experiment ($p < 0.02$ sheep 5 and $p < 0.002$ sheep 6; unpaired Student t-test). IL-1β transcripts were approximately 70 fold higher (range 22.4–156.6) in skin after gene-gun vaccination with pGM-CSF than in NF-control vaccinated skin in sheep 5, and 46 fold higher (range 25–67.5) in sheep 6. Maximal expression of IL-1β mRNA was evident 72 hours after pGM-CSF administration in both animals (mean 157 fold difference (sheep 5) and 68 fold difference (sheep 6)). When IL-1β mRNA expression in pGM-CSF vaccinated skin is compared to endogenous IL-1β expression, a ~200 fold induction is apparent (range 173–234; sheep 6) over the first 72 hours. Moreover, expression was still 100 fold higher than endogenous levels up to 96 hours after gene-gun delivery.

IL-1β mRNA was detected at low levels in normal skin in both animals and is also represented in Figure 3.45. IL-1β mRNA expression was elevated in NF-control vaccinated skin 16 hours p/v in sheep 5. Levels thereafter were comparable to endogenous IL-1β mRNA expression. In sheep 6, administration of the NF-control plasmid caused (approximately) a 5 fold increase in IL-1β transcripts over the first 72 hours, although some variability is evident between skin samples which had been vaccinated at the same time (Figure 3.45c).

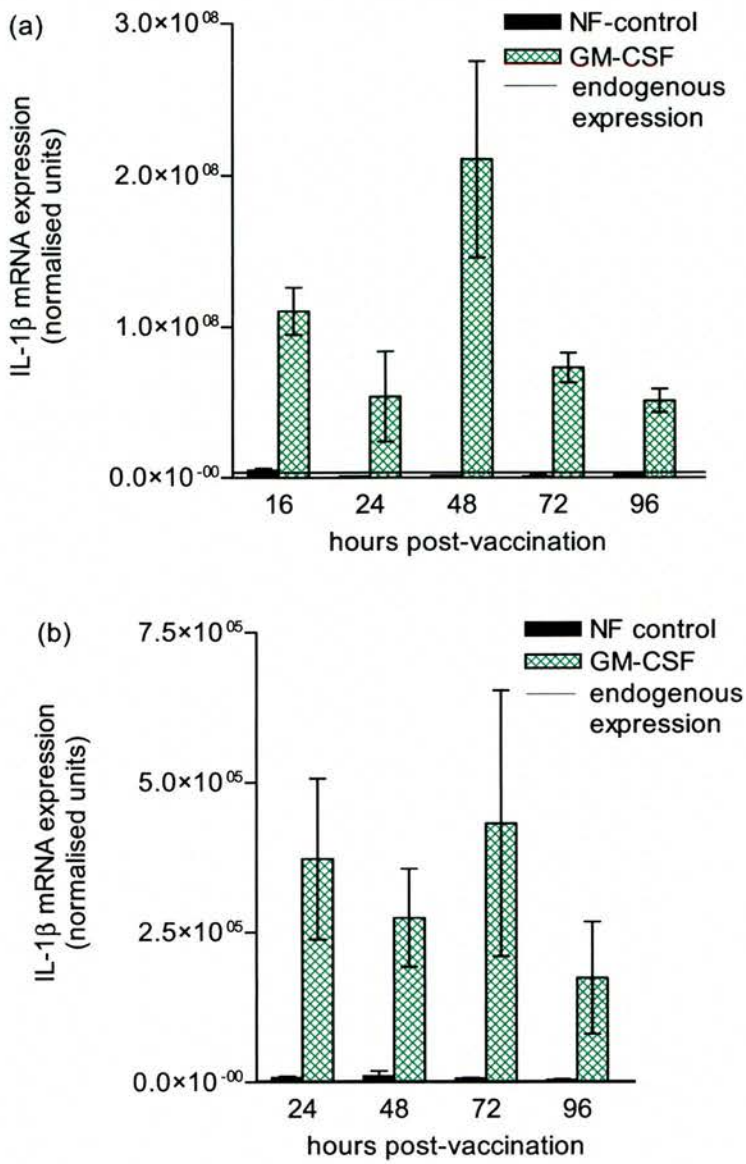

Figure 3.45 IL-1β mRNA expression in skin over 96 hours after gene-gun delivery of pGM-CSF and the NF-control. (a) Sheep 5 (biopsy experiment C); (b) and (c) sheep 6 (biopsy experiment D). Endogenous expression of IL-1β mRNA is represented as a solid line in (a); n = 2–3 biological samples (data are presented as mean ± SEM); $p < 0.02$ (0.012, unpaired Student t-test). In (b), n=3 biological samples and $p < 0.002$ (0.0017), unpaired Student t-test. Endogenous expression of IL-1β mRNA is too low to be represented in (b), and is shown as a solid line in (c) alongside values obtained after gene-gun administration of the NF-control.

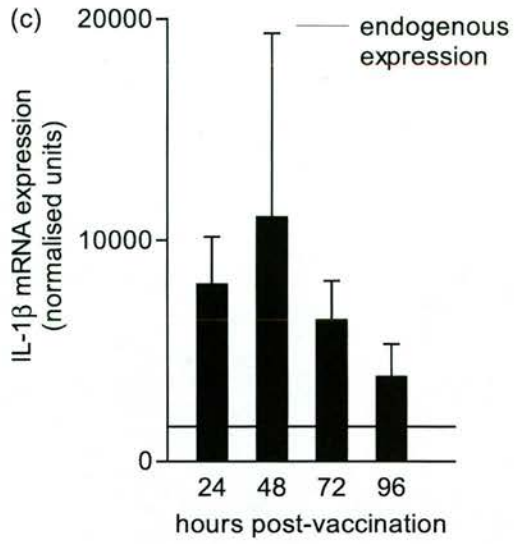

Figure 3.45 (cont.)

IL-18 mRNA expression

The kinetics of IL-18 mRNA expression over 96 hours was investigated after administration of both pGM-CSF and the NF-control (Figure 3.46). In both animals, no statistically significant difference was evident in skin vaccinated with pGM-CSF when compared to biopsies vaccinated with NF-control at any of the time-points investigated ($p > 0.05$, sheep 5 and 6). Endogenous expression of IL-18 mRNA was approximately 2 fold higher than in skin vaccinated with either plasmid from 24–96 hours p/v-in sheep 5 (Figure 3.46a) and expression remained at a similar level in all biopsies evaluated over the time-course in this animal. Gene-gun administration of both plasmids also resulted in decreased IL-18 mRNA expression in sheep 6 from 24–72 hours, although by 96 hours p/v, IL-18 mRNA expression was comparable to levels quantified in normal skin.

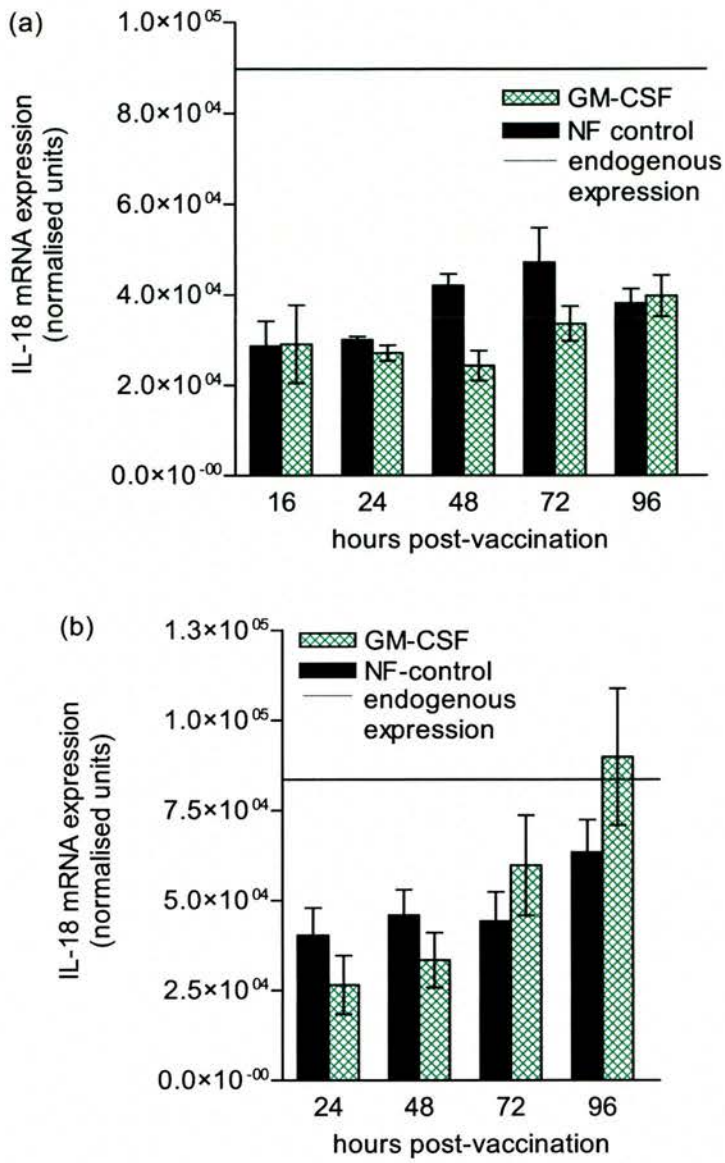

Figure 3.46 IL-18 mRNA expression in skin over 96 hours after gene-gun vaccination with pGM-CSF and the NF-control. (a) Sheep 5 (biopsy experiment C), (b) sheep 6 (biopsy experiment D). Endogenous IL-18 mRNA expression is represented as a solid line. Data are presented as mean ± SEM.

TNF-α mRNA expression

In both animals, expression of TNF-α mRNA was consistently higher after pGM-CSF administration than after administration of the NF-control plasmid at all of the time-points investigated (Figure 3.47). Furthermore, this difference in TNF-α mRNA expression was statistically significant ($p < 0.003$, sheep 5; $p < 0.002$, sheep 6). Variability in the expression of TNF-α was however evident in biopsies from the same time-points. Expression of TNF-α mRNA was also analysed in normal skin obtained from sheep 6 (b). This revealed that there was a mean 3 fold increase (range 2.9–3.4) in TNF-α mRNA expression up to 72 hours after vaccination with the NF-control. Expression of TNF-α then declined to levels expressed in normal skin. Conversely, expression of TNF-α was still highly elevated in the pGM-CSF vaccinated skin biopsies up to 96 hours p/v (mean 7.8 fold increase, range 3.0–15.3).

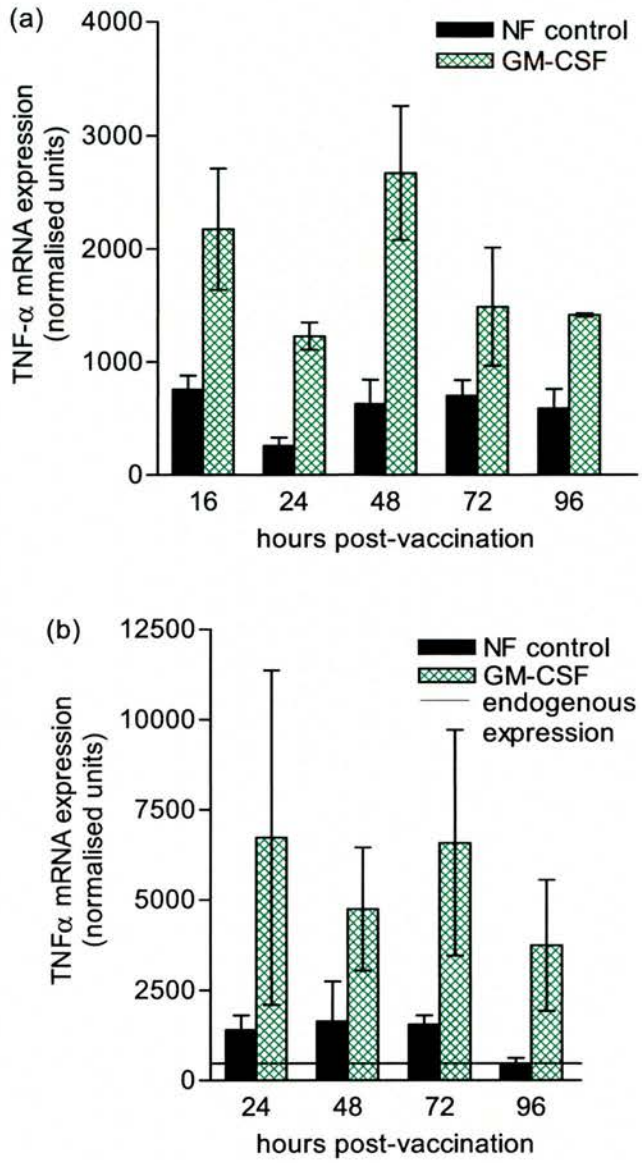

Figure 3.47 TNF-α mRNA expression in skin over 96 hours after gene-gun delivery of pGM-CSF and the NF-control. (a) Sheep 5, (b) sheep 6. Expression of TNF-α was significantly higher in pGM-CSF vaccinated biopsies than in NF-control vaccinated skin in both animals ($p < 0.003$, sheep 5; $p < 0.002$, sheep 6, unpaired Student t-test). Endogenous expression was also analysed and is represented by the solid line. Data are presented as mean ± SEM.

IL-12p40 mRNA expression

Expression of IL-12p40 mRNA was analysed by quantitative real-time RT-PCR. IL-12p40 transcripts were not detected in any of the samples obtained from pGM-CSF or NF-control vaccinated skin biopsies. In addition, IL-12p40 was undetectable in normal skin removed from two different animals (animals 4 and 6; biopsy experiments E and D, respectively). Only non-specific product accumulated during the amplification stage, whereas specific product was detected in the positive control sample (diluted 1° PCR product) and is shown in Figure 3.48.

IL-10 mRNA expression

IL-10 mRNA expression was also analysed by quantitative RT-PCR. IL-10 transcripts were not detected in any of the biopsy samples evaluated from sheep 6 (biopsy experiment D), or indeed in sheep 4 (biopsy experiment E) after gene-gun delivery of pGM-CSF or the NF-control. Furthermore, IL-10 transcripts could not be detected in normal skin. Results are shown in Figure 3.48.

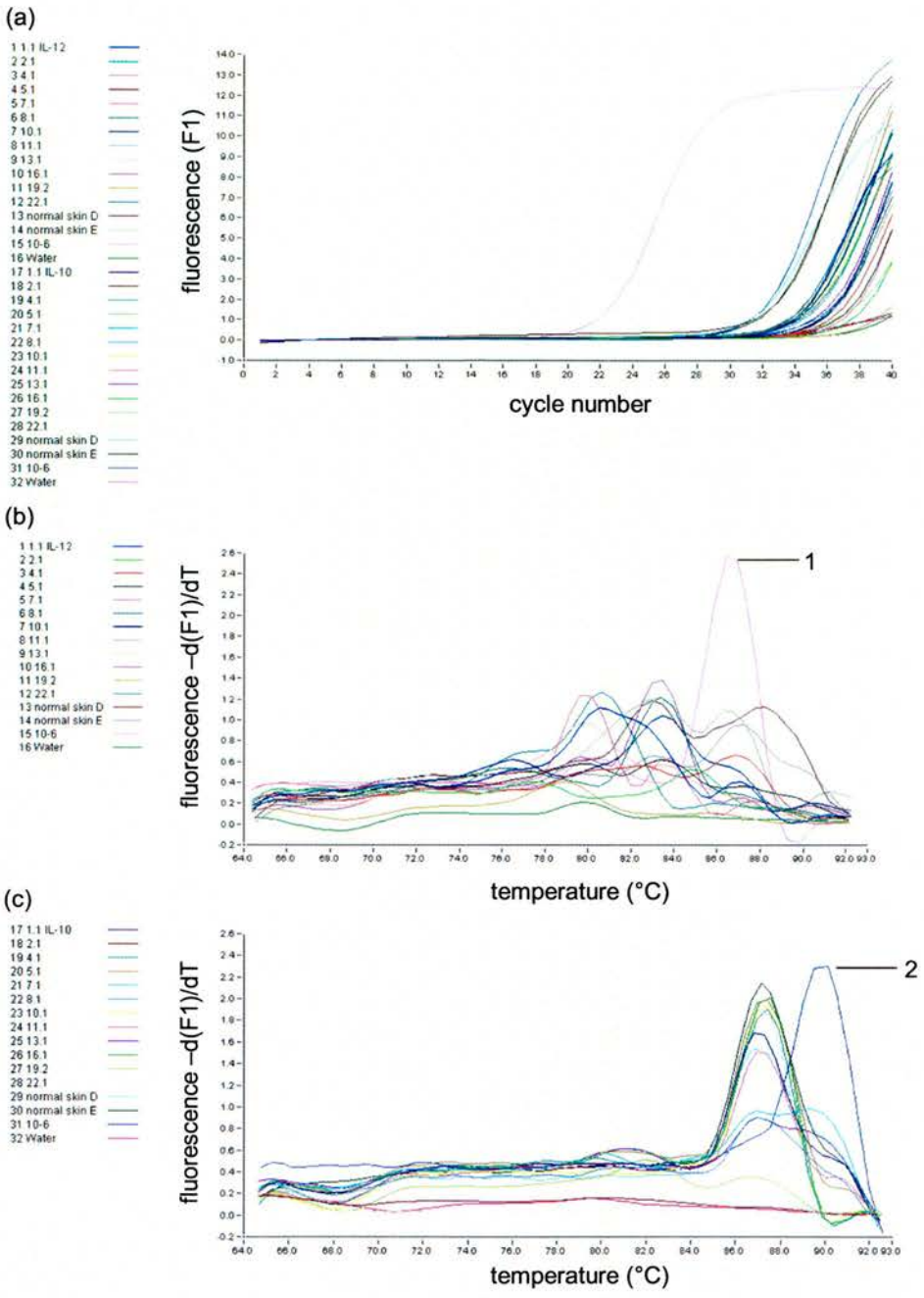

Figure 3.48 IL-12p40 and IL-10 transcripts are not detected in normal skin, pGM-CSF vaccinated or NF-control vaccinated skin. (a) Amplification plot of cDNA samples amplified with IL-12p40 and IL-10-specific primers. (b and c) Only non-specific products have accumulated since amplicons do not melt at the same temperature as the IL-12p40 (1) or IL-10 (2) standards (diluted 1° PCR products).

3.6.2 Effects of pIL-3 in skin over 4 days

3.6.2.1 Histological analysis of pIL-3 vaccinated skin

Gene-gun vaccination with pIL-3 (without the GFP gene) caused severe inflammation over the time-course in all biopsy sections evaluated from both animals. Comparatively little inflammation was induced after administration of the NF-control in most of the sections screened (Figure 3.49). Inflammation was however observed in some of the skin sections where the NF-control was administered in sheep 5 (data not shown) from 16–24 hours, whereas only low-grade inflammation was observed in sheep 6 (biopsy experiment D).

By 24 hours, a pronounced eosinophilic infiltration in both the epidermis and dermis was apparent after gene-gun administration of pIL-3. Neutrophils were also present within the developing pustule and small mononuclear cells had also accumulated in the upper part of the dermis by 24 hours. The reaction did not appear to increase in severity over the time-course, and it is likely that the peak inflammatory reaction occurred within the first 24 hours. Perhaps the most striking observation after pIL-3 administration in both animals was an overlying epidermal oedema which started to form approximately 48 hours p/v and was still evident up to 4 days p/v. This fluid filled pustule was evident by eye (Figure 3.50) and in some of the sections measured up to 800 μm. The H & E stained skin sections also revealed a pronounced infiltration of mononuclear cells in the dermis 3 days p/v in sheep 5 (biopsy experiment C) and 4 days p/v in sheep 6 (biopsy experiment D).

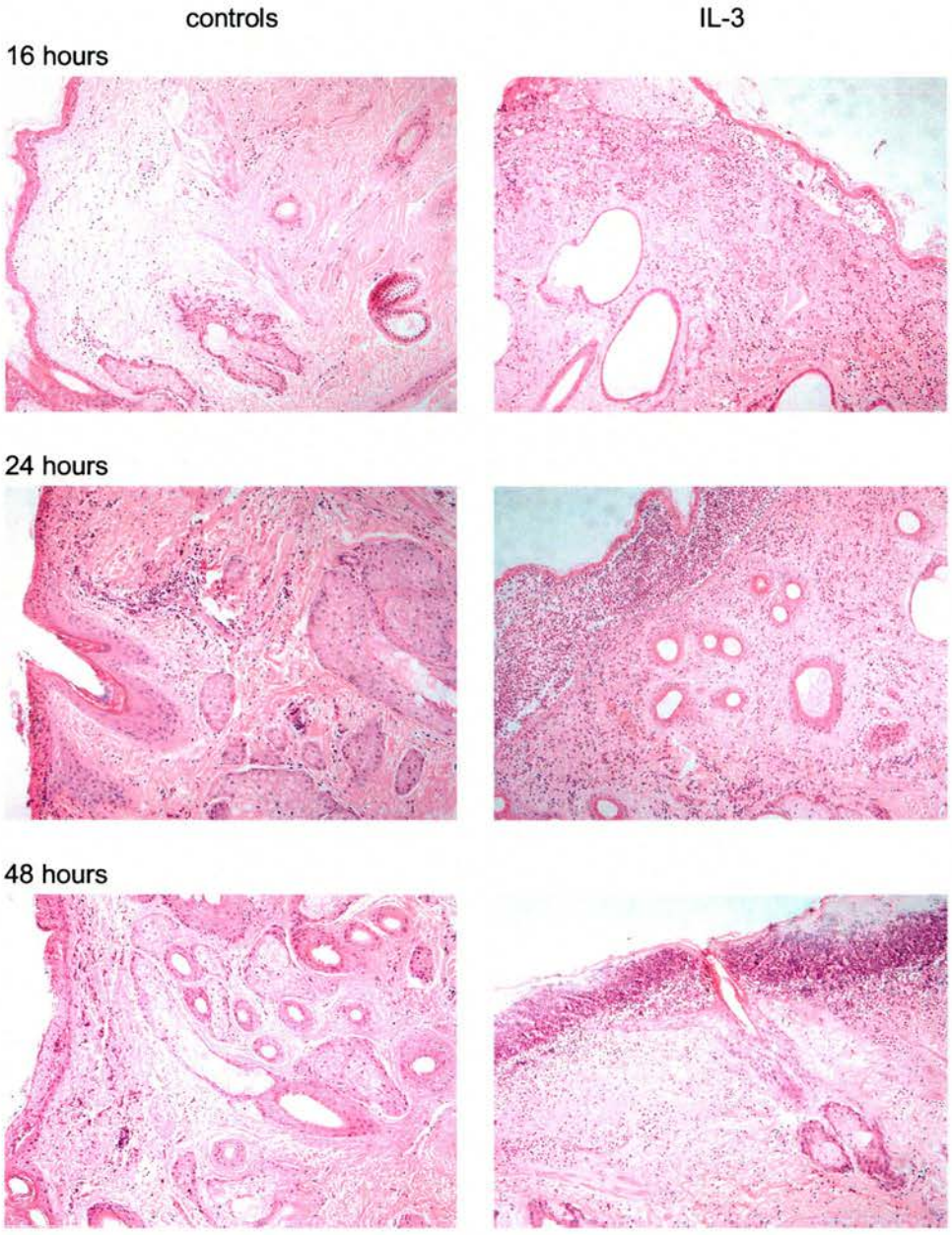

Figure 3.49 Comparison of the inflammatory events induced in the skin 16–96 hours after gene-gun administration of pIL-3 and the NF-control. Skin biopsies were removed immediately at post mortem, fixed in ZSF and stained with H & E. Representative images from each of the time-points are shown. (Original magnification, ×80.)

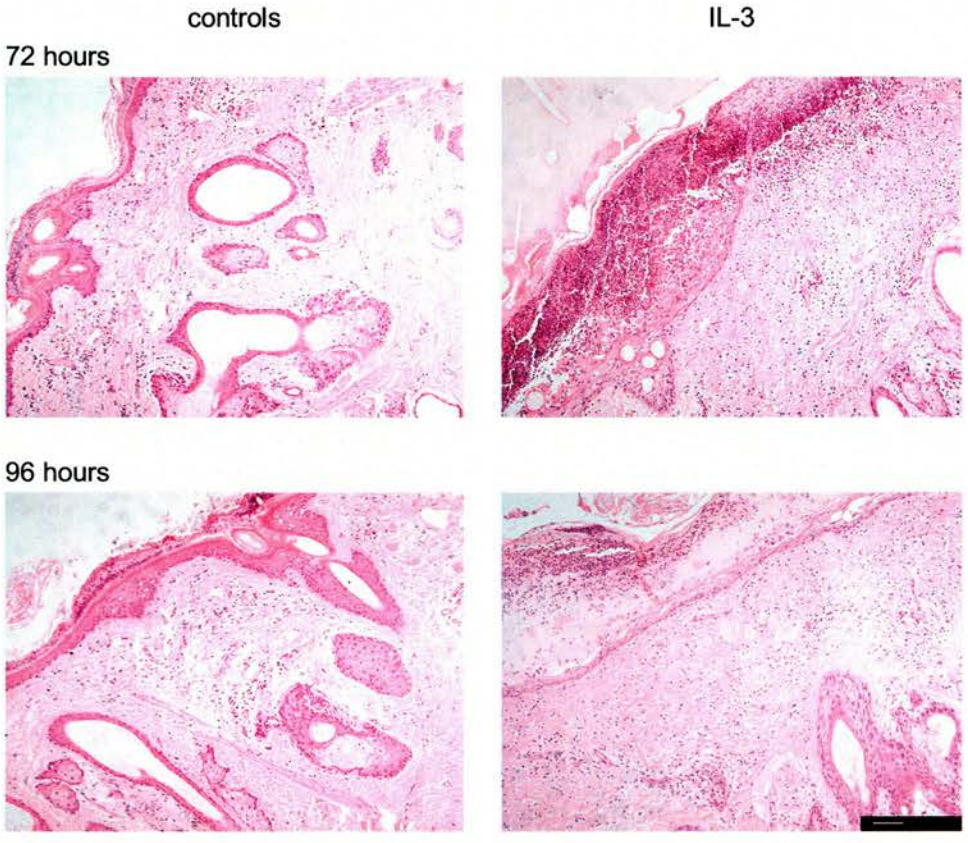

Figure 3.49 (cont.)

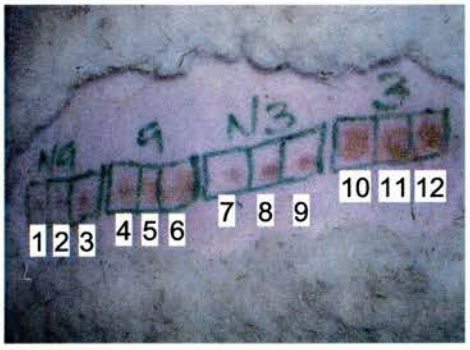

Figure 3.50 Development of erythematic reaction 4 days after gene-gun administration with four plasmid constructs. DNA vaccination was carried out on adjacent skin sites with the following plasmids: NF-GM-CSF (sites 1–3), pGM-CSF (sites 4–6), NF-IL-3 (sites 7–9) and pIL-3 (sites 10–12). Note the severe inflammatory reaction (pustule formation) caused by gene-gun vaccination with pGM-CSF and pIL-3. Gold dust is still clearly visible on skin where NF constructs have been delivered and little swelling is evident.

3.6.2.2 Immunohistological analysis of pIL-3 vaccinated skin

MHC class II DRα^+ cells infiltrated skin approximately 16–24 hours after gene-gun vaccination with pIL-3 (Figure 3.51). MHC class II DRα^+ cells accumulated just under the epidermis and high magnification revealed that these cells possessed a small and round morphology (Figure 3.52a). Some infiltration of DR$^+$ cells was observed in the NF-control vaccinated site but this was not nearly as pronounced as observed after pIL-3 delivery. DR$^+$ cells appeared to continue to traffick into the skin up to 2 days after pIL-3 administration and cells were evident in the deeper regions of the dermis. The most striking observation in this 4 day experiment was a pronounced accumulation of DR$^+$ cells 3 days p/v (sheep 5, Figure 3.51) and 4 days p/v (sheep 6; data not shown). On closer examination, some of the cells had a dendritic morphology. In addition, MHC class II$^+$ cells with the appearance of fibroblasts were present in the deeper regions of the dermis in skin removed 3 days p/v with pIL-3 (Figure 3.52b). This was not observed in any of the NF-control vaccinated skin sections.

An increase in CD45RA$^+$ cells was also evident 24 hours p/v with pIL-3 (Figure 3.53), but not after vaccination with the NF-control. Serial sections again showed a similar pattern of staining with mAbs VPM 54 and 73B. CD45RA$^+$ cells continued to traffic over the next 24 hours and could be observed deep within the dermis and surrounding blood vessels and numbers remained slightly elevated up to 4 days p/v. With the exception of the 24 hour time-point p/v with pIL-3 (where numbers of $\gamma\delta$ T cells were slightly increased relative to normal skin) there was little change in the prevalence of these cells over the time-course of the experiment (data not shown).

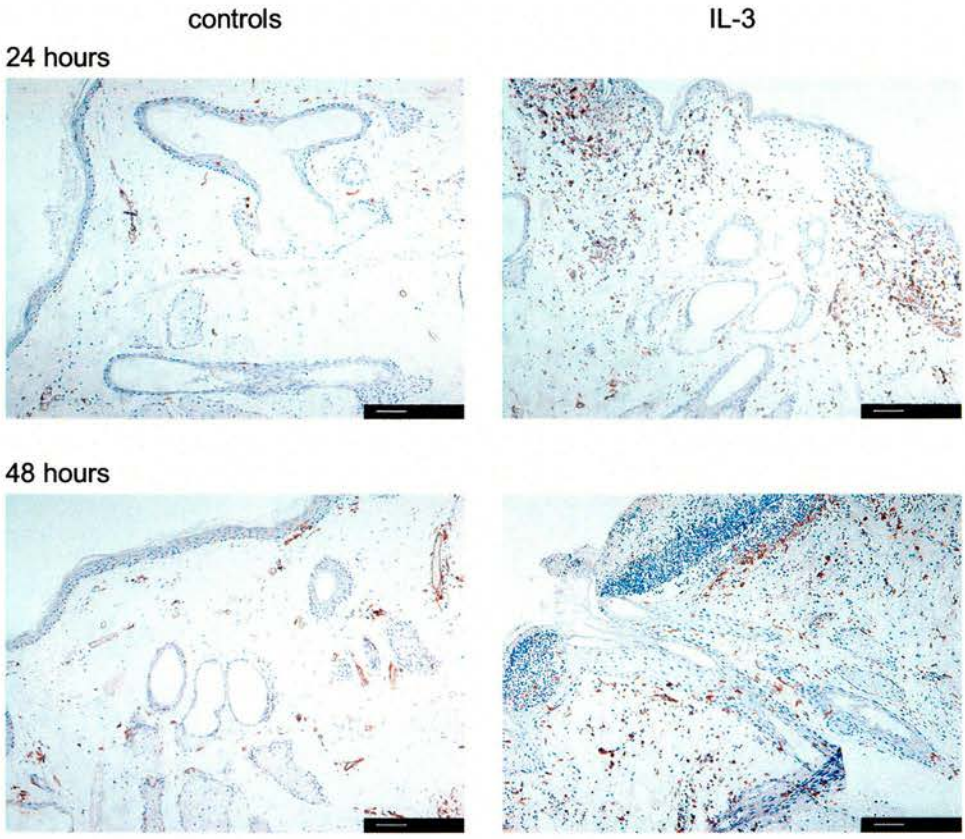

Figure 3.51 Infiltration of MHC class II^+ cells in pIL-3 vaccinated skin. Immunolabelling of MHC class II $DR\alpha^+$ cells was carried out with mAb VPM 54. Representative images are shown after staining pIL-3 vaccinated skin section (right panels) and NF-control vaccinated skin sections (left panels). Note the infiltration of small, round DR^+ cells 24 hours after pIL-3 administration and infiltration of DR^+ cells with a dendritic morphology 48 hours later. Sections were counterstained with haematoxylin. (Scale bar = 250µm.)

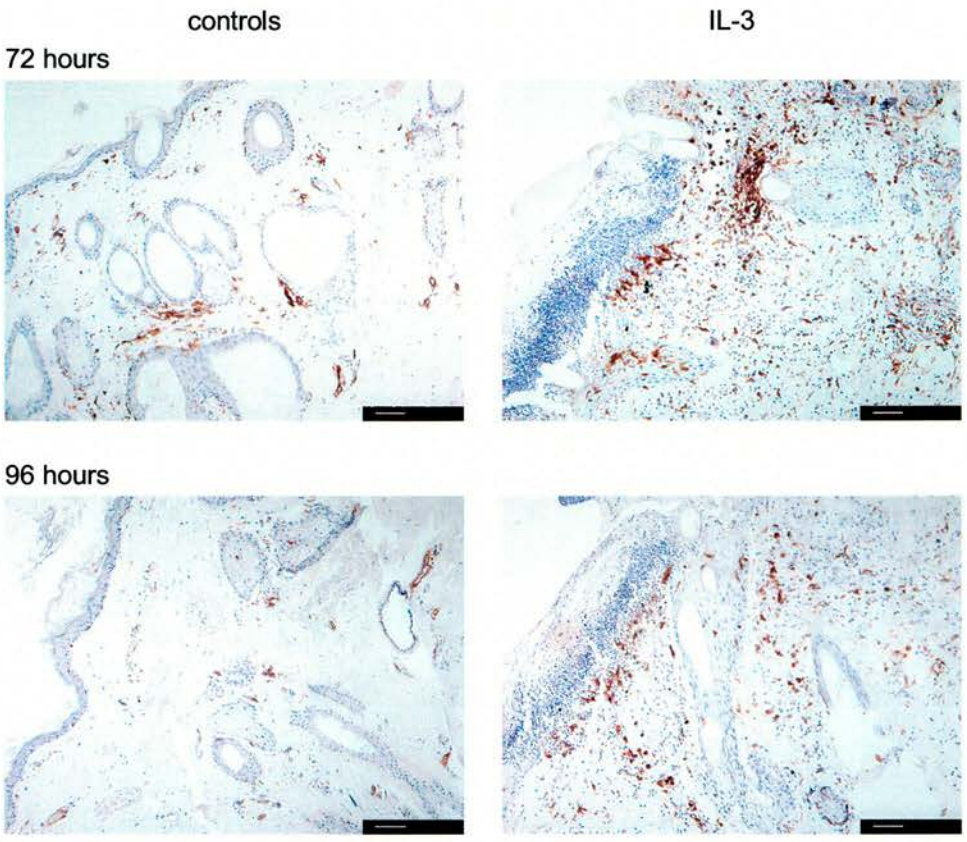

Figure 3.51 (cont.) (Scale bar = 250μm.)

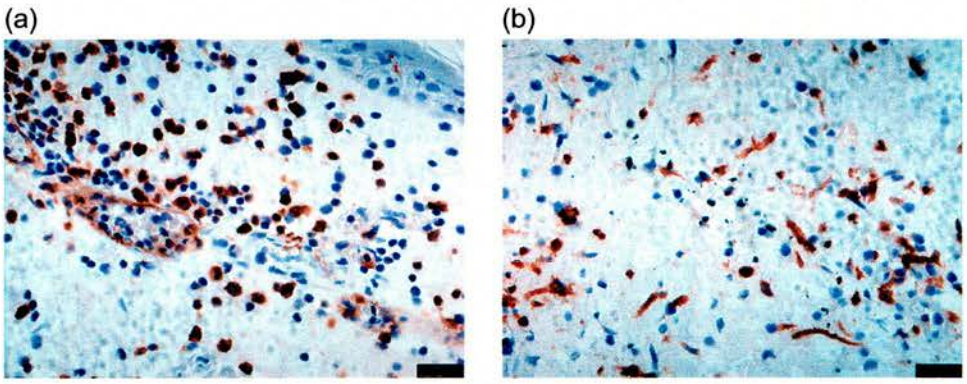

Figure 3.52 High power magnification of skin sections immunolabelled with mAb VPM 54 (anti MHC class II DRα). (a) 24 hours p/v; note the small MHC class II^+ mononuclear cells infiltrating the superficial dermis. (b) 72 hours p/v; note MHC class II^+ cells with the morphological appearance of fibroblasts located deep within the dermis. (Original magnification, ×250.)

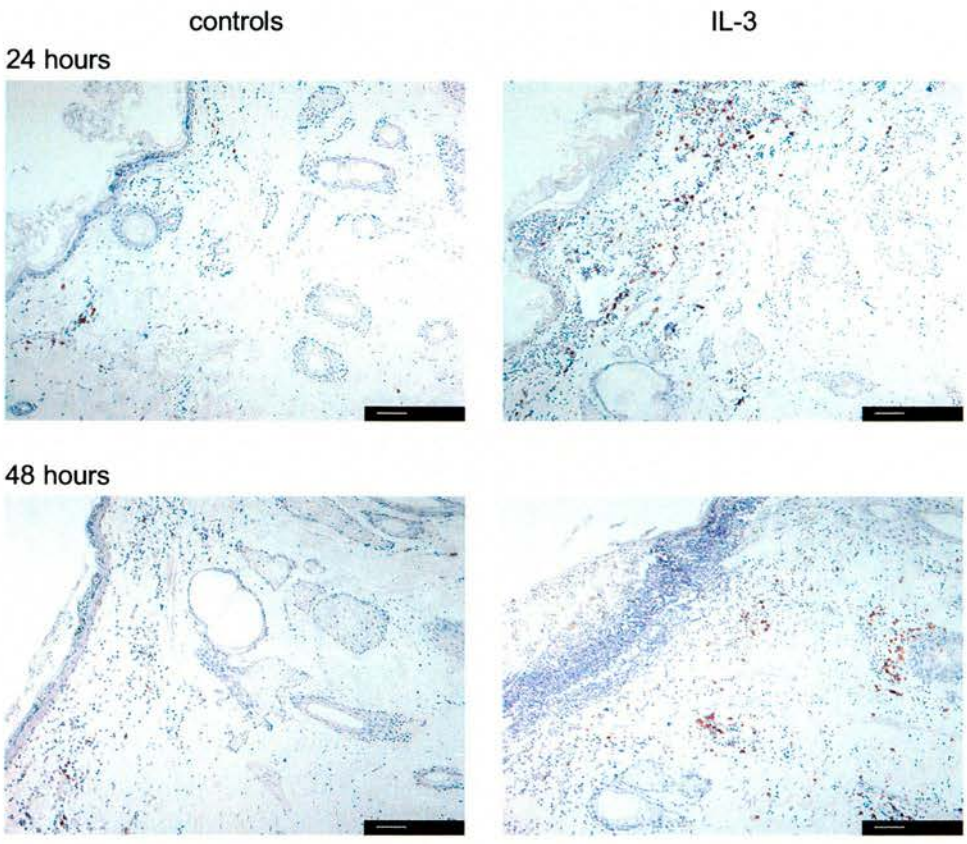

Figure 3.53 Immunostaining of $CD45RA^+$ lymphocytes in pIL-3 and NF-control vaccinated skin with mAb 73B. An increase in $CD45RA^+$ cells (B cells and naïve T cells) is evident 24 hours after pIL-3 administration. (Scale bar = 250μm.)

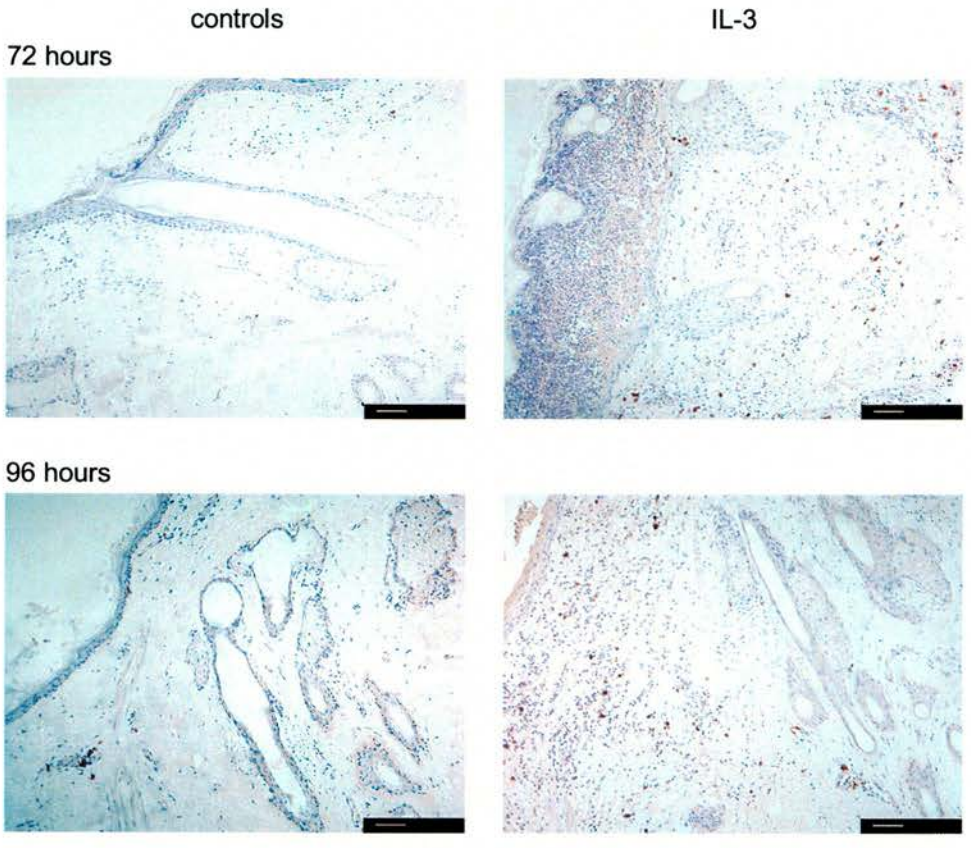

Figure 3.52 (cont.) (Scale bar = 200μm.)

3.6.2.3 Cytokine mRNA expression in skin after gene-gun delivery of pIL-3

Quantitative RT-PCR was employed to assess the kinetics of IL-3 mRNA expression in the skin from 16–96 hours and the kinetics of proinflammatory cytokine mRNA expression. RNA samples were treated as already described (Section 3.5.2.3) and validated to remove residual plasmid prior to the evaluation of samples by quantitative real-time RT-PCR (data not shown). Unfortunately, only two biopsies were available for the 48–96 hour time-points after pIL-3 administration in sheep 5 (biopsy experiment C), due to problems encountered with plasmid delivery in this experiment.

IL-3 mRNA expression

IL-3 mRNA expression remained at an almost constant level 16–24 hours after gene-gun bombardment with pIL-3 in sheep 5 (Figure 3.54a). Expression of IL-3 mRNA dropped markedly by 48 hours and remained at a similar level until the last sampling time-point (96 hours p/v). In sheep 6, expression of IL-3 mRNA declined in an almost linear fashion from 24 to 96 hours (Figure 3.54b). Expression of IL-3 mRNA was again undetectable in normal skin sections and in skin sections where the NF-control had been administered (data not shown), possibly as a result of the lack of specificity of the IL-3 primers employed in the assay (extensive primer-dimerisation was a consistent problem).

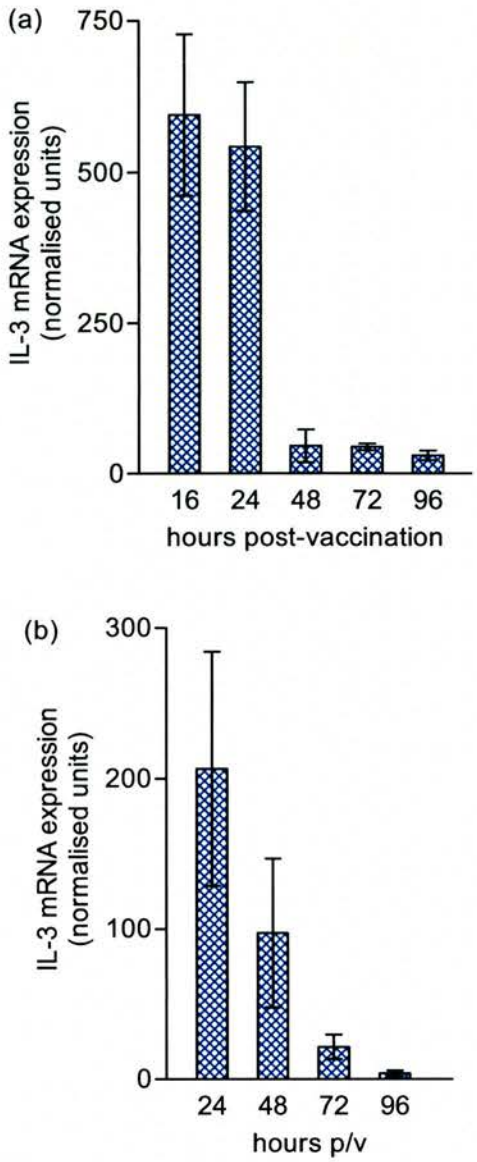

Figure 3.54 IL-3 mRNA expression in skin over 96 hours after gene-gun vaccination with pIL-3. (a) Sheep 5, (b) sheep 6. Data are presented as mean ± SEM.

IL-1β mRNA expression

Expression of IL-1β mRNA was consistently higher in pIL-3 vaccinated skin when compared to NF-control vaccinated skin (and normal skin) at all time points investigated in sheep 5. Furthermore, this difference was statistically significant ($p < 0.005$), where mean values for each time-point have been calculated and values obtained after pIL-3 vaccination compared with values obtained after NF-control vaccination (Figure 3.55a). There was however considerable variation in IL-1β expression in different skin sites vaccinated with pIL-3 at the 16 hour and 96 hour time-points. In addition, only one cDNA sample from the 48 hour time-point was available for analysis in this LightCycler® experiment. In sheep 6 (Figure 3.55b), IL-1β transcripts were highly elevated in pIL-3 vaccinated skin biopsies when compared to transcripts measured in normal skin and in NF-control vaccinated skin at 3 of the 4 time-points investigated. Furthermore, this difference was highly significant 48 hours after pIL-3 administration ($p < 0.001$).

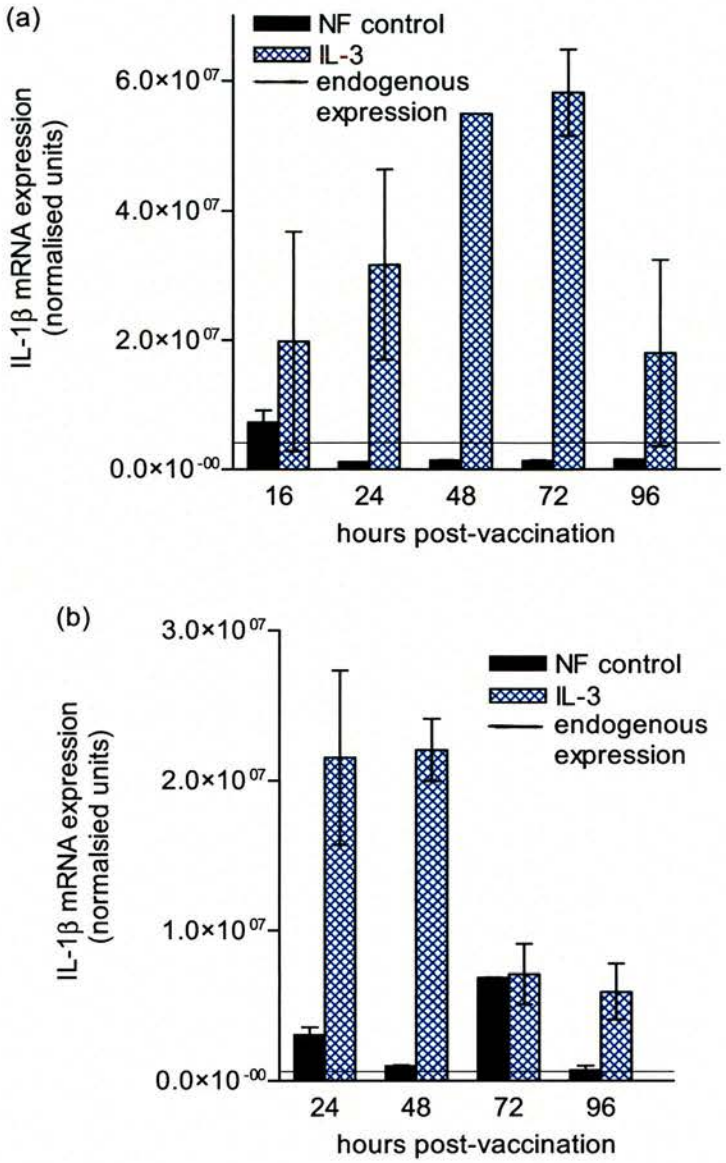

Figure 3.55 IL-1β mRNA expression in skin over 96 hours after gene-gun vaccination with pIL-3 and the NF-control. (a) sheep 5, (b) sheep 6. Note that only one biopsy cDNA sample from the 48 hour time-point was available from sheep 5 for analysis in this LightCycler® experiment. Data are presented as mean ± SEM.

IL-18 mRNA expression

As demonstrated in the previous experiments carried out in this study, IL-18 mRNA expression was lower in skin vaccinated with either plasmid (cytokine construct or the NF-control) than expressed in normal skin. A 2-3 fold reduction in IL-18 transcripts was apparent after administration of both plasmids 24 hours p/v. This was evident in both animals in this part of the study. In addition, expression of IL-18 mRNA was higher in the NF-control vaccinated skin biopsies harvested at 24, 72 and 96 hours than in those vaccinated with pIL-3 in sheep 5 (Figure 3.56a). Furthermore, this difference in IL-18 expression was statistically significant ($p < 0.03$). In contrast, IL-18 transcripts were comparable in skin after administration of either pIL-3 or the NF-control plasmid in sheep 6 (Figure 3.56b) with the exception of the 72 hour time-point, where levels were higher in the NF-control vaccinated skin biopsies. No statistically significant difference was apparent over the time-course in this animal ($p > 0.05$).

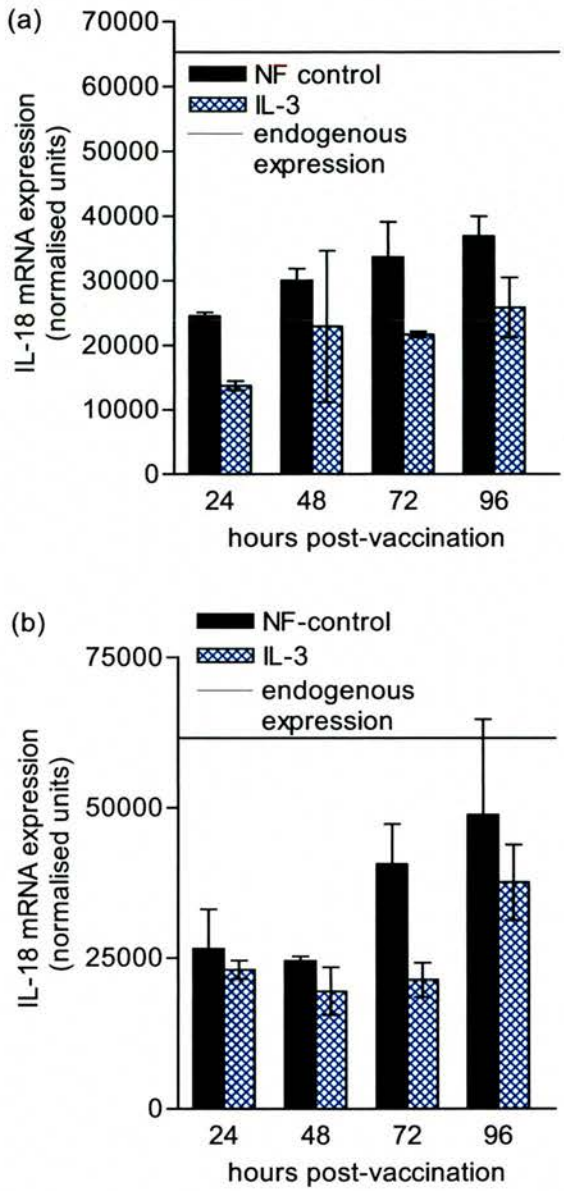

Figure 3.56 IL-18 mRNA expression in skin 24–96 hours after gene-gun vaccination with pIL-3 and the NF-control in sheep 5 (a) and in sheep 6 (b). Endogenous IL-18 expression is represented as a solid line. Data are presented as mean ± SEM.

TNF-α mRNA expression

The kinetics of TNF-α mRNA expression was also investigated after DNA vaccination with pIL-3 and the NF-control. Data are shown from both animals in Figure 3.57. TNF-α mRNA was expressed at higher levels from 24–96 hours in the pIL-3 vaccinated biopsies than in NF-control vaccinated skin in both sheep. In addition, administration of the NF-control plasmid resulted in an upregulation of TNF-α mRNA at most of the time-points investigated when compared to endogenous TNF-α expression (Figure 3.57a); however, it is evident in this experiment that the expression of TNF-α mRNA was significantly higher in biopsies obtained from pIL-3 vaccinated skin (sheep 6) than in NF-control vaccinated biopsies ($p < 0.002$). Although increased expression of TNF-α mRNA was evident after gene-gun delivery of pIL-3 when compared to NF-control vaccinated skin in sheep 5, this was not statistically significant ($p > 0.05$, Figure 3.57).

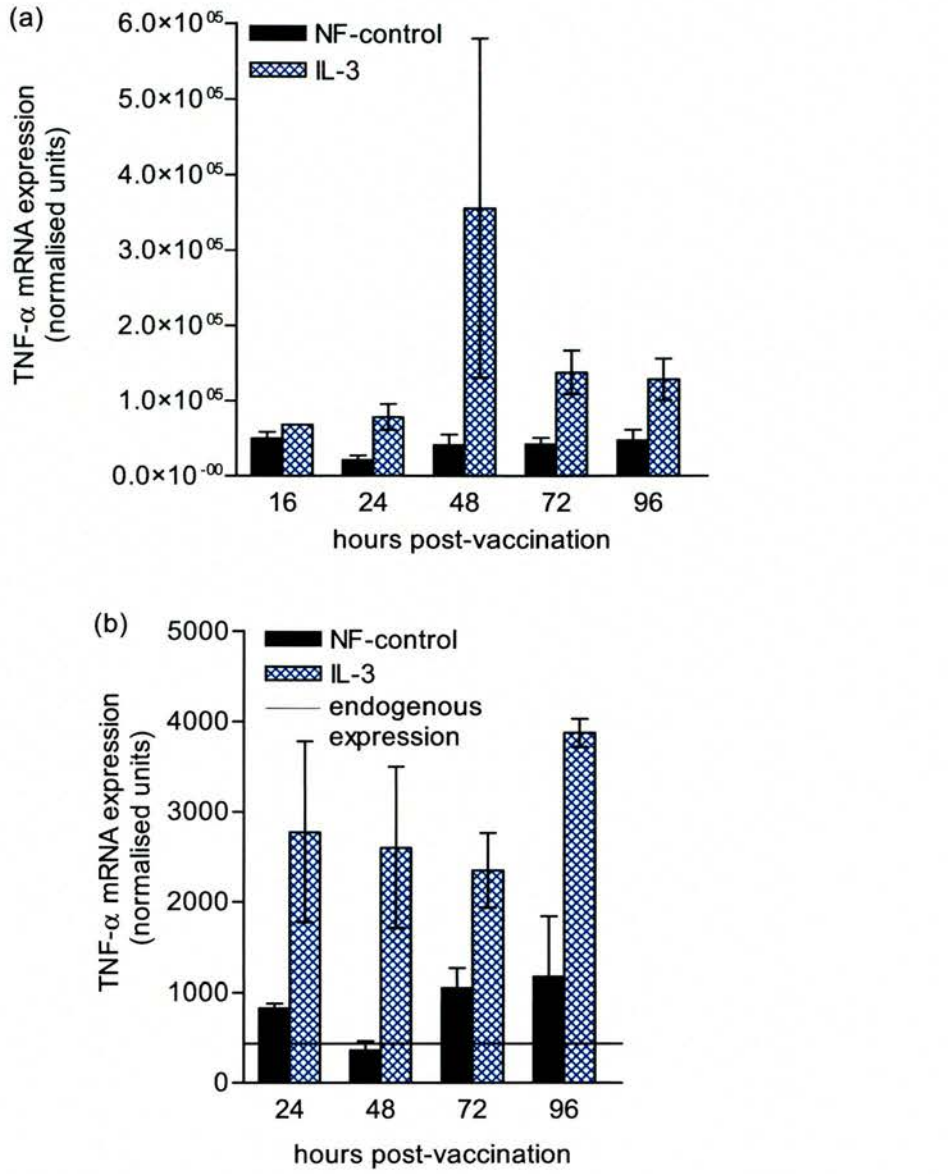

Figure 3.57 Expression of TNF-α mRNA in skin over 96 hours after gene-gun vaccination with pIL-3 and the NF-control. (a) Sheep 5, (b) sheep 6. Endogenous expression of TNF-α is represented as a solid line. Data are presented as mean ± SEM.

3.7 Discussion

3.7.1 Immunopathology of pGM-CSF vaccinated skin

3.7.1.1 Biopsy experiment A (1–7 days)

It was evident from biopsy experiment A that pGM-CSF caused a severe inflammatory reaction in the skin 24 hours after gene-gun delivery. This was characterised by the formation of epidermal microabscesses which were composed predominantly of neutrophils. In contrast, the dermal infiltrate was composed of some mononuclear cells and a large number of eosinophils 24 hours p/v. GM-CSF is indeed a chemoattractant for eosinophils (Warringa et al., 1991) and this early recruitment is in agreement with observations by Haig and colleagues (Haig et al, 1995a) following intradermal administration of recombinant GM-CSF. At later time-points the dermal infiltrate became largely composed of mononuclear cells and an infiltration of MHC class II^+ cells with the morphological appearance of DC was apparent 3–4 days after pGM-CSF administration. Whilst an inflammatory response was also induced after administration of control plasmid pEGFP-N1 (characterised by a mixed dermal infiltrate over the time-course), large foci of MHC class II DR^+ DC were not observed. Immunohistochemical staining revealed an infiltration of $CD45RA^+$ lymphocytes (expressed by both naïve T cells and B cells) at later time-points (5–6 days) after pGM-CSF administration. Since there are essentially no $CD45RA^+$ T cells in afferent lymph draining skin (Mackay et al, 1990), these cells are most likely to be B cells. Another interesting finding from this experiment was an apparent increase in γδ T cells 24 hours after administration of all of the plasmids.

3.7.1.2 Gene-gun delivery of NF-(GM-CSF) control induces mild inflammatory changes in ovine skin

To further understand the adjuvant mechanisms of GM-CSF DNA, an examination into the early events (1–24 hours) was required in order to assess the earlier events (i.e. before the peak inflammatory reaction had taken place). In addition, later time-points (up to 4 days p/v) were required in order to confirm DC infiltration and also to correlate the histological findings with cytokine expression in the skin. It was evident that the NF-control induced a mild inflammatory response in the first 24 hours; the biopsies taken from the NF-control vaccinated sites exhibited low-grade infiltration of neutrophils at the earlier time-points (2–24 hours), however no pustule formation was evident over the 4 days as was observed after pEGFP-N1 administration. Unfortunately, no direct comparison of the inflammatory effects induced after delivery of either pEGFP-N1 or the NF-control was made in this study.

Neutrophilic recruitment and pustule formation was documented by Braun and colleagues (Braun et al, 1999) and occurred regardless of the presence of plasmid on the gold beads, suggesting that the response was due to the delivery of gold, and not a response to bacterial DNA. The lesions were composed largely of neutrophils following vaccination with both pGM-CSF and pEGFP-N1 and it is likely that neutrophils represent the first cell population to be recruited to the vaccination site. The results from this study are in agreement with previous studies indicating that granulocytes are the first cells migrating into the tissue during inflammation (Braun et al, 1999; Van Der et al., 2001).

Keratinocytes, which comprise 95% of the cells in the epidermis, form the first line of defence in skin and alert the host to danger by the production of a number of cytokines (including GM-CSF, IL-1β and TNF-α; (Kimber et al., 2000). In accord with a mild inflammatory response was an increase in GM-CSF mRNA in NF-control vaccinated skin biopsies, possibly as a result of the damage elicited to the keratin layer by the gene-gun procedure. An increase in TNF-α and IL-1β transcripts was apparent as early as one hour after delivery of the control plasmid and levels were slightly elevated (when compared to endogenous levels) for up to 96 hours in some of the biopsies. Thereafter, levels of TNF-α and IL-1β declined to baseline levels. A slight increase in MHC class II^+ staining was evident at some of the early time-points (16–24 hours) and may be due to activation of resident skin cells and even endothelial cells; however, a pronounced infiltration of DC-like cells was not observed in any of the sections analysed.

3.7.1.3 pGM-CSF recruits neutrophils into the skin

In marked contrast to the effects elicited by the NF-control plasmid, was a pronounced infiltration of neutrophils as early as 2–4 hours after pGM-CSF delivery. The histological findings correlated well with the expression of GM-CSF mRNA, where transcripts peaked at approximately 4 hours in both animals. At this time-point neutrophils accumulated under the keratin layer and development of a micro abscess was evident as early as 6 hours p/v. GM-CSF mRNA progressively declined but was still slightly elevated at the 96 hour time-point, consistent with the sloughing of the epidermal layer. Quantification of TNF-α and IL-1β transcripts revealed differential expression patterns over time. TNF-α expression did not differ markedly from NF-control vaccinated skin biopsies at early time-points (1–6 hours) after pGM-CSF delivery; however, at later time-points (24–96 hours), TNF-α mRNA expression was elevated in skin vaccinated with pGM-CSF, consistent with a more pronounced inflammatory reaction. Perhaps the most striking observation with regard to cytokine expression in this study was the highly pronounced increase in IL-1β transcripts

after pGM-CSF administration, where levels increased in a linear fashion over the first 24 hours and remained highly elevated up to 4 days p/v. Expression of IL-1β mRNA was 200–300 fold higher in pGM-CSF vaccinated biopsies than in normal skin. Moreover, IL-1β transcripts remained sustained over the 4 days after pGM-CSF delivery, whereas levels had returned to those measured in normal skin 48 hours after delivery of the NF-control plasmid.

It is interesting to speculate which cells are the major source of IL-1β transcripts. IL-1β is produced almost exclusively by LC in murine epidermis (Heufler et al, 1992; Schreiber et al, 1992) however, IL-1β is also an inducible product of human keratinocytes (Kupper et al., 1986). GM-CSF has indeed been reported to promote the transcription and synthesis of IL-1β in mouse dendritic cell clones (Granucci et al., 1994) and human monocytes (Smith et al., 1990). Furthermore, GM-CSF induces IL-1β message accumulation in PMN (Fernandez et al., 1996) and is a well-known survival factor for PMN (Brach et al., 1992; Colotta et al., 1992). PMN are now known to play an important role in inflammation, immune responses, and tissue repair by secreting IL-1β (reviewed in Yamashiro et al., 2001). In this study, a pronounced accumulation of neutrophils was evident as early as 4 hours and it is possible that neutrophils are responsible for such high levels of IL-1β transcripts. *In situ* hybridisation in combination with immunohistochemistry would help to address the source of IL-1β.

3.7.1.4 pGM-CSF recruits DC into the skin

In agreement with biopsy experiment A, a pronounced infiltration of MHC class II^+ cells 4 days after pGM-CSF administration was evident in both animals. Unfortunately, attempts to further characterise MHC class II^+ infiltrates proved difficult; staining with anti-CD14 mAb in order to differentiate infiltrating macrophages from DC was unsuccessful. Staining with anti-CD1b was also unsuccessful and whilst mAb successfully stained cells in cytospins (results not shown), the morphology of the cells and tissue was poor. Further analysis of MHC class II^+ infiltrates is imperative to confirm that these cells are indeed DC.

It could be envisaged that GM-CSF is first chemotactic for PMN resulting in their early recruitment into the skin. PMN start to accumulate where abundant GM-CSF protein is present which in turn induces IL-1β expression in PMN, thereby amplifying the acute inflammatory responses by recruiting additional PMN into inflammatory sites. Recently, it has been reported that defensins and other peptides pre-stored in PMN granules attract monocytes, dendritic cells and T cells, leading to the hypothesis that the release of PMN granular peptides may link innate and adaptive immunity (Yamashiro et al, 2001). It is now coming to light that there is first a requirement for "priming" of PMN by cytokines to induce the delayed expression of monocyte chemoattractant protein-1 (MCP-1), which is a signal

for mononuclear cells (Rand et al., 1996). As a result of the chemokines and cytokines expressed by infiltrating PMN and the increased permeability of endothelium, recruitment of DC takes place. In line with this was an upregulation of MCP-1 protein which coincided with maximal DC infiltration after DNA vaccination with pGM-CSF (Perales et al, 2002).

3.7.2 Immunopathology of pIL-3 vaccinated skin

In the first study conducted, the histological effects elicited after pIL-3 administration were not nearly as pronounced as the histological changes induced by pGM-CSF. Indeed, at some of the time-points investigated, the effects of pIL-3 were only slightly more pronounced than observed with pEGFP-N1 (control plasmid). Consistent with the known *in vivo* effects of pIL-3 was an increase in the number of eosinophils, particularly within the first 48 hours (Warringa et al, 1991). Immunohistochemical staining revealed a modest increase in small MHC class II^+ mononuclear cells by approximately 24 hours. Serial sections were compared after staining with mAb specific for both MHC class II and CD45RA and a similar staining pattern was apparent. It is likely that these MHC class II^+ $CD45RA^+$ cells were B cells (as discussed in 3.7.1.1). It is known that IL-3 receptors are expressed at low levels on the majority of peripheral blood B-lymphocytes (Macardle et al., 1996) and perhaps B cells are recruited from the blood to the skin after pIL-3 administration. Further analysis is required in order to confirm this preliminary finding. No apparent infiltration of DC was observed after pIL-3 administration in biopsy experiment A.

For subsequent analysis of pIL-3 effects, the GFP gene was removed from the construct. Since no comparison was made using the same animals with pIL-3 containing the GFP gene and the construct where GFP had been removed, it is impossible to confirm if removal of GFP gene had any effect; however, in all subsequent experiments a more pronounced inflammatory reaction was evident after pIL-3 (–GFP gene) than observed in biopsy experiment A. In addition a more pronounced infiltration of eosinophils and mononuclear cells was apparent by 24 hours, when compared to biopsy experiment A. Furthermore, large infiltrates of MHC class II^+ cells were identified 3–4 days after pIL-3 administration. It remains to be determined if the cells expressing MHC class II 3 days after pIL-3 administration were indeed DC.

The kinetics of pIL-3 mRNA expression followed a similar trend observed after pGM-CSF administration, notably where peak expression was observed approximately 4 hours after administration and declined thereafter. IL-3 transcripts were detected up to 96 hours p/v, whereas IL-3 transcripts could not be detected in normal skin or in the NF-control vaccinated

skin biopsies. Consistent with a pronounced inflammatory reaction was a marked increase in TNF-α and IL-1β transcripts over the time-course. It should however be acknowledged that attempts to detect recombinant IL-3 were largely unsuccessful. If further work is to be carried out with this cytokine, it is imperative that functional protein is demonstrated to be expressed. Since problems were encountered using the anti-IL-3 mAb, an alternative is to measure the *in vitro* stimulatory capacity of supernatants collected from IL-3-transfected cells using bone marrow cultures.

3.7.3 IL-18 mRNA decreases after gene-gun vaccination

In this study, gene-gun bombardment with all plasmids caused a decrease in IL-18 transcripts in skin (relative to endogenous expression). IL-18 is expressed by both keratinocytes and LC (Stoll et al., 1997; Stoll et al., 1998) and gene-gun vaccination with pGM-CSF has been documented to result in an increase in IL-18 protein (Perales et al, 2002). This present study relied on the quantification of mRNA transcripts to assess changes in gene expression after DNA vaccination. Whilst quantitative RT-PCR is a powerful method and gave some insight into the changes induced in tissues after adjuvant administration, some caution in the interpretation of the data is imperative. What this study fails to show is how mRNA expression is related to protein expression and secretion, and so in the case of IL-18 expression, the number of relative transcripts may be less shortly after DNA vaccination, but levels of protein could indeed be higher. In addition, it has been reported that cells harbour high levels of IL-18 mRNA which is rapidly translated upon stimulation, thus the level of mRNA may not correlate with the level of protein expression. It would therefore be more informative if this study had also included some evaluation of protein expression.

IL-12p40 transcripts are reported to be expressed at low levels in normal skin (Scarozza et al., 1998) and purified LC are known to spontaneously produce IL-12p40 (Tada et al., 2000). Since IL-12 promotes the accessory cell function of epidermal LC (Suemoto et al., 1998), expression of this cytokine after pGM-CSF administration was analysed. In this study, mRNAs encoding IL-12p40 were detected in normal skin (by conventional RT-PCR), but rarely after pGM-CSF vaccination which is in line with the observation that GM-CSF inhibits IL-12p40 production by stimulated LC (Tada et al, 2000). In contrast, Perales and colleagues detected IL-12 protein within 24–48 hours in skin following gene-gun vaccination with pGM-CSF (Perales et al, 2002). In addition, IL-10 transcripts could not be detected by

quantitative RT-PCR in this study; however, conventional RT-PCR using undiluted cDNA samples revealed that IL-10 was indeed expressed in normal skin and in all of the pGM-CSF vaccinated samples. Quantification of this anti-inflammatory cytokine merits further investigation; in particular it would be of interest to determine if IL-10 expression is upregulated when expression of proinflammatory genes is at maximal levels.

3.7.4 DC migration and maturation

During infection, microbial components provide signals that alert the immune system to danger and promote the generation of immunity by stimulating DC to mature so that they can present foreign antigens and stimulate T cells. In the absence of danger signals, there is often no immune response or tolerance may develop. This has led to the concept that the immune system responds only to antigens perceived to be associated with a dangerous situation such as infection. GM-CSF is not only a growth factor of DC but is thought to exert its adjuvant activity by acting as a danger signal. In agreement with this latter statement, a pronounced upregulation of IL-1β and TNF-α was induced after gene-gun delivery of pGM-CSf (and pIL-3) and levels remained elevated over 4 days. Both of these cytokines are pivotal in DC maturation and migration. Moreover, GM-CSF and IL-1β mediate the maturation of murine epidermal LC into potent immunostimulatory DC (Heufler et al., 1988). DC were observed to enter the skin 3−4 days after pGM-CSF delivery and accumulated in the dermis and then disappeared, presumably having migrated to the DLN. Isolation of DC after gene-gun delivery of pGM-CSF or pIL-3 was therefore the next logical step to take, since hyperelevated levels of IL-1β in the skin 3−4 days after pGM-CSF administration may cause maturation and migration of DC.

4 Effects of pGM-CSF on ALDC draining the site of gene gun delivery

4.1 Introduction

Recent studies indicate that the nature of maturation stimuli and the kinetics of activation have a quantitative and qualitative impact on T cell stimulation. Understanding how DC interpret different stimuli is pivotal to our understanding of the generation of immune responses following infection and vaccination. Interest in GM-CSF as a molecular adjuvant is due to its dual role as a growth factor for DC and as an inducer of inflammation or "danger", resulting in the activation and maturation of DC. Indeed, enhancement of humoral and cell-mediated immune responses has been well documented after vaccination with plasmids encoding poorly immunogenic antigens in combination with GM-CSF in mice. This enhancement has been attributed to the recruitment of DC to the site of vaccination. Some enhancement of immune response has also been documented in outbred species; however, further optimisation is still required if GM-CSF is to be successfully employed in vaccination procedures.

The mechanisms by which GM-CSF enhances the immune response are not fully understood. Studies in mice and humans have focused on the administration of large quantities of recombinant GM-CSF and the preferential expansion and activation of myeloid DC has been reported in both species (reviewed in Chapter 1). Attempts to directly isolate and study *ex vivo* DC after DNA vaccination with pGM-CSF are currently lacking and would further our understanding of the mechanisms by which this adjuvant works *in vivo*. Alterations in the type and quantity of cytokines expressed by DC are likely to be a major influence in T cell sub-population activation. In addition, changes in the expression of antigen presentation molecules and costimulatory markers (CD80 and CD86) need to be further addressed after DNA vaccination with pGM-CSF, since upregulation of these markers would equip DC with a greater capacity to stimulate T cells. If GM-CSF is to be fully exploited as a molecular adjuvant, it is essential to understand both the changes in DC subpopulation balance and the characteristics of expanded DC relative to those of steady-state DC after vaccination with pGM-CSF.

Experiments on the physiology of DC require access to DC closest to their native, non-activated form. Human and mouse systems rely on complex and lengthy cultures or isolation of DC from tissues and it is therefore difficult to equate DC to physiological conditions. Cannulation of the pseudoafferent lymphatics in sheep provides an efficient method to

directly access unmanipulated DC closest to their natural form as they traffic from the skin to the lymph node. This technique is performed by first removing the DLN and allowing anastomosis of the afferent vessels with the remaining efferent duct. Approximately eight weeks later, the "efferent" vessel can be cannulated and afferent lymph obtained for periods sometimes in excess of 2 months. Although this technique is feasible in both rats and in cattle, only intestinal lymph is available in the former and in both species cannulations remain patent for only a few days (John Hopkins, personal communication). By pseudoafferent lymphatic cannulation of sheep, it is possible to monitor phenotypic and functional changes in DC draining from the skin after DNA vaccination with pGM-CSF over a longer time-period. This is therefore a potentially useful model in order to further investigate the biology of DC which infiltrate the skin approximately 4 days after DNA vaccination with pGM-CSF in sheep (chapter 3). A further advantage of the ruminant model is that it enables collection of large numbers of cells for more detailed analysis throughout the duration of any response.

Two ALDC subpopulations have been well characterised in both cattle (Howard et al, 1997) and in rats (Liu et al, 1998c) and appear to have different roles *in vivo*. Bovine SIRPα^+ ALDC are more effective at stimulating proliferative responses in allogeneic CD4$^+$ and CD8$^+$ T cells (Howard et al, 1997). Differences in function of bovine ALDC have been related to differences in constitutive cytokine expression by the two populations as defined by the expression of SIRPα and not due to a difference in expression of costimulatory markers (Stephens et al, 2003). Bovine SIRPα^- ALDC constitutively express high levels of IL-12p40, whereas IL-10 transcripts are rare or absent in this subpopulation. Conversely, SIRPα^+ ALDC express low levels of IL-12p40 but constitutively express high levels of pro-inflammatory IL-6, IL-1α and IL-1β and occasionally, low levels of IL-10. Moreover, the induction of strong CD8$^+$ T cell responses by SIRPα^+ ALDC is related to the high level of expression of IL-1α (Hope et al, 2001).

Cytokine profiles of rat ALDC have not as yet been ascertained; however, rat splenic CD4$^-$ /SIRPα^- DC were reported to produce large quantities of IL-12 and TNF-α and induced Th1 responses in allogeneic CD4$^+$ T cells, whereas CD4$^+$/SIRPα^+ DC produced low amounts of IL-12 and no TNF-α, but induced both Th1 and Th2 responses (Voisine et al, 2002). As described in cattle, rat splenic and afferent lymph SIRPα^+ DC are highly immunostimulatory, whereas CD4$^-$/SIRPα^- DC exhibit a poor CD8$^+$ T cell stimulatory capacity (Liu et al, 1998c; Voisine et al, 2002). Furthermore, a recent study indicates that SIRPα^- ALDC transport material from apoptotic enterocytes to T cell areas of mesenteric lymph nodes and a role in the maintenance of tolerance has thus been proposed (Huang et al, 2000).

Ovine ALDC subpopulations have been partially characterised (Bailey, 2003); however, the cytokine profiles of steady-state ovine ALDC have not as yet been determined. Further characterisation of the two subpopulations was therefore essential in order to ascertain any changes in cytokine expression after DNA vaccination with pGM-CSF and also to further our understanding of ovine ALDC based on expression of the SIRPα molecule.

4.2 Aims

The aims of this part of the study were to isolate ovine ALDC based on the expression of SIRPα and to:

Characterise ovine SIRPα$^+$ and SIRPα$^-$ ALDC subpopulations in the steady-state flux from the skin

(i) Characterise the morphology and cell-surface marker expression

(ii) Quantify expression of cytokine transcripts (IL-12p40, IL-18, IL-10, TNF-α and IL-1β)

(iii) Investigate TLR expression and LC-specific transcripts

Characterise SIRPα$^+$ and SIRPα$^-$ DC subpopulations after pGM-CSF administration

(i) Quantify cytokine mRNA expression in SIRPα$^+$ and SIRPα$^-$ ALDC at intervals after gene-gun vaccination with pGM-CSF

(ii) Determine if GM-CSF causes expansion of SIRPα$^+$ and SIRPα$^-$ ALDC

(iii) Determine changes in cell-surface markers on MHC class II$^+$ ALDC

4.3 Phenotypic characterisation of ALDC

4.3.1 Isolation of SIRPα$^+$ and SIRPα$^-$ subpopulations of ALDC by cell sorting

ALDC were obtained by cannulation of afferent lymphatics as described in chapter 2 (Section 2.2.4.1). This technique allows the collection of lymph with a cellular composition identical to true afferent fluid. Experiments were not started until at least seven days after cannulation to guarantee access to cells unaffected by surgical trauma. A typical 24-hour collection of 100ml of lymph contains approximately 1×10^6 cells/ml of which 1–10% are non-lymphoid MHC class II$^+$ DC (Hopkins et al, 1989). A 24 hour collection of lymph may therefore contain between 10^6 and 10^7 DC. There is no single surface marker that is both specific for DC and is expressed by all DC; therefore it is imperative that attempts to isolate DC are not based solely on the expression of a single marker. There are several "pan"-DC surface markers for which there are antibodies available for sheep (Table 4.1) and one such marker is MHC class II. Constitutive expression of MHC class II is usually restricted to professional APC (Puri et al, 1987), although in sheep afferent lymph the majority of CD4$^+$, CD8$^+$ and γδ T cells express both DQ and DR molecules (Dutia et al, 1993a). In addition, MHC class II expression is inducible in (human) neutrophils (Radsak et al., 2000). MHC class II is however expressed at significantly higher levels on ALDC than expressed on other cell types, including both macrophages (Santin et al., 1999) and B cells (Hopkins et al, 1986); indeed the level of MHC class II expression on ALDC is 3–10 greater than on resting B cells.

ALDC were enriched to approximately 60% (when examined by light microscopy) using the density-gradient medium, OptiPrep™, as outlined in chapter 2 (Section 2.2.4.6). OptiPrep™ was used to enrich for DC as it does not appear to cause activation of APC unlike Percoll gradients which cause activation following ingestion of silica particles (Graziani-Bowering et al, 1997). ALDC were double immunolabelled using IL-A24 mAb that recognises the SIRPα molecule (Brooke et al, 1998; Ellis et al., 1988) followed by a biotinylated mAb (SW73.2) that is specific for a nonpolymorphic determinant on sheep class II (MHC class II DR DQβ) (Hopkins et al, 1986) since this combination of mAb resulted in clearly defined populations of ALDC (Section 2.2.4.7).

Table 4.1 Cell surface markers expressed by ALDC and available ruminant-specific mAb. The table also lists potential uses and/or limitations in using the listed mAb in cell sorting of ALDC populations.

surface marker	mAb(s)	cell types expressing surface marker	uses/limitations for cell sorting	references
CD1b	VPM 5	dermal DC, cortical thymocytes	DC express different levels of CD1	Rhind et al (1996b)
panCD1	SBU-T6	LC, dermal DC, B cells mammary mϕs, lamina propria mϕs		
CD11c	OM1	interstitial DC mϕs	+/– expression on DC	Gupta et al (1993)
DEC-205 (WC6)	(i) IAH CC98 (ii) IL-A114 (ii) IL-A53	(i) stains <30% lymphocytes from blood & lymph (ii) stains majority of DC. Weak reactivity with granulocytes (iii) staining of B cell areas and macrophages in Peyer's patch and lamina propria	ALDC express higher WC6 antigen (DEC-205) than expressed on other cells (Gliddon et al, 2004)	Dutia et al (1993b)
MHC class IIβ MHC class IIα	SW73.2 VPM 54	DC, mϕs, activated lymphocytes, monocytes	DC express higher MHC class II than on other cells, including B cells and mϕs	Hopkins et al (1986)

For subsequent cell sorting, DC were defined by:

(i) High FSC and SSC (due to their large size and granularity)

(ii) High MHC class II (channel number > 10^3)

100% of ALDC express high levels (channel number $\geq 10^3$) of surface MHC class II. Individual gates were therefore positioned around the MHC class II^{hi} $SIRP\alpha^+$ and MHC Class II^{hi} $SIRP\alpha^-$ populations. A representative experiment illustrating the gate criteria for cell sorting is shown in Figure 4.1. The $SIRP\alpha^+$ population is the larger of the two populations of ovine ALDC; approximately 80% (range 71–86%) of ovine ALDC express SIRPα (Table 4.2), as was reported with bovine ALDC (Brooke et al, 1998). This is also in agreement with an earlier study, where the SIRPα molecule was expressed on the majority

(approximately 58%) of ovine ALDC using an immunoperoxidase staining method (Haig et al., 1995b).

It was then deemed necessary to confirm that ALDC purified by FACS were indeed DC, since MHC class II expression is not restricted to these cells. In addition, the SIRPα molecule is expressed on bovine monocytes as well as DC (Brooke et al, 1998). Expression of SIRPα by a subset of ovine lymphocytes is evident in Figure 4.2. It was therefore vital that purified ALDC populations were analysed by employing a variety of different techniques to confirm that cells displayed characteristics typical of DC prior to carrying out further work. It was also of interest to compare morphological characteristics of $SIRP\alpha^{+}$ and $SIRP\alpha^{-}$ ALDC subpopulations with those already described in cattle and rats.

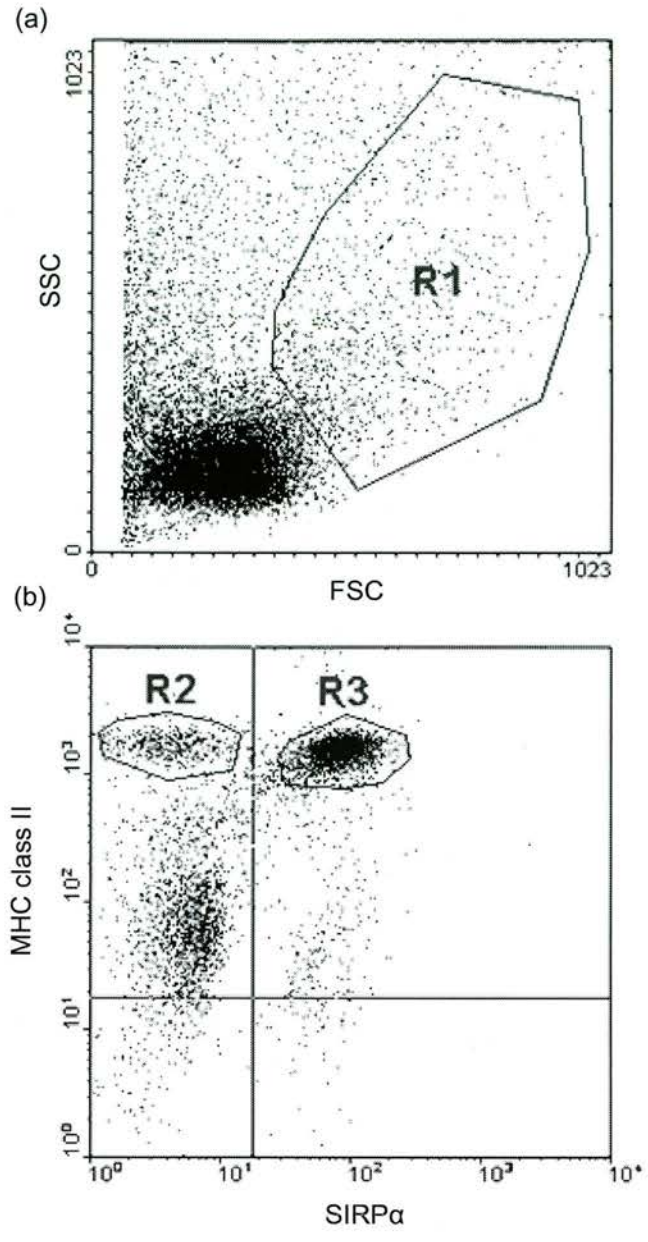

Figure 4.1 Two-colour flow cytometry of ALDC. (a) ALDC were gated based on high FSC and SSC (gate R1). (b) DC were immunolabelled with mAb IL-A24 (anti-SIRPα) followed by the biotinylated mAb SW73.2 (anti-MHC class II β). To isolate the two populations of ALDC, gates (R2 and R3) were positioned around cells, which express high MHC class II (channel number > 10^3).

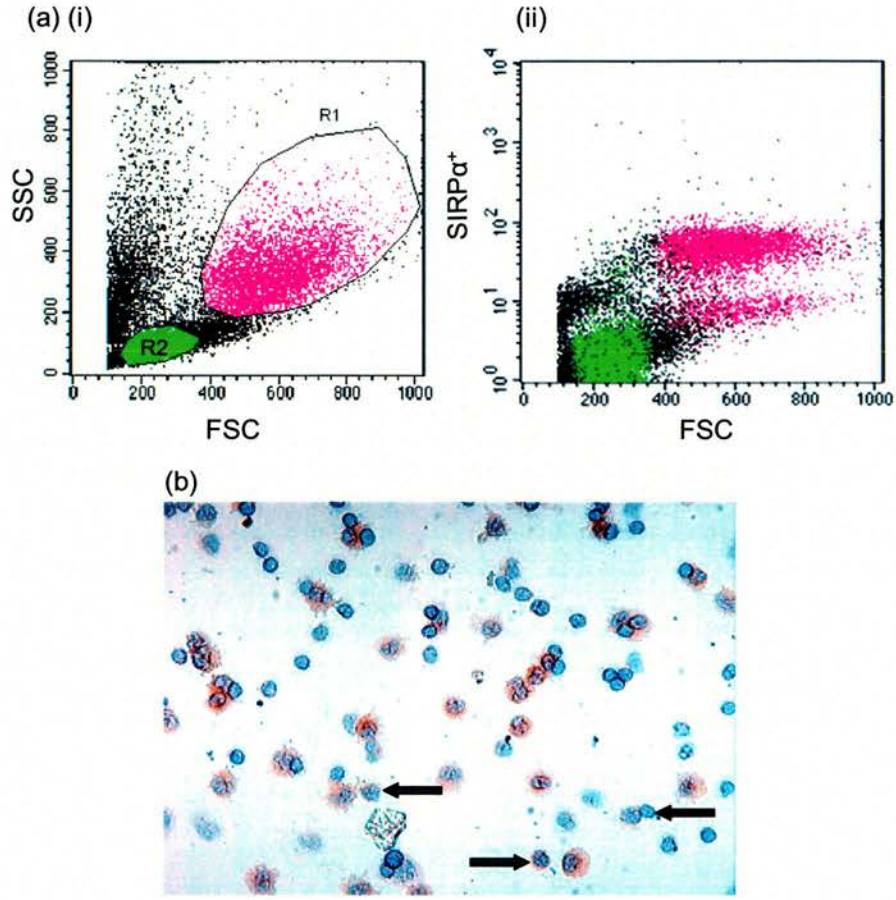

Figure 4.2 ALC stained with mAb IL-A24 (anti-SIRPα). (a) Flow cytometry analysis of ALC stained with mAb IL-A24 (detected with a FITC-conjugated mAb). (i) FSC and SSC profiles of ALC. For FACS analysis, gates were routinely set to exclude dead cells and discriminate between two regions containing predominantly APC and large blasts (R1) or small lymphocytes (R2). (ii) Two populations of cells (SIRPα$^+$ and SIRPα$^-$) are evident in R1 (pink). A small population of cells in the lymphocyte-gate (R2) are also SIRPα$^+$ (green). (b) DC-enriched fraction (fraction 1 after centrifugation with OptiPrep™) immunolabelled with mAb IL-A24 (detected with a peroxidase-conjugated mAb) and counterstained with haematoxylin. Most ALDC react with mAb IL-A24 (large veiled brown cells). Smaller mononuclear cells (black arrows) also react with this mAb.

Table 4.2 Cell sorting experiments carried out with the DC-enriched fraction obtained from "resting" lymph. The percentages of SIRPα$^{+/-}$ ALDC are derived from the number of cells recorded in each gate (R2 and R3) upon initial analysis and not from the total numbers of each FACS–sorted population isolated. Approximately 80% (range 71–86%) of ALDC express the SIRPα antigen. The table also lists the total number of SIRPα^{+} and SIRPα^{-} ALDC obtained from each cell sort. Cell sorting experiments 5.0–10.0; cell sorts after DNA vaccination with pGM-CSF (Section 4.6) are omitted. (NA, not assessed; *, no further work was carried out with this sample due to low purity.)

sort number	sheep ID	SIRPα^{+} (%)	SIRPα^{-} (%)	number of SIRPα^{+}	number of SIRPα^{-}	SIRPα^{+} purity (%)	SIRPα^{-} purity (%)
1.0	JH1	85	15	56, 511	9891	95	96
2.0	JH1	79	21	446, 651	114, 442	99	96
3.0	JH2	75	25	343, 137	160, 165	96	NA
4.0	JH2	71	29	640, 223	313, 367	99	NA
11.0	JH3	79	21	401, 816	362, 824	93	*42
12.0	JH3	71	29	564, 372	159, 526	95	90
13.0	JH3	77	23	140, 000	40, 000	96	95
14.0	JH4	77	23	648, 952	156, 993	97	97
15.0	JH4	79	21	258, 962	78, 401	95	90
16.0	JH5	86	16	2.69×10^6	326, 607	100	96
17.0	JH6	80	20	158, 742	29, 671	NA	NA
18.0	JH6	78	22	233, 398	54, 346	98	97
19.0	JH6	82	18	122, 881	24, 992	NA	NA
20.0	JH6	77	23	NA	NA	96	95

4.3.2 Morphological characterisation of SIRPα$^+$ and SIRPα$^-$ ALDC

Experiments were then undertaken in order to compare the morphology of the purified SIRPα$^+$ and SIRPα$^-$ ALDC. Immediately after cell sorting, cytospins were prepared from each collection (Section 2.2.2.3). Cells were fixed in ice-cold acetone and either stained with Giemsa, or were restained with mAb IL-A24 and counterstained with haematoxylin. Representative images are shown in Figure 4.3. DC were defined by reported criteria, notably that they are typically large mononuclear cells with round or indented nuclei with prominent dendritic processes (Steinman, 1991). Both populations of cells have typical features of DC, as illustrated by their large size (>10μm) and prominent nuclei. Furthermore, both populations show pronounced protrusions and microvillous projections of their plasma membrane typical of DC (Drexhage et al., 1979).

Differences in morphology are apparent between the two populations. SIRPα$^+$ ALDC contain large nuclei with relatively sparse cytoplasm and multiple blunt processes (pseudopodia) (Figure 4.3a). In contrast, many SIRPα$^-$ ALDC display a frilly or veiled appearance, which is particularly evident in Figure 4.3f. In addition, SIRPα$^-$ ALDC appear to be a relatively homogeneous population of cells, in contrast to the heterogeneous SIRPα$^+$ ALDC subpopulation. When viewed by light microscopy, SIRPα$^-$ cells are slightly larger than SIRPα$^+$ ALDC and this difference is confirmed by analysis of light scatter profiles by flow cytometry (Figure 4.4). These morphological distinctions are not absolute, and DC with intermediate morphology are present in both populations.

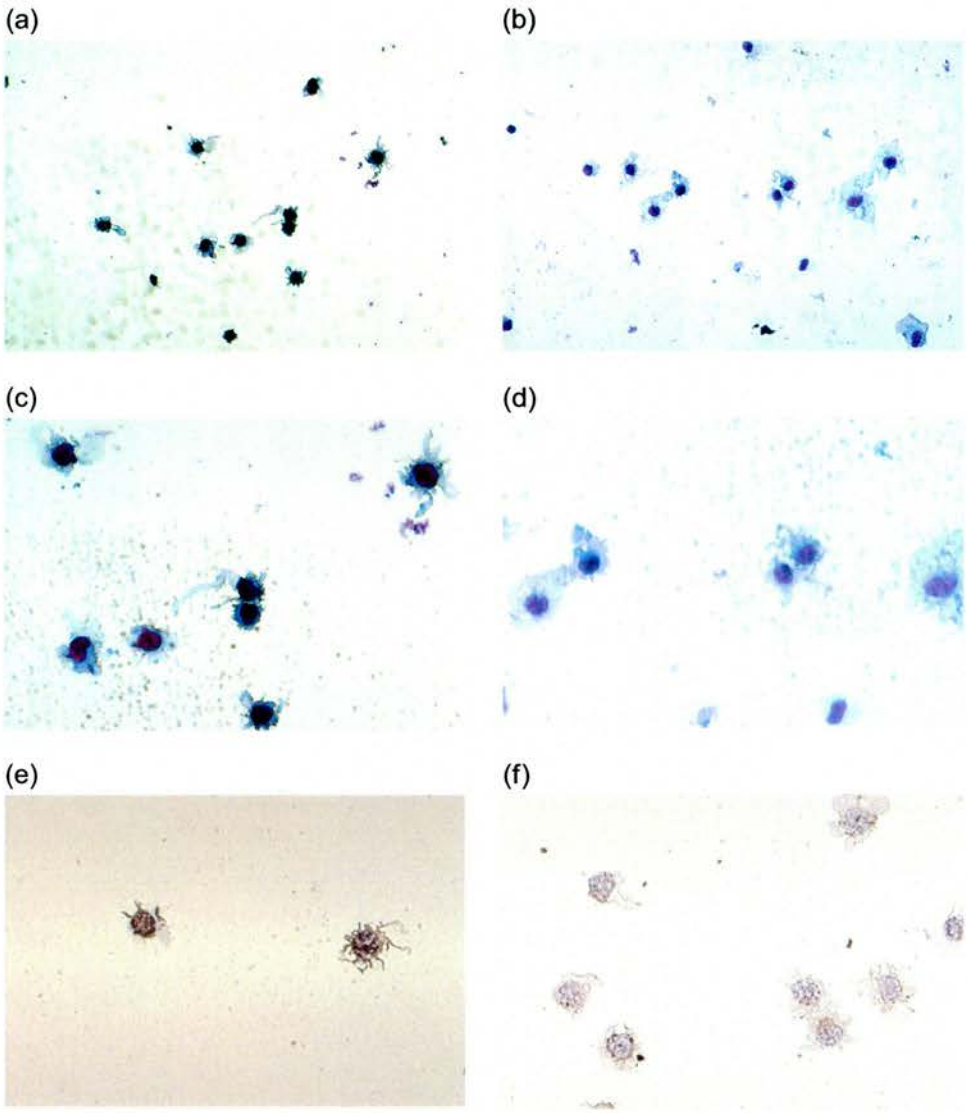

Figure 4.3 Morphology of SIRPα$^+$ and SIRPα$^-$ ALDC. FACS-sorted ALDC were cytocentrifuged and either stained with Giemsa or re-immunolabelled with IL-A24 and counterstained with haematoxylin. SIRPα$^+$ (a, c & e) and SIRPα$^-$ (b, d & f) ALDC were then examined by light microscopy.

(a) SIRPα$^+$ ALDC stained with Giemsa (original magnification, ×80)
(b) SIRPα$^-$ ALDC stained with Giemsa (original magnification, ×80)
(c) SIRPα$^+$ ALDC stained with Giemsa (original magnification, ×250)
(d) SIRPα$^-$ ALDC stained with Giemsa (original magnification, ×250)
(e) SIRPα$^+$ ALDC stained with IL-A24 (original magnification, ×250)
(f) SIRPα$^-$ ALDC stained with IL-A24 (original magnification, ×250)

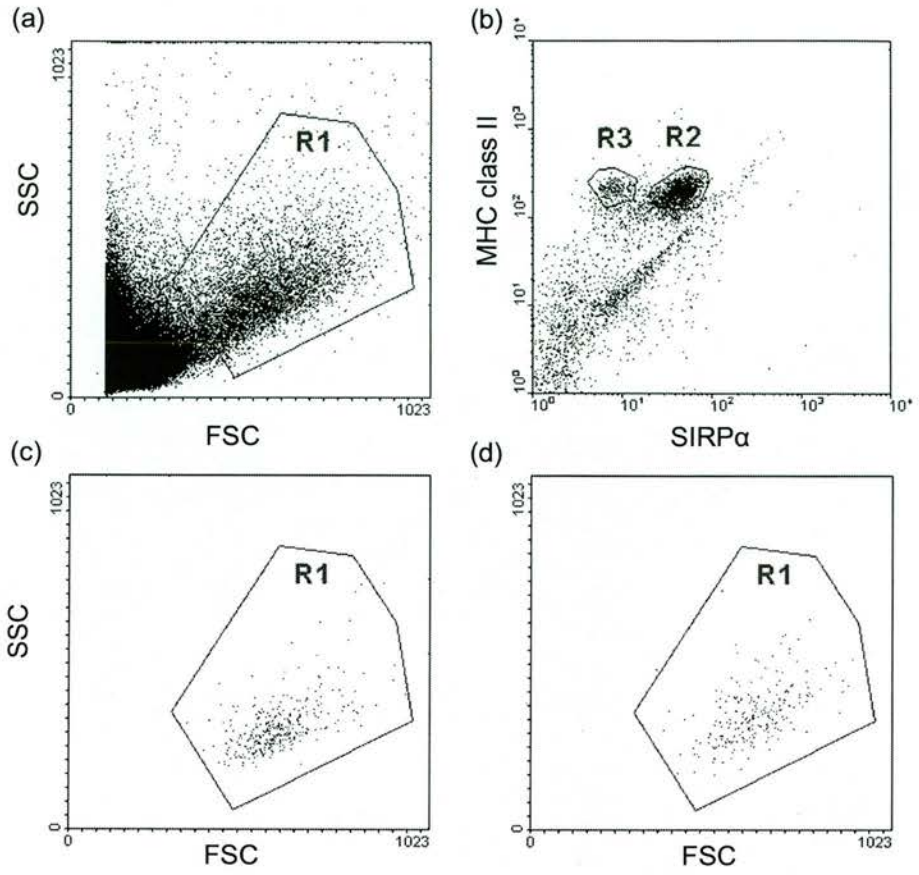

Figure 4.4 Comparison of SIRPα$^+$ and SIRPα$^-$ ALDC populations for light scatter characteristics.

(a) FSC and SSC profiles of unfractionated lymph cells
(b) Unfractionated lymph cells stained using mAb IL-A24 (SIRPα) and biotinylated SW73.2 (MHC class II β)
(c) back-gated FSC × SSC profiles for SIRPα$^+$ DC defined by R1 (a) and R2 (b)
(d) back-gated FSC × SSC profile of SIRPα$^-$ DC defined by R1 (a) and R3 (b)

4.3.3 Ultrastructural characterisation of ALDC

Transmission Electron Microscopy (TEM) was next employed in order to determine ultrastructural characteristics of isolated SIRPα$^+$ and SIRPα$^-$ ALDC. Purified ALDC were fixed in glutaraldehyde immediately after cell sorting. In addition, unfractionated lymph was washed and fixed for TEM. Overall, SIRPα$^+$ and SIRPα$^-$ ALDC show some ultrastructural features characteristic of DC (Figure 4.5a,b). Since sorted DC were not freshly fixed (i.e. soon after collection from the animal), it is possible that some of the ultrastructural features may in fact be lost or induced from the experimental procedure itself. Loss of some of the pronounced protrusions (observed previously in the Giemsa stained ALDC) is particularly evident when sorted DC are compared with freshly fixed ALC (Figure 4.5c,d). Occasionally many atypical mitochondria were observed in some SIRPα$^+$ cells; however, this may in fact be artefact (Steven Mitchell, personal communication). Cells were also closely examined for the presence of Birbeck granules, which are characteristic of human LC (Birbeck et al., 1961) and also for the presence of apoptotic body inclusions, since rat SIRPα$^-$ ALDC have been reported to contain apoptotic DNA (Huang et al, 2000). Due to low cell yields after the sorting procedure, few SIRPα$^-$ ALDC were present on the cut sections; however, intracellular vesicles which resembled apoptotic bodies were observed in two SIRPα$^-$ cells (Figure 4.5b (V)). The main observations for both ALDC populations are:

(i) A large diameter (when compared to lymph-derived lymphocytes),

(ii) Abundant cytoplasmic vesicles were present in some of the cells (possibly lysosomes, phagolysosomes and endocytic vacuoles),

(iii) No Birbeck granules (a unique feature of epidermal LC) were observed in either subpopulation of ALDC,

(iv) Pleomorphic and deeply convoluted nuclei with marginated heterochromatin characteristic of DC (Drexhage et al, 1979; Gregg et al., 1995) and

(v) Nucleoli were not obvious in either population.

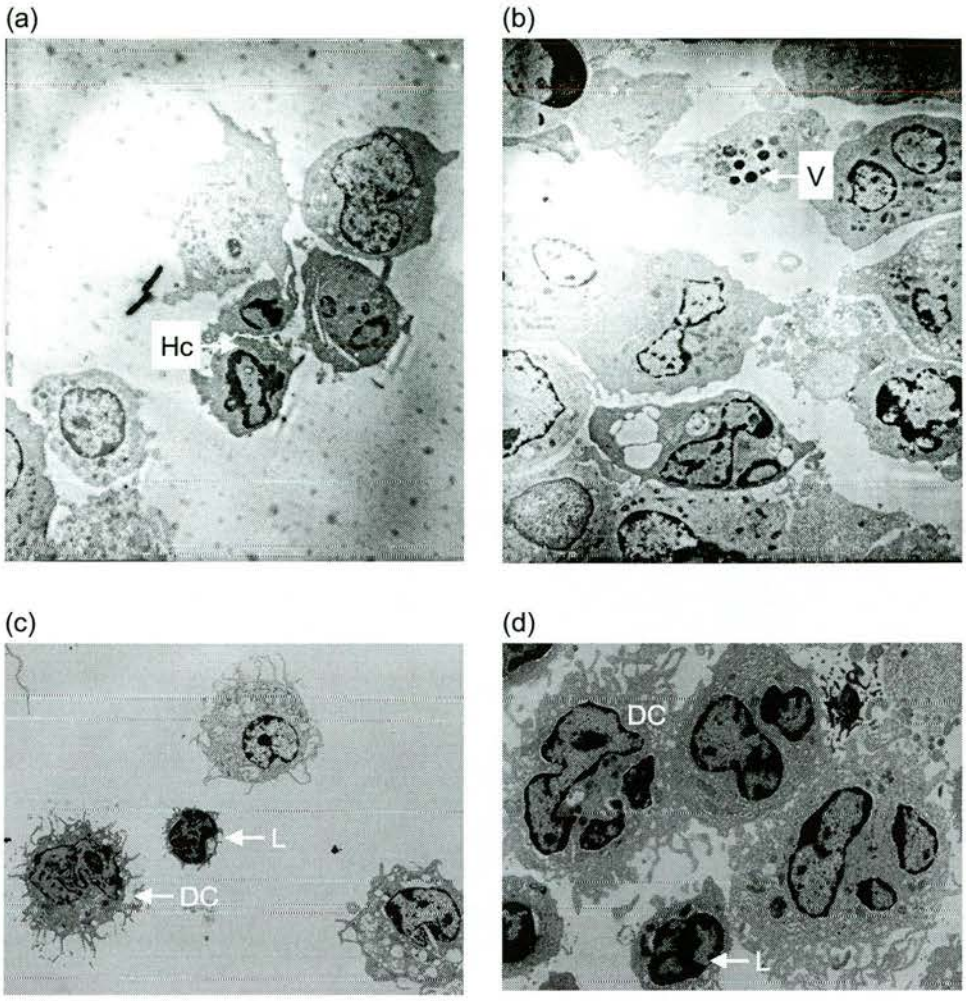

Figure 4.5 Transmission electron microscopy (TEM) of FACS–sorted DC. (a) SIRPα^{+} MHC class II^{hi} ALDC, (b) SIRPα^{-} MHC class II^{hi} ALDC, (c & d) lymph enriched for DC. ALDC were separated by FACS, fixed in glutaraldehyde, and examined by TEM. SIRPα^{-} ALDC contain numerous electron-dense and -lucent inclusions (b, label V). Both populations contain heterochromatic nuclei and electron-lucent cytoplasm, characteristic of DC. (DC, dendritic cell; Hc, heterochromatic nuclei; L, lymphocyte; V, vesicle.)

4.3.4 Immunostaining of purified ALDC subpopulations

To assess more specifically the phenotype of SIRPα$^+$ and SIRPα$^-$ ALDC, several mAb directed against cell surface markers were tested for reactivity by immunochemistry. A range of mAb was applied to cytospins prepared from sorted cells. Neither subpopulation of DC appeared to express T- or B cell surface markers by immunochemistry (data not shown). It is known that DC and macrophages share many cell surface antigens such as MHC class II, CD11b, CD11c and mannose receptors including DEC-205 (CD205). However, ovine ALDC express CD1b but very little CD14 (Hopkins and Dutia, 1991; Hopkins and Gupta, 1996), while ovine macrophages express little or no CD1b but low to high levels of CD14 (Gupta et al., 1996; Rhind et al., 1996a).

Humans possess five distinct CD1 genes (CD1A, B, C, D and E) which encode four protein products, CD1a, CD1b and CD1c (group 1) and CD1d (group 2); and sheep possess at least 7 CD1 genes including CD1B, D and E (Hopkins et al., 2000). Previous studies in sheep have shown that the majority of mAb recognise a 46 kDa antigen with a distribution similar to that of human CD1b (expressed by thymocytes and DC). The mAb SBU-T6 has a wider tissue distribution (Mackay et al., 1988b) and is considered to recognise a CD1c-like molecule or to represent a "pan-CD1" mAb (Hopkins and Dutia, 1991). Importantly, mAb SBU-T6 stains both LC and dermal DC in sheep, whereas VPM 5 and CC118 stain dermal DC only (Rhind, 1996). Both subpopulations stain strongly with mAb SBU-T6 (Figure 4.6), suggesting that either population may be derived from either LC or dermal DC. Insufficient material was available to assess reactivity of all anti-CD1 mAb with ALDC by immunochemistry.

Cytospins were also stained with a mAb that recognises γδ T cells in ovine skin (CC15; Table 2.1). The γδ$^+$ DC found in the skin of many rodent species were first described by Bergstresser (Bergstresser et al, 1983) and Tschachler (Tschachler et al, 1983). γδ cells were initially described as Thy-1$^+$ DC and have been reported to express the γδ T cell receptor and to present antigen (Welsh and Kripke, 1990). Indeed, ovine γδ DC have been isolated from lymph and were found to have ultrastructural features characteristic of DC (Welsh and Kripke, 1990). In my work, neither population stained with this antibody, suggesting that neither population has arisen from this type of "DC" in the skin (data not shown).

Weak reactivity was observed with mAb VPM 65 (anti-CD14) in a small fraction of SIRPα$^+$ ALDC by immunochemistry (Figure 4.7), as observed previously with ovine ALDC (Gupta et al, 1996). None of the cells in the SIRPα$^-$ fraction stained positive with mAb VPM 65 in any of the cytospins tested.

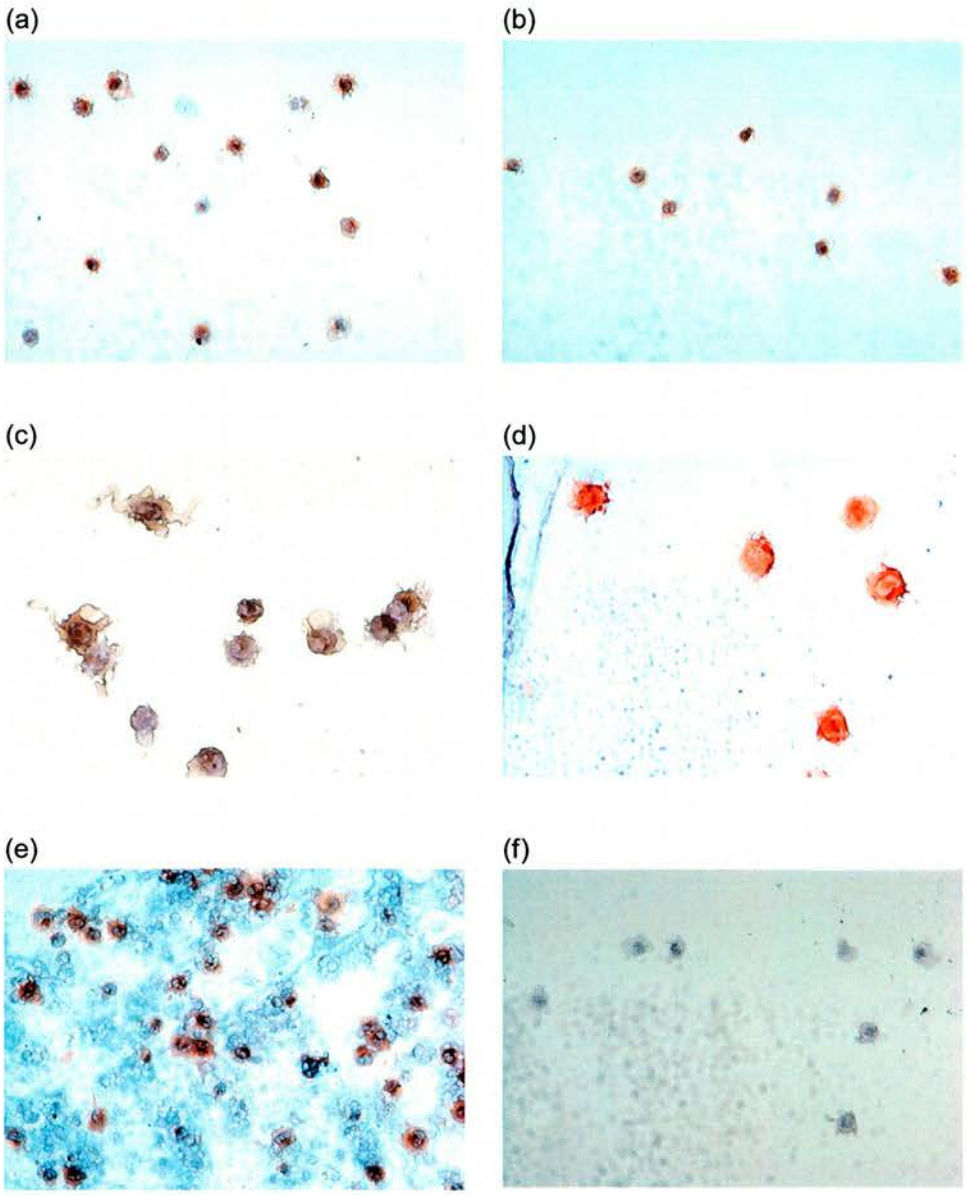

Figure 4.6 Reactivity of purified SIRPα$^+$ and SIRPα$^-$ ALDC with an anti-CD1 mAb. Cytospins were prepared from purified ALDC and immunostaining was carried out with mAb SBU-T6 followed by counterstaining with haematoxylin. Reactivity is observed with both SIRPα$^+$ and SIRPα$^-$ ALDC.

(a) SIRPα$^-$ DC (original magnification, ×80)
(b) SIRPα$^+$ DC (original magnification, ×80)
(c) SIRPα$^-$ DC (original magnification, ×250)
(d) SIRPα$^+$ (original magnification, ×250)
(e) Positive control: lymph cells stained with SBU-T6 mAb
(f) Negative control: immunolabelled SIRPα$^-$ DC with secondary mAb only

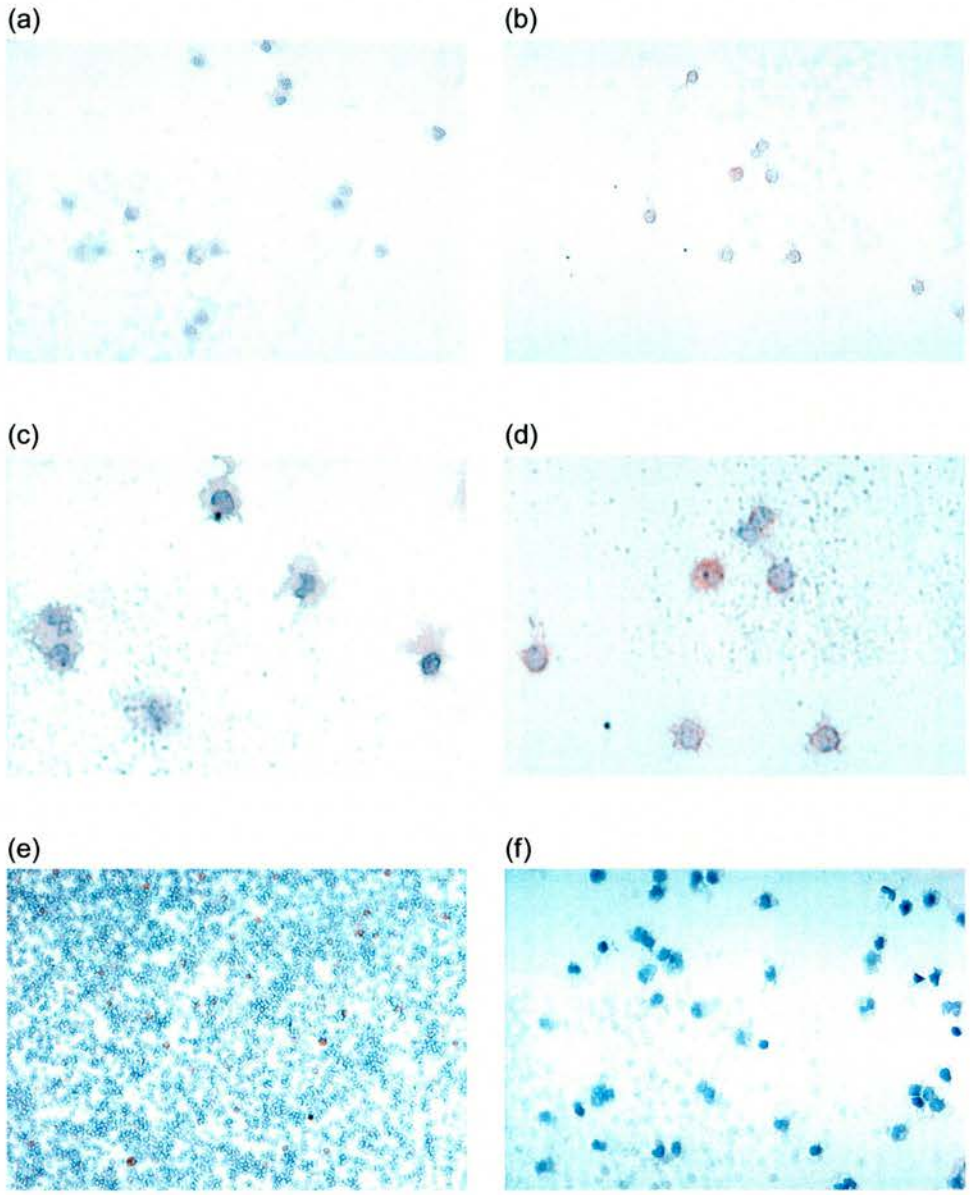

Figure 4.7 Reactivity of purified SIRPα$^+$ and SIRPα$^-$ ALDC with an anti-CD14 mAb. Cytospins were prepared from purified ALDC and immunostaining was carried out with mab VPM 65. Reactivity is observed with some SIRPα$^+$ ALDC.

(a) SIRPα$^-$ DC (original magnification, ×80)
(b) SIRPα$^+$ DC (original magnification, ×80)
(c) SIRPα$^-$ DC (original magnification, ×250)
(d) SIRPα$^+$ (original magnification, ×250)
(e) Positive control: lymphocyte-enriched fraction stained with VPM 65 mAb
(f) Negative control: sorted cells immunolabelled with secondary mAb only

4.3.5 Flow cytometric analysis of ALDC

In order to further investigate the phenotype of SIRPα$^+$ and SIRPα$^-$ ALDC, flow cytometry was carried out on unfractionated ALC. ALC were immunolabelled with several mAb (listed in Table 2.2) and biotinylated IL-A24 (anti-SIRPα). Since weak reactivity was observed with mAb VPM 65 (anti-CD14) in a fraction of SIRPα$^+$ ALDC when assessed by immunochemistry (Section 4.3.4), ALDC were again evaluated for surface expression of CD14 by flow cytometry. Figure 4.8 is representative of data obtained from three animals. Approximately 15% (range 13–21%) of SIRPα$^+$ ALDC express CD14 (as determined by FL1, Figure 4.8a). Conversely, CD14 was not detected on any of the SIRPα$^-$ ALDC in any of the animals used in this study. The phenotype of ovine SIRPα$^+$ and SIRPα$^-$ ALDC has been extensively characterised by flow cytometry in a previous study (Bailey, 2003). In agreement with these findings, approximately 40% of SIRPα$^+$ ALDC were reported to express CD14. Interestingly, both studies show that SIRPα$^-$ ALDC express higher levels of CD45RA than SIRPα$^+$ ALDC (Figure 4.8b), whereas expression of MHC class II and CD40 is similar in both ALDC populations (Figure 4.8c,d).

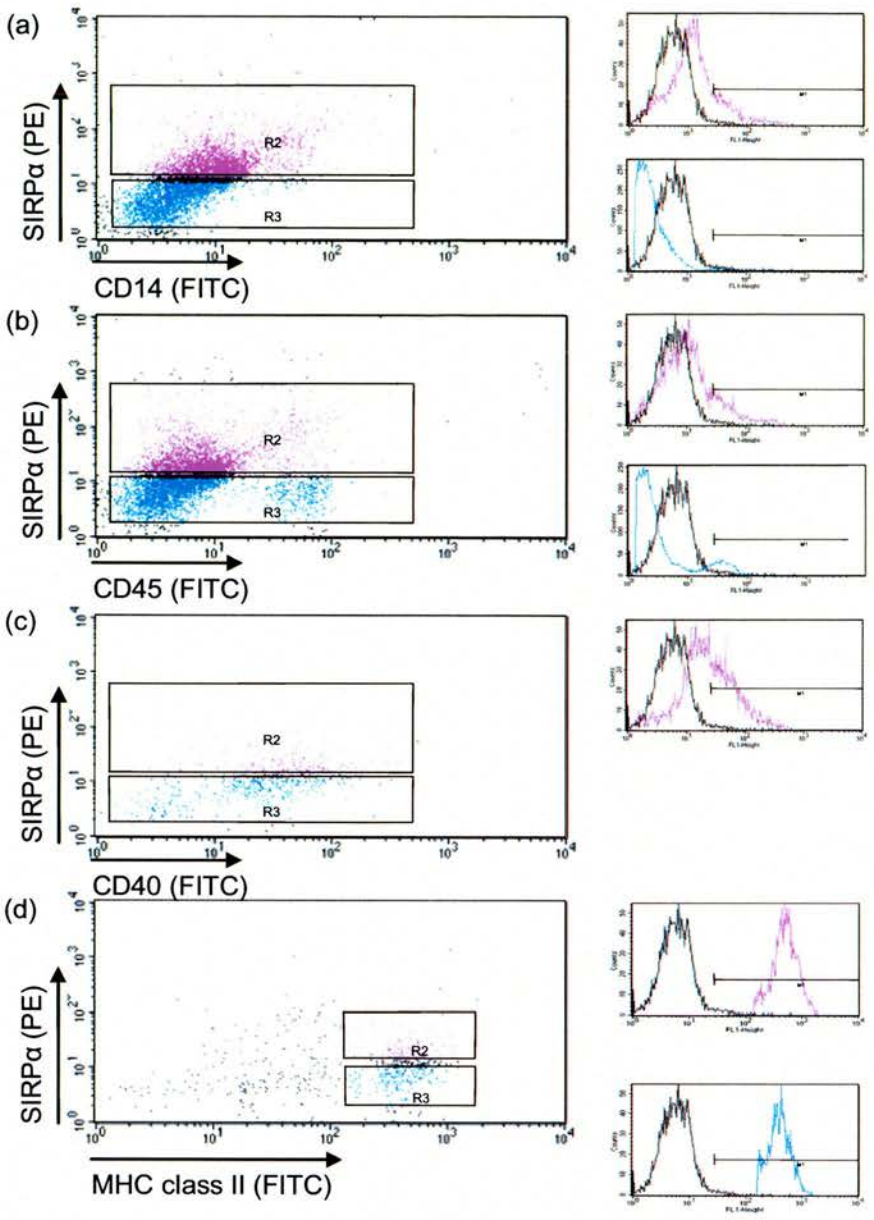

Figure 4.8 Two-colour flow cytometry of ALDC populations. Expression of (a) CD14, (b) CD45RA, (c) CD40 and (d) MHC class II on SIRPα$^+$ (R2, purple) and SIRPα$^-$ (R3, blue) ALDC. Negative controls (NMS) are shown in black (histograms).

4.3.6 ATPase staining of purified ALDC subpopulations

Veiled cells in lymph form a heterogeneous population, some of which have been proposed to belong to the LC lineage based on morphological analysis (Brand et al., 1993); surface expression of CD1 (Bujdoso et al, 1989) and possession of Birbeck granules (Hoefsmit et al., 1982), a unique feature of LC (Birbeck et al, 1961). LC can be further differentiated by a variety of other criteria including expression of ATPase (Steinman, 1991) or acetylcholinesterase (Hollis and Lyne, 1972; Lyne and Chase, 1966). Acetylcholinesterase staining has been reported to be a more reliable method of quantifying ovine LC than using mAb which recognise MHC class II antigens or CD1 (Townsend et al, 1997). LC also possess strong ATPase activity; this enzyme is described as being an ectoenzyme, localised within or at the surface of the plasma membrane and not within cells, in both human (Zelickson and Mottaz, 1968) and guinea pig epidermal LC (Wolff and Winkelmann, 1967).

In order to investigate if either sub-population of ALDC is derived from epidermal LC, ATPase staining was carried out on cytospin preparations from FACS–sorted DC. FACS-sorted DC were not fixed in ice-cold acetone following cytocentrifugation, but instead were air-dried and stored at –20°C until the ATPase procedure was carried out. Sections of equine muscle were simultaneously stained (by Neil McIntyre, EBVC) and served as positive controls for the staining procedure (results not shown). FACS–sorted ALDC and muscle sections were then fixed in cacodylate buffer and ATPase staining was carried out. Faint ATPase staining was observed in some SIRPα^+ ALDC (obtained from cell sorting experiment 3.0) as indicated by the dark grey peripheral staining of DC processes (Figure 4.9). No ATPase positive cells were observed in purified SIRPα^- ALDC.

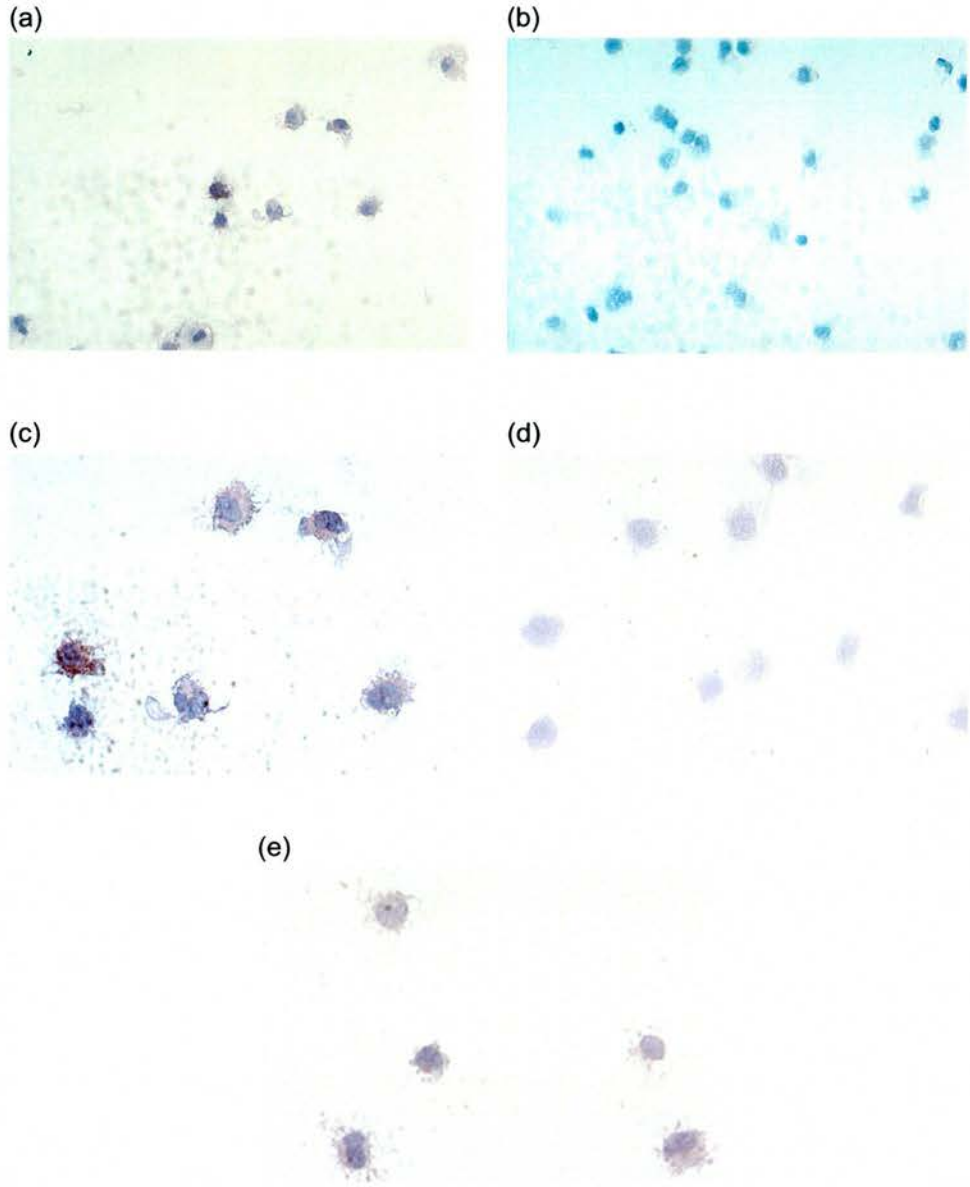

Figure 4.9 ATPase staining of highly purified ALDC populations. After sorting by FACS, cells were cytocentrifuged and air-dried prior to storage at –20°C. ATPase staining was carried out and cells were lightly counterstained with Giemsa. A fraction of SIRPα$^+$ ALDC appear ATPase positive (dark grey); staining of cell membrane and dendrites can be observed.

(a) SIRPα$^+$ cells (original magnification, ×80)
(b) SIRPα$^-$ cells (original magnification, ×80)
(c) SIRPα$^+$ cells (original magnification, ×250)
(d) SIRPα$^-$ cells (original magnification, ×250)
(e) SIRPα$^+$ cells (original magnification, ×250)

4.4 Molecular analysis of purified ALDC populations

RNA was extracted from freshly sorted ALDC stored in FACS buffer supplemented with actinomycin D in order to prevent *de novo* transcription. From an average 16 hour collection, approximately 0.5μg (range 0.2–2.7μg) of RNA was extracted from purified SIRPα$^+$ ALDC; RNA could not be quantified in the majority of SIRPα$^-$ ALDC samples. RNA was concentrated under vacuum in order to perform a RT reaction with as much available RNA as possible. Conventional RT-PCR was first employed using GAPDH primers to confirm that amplifiable material was present and genomic DNA had been fully degraded. Occasionally, no signal was observed after 40 cycles of amplification of cDNA samples with GAPDH-specific primers (both ALDC samples obtained from sort 1.0; Figure 4.10) or only a very weak signal (samples obtained from cell sorting experiment 13.0, results not shown) indicating that either insufficient RNA was extracted, or that RNA had degraded during the extraction procedure.

GAPDH transcripts were present in samples from sorting experiments 2.0 and 3.0 (Figure 4.11), and in all the samples that followed, where the cell yields were generally higher than those obtained from the first sorting experiment. Agilent analysis of samples 2.0 and 3.0 revealed that the concentration of RNA was low and of poor quality (results not shown); however, it was still possible to quantify cytokine expression in these samples (Section 4.4.3).

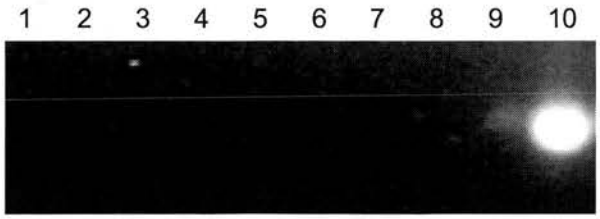

Figure 4.10 Analysis of GAPDH transcripts in purified ALDC by RT-PCR. GAPDH RT-PCR was carried out with cDNA samples obtained from SIRPα$^+$ and SIRPα$^-$ ALDC purified from cell sorting experiment 1.0. No GAPDH transcripts are evident after 40 cycles of amplification.

Lane 1 SIRPα$^+$ ALDC (+RT)
Lane 2 SIRPα$^-$ ALDC (+RT)
Lane 5 SIRPα$^+$ ALDC (–RT)
Lane 6 SIRPα$^-$ ALDC (–RT)
Lane 8 Negative control (nuclease-free water)
Lane 10 Positive control (1:1000 dilution of GAPDH 1° PCR product)

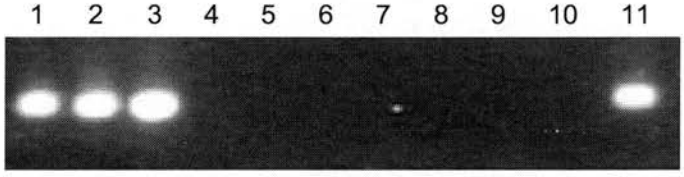

Figure 4.11 Analysis of GAPDH transcripts in purified ALDC by RT-PCR. GAPDH RT-PCR was carried out with SIRPα$^+$ and SIRPα$^-$ cDNA samples obtained from cell sorting experiment 2.0. Specific transcripts are evident after 40 cycles of amplification.

Lane 1 SIRPα$^-$ (+RT)
Lane 2 SIRPα$^+$ (+RT)
Lane 3 enriched DC fraction (+RT)
Lane 5 SIRPα$^-$ (–RT)
Lane 6 SIRPα$^+$ (–RT)
Lane 7 enriched DC fraction (–RT)
Lane 9 Negative control (nuclease-free water)
Lane 11 Positive control (1:1000 dilution of GAPDH 1° PCR product)

4.4.1 Reverse transcription-polymerase chain reaction (RT-PCR) for Langerhans'-cell specific transcripts in FACS–sorted DC

Since a fraction of SIRPα$^+$ ALDC stained weakly with ATPase (Figure 4.9), further analysis was required to determine if cells within this population represent migratory epidermal LC. In humans, CD1a is a reliable marker of LC (Ruco et al., 1989). However, sheep CD1a – specific antibodies have not yet been defined as most seem to react with both LC and dermal DC. Both ALDC subpopulations react with mAb SBU-T6 (pan anti-CD1) and could therefore contain DC derived from either lineage. CD1A has not as yet been identified in sheep or in cattle and is completely lacking in mice, although a partial sequence for equine CD1a cDNA is now available (Steinbach and Walter 2003, unpublished data; accession number AY376269). A molecular approach was therefore adopted to ascertain if either ALDC population contain CD1a transcripts.

CD1a-specific primers were designed from available human cDNA sequences and analysed by Premier Biosoft software (Section 2.3.5.2). Initial attempts to amplify ovine CD1a used annealing temperatures of 55°C and 52°C; however, no products were observed using cDNA from ovine spleen, skin or from enriched DC which had been verified to contain amplifiable material by GAPDH RT-PCR (data not shown). A source of material was thus required in order to determine the specificity of the CD1a primers. DNA extracted from human skin was pooled with human skin-derived cDNA (a kind gift from Kirsty Newman, University of Edinburgh) and amplified for 40 cycles at 52°C. To ensure that ovine transcripts were not a limiting factor in this system, 5μg of RNA from the skin of two different sheep was reverse transcribed. Specific PCR products were only observed with the human DNA/cDNA mix (Figure 4.12). A ~1500bp amplicon (1480bp) corresponds to the amplification of the human CD1a gene and a ~400bp amplicon (384bp) corresponds to the amplification of CD1a cDNA. Two non-specific bands were observed in both ovine skin cDNA samples at approximately 600bp and 700bp. Attempts to optimise the PCR reaction proved unsuccessful. No further work was carried out with this set of primers.

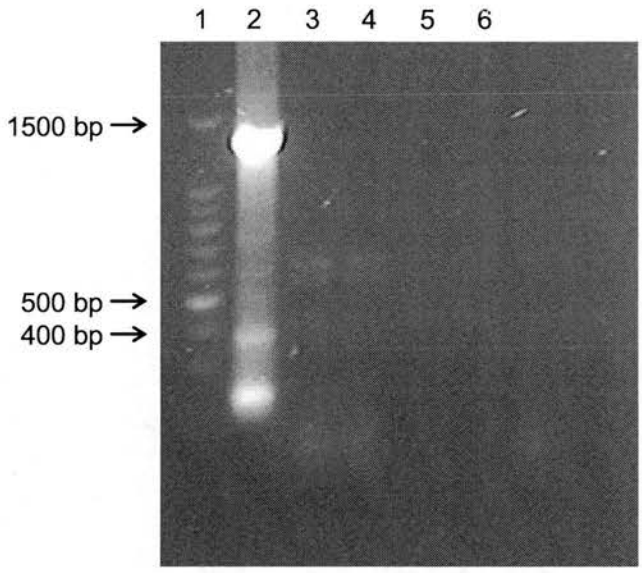

Figure 4.12 CD1a (RT)-PCR optimisation. Primer pairs were tested on human DNA and also on SSk and spleen cDNA samples. Amplification was carried out for 40 cycles at 50°C.

Lane 1 100bp marker
Lane 2 Human skin-derived genomic material (DNA and RNA) amplified with CD1a-specific primers
Lane 3 Ovine skin (from biopsy experiment D) cDNA amplified with CD1a primers
Lane 4 Ovine skin (from biopsy experiment E) cDNA amplified with CD1a primers
Lane 6 Negative control (nuclease-free water)

A molecular approach was again adopted to ascertain if either ALDC subpopulation contain transcripts for langerin (CD207), which is expressed by both human and murine LC (Valladeau et al., 2000; Valladeau et al., 2002). Langerin (CD207) is a novel C-type lectin and acts as a potent inducer of Birbeck granule formation (BG) and is a nonconventional endocytic receptor routing into these organelles in LC (Valladeau et al, 2002). Although Birbeck granules appeared to be absent from both populations when viewed by electron microscopy (Figure 4.5), langerin (which is the major component of Birbeck granules) may still be expressed by ALDC. In line with this hypothesis, murine DC within lymph nodes and spleen and also in some non-lymphoid tissues (lung, liver, heart) have been reported to express langerin (Valladeau et al, 2002), suggesting that migrating DC may still contain langerin transcripts.

At the time of writing, there were no available sequences for langerin in sheep, or indeed any other ruminant. Human and murine langerin (CD207) sequences were therefore aligned and consensus primers were designed from homologous regions. Murine skin (and spleen) contain abundant mRNA transcripts of langerin (Takahara et al., 2002). In line with this observation, RNA (and DNA) were extracted from murine spleen to serve as positive control

material (kindly supplied by Miss Clemence Hindley, University of Edinburgh). RNA was also extracted from (normal/non-vaccinated) skin biopsies obtained from two different sheep (collected from biopsy experiments D and E). Langerin primers were tested on skin cDNA samples where different amounts (1–5μg) of RNA were reverse transcribed. A 400bp product was observed after 40 rounds of amplification with all ovine skin cDNA samples tested and also in murine cDNA derived from spleen (Figure 4.13). The expected amplicon size of genomic (human) langerin is 1580bp following PCR with this set of primers; a >1000bp product was detected after amplification with human and sheep DNA and may correspond to amplification of genomic material. Primary PCR product was then purified and cloned into into pGEM®-T Easy (Section 2.3.7.2) and sequenced. Sequencing revealed that ovine langerin (CD207) shares 94% homology with bovine CD207 (accession number XM_588243; sequence submitted March 2005), and shares 85% homology with human CD207 (accession number AJ242859) (Appendix III). RT-PCR was then carried out with purified ALDC cDNA samples. Importantly, 400bp products were detected in two out of the four SIRPα$^+$ ALDC samples tested. No transcripts were detected in any of the four SIRPα$^-$ ALDC samples evaluated (Figure 4.14).

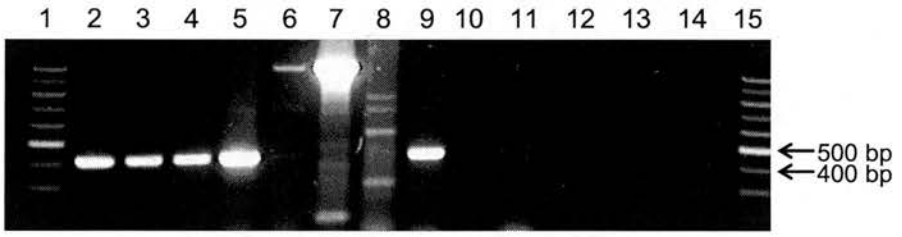

Figure 4.13 Optimisation of langerin RT-PCR. RNA was extracted from ovine skin and spleen biopsies and reverse transcribed. Positive control material consisted of DNA and cDNA obtained from murine spleen and human skin. cDNA was amplified for 40 cycles with an annealing temperature of 53°C. 400bp products correspond to amplification of langerin mRNA and can be detected in both normal ovine skin and murine spleen.

Lane 1 100bp marker
Lane 2 ovine skin (1 μg, biopsy experiment E)
Lane 3 ovine skin (5 μg biopsy experiment E)
Lane 4 ovine skin (1 μg biopsy experiment D)
Lane 5 ovine skin (5 μg biopsy experiment D)
Lane 6 ovine spleen DNA
Lane 7 human skin
Lane 8 murine spleen DNA
Lane 9 murine spleen cDNA
Lane 11 water (negative control)
Lane 15 100bp marker

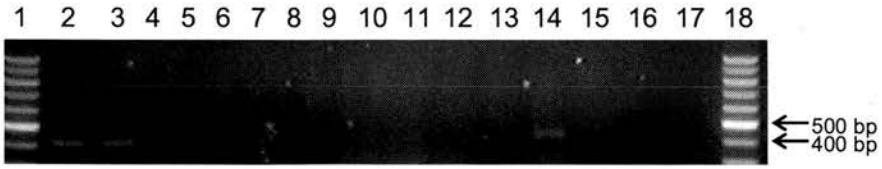

Figure 4.14 Analysis of langerin transcripts in purified ALDC by RT-PCR. RT-PCR was carried out for 40 cycles with freshly sorted SIRPα$^+$ and SIRPα$^-$ ALDC. Langerin transcripts (400bp fragments) are present in two out of the four SIRPα$^+$ ALDC populations evaluated.

Lane 1 100bp ladder
Lane 2 SIRPα$^+$ ALDC (JH4 sort 14.0; purity: 97%)
Lane 3 SIRPα$^+$ ALDC (JH4 sort 15.0; purity: 95%)
Lane 4 SIRPα$^+$ ALDC (JH5 sort 16.0; purity: 100%)
Lane 5 SIRPα$^+$ ALDC (JH6 sort 20.0; purity: 96%)
Lane 8 SIRPα$^-$ ALDC (JH4 sort 14.0; purity: 97%)
Lane 9 SIRPα$^-$ ALDC (JH4 sort 15.0; purity: 90%)
Lane 10 SIRPα$^-$ ALDC (JH5 sort 16.0; purity: 96%)
Lane 11 SIRPα$^-$ ALDC (JH6 sort 20.0; purity: 95%)
Lane 14 positive control (ovine skin)
Lane 16 negative control (nuclease-free water)
Lane 18 100bp marker

4.4.2 Expression of toll-like receptors in purified ALDC subpopulations

Different subsets of murine and human DC express different TLR and consequently respond to different PAMP. Expression of TLR family members has been investigated in human blood CD11c$^-$ pDC and CD11c$^+$ myeloid DC (Jarrossay et al, 2001; Kadowaki et al., 2001; Krug et al., 2001). These studies have shown that myeloid DC preferentially express TLR4, whereas pDC uniquely express TLR9. TLR9 is involved in the recognition of CpG motifs (Hemmi et al, 2000), which is of particular interest with regard to DNA vaccination where CpG motifs are present within the bacterial DNA of the plasmid. Experiments were thus undertaken in order to identify any differences in TLR expression between the two ALDC populations, which may help to further understand their biology. Due to the availability of (bovine) sequences, TLR3, TLR4 and TLR9 were investigated in this study.

RNA was extracted from ovine PBMC, spleen and skin obtained from clinically normal (non-vaccinated) sheep and analysed by RT-PCR to optimise primers. TLR3, TLR4 and TLR9 transcripts were detected in PBMC after 35 cycles of amplification (Figure 4.15). After 40 cycles, TLR3 and TLR4 transcripts were detected in spleen samples (Figure 4.16). Conversely, TLR9 transcripts were absent in spleen samples in this study. TLR9 mRNA was however detected in normal skin obtained from two different sheep and where 5μg of total RNA was reverse transcribed.

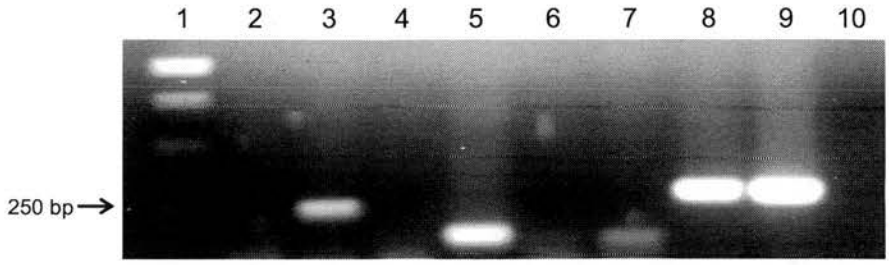

Figure 4.15 Optimisation of TLR primers with ovine PBMC and spleen cDNA. Amplification was carried out for 35 cycles with an annealing temperature of 55°C. Expected sizes of amplicons are as follows: ovine TLR9, 239bp; ovine TLR4, 151bp; ovine TLR3, 139bp.

Lane 1 1kb ladder
Lane 2 spleen cDNA amplified with TLR9 primers
Lane 3 PBMC cDNA amplified with TLR9 primers
Lane 4 spleen cDNA amplified with TLR4 primers
Lane 5 PBMC cDNA amplified with TLR4 primers
Lane 6 spleen cDNA amplified with TLR3 primers
Lane 7 PBMC cDNA amplified with TLR3 primers
Lane 8 spleen cDNA amplified with murine TLR4 primers (250bp product)
Lane 9 PBMC cDNA amplified with murine TLR4 primers (250bp product)
Lane 10 negative control (nuclease-free water amplified with 3 sets of primers)

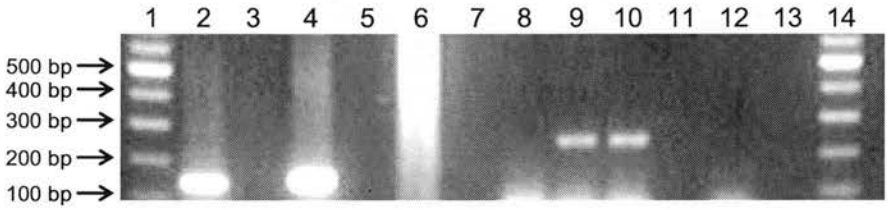

Figure 4.16 Optimisation of TLR primers with ovine skin and spleen cDNA. Amplification was carried out for 40 cycles with an annealing temperature of 55°C. Expected sizes of amplicons are as follows: ovine TLR9, 239bp; ovine TLR4, 151bp; ovine TLR3, 139bp.

Lane 1 100bp marker
Lane 2 TLR3 amplification of spleen (139bp)
Lane 4 TLR4 amplification of spleen (151bp)
Lane 6 TLR9 amplification of spleen (239bp)
Lane 8 TLR9 amplification of skin cDNA (1µg RNA)
Lane 9 TLR9 amplification of skin cDNA (5µg RNA); biopsy experiment D
Lane 10 TLR9 amplification of skin cDNA (5µg RNA); biopsy experiment E
Lane 12 Negative control (nuclease-free water)
Lane 14 100bp marker

4.4.2.1 TLR4 mRNA expression in purified ALDC subpopulations

TLR4 is expressed by both human and murine myeloid DC (Boonstra et al, 2003; Jarrossay et al, 2001) and also in monocyte-derived pre-DC1 (Kadowaki et al, 2001). Since a small proportion of SIRPα$^+$ ALDC expressed surface CD14 (as shown by both immunochemistry and flow cytometry analysis), it was postulated that this population may also express TLR4, since TLR4 and CD14 work in conjunction with one another in the recognition of LPS (Poltorak et al, 1998), a characteristic of Gram-negative bacteria.

Primers were designed from available bovine sequences and primer pairs were first optimised. In this set of experiments, cDNA derived from (i) enriched-DC fraction and (ii) PBMC served as positive control material. TLR4 transcripts were detected in purified SIRPα$^+$ ALDC following amplification of mRNA derived from three different cell-sorted preparations obtained from "resting" lymph from three different animals. Figure 4.17a is representative of three independent RT-PCR experiments carried out with cDNA derived from sorting experiments 2.0, 3.0 and 15.0. TLR4 transcripts were not detected in the SIRPα$^-$ ALDC population, even after 40–45 rounds of amplification. GAPDH RT-PCR indicated that there was amplifiable material present within each of the SIRPα$^-$ ALDC samples chosen (Figure 4.17b), indeed cDNA samples were chosen from cell sorting experiments with high cell yields (Table 4.2). TLR4 PCR products were subsequently purified using a PCR clean-up kit (Qiagen™), cloned into pGEM®-T Easy (Section 2.3.7.2) and sequenced by Mr. Ian Bennett (Appendix III). Ovine TLR4 shares 95% homology with bovine TLR4 (accession number AY297043) and 90% homology with human TLR4 (accession number BC025294).

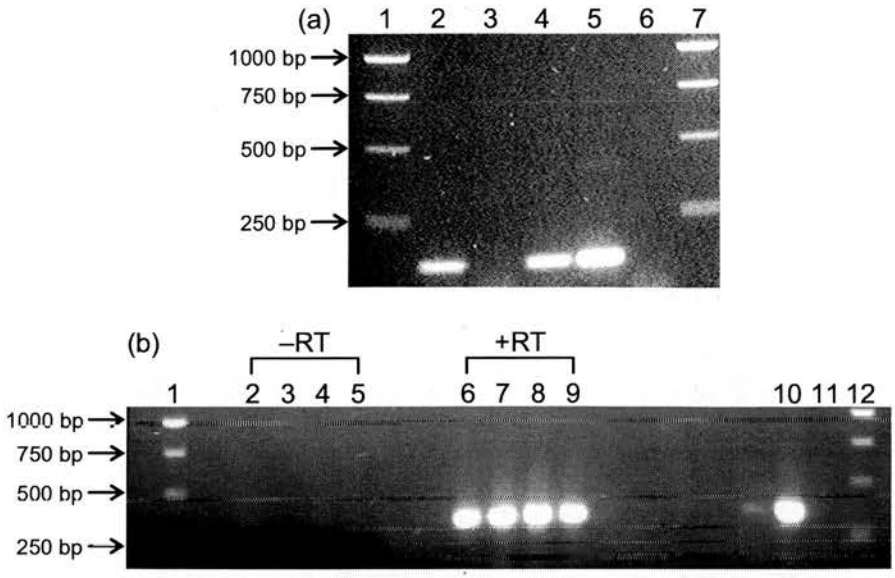

Figure 4.17 Analysis of TLR4 transcripts in freshly isolated SIRPα$^+$ and SIRPα$^-$ ALDC by RT-PCR. (a) Fragments <250bp are evident after amplification of mRNA obtained from SIRPα$^+$ ALDC, PBMC and the DC-enriched fraction (OptiPrep™ fraction 1), but not in SIRPα$^-$ ALDC (anticipated TLR4 product size is 151bp; Table 2.5). ALDC subpopulations were isolated by cell sorting to a purity of >90%. cDNAs were amplified for 40 cycles and were separated on a 2% agarose gel containing ethidium bromide. The data shown are representative of three independent RT-PCR experiments from three different animals. Total RNA was extracted from 10^6 PBMC and 10^6 cells from fraction 1 (enriched DC-fraction, Figure 2.4). (b) Amplifiable material was confirmed by GAPDH RT-PCR (b) where amplicons of approximately 400bp are evident (expected size of amplicon is 366bp with GAPDH specific primers, Table 2.5).

(a) TLR4 RT-PCR
Lane 1 1kb ladder
Lane 2 SIRPα$^+$ ALDC (sort 15.0; purity 95%)
Lane 3 SIRPα$^-$ ALDC (sort 15.0; purity 90%)
Lane 4 DC-enriched fraction
Lane 5 PBMC
Lane 6 Negative control (nuclease-free water)
Lane 7 1kb ladder

(b) GAPDH RT-PCR
Lane 1 1kb ladder
Lane 2 SIRPα$^-$ ALDC (15.0) –RT
Lane 3 SIRPα$^+$ ALDC (15.0) –RT
Lane 4 PBMC –RT
Lane 5 DC –RT
Lane 6 SIRPα$^-$ ALDC (15.0) +RT
Lane 7 SIRPα$^-$ ALDC (15.0) +RT
Lane 8 PBMC +RT
Lane 9 DC +RT
Lane 10 positive control (1:1000 1° GAPDH PCR product)
Lane 11 negative control (water)
Lane 12 1kb ladder

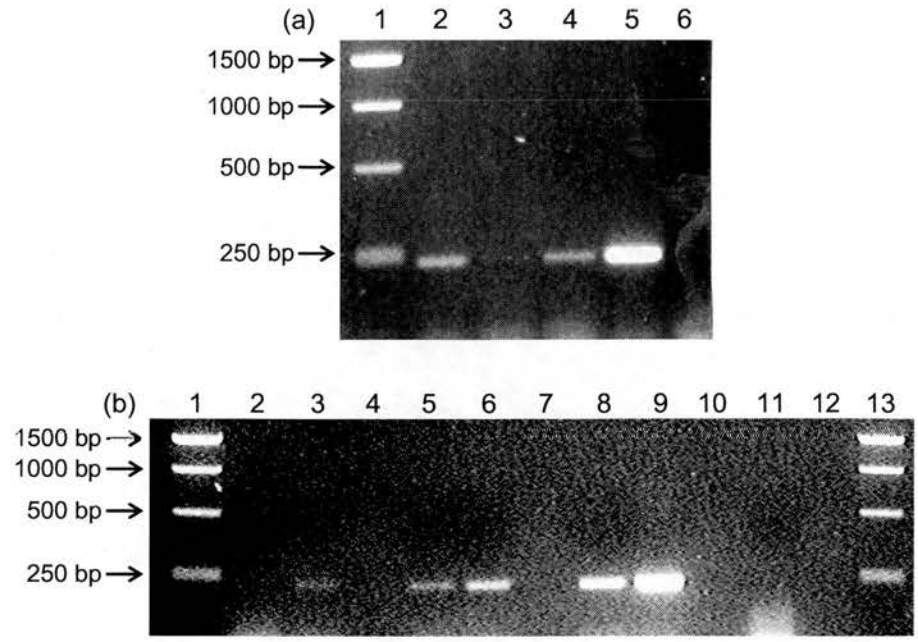

Figure 4.18 Analysis of TLR9 transcripts in freshly isolated SIRPα$^+$ and SIRPα$^-$ ALDC by RT-PCR. ALDC subpopulations were isolated by cell sorting to a purity of >95%. cDNAs were amplified for 40 cycles with an annealing temperature of 55°C. The data shown (a and b) are representative of three experiments from three different animals. TLR9 mRNA expression was also analysed in DC-enriched fraction and in PBMC. Fragments of approximately 250bp are evident after PCR amplification of cDNA (expected size of TLR9 is 239bp, Table 2.5).

(a)
Lane 1 1kb ladder
Lane 2 SIRPα$^+$ ALDC (sort 15.0)
Lane 3 SIRPα$^-$ ALDC (sort 15.0)
Lane 4 DC-enriched fraction
Lane 5 PBMC
Lane 6 Negative control (nuclease-free water)

(b)
Lane 1 1kb ladder
Lane 2 SIRPα$^-$ ALDC (sort 3.0)
Lane 3 SIRPα$^-$ ALDC (sort 4.0)
Lane 5 SIRPα$^+$ ALDC (sort 3.0)
Lane 6 SIRPα$^+$ ALDC (sort 4.0)
Lane 8 DC-enriched fraction
Lane 9 PBMC
Lane 11 Negative control (nuclease-free water)
Lane 13 1 kb ladder

4.4.2.2 TLR9 mRNA expression in purified ALDC subpopulations

Several factors are likely to influence the magnitude of the immune response generated after DNA vaccination, including optimal gene expression and the immunogenicity of the expressed gene. Indeed, there is compelling evidence that the immunogenicity of plasmid DNA is influenced by CpG motifs contained within the plasmid backbone, for example within the antibiotic resistance gene and the non-coding region of the plasmid. (Klinman et al., 1999; Sato et al, 1996). Recently, it has been demonstrated that TLR9 is essential for CpG-induced innate immune cell activation, since TLR9 knockout mice are refractory (Hemmi et al, 2000). From the current literature, it appears that TLR9 is preferentially expressed by pDC (Jarrossay et al, 2001; Kadowaki et al, 2001), although an equivalent cell type has not yet been described in ruminants.

To further characterise the SIRPα^+ and SIRPα^- ALDC populations in sheep, primers were designed for TLR9 using available bovine sequences (*ovine sequences were not available at the time of writing). The expression of TLR9 was investigated by RT-PCR on freshly isolated, highly purified (> 90% purity) SIRPα^+ and SIRPα^- ALDC. TLR9 transcripts were detected in SIRPα^+ ALDC obtained from three different animals (Figure 4.18a,b). TLR9 transcripts were also present in SIRPα^- ALDC obtained from cell sorting experiments 4.0 and 15.0, although only weak expression of TLR9 was evident in sample 15.0. TLR9 transcripts were absent in SIRPα^- ALDC obtained from cell sorting experiment 3.0. TLR9 PCR products were purified using a PCR clean-up kit (Qiagen^{TM}), cloned into pGEM$^{®}$-T Easy (Section 2.3.7.2) and sequenced by Mr. Ian Bennett (Appendix III). The selected clone shares 98% homology with the available *ovine TLR9 sequence (accession number NM_001011555 submitted by Brownlie et al., February 2005, unpublished data) and 96% homology with bovine TLR9 (accession number AY859726).

4.4.2.3 TLR3 mRNA expression in purified ALDC subpopulations

TLR3 is involved in the recognition of dsRNA (Alexopoulou et al, 2001) contained within some viruses, for example, reovirus, and in the recognition of dsRNA produced during the viral lifecycle (West Nile virus). TLR3 is expressed by both human myeloid and pDC (outlined in the Introduction).

RT-PCR was carried out essentially as already described with cDNA derived from sorted ALDC populations. Weak expression of TLR3 was observed in both SIRPα^+ and SIRPα^- ALDC and also in PBMC and enriched DC after 40 cycles of amplification. A representative example is shown in Figure 4.19.

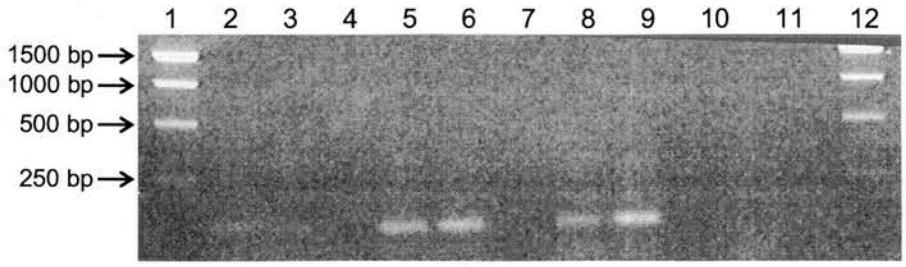

Figure 4.19 Analysis of TLR3 transcripts in SIRPα$^+$ and SIRPα$^-$ ALDC by RT-PCR. cDNA was amplified for 40 cycles with an annealing temperature of 58°C. Fragments <250bp are evident after amplification of cDNA obtained from SIRPα$^+$ ALDC samples, PBMC and in the enriched-DC fraction, (expected size of amplicon is 139bp with TLR3 primers). TLR3 transcripts are only weakly detected in SIRPα$^-$ ALDC.

Lane 1 1kb ladder
Lane 2 SIRPα$^-$ ALDC (sort 3.0)
Lane 3 SIRPα$^-$ ALDC (sort 4.0)
Lane 5 SIRPα$^+$ ALDC (sort 3.0)
Lane 6 SIRPα$^+$ ALDC (sort 4.0)
Lane 8 PBMC
Lane 9 DC-enriched fraction
Lane 11 Negative control (nuclease-free water)
Lane 12 1kb ladder

4.4.3 Cytokine expression in freshly isolated ALDC populations

The purpose of this part of the study was to investigate whether differences in cytokine production between the two ALDC subpopulations are present, which could influence the bias of the immune response they stimulate in the steady-state flux from the skin. In addition, characterisation of cytokine expression for each population was imperative in order to accurately assess any change(s) in the cytokine profile after DNA vaccination with pGM-CSF. Quantitative polymerase chain reactions were carried out to measure specific cytokine transcripts. Although GAPDH transcripts were detected in some sort samples by conventional RT-PCR, transcripts for some cytokines could not be quantified (for all cytokines evaluated with sample 13.0, as transcripts were either below the level of quantification (>40 cycles of amplification were required in order to quantify products which was not always possible due to availability of the LightCycler® machine) or were absent altogether. Cytokine expression was normalised against the universal housekeeping gene GAPDH. Figures are representative of 2–4 independent experimental runs on the LightCycler®. cDNA derived from fresh, unstimulated ALDC revealed that distinct differences in cytokine expression were indeed evident.

4.4.3.1 IL-12p40 mRNA expression in purified SIRPα$^+$ and SIRPα$^-$ ALDC

For quantification of IL-12 transcripts, only the production of the p40 subunit was evaluated, as production of p35 is generally considered to be constitutive in most cells (Schoenhaut et al., 1992). ALDC samples were analysed on 3–4 separate occasions by quantitative RT-PCR with the exception of ALDC samples obtained from sorting experiment 16.0, where only two quantitative RT-PCR experiments were carried out due to time constraints. Data are presented as mean ± SEM (arbitrary normalised units) calculated from 2–4 experiments. IL-12p40 mRNA was detected in all ALDC samples analysed (Figure 4.20a). There was however considerable variability in IL-12p40 expression between different animals, and may reflect the outbred nature of this population. In addition, the level of IL-12p40 expression varied between samples collected from the same animal but on different days (sheep JH3 and JH9); however there was limited variation in expression of IL-12p40 in samples collected from sheep JH2 on consecutive days (sort samples 3.0 and 4.0) and importantly this animal was later vaccinated with pGM-CSF (Section 4.6) immediately after "resting" lymph (4.0) was collected.

Although considerable variability in IL-12p40 mRNA expression was evident between different animals and samples, constitutive production of IL-12p40 was consistently higher in SIRPα$^-$ ALDC than in SIRPα$^+$ ALDC from each afferent lymph sample in all six animals analysed (Figure 4.20a). Statistical analysis using the paired (two-tailed) Student t-test revealed that there is a statistically significant difference in IL-12p40 expression in SIRPα$^-$ and SIRPα$^+$ ALDC obtained from the following cell sorting experiments: 2.0 (JH1, $p < 0.02$); 3.0 (JH2, $p < 0.04$); 4.0 (JH2, $p < 0.04$); 12.0 (JH2, $p < 0.05$); 15.0 (JH4, $p < 0.03$); 19.0 (JH6, $p < 0.02$); 20.0 (JH6, $p < 0.03$). No statistically significant difference in IL-12p40 expression is apparent between SIRPα$^+$ and SIRPα$^-$ ALDC obtained from sorting experiment 14.0 ($p > 0.05$).

A way to overcome the issue of non-independence in this data set is to calculate mean values for each ALDC sample from each animal (excluding the second set of measurements from samples obtained from the same animal) and to compare values from all six animals (Figure 4.20b). Using this type of analysis, IL-12p40 expression is significantly higher in SIRPα$^-$ ALDC ($p < 0.03$, paired Student t-test; $p < 0.04$, Wilcoxon matched pairs test). On average, freshly isolated SIRPα$^-$ ALDC express 24-fold more p40 transcripts than SIRPα$^+$ ALDC (mean difference of 24; range 5.7–68-fold).

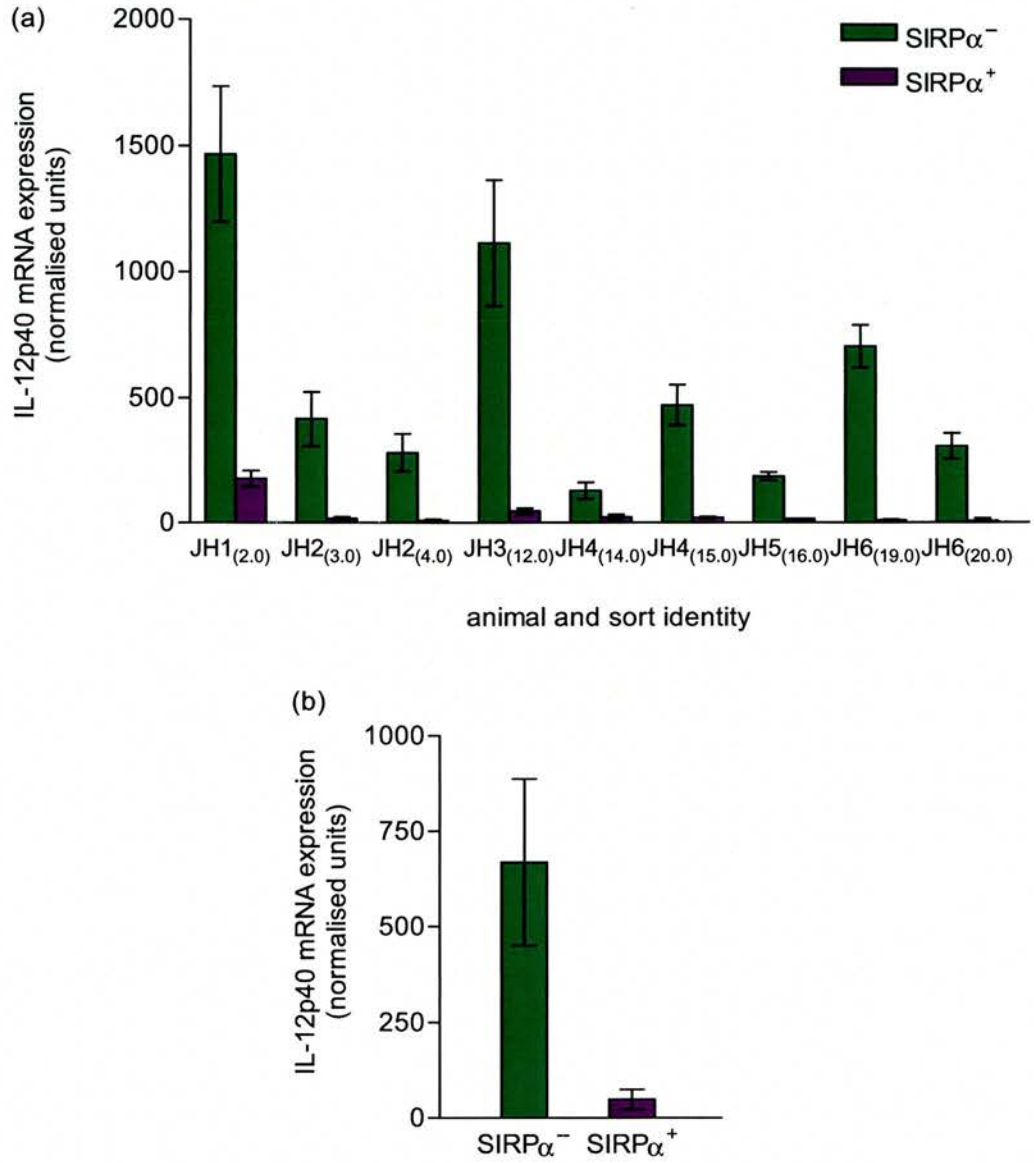

Figure 4.20 Expression of IL-12p40 mRNA in freshly sorted ALDC subpopulations. IL-12p40 mRNA expression was analysed in six animals (a, JH1–JH6). Subscript numbers in brackets correspond to individual cell sorting experiments. Data are presented as mean ± SEM (n = 2–4 independent quantitative RT-PCR experiments; $JH1_{(2.0)}$, $p < 0.02$; $JH2_{(3.0)}$, $p < 0.04$; $JH2_{(4.0)}$, $p < 0.04$; $JH3_{(12.0)}$, $p < 0.05$; $JH4_{(14.0)}$, $p > 0.05$; $JH4_{(15.0)}$, $p < 0.03$; $JH5_{(16.0)}$, $n = 2$, p cannot be determined; $JH6_{(19.0)}$, $p < 0.02$; $JH6_{(20.0)}$, $p < 0.03$.) (b) Mean values for each ALDC sample have been calculated for each of the six animals and compared as one data set, presented as mean ± SEM ($p < 0.03$, paired Student t-test; $p < 0.04$, Wilcoxon paired test)). Results show that freshly sorted $SIRP\alpha^-$ ALDC express significantly more IL-12p40 transcripts than $SIRP\alpha^+$ ALDC.

4.4.3.2 IL-10 mRNA expression in purified SIRPα$^+$ and SIRPα$^-$ ALDC

Transcripts for IL-10 were undetectable in SIRPα$^-$ ALDC in all six animals analysed. Figure 4.21a,b is representative of several melting curve analyses performed after the amplification stage and show that only non-specific products have accumulated with cDNA samples derived from SIRPα$^-$ ALDC after 40 cycles of amplification. Conversely, constitutive production of IL-10 mRNA was detected in the majority of SIRPα$^+$ samples (Figure 4.21c). In four of the six sheep analysed (SIRPα$^+$ samples 2.0–4.0 and 14.0–16.0), specific IL-10 transcripts were consistently detected, since amplicons melt at the same temperature as IL-10 standards (diluted 1° PCR products, verified to be IL-10 amplicons by sequence analysis, Appendix III). No IL-10 transcripts were detected in SIRPα$^+$ samples obtained from sheep JH3 (sorts 12.0 and 13.0) or sheep JH6 (sort 20.0) in any of the experiments undertaken. Specific IL-10 transcripts were detected in one LightCycler® experimental run carried out with sample 19.0 but were below the level of quantification of the assay.

Figure 4.22 shows data obtained from each SIRPα$^+$ ALDC sample, where mean values have been calculated from 2–3 independent experiments carried out on the LightCycler®. There was considerable variation in IL-10 expression between different animals and even in samples collected on different days from the same animal; considerable variation in IL-10 transcripts was apparent in SIRPα$^+$ ALDC obtained from sheep JH4 (14.0 and 15.0). There was however limited variation in expression of IL-10 in SIRPα$^+$ ALDC samples collected from sheep JH2 (SIRPα$^+$ samples 3.0 and 4.0) 24 hours apart, which is of relevance to this study, since pGM-CSF was subsequently administered to this animal (Section 4.6).

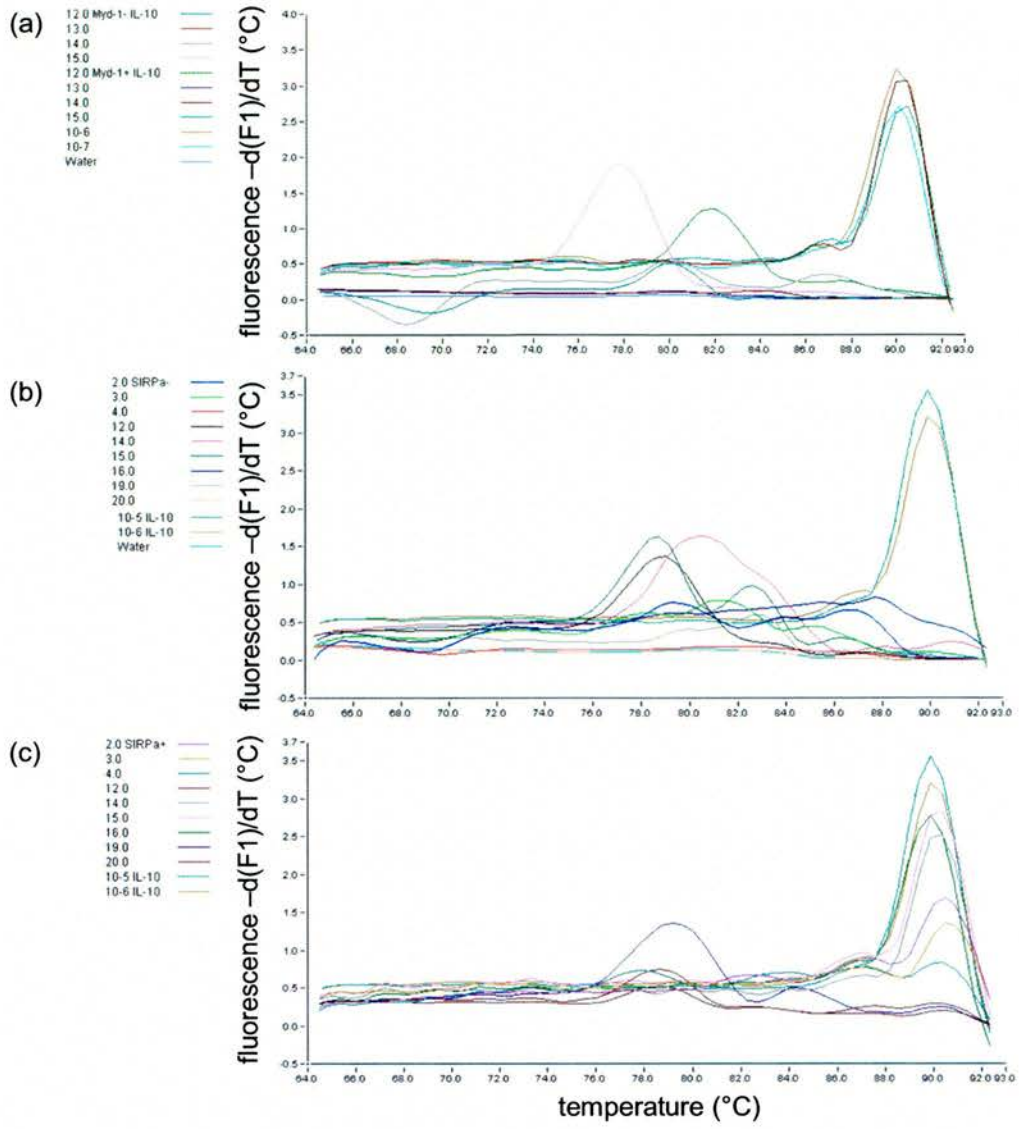

Figure 4.21 SIRPα$^+$ ALDC uniquely express IL-10 transcripts. Melting curve analysis performed on amplicons generated during amplification with freshly sorted ALDC cDNA samples. Specific IL-10 transcripts were detected in most of the SIRPα$^+$ ALDC samples analysed, with the exception of samples obtained from sheep JH3 (sort samples 12.0 and 13.0; (a & c)) and sheep JH6 (sort samples 19.0 and 20.0; (c)). No IL-10 transcripts were detected in any of the SIRPα$^-$ ALDC samples tested (a & b). Note that in (a) MyD-1 corresponds to SIRPα antigen.

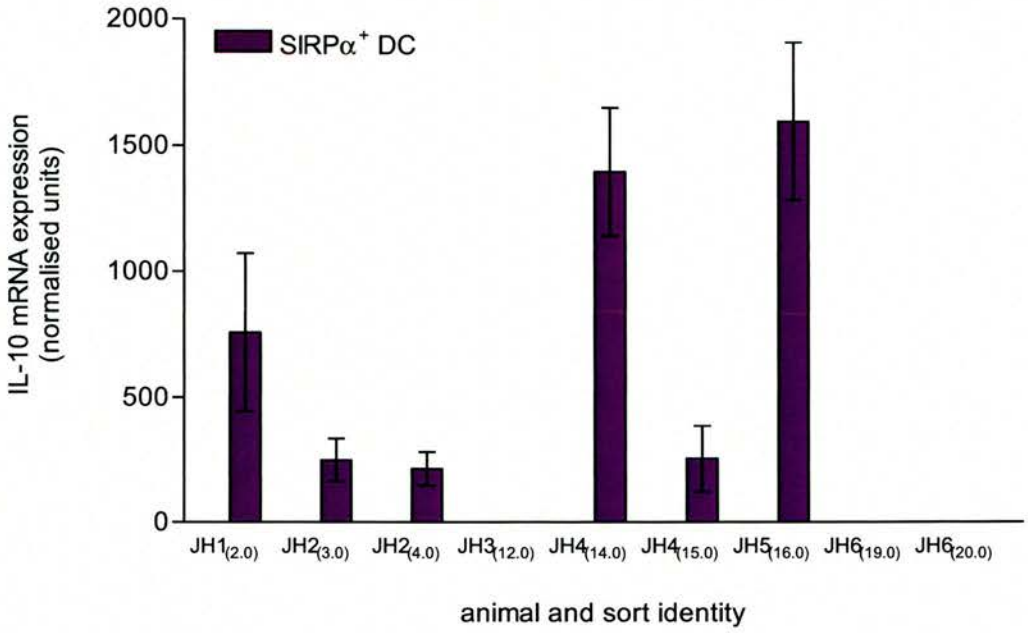

Figure 4.22 Expression levels of IL-10 mRNA in freshly sorted SIRPα$^+$ ALDC. IL-10 transcripts were undetectable in all SIRPα$^-$ samples studied and were absent or below the level of quantification for several SIRPα$^+$ ALDC samples (sheep JH3 and JH6). n = 3 independent quantitative RT-PCR experiments (JH1 and JH2); n = 2 (JH4 and JH5). Data are presented as mean ± SEM.

4.4.3.3 IL-1β mRNA expression in purified SIRPα$^+$ and SIRPα$^-$ ALDC

The expression of pro-inflammatory IL-1β was also investigated by quantitative RT-PCR. IL-1β transcripts were evident in both ALDC subpopulations, with the exception of SIRPα$^-$ ALDC samples obtained from sheep JH6 (sort samples 19.0 and 20.0), where transcripts were undetectable. In general, fresh SIRPα$^+$ ALDC produce considerably more IL-1β transcripts than SIRPα$^-$ ALDC (Figure 4.23a). There was, however, considerable variation between the results for different animals and values for IL-1β were substantially higher in SIRPα$^+$ ALDC samples obtained from sheep JH4 (samples 14.0 and 15.0) and JH5 (sample 16.0) than in SIRPα$^+$ samples obtained from the other animals. Where data from sheep JH4 and JH5 are not presented (Figure 4.23b), a pronounced difference in IL-1β expression is also evident with samples obtained from other animals, with the exception of ALDC samples obtained from sheep JH2 (sort samples 3.0 and 4.0).

On average SIRPα$^+$ ALDC produce 13 fold (range 1.2–32.5) more IL-1β transcripts than SIRPα$^-$ ALDC (Figure 4.23c) and importantly this difference is of statistical significance ($p < 0.008$, Wilcoxon paired t-test). Mean fold differences have been calculated for ALDC samples obtained from the same lymph and are presented in Table 4.3. Since IL-1β was not

detected in either of the SIRPα⁻ ALDC samples from sheep JH6, fold differences cannot be calculated.

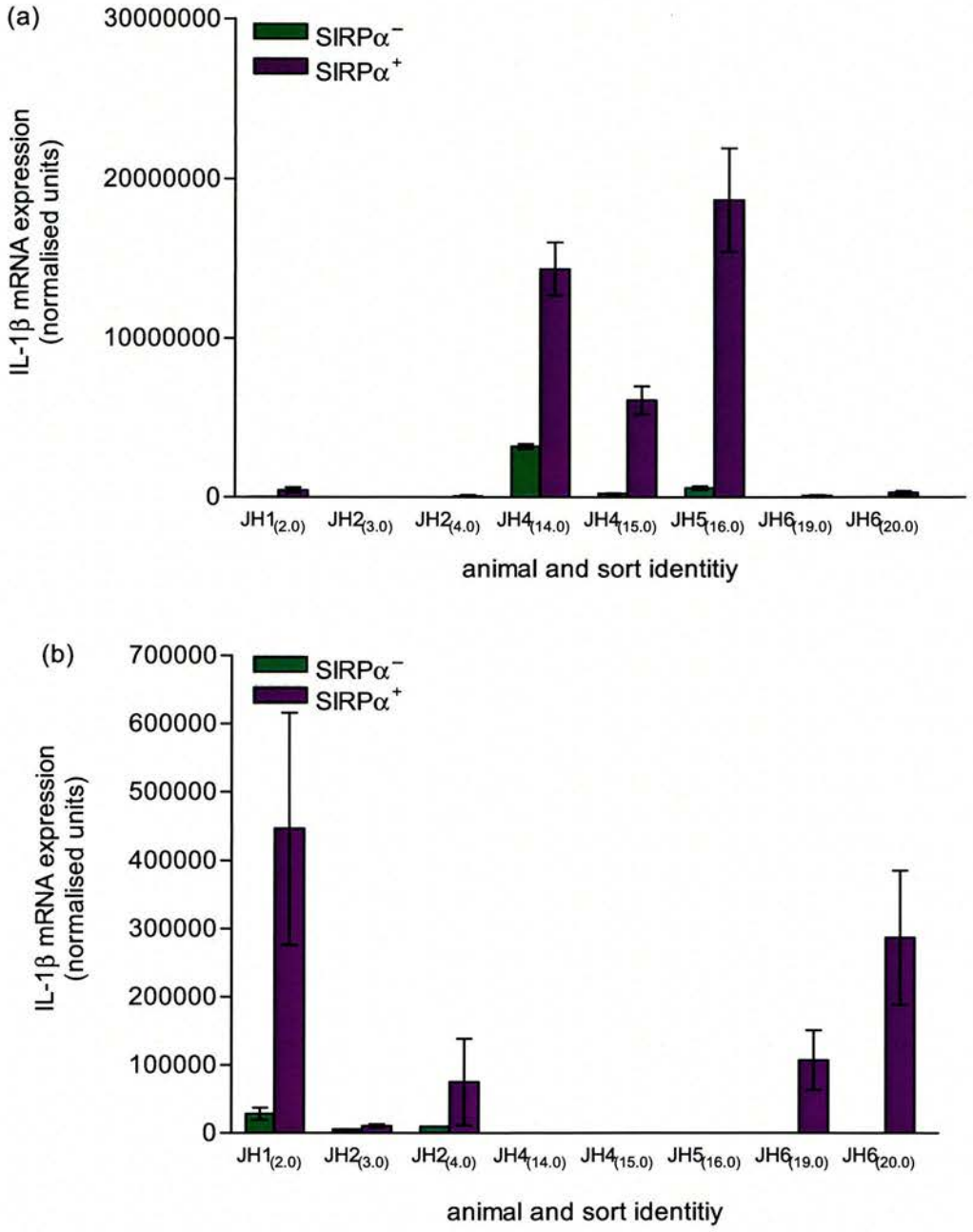

Figure 4.23 Expression of IL-1β mRNA in freshly sorted ALDC subpopulations. (a) Expression of IL-1β mRNA in freshly sorted ALDC from six animals. Mean values have been calculated for each ALDC population from each animal and presented as mean ± SEM. (b) Expression of IL-1β mRNA in freshly sorted ALDC without data obtained from animals JH4 and JH5 presented; c, SIRPα⁺ ALDC express significantly more IL-β transcripts than SIRPα⁻ ALDC. There is a statistically significant difference in IL-1β expression by SIRPα⁺ and SIRPα⁻ ALDC ($p < 0.008$).

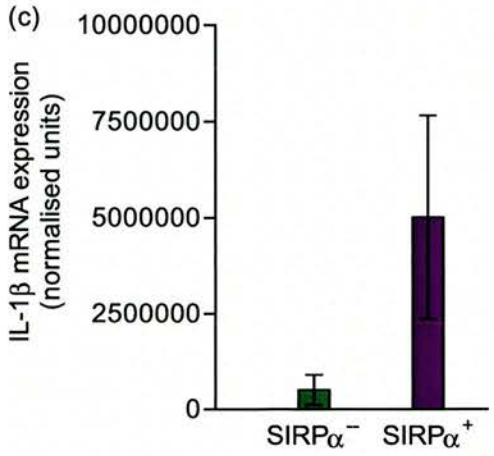

Figure 4.23 (cont.)

Table 4.3 Mean fold difference in IL-1β mRNA expression in highly purified ALDC subpopulations. (*, difference calculated from one experiment only, where IL-1β expression in the SIRPα⁻ ALDC subpopulation was within the quantification limit of the assay; –, cannot be assessed: IL-1β transcripts were absent in SIRPα⁻ ALDC samples obtained from sorts 19.0 and 20.0 (sheep JH6).)

animal	sort id	mean fold difference	range
JH1	2.0	15	9.9–20.1
JH2	3.0	1.5*	–
JH2	4.0	1.2*	–
JH4	14.0	4.5	4.2–4.9
JH4	15.0	26.65	20.8–32.5
JH5	16.0	31.83	31.8–31.9
JH6	19.0	–	–
JH6	20.0	–	–

4.4.3.4 IL-18 mRNA expression in purified SIRPα$^+$ and SIRPα$^-$ ALDC

IL-18 transcripts were detected in both ALDC subpopulations by quantitative RT-PCR in this study. Figure 4.24a shows data obtained from three independent experimental runs on the LightCycler®, with the exception of ALDC samples obtained from cell sorting experiment 19.0 (n = 2 independent experiments). Data are presented as mean ± SEM. With the exception of samples 4.0 and 16.0, where IL-18 transcripts are significantly higher in the SIRPα$^+$ ALDC population ($p < 0.03$ (4.0) and $p < 0.02$ (16.0)), no obvious difference in expression of IL-18 is apparent between SIRPα$^+$ and SIRPα$^-$ ALDC when data obtained from the three independent LightCycler® runs are presented in this way.

Due to the lack of reproducibility of the quantitative RT-PCR experiments, data are also displayed as individual plots for each of the five sheep analysed showing all of the replicate values for each quantitative RT-PCR experiment carried out (Figure 4.24b). This better illustrates that there is indeed a difference in IL-18 expression between SIRPα$^+$ and SIRPα$^-$ ALDC in four out of five animals analysed in this study; on average, SIRPα$^+$ ALDC express 2 fold more IL-18 transcripts than SIRPα$^-$ ALDC. This is particularly evident in sample 2.0 (sheep JH1), samples 3.0 and 4.0 (sheep JH2) and sample 16.0 (sheep JH6). In 2 out of 3 LightCyler® experiments, more abundant IL-18 transcripts were quantified in the SIRPα$^+$ ALDC derived from sample 14.0; however, on the third analysis, levels of IL-18 were approximately the same. The mean fold differences in IL-18 expression are presented in Table 4.4 for each set of samples.

Importantly, where mean values are calculated for each SIRPα$^+$ and SIRPα– ALDC sample for each animal and are compared as one data set, the difference in IL-18 expression between the two ALDC populations is statistically significant ($p < 0.03$; Figure 4.24c).

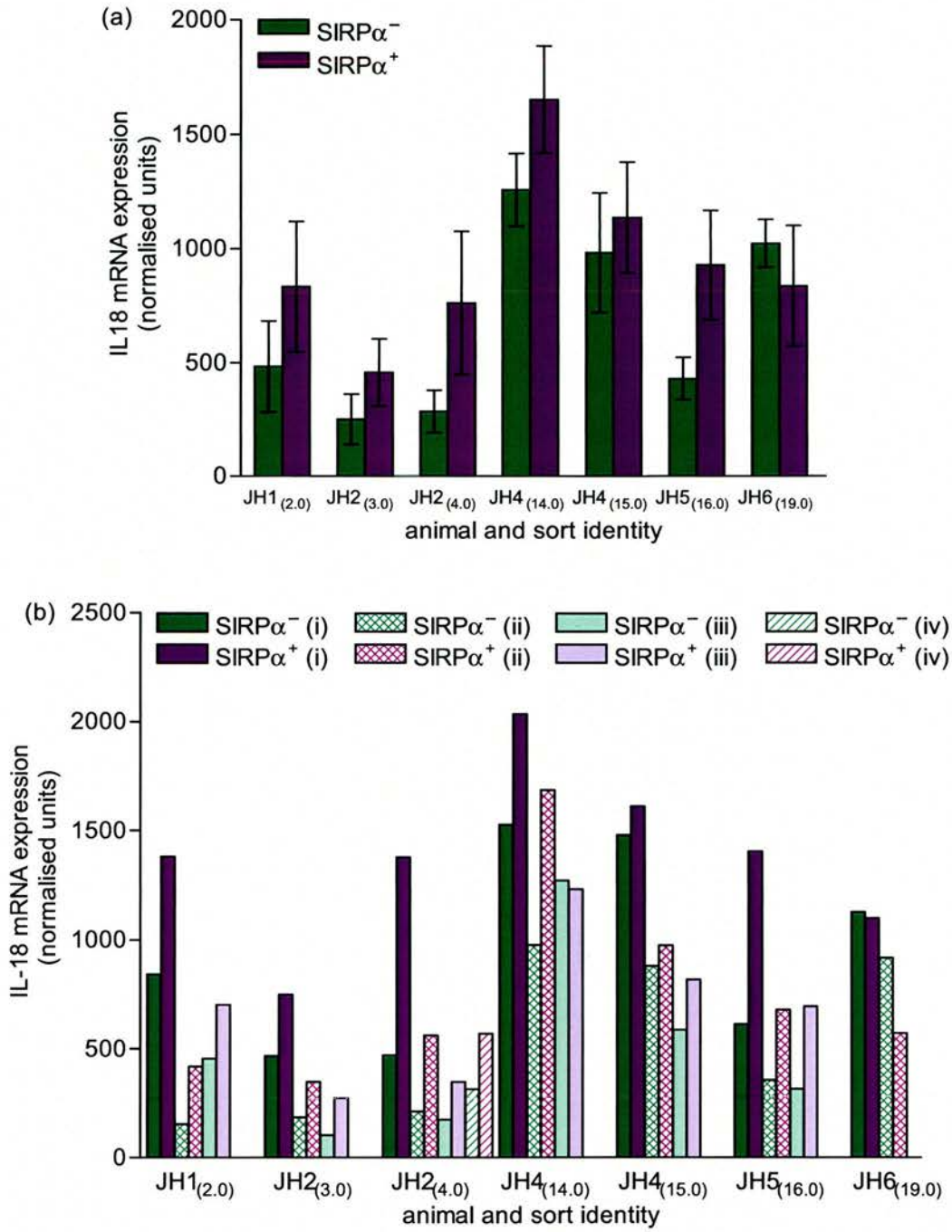

Figure 4.24 Expression of IL-18 mRNA in freshly sorted ALDC subpopulations. (a) Data are presented as mean ± SEM of three independent LightCycler® experiments (JH1, JH2, JH4 & JH5) or mean ± SEM of two experiments (JH6). (b) Normalised values for each cDNA sample and from each LightCycler® experiment carried out (i–iv). (c) SIRPα$^+$ ALDC express significantly more IL-18 transcripts than SIRPα$^-$ ALDC. Mean values have been calculated for each animal and values obtained from SIRPα$^+$ ALDC compared with mean values obtained from SIRPα$^-$ ALDC samples.

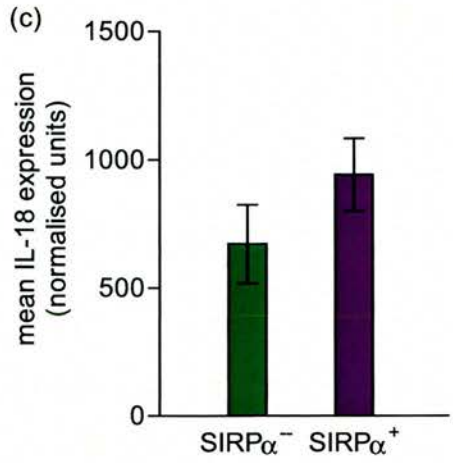

Figure 4.24 (cont.)

Table 4.4 Mean fold differences in IL-18 mRNA expression in highly purified ALDC populations

animal	cell sorting experiment	mean fold difference ($SIRP\alpha^+$/ $SIRP\alpha^-$)	range	p value (Student paired t-test)
JH1	2.0	2.0	1.6–2.8	–
JH2	3.0	2.1	1.6–2.7	–
JH2	4.0	2.5	2.0–2.9	0.03
JH4	14.0	1.46	1.3–1.73	–
JH4	15.0	1.2	1.1–1.4	–
JH5	16.0	2.1	1.9–2.3	0.01

4.4.3.5 TNF-α mRNA expression in purified $SIRP\alpha^+$ and $SIRP\alpha^-$ ALDC

TNF-α transcripts were detected in all ALDC samples examined, although transcripts were below the level of quantification in samples obtained from cell sorting experiments 12.0 and 20.0. TNF-α mRNA expression was highly variable in all five animals analysed in this study (Figure 4.25). For example, expression of TNF-α was higher in $SIRP\alpha^-$ ALDC than in $SIRP\alpha^+$ ALDC isolated from sorting experiments 15.0 (sheep JH4, mean 1.6 fold difference) and 16.0 (sheep JH6, mean 3.2 fold difference), calculated from two independent quantitative RT-PCR experiments (Figure 4.25a). Conversely, TNF-α expression was higher in $SIRP\alpha^+$ ALDC obtained from sorting experiment 3.0 (sheep JH2, mean 1.4 fold difference; calculated from three independent LightCycler® runs) and 14.0 (sheep JH4, mean

5 fold difference; calculated from two LightCycler® runs). With the exception of samples obtained from sheep JH2 (sort samples 3.0 and 4.0), where levels of TNF-α mRNA remained at a similar level in samples collected on different days, differences in the expression of TNF-α in ALDC subsets collected from sheep JH4 were inconsistent. Samples 14.0 and 15.0 represent 24-hour samples collected on different days from this animal, and notably, $SIRP\alpha^+$ ALDC contain more TNF-α transcripts from one collection, whereas $SIRP\alpha^-$ ALDC contain more abundant transcripts 24 hours later. In addition, differences in levels of TNF-α between $SIRP\alpha^+$ and $SIRP\alpha^-$ ALDC (from the same lymph sample) were inconsistent when analysed on separate occasions, as illustrated in Figure 4.25b, where values obtained from individual analyses are compared. For instance, in one quantitative RT-PCR assay, levels of TNF-α transcripts were approximately the same in $SIRP\alpha^+$ and $SIRP\alpha^-$ ALDC obtained from sheep JH2 (sorting experiment 4.0), whereas in another assay (ii), $SIRP\alpha^+$ ALDC expressed 1.9 fold more TNF-α transcripts than $SIRP\alpha^-$ ALDC and in the third assay (iii), $SIRP\alpha^-$ ALDC expressed 2.7 fold more TNF-α transcripts than $SIRP\alpha^+$ ALDC.

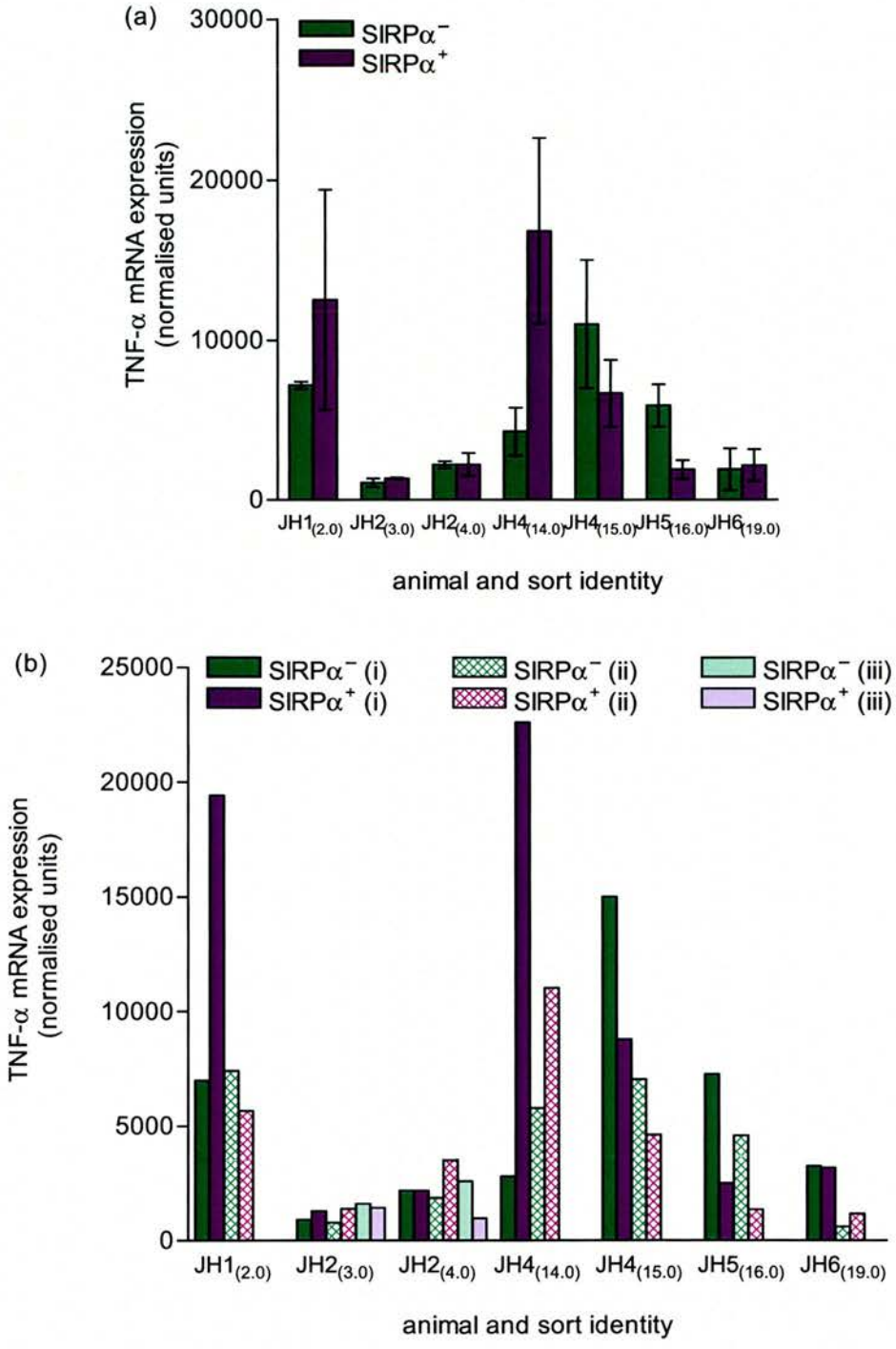

Figure 4.25 Expression of TNF-α mRNA in freshly sorted ALDC subpopulations. (a) Data are presented as mean ± SEM calculated from 2–3 independent experiments. (b) Data are displayed from each individual LightCycler® experiment (experiments i–iii) carried out with each cDNA sample.

4.5 Discussion (part 1)

4.5.1 Morphology of SIRPα$^+$ and SIRPα$^-$ ALDC

Two phenotypically distinct subpopulations of ALDC were identified in ovine afferent lymph based on differential expression of the SIRPα molecule. Microscopy of the sorted ALDC revealed a classical DC morphology, with many dendrites, abundant veils, prominent nuclei and a large size (>10μm diameter). It is of interest to note that there are indeed morphological differences between the two populations, as has been reported in studies involving both rats (Liu et al, 1998c) and cattle (Howard et al., 2002). In all three species, SIRPα$^-$ ALDC are larger than SIRPα$^+$ ALDC and appear to be a homogeneous population, whereas the SIRPα$^+$ ALDC appear to be more heterogeneous. In addition, ovine SIRPα$^+$ DC display blunt pseudopodia and have a "spiky" appearance, whereas SIRPα$^-$ ALDC have a more veiled or frilly appearance.

Ultrastructural analysis by TEM showed that both populations possess some ultrastructural features common to DC of other species, including abundant cytoplasmic inclusions and heterochromatic nuclei. MacPherson and colleagues demonstrated that OX41$^-$ ALDC contain apoptotic DNA and have suggested a role for this subpopulation in the induction and maintenance of peripheral tolerance (Huang et al, 2000). Structures that resemble apoptotic bodies were identified in ovine SIRPα$^-$ ALDC; however, this observation must be interpreted with caution as only a small number of SIRPα$^-$ DC were present on sections. Furthermore, electron microscopy was carried out with only two available SIRPα$^-$ samples from two animals. Staining with the fluorescent dye 4', 6–diamidino–2–phenylindole (DAPI) was also carried out on cytospin preparations of sorted cells to attempt to identify DNA contained within apoptotic bodies. The results from this experiment were inconclusive (data not shown). Further analysis by TEM, TUNEL and DAPI staining would help to clarify if ovine SIRPα$^-$ cells contain apoptotic bodies and are potentially involved in the traffic of self-antigens from the skin to the DLN.

4.5.2 Origin of SIRPα$^+$ and SIRPα$^-$ ALDC

It is of paramount interest to determine the origin of the SIRPα$^+$ and SIRPα$^-$ ALDC subpopulations and to determine if expansion of a particular DC subset is required for the generation of a type 1 or type 2 immune response following DNA vaccination. Gene-gun vaccination targets the skin, which harbours two populations of immature DC; LC and dermal DC. The origin of ALDC populations in sheep is not yet known, although expression

of CD1 suggests that either population could be derived from LC and/or dermal DC. Since DNA vaccination by gene-gun targets the skin and LC are a major target, further analysis of ALDC populations was necessary. In cattle there is some evidence that the SIRPα$^+$ ALDC population contains migratory LC, since acetylcholinesterase positive cells are evident within this population (Howard and Hope, 2000; Yirrell et al., 1991). Furthermore, cells in the epidermis and dermis express SIRPα (Adams et al, 1998), indicating that SIRPα$^+$ lymph DC are derived from these locations. In this study, no staining of any cells occurred with mAb IL-A24 on paraffin wax embedded ovine skin or lymph node tissue (results not shown) and further studies should be carried out with frozen sections.

A unique feature of epidermal-derived LC is the presence of Birbeck granules (Birbeck et al, 1961), which are disks of two limiting membranes, separated by leaflets with periodic "zipper like" striations (Valladeau et al., 2003). Birbeck granules, which often described as resembling tennis-racket like structures, could not be observed in either DC subpopulation by electron microscopy. Ovine LC have been reported to contain fewer Birbeck granules than other mammals (Hollis and Lyne, 1972). Furthermore, LC in lymph contain no or markedly fewer Birbeck granules (Brand et al, 1993). ATPase staining is often employed to identify LC in the epidermis and is also reported to be a reliable marker of epidermal LC (Steinman, 1991). ATPase staining revealed that some SIRPα$^+$ ALDC stained weakly for ATPase. This preliminary result necessitated further analysis to determine if SIRPα$^+$ DC possessed any other features characteristic of LC such as expression of CD1a, langerin or S100.

Immunohistochemical labelling of cytospins prepared from sorted cells revealed that an equal proportion (approximately 80%) of both subpopulations express CD1, a surface marker associated with both LC and dermal DC. mAbs specific for CD1a are currently lacking in the sheep system. A molecular approach was therefore adopted to investigate if either population expressed CD1a and/or langerin, both of which are exclusively expressed by human LC. Birbeck granules were absent from both populations when viewed by electron microscopy; however, langerin (a major component of Birbeck granules) could still be expressed by LC-derived ALDC. Importantly, langerin transcripts were detected in two out of the four SIRPα$^+$ samples analysed, but absent in all four of the SIRPα$^-$ samples which had been verified to contain amplifiable material by GAPDH RT-PCR. It is interesting that transcripts were lacking in some of the SIRPα$^+$ DC. It is possible that the PCR system was not sufficiently sensitive even though cDNA samples chosen for RT-PCR were those derived from sorting experiments where high cell yields/RNA were obtained. Alternatively, langerin transcripts may be quite rare or even absent in migratory LC. Indeed, langerin is down-regulated upon culture of mouse epidermal LC and this is in line with the notion that it

represents a feature of immature cells (Larregina et al., 2001a; Valladeau et al., 1999). From this preliminary analysis, it is possible that the SIRPα$^+$ ALDC population contains a migratory population of DC derived from epidermal LC (due to expression of both langerin and ATPase).

Indeed the SIRPα$^+$ population appears to be a heterogeneous group of DC, in which some CD14 expressing cells were detected. Whilst it was not proven that the SIRPα$^+$ subpopulation was completely devoid of monocytes and tissue macrophages, it is possible that CD14 is expressed by (SIRPα$^+$) ALDC as reported previously (Bailey, 2003; Gupta et al, 1996), rather than due to adsorption of this molecule. RT-PCR using ovine-specific CD14 primers would help to clarify this matter. Although no direct comparison was made, macrophages express higher levels of CD14 than DC (Gupta et al, 1996) and the level expressed by the SIRPα$^+$ ALDC in this study appears to be rather low. It is of relevance to this study that MoDC retain low-level expression of CD14 in culture (Manna et al., 2001) and freshly isolated LC can express low levels of CD14 (Caux et al., 1992a). Moreover, dermal resident CD14$^+$ cells have been shown to differentiate into LC (Larregina et al, 2001a) and in the steady-state LC have been demonstrated to be mostly derived from a skin resident cell, rather than a blood or bone marrow precursor (Merad et al., 2002). Importantly, langerin is also expressed by dermal LC precursors and so it is possible that this SIRPα$^+$ ALDC population contains cells derived from dermal LC precursors and/or LC. It is interesting that neither fresh nor cultured ALDC express coagulation factor XIIIa, a marker associated with dermal DC (Haig et al, 1995b), suggesting that LC represent the migratory population and not dermal DC.

Alternatively, these CD14$^+$ SIRPα$^+$ ALDC may be directly derived from a monocyte precursor, as the physiological factors involved in the regulation of DC differentiation are still unknown and there appears to be a fine line between monocytes differentiating into macrophages or DC; Randolph and colleagues (Randolph et al., 1998) first demonstrated the ability of human endothelial cells to mature adherent peripheral blood CD14$^+$ monocytes into DC in a reverse transmigration assay, a process that is reminiscent of the movement of cells from tissue into lymphatic vessels. It has also recently been demonstrated that macrophages can differentiate into DC *in vitro* (Ichikawa et al., 2003), suggesting that macrophages are not as fully differentiated as has been proposed. Both ALDC populations probably arise from myeloid precursors, since they express myeloid markers, namely CD11c (Bailey, 2003). It does not appear to be the case that either population is the equivalent of the pDC found in humans, although high expression of CD45RA by SIRPα$^-$ ALDC is a characteristic of pDC (Liu et al, 2001).

4.5.3 TLR mRNA expression in ALDC subpopulations

Since a fraction of SIRPα$^+$ DC expressed CD14, it was postulated that this population might also express TLR4, since CD14 and TLR4 work in conjunction with one another in the recognition of LPS, a component of Gram-negative bacteria (Poltorak et al, 1998). In line with this, TLR4 transcripts were detected in SIRPα$^+$ ALDC, whereas transcripts for this receptor could not be detected by conventional RT-PCR in SIRPα$^-$ ALDC. TLR4 is expressed by myeloid DC in humans, and more recently, TLR4 has also been reported to be expressed by murine LC (Mitsui et al, 2004). Bovine DC derived from blood monocytes have also been reported to express TLR4, but at lower levels than in monocytes and monocyte-derived macrophages (Werling et al., 2004). It is difficult to draw upon any similarities with *ex vivo*-derived cells, since Werling's group employed an *in vitro* system where many factors, including cytokines could affect TLR expression. In another study which employed xenogeneic endothelial cells to maturate DC, maturation of adherent monocytes into DC was accompanied by an upregulation of message for TLR4 (Manna et al., 2002).

It then became apparent that further investigation of expression of other TLR was required, as any differences in the expression of these receptors may highlight differences in the biology of these DC and how they are likely to respond to a pathogen or stimulus such as CpG motifs contained within DNA vaccines. From those samples tested, both populations were found to express TLR3 and whilst all SIRPα$^+$ ALDC samples analysed expressed TLR9, weak expression was detected in only some of the SIRPα$^-$ ALDC. Due to time constraints, no quantification of TLR was carried out and this would be a logical approach to take, since RNA yields were typically low for the smaller SIRPα$^-$ ALDC population. High-quality antibodies are still not available for many TLR, and are completely lacking for the ovine system; many reports therefore rely on mRNA expression profiles. In principle, either population could be regarded as being capable of responding to prokaryotic dsRNA or CpG motifs. Functional studies now need to be adopted in order to assess how each DC population would respond to these ligands.

Expression of TLR9 by myeloid DC is a contentious issue. Indeed Werling and colleagues did not detect TLR3 or TLR9 from bovine MoDC, although transcripts for TLR2 and TLR4 were detected, albeit at lower levels than on monocytes or macrophages. Human monocytes are believed to be unresponsive to CpG motifs because they lack expression of TLR9 (Hornung et al., 2002). The lack of mRNA transcripts for TLR9 in bovine myeloid DC is in accordance with several other reports. However, expression of TLR9 may not be restricted to cells of the lymphoid origin/pDC as illustrated by work carried out by Spies and colleagues

(2003) in which they demonstrated that plasmid DNA can activate both pDC ($CD11c^{hi}$ $CD45RA^{hi}$ $CD11b^{lo}$) and conventional myeloid ($CD11c^{hi}$ $CD45RA^{lo}$ $CD11b^{hi}$) DC via TLR9. Furthermore, freshly isolated murine LC (myeloid DC) express TLR9 (Mitsui et al, 2004). These examples illustrate the difficulties of translating functional findings between DC subsets in different species.

4.5.4 Cytokine mRNA expression in ALDC subpopulations

This study provides evidence that distinct quantitative differences in cytokine production exist between two ALDC subpopulations in sheep. There was substantial variation in cytokine mRNA levels between sheep and this may reflect the nature of an outbred population; however, cytokine profiles of $SIRP\alpha^+$ and $SIRP\alpha^-$ ALDC were similar in the six sheep analysed. Differences in cytokine expression were also observed with some samples collected on different days from the same sheep (with the exception of samples collected from JH2; 3.0 and 4.0). Such inconsistencies may reflect changes in the lymph after surgery, or that there is some natural (but unknown) stimulation or perhaps insufficient prevention of *de novo* transcription. Actinomycin D was added to prevent *de novo* transcription and concentrations of actinomycin D had to be estimated from the volume of lymph collected 24 hours earlier and thus it was not always possible to obtain the optimal concentration. Alternatively, although expression of the housekeeping gene GAPDH should be consistent, changes in the expression of GAPDH have been reported (Bustin, 2000). Normalisation with another housekeeping gene such as ribosomal 18S may help to clarify this matter.

Quantitative RT-PCR revealed that $SIRP\alpha^-$ ALDC express significantly higher levels of IL-12p40 than $SIRP\alpha^+$ ALDC, which is in agreement with findings from cattle (Howard et al, 2002; Stephens et al, 2003) and rat splenic $SIRP\alpha^-$ DC (Voisine et al, 2002). IL-12 drives T cells towards Th1-type responses (Heufler et al, 1996; Macatonia et al, 1995; Seder et al, 1993). On this basis, $SIRP\alpha^-$ ALDC could be anticipated to polarise naïve $CD4^+$ T cells into Th1 cells. However, in this study, only the expression of the p40 subunit was quantified; no assessment of p35 was made. In addition, IL-12 has been described as the mandatory molecule secreted by activated DC that promotes the differentiation of naïve B cells into plasma cells (Dubois et al., 1998). Further studies must be conducted in order to determine if indeed bioactive IL-12 is produced by both $SIRP\alpha^-$ and $SIRP\alpha^+$ DC, since p40 is the common subunit of both IL-12 and IL-23 (Brombacher et al., 2003; Oppmann et al., 2000). Currently there are no commercially available ELISAs for ovine IL-12 and hence many studies rely on mRNA profiles. A capture ELISA for bovine IL-12 has been described (Hope

et al., 2002); however, the mAb available do not distinguish between IL-12p40 and the IL-12 p75 heterodimer.

Polarisation of Th cells into Th1 cells also depends on IL-18, which potentiates the effects of IL-12, resulting in higher levels of IFN-γ (Okamura et al., 1995). IL-18 has been demonstrated to be constitutively expressed by human MoDC (Gardella et al., 1999). Both ALDC populations were reported to express IL-18 in cattle, but transcripts were not quantified (Stephens et al, 2003). In this study it was evident that both ALDC populations constitutively express IL-18 mRNA. Levels of IL-18 expression were similar in some of the $SIRP\alpha^+$ and $SIRP\alpha^-$ samples derived from the same lymph; however, in most samples analysed, IL-18 transcripts were approximately 2 fold higher in the $SIRP\alpha^+$ ALDC subpopulation. High constitutive expression of IL-12p40 in conjunction with IL-18 expression may favour the development of a Th1-type immune response by $SIRP\alpha^-$ ALDC. It would be of interest to assess the Th types induced by means of a mixed lymphocyte reaction, where allogeneic naïve $CD4^+$ T cells are incubated with $SIRP\alpha^-$ (/$SIRP\alpha^+$) ALDC and IFN-γ production is quantified. In addition the stimulatory capacity of ovine $SIRP\alpha^+$ and $SIRP\alpha^-$ ALDC requires investigation as it remains to be elucidated if $SIRP\alpha^-$ DC, like rat and bovine $SIRP\alpha^-$ DC are poor at stimulating $CD4^+$ and $CD8^+$ T cells in comparison to the highly immunostimulatory $SIRP\alpha^+$ ALDC.

Quantitative RT-PCR revealed that $SIRP\alpha^+$ ALDC exclusively express IL-10 whereas IL-10 transcripts were undetectable for the entire collection of $SIRP\alpha^-$ ALDC sort samples in all six of the animals studied. This is in agreement with work carried out in cattle, where IL-10 transcripts are more abundant in $SIRP\alpha^+$ ALDC than in $SIRP\alpha^-$ ALDC (Stephens et al, 2003). The presence of both IL-10 and IL-6 during T cell stimulation has been linked to the generation of Th2-type responses in mice (Liu et al, 1998b; Rincon et al, 1997). Conversely, IL-10 has been demonstrated to have a down-regulatory effect in humans and in ruminants, reducing the proliferation of both Th1- and Th2-type clones (Brown and Estes, 1997; Del Prete et al, 1993). IL-10 is also reported to down regulate IL-12 production (D'Andrea et al., 1993) and this could help to explain the low IL-12p40 expression by $SIRP\alpha^+$ ALDC. It is also interesting to speculate that high expression of IL-10 by $SIRP\alpha^+$ ALDC may have an effect on the production of IL-12p40 by $SIRP\alpha^-$ ALDC. This could explain the difference in IL-12p40 expression observed in $SIRP\alpha^-$ ALDC collected on different days from sheep JH4, where lower expression of IL-12p40 correlated with high IL-10 mRNA expression in $SIRP\alpha^+$ ALDC, whereas increased expression of IL-12p40 by $SIRP\alpha^-$ ALDC 24 hours later correlated with a reduced number of IL-10 transcripts in $SIRP\alpha^+$ ALDC.

IL-10 has also been demonstrated to act on a variety of cell types to suppress the production of proinflammatory mediators, although the ability of IL-10 to inhibit proinflammatory activation has been shown to be selective with respect to stimulus and effector responses (Lisinski and Furie, 2002). It is possible that the SIRPα$^+$ ALDC, or indeed cells within this population have an anti-inflammatory role as has been proposed by Howard and colleagues (Howard et al, 2002). This is an attractive theory since constitutive expression of proinflammatory IL-1β and IL-18 was significantly higher in SIRPα$^+$ ALDC analysed in this study. IL-18 is a member of the IL-1 family and is also commonly described as a proinflammatory cytokine, (Sims, 2002). It is conceivable that the expression of IL-10 by SIRPα$^+$ ALDC exerts a regulatory effect on T cells whilst production of proinflammatory IL-1β, in conjunction with high levels of IL-18, may be beneficial for an efficient host immune response against infections. It is interesting that the cytokine profile of steady-state SIRPα$^+$ ALDC is similar to that observed with monocytes which differentiate into TLR7 expressing DC with potent functional activities in the presence of IFN-1 (Mohty et al., 2003), which also secrete large amounts of IL-10, IL-1β, (IL-6) and IL-18, when compared with immature and mature (IL-4 stimulated) DC. Furthermore, these DC promote a Th1 response that is independent of IL-12p70 and IL-18, but is substantially inhibited by IFN-α neutralisation. SIRPα$^+$ ALDC through IL-18 and other inflammatory cytokines may play an important role in regulating the immune response, especially at the early steps of cell-mediated immunity.

Most SIRPα$^+$ DC analysed in this study expressed IL-12p40, but at significantly lower levels than expressed by SIRPα$^-$ ALDC. It is tempting to draw upon similarities of the SIRPα$^+$ population with LC due to the possible expression of langerin and/or ATPase in this preliminary study and the expression of acetycholinesterase demonstrated by a subset of these cells by Howard and colleagues (Howard and Hope, 2000). LC produce constitutively and/or inducibly, a variety of cytokines including IL-1β, IL-6, IL-12, IL-15 and IL-18 (Kimber et al, 2000), indeed murine LC are the major source of mRNA for IL-1β among unstimulated epidermal cells (Cumberbatch et al., 1996). Constitutive expression of IL-12 mRNA by CD1a$^+$ ALDC (proposed to be LC) isolated from humans has been reported (Yawalkar et al., 1996), however, this study made no comparison of IL-12 mRNA expression in other DC-types (for instance, in lymph or in blood) and IL-12 transcripts were detected in only 4 out of the 10 samples by nested PCR.

Recent studies have generated considerable debate as to how DC regulate distinct types of T cell responses. An evolutionary theory suggests that DC lineages or subsets can induce Th1 or Th2 immune responses. However, several studies have demonstrated that a given DC subset can demonstrate a remarkable functional plasticity and induce either Th1 or Th2 immune responses depending on the types of stimulation (Kalinski et al., 1999b; Kalinski et

al., 1999a; Liu et al., 2000). However, the expression of limited sets of pattern recognition receptors on human pDC and myeloid DC suggest that neither can respond to all microbial antigens, and do not therefore have unrestricted functional plasticity. It would be interesting to expose ALDC subpopulations to various PAMP and quantify the cytokines produced before and after stimulation. For instance, functional *in vitro* studies would determine if exposure of SIRPα$^+$ ALDC to LPS resulted in an upregulation of bioactive IL-12 and indeed, if both populations respond "equally" to CpG motifs and dsRNA by producing similar cytokine profiles, thereby demonstrating the plasticity of DC. For instance, can PAMP interaction with PRR change a SIRPα$^-$ ALDC into a DC that stimulates a Th2 response, as a result of IL-10 expression? Such studies could also be extended to address if Th1 or Th2 cells are always stimulated by one subpopulation rather than the other in the steady-state, and if this is still evident after exposure to microbial stimuli.

Whether SIRPα$^+$ and SIRPα$^-$ ALDC represent distinct lineages of DC or different maturational/developmental stages is not known. In the rat model, it has been argued that SIRPα$^+$ and SIRPα$^-$ ALDC are not precursors of each other, since CD4$^+$ SIRPα$^+$ and CD4$^-$ SIRPα$^-$ ALDC have similar turnover times *in vivo* (Liu et al, 1998c). Indeed, SIRPα$^+$ and SIRPα$^-$ ALDC appear to be two separate populations as they differ both phenotypically and functionally in both rats and cattle (Howard et al, 1997). Observations from this study and from other studies conducted with DC in other species (cattle, rats, mice and humans) are summarised in Table 4.5. Functional studies are now required to assess how ovine SIRPα$^+$ and SIRPα$^-$ ALDC compare with rat and bovine subpopulations.

Table 4.5 Comparison of phenotype and cytokine expression in DC subsets in different species. Information regarding DC subsets in sheep, cattle and rats refers to ALDC (with the exception of cytokine profiles of rat SIRPα$^+$ and SIRPα$^-$ DC where the only information currently available is obtained from splenic DC). Cytokine expression refers to the cytokine profile in freshly isolated ALDC or the reported "bias" in cytokine expression (human and murine DC subsets[†]), although it is now established that the cytokine expression is not fixed and ultimately depends on the extracellular milieu/stimulus used. ND = not determined; *, splenic DC only; PRR = pattern-recognition receptors.

surface phenotype	PRRs	other characteristics	cytokine expression	allostimulatory capacity
(a) sheep				
(i) SIRPα+				
HLA-DR^{hi} CD11c$^+$ CD40$^+$ CD80$^+$ CD14$^{+/-}$	TLR3$^+$ TLR4$^+$ TLR9$^+$ DEC205$^+$	spiky, heterogeneous langerin$^+$ ATPase$^+$	IL-10 IL-1β IL-18 TNF-α (variable)	ND
(ii) SIRPα$^-$				
HLA-DR^{hi} CD11c$^{+/-}$ CD40$^+$ CD80$^{lo/-}$ CD86$^{lo/-}$ CD45$^{RA(hi)}$ CD8$^{+/lo}$	TLR3$^+$ TLR9$^+$ TLR4$^-$	"frilly"/veiled, large, homogeneous, apoptotic bodies (?)	IL-12p40 IL-18 TNF-α (variable)	ND
(b) cattle				
(i) SIRPα$^+$				
HLA-DR^{hi} CD26$^-$ CC81Ag$^-$ CD11a$^-$/lo	ND	heterogeneous, acetycholinesterase$^+$, (note that LC in cattle are SIRPα$^+$)	IL-10$^{+/-}$ IL-1α IL-1β IL-6 TNF-α (variable)	high CD8$^+$ T cell proliferation (due to IL-1α)
(ii) SIRPα$^-$				
HLA-DR^{hi} CD26$^+$ CC81Ag$^+$ CD11a^{hi}	ND	homogeneous	IL-12p40 & p75 TNF-α (variable)	low

Table 4.5 (Cont.)

(c) rat*				
(ii) SIRPα$^+$				
class II^{hi} CD4$^+$	ND	heterogeneous, short fine processes	IL-1β* L-10*	high promote IL-12 independent Th1 response & IL-13 producing CD4+ T cells (Th2) *
(ii) SIRPα$^-$				
class II^{hi} CD4$^-$ CD80^{hi} invariant chain$^+$	ND	homogeneous, apoptotic bodies/ & epithelial cell-restricted cytokeratins, NSE$^+$	IL-12p40* TNF-α* (Th1 induction)	low promote Th1 immune responses*
(d) mouse DC				
(i) "lymphoid"CD8α$^+$ splenic DC				
CD11c$^+$ CD11b$^{lo/dull}$ CD8α$^+$ DEC-205$^+$	TLR3$^+$ TLR9$^+$ TLR4$^-$ TLR7$^-$	large size, poor viability *in vitro*, uptake of apoptotic bodies and cross-presentation to CD8$^+$ T cells → cross-tolerance vs. cross-priming	IL-12p70 TNF-α *Note*: can produce IL-10 with certain stimuli	promote Th1† (& Th2) responses
(ii) "myeloid" splenic DC. Note that in the spleen there are at least two myeloid DC populations: (1) CD8α$^-$/CD4$^+$ and (2)CD8α$^-$/CD4$^-$)				
CD11c$^+$ CD11b$^+$ CD8α$^-$ DEC-205$^-$	(1) TLR7$^+$ TLR9$^+$		IL-10 CD8α$^-$/CD4$^+$ can produce IL-12p70 with certain stimuli	promote Th2† (& Th1) responses
	(2) TLR2$^+$ TLR4$^+$ TLR9$^+$		*Note*: CD4$^+$ DC seem incapable of producing IL-12p70 even with different/additional stimuli	

Table 4.5 (Cont.)

(iii) LC (myeloid)

MHC class II$^+$ CD11c$^+$ DEC-205$^+$ CD11b$^-$	TLR2$^+$ TLR4$^+$ TLR9$^+$ TLR7$^-$	ATPase$^+$, acetycholinesterase$^+$, Birbeck granules (langerin$^+$/CD207$^+$), E-cadherin	IL-1β IL-6 IL-12 IL-15 IL-18	freshly isolated LC have a low stimulatory capacity, but can be matured into potent APC

(iv) pDC

B220$^+$/CD45R CD11c$^+$ GR-1 MHC class III^o CD80$^-$ CD86$^{-/lo}$	TLR7$^+$, TLR9$^+$ TLR3$^-$ TLR4$^-$		Type I IFNs (IFN-α/β/ω) IL-6 TNF-α IP-10 IL-12p75	low (↑ Th1 capacity if stimulated with CpG)

(e) human

(i) myeloid blood DC (note this population contains several DC subsets, including BDCA-1$^+$ (CD1c) DC and the smaller BDCA-3+ population)

HLA-DR^{high} CD11c^{high} CD1b/c$^+$ CD13^{+-} CD33$^+$ CD45RO$^+$ CD14$^{+/-}$ (BDCA-1$^+$ DC only)	TLR2$^+$ TLR3$^+$ TLR4$^+$ TLR7$^-$ TLR9$^-$	heterogeneous	IL-12 IL-6 TNF-α	high (BDCA-1$^+$ DC > BDCA-3$^+$)

(ii) pDC

CD11c$^-$ CD123^{hi} BDCA-2$^+$ BDCA-4$^+$ HLA-DR^{++} CD45RA$^+$ CD80$^{-/lo}$ CD86$^{-/lo}$	TLR7$^+$ TLR9$^+$ TLR3$^-$ TLR4$^-$	small size, oval nucleus	IFN-α IL-6 TNF-α IP-10 IL-12p75 (if stimulated with CD40 & CpG)	low tolerogenic(?)

4.6 DNA vaccination of cannulated sheep Experiment 1 – vaccination with pGM-CSF

From the earlier work carried out on pGM-CSF vaccinated skin (chapter 3), it was apparent that GM-CSF was a potent inducer of inflammation, as demonstrated by the formation of a microabscess by approximately 6 hours and significantly elevated expression of proinflammatory TNF-α and IL-1β mRNA. Furthermore, administration of pGM-CSF consistently caused a pronounced infiltration of MHC class II^+ DC into the skin approximately 3–4 days p/v. For these reasons, it was decided to administer pGM-CSF to a cannulated animal rather than with pIL-3. Sheep JH2 was used for this preliminary experiment. Two 24-hour lymph samples were collected from this sheep prior to DNA vaccination (sort samples 3.0 and 4.0). Lymph volumes were carefully measured as the volume of actinomycin D was crucial to prevent *de novo* transcription in order to quantify any changes in cytokine expression after DNA vaccination with pGM-CSF. The sheep was prepared (Section 2.4) and vaccinated five times (0.5–1.0μg of pGM-CSF per shot) in the drainage area of the cannula. An overview of this experiment is illustrated in Figure 4.26.

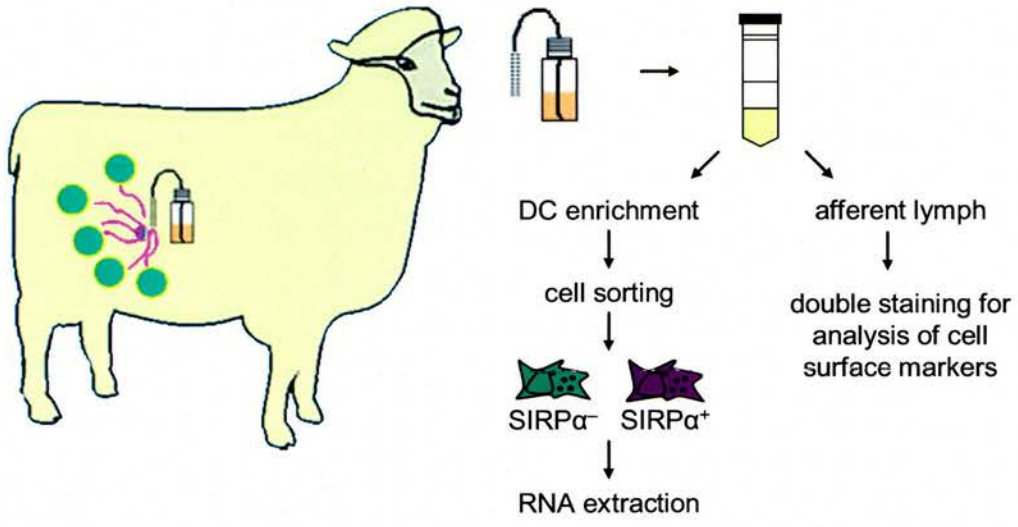

Figure 4.26 Gene-gun administration of pGM-CSF to a cannulated sheep. The animal was vaccinated five times in the drainage area of the cannula and lymph was collected every 24 hours. 90% of the lymph was committed to the enrichment procedure and cell sorting. The remaining unfractionated lymph was used for double immunolabelling and analysis of cell surface markers.

Approximately 24 hours p/v, 5–10ml of lymph was removed for double immunolabelling of ALC for a variety of cell surface markers followed by staining with biotinylated SW73.2 (anti-MHC class IIβ). The remaining lymph (approximately 90ml) was washed and enriched for DC and stained for sorting (as already described). After sorting, RNA was extracted and stored at –80°C until required. The lymph continued to flow for six days after gene-gun vaccination with pGM-CSF.

4.6.1 Expansion of ALDC subsets after pGM-CSF administration

Development of an epidermal lesion was evident after pGM-CSF administration (not shown). Concurrent with the onset of inflammation was an increase in the total number of leukocytes migrating through the draining afferent lymph (Table 4.6). The absolute numbers of purified ALDC are also listed in Table 4.6. From this, it appears that gene-gun administration of pGM-CSF expands both sub-populations of ALDC 4 days p/v. In addition, relative percentages of purified SIRPα$^+$ and SIRPα$^-$ ALDC (as a % of total leukocytes) have been calculated. A 2.6 fold increase in SIRPα$^+$ ALDC and a 1.9 fold increase in SIRPα$^-$ ALDC was recorded 4 days after pGM-CSF administration (relative to percentages calculated prior to DNA vaccination).

Relative percentages of SIRPα$^+$ and SIRPα$^-$ ALDC (as a % of enriched DC immunolabelled for subsequent cell sorting) have also been calculated (Figure 4.27a,b), where an increase in the percentage of SIRPα$^+$ ALDC was observed 3–4 days after pGM-CSF administration and an increase in the percentage of SIRPα$^-$ ALDC was observed at days 5–6 p/v. In addition, the relative frequencies of PMN, lymphocytes and ALDC in afferent lymph are presented before and after pGM-CSF administration (Figure 4.27c and Figure 2.1 for gate criteria). The scatterplots clearly show that the number of PMN increased quite dramatically 24 hours after pGM-CSF administration; the number of neutrophils represented approximately 9% of total ALC in the steady-state and increased to approximately 21% 24 hours p/v. Changes in the number of lymphocytes were also evident; where the proportion of lymphocytes was lower (range 51–54%) at days 1, 5 and 6 p/v compared with the proportion of lymphocytes observed in the steady-state (approximately 65% of lymph cells). Conversely, only small changes were evident in the proportion of ALDC (ranged from approximately 7%–11% of total ALC).

Table 4.6 Total leukocyte output and absolute numbers of SIRPα$^+$ and SIRPα$^-$ ALDC isolated by FACS pre- and post-vaccination with pGM-CSF. (NA, not assessed.)

time-point	cell output per 24 hours	total no. SIRPα$^+$ ALDC	total no. SIRPα$^-$ ALDC	% SIRPα$^+$ ALDC	% SIRPα$^-$ ALDC
pre	1.32×10^8	343,137	160,165	0.26	0.12
pre	1.55×10^8	640,223	213,367	0.4	0.14
1 day p/v	2.08×10^8		170,000		0.08
2 days p/v	2.36×10^8	446,068	99,000	0.19	0.04
3 days p/v	NA	921,820	239,552	NA	NA
4 days p/v	**1.96×10^8**	**2×10^6**	**500,000**	**1.02**	**0.26**
5 days p/v	1.93×10^8	1,166,700	423,440	0.6	0.22
6	1.1×10^8	330,000	210,000	0.3	0.19

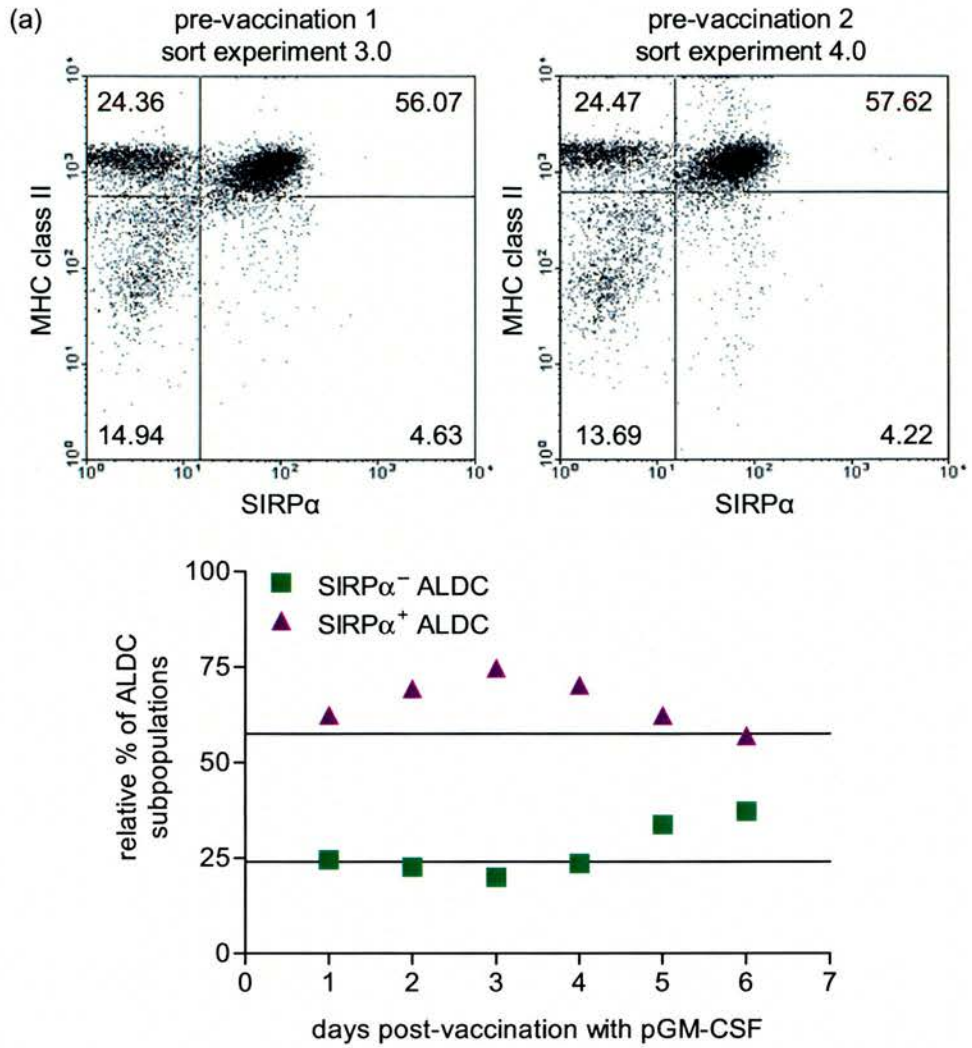

Figure 4.27 Expansion of SIRPα$^+$ and SIRPα$^-$ ALDC populations after gene-gun delivery of pGM-CSF. (a) Lymph was collected from sheep JH2 for 2 days prior to vaccination with pGM-CSF. For each 24-hour collection, lymph was enriched for DC and double immunolabelling was carried out with mAb IL-A24 (anti-SIRPα) and SW73.2 (anti-MHC class II β), where the SIRPα$^+$ DC comprised 56–58% of enriched cells and SIRPα$^-$ DC comprised ~24% (represented in (b) as solid lines). (b) Relative percentages of SIRPα$^+$ and SIRPα$^-$ ALDC after administration of pGM-CSF. (c) Percentage of PMN, lymphocytes and ALDC (calculated as a % of total ALC) before and after administration of pGM-CSF (refer to Figure 2.1 for gate criteria).

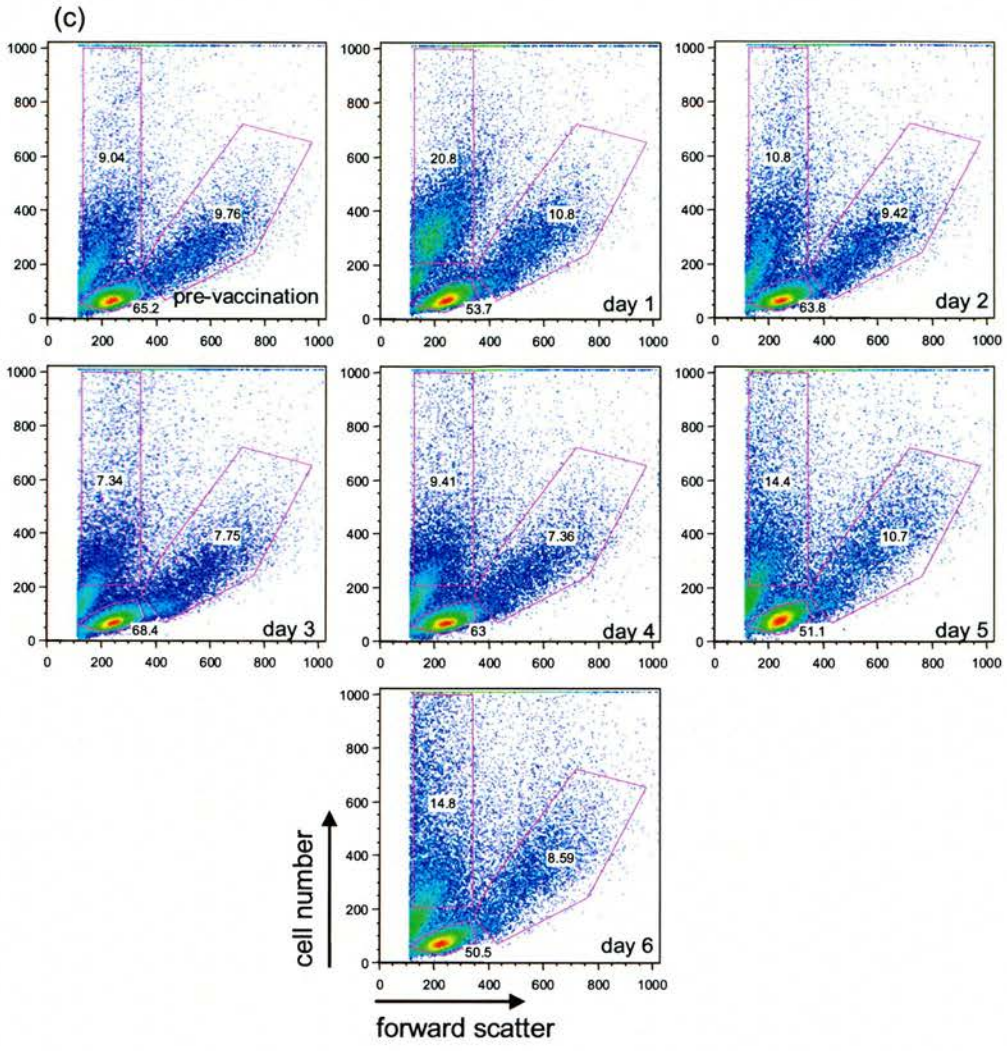

Figure 4.27 (cont.)

4.6.2 Flow cytometric analysis of ALDC cell surface marker expression after gene-gun delivery of pGM-CSF

In experiment 1, the expression of several surface markers on ALDC was analysed by flow cytometry pre- and post-administration of pGM-CSF. The aim of this experiment was to define any changes in the expression of surface markers so that future experiments could be more carefully designed to assess changes in surface expression in SIRPα^{+} and SIRPα^{-} ALDC. Furthermore, biotinylated mAb IL-A24 (anti-SIRPα) was not available at this point in the study. Results from experiment 1 are represented in Figure 4.28–4.35 and the recorded mean fluorescence intensities and percentage of gated cells are also listed. Unfractionated lymph cells (1×10^7 cells/ml) were first immunolabelled with antibodies specific for ovine CD1b, CD40, CD80, CD86, CD11c, CD2, and LFA-3. Bound antibody was detected with

FITC-conjugated anti-mouse Ig. Lymph cells were then stained with biotinylated SW73.2 (anti-MHC class II β) which was detected with streptavidin-PE. ALDC were electronically gated based on high SSC and FSC (R1) and then gated on the population of cells expressing high MHC class II (channel number $>10^3$, R2).

4.6.2.1 Expression of antigen presentation molecules on ALDC after gene-gun delivery of pGM-CSF

In experiment 1, a pronounced increase in the expression of several surface markers on ALDC occurred after gene-gun vaccination with pGM-CSF. A marked increase in the expression of surface CD1b was particularly evident from 1–6 days p/v (Figure 4.28). The increase in expression of CD1b was similar 1–4 days p/v; however, a further shift in fluorescence was evident 5 days p/v and levels then declined slightly by day 6 to levels observed 1–4 days p/v. Importantly, the mAb used to detect CD1b (VPM 5) was previously titrated and a concentration of 1:100 of VPM 5 was shown to be at saturating levels and thus used for all subsequent experiments (Section 2.2.4.5).

A pronounced increase in the expression of surface MHC class II was observed on ALDC for the first 48 hours after gene-gun delivery of pGM-CSF (Figure 4.29), whereas expression was comparable to levels observed pre-vaccination at days 3–4 p/v. Interestingly, an increase in MHC class II expression was again evident 5 days p/v and then declined to levels lower than expressed on ALDC in the steady-state flux.

4.6.2.2 Expression of costimulatory molecules on ALDC after gene-gun delivery of pGM-CSF

Expression of the costimulatory molecules CD40, CD86 and CD80 was also investigated, since upregulation of these molecules would suggest enhanced accessory function of ALDC in the lymph node. Expression of surface CD40 essentially mirrored surface MHC class II expression. A slight upregulation in CD40 surface expression was observed for the first 48 hours after pGM-CSF delivery (Figure 4.30). A reduction in surface CD40 to levels observed prior to DNA vaccination was then evident 3–4 days p/v, which was followed by an increase in CD40 at days 5-6 p/v. Staining of cell surface CD86 revealed an increase in the expression of this costimulatory molecule for the first 48 hours p/v (Figure 4.31). Expression of CD86 then returned to pre-vaccination levels at days 3–4. A similar shift in fluorescence was again observed at days 5–6 and a proportion of these cells expressed CD86 at high levels (channel number 10^2–10^3). In contrast to the expression of CD40 and CD86, there was little change in

surface expression of CD80 on the majority of ALDC over the time-course (Figure 4.32); high CD80 expression was however evident in a small proportion of ALDC from days 1–2 and days 5–6 following pGM-CSF administration.

LFA-3 expression remained unchanged over the time-course of the experiment, with the exception of the 5-day time-point, where LFA-3 expression increased slightly (Figure 4.33). Levels of LFA-3 were not assessed at the 4 days p/v time-point in this experiment. ALDC have been reported to express CD2 on their cell surface (Bujdoso et al, 1989), a ligand for LFA-3 (Selvaraj et al., 1987), although it is possible that this may be due to adsorption of the CD2 molecules as a consequence of the high level of LFA-3 shown by afferent DC (Bujdoso et al, 1989), rather than due to expression of a CD2 gene. No change in CD2 expression was observed at any of the time-points investigated (Figure 4.34). Conversely, a marked increase in the expression of the integrin CD11c was observed (detected with mAb OM1) at days 1–2 p/v and a further increase in CD11c expression was observed at days 5–6 p/v (Figure 4.35).

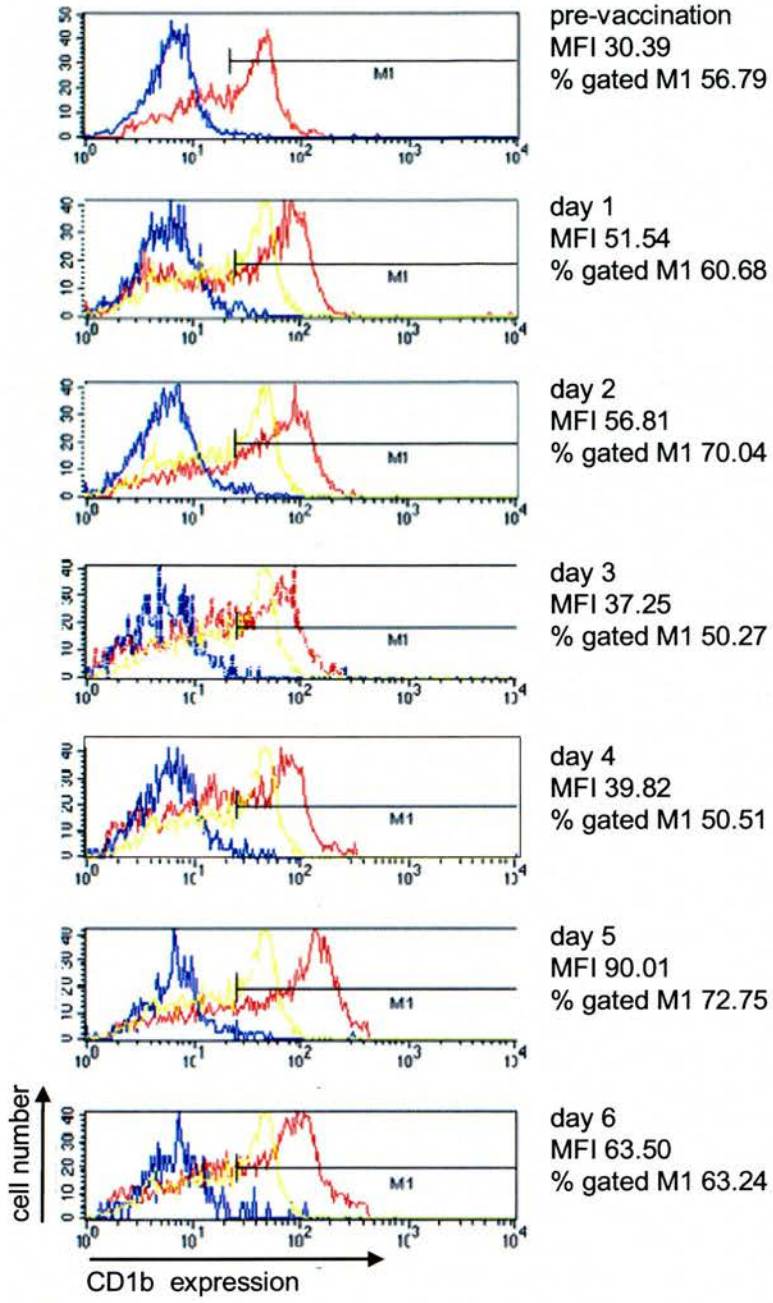

Figure 4.28 Cell-surface expression of CD1b on ALDC before and after gene-gun vaccination with pGM-CSF. Non-specific staining with NMS (negative control) is shown (blue histogram); expression of CD1b at that time-point (red histogram) and expression of CD1b prior to vaccination is represented again at each time-point after DNA vaccination with pGM-CSF (yellow histograms).

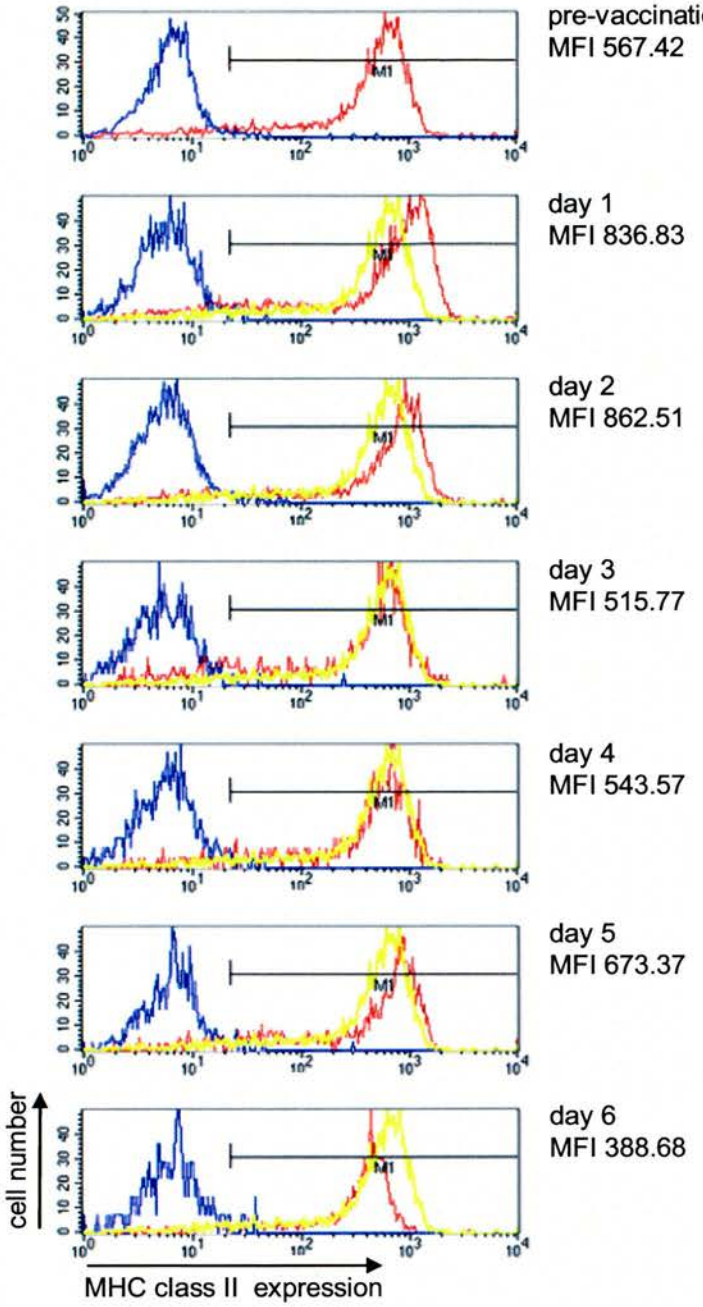

Figure 4.29 Cell-surface expression of MHC class II DRα on ALDC before and after gene-gun vaccination with pGM-CSF. Non-specific staining with NMS (negative control) is shown (blue histogram); expression of MHC class II at that time-point (red histogram) and expression of MHC class II prior to vaccination is represented again at each time-point after DNA vaccination with pGM-CSF (yellow histograms).

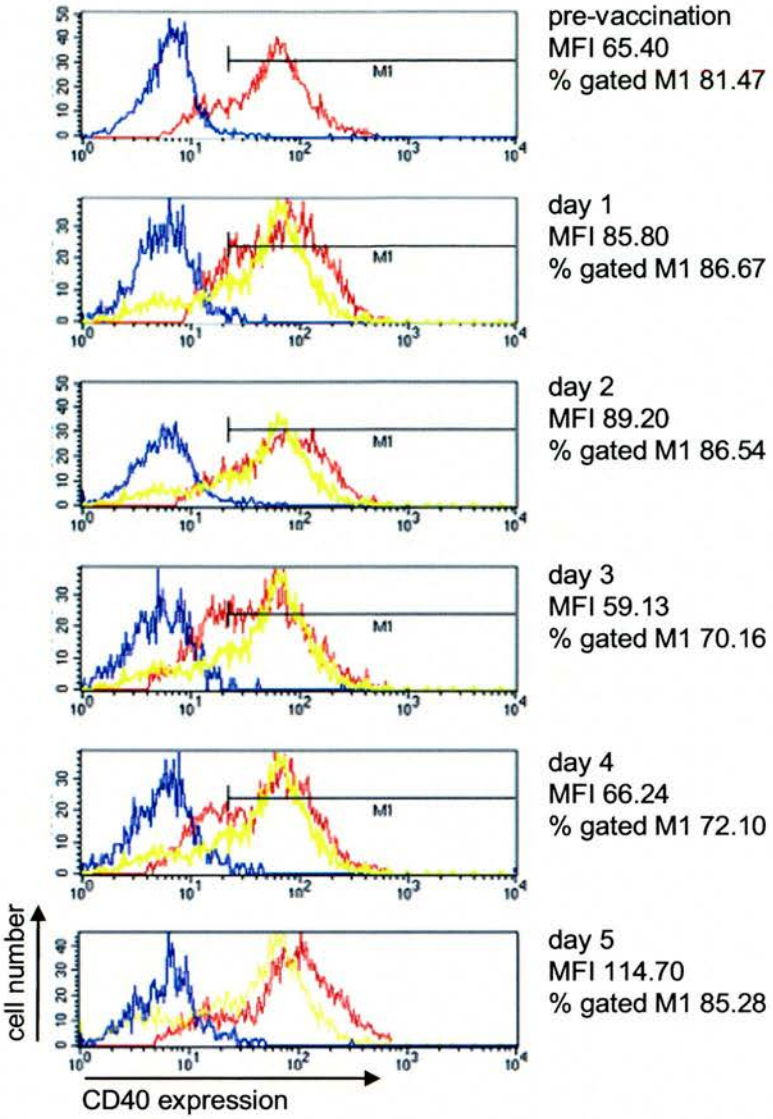

Figure 4.30 Cell-surface expression of CD40 on ALDC before and after gene-gun vaccination with pGM-CSF. Non-specific staining with NMS (negative control) is shown (blue histogram); expression of CD40 at that time-point (red histogram) and expression of CD40 prior to vaccination is represented again at each time-point after DNA vaccination with pGM-CSF (yellow histograms).

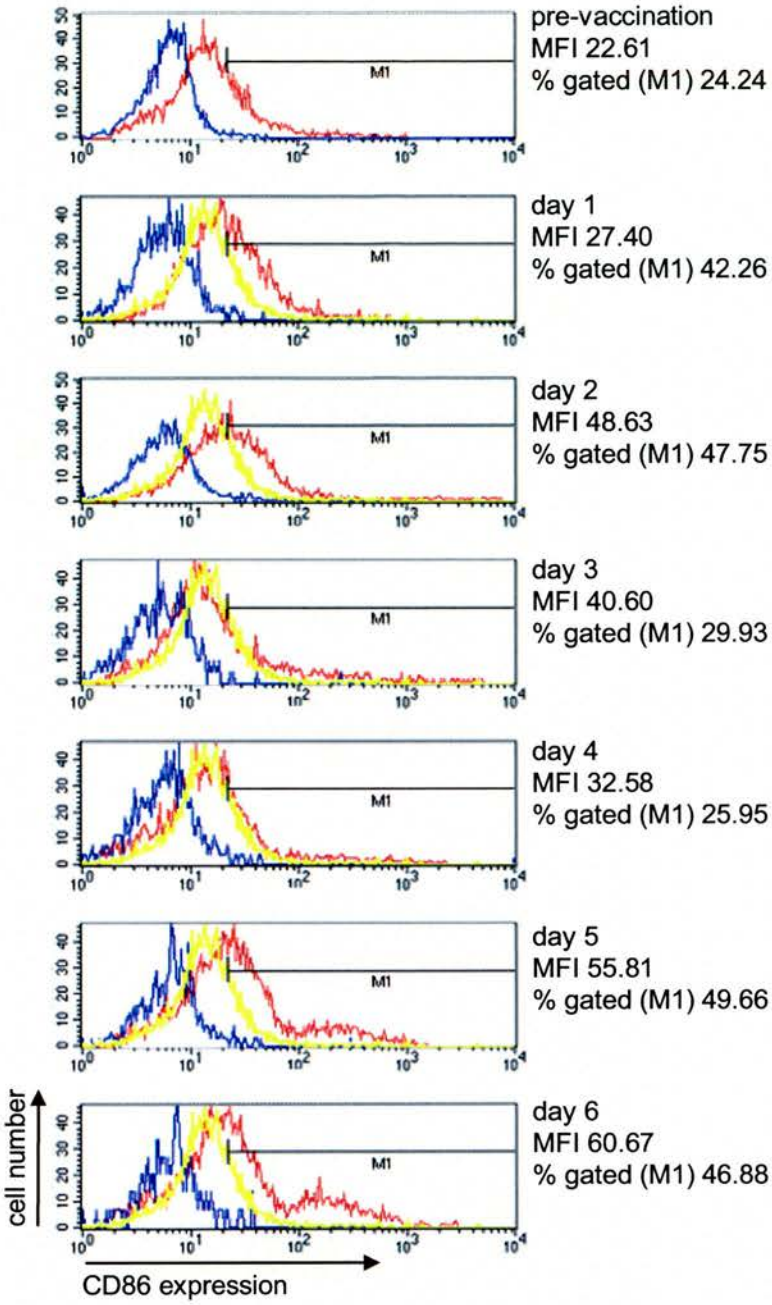

Figure 4.31 Cell-surface expression of CD86 on ALDC before and after gene-gun vaccination with pGM-CSF. Non-specific staining with NMS (negative control) is shown (blue histogram); expression of CD86 at that time-point (red histogram) and expression of CD86 prior to vaccination is represented again at each time-point after DNA vaccination with pGM-CSF (yellow histograms).

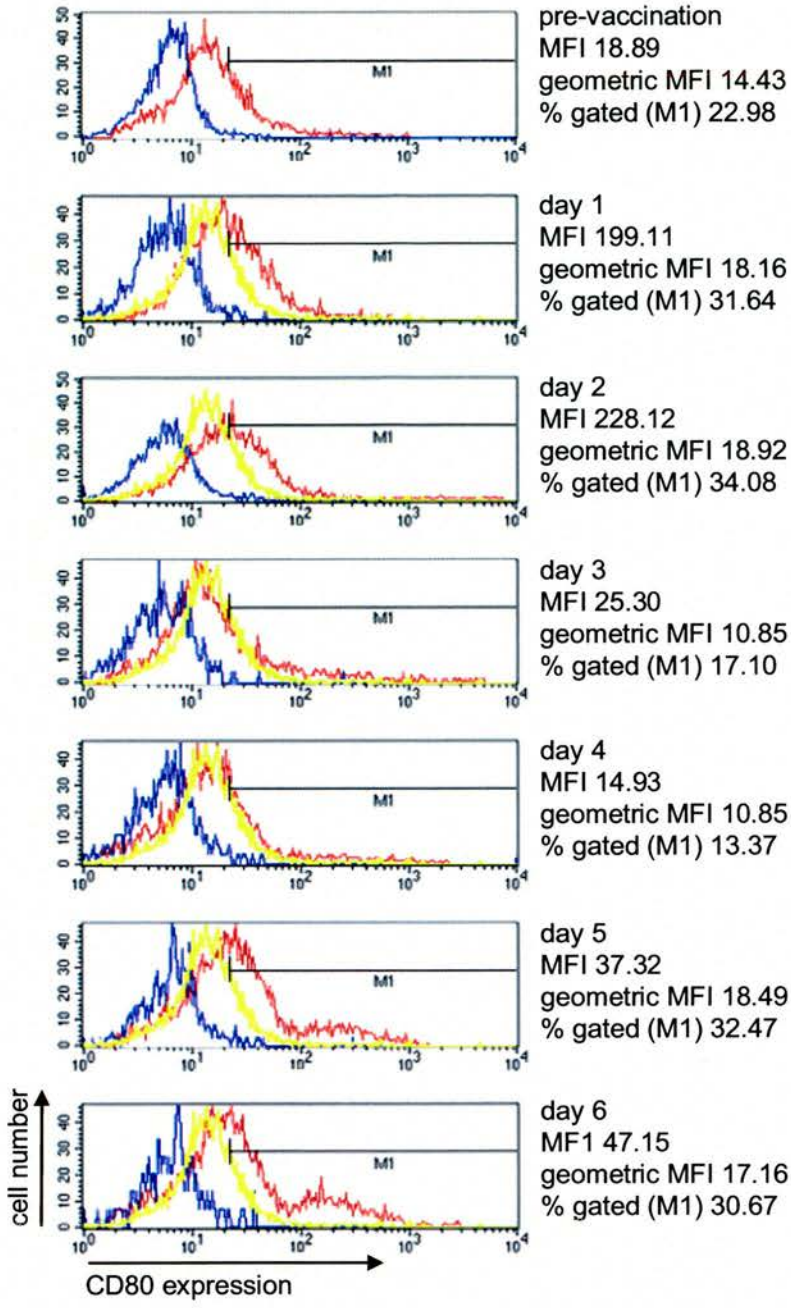

Figure 4.32 Cell-surface expression of CD80 on ALDC before and after gene-gun vaccination with pGM-CSF. Non-specific staining with NMS (negative control) is shown (blue histogram); expression of CD80 at that time-point (red histogram) and expression of CD80 prior to vaccination is represented again at each time-point after DNA vaccination with pGM-CSF (yellow histograms).

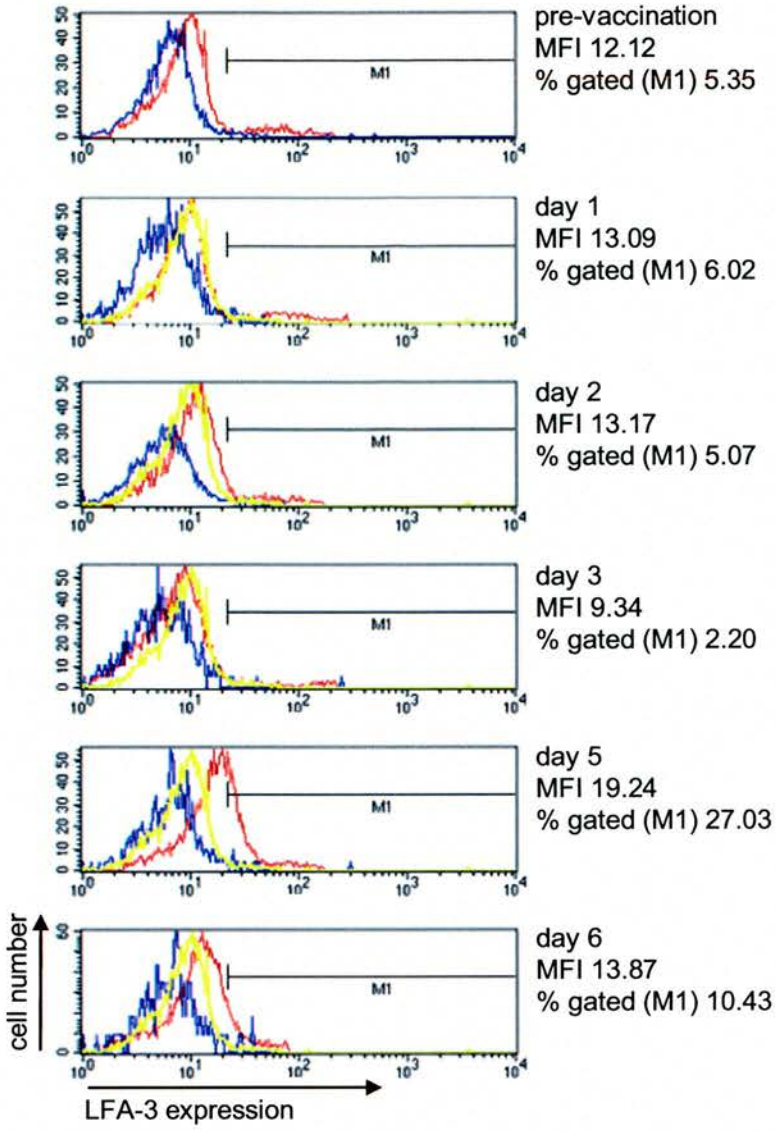

Figure 4.33 Cell-surface expression of LFA-3 on ALDC before and after gene-gun vaccination with pGM-CSF. Non-specific staining with NMS (negative control) is shown (blue histogram); expression of LFA-3 at that time-point (red histogram) and expression of LFA-3 prior to vaccination is represented again at each time-point after DNA vaccination with pGM-CSF (yellow histograms). Expression of LFA-3 was not assessed 4 days p/v.

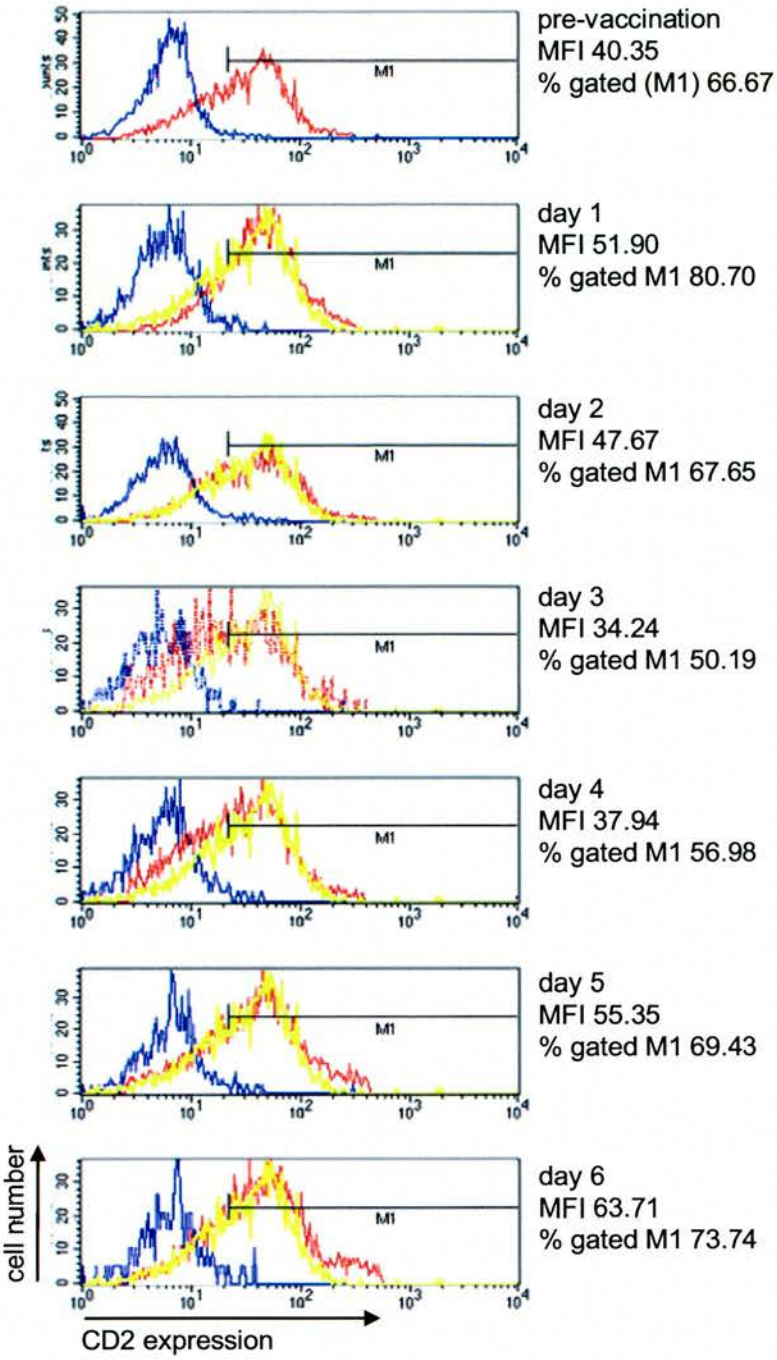

Figure 4.34 Cell-surface expression of CD2 on ALDC before and after gene-gun vaccination with pGM-CSF. Non-specific staining with NMS (negative control) is shown (blue histogram); expression of CD2 at that time-point (red histogram) and expression of CD2 prior to vaccination is represented again at each time-point after DNA vaccination with pGM-CSF (yellow histograms).

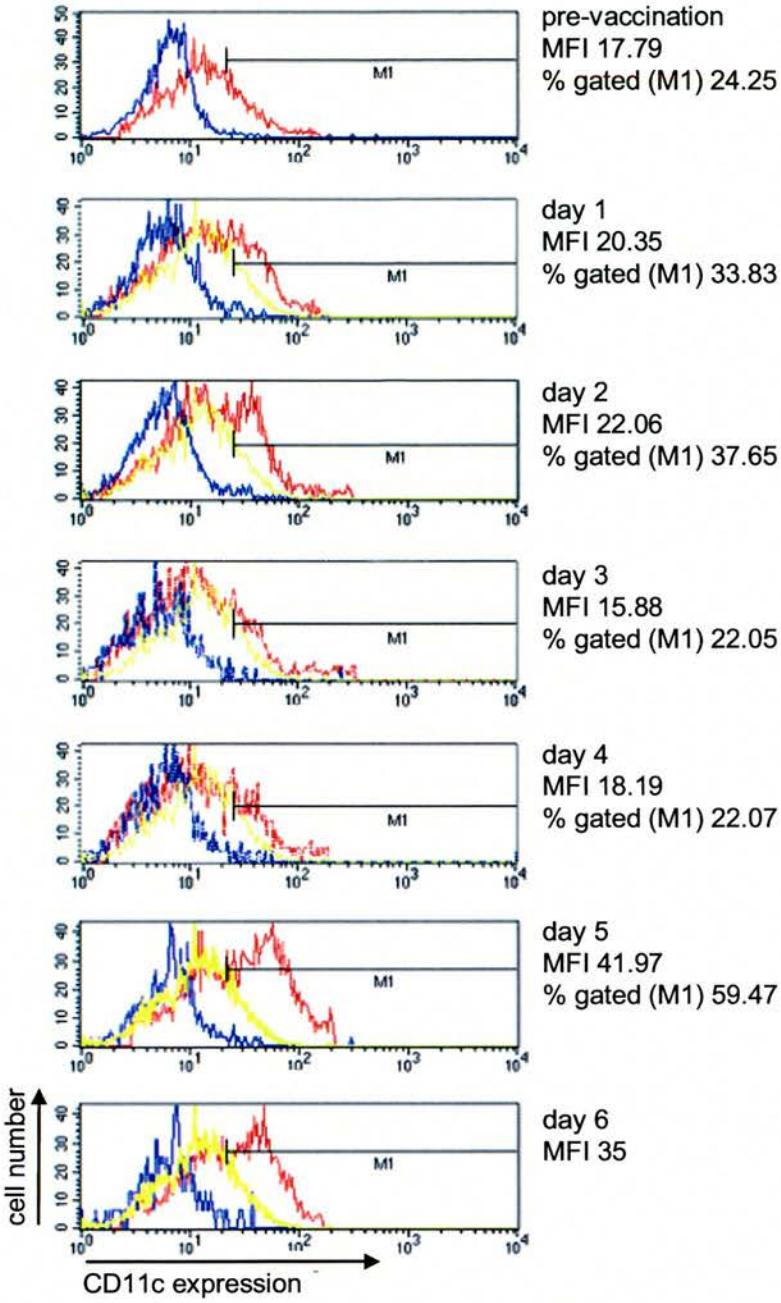

Figure 4.35 Cell-surface expression of CD11c on ALDC before and after gene-gun vaccination with pGM-CSF. Non-specific staining with NMS (negative control) is shown (blue histogram); expression of CD11c at that time-point (red histogram) and expression of CD11c prior to vaccination is represented again at each time-point after DNA vaccination with pGM-CSF (yellow histograms).

4.6.3 Cytokine expression in purified ALDC subpopulations after gene-gun delivery of pGM-CSF

Cytokine mRNA synthesis in migrating afferent DC pre- and post-pGM-CSF administration was examined by quantitative real-time RT-PCR analysis. RNA was extracted from each ALDC subpopulation purified from lymph collected at 24-hour intervals over the time-course of the experiment. ALDC were purified by FACS as described previously and RNA was concentrated under vacuum. All of the RNA was committed to the reverse transcription reaction. Prior to quantitative analysis conventional GAPDH RT-PCR was carried out to ensure that genomic DNA was fully degraded and that amplifiable material was present in each sample (Figure 4.36). The purities of each collection are listed in Table 4.7. Importantly, there was little variation in expression of transcripts in purified ALDC populations collected on two separate occasions (48 and 24 hours prior to vaccination with pGM-CSF, Section 4.4.3), therefore a suitable "baseline" was established for comparison of cytokine transcripts in each ALDC population after pGM-CSF vaccination.

Table 4.7 Purity of each cell-sorted ALDC population. Immediately after cell sorting a sample from each collection was analysed by flow cytometry. This is expressed as a % of cells which fall into the correct (previously defined) gate (either the MHC class II^{hi} $SIRP\alpha^{+}$ gate or the MHC class II^{hi} $SIRP\alpha^{-}$ gate).

Time-point	$SIRP\alpha^{-}$ purity	$SIRP\alpha^{+}$ purity
day 1	97%	100%
day 2	99%	97%
day 3	99%	99%
day 4	100%	99%
day 5	99%	99%
day 6	97%	99%

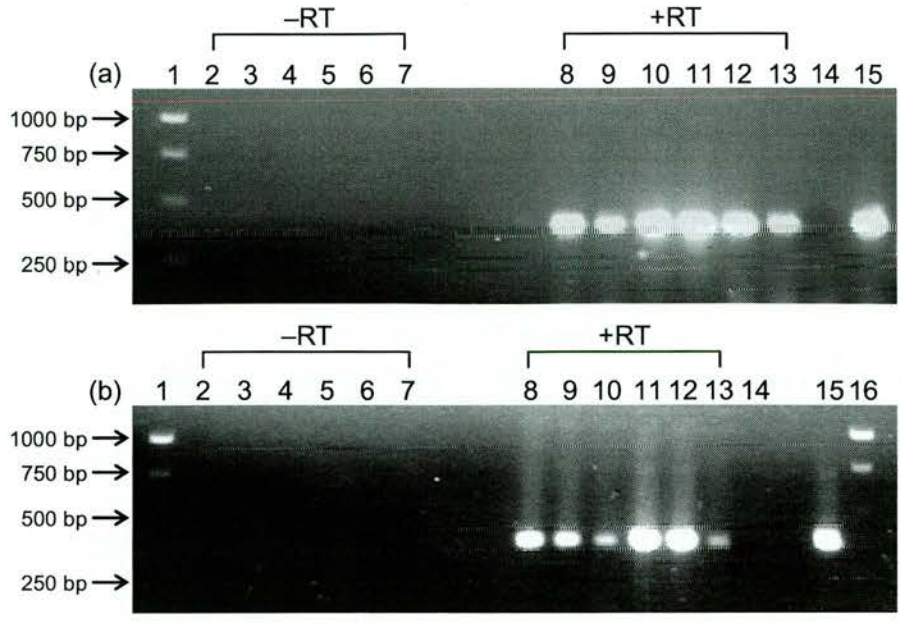

Figure 4.36 Analysis of GAPDH transcripts in purified ALDC by RT-PCR. RNA was extracted from each ALDC population after gene-gun delivery of pGM-CSF. RNA was concentrated under vacuum and reverse transcribed both with and without reverse transcriptase (-RT) to confirm that genomic DNA had been sufficiently degraded by the DNase step included in the protocol. ~350bp fragments are evident after amplification of cDNA samples obtained from SIRPα$^+$ and SIRPα$^-$ ALDC with GAPDH-specific primers (expected amplicon size is 366bp, Table 2.12) but not in samples where the RT enzyme was omitted, indicating that there are no genomic contaminants.

(a)
Lane 1 1kb ladder
Lanes 2–7 D1-D6 p/v –RT SIRPα$^+$ samples
Lanes 8–13 D1-D6 p/v +RT SIRPα$^+$ samples
Lane 14 Negative control
Lane 15 Positive control (1:1000 dilution of GAPDH 1° PCR product)

(b)
Lanes 1 & 16 1kb ladder
Lanes 2–7 D1-D6 p/v-RT SIRPα$^-$ samples
Lanes 8–13 D1-D6 p/v SIRPα$^-$ samples
Lane 14 Negative control
Lane 15 Positive control (1:1000 dilution of GAPDH 1° PCR product)

4.6.3.1 IL-12p40 mRNA expression in ALDC populations after pGM-CSF administration

IL-12p40 transcripts were quantified in each ALDC population before and after gene-gun delivery of pGM-CSF. Due to the number of cDNA samples obtained from this experiment, it was not possible to analyse each cDNA sample in triplicate, therefore quantitative RT-PCR was carried out on three separate occasions and data are presented as mean ± SEM (Figure 4.37). In this experiment, pGM-CSF caused a 1.7 fold increase (range 1.6-1.9) in IL-12p40 transcripts in SIRPα$^-$ ALDC 4 days after pGM-CSF administration ($p < 0.03$; paired Student t-test) and a similar increase in IL-12p40 transcripts was recorded at day 6 p/v ($p < 0.03$; range 1.5–2.0) In addition, an increase in IL-12p40 mRNA expression was observed in SIRPα$^+$ ALDC when compared to pre-vaccination levels. This was particularly evident at days 3 (mean 2.7 fold increase; range 2.5–2.8; $p < 0.004$) and 4 days p/v (mean 2.8 fold increase; range 2.0–3.3).

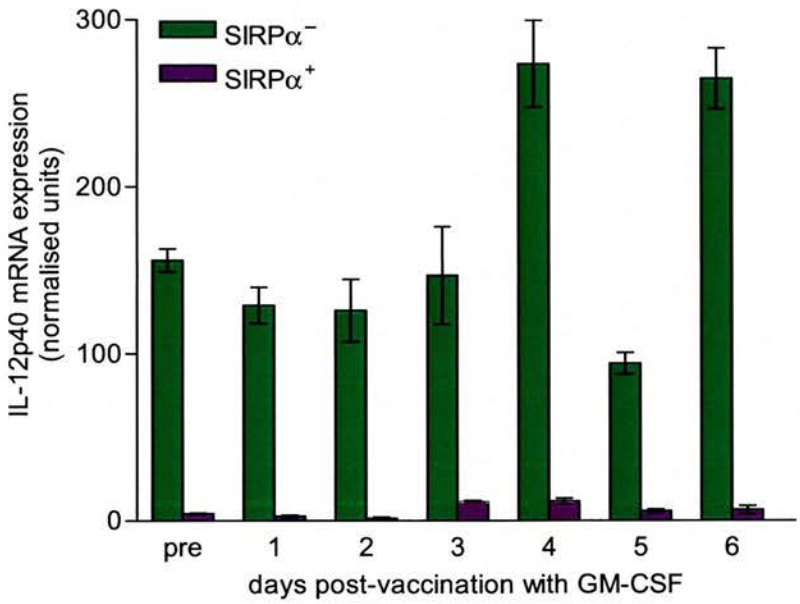

Figure 4.37 Expression of IL-12p40 mRNA in freshly sorted ALDC populations before and after gene-gun vaccination with pGM-CSF. Data are presented as mean ± SEM calculated from three independent quantitative RT-PCR experiments.

4.6.3.2 IL-10 mRNA expression in ALDC populations after pGM-CSF administration

IL-10 mRNA expression was also evaluated in both populations of ALDC by quantitative RT-PCR (Figure 4.38). Three independent experiments were carried out on the LightCycler® with each of the cDNA samples. A slight increase in IL-10 expression was observed in SIRPα$^+$ ALDC 3 days p/v (mean 2.4 fold increase; range 1.9–2.9) and 4 days p/v (mean 2.1 fold increase; range 1.5–2.4). Interestingly, IL-10 transcripts were also detected in SIRPα$^-$ ALDC 5 days after pGM-CSF administration and notably the purity of this sample was 99% (Table 4.7). Specific transcripts were also detected in one out of the three assays carried out with SIRPα$^-$ ALDC samples obtained at days 1 and 2 p/v, however, transcripts could not be quantified as the assay was not sufficiently sensitive to be able to quantify Ct values over 40 cycles of amplification (data not shown).

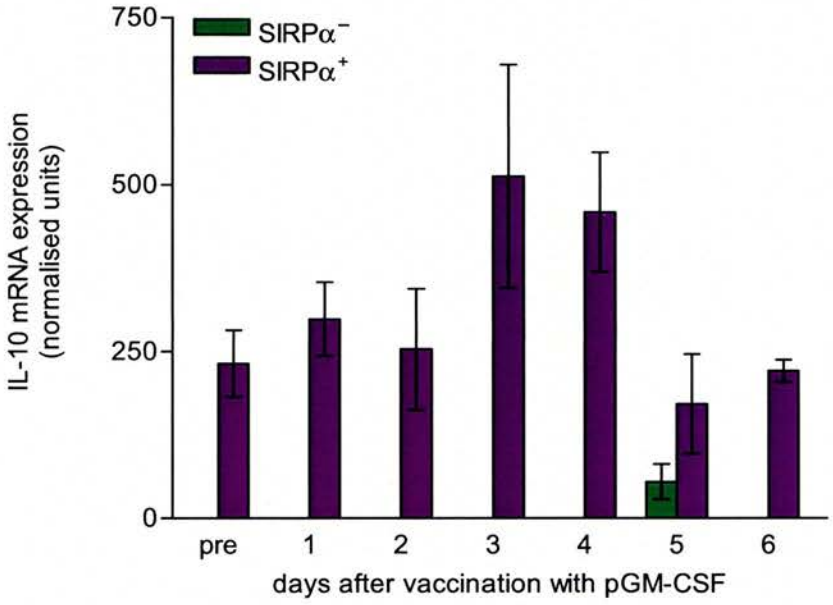

Figure 4.38 Quantification of IL-10 transcripts in freshly sorted ALDC populations before and after gene-gun vaccination with pGM-CSF. Data are presented as mean ± SEM.

4.6.3.3 IL-1β mRNA expression in ALDC populations after pGM-CSF administration

A marked increase in IL-1β mRNA expression was observed in SIRPα$^+$ ALDC after gene-gun administration of pGM-CSF, peaking at approximately 24 hours (mean fold increase of 22.7%). IL-1β expression remained elevated over the time-course of the experiment in SIRPα$^+$ ALDC and was sustained even at six days p/v, where transcripts were three times higher than those observed prior to pGM-CSF administration. Figure 4.39 is representative of two independent experiments carried out on the LightCycler®. It was not always possible to quantify levels of IL-1β expressed by SIRPα$^-$ ALDC (levels were below the level of quantification of the assay), although specific transcripts were present in all samples analysed. A 2.4 fold increase in IL-1β expression was evident in SIRPα$^-$ ALDC at days 1 and 3 after pGM-CSF administration.

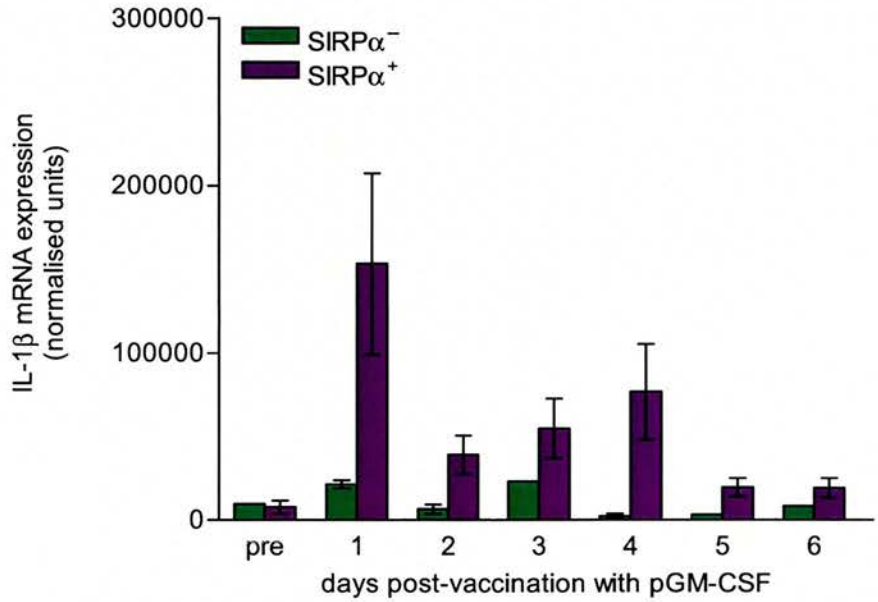

Figure 4.39 Expression of IL-1β mRNA in freshly sorted ALDC populations before and after administration of pGM-CSF. Data are representative of two separate quantitative RT-PCR experiments and are presented as mean ± SEM.

4.6.3.4 IL-18 mRNA expression in ALDC populations after pGM-CSF administration

Quantification of IL-18 transcripts in purified ALDC was also carried out. Figure 4.40a is representative of three independent quantitative RT-PCR experiments (data are presented as mean ± SEM). From these experiments it is apparent that IL-18 mRNA expression was elevated in both SIRPα$^+$ and SIRPα$^-$ ALDC populations 6 days after gene-gun delivery of pGM-CSF. However, this difference is not statistically significant and there is some variability in the values obtained from the quantitative RT-PCR assays. To compensate for such variability between experiments, data obtained from one experiment are presented, where each ALDC cDNA sample has been analysed in duplicate (Figure 4.40b). It was not possible to perform this assay with triplicates of each cDNA sample as only 32 reactions can be carried out at any one time on the LightCycler®. The trend is similar to that obtained from the three independent experiments (Figure 4.40a). Notably, IL-18 mRNA expression was increased approximately two-fold in SIRPα$^+$ ALDC (when compared to pre-vaccination levels) isolated at days 3, 4 and 6 p/v. A two-fold increase in IL-18 mRNA expression was also observed in the SIRPα$^-$ ALDC population at all time-points investigated with the exception of the day 3 time-point.

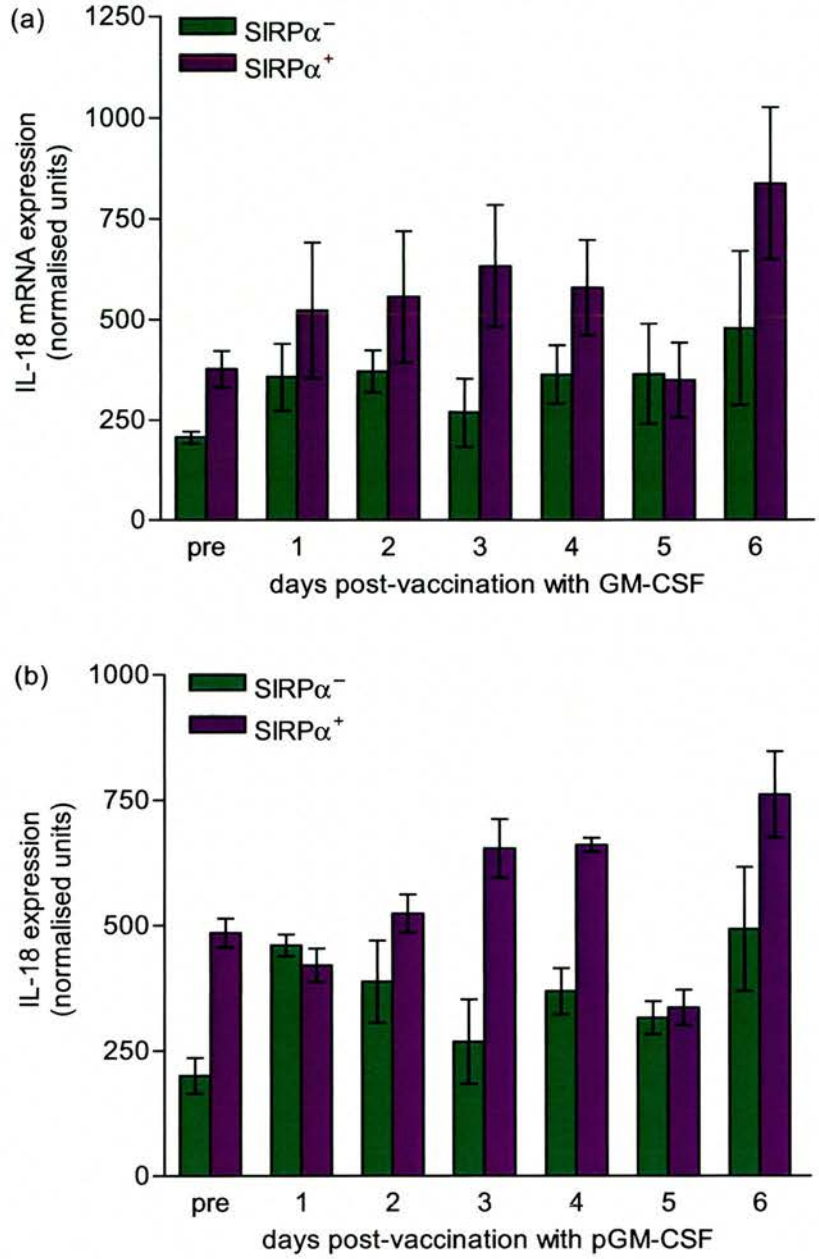

Figure 4.40 Expression of IL-18 mRNA in freshly sorted ALDC populations before and after gene-gun delivery of pGM-CSF. (a) Representative of three independent experimental runs on the LightCycler®. Data are presented as mean ± SEM. There are no significant differences between pre- and post-vaccination levels of IL-18 mRNA in either subpopulation. (b) Expression of IL-18 mRNA before and after vaccination with pGM-CSF. Each cDNA sample was analysed in duplicate on the LightCycler® and data are presented as mean ± SEM.

4.6.3.5 TNF-α mRNA expression in ALDC populations after pGM-CSF administration

TNF-α mRNA expression was analysed in each ALDC subpopulation before and after administration of pGM-CSF and data are displayed in Figure 4.41a,b. Figure 4.41a represents data from three independent LightCycler® experiments (data are presented as mean ± SEM). From these experiments, it is evident that pGM-CSF resulted in increased TNF-α mRNA expression in SIRPα$^-$ ALDC 24 hours p/v ($p < 0.03$). Levels of TNF-α were elevated in both ALDC populations 4 days after administration of pGM-CSF and this increase is statistically significant ($p < 0.04$ (SIRPα$^+$ ALDC); $p < 0.02$ (SIRPα$^-$ ALDC). Due to the variability between quantitative RT-PCR assays, expression of TNF-α mRNA was also assessed by analysing each cDNA sample in duplicate in the same quantitative RT-PCR assay (Figure 4.41b), and importantly the overall pattern of TNF-α mRNA expression was comparable to the results obtained from the three independent experiments carried out.

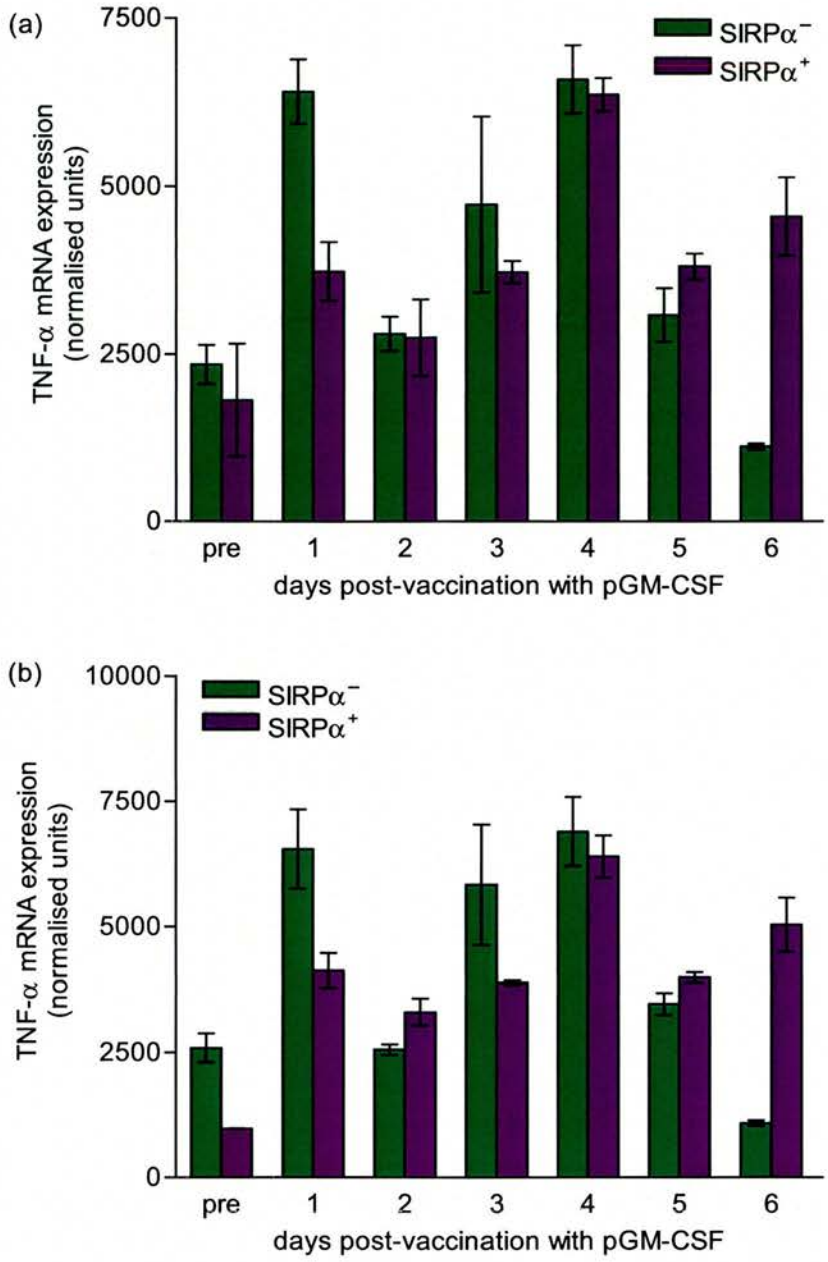

Figure 4.41 TNF-α mRNA expression in freshly sorted ALDC populations before and after gene-gun vaccination with pGM-CSF. (a) Data obtained from three independent experiments using the LightCycler®. There is a statistically significant difference between TNF-α expression between pre-vaccination samples and samples collected 4 days p/v ($SIRP\alpha^+$ samples, $p < 0.04$; $SIRP\alpha^-$ samples, $p < 0.02$; paired Student t-test). There is also a statistically significant difference 24 hours p/v in the $SIRP\alpha^-$ population ($p < 0.03$); (b) Expression of TNF-α mRNA before and after gene-gun vaccination with pGM-CSF and where each sample was analysed in duplicate. Data are presented as mean ± SEM.

4.6.4 DNA vaccination of cannulated sheep Experiment 2

It was imperative that pGM-CSF was administered to other cannulated sheep to confirm the findings from experiment 1. It was also imperative that vaccination with NF-control plasmid was carried out in order to assess if the changes in (i) surface marker expression on MHC class II^+ ALDC and (ii) cytokine expression by the $SIRP\alpha^+$ and $SIRP\alpha^-$ populations are indeed due to the biological effects of GM-CSF and not due to immunostimulatory CpG motifs and/or the physical trauma of the vaccination procedure. CpG motifs can cause LC migration and activation of DC (Ban et al, 2000). The trauma of the DNA vaccination procedure itself induces some changes in the cytokine milieu of the skin, for instance, an upregulation of TNF-α and IL-1β mRNA was documented in control-vaccinated skin sites (discussed in chapter 3), even though there appeared to be only low-grade pathology at these sites. Upregulation of proinflammatory cytokines may affect the biology of resident skin DC. Attempts to repeat the gene-gun experiment with pGM-CSF with cannulated sheep proved difficult (Table 4.8); the lymph stopped flowing three times in the first 16-hours after gene-gun vaccination with pGM-CSF.

Table 4.8 DNA vaccination experiments carried out on cannulated sheep.

sheep ID	plasmid	outcome	experimental information
	pGM-CSF	–	lymph became infected
JH2	pGM-CSF	+	lymph flowed for 1 week
	pGM-CSF	–	lymph stopped after DNA vaccination
	pGM-CSF	–	lymph stopped after DNA vaccination
	pGM-CSF	–	lymph stopped after DNA vaccination
JH6	NF-control	+/–	lymph flowed for 5 days (bloody lymph)
JH6	pGM-CSF	+/–	lymph flowed for 4 days (bloody lymph)

Sheep JH6 was vaccinated with the NF-control construct and lymph was collected at 24-hour intervals over 5 days and SIRPα$^+$ and SIRPα$^-$ ALDC were purified by FACS. On the fifth day, the animal was vaccinated with the pGM-CSF. The lymph was collected from this sheep for the following four days. At all time-points investigated, the lymph contained many erythrocytes and lymph volumes were low (<35ml) and stopped flowing several times over the time-course. Due to the fact that previous experiments had been unsuccessful and due to time constraints, heparin was administered to the animal several times to maintain the flow of lymph.

4.6.4.1 Expression of surface markers on ALDC after gene-gun vaccination

Expression of surface markers (CD40, MHC class II, CD1b, CD80, CD86 and LFA-3) was analysed after gene-gun vaccination with both pGM-CSF and the NF-control. Some of the data are displayed in Figure 4.42 and Figure 4.43.

In contrast to experiment 1, where a marked increase in several surface markers (MHC class II, CD1b, CD40, CD86 and CD11c) was observed on ALDC 24 hours after vaccination with pGM-CSF, there was no change in surface expression in this experiment. Figure 4.42 shows ALDC surface expression of CD1b, CD11c and MHC class II before and 24 hours after administration of pGM-CSF. Although no change in the level of expression of MHC class II was apparent, the number of cells expressing MHC class II at lower levels (10^1–10^2 $\log_{10}$ fluorescence) increased p/v (this was not observed previously) and may correspond to an increase in the number of activated lymphocytes (blasts) in the R1 (DC) gate.

Expression of surface markers remained unchanged throughout the time-course. No increase in expression of CD40, CD11c or MHC class II (Figure 4.43) or CD1b (data not shown) was evident 4–5 days after vaccination with pGM-CSF (or NF-control), which again contrasts markedly with experiment 1. Cytokine expression by ALDC populations was also evaluated by quantitative RT-PCR (data not shown). mRNA expression of proinflammatory TNF-α and IL-1β was highly elevated in ALDC samples after administration of either plasmid (data not shown), whereas IL-10 transcripts were rare or absent.

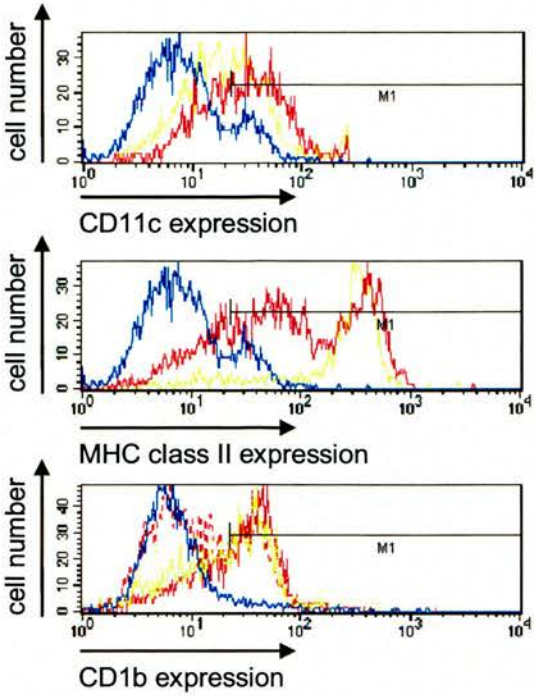

Figure 4.42 Representative data from vaccine experiment 2, 24 hours after vaccination with pGM-CSF. Blue histogram: negative control (NMS); yellow: pre-vaccination levels; red: pGM-CSF vaccinated.

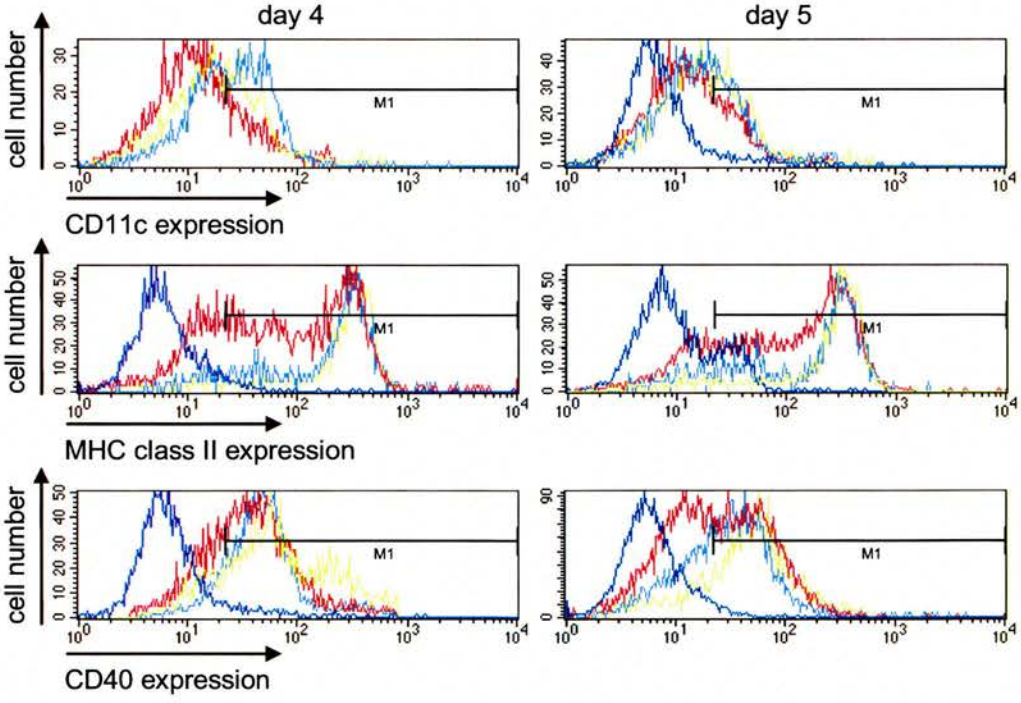

Figure 4.43 Representative data from vaccine experiment 2, 96 hours after gene-gun vaccination with pGM-CSF and the NF-control. Blue histogram: negative control (NMS); yellow histogram: pre-vaccination levels; red histogram: pGM-CSF vaccinated; light blue histogram: NF-control vaccinated.

4.7 Discussion (part 2)

To assess the *in vivo* effects of pGM-CSF on ALDC, a pseudo-afferent lymph cannulation model was employed, enabling access to pure unmanipulated DC after gene-gun vaccination. In this study the immunophenotype of MHC class II^+ ALDC was investigated. In addition, cytokine expression was quantified in purified $SIRP\alpha^+$ and $SIRP\alpha^-$ ALDC and compared to levels prior to vaccination. Maintaining the lymph flow after gene-gun vaccination of cannulated sheep proved difficult for reasons that remain to be elucidated, although it seems likely that since GM-CSF induces acute inflammation and oedema (fibrinous exudate), one might expect the lymph to clot. The first experiment where pGM-CSF was administered to a cannulated sheep revealed some interesting findings. Nonetheless, these data must be interpreted with considerable caution since this experiment was not successfully repeated, nor was the experiment involving gene-gun administration of the NF-control carried out successfully. Further experiments must be conducted to further define the activities of pGM-CSF (and the effects of CpG motifs/vaccination trauma) on ALDC populations *in vivo*. However, data obtained from this preliminary experiment are consistent with some previously reported activities of recombinant GM-CSF and may therefore shed some light on the *in vivo* activities of this cytokine and help to design future experiments.

4.7.1 Expression of surface molecules on ALDC after gene-gun delivery of pGM-CSF

Several of the cell surface markers investigated in this preliminary study were upregulated after gene-gun delivery of pGM-CSF. An increase in surface expression of CD1b and CD11c was particularly evident at all time-points investigated with the most pronounced increase observed 5 days p/v. An increase in surface expression of MHC class II by ALDC was also apparent 24–48 hours after DNA vaccination. In addition, an increase in CD40 and CD86 was observed at days 1–2 and also at days 5–6 after administration of pGM-CSF, whereas surface expression of LFA-3 was increased six days p/v. An upregulation of these molecules would suggest that DC draining the skin after pGM-CSF administration are of a mature phenotype and have enhanced accessory function in the lymph node.

GM-CSF is well documented to cause an increase in cell surface markers; for instance *in vitro* exposure of isolated LC to GM-CSF results in upregulation of CD80, CD86 and CD40 (Salgado et al., 1999) and exposure of human monocytes and alveolar macrophages to recombinant GM-CSF has been demonstrated to increase surface expression of CD11c (Rivier et al., 1994). There is also evidence from *in vivo* studies that GM-CSF increases the

expression of a number of surface markers, which may explain the enhanced function of DC after exposure to GM-CSF. Indeed preferentially expanded DC1 cells identified after *in vivo* GM-CSF/IL-4 therapy were reported to express higher levels of HLA-DR, CD11c and CD80 than pre-treatment DC (Kiertscher et al, 2003). Interestingly, an increase in CD1d was reported on GM-CSF expanded DC in a study by Daro and colleagues (Daro et al, 2000) and the authors concluded that this would enhance antigen presentation. Furthermore, an increase in both CD1d and CD80 on expanded $CD11c^{+}$ $CD8\alpha^{-}$ has also been reported by Mach and colleagues after injection of murine tumour cells engineered to secrete GM-CSF (Mach et al., 2000). With the exception of some $CD80^{hi}$ expressing ALDC 24 hours after pGM-CSF administration, levels of CD80 expressed by ALDC remained unchanged throughout the time-course in this study. Conversely, an increase in CD86 expression was observed and this is of particular interest since CD86-CD28 interaction plays a critical role during the activation of naïve T cells. In addition, an upregulation of LFA-3 on ALDC would suggest that interaction with T cells may be enhanced.

Upregulation of CD1b and MHC class II is suggestive of an enhanced antigen-presenting activity of ALDC, providing a mechanism by which pGM-CSF could boost immune responses. An increase in costimulatory marker expression would be anticipated to further enhance the immune response. Upregulation of CD11c was also observed in this experiment. Importantly, CD11c is an integrin on DC, macrophages and neutrophils and is a member of a family of surface glycoproteins that is essential for adhesion-dependent functions. CD11c binds to cell-adhesion molecules and extracellular matrix (fibrinogen). It is possible that the observed increase in the level of surface expression of CD11c may aid trafficking of DC to the lymph node.

The STAT6 signalling pathway is constitutively activated in immature DC (iDC), whereas STAT1 signalling is most robust in mature DC and optimal activation of STAT1 during DC maturation requires both IL-4 and GM-CSF (Jackson et al., 2004). Analyses of $STAT1^{-/-}$ DC reveal a role for STAT1 in repressing CD86 expression in pre-DC and up-regulating CD40 and CD11c expression in mature DC. It would be of interest to this study to evaluate the effects of pGM-CSF on STAT6 and STAT1 signalling pathways.

4.7.2 Cytokine mRNA expression in purified SIRPα$^+$ and SIRPα$^-$ ALDC populations after pGM-CSF delivery

A modest increase in IL-10 and IL-12p40 mRNA expression was observed in SIRPα$^+$ and SIRPα$^-$ ALDC respectively, approximately 4 days after pGM-CSF administration. A further increase in IL-12p40 was observed 6 days p/v. It was particularly interesting that IL-10 transcripts were detected at low levels in highly purified (>98%) SIRPα$^-$ ALDC 5 days after gene-gun vaccination with pGM-CSF. Analysis of SIRPα$^-$ ALDC in the steady-state flux showed that IL-10 was not expressed by this subset. Perhaps IL-10 is upregulated in SIRPα$^-$ ALDC to dampen down proinflammatory cytokine production. It is also possible that this induction of IL-10 in SIRPα$^-$ ALDC is responsible for the marked decrease in IL-12p40 in this DC subset 5 days after pGM-CSF vaccination, since IL-10 downregulates IL-12 expression (Murphy et al., 1994). The observed increase in IL-12p40, IL-10 and TNF-α transcripts in ALDC 4 days p/v with pGM-CSF may correspond to activated DC recruited into the skin approximately 4 days after pGM-CSF administration. This is interesting since no upregulation of surface MHC class II, CD40, CD80 or CD86 was observed 4 days p/v, yet increased expression of these surface molecules was observed 5–6 days p/v. For future studies, it would be of interest to remove biopsies and confirm the infiltration of DC into the skin by immunostaining in order to correlate the findings obtained with ALDC with the kinetics of DC infiltration into the skin.

It is particularly interesting to note that mRNA expression of IL-1β was highly elevated in SIRPα$^+$ ALDC isolated 24 hours after pGM-CSF administration. From the earlier part of this study (sections 4.3.6 and 4.4.1) and studies conducted by others (Adams et al, 1998; Howard and Hope, 2000; Yirrell et al, 1991), it seems likely that SIRPα$^+$ ALDC contain a subset of migratory LC and that this highly elevated expression of IL-1β is due to activated LC migrating to the lymph node as a consequence of inflammation in the skin (discussed in chapter 3). Indeed, LC are the major source of IL-1β in murine skin (Heufler et al, 1992; Schreiber et al, 1992). Although levels of IL-1β mRNA remained slightly elevated in both ALDC subpopulations over the first four days p/v, transcripts were considerably lower in SIRPα$^-$ ALDC than in SIRPα$^+$ ALDC at the 24 hour time-point. In addition, whilst an increase in IL-1β transcripts was observed in SIRPα$^-$ ALDC, a pronounced difference between the two populations was still evident as observed prior to administration of pGM-CSF. TNF-α and IL-18 transcripts were also elevated in both ALDC populations at all time-points investigated when compared to pre-vaccination levels. It is interesting to observe that pGM-CSF administration does not appear to skew the cytokines produced by either DC subset (with the possible exception of low-level IL-10 expression in SIRPα$^-$ ALDC 5 days

p/v), but perhaps by activating these cells (by acting as a "danger signal"), expression of these constitutively produced cytokines is enhanced.

In agreement with these findings, administration of recombinant GM-CSF in mice resulted in increased production of IL-10 in murine myeloid DC, whereas IL-12p40 expression was increased in the lymphoid DC subset (Parajuli et al, 2001). The increase in cytokine production was however more pronounced in Parajuli's study; however, this could be due to the route of administration, differences in the biological activities of GM-CSF or even the concentration of GM-CSF. In the latter study, high concentrations of recombinant GM-CSF were administered systemically to mice (6μg/kg/day of GM-CSF). In this study, DNA coated on bullets was quantified in each batch and ranged from 0.25–1.0μg of pGM-CSF per shot. No assessment of the concentration of GM-CSF after gene-gun vaccination of ovine fibroblasts was made in this study and so it is difficult to compare the findings. Turner and colleagues reported that normal human skin fibroblasts transfected by the gene-gun produce high levels of human recombinant GM-CSF (250ng/10^6 cells/24 hours) (Turner et al., 1998), suggesting that gene-gun vaccination is an efficient method to deliver cytokine genes. GM-CSF has been shown to inhibit IL-12 production of murine LC (Tada et al, 2000), but no inhibition of IL-12p40 was evident in this nor in Pulendran's study.

Kiertscher and colleagues demonstrated a preferential expansion of myeloid HLA-DR^+/$CD11c^+$ DC1 cells (IL-12 producing) after GM-CSF administration in humans (Kiertscher et al, 2003) and argue that expansion of the DC1 subset may augment cell mediated immune responses, where Th1 polarisation is required. In this study, whilst an increase in both $SIRP\alpha^+$ and $SIRP\alpha^-$ ALDC was evident 4 days after vaccination with pGM-CSF, (which is of interest since DC were previously identified in the skin at this time-point (chapter 3)), $SIRP\alpha^+$ ALDC were still the predominant population. It would therefore be of interest to determine the overall bias of the immune response and compare findings with observations in humans and in mice.

4.7.3 Gene-gun vaccination with the NF-(GM-CSF)-control

It is necessary to determine to what extent the vaccination procedure itself and CpG motifs contained in the plasmid are responsible for upregulation of surface markers on DC draining from the skin. It was concluded from earlier work conducted (chapter 3), that pGM-CSF is expressed in the skin within 2 hours after gene-gun administration (mRNA levels peaking at 4 hours p/v). It is interesting that surface expression of CD1b, MHC class II and CD11c was increased (in comparison to pre-vaccination levels) on ALDC collected 24 hours p/v,

suggesting that GM-CSF (and/or CpG motifs) causes maturation and migration of skin resident cells such as LC and dermal DC. CpG sequences are present in plasmids and might contribute to the immune response generated by DNA vaccination. Ban and co-workers demonstrated that intradermal injection of 10μg of CpG-containing oligonucleotides into murine skin induced the local depletion of LC within 2 hours of exposure. In addition, *in vitro* unmethylated CpG motifs were found to directly activate splenocytes, monocytes, macrophages and DC to secrete a variety of cytokines such as IFN, IL-1β, TNF-α, IL-18 and IL-12 and activate B cells for IL-5 secretion and proliferation (Ban et al, 2000). Therefore it was essential that gene-gun administration of the NF-control plasmid was carried out.

The only other animal, which remained patent after DNA vaccination was sheep JH6. However, lymph volumes were low and the lymph contained both erythrocytes and PMN. Due to time constraints, the NF-control was administered to this animal and lymph was collected over 5 days. Gene-gun administration of pGM-CSF was then carried out on the fifth day. No changes in cell surface markers were observed in ALDC obtained from the control experiment or in the repeat of the pGM-CSF experiment. The data for this set of experiments must be interpreted with caution. Lymph that contains blood is not normally used for experiments, as this implies that surgical trauma has occurred, resulting in conditions which would not reflect the physiological conditions and indeed such conditions may cause activation of DC. Indeed, for all other experiments, lymph was analysed for PMN and erythrocytes prior to usage. Heparin was used several times throughout the course of the experiment and heparin itself is known to cause changes in DC. For instance, heparin induces differentiation of $CD1a^+$ DC from monocytes and heparin-treated DC respond to LPS or LPS plus IFN-γ with higher IL-10 and less IL-12 production than heparin-untreated DC (Xia and Kao, 2002). In addition, LC migration is modulated by N-sulphated glucosamine moieties in heparin (O'Sullivan et al., 2000).

Further studies are therefore required to compare the adjuvant effects of pGM-CSF with the effects of vector backbone DNA. These preliminary findings do, however, reveal the ability of pGM-CSF to enhance the function of DC *in vivo* and further studies using the cannulation model should now be conducted.

5 Final Discussion

One method to enhance the immunogenicity of DNA vaccines is to employ cytokines as molecular adjuvants. Studies have shown that GM-CSF and IL-3 are implicated in DC development/ontogeny and both cytokines have been documented to cause expansion of DC with enhanced accessory function (Section 1.3.3.3). pGM-CSF has been extensively investigated as a molecular adjuvant and shown to augment both CTL and antibody responses in a number of animal models, whereas pIL-3 has received little attention. The mechanisms by which pGM-CSF exerts its effects *in vivo* have not been fully characterised, although recruitment and activation of DC have been demonstrated and are believed to be responsible. Recent studies have demonstrated the remarkable flexibility of DC and that inflammatory signals in the periphery (danger signals) may have important consequences in terms of DC phenotype and function. GM-CSF is not only a growth factor of DC but is thought to exert its adjuvant activity by causing inflammation, thus acting as a danger signal. Understanding the inflammatory events in the skin after gene-gun administration of pGM-CSF and pIL-3 may further our understanding of the adjuvant effects of these cytokines.

The initial experiments described in this thesis were designed to extend our knowledge of the inflammatory response in the skin after administration of pGM-CSF and pIL-3 (chapter 3). These experiments were aimed at determining when cells of the immune system were recruited in relation to expression of plasmid DNA and proinflammatory cytokines (TNF-α, IL-1β and IL-18), which are implicated in DC migration and maturation. Subsequent studies involved further characterisation of DC draining from the skin using the pseudo-afferent lymph model, in order to compare the phenotype of steady-state DC with those after administration of a cytokine gene (chapter 4). This final chapter will attempt to bring together the main findings of this thesis.

Both pGM-CSF and pIL-3 caused a severe inflammatory reaction in ovine skin, characterised by the formation of large pustules by 24 hours, composed predominantly of neutrophils. Whilst some infiltration of neutrophils was also apparent in NF-control vaccinated skin, the inflammatory reaction was substantially less severe than those associated with either pGM-CSF or pIL-3. Peak expression of GM-CSF and IL-3 transcripts was observed approximately 4 hours after gene-gun vaccination which correlated with the kinetics of neutrophil infiltration; pronounced trafficking of neutrophils was evident as early as 2–4 hours p/v. Interestingly, IL-1β expression mirrored the pattern of IL-3 expression, peaking at approximately 4 hours, yet remaining elevated up to 4 days p/v. TNF-α transcripts were elevated in pIL-3 vaccinated skin from 24–96 hours. Infiltration of B cells was evident

by 24 hours whereas eosinophils continued to traffic into the skin for up to 48 hours after vaccination with pIL-3, consistent with known *in vivo* effects of this cytokine. B cell infiltration was also evident in pGM-CSF vaccinated skin sections at later time-points (> 3–6 days).

Perhaps the most striking observation with regard to cytokine expression in the early study was the highly pronounced increase in IL-1β transcripts after pGM-CSF administration, where levels increased in a linear fashion over the first 24 hours and remained highly elevated up to 4 days (200–300 fold higher than in normal skin). TNF-α mRNA expression was also highly elevated from 1–4 days p/v. This is consistent with the hypothesis that GM-CSF causes maturation and migration of DC by inducing the release of proinflammatory cytokines (danger signals) from other cells. Interestingly, MHC class II^+ DC entered the skin at later time points; on average 4 days after gene-gun vaccination with pGM-CSF and 3–4 days after pIL-3 (where GFP had been removed from constructs), indicating that the inflammatory milieu in the skin at these time-points is chemotactic for DC. Since TNF-α and IL-1β transcripts were still elevated when DC entered the skin, it seems logical to assume that infiltrating DC would be highly activated, responding as if an infection was taking place within the skin, resulting in an increase in costimulatory molecules and antigen presentation molecules.

From these studies it appears that both GM-CSF and IL-3 are first chemotactic for PMN (predominantly neutrophils) and that GM-CSF (and to a lesser extent IL-3) induces IL-1β mRNA expression in PMN, thereby amplifying the acute inflammatory response. It is a plausible theory that defensins and other peptides pre-stored in PMN granules attract DC, in agreement with the hypothesis that the release of PMN granular peptides may link innate and adaptive immunity (Yamashiro et al, 2001). Such "priming" of PMN by GM-CSF/IL-3 may then induce the delayed expression of MCP-1, a signal for mononuclear cells (Rand et al, 1996). An analysis of the expression of IL-8 (an inflammatory cytokine produced by neutrophils) in combination with the chemokines MCP-1 and CCR6, both of which are highly chemotactic for DC, may well reveal more about the mechanisms by which GM-CSF exerts its adjuvant effects.

An investigation into steady-state ALDC was next conducted. It seems likely that $SIRP\alpha^-$ ALDC are comparable to the $CD8\alpha^+$ ("lymphoid") subset described in mice. Indeed $CD8\alpha^+$ DC express high levels of IL-12p40 (Maldonado-Lopez et al, 1999; Pulendran et al, 1999), as described in bovine $SIRP\alpha^-$ ALDC (Howard et al, 2002; Stephens et al, 2003), rat splenic $SIRP\alpha^-$ ALDC (Voisine et al, 2002) and now in ovine $SIRP\alpha^-$ ALDC. Interestingly, murine $CD8\alpha^+$ DC have a unique ability to take up apoptotic cells and to cross present cytosolic

antigens to $CD8^+$ T cells (den Haan et al., 2000). $CD8\alpha^+$ DC have also been demonstrated to be particularly efficient at inducing antigen-specific tolerance *in vivo* (Liu et al., 2002). Similarly, apoptotic bodies have been observed in rat (Huang et al, 2000) and more recently in ovine $SIRP\alpha^-$ ALDC (Epardaud et al., 2004) and a role in the maintenance of tolerance has been proposed. Another feature shared by $SIRP\alpha^-$ ALDC and murine $CD8\alpha^+$ DC is the large size and homogeneity of these cells, and the short half-life *in vitro* (Liu et al, 1998c; Voisine et al, 2002). The TLR profile of ovine $SIRP\alpha^-$ ALDC is also similar to that described in $CD8\alpha^+$ DC, where both TLR3 and TLR9 are expressed, whereas TLR4 transcripts are absent. $SIRP\alpha^-$ ALDC may have an intrinsic ability to polarise naïve $CD4^+$ T cells into Th1 cells but also appear to have a role in the maintenance of tolerance in the steady-state. The flexibility of murine DC subsets has been well demonstrated and whilst $CD8\alpha^+$ DC have an intrinsic ability to polarise $CD4^+$ T cells into Th1 cells, this capacity can be overridden by microbial signals (Section 1.4.4.2). Whether exogenous (microbial/inflammatory) signals can skew the cytokine profile of $SIRP\alpha^-$ ALDC remains to be determined and would be a logical step to take.

$SIRP\alpha^+$ ALDC are indeed a heterogeneous population of DC and it is this population which appears to contain a subset of migratory LC, since a fraction of ovine $SIRP\alpha^+$ ALDC are $ATPase^+$ and langerin transcripts appear to be uniquely expressed in this subset. These findings are also in agreement with previous studies; bovine $SIRP\alpha^+$ ALDC contain a population of acetylcholinesterase positive cells (Howard and Hope, 2000; Yirrell et al, 1991) and $SIRP\alpha^+$ cells have been detected in the epidermis by immunohistochemistry (Adams et al, 1998). In this study, purified ovine $SIRP\alpha^+$ ALDC uniquely expressed TLR4 mRNA and CD14. These findings bear similarities with those described with murine LC; TLR4 is expressed by murine LC (Mitsui et al, 2004) and interestingly, dermal resident $CD14^+$ cells differentiate into LC, suggesting that migratory LC may continue to express low surface CD14 (Larregina et al, 2001a)). LC are known to produce constitutively and/or inducibly, a variety of cytokines including IL-1β, IL-6, IL-12, IL-15 and IL-18 (Kimber et al, 2000), indeed murine LC are the major source of mRNA for IL-1β among unstimulated epidermal cells (Cumberbatch et al, 1996), which is also in line with the high constitutive expression of IL-1β by $SIRP\alpha^+$ ALDC in this study. Notably, IL-10 transcripts were only detected in $SIRP\alpha^+$ ALDC (in the steady-state flux). It is possible that the $SIRP\alpha^+$ ALDC, or indeed cells within this population have an anti-inflammatory role as has been proposed by Howard and co-workers (Howard et al, 2002). This is an attractive theory since $SIRP\alpha^+$ ALDC constitutively express high levels of proinflammatory IL-1β and IL-18.

It seems unlikely that either population is the equivalent of the pDC found in humans and more recently identified in mice (Asselin-Paturel et al., 2001; Nakano et al., 2001), although

high expression of CD45RA by SIRPα$^-$ ALDC is a characteristic of pDC (Liu et al, 2001). Howard and colleagues did not however detect IFN-α/β transcripts in either population, and suggest that neither SIRPα$^+$ nor SIRPα$^-$ ALDC are equivalent to the pDC (Howard et al, 2002; Stephens et al, 2003), which is in accord with the finding that pDC circulate in the blood and enter the lymph nodes from the blood via the high endothelial venules (Cella et al., 1999) and would not therefore be present in lymph. Both ALDC subsets are likely to be derived from a myeloid progenitor, based on the myeloid-like morphology and the lack of lymphoid-related markers. Furthermore, SIRPα is a myeloid-restricted antigen (Adams et al, 1998).

The latter part of this study partly addressed the effects of pGM-CSF on DC draining from the vaccination site. The number of leukocytes in afferent lymph increased over the first 48 hours, consistent with an acute inflammatory reaction in the skin. Furthermore, a pronounced upregulation of surface antigen presentation molecules (CD1b and MHC class IIα), costimulatory molecules (CD40 and CD86) and accessory molecules, CD11c and LFA-3 was observed on ALDC draining from the vaccination area at various time-points. Notably, CD1b and CD11c were upregulated at all time points investigated. Interestingly, an increase in surface expression of MHC class II, CD40 and CD86 was observed at earlier time-points (24–48 hours) and this is likely due to the activation of resident DC within the first 24 hours, possibly due to increased expression of IL-1β and TNF-α. Upregulation of surface CD40 and CD86 was again observed 5 days p/v, coinciding with the most pronounced increase in surface CD1b and CD11c expression. A second "wave" of upregulation of surface markers may correspond to DC which have infiltrated the skin (approximately 4 days p/v) and which are activated by the highly elevated levels of IL-1β and TNF-α in the skin. Upregulation of surface markers would suggest that DC draining the skin after pGM-CSF administration are of a mature phenotype and have enhanced accessory function in the lymph node.

As observed by others (Section 1.3.3.3), pGM-CSF does not appear to skew the cytokine profiles of DC subsets but rather augments cytokine production. At 4 and 6 days p/v, increased IL-10 and IL-12p40 expression was observed in SIRPα$^+$ and SIRPα$^-$ ALDC, respectively. Expression of TNF-α and IL-18 mRNA was also elevated in both ALDC populations at all time-points investigated, suggesting that both populations were activated by pGM-CSF and/or the gene-gun procedure itself. The observed increase in IL-12p40, IL-10 and TNF-α transcripts in ALDC 4 days after vaccination with pGM-CSF may correspond to activated DC recruited into the skin at this time-point. Conversely, IL-1β transcripts were highly elevated in SIRPα$^+$ ALDC isolated 24 hours after pGM-CSF administration and declined from there on. Such highly elevated IL-1β expression may be due to activation of resident LC collected in the first 24 hours after pGM-CSF vaccination, as SIRPα$^+$ ALDC

appear to contain migratory LC. Since DNA vaccination on other cannulated animals was unsuccessful, the role of CpG and the gene-gun procedure in the activation of DC is not known. Increased IL-1β and TNF-α transcripts were documented up to 72 hours after administration of the NF-control, and may also result in activation and migration of resident DC such as LC; however, an infiltration of DC was not observed 3–4 days after vaccination with control plasmids in the previous studies and so it seems somewhat unlikely that the observed upregulation of surface markers observed 5 days p/v and the increase in cytokine expression (days 4 and 6) was entirely due to administration of plasmid DNA and/or the gene gun bombardment procedure.

5.1 Future work

Future work should focus on further defining the cytokine and chemokine milieu at the time that DC infiltrate the skin after pGM-CSF/pIL-3 administration. In particular other proinflammatory cytokines, such as IL-6 and IL-8 should be investigated in relationship to the expression of the DC-chemotactic chemokines, MCP-1 and CCR6. The kinetics of DC infiltration needs to be more closely addressed in order to ascertain when SIRPα^{+} and SIRPα^{-} DC are recruited into the skin and/or if there is proliferation of resident DC population(s) within the skin. This could be achieved by quantification of double immunolabelled DC (SIRPα$^{+/-}$ and MHC class II) in conjunction with ATPase staining at various time-points p/v. Proliferation of DC could also be addressed using immunostaining in combination with a mAb to proliferating cell nuclear antigen (PCNA). Infiltration of B cells after pIL-3 administration (and to a lesser extent with pGM-CSF), necessitates further investigation. DNA vaccine-induced antibody responses in outbred species have been problematic and the ability of IL-3 to recruit B cells may therefore be advantageous. Whilst DC are required to activate Th2 cells which ultimately induce secretion of antibody by B cells, perhaps creating an environment where both B cells and DC are exposed to the vaccine encoded antigen may induce a more effective antibody response. Indeed, it has been proposed that binding of CpG motifs through TLR9 on B cells may initiate or amplify early T cell-independent IgG responses (He et al., 2004). The adjuvant effects of pIL-3 therefore merit closer attention.

The cannulation model provides an excellent system in which to investigate the way in which DC respond to various stimuli including the effects of molecular adjuvants. From the preliminary work involving DNA vaccination of cannulated sheep with pGM-CSF, it appeared that the cytokine profiles were augmented, rather than skewed with pGM-CSF,

although activation of DC by CpG motifs could be responsible for enhanced cytokine induction, since both populations express TLR9 and increased expression of proinflammatory cytokines was evident in NF-control vaccinated skin. It would be extremely valuable (and a rational approach to vaccine design) to determine the extent of plasticity of these DC subpopulations. This could be achieved by isolating SIRPα^+ and SIRPα^- ALDC populations after *in vivo* exposure to microbial stimuli. Since, both populations express TLR3 and TLR9, it remains to be determined if both populations respond "equally" by expressing the same cytokine profiles if exposed to microbial stimuli alone. For instance, do SIRPα^+ ALDC respond by producing more Th1-biasing IL-12p40 after exposure to dsRNA (poly I: C)?

The *in vivo* effects of pGM-CSF and pIL-3 on ALDC require further study. It is imperative that gene-gun vaccination with NF-control plasmids is carried out to assess the effects of administration of CpG motifs and/or the gene-gun procedure on DC draining the skin. It would also be of interest to remove biopsies and confirm DC infiltration by immunostaining, in order to correlate the findings obtained with ALDC with the kinetics of DC infiltration into the skin after pGM-CSF/pIL-3 vaccination. Increased surface expression of several surface markers on ALDC, including CD1, and CD11c was evident in this study; however, no comparison of ALDC subsets was carried out. It would be particularly valuable to ascertain if upregulation of cell surface markers is evident in both subpopulations. In particular, ascertaining which costimulatory molecules are expressed by each DC subset after administration of pGM-CSF/pIL-3 is vital, as a lack of costimulatory molecules can ultimately lead to tolerance to the DNA vaccine encoded antigen (Steinman and Nussenzweig, 2002).

It would be particularly valuable to investigate the functional capacity of each ALDC subset in allogeneic reactions *in vitro* before and after DNA vaccination with pGM-CSF/pIL-3. The stimulatory capacity of both ALDC subsets has been investigated in both rats (Liu et al, 1998c) and in cattle (Howard et al, 1997) and both studies revealed that the SIRPα^+ ALDC possessed superior immunostimulatory capacity compared to SIRPα^- ALDC. It would be fascinating to study the responses after administration of pGM-CSF and to assess if SIRPα^- ALDC have enhanced immunostimulatory capacity in comparison to those isolated from the steady-state flux. Whilst it appears from this preliminary study and others that GM-CSF does not skew the cytokine production produced by DC subsets, it would be of interest to determine cytokine expression in allogeneic CD4$^+$ T cells after *in vitro* stimulation with freshly isolated ALDC before and after pGM-CSF administration. Cytokine profiles of CD4$^+$ and CD8$^+$ T cells isolated from afferent lymph before and after pGM-CSF vaccination would also be particularly valuable. Knowing which DC subset has enhanced accessory function

(upregulated antigen presentation and costimulatory molecules) and knowledge of the Th polarising capacity of each subset could provide a basis for selective targeting of DC *in vivo* after DNA vaccination with pGM-CSF.

It would also be of interest to determine if pIL-3 and pGM-CSF enhance uptake and presentation of antigen *in vivo* as has been suggested by other studies (Section 1.3.3.3). Gene-gun vaccination does not result in long lived expression of the encoded "antigen", although in this study the fact that cytokines rather than a foreign antigen were investigated complicates matters, since GM-CSF is constitutively expressed in the skin. In this study, peak expression of both cytokines occurred at approximately 4 hours p/v and levels thereafter declined and were only just detectable up to 96 hours. While further characterisation of the cytokine and chemokine milieu is necessary, studies must also focus on the kinetics of antigen (protein) expression. If little antigen is available for DC uptake, or peak antigen expression has occurred, DC may well become activated and capable of stimulating T cells, but may not actually be presenting the target antigen. Ensuring that plasmid DNA is expressed in sufficient quantities until maximal DC infiltration ensues may be pivotal in the optimisation of DNA vaccines. Since the "antigen-producing factories" after gene-gun vaccination are predominantly keratinocytes and (to a lesser extent) fibroblasts (Section 1.2.1), ensuring antigen expression may be difficult since sloughing of the skin is inevitable by 4 days when maximal infiltration of DC occurs with pGM-CSF. Perhaps studies should focus on administering GM-CSF and administering a second antigen-encoding plasmid when DC infiltration takes place, therefore maximising direct transfection of infiltrating DC and resident LC/dermal DC. Using plasmids which promote apoptosis of transfected keratinocytes and fibroblasts may also increase the opportunity for DC to acquire antigen in the periphery, where the presence of danger signals will promote stimulatory DC rather than tolerogenic DC.

References

Adams, S., van der Laan, L. J., Vernon-Wilson, E., Renardel, d. L., Dopp, E. A., Dijkstra, C. D., Simmons, D. L., and van den Berg, T. K. (1998). Signal-regulatory protein is selectively expressed by myeloid and neuronal cells. *J.Immunol.* **161**, 1853-1859.

Ahmad-Nejad, P., Hacker, H., Rutz, M., Bauer, S., Vabulas, R. M., and Wagner, H. (2002). Bacterial CpG-DNA and lipopolysaccharides activate Toll-like receptors at distinct cellular compartments. *Eur.J.Immunol.* **32**, 1958-1968.

Akbari, O., Panjwani, N., Garcia, S., Tascon, R., Lowrie, D., and Stockinger, B. (1999). DNA vaccination: transfection and activation of dendritic cells as key events for immunity. *J.Exp.Med.* **189**, 169-178.

Akira, S., Hoshino, K., and Kaisho, T. (2000). The role of Toll-like receptors and MyD88 in innate immune responses. *J.Endotoxin.Res.* **6**, 383-387.

Albert, M. L., Sauter, B., and Bhardwaj, N. (1998). Dendritic cells acquire antigen from apoptotic cells and induce class I-restricted CTLs. *Nature* **392**, 86-89.

Alexopoulou, L., Holt, A. C., Medzhitov, R., and Flavell, R. A. (2001). Recognition of double-stranded RNA and activation of NF-kappaB by Toll-like receptor 3. *Nature* **413**, 732-738.

Appelmelk, B. J., van, D., I, van Vliet, S. J., Vandenbroucke-Grauls, C. M., Geijtenbeek, T. B., and van Kooyk, Y. (2003). Cutting edge: carbohydrate profiling identifies new pathogens that interact with dendritic cell-specific ICAM-3-grabbing nonintegrin on dendritic cells. *J.Immunol.* **170**, 1635-1639.

Armengol, G., Ruiz, L. M., and Orduz, S. (2004). The injection of plasmid DNA in mouse muscle results in lifelong persistence of DNA, gene expression, and humoral response. *Mol.Biotechnol.* **27**, 109-118.

Armitage, J. O. (1998). Emerging applications of recombinant human granulocyte-macrophage colony-stimulating factor. *Blood* **92**, 4491-4508.

Asea, A., Kraeft, S. K., Kurt-Jones, E. A., Stevenson, M. A., Chen, L. B., Finberg, R. W., Koo, G. C., and Calderwood, S. K. (2000). HSP70 stimulates cytokine production through a CD14-dependant pathway, demonstrating its dual role as a chaperone and cytokine. *Nat.Med.* **6**, 435-442.

Asselin-Paturel, C., Boonstra, A., Dalod, M., Durand, I., Yessaad, N., Dezutter-Dambuyant, C., Vicari, A., O'Garra, A., Biron, C., Briere, F., and Trinchieri, G. (2001). Mouse type I IFN-producing cells are immature APCs with plasmacytoid morphology. *Nat.Immunol.* **2**, 1144-1150.

Athman, R. and Philpott, D. (2004). Innate immunity via Toll-like receptors and Nod proteins. *Curr.Opin.Microbiol.* **7**, 25-32.

Avigan, D., Wu, Z., Gong, J., Joyce, R., Levine, J., Elias, A., Richardson, P., Milano, J., Kennedy, L., Anderson, K., and Kufe, D. (1999). Selective in vivo mobilization with granulocyte macrophage colony-stimulating factor (GM-CSF)/granulocyte-CSF as compared to G-CSF alone of dendritic cell

progenitors from peripheral blood progenitor cells in patients with advanced breast cancer undergoing autologous transplantation. *Clin.Cancer Res.* **5**, 2735-2741.

Babiuk, L. A., Lewis, J., van den, H. S., and Braun, R. (1999). DNA immunization: present and future. *Adv.Vet.Med.* **41**, 163-179.

Babiuk, L. A., Pontarollo, R., Babiuk, S., Loehr, B., and van Drunen Littel-van den Hurk (2003). Induction of immune responses by DNA vaccines in large animals. *Vaccine* **21**, 649-658.

Bagley, C. J., Woodcock, J. M., Stomski, F. C., and Lopez, A. F. (1997). The structural and functional basis of cytokine receptor activation: lessons from the common beta subunit of the granulocyte-macrophage colony-stimulating factor, interleukin-3 (IL-3), and IL-5 receptors. *Blood* **89**, 1471-1482.

Bailey, S. L. Phenotype and cytokine expression profiles of ovine dendritic cells migrating to lymph nodes. Development of a ribonuclease protection assay to quantify IL-18 and other cytokines. 2003. University of Edinburgh.

Ref Type: Thesis/Dissertation

Ban, E., Dupre, L., Hermann, E., Rohn, W., Vendeville, C., Quatannens, B., Ricciardi-Castagnoli, P., Capron, A., and Riveau, G. (2000). CpG motifs induce Langerhans cell migration in vivo. *Int.Immunol.* **12**, 737-745.

Banchereau, J., Briere, F., Caux, C., Davoust, J., Lebecque, S., Liu, Y. J., Pulendran, B., and Palucka, K. (2000). Immunobiology of dendritic cells. *Annu.Rev.Immunol.* **18**, 767-811.

Banchereau, J. and Steinman, R. M. (1998). Dendritic cells and the control of immunity. *Nature* **392**, 245-252.

Barouch, D. H., Santra, S., Tenner-Racz, K., Racz, P., Kuroda, M. J., Schmitz, J. E., Jackson, S. S., Lifton, M. A., Freed, D. C., Perry, H. C., Davies, M. E., Shiver, J. W., and Letvin, N. L. (2002). Potent CD4+ T cell responses elicited by a bicistronic HIV-1 DNA vaccine expressing gp120 and GM-CSF. *J.Immunol.* **168**, 562-568.

Basu, S., Binder, R. J., Suto, R., Anderson, K. M., and Srivastava, P. K. (2000). Necrotic but not apoptotic cell death releases heat shock proteins, which deliver a partial maturation signal to dendritic cells and activate the NF-kappa B pathway. *Int.Immunol.* **12**, 1539-1546.

Benvenisti, L., Rogel, A., Kuznetzova, L., Bujanover, S., Becker, Y., and Stram, Y. (2001). Gene gun-mediate DNA vaccination against foot-and-mouth disease virus. *Vaccine* **19**, 3885-3895.

Benvenuti, F. and Burrone, O. R. (2001). Anti-idiotypic antibodies induced by genetic immunisation are directed exclusively against combined V(L)/V(H) determinants. *Gene Ther.* **8**, 1555-1561.

Bergstresser, P. R., Fletcher, C. R., and Streilein, J. W. (1980). Surface densities of Langerhans cells in relation to rodent epidermal sites with special immunologic properties. *J.Invest Dermatol.* **74**, 77-80.

Bergstresser, P. R., Tigelaar, R. E., Dees, J. H., and Streilein, J. W. (1983). Thy-1 antigen-bearing dendritic cells populate murine epidermis. *J.Invest Dermatol.* **81**, 286-288.

Binder, R. J., Anderson, K. M., Basu, S., and Srivastava, P. K. (2000). Cutting edge: heat shock protein gp96 induces maturation and migration of CD11c+ cells in vivo. *J.Immunol.* **165**, 6029-6035.

Birbeck, M. S., Breathnack, A. S., and Everall, J. D. (1961). An electron microscope study of basal melanocytes and high level clear cells (Langerhans cells) in vitiligo. *J.Invest.Dermatol.* **37**, 51-64.

Birnboim, H. C. and Doly, J. (1979). A rapid alkaline extraction procedure for screening recombinant plasmid DNA. *Nucleic Acids Res.* **7**, 1513-1523.

Boonstra, A., Asselin-Paturel, C., Gilliet, M., Crain, C., Trinchieri, G., Liu, Y. J., and O'Garra, A. (2003). Flexibility of mouse classical and plasmacytoid-derived dendritic cells in directing T helper type 1 and 2 cell development: dependency on antigen dose and differential toll-like receptor ligation. *J.Exp.Med.* **197**, 101-109.

Bot, A., Stan, A. C., Inaba, K., Steinman, R., and Bona, C. (2000). Dendritic cells at a DNA vaccination site express the encoded influenza nucleoprotein and prime MHC class I-restricted cytolytic lymphocytes upon adoptive transfer. *Int.Immunol.* **12**, 825-832.

Bouloc, A., Walker, P., Grivel, J. C., Vogel, J. C., and Katz, S. I. (1999). Immunization through dermal delivery of protein-encoding DNA: a role for migratory dendritic cells. *Eur.J.Immunol.* **29**, 446-454.

Bowne, W. B., Wolchok, J. D., Hawkins, W. G., Srinivasan, R., Gregor, P., Blachere, N. E., Moroi, Y., Engelhorn, M. E., Houghton, A. N., and Lewis, J. J. (1999). Injection of DNA encoding granulocyte-macrophage colony-stimulating factor recruits dendritic cells for immune adjuvant effects. *Cytokines Cell Mol.Ther.* **5**, 217-225.

Boyle, C. M. and Robinson, H. L. (2000). Basic mechanisms of DNA-raised antibody responses to intramuscular and gene gun immunizations. *DNA Cell Biol.* **19**, 157-165.

Brach, M. A., deVos, S., Gruss, H. J., and Herrmann, F. (1992). Prolongation of survival of human polymorphonuclear neutrophils by granulocyte-macrophage colony-stimulating factor is caused by inhibition of programmed cell death. *Blood* **80**, 2920-2924.

Brand, C. U., Gerber, H. A., Hunziker, T., Schaffner, T., Limat, A., and Brathen, L. R. (1993). Phenotype of Langerhans cells in human afferent skin lymph derived from allergic contact dermatitis. *Exp.Dermatol.* **2**, 274-279.

Braun, R. P., Babiuk, L. A., Loehr, B. I., and van Drunen Littel-van den Hurk (1999). Particle-mediated DNA immunization of cattle confers long-lasting immunity against bovine herpesvirus-1. *Virology* **265**, 46-56.

Brawand, P., Fitzpatrick, D. R., Greenfield, B. W., Brasel, K., Maliszewski, C. R., and De Smedt, T. (2002). Murine plasmacytoid pre-dendritic cells generated from Flt3 ligand-supplemented bone marrow cultures are immature APCs. *J.Immunol.* **169**, 6711-6719.

Brombacher, F., Kastelein, R. A., and Alber, G. (2003). Novel IL-12 family members shed light on the orchestration of Th1 responses. *Trends Immunol.* **24**, 207-212.

Brooke, G. P., Parsons, K. R., and Howard, C. J. (1998). Cloning of two members of the SIRP alpha family of protein tyrosine phosphatase binding proteins in cattle that are expressed on monocytes and a subpopulation of dendritic cells and which mediate binding to CD4 T cells. *Eur.J.Immunol.* **28**, 1-11.

Brossart, P. and Bevan, M. J. (1997). Presentation of exogenous protein antigens on major histocompatibility complex class I molecules by dendritic cells: pathway of presentation and regulation by cytokines. *Blood* **90**, 1594-1599.

Brown, G. D., Herre, J., Williams, D. L., Willment, J. A., Marshall, A. S., and Gordon, S. (2003). Dectin-1 mediates the biological effects of beta-glucans. *J.Exp.Med.* **197**, 1119-1124.

Brown, W. C. and Estes, D. M. (1997). 2 Type 1 and Type 2 Responses in Cattle and their Regulation. *In* "Cytokines In Veterinary Medicine" (V. E. C. J. Schijns and M. C. Horzinek, Eds.), pp. 15-34. CABI Publishing, Wallingford, UK.

Bujdoso, R., Hopkins, J., Dutia, B. M., Young, P., and McConnell, I. (1989). Characterization of sheep afferent lymph dendritic cells and their role in antigen carriage. *J.Exp.Med.* **170**, 1285-1301.

Burger, J. A., Mendoza, R. B., and Kipps, T. J. (2001). Plasmids encoding granulocyte-macrophage colony-stimulating factor and CD154 enhance the immune response to genetic vaccines. *Vaccine* **19**, 2181-2189.

Bustin, S. A. (2000). Absolute quantification of mRNA using real-time reverse transcription polymerase chain reaction assays. *J.Mol.Endocrinol.* **25**, 169-193.

Campbell, K., Diao, H., Ji, J., and Soong, L. (2003). DNA immunization with the gene encoding P4 nuclease of Leishmania amazonensis protects mice against cutaneous Leishmaniasis. *Infect.Immun.* **71**, 6270-6278.

Casares, S., Inaba, K., Brumeanu, T. D., Steinman, R. M., and Bona, C. A. (1997). Antigen presentation by dendritic cells after immunization with DNA encoding a major histocompatibility complex class II-restricted viral epitope. *J.Exp.Med.* **186**, 1481-1486.

Caux, C., Dezutter-Dambuyant, C., Schmitt, D., and Banchereau, J. (1992a). GM-CSF and TNF-alpha cooperate in the generation of dendritic Langerhans cells. *Nature* **360**, 258-261.

Caux, C., Massacrier, C., Vanbervliet, B., Dubois, B., Van Kooten, C., Durand, I., and Banchereau, J. (1994). Activation of human dendritic cells through CD40 cross-linking. *J.Exp.Med.* **180**, 1263-1272.

Caux, C., Moreau, I., Saeland, S., and Banchereau, J. (1992b). Interferon-gamma enhances factor-dependent myeloid proliferation of human CD34+ hematopoietic progenitor cells. *Blood* **79**, 2628-2635.

Caux, C., Vanbervliet, B., Massacrier, C., Dezutter-Dambuyant, C., Saint-Vis, B., Jacquet, C., Yoneda, K., Imamura, S., Schmitt, D., and Banchereau, J. (1996a). CD34+ hematopoietic progenitors from human cord blood differentiate along two independent dendritic cell pathways in response to GM-CSF+TNF alpha. *J.Exp.Med.* **184**, 695-706.

Caux, C., Vanbervliet, B., Massacrier, C., Durand, I., and Banchereau, J. (1996b). Interleukin-3 cooperates with tumor necrosis factor alpha for the development of human dendritic/Langerhans cells from cord blood CD34+ hematopoietic progenitor cells. *Blood* **87**, 2376-2385.

Cella, M., Jarrossay, D., Facchetti, F., Alebardi, O., Nakajima, H., Lanzavecchia, A., and Colonna, M. (1999). Plasmacytoid monocytes migrate to inflamed lymph nodes and produce large amounts of type I interferon. *Nat.Med.* **5**, 919-923.

Chiodoni, C., Paglia, P., Stoppacciaro, A., Rodolfo, M., Parenza, M., and Colombo, M. P. (1999). Dendritic cells infiltrating tumors cotransduced with granulocyte/macrophage colony-stimulating factor (GM-CSF) and CD40 ligand genes take up and present endogenous tumor-associated antigens, and prime naive mice for a cytotoxic T lymphocyte response. *J.Exp.Med.* **190**, 125-133.

Chow, J. C., Young, D. W., Golenbock, D. T., Christ, W. J., and Gusovsky, F. (1999). Toll-like receptor-4 mediates lipopolysaccharide-induced signal transduction. *J.Biol.Chem.* **274**, 10689-10692.

Chow, Y. H., Chiang, B. L., Lee, Y. L., Chi, W. K., Lin, W. C., Chen, Y. T., and Tao, M. H. (1998). Development of Th1 and Th2 populations and the nature of immune responses to hepatitis B virus DNA vaccines can be modulated by codelivery of various cytokine genes. *J.Immunol.* **160**, 1320-1329.

Clevers, H., MacHugh, N. D., Bensaid, A., Dunlap, S., Baldwin, C. L., Kaushal, A., Iams, K., Howard, C. J., and Morrison, W. I. (1990). Identification of a bovine surface antigen uniquely expressed on CD4-CD8- T cell receptor gamma/delta+ T lymphocytes. *Eur.J.Immunol.* **20**, 809-817.

Colotta, F., Re, F., Polentarutti, N., Sozzani, S., and Mantovani, A. (1992). Modulation of granulocyte survival and programmed cell death by cytokines and bacterial products. *Blood* **80**, 2012-2020.

Condon, C., Watkins, S. C., Celluzzi, C. M., Thompson, K., and Falo, L. D., Jr. (1996). DNA-based immunization by in vivo transfection of dendritic cells. *Nat.Med.* **2**, 1122-1128.

Conry, R. M., Curiel, D. T., Strong, T. V., Moore, S. E., Allen, K. O., Barlow, D. L., Shaw, D. R., and LoBuglio, A. F. (2002). Safety and immunogenicity of a DNA vaccine encoding carcinoembryonic antigen and hepatitis B surface antigen in colorectal carcinoma patients. *Clin.Cancer Res.* **8**, 2782-2787.

Corr, M., Lee, D. J., Carson, D. A., and Tighe, H. (1996). Gene vaccination with naked plasmid DNA: mechanism of CTL priming. *J.Exp.Med.* **184**, 1555-1560.

Coughlan, S., Harkiss, G. D., and Hopkins, J. (1996). Enhanced proliferation of CD4+ T cells induced by dendritic cells following antigen uptake in the presence of specific antibody. *Vet.Immunol.Immunopathol.* **49**, 321-330.

Cumberbatch, M., Dearman, R. J., Antonopoulos, C., Groves, R. W., and Kimber, I. (2001). Interleukin (IL)-18 induces Langerhans cell migration by a tumour necrosis factor-alpha- and IL-1beta-dependent mechanism. *Immunology* **102**, 323-330.

Cumberbatch, M., Dearman, R. J., and Kimber, I. (1996). Constitutive and inducible expression of interleukin-6 by Langerhans cells and lymph node dendritic cells. *Immunology* **87**, 513-518.

Cumberbatch, M., Dearman, R. J., and Kimber, I. (1997a). Interleukin 1 beta and the stimulation of Langerhans cell migration: comparisons with tumour necrosis factor alpha. *Arch.Dermatol.Res.* **289**, 277-284.

Cumberbatch, M., Dearman, R. J., and Kimber, I. (1997b). Langerhans cells require signals from both tumour necrosis factor alpha and interleukin 1 beta for migration. *Adv.Exp.Med.Biol.* **417**, 125-128.

Cumberbatch, M., Dearman, R. J., and Kimber, I. (1997c). Stimulation of Langerhans cell migration in mice by tumour necrosis factor alpha and interleukin 1 beta. *Adv.Exp.Med.Biol.* **417**, 121-124.

Cumberbatch, M., Dearman, R. J., and Kimber, I. (1998). Characteristics and regulation of the expression on interleukin 1 receptors by murine Langerhans cells and keratinocytes. *Arch.Dermatol.Res.* **290**, 688-695.

Cumberbatch, M., Griffiths, C. E., Tucker, S. C., Dearman, R. J., and Kimber, I. (1999). Tumour necrosis factor-alpha induces Langerhans cell migration in humans. *Br.J.Dermatol.* **141**, 192-200.

Cumberbatch, M. and Kimber, I. (1992). Dermal tumour necrosis factor-alpha induces dendritic cell migration to draining lymph nodes, and possibly provides one stimulus for Langerhans' cell migration. *Immunology* **75**, 257-263.

Cumberbatch, M., Scott, R. C., Basketter, D. A., Scholes, E. W., Hilton, J., Dearman, R. J., and Kimber, I. (1993). Influence of sodium lauryl sulphate on 2,4-dinitrochlorobenzene-induced lymph node activation. *Toxicology* **77**, 181-191.

D'Andrea, A., Aste-Amezaga, M., Valiante, N. M., Ma, X., Kubin, M., and Trinchieri, G. (1993). Interleukin 10 (IL-10) inhibits human lymphocyte interferon gamma-production by suppressing natural killer cell stimulatory factor/IL-12 synthesis in accessory cells. *J.Exp.Med.* **178**, 1041-1048.

d'Ostiani, C. F., Del Sero, G., Bacci, A., Montagnoli, C., Spreca, A., Mencacci, A., Ricciardi-Castagnoli, P., and Romani, L. (2000). Dendritic cells discriminate between yeasts and hyphae of the fungus Candida albicans. Implications for initiation of T helper cell immunity in vitro and in vivo. *J.Exp.Med.* **191**, 1661-1674.

Dalod, M., Hamilton, T., Salomon, R., Salazar-Mather, T. P., Henry, S. C., Hamilton, J. D., and Biron, C. A. (2003). Dendritic cell responses to early murine cytomegalovirus infection: subset functional specialization and differential regulation by interferon alpha/beta. *J.Exp.Med.* **197**, 885-898.

Dandie, G. W., Clydesdale, G. J., Radcliff, F. J., and Muller, H. K. (2001). Migration of Langerhans cells and gammadelta dendritic cells from UV-B-irradiated sheep skin. *Immunol.Cell Biol.* **79**, 41-48.

Daro, E., Pulendran, B., Brasel, K., Teepe, M., Pettit, D., Lynch, D. H., Vremec, D., Robb, L., Shortman, K., McKenna, H. J., Maliszewski, C. R., and Maraskovsky, E. (2000). Polyethylene glycol-modified GM-CSF expands CD11b(high)CD11c(high) but notCD11b(low)CD11c(high) murine dendritic cells in vivo: a comparative analysis with Flt3 ligand. *J.Immunol.* **165**, 49-58.

De Rose, R., Scheerlinck, J. P., Casey, G., Wood, P. R., Tennent, J. M., and Chaplin, P. J. (2000). Ovine interleukin 12: analysis of biologic function and species comparison. *J.Interferon Cytokine Res.* **20**, 557-564.

De Rose, R., Tennent, J., McWaters, P., Chaplin, P. J., Wood, P. R., Kimpton, W., Cahill, R., and Scheerlinck, J. P. (2002). Efficacy of DNA vaccination by different routes of immunisation in sheep. *Vet.Immunol.Immunopathol.* **90**, 55-63.

Del Prete, G., de Carli, M., Almerigogna, F., Giudizi, M. G., Biagiotti, R., and Romagnani, S. (1993). Human IL-10 is produced by both type 1 helper (Th1) and type 2 helper (Th2) T cell clones and inhibits their antigen-specific proliferation and cytokine production. *J.Immunol.* **150**, 353-360.

den Haan, J. M., Lehar, S. M., and Bevan, M. J. (2000). CD8(+) but not CD8(-) dendritic cells cross-prime cytotoxic T cells in vivo. *J.Exp.Med.* **192**, 1685-1696.

Diebold, S. S., Kaisho, T., Hemmi, H., Akira, S., and Reis e Sousa (2004). Innate antiviral responses by means of TLR7-mediated recognition of single-stranded RNA. *Science* **303**, 1529-1531.

Diebold, S. S., Montoya, M., Unger, H., Alexopoulou, L., Roy, P., Haswell, L. E., Al Shamkhani, A., Flavell, R., Borrow, P., and Reis e Sousa (2003). Viral infection switches non-plasmacytoid dendritic cells into high interferon producers. *Nature* **424**, 324-328.

Doe, B., Selby, M., Barnett, S., Baenziger, J., and Walker, C. M. (1996). Induction of cytotoxic T lymphocytes by intramuscular immunization with plasmid DNA is facilitated by bone marrow-derived cells. *Proc.Natl.Acad.Sci.U.S.A* **93**, 8578-8583.

Donnelly, J., Berry, K., and Ulmer, J. B. (2003). Technical and regulatory hurdles for DNA vaccines. *Int.J.Parasitol.* **33**, 457-467.

Dowty, M. E., Williams, P., Zhang, G., Hagstrom, J. E., and Wolff, J. A. (1995). Plasmid DNA entry into postmitotic nuclei of primary rat myotubes. *Proc.Natl.Acad.Sci.U.S.A* **92**, 4572-4576.

Doxsee, C. L., Riter, T. R., Reiter, M. J., Gibson, S. J., Vasilakos, J. P., and Kedl, R. M. (2003). The immune response modifier and Toll-like receptor 7 agonist S-27609 selectively induces IL-12 and TNF-alpha production in CD11c+CD11b+CD8- dendritic cells. *J.Immunol.* **171**, 1156-1163.

Dranoff, G., Jaffee, E., Lazenby, A., Golumbek, P., Levitsky, H., Brose, K., Jackson, V., Hamada, H., Pardoll, D., and Mulligan, R. C. (1993). Vaccination with irradiated tumor cells engineered to secrete murine granulocyte-macrophage colony-stimulating factor stimulates potent, specific, and long-lasting anti-tumor immunity. *Proc.Natl.Acad.Sci.U.S.A* **90**, 3539-3543.

Drew, D. R., Lightowlers, M. W., and Strugnell, R. A. (2000). A comparison of DNA vaccines expressing the 45W, 18k and 16k host-protective antigens of Taenia ovis in mice and sheep. *Vet.Immunol.Immunopathol.* **76**, 171-181.

Drexhage, H. A., Mullink, H., de Groot, J., Clarke, J., and Balfour, B. M. (1979). A study of cells present in peripheral lymph of pigs with special reference to a type of cell resembling the Langerhans cell. *Cell Tissue Res.* **202**, 407-430.

Dubois, B., Massacrier, C., Vanbervliet, B., Fayette, J., Briere, F., Banchereau, J., and Caux, C. (1998). Critical role of IL-12 in dendritic cell-induced differentiation of naive B lymphocytes. *J.Immunol.* **161**, 2223-2231.

Dutia, B. M., MacCarthy-Morrogh, L., Glass, E. J., Knowles, G., Spooner, R. L., and Hopkins, J. (1995). Discrimination between major histocompatibility complex class II DQ and DR locus products in cattle. *Anim Genet.* **26**, 111-114.

Dutia, B. M., McConnell, I., Bird, K., Keating, P., and Hopkins, J. (1993a). Patterns of major histocompatibility complex class II expression on T cell subsets in different immunological compartments. 1. Expression on resting T cells. *Eur.J.Immunol.* **23**, 2882-2888.

Dutia, B. M., Ross, A. J., and Hopkins, J. (1993b). Analysis of the monoclonal antibodies comprising WC6. *Vet.Immunol.Immunopathol.* **39**, 193-199.

Dutia, B. M., Ross, A. J., and Hopkins, J. (1993c). Comparison of workshop CD45R monoclonal antibodies with OvCD45R monoclonal antibodies in sheep. *Vet.Immunol.Immunopathol.* **39**, 121-128.

Ebner, S., Hofer, S., Nguyen, V. A., Furhapter, C., Herold, M., Fritsch, P., Heufler, C., and Romani, N. (2002). A novel role for IL-3: human monocytes cultured in the presence of IL-3 and IL-4 differentiate into dendritic cells that produce less IL-12 and shift Th cell responses toward a Th2 cytokine pattern. *J.Immunol.* **168**, 6199-6207.

Edwards, A. D., Diebold, S. S., Slack, E. M., Tomizawa, H., Hemmi, H., Kaisho, T., Akira, S., and Reis e Sousa (2003). Toll-like receptor expression in murine DC subsets: lack of TLR7 expression by CD8 alpha+ DC correlates with unresponsiveness to imidazoquinolines. *Eur.J.Immunol.* **33**, 827-833.

Eisenbraun, M. D., Fuller, D. H., and Haynes, J. R. (1993). Examination of parameters affecting the elicitation of humoral immune responses by particle bombardment-mediated genetic immunization. *DNA Cell Biol.* **12**, 791-797.

Ellis, J. A., Davis, W. C., MacHugh, N. D., Emery, D. L., Kaushal, A., and Morrison, W. I. (1988). Differentiation antigens on bovine mononuclear phagocytes identified by monoclonal antibodies. *Vet.Immunol.Immunopathol.* **19**, 325-340.

Emery, D. L., MacHugh, N. D., and Ellis, J. A. (1987). The properties and functional activity of non-lymphoid cells from bovine afferent (peripheral) lymph. *Immunology* **62**, 177-183.

Engering, A., Geijtenbeek, T. B., van Vliet, S. J., Wijers, M., van Liempt, E., Demaurex, N., Lanzavecchia, A., Fransen, J., Figdor, C. G., Piguet, V., and van Kooyk, Y. (2002). The dendritic cell-specific adhesion receptor DC-SIGN internalizes antigen for presentation to T cells. *J.Immunol.* **168**, 2118-2126.

Entrican, G., Deane, D., MacLean, M., Inglis, L., Thomson, J., McInnes, C., and Haig, D. M. (1996). Development of a sandwich ELISA for ovine granulocyte/macrophage colony-stimulating factor. *Vet.Immunol.Immunopathol.* **50**, 105-115.

Epardaud, M., Bonneau, M., Payot, F., Cordier, C., Megret, J., Howard, C., and Schwartz-Cornil, I. (2004). Enrichment for a CD26hi SIRP- subset in lymph dendritic cells from the upper aero-digestive tract. *J.Leukoc.Biol.* **76**, 553-561.

Fadok, V. A., Bratton, D. L., Konowal, A., Freed, P. W., Westcott, J. Y., and Henson, P. M. (1998). Macrophages that have ingested apoptotic cells in vitro inhibit proinflammatory cytokine production

through autocrine/paracrine mechanisms involving TGF-beta, PGE2, and PAF. *J.Clin.Invest* **101**, 890-898.

Feltquate, D. M., Heaney, S., Webster, R. G., and Robinson, H. L. (1997). Different T helper cell types and antibody isotypes generated by saline and gene gun DNA immunization. *J.Immunol.* **158**, 2278-2284.

Fernandez, M. C., Walters, J., and Marucha, P. (1996). Transcriptional and post-transcriptional regulation of GM-CSF-induced IL-1 beta gene expression in PMN. *J.Leukoc.Biol.* **59**, 598-603.

Fonteneau, J. F., Gilliet, M., Larsson, M., Dasilva, I., Munz, C., Liu, Y. J., and Bhardwaj, N. (2003). Activation of influenza virus-specific CD4+ and CD8+ T cells: a new role for plasmacytoid dendritic cells in adaptive immunity. *Blood* **101**, 3520-3526.

Foulds, K. E., Zenewicz, L. A., Shedlock, D. J., Jiang, J., Troy, A. E., and Shen, H. (2002). Cutting edge: CD4 and CD8 T cells are intrinsically different in their proliferative responses. *J.Immunol.* **168**, 1528-1532.

Fynan, E. F., Webster, R. G., Fuller, D. H., Haynes, J. R., Santoro, J. C., and Robinson, H. L. (1993). DNA vaccines: protective immunizations by parenteral, mucosal, and gene-gun inoculations. *Proc.Natl.Acad.Sci.U.S.A* **90**, 11478-11482.

Gallucci, S., Lolkema, M., and Matzinger, P. (1999). Natural adjuvants: endogenous activators of dendritic cells. *Nat.Med.* **5**, 1249-1255.

Gallucci, S. and Matzinger, P. (2001). Danger signals: SOS to the immune system. *Curr.Opin.Immunol.* **13**, 114-119.

Galvin, T. A., Muller, J., and Khan, A. S. (2000). Effect of different promoters on immune responses elicited by HIV-1 gag/env multigenic DNA vaccine in Macaca mulatta and Macaca nemestrina. *Vaccine* **18**, 2566-2583.

Gardella, S., Andrei, C., Costigliolo, S., Poggi, A., Zocchi, M. R., and Rubartelli, A. (1999). Interleukin-18 synthesis and secretion by dendritic cells are modulated by interaction with antigen-specific T cells. *J.Leukoc.Biol.* **66**, 237-241.

Geijtenbeek, T. B., Kwon, D. S., Torensma, R., van Vliet, S. J., van Duijnhoven, G. C., Middel, J., Cornelissen, I. L., Nottet, H. S., KewalRamani, V. N., Littman, D. R., Figdor, C. G., and van Kooyk, Y. (2000). DC-SIGN, a dendritic cell-specific HIV-1-binding protein that enhances trans-infection of T cells. *Cell* **100**, 587-597.

Geijtenbeek, T. B. and van Kooyk, Y. (2003). Pathogens target DC-SIGN to influence their fate DC-SIGN functions as a pathogen receptor with broad specificity. *APMIS* **111**, 698-714.

Geissler, M., Gesien, A., Tokushige, K., and Wands, J. R. (1997). Enhancement of cellular and humoral immune responses to hepatitis C virus core protein using DNA-based vaccines augmented with cytokine-expressing plasmids. *J.Immunol.* **158**, 1231-1237.

Geissmann, F., Revy, P., Regnault, A., Lepelletier, Y., Dy, M., Brousse, N., Amigorena, S., Hermine, O., and Durandy, A. (1999). TGF-beta 1 prevents the noncognate maturation of human dendritic Langerhans cells. *J.Immunol.* **162**, 4567-4575.

Gilliet, M., Boonstra, A., Paturel, C., Antonenko, S., Xu, X. L., Trinchieri, G., O'Garra, A., and Liu, Y. J. (2002). The development of murine plasmacytoid dendritic cell precursors is differentially regulated by FLT3-ligand and granulocyte/macrophage colony-stimulating factor. *J.Exp.Med.* **195**, 953-958.

Gliddon, D. R., Hope, J. C., Brooke, G. P., and Howard, C. J. (2004). DEC-205 expression on migrating dendritic cells in afferent lymph. *Immunology* **111**, 262-272.

Gonzalez, L., Anderson, I., Deane, D., Summers, C., and Buxton, D. (2001). Detection of immune system cells in paraffin wax-embedded ovine tissues. *J.Comp Pathol.* **125**, 41-47.

Granucci, F., Girolomoni, G., Lutz, M. B., Foti, M., Marconi, G., Gnocchi, P., Nolli, L., and Ricciardi-Castagnoli, P. (1994). Modulation of cytokine expression in mouse dendritic cell clones. *Eur.J.Immunol.* **24**, 2522-2526.

Graziani-Bowering, G. M., Graham, J. M., and Filion, L. G. (1997). A quick, easy and inexpensive method for the isolation of human peripheral blood monocytes. *J.Immunol.Methods* **207**, 157-168.

Gregg, D. A., Mebus, C. A., and Schlafer, D. H. (1995). Early infection of interdigitating dendritic cells in the pig lymph node with African swine fever viruses of high and low virulence: immunohistochemical and ultrastructural studies. *J.Vet.Diagn.Invest* **7**, 23-30.

Grouard, G., Rissoan, M. C., Filgueira, L., Durand, I., Banchereau, J., and Liu, Y. J. (1997). The enigmatic plasmacytoid T cells develop into dendritic cells with interleukin (IL)-3 and CD40-ligand. *J.Exp.Med.* **185**, 1101-1111.

Gupta, V. K., McConnell, I., Dalziel, R. G., and Hopkins, J. (1996). Identification of the sheep homologue of the monocyte cell surface molecule--CD14. *Vet.Immunol.Immunopathol.* **51**, 89-99.

Gupta, V. K., McConnell, I., and Hopkins, J. (1993). Reactivity of the CD11/CD18 workshop monoclonal antibodies in the sheep. *Vet.Immunol.Immunopathol.* **39**, 93-102.

Gurunathan, S., Klinman, D. M., and Seder, R. A. (2000). DNA vaccines: immunology, application, and optimization*. *Annu.Rev.Immunol.* **18**, 927-974.

Haddad, D., Ramprakash, J., Sedegah, M., Charoenvit, Y., Baumgartner, R., Kumar, S., Hoffman, S. L., and Weiss, W. R. (2000). Plasmid vaccine expressing granulocyte-macrophage colony-stimulating factor attracts infiltrates including immature dendritic cells into injected muscles. *J.Immunol.* **165**, 3772-3781.

Haig, D. M., Hutchison, G., Green, I., Sargan, D., and Reid, H. W. (1995a). The effect of intradermal injection of GM-CSF and TNF-alpha on the accumulation of dendritic cells in ovine skin. *Vet.Dermatol.* **6**, 211-220.

Haig, D. M., Percival, A., Mitchell, J., Green, I., and Sargan, D. (1995b). The survival and growth of ovine afferent lymph dendritic cells in culture depends on tumour necrosis factor-alpha and is

enhanced by granulocyte-macrophage colony-stimulating factor but inhibited by interferon-gamma. *Vet.Immunol.Immunopathol.* **45**, 221-236.

Hall, J. G. (1967). A method for collecting lymph from the prefemoral lymph node of unanaesthetised sheep. *Q.J.Exp.Physiol Cogn Med.Sci.* **52**, 200-205.

Han, R., Reed, C. A., Cladel, N. M., and Christensen, N. D. (2000). Immunization of rabbits with cottontail rabbit papillomavirus E1 and E2 genes: protective immunity induced by gene gun-mediated intracutaneous delivery but not by intramuscular injection. *Vaccine* **18**, 2937-2944.

Hanada, K., Tsunoda, R., and Hamada, H. (1996). GM-CSF-induced in vivo expansion of splenic dendritic cells and their strong costimulation activity. *J.Leukoc.Biol.* **60**, 181-190.

Harkiss, G. D., Hopkins, J., and McConnell, I. (1990). Uptake of antigen by afferent lymph dendritic cells mediated by antibody. *Eur.J.Immunol.* **20**, 2367-2373.

Harrison, R. A., Richards, A., Laing, G. D., and Theakston, R. D. (2002). Simultaneous GeneGun immunisation with plasmids encoding antigen and GM-CSF: significant enhancement of murine antivenom IgG1 titres. *Vaccine* **20**, 1702-1706.

Hartmann, G., Weiner, G. J., and Krieg, A. M. (1999). CpG DNA: a potent signal for growth, activation, and maturation of human dendritic cells. *Proc.Natl.Acad.Sci.U.S.A* **96**, 9305-9310.

He, B., Qiao, X., and Cerutti, A. (2004). CpG DNA induces IgG class switch DNA recombination by activating human B cells through an innate pathway that requires TLR9 and cooperates with IL-10. *J.Immunol.* **173**, 4479-4491.

Heil, F., Hemmi, H., Hochrein, H., Ampenberger, F., Kirschning, C., Akira, S., Lipford, G., Wagner, H., and Bauer, S. (2004). Species-specific recognition of single-stranded RNA via toll-like receptor 7 and 8. *Science* **303**, 1526-1529.

Hemmi, H., Takeuchi, O., Kawai, T., Kaisho, T., Sato, S., Sanjo, H., Matsumoto, M., Hoshino, K., Wagner, H., Takeda, K., and Akira, S. (2000). A Toll-like receptor recognizes bacterial DNA. *Nature* **408**, 740-745.

Hengge, U. R., Walker, P. S., and Vogel, J. C. (1996). Expression of naked DNA in human, pig, and mouse skin. *J.Clin.Invest* **97**, 2911-2916.

Henn, V., Slupsky, J. R., Grafe, M., Anagnostopoulos, I., Forster, R., Muller-Berghaus, G., and Kroczek, R. A. (1998). CD40 ligand on activated platelets triggers an inflammatory reaction of endothelial cells. *Nature* **391**, 591-594.

Heufler, C., Koch, F., and Schuler, G. (1988). Granulocyte/macrophage colony-stimulating factor and interleukin 1 mediate the maturation of murine epidermal Langerhans cells into potent immunostimulatory dendritic cells. *J.Exp.Med.* **167**, 700-705.

Heufler, C., Koch, F., Stanzl, U., Topar, G., Wysocka, M., Trinchieri, G., Enk, A., Steinman, R. M., Romani, N., and Schuler, G. (1996). Interleukin-12 is produced by dendritic cells and mediates T helper 1 development as well as interferon-gamma production by T helper 1 cells. *Eur.J.Immunol.* **26**, 659-668.

Heufler, C., Topar, G., Koch, F., Trockenbacher, B., Kampgen, E., Romani, N., and Schuler, G. (1992). Cytokine gene expression in murine epidermal cell suspensions: interleukin 1 beta and macrophage inflammatory protein 1 alpha are selectively expressed in Langerhans cells but are differentially regulated in culture. *J.Exp.Med.* **176**, 1221-1226.

Higuchi, R., Fockler, C., Dollinger, G., and Watson, R. (1993). Kinetic PCR analysis: real-time monitoring of DNA amplification reactions. *Biotechnology (N.Y.)* **11**, 1026-1030.

Hikino, H., Miyagi, T., Hua, Y., Hirohisa, S., Gold, D. P., Li, X. K., Fujino, M., Tetsuya, T., Amemiya, H., Suzuki, S., Robb, L., Miyata, M., and Kimura, H. (2000). GM-CSF-independent development of dendritic cells from bone marrow cells in the GM-CSF-receptor-deficient mouse. *Transplant.Proc.* **32**, 2458-2459.

Hoefsmit, E. C., Duijvestijn, A. M., and Kamperdijk, E. W. (1982). Relation between langerhans cells, veiled cells, and interdigitating cells. *Immunobiology* **161**, 255-265.

Hollis, D. E. and Lyne, A. G. (1972). Acetylcholinesterase-positive langerhans cells in the epidermis and wool follicles of the sheep. *J.Invest Dermatol.* **58**, 211-217.

Hope, J. C., Kwong, L. S., Entrican, G., Wattegedera, S., Vordermeier, H. M., Sopp, P., and Howard, C. J. (2002). Development of detection methods for ruminant interleukin (IL)-12. *J.Immunol.Methods* **266**, 117-126.

Hope, J. C., Sopp, P., Collins, R. A., and Howard, C. J. (2001). Differences in the induction of CD8+ T cell responses by subpopulations of dendritic cells from afferent lymph are related to IL-1 alpha secretion. *J.Leukoc.Biol.* **69**, 271-279.

Hopkins, J. and Dutia, B. M. (1991). Workshop studies on the ovine CD1 homologue. *Vet.Immunol.Immunopathol.* **27**, 97-99.

Hopkins, J., Dutia, B. M., Bujdoso, R., and McConnell, I. (1989). In vivo modulation of CD1 and MHC class II expression by sheep afferent lymph dendritic cells. Comparison of primary and secondary immune responses. *J.Exp.Med.* **170**, 1303-1318.

Hopkins, J., Dutia, B. M., and McConnell, I. (1986). Monoclonal antibodies to sheep lymphocytes. I. Identification of MHC class II molecules on lymphoid tissue and changes in the level of class II expression on lymph-borne cells following antigen stimulation in vivo. *Immunology* **59**, 433-438.

Hopkins, J., Dutia, B. M., and Rhind, S. M. (2000). Sheep CD1 genes and proteins. *Vet.Immunol.Immunopathol.* **73**, 3-14.

Hopkins, J. and Gupta, V. K. (1996). Identification of three myeloid-specific differentiation antigens in sheep. *Vet.Immunol.Immunopathol.* **52**, 329-339.

Hornung, V., Rothenfusser, S., Britsch, S., Krug, A., Jahrsdorfer, B., Giese, T., Endres, S., and Hartmann, G. (2002). Quantitative expression of toll-like receptor 1-10 mRNA in cellular subsets of human peripheral blood mononuclear cells and sensitivity to CpG oligodeoxynucleotides. *J.Immunol.* **168**, 4531-4537.

Hoshino, K., Takeuchi, O., Kawai, T., Sanjo, H., Ogawa, T., Takeda, Y., Takeda, K., and Akira, S. (1999). Cutting edge: Toll-like receptor 4 (TLR4)-deficient mice are hyporesponsive to lipopolysaccharide: evidence for TLR4 as the Lps gene product. *J.Immunol.* **162**, 3749-3752.

Howard, C. J. and Hope, J. C. (2000). Dendritic cells, implications on function from studies of the afferent lymph veiled cell. *Vet.Immunol.Immunopathol.* **77**, 1-13.

Howard, C. J., Hope, J. C., Stephens, S. A., Gliddon, D. R., and Brooke, G. P. (2002). Co-stimulation and modulation of the ensuing immune response. *Vet.Immunol.Immunopathol.* **87**, 123-130.

Howard, C. J., Morrison, W. I., Bensaid, A., Davis, W., Eskra, L., Gerdes, J., Hadam, M., Hurley, D., Leibold, W., Letesson, J. J., and . (1991). Summary of workshop findings for leukocyte antigens of cattle. *Vet.Immunol.Immunopathol.* **27**, 21-27.

Howard, C. J., Sopp, P., Bembridge, G., Young, J., and Parsons, K. R. (1993). Comparison of CD1 monoclonal antibodies on bovine cells and tissues. *Vet.Immunol.Immunopathol.* **39**, 77-83.

Howard, C. J., Sopp, P., Brownlie, J., Kwong, L. S., Parsons, K. R., and Taylor, G. (1997). Identification of two distinct populations of dendritic cells in afferent lymph that vary in their ability to stimulate T cells. *J.Immunol.* **159**, 5372-5382.

Howard, C. J., Sopp, P., Brownlie, J., Parsons, K. R., Kwong, L. S., and Collins, R. A. (1996). Afferent lymph veiled cells stimulate proliferative responses in allogeneic CD4+ and CD8+ T cells but not gamma delta TCR+ T cells. *Immunology* **88**, 558-564.

Hsu, S. C., Obeid, O. E., Collins, M., Iqbal, M., Chargelegue, D., and Steward, M. W. (1998). Protective cytotoxic T lymphocyte responses against paramyxoviruses induced by epitope-based DNA vaccines: involvement of IFN-gamma. *Int.Immunol.* **10**, 1441-1447.

Huang, F. P. and MacPherson, G. G. (2001). Continuing education of the immune system--dendritic cells, immune regulation and tolerance. *Curr.Mol.Med.* **1**, 457-468.

Huang, F. P., Platt, N., Wykes, M., Major, J. R., Powell, T. J., Jenkins, C. D., and MacPherson, G. G. (2000). A discrete subpopulation of dendritic cells transports apoptotic intestinal epithelial cells to T cell areas of mesenteric lymph nodes. *J.Exp.Med.* **191**, 435-444.

Huang, Q., Liu, D., Majewski, P., Schulte, L. C., Korn, J. M., Young, R. A., Lander, E. S., and Hacohen, N. (2001). The plasticity of dendritic cell responses to pathogens and their components. *Science* **294**, 870-875.

Hudson, L. and Hay, F. C. (1989). "Practical Immunology." Blackwell, Oxford.

Ichikawa, M., Sugita, M., Takahashi, M., Satomi, M., Takeshita, T., Araki, T., and Takahashi, H. (2003). Breast milk macrophages spontaneously produce granulocyte-macrophage colony-stimulating factor and differentiate into dendritic cells in the presence of exogenous interleukin-4 alone. *Immunology* **108**, 189-195.

Inaba, K., Inaba, M., Romani, N., Aya, H., Deguchi, M., Ikehara, S., Muramatsu, S., and Steinman, R. M. (1992a). Generation of large numbers of dendritic cells from mouse bone marrow cultures supplemented with granulocyte/macrophage colony-stimulating factor. *J.Exp.Med.* **176**, 1693-1702.

Inaba, K., Schuler, G., Witmer, M. D., Valinksy, J., Atassi, B., and Steinman, R. M. (1986). Immunologic properties of purified epidermal Langerhans cells. Distinct requirements for stimulation of unprimed and sensitized T lymphocytes. *J.Exp.Med.* **164**, 605-613.

Inaba, K., Steinman, R. M., Pack, M. W., Aya, H., Inaba, M., Sudo, T., Wolpe, S., and Schuler, G. (1992b). Identification of proliferating dendritic cell precursors in mouse blood. *J.Exp.Med.* **175**, 1157-1167.

Inaba, K., Turley, S., Yamaide, F., Iyoda, T., Mahnke, K., Inaba, M., Pack, M., Subklewe, M., Sauter, B., Sheff, D., Albert, M., Bhardwaj, N., Mellman, I., and Steinman, R. M. (1998). Efficient presentation of phagocytosed cellular fragments on the major histocompatibility complex class II products of dendritic cells. *J.Exp.Med.* **188**, 2163-2173.

Ish-Horowicz, D. and Burke, J. F. (1981). Rapid and efficient cosmid cloning. *Nucleic Acids Res.* **9**, 2989-2998.

Ismaili, J., Olislagers, V., Poupot, R., Fournie, J. J., and Goldman, M. (2002). Human gamma delta T cells induce dendritic cell maturation. *Clin.Immunol.* **103**, 296-302.

Iwasaki, A., Torres, C. A., Ohashi, P. S., Robinson, H. L., and Barber, B. H. (1997). The dominant role of bone marrow-derived cells in CTL induction following plasmid DNA immunization at different sites. *J.Immunol.* **159**, 11-14.

Jackson, S. H., Yu, C. R., Mahdi, R. M., Ebong, S., and Egwuagu, C. E. (2004). Dendritic cell maturation requires STAT1 and is under feedback regulation by suppressors of cytokine signaling. *J.Immunol.* **172**, 2307-2315.

Jarrossay, D., Napolitani, G., Colonna, M., Sallusto, F., and Lanzavecchia, A. (2001). Specialization and complementarity in microbial molecule recognition by human myeloid and plasmacytoid dendritic cells. *Eur.J.Immunol.* **31**, 3388-3393.

Jolles, S., Christensen, J., Holman, M., Klaus, G. B., and Ager, A. (2002). Systemic treatment with anti-CD40 antibody stimulates Langerhans cell migration from the skin. *Clin.Exp.Immunol.* **129**, 519-526.

Kadowaki, N., Ho, S., Antonenko, S., Malefyt, R. W., Kastelein, R. A., Bazan, F., and Liu, Y. J. (2001). Subsets of human dendritic cell precursors express different toll-like receptors and respond to different microbial antigens. *J.Exp.Med.* **194**, 863-869.

Kalinski, P., Hilkens, C. M., Wierenga, E. A., and Kapsenberg, M. L. (1999a). T-cell priming by type-1 and type-2 polarized dendritic cells: the concept of a third signal. *Immunol.Today* **20**, 561-567.

Kalinski, P., Schuitemaker, J. H., Hilkens, C. M., Wierenga, E. A., and Kapsenberg, M. L. (1999b). Final maturation of dendritic cells is associated with impaired responsiveness to IFN-gamma and to bacterial IL-12 inducers: decreased ability of mature dendritic cells to produce IL-12 during the interaction with Th cells. *J.Immunol.* **162**, 3231-3236.

Kamath, A. T., Hanke, T., Briscoe, H., and Britton, W. J. (1999). Co-immunization with DNA vaccines expressing granulocyte-macrophage colony-stimulating factor and mycobacterial secreted

proteins enhances T cell immunity, but not protective efficacy against Mycobacterium tuberculosis. *Immunology* **96**, 511-516.

Karpati, G., Pouliot, Y., and Carpenter, S. (1988). Expression of immunoreactive major histocompatibility complex products in human skeletal muscles. *Ann.Neurol.* **23**, 64-72.

Kawai, K., Shimura, H., Minagawa, M., Ito, A., Tomiyama, K., and Ito, M. (2002). Expression of functional Toll-like receptor 2 on human epidermal keratinocytes. *J.Dermatol.Sci.* **30**, 185-194.

Kelly, K. A., Lucas, K., Hochrein, H., Metcalf, D., Wu, L., and Shortman, K. (2001). Development of dendritic cells in culture from human and murine thymic precursor cells. *Cell Mol.Biol.(Noisy.-le-grand)* **47**, 43-54.

Kelso, A. (1995). Th1 and Th2 subsets: paradigms lost? *Immunol.Today* **16**, 374-379.

Kiertscher, S. M., Gitlitz, B. J., Figlin, R. A., and Roth, M. D. (2003). Granulocyte/macrophage-colony stimulating factor and interleukin-4 expand and activate type-1 dendritic cells (DC1) when administered in vivo to cancer patients. *Int.J.Cancer* **107**, 256-261.

Kim, J. J., Trivedi, N. N., Nottingham, L. K., Morrison, L., Tsai, A., Hu, Y., Mahalingam, S., Dang, K., Ahn, L., Doyle, N. K., Wilson, D. M., Chattergoon, M. A., Chalian, A. A., Boyer, J. D., Agadjanyan, M. G., and Weiner, D. B. (1998). Modulation of amplitude and direction of in vivo immune responses by co-administration of cytokine gene expression cassettes with DNA immunogens. *Eur.J.Immunol.* **28**, 1089-1103.

Kim, J. J. and Weiner, D. B. (1997). DNA gene vaccination for HIV. *Springer Semin.Immunopathol.* **19**, 175-194.

Kim, S. H., Cho, D., and Kim, T. S. (2001). Induction of in vivo resistance to Mycobacterium avium infection by intramuscular injection with DNA encoding interleukin-18. *Immunology* **102**, 234-241.

Kimber, I., Cumberbatch, M., Dearman, R. J., Bhushan, M., and Griffiths, C. E. (2000). Cytokines and chemokines in the initiation and regulation of epidermal Langerhans cell mobilization. *Br.J.Dermatol.* **142**, 401-412.

Kirschning, C. J., Wesche, H., Merrill, A. T., and Rothe, M. (1998). Human toll-like receptor 2 confers responsiveness to bacterial lipopolysaccharide. *J.Exp.Med.* **188**, 2091-2097.

Klencke, B., Matijevic, M., Urban, R. G., Lathey, J. L., Hedley, M. L., Berry, M., Thatcher, J., Weinberg, V., Wilson, J., Darragh, T., Jay, N., Da Costa, M., and Palefsky, J. M. (2002). Encapsulated plasmid DNA treatment for human papillomavirus 16 associated anal dysplasia: a Phase I study of ZYC101. *Clin.Cancer Res.* **8**, 1028-1037.

Klinman, D. M., Barnhart, K. M., and Conover, J. (1999). CpG motifs as immune adjuvants. *Vaccine* **17**, 19-25.

Klinman, D. M., Sechler, J. M., Conover, J., Gu, M., and Rosenberg, A. S. (1998). Contribution of cells at the site of DNA vaccination to the generation of antigen-specific immunity and memory. *J.Immunol.* **160**, 2388-2392.

Klinman, D. M., Yi, A. K., Beaucage, S. L., Conover, J., and Krieg, A. M. (1996). CpG motifs present in bacteria DNA rapidly induce lymphocytes to secrete interleukin 6, interleukin 12, and interferon gamma. *Proc.Natl.Acad.Sci.U.S.A* **93**, 2879-2883.

Knight, S. C. (1984). Veiled cells--"dendritic cells" of the peripheral lymph. *Immunobiology* **168**, 349-361.

Kobayashi, Y., Matsumoto, M., Kotani, M., and Makino, T. (1999). Possible involvement of matrix metalloproteinase-9 in Langerhans cell migration and maturation. *J.Immunol.* **163**, 5989-5993.

Kohrgruber, N., Halanek, N., Groger, M., Winter, D., Rappersberger, K., Schmitt-Egenolf, M., Stingl, G., and Maurer, D. (1999). Survival, maturation, and function of CD11c- and CD11c+ peripheral blood dendritic cells are differentially regulated by cytokines. *J.Immunol.* **163**, 3250-3259.

Kronin, V., Winkel, K., Suss, G., Kelso, A., Heath, W., Kirberg, J., von Boehmer, H., and Shortman, K. (1996). A subclass of dendritic cells regulates the response of naive CD8 T cells by limiting their IL-2 production. *J.Immunol.* **157**, 3819-3827.

Krug, A., Luker, G. D., Barchet, W., Leib, D. A., Akira, S., and Colonna, M. (2004). Herpes simplex virus type 1 activates murine natural interferon-producing cells through toll-like receptor 9. *Blood* **103**, 1433-1437.

Krug, A., Towarowski, A., Britsch, S., Rothenfusser, S., Hornung, V., Bals, R., Giese, T., Engelmann, H., Endres, S., Krieg, A. M., and Hartmann, G. (2001). Toll-like receptor expression reveals CpG DNA as a unique microbial stimulus for plasmacytoid dendritic cells which synergizes with CD40 ligand to induce high amounts of IL-12. *Eur.J.Immunol.* **31**, 3026-3037.

Kumaraguru, U., Rouse, R. J., Nair, S. K., Bruce, B. D., and Rouse, B. T. (2000). Involvement of an ATP-dependent peptide chaperone in cross-presentation after DNA immunization. *J.Immunol.* **165**, 750-759.

Kupper, T. S., Ballard, D. W., Chua, A. O., McGuire, J. S., Flood, P. M., Horowitz, M. C., Langdon, R., Lightfoot, L., and Gubler, U. (1986). Human keratinocytes contain mRNA indistinguishable from monocyte interleukin 1 alpha and beta mRNA. Keratinocyte epidermal cell-derived thymocyte-activating factor is identical to interleukin 1. *J.Exp.Med.* **164**, 2095-2100.

Kusakabe, K., Xin, K. Q., Katoh, H., Sumino, K., Hagiwara, E., Kawamoto, S., Okuda, K., Miyagi, Y., Aoki, I., Nishioka, K., Klinman, D., and Okuda, K. (2000). The timing of GM-CSF expression plasmid administration influences the Th1/Th2 response induced by an HIV-1-specific DNA vaccine. *J.Immunol.* **164**, 3102-3111.

Lappin, M. B., Kimber, I., and Norval, M. (1996). The role of dendritic cells in cutaneous immunity. *Arch.Dermatol.Res.* **288**, 109-121.

Larregina, A. T., Morelli, A. E., Spencer, L. A., Logar, A. J., Watkins, S. C., Thomson, A. W., and Falo, L. D., Jr. (2001a). Dermal-resident CD14+ cells differentiate into Langerhans cells. *Nat.Immunol.* **2**, 1151-1158.

Larregina, A. T., Watkins, S. C., Erdos, G., Spencer, L. A., Storkus, W. J., Beer, S. D., and Falo, L. D., Jr. (2001b). Direct transfection and activation of human cutaneous dendritic cells. *Gene Ther.* **8**, 608-617.

Latour, S., Tanaka, H., Demeure, C., Mateo, V., Rubio, M., Brown, E. J., Maliszewski, C., Lindberg, F. P., Oldenborg, A., Ullrich, A., Delespesse, G., and Sarfati, M. (2001). Bidirectional negative regulation of human T and dendritic cells by CD47 and its cognate receptor signal-regulator protein-alpha: down-regulation of IL-12 responsiveness and inhibition of dendritic cell activation. *J.Immunol.* **167**, 2547-2554.

Lee, S. W., Cho, J. H., and Sung, Y. C. (1998). Optimal induction of hepatitis C virus envelope-specific immunity by bicistronic plasmid DNA inoculation with the granulocyte-macrophage colony-stimulating factor gene. *J.Virol.* **72**, 8430-8436.

Lens, J. W., Drexhage, H. A., Benson, W., and Balfour, B. M. (1983). A study of cells present in lymph draining from a contact allergic reaction in pigs sensitized to DNFB. *Immunology* **49**, 415-422.

Lisinski, T. J. and Furie, M. B. (2002). Interleukin-10 inhibits proinflammatory activation of endothelium in response to Borrelia burgdorferi or lipopolysaccharide but not interleukin-1beta or tumor necrosis factor alpha. *J.Leukoc.Biol.* **72**, 503-511.

Liu, H. M., Newbrough, S. E., Bhatia, S. K., Dahle, C. E., Krieg, A. M., and Weiner, G. J. (1998a). Immunostimulatory CpG oligodeoxynucleotides enhance the immune response to vaccine strategies involving granulocyte-macrophage colony-stimulating factor. *Blood* **92**, 3730-3736.

Liu, K., Iyoda, T., Saternus, M., Kimura, Y., Inaba, K., and Steinman, R. M. (2002). Immune tolerance after delivery of dying cells to dendritic cells in situ. *J.Exp.Med.* **196**, 1091-1097.

Liu, L., Rich, B. E., Inobe, J., Chen, W., and Weiner, H. L. (1998b). Induction of Th2 cell differentiation in the primary immune response: dendritic cells isolated from adherent cell culture treated with IL-10 prime naive CD4+ T cells to secrete IL-4. *Int.Immunol.* **10**, 1017-1026.

Liu, L., Zhang, M., Jenkins, C., and MacPherson, G. G. (1998c). Dendritic cell heterogeneity in vivo: two functionally different dendritic cell populations in rat intestinal lymph can be distinguished by CD4 expression. *J.Immunol.* **161**, 1146-1155.

Liu, L., Zhou, X., Shi, J., Xie, X., and Yuan, Z. (2003). Toll-like receptor-9 induced by physical trauma mediates release of cytokines following exposure to CpG motif in mouse skin. *Immunology* **110**, 341-347.

Liu, Y. J., Kadowaki, N., Rissoan, M. C., and Soumelis, V. (2000). T cell activation and polarization by DC1 and DC2. *Curr.Top.Microbiol.Immunol.* **251**, 149-159.

Liu, Y. J., Kanzler, H., Soumelis, V., and Gilliet, M. (2001). Dendritic cell lineage, plasticity and cross-regulation. *Nat.Immunol.* **2**, 585-589.

Lord, E. M., Yeh, K. Y., Moran, J. A., Storozynsky, E., and Frelinger, J. G. (1998). IL-3-mediated enhancement of particulate antigen presentation by macrophages. *J.Immunother.* **21**, 205-210.

Luger, T. A., Bhardwaj, R. S., Grabbe, S., and Schwarz, T. (1996). Regulation of the immune response by epidermal cytokines and neurohormones. *J.Dermatol.Sci.* **13**, 5-10.

Lukas, M., Stossel, H., Hefel, L., Imamura, S., Fritsch, P., Sepp, N. T., Schuler, G., and Romani, N. (1996). Human cutaneous dendritic cells migrate through dermal lymphatic vessels in a skin organ culture model. *J.Invest Dermatol.* **106**, 1293-1299.

Lund, J., Sato, A., Akira, S., Medzhitov, R., and Iwasaki, A. (2003). Toll-like receptor 9-mediated recognition of Herpes simplex virus-2 by plasmacytoid dendritic cells. *J.Exp.Med.* **198**, 513-520.

Lund, J. M., Alexopoulou, L., Sato, A., Karow, M., Adams, N. C., Gale, N. W., Iwasaki, A., and Flavell, R. A. (2004). Recognition of single-stranded RNA viruses by Toll-like receptor 7. *Proc.Natl.Acad.Sci.U.S.A* **101**, 5598-5603.

Lutz, M. B., Assmann, C. U., Girolomoni, G., and Ricciardi-Castagnoli, P. (1996). Different cytokines regulate antigen uptake and presentation of a precursor dendritic cell line. *Eur.J.Immunol.* **26**, 586-594.

Lyne, A. G. and Chase, H. B. (1966). Branched cells in the epidermis of the sheep. *Nature* **209**, 1357-1358.

Macardle, P. J., Chen, Z., Shih, C. Y., Huang, C. M., Weedon, H., Sun, Q., Lopez, A. F., and Zola, H. (1996). Characterization of human leucocytes bearing the IL-3 receptor. *Cell Immunol.* **168**, 59-68.

Macatonia, S. E., Hosken, N. A., Litton, M., Vieira, P., Hsieh, C. S., Culpepper, J. A., Wysocka, M., Trinchieri, G., Murphy, K. M., and O'Garra, A. (1995). Dendritic cells produce IL-12 and direct the development of Th1 cells from naive CD4+ T cells. *J.Immunol.* **154**, 5071-5079.

Macatonia, S. E., Knight, S. C., Edwards, A. J., Griffiths, S., and Fryer, P. (1987). Localization of antigen on lymph node dendritic cells after exposure to the contact sensitizer fluorescein isothiocyanate. Functional and morphological studies. *J.Exp.Med.* **166**, 1654-1667.

Mach, N., Gillessen, S., Wilson, S. B., Sheehan, C., Mihm, M., and Dranoff, G. (2000). Differences in dendritic cells stimulated in vivo by tumors engineered to secrete granulocyte-macrophage colony-stimulating factor or Flt3-ligand. *Cancer Res.* **60**, 3239-3246.

MacHugh, N. D., Bensaid, A., Davis, W. C., Howard, C. J., Parsons, K. R., Jones, B., and Kaushal, A. (1988). Characterization of a bovine thymic differentiation antigen analogous to CD1 in the human. *Scand.J.Immunol.* **27**, 541-547.

Mackay, C. R. and Hein, W. R. (1989). A large proportion of bovine T cells express the gamma delta T cell receptor and show a distinct tissue distribution and surface phenotype. *Int.Immunol.* **1**, 540-545.

Mackay, C. R., Hein, W. R., Brown, M. H., and Matzinger, P. (1988a). Unusual expression of CD2 in sheep: implications for T cell interactions. *Eur.J.Immunol.* **18**, 1681-1688.

Mackay, C. R., Kimpton, W. G., Brandon, M. R., and Cahill, R. N. (1988b). Lymphocyte subsets show marked differences in their distribution between blood and the afferent and efferent lymph of peripheral lymph nodes. *J.Exp.Med.* **167**, 1755-1765.

Mackay, C. R., Marston, W. L., and Dudler, L. (1990). Naive and memory T cells show distinct pathways of lymphocyte recirculation. *J.Exp.Med.* **171**, 801-817.

MacPherson, G. G., Jenkins, C. D., Stein, M. J., and Edwards, C. (1995). Endotoxin-mediated dendritic cell release from the intestine. Characterization of released dendritic cells and TNF dependence. *J.Immunol.* **154**, 1317-1322.

Macpherson, I. and Stoker, M. (1962). Polyoma transformation of hamster cell clones--an investigation of genetic factors affecting cell competence. *Virology* **16**, 147-151.

Maddox, J. F., Mackay, C. R., and Brandon, M. R. (1985). Surface antigens, SBU-T4 and SBU-T8, of sheep T lymphocyte subsets defined by monoclonal antibodies. *Immunology* **55**, 739-748.

Maecker, H. T., Umetsu, D. T., DeKruyff, R. H., and Levy, S. (1998). Cytotoxic T cell responses to DNA vaccination: dependence on antigen presentation via class II MHC. *J.Immunol.* **161**, 6532-6536.

Maeda, N., Nigou, J., Herrmann, J. L., Jackson, M., Amara, A., Lagrange, P. H., Puzo, G., Gicquel, B., and Neyrolles, O. (2003). The cell surface receptor DC-SIGN discriminates between Mycobacterium species through selective recognition of the mannose caps on lipoarabinomannan. *J.Biol.Chem.* **278**, 5513-5516.

Maldonado-Lopez, R., De Smedt, T., Michel, P., Godfroid, J., Pajak, B., Heirman, C., Thielemans, K., Leo, O., Urbain, J., and Moser, M. (1999). CD8alpha+ and CD8alpha- subclasses of dendritic cells direct the development of distinct T helper cells in vivo. *J.Exp.Med.* **189**, 587-592.

Maldonado-Lopez, R., Maliszewski, C., Urbain, J., and Moser, M. (2001). Cytokines regulate the capacity of CD8alpha(+) and CD8alpha(-) dendritic cells to prime Th1/Th2 cells in vivo. *J.Immunol.* **167**, 4345-4350.

Manickasingham, S. P., Edwards, A. D., Schulz, O., and Reis e Sousa (2003). The ability of murine dendritic cell subsets to direct T helper cell differentiation is dependent on microbial signals. *Eur.J.Immunol.* **33**, 101-107.

Manigold, T., Bocker, U., Traber, P., Dong-Si, T., Kurimoto, M., Hanck, C., Singer, M. V., and Rossol, S. (2000). Lipopolysaccharide/endotoxin induces IL-18 via CD14 in human peripheral blood mononuclear cells in vitro. *Cytokine* **12**, 1788-1792.

Manna, P. P., Duffy, B., Olack, B., Lowell, J., and Mohanakumar, T. (2001). Activation of human dendritic cells by porcine aortic endothelial cells: transactivation of naive T cells through costimulation and cytokine generation. *Transplantation* **72**, 1563-1571.

Manna, P. P., Steward, N., Lowell, J., and Mohanakumar, T. (2002). Differentiation and functional maturation of human CD14(+) adherent peripheral blood monocytes by xenogeneic endothelial cells: up-regulation of costimulation, cytokine generation, and toll-like receptors. *Transplantation* **74**, 243-252.

Manz, M. G., Traver, D., Miyamoto, T., Weissman, I. L., and Akashi, K. (2001). Dendritic cell potentials of early lymphoid and myeloid progenitors. *Blood* **97**, 3333-3341.

Martinez-Moczygemba, M. and Huston, D. P. (2003). Biology of common beta receptor-signaling cytokines: IL-3, IL-5, and GM-CSF. *J.Allergy Clin.Immunol.* **112**, 653-665.

Matzinger, P. (1994). Tolerance, danger, and the extended family. *Annu.Rev.Immunol.* **12**, 991-1045.

Mawby, W. J., Holmes, C. H., Anstee, D. J., Spring, F. A., and Tanner, M. J. (1994). Isolation and characterization of CD47 glycoprotein: a multispanning membrane protein which is the same as integrin-associated protein (IAP) and the ovarian tumour marker OA3. *Biochem.J.* **304 (Pt 2)**, 525-530.

McInnes, C., Haig, D., and Logan, M. (1993). The cloning and expression of the gene for ovine interleukin-3 (multi-CSF) and a comparison of the in vitro hematopoietic activity of ovine IL-3 with ovine GM-CSF and human M-CSF. *Exp.Hematol.* **21**, 1528-1534.

McKeever, D. J., Awino, E., and Morrison, W. I. (1992). Afferent lymph veiled cells prime CD4+ T cell responses in vivo. *Eur.J.Immunol.* **22**, 3057-3061.

McKeever, D. J., MacHugh, N. D., Goddeeris, B. M., Awino, E., and Morrison, W. I. (1991). Bovine afferent lymph veiled cells differ from blood monocytes in phenotype and accessory function. *J.Immunol.* **147**, 3703-3709.

Medzhitov, R. and Janeway, C. A., Jr. (1999). Innate immune induction of the adaptive immune response. *Cold Spring Harb.Symp.Quant.Biol.* **64**, 429-435.

Medzhitov, R., Preston-Hurlburt, P., Kopp, E., Stadlen, A., Chen, C., Ghosh, S., and Janeway, C. A., Jr. (1998). MyD88 is an adaptor protein in the hToll/IL-1 receptor family signaling pathways. *Mol.Cell* **2**, 253-258.

Mellman, I. and Steinman, R. M. (2001). Dendritic cells: specialized and regulated antigen processing machines. *Cell* **106**, 255-258.

Mena, A., Andrew, M. E., and Coupar, B. E. (2001). Rapid dissemination of intramuscularly inoculated DNA vaccines. *Immunol.Cell Biol.* **79**, 87-89.

Merad, M., Manz, M. G., Karsunky, H., Wagers, A., Peters, W., Charo, I., Weissman, I. L., Cyster, J G., and Engleman, E. G. (2002). Langerhans cells renew in the skin throughout life under steady-state conditions. *Nat.Immunol.* **3**, 1135-1141.

Mincheff, M., Tchakarov, S., Zoubak, S., Loukinov, D., Botev, C., Altankova, I., Georgiev, G., Petrov, S., and Meryman, H. T. (2000). Naked DNA and adenoviral immunizations for immunotherapy of prostate cancer: a phase I/II clinical trial. *Eur.Urol.* **38**, 208-217.

Mitsui, H., Watanabe, T., Saeki, H., Mori, K., Fujita, H., Tada, Y., Asahina, A., Nakamura, K., and Tamaki, K. (2004). Differential expression and function of Toll-like receptors in Langerhans cells: comparison with splenic dendritic cells. *J.Invest Dermatol.* **122**, 95-102.

Miyake, K. (2004). Endotoxin recognition molecules, Toll-like receptor 4-MD-2. *Semin.Immunol.* **16**, 11-16.

Mohty, M., Vialle-Castellano, A., Nunes, J. A., Isnardon, D., Olive, D., and Gaugler, B. (2003). IFN-alpha skews monocyte differentiation into Toll-like receptor 7-expressing dendritic cells with potent functional activities. *J.Immunol.* **171**, 3385-3393.

Mollah, Z. U., Aiba, S., Nakagawa, S., Mizuashi, M., Ohtani, T., Yoshino, Y., and Tagami, H. (2003). Interleukin-3 in cooperation with transforming growth factor beta induces granulocyte macrophage colony stimulating factor independent differentiation of human CD34+ hematopoietic progenitor cells into dendritic cells with features of Langerhans cells. *J.Invest Dermatol.* **121**, 1397-1401.

Montgomery, D. L., Huygen, K., Yawman, A. M., Deck, R. R., DeWitt, C. M., Content, J., Liu, M. A., and Ulmer, J. B. (1997). Induction of humoral and cellular immune responses by vaccination with M. tuberculosis antigen 85 DNA. *Cell Mol.Biol.(Noisy.-le-grand)* **43**, 285-292.

Moore, A. C., Kong, W. P., Chakrabarti, B. K., and Nabel, G. J. (2002). Effects of antigen and genetic adjuvants on immune responses to human immunodeficiency virus DNA vaccines in mice. *J.Virol.* **76**, 243-250.

Morse, M. A., Mosca, P. J., Clay, T. M., and Lyerly, H. K. (2002). Dendritic cell maturation in active immunotherapy strategies. *Expert.Opin.Biol.Ther.* **2**, 35-43.

Murphy, E. E., Terres, G., Macatonia, S. E., Hsieh, C. S., Mattson, J., Lanier, L., Wysocka, M., Trinchieri, G., Murphy, K., and O'Garra, A. (1994). B7 and interleukin 12 cooperate for proliferation and interferon gamma production by mouse T helper clones that are unresponsive to B7 costimulation. *J.Exp.Med.* **180**, 223-231.

Mwangi, W., Brown, W. C., Lewin, H. A., Howard, C. J., Hope, J. C., Baszler, T. V., Caplazi, P., Abbott, J., and Palmer, G. H. (2002). DNA-encoded fetal liver tyrosine kinase 3 ligand and granulocyte macrophage-colony-stimulating factor increase dendritic cell recruitment to the inoculation site and enhance antigen-specific CD4+ T cell responses induced by DNA vaccination of outbred animals. *J.Immunol.* **169**, 3837-3846.

Mwau, M., Cebere, I., Sutton, J., Chikoti, P., Winstone, N., Wee, E. G., Beattie, T., Chen, Y. H., Dorrell, L., McShane, H., Schmidt, C., Brooks, M., Patel, S., Roberts, J., Conlon, C., Rowland-Jones, S. L., Bwayo, J. J., McMichael, A. J., and Hanke, T. (2004). A human immunodeficiency virus 1 (HIV-1) clade A vaccine in clinical trials: stimulation of HIV-specific T-cell responses by DNA and recombinant modified vaccinia virus Ankara (MVA) vaccines in humans. *J.Gen.Virol.* **85**, 911-919.

Naessens, J. and Howard, C. J. (1991). Individual antigens of cattle. Monoclonal antibodies reacting with bovine B cells (BoWC3, BoWC4 and BoWC5). *Vet.Immunol.Immunopathol.* **27**, 77-85.

Nakano, H., Yanagita, M., and Gunn, M. D. (2001). CD11c(+)B220(+)Gr-1(+) cells in mouse lymph nodes and spleen display characteristics of plasmacytoid dendritic cells. *J.Exp.Med.* **194**, 1171-1178.

Nasi, M. L., Lieberman, P., Busam, K. J., Prieto, V., Panageas, K. S., Lewis, J. J., Houghton, A. N., and Chapman, P. B. (1999). Intradermal injection of granulocyte-macrophage colony-stimulating factor (GM-CSF) in patients with metastatic melanoma recruits dendritic cells. *Cytokines Cell Mol.Ther.* **5**, 139-144.

Nestle, F. O., Alijagic, S., Gilliet, M., Sun, Y., Grabbe, S., Dummer, R., Burg, G., and Schadendorf, D. (1998). Vaccination of melanoma patients with peptide- or tumor lysate-pulsed dendritic cells. *Nat.Med.* **4**, 328-332.

Nichols, W. W., Ledwith, B. J., Manam, S. V., and Troilo, P. J. (1995). Potential DNA vaccine integration into host cell genome. *Ann.N.Y.Acad.Sci.* **772**, 30-39.

Nobiron, I., Thompson, I., Brownlie, J., and Collins, M. E. (2003). DNA vaccination against bovine viral diarrhoea virus induces humoral and cellular responses in cattle with evidence for protection against viral challenge. *Vaccine* **21**, 2082-2092.

O'Keeffe, M., Hochrein, H., Vremec, D., Pooley, J., Evans, R., Woulfe, S., and Shortman, K. (2002). Effects of administration of progenipoietin 1, Flt-3 ligand, granulocyte colony-stimulating factor, and pegylated granulocyte-macrophage colony-stimulating factor on dendritic cell subsets in mice. *Blood* **99**, 2122-2130.

O'Neill, L. A. (2004). TLRs: Professor Mechnikov, sit on your hat. *Trends Immunol.* **25**, 687-693.

O'Sullivan, G. M., Boswell, C. M., and Halliday, G. M. (2000). Langerhans cell migration is modulated by N-sulfated glucosamine moieties in heparin. *Exp.Dermatol.* **9**, 25-33.

Okamura, H., Tsutsi, H., Komatsu, T., Yutsudo, M., Hakura, A., Tanimoto, T., Torigoe, K., Okura, T., Nukada, Y., Hattori, K., and . (1995). Cloning of a new cytokine that induces IFN-gamma production by T cells. *Nature* **378**, 88-91.

Olweus, J., BitMansour, A., Warnke, R., Thompson, P. A., Carballido, J., Picker, L. J., and Lund-Johansen, F. (1997). Dendritic cell ontogeny: a human dendritic cell lineage of myeloid origin. *Proc.Natl.Acad.Sci.U.S.A* **94**, 12551-12556.

Oppmann, B., Lesley, R., Blom, B., Timans, J. C., Xu, Y., Hunte, B., Vega, F., Yu, N., Wang, J., Singh, K., Zonin, F., Vaisberg, E., Churakova, T., Liu, M., Gorman, D., Wagner, J., Zurawski, S., Liu, Y., Abrams, J. S., Moore, K. W., Rennick, D., Waal-Malefyt, R., Hannum, C., Bazan, J. F., and Kastelein, R. A. (2000). Novel p19 protein engages IL-12p40 to form a cytokine, IL-23, with biological activities similar as well as distinct from IL-12. *Immunity.* **13**, 715-725.

Ostman, A. and Bohmer, F. D. (2001). Regulation of receptor tyrosine kinase signaling by protein tyrosine phosphatases. *Trends Cell Biol.* **11**, 258-266.

Ou-Yang, P., Hwang, L. H., Tao, M. H., Chiang, B. L., and Chen, D. S. (2002). Co-delivery of GM-CSF gene enhances the immune responses of hepatitis C viral core protein-expressing DNA vaccine: role of dendritic cells. *J.Med.Virol.* **66**, 320-328.

Ozinsky, A., Underhill, D. M., Fontenot, J. D., Hajjar, A. M., Smith, K. D., Wilson, C. B., Schroeder, L., and Aderem, A. (2000). The repertoire for pattern recognition of pathogens by the innate immune system is defined by cooperation between toll-like receptors. *Proc.Natl.Acad.Sci.U.S.A* **97**, 13766-13771.

Parajuli, P., Mosley, R. L., Pisarev, V., Chavez, J., Ulrich, A., Varney, M., Singh, R. K., and Talmadge, J. E. (2001). Flt3 ligand and granulocyte-macrophage colony-stimulating factor preferentially expand and stimulate different dendritic and T-cell subsets. *Exp.Hematol.* **29**, 1185-1193.

Parajuli, P., Nishioka, Y., Nishimura, N., Singh, S. M., Hanibuchi, M., Nokihara, H., Yanagawa, H., and Sone, S. (1999). Cytolysis of human dendritic cells by autologous lymphokine-activated killer cells: participation of both T cells and NK cells in the killing. *J.Leukoc.Biol.* **65**, 764-770.

Parsons, K. R., Bembridge, G., Sopp, P., and Howard, C. J. (1993). Studies of monoclonal antibodies identifying two novel bovine lymphocyte antigen differentiation clusters: workshop clusters (WC) 6 and 7. *Vet.Immunol.Immunopathol.* **39**, 187-192.

Patel, V., Smith, R. E., Serra, A., Brooke, G., Howard, C. J., and Rigley, K. P. (2002). MyD-1 (SIRPalpha) regulates T cell function in the absence of exogenous danger signals, via a TNFalpha-dependent pathway. *Eur.J.Immunol.* **32**, 1865-1872.

Perales, M. A., Fantuzzi, G., Goldberg, S. M., Turk, M. J., Mortazavi, F., Busam, K., Houghton, A. N., Dinarello, C. A., and Wolchok, J. D. (2002). GM-CSF DNA induces specific patterns of cytokines and chemokines in the skin: implications for DNA vaccines. *Cytokines Cell Mol.Ther.* **7**, 125-133.

Pillarisetty, V. G., Miller, G., Shah, A. B., and DeMatteo, R. P. (2003). GM-CSF expands dendritic cells and their progenitors in mouse liver. *Hepatology* **37**, 641-652.

Pinedo, H. M., Buter, J., Luykx-de Bakker, S. A., Pohlmann, P. R., van Hensbergen, Y., Heideman, D. A., van Diest, P. J., de Gruijl, T. D., and van der, W. E. (2003). Extended neoadjuvant chemotherapy in locally advanced breast cancer combined with GM-CSF: effect on tumour-draining lymph node dendritic cells. *Eur.J.Cancer* **39**, 1061-1067.

Pober, J. S., Gimbrone, M. A., Jr., Collins, T., Cotran, R. S., Ault, K. A., Fiers, W., Krensky, A. M., Clayberger, C., Reiss, C. S., and Burakoff, S. J. (1984). Interactions of T lymphocytes with human vascular endothelial cells: role of endothelial cells surface antigens. *Immunobiology* **168**, 483-494.

Poltorak, A., He, X., Smirnova, I., Liu, M. Y., Van Huffel, C., Du, X., Birdwell, D., Alejos, E., Silva, M., Galanos, C., Freudenberg, M., Ricciardi-Castagnoli, P., Layton, B., and Beutler, B. (1998). Defective LPS signaling in C3H/HeJ and C57BL/10ScCr mice: mutations in Tlr4 gene. *Science* **282**, 2085-2088.

Porgador, A., Irvine, K. R., Iwasaki, A., Barber, B. H., Restifo, N. P., and Germain, R. N. (1998). Predominant role for directly transfected dendritic cells in antigen presentation to CD8+ T cells after gene gun immunization. *J.Exp.Med.* **188**, 1075-1082.

Powell, T. J., Jenkins, C. D., Hattori, R., and MacPherson, G. G. (2003). Rat bone marrow-derived dendritic cells, but not ex vivo dendritic cells, secrete nitric oxide and can inhibit T-cell proliferation. *Immunology* **109**, 197-208.

Pugh, C. W., MacPherson, G. G., and Steer, H. W. (1983). Characterization of nonlymphoid cells derived from rat peripheral lymph. *J.Exp.Med.* **157**, 1758-1779.

Pulendran, B., Smith, J. L., Caspary, G., Brasel, K., Pettit, D., Maraskovsky, E., and Maliszewski, C. R. (1999). Distinct dendritic cell subsets differentially regulate the class of immune response in vivo. *Proc.Natl.Acad.Sci.U.S.A* **96**, 1036-1041.

Puri, N. K., Gogolin-Ewens, K. J., and Brandon, M. R. (1987). Monoclonal antibodies to sheep MHC class I and class II molecules: biochemical characterization of three class I gene products and four distinct subpopulations of class II molecules. *Vet.Immunol.Immunopathol.* **15**, 59-86.

Qureshi, S. T., Lariviere, L., Leveque, G., Clermont, S., Moore, K. J., Gros, P., and Malo, D. (1999). Endotoxin-tolerant mice have mutations in Toll-like receptor 4 (Tlr4). *J.Exp.Med.* **189**, 615-625.

Radsak, M., Iking-Konert, C., Stegmaier, S., Andrassy, K., and Hansch, G. M. (2000). Polymorphonuclear neutrophils as accessory cells for T-cell activation: major histocompatibility complex class II restricted antigen-dependent induction of T-cell proliferation. *Immunology* **101**, 521-530.

Rand, M. L., Warren, J. S., Mansour, M. K., Newman, W., and Ringler, D. J. (1996). Inhibition of T cell recruitment and cutaneous delayed-type hypersensitivity-induced inflammation with antibodies to monocyte chemoattractant protein-1. *Am.J.Pathol.* **148**, 855-864.

Randolph, G. J., Beaulieu, S., Lebecque, S., Steinman, R. M., and Muller, W. A. (1998). Differentiation of monocytes into dendritic cells in a model of transendothelial trafficking. *Science* **282**, 480-483.

Raviprakash, K., Ewing, D., Simmons, M., Porter, K. R., Jones, T. R., Hayes, C. G., Stout, R., and Murphy, G. S. (2003). Needle-free Biojector injection of a dengue virus type 1 DNA vaccine with human immunostimulatory sequences and the GM-CSF gene increases immunogenicity and protection from virus challenge in Aotus monkeys. *Virology* **315**, 345-352.

Raz, E., Carson, D. A., Parker, S. E., Parr, T. B., Abai, A. M., Aichinger, G., Gromkowski, S. H., Singh, M., Lew, D., and Yankauckas, M. A. (1994). Intradermal gene immunization: the possible role of DNA uptake in the induction of cellular immunity to viruses. *Proc.Natl.Acad.Sci.U.S.A* **91**, 9519-9523.

Reinhold, M. I., Lindberg, F. P., Kersh, G. J., Allen, P. M., and Brown, E. J. (1997). Costimulation of T cell activation by integrin-associated protein (CD47) is an adhesion-dependent, CD28-independent signaling pathway. *J.Exp.Med.* **185**, 1-11.

Reis e Sousa (2004). Activation of dendritic cells: translating innate into adaptive immunity. *Curr.Opin.Immunol.* **16**, 21-25.

Reis e Sousa, Stahl, P. D., and Austyn, J. M. (1993). Phagocytosis of antigens by Langerhans cells in vitro. *J.Exp.Med.* **178**, 509-519.

Rhind, S. M. Molecular analysis of ovine CD1 expression. 1996. University of Edinburgh.

Ref Type: Thesis/Dissertation

Rhind, S. M., Dutia, B. M., Howard, C. J., and Hopkins, J. (1996b). Discrimination of two subsets of CD1 molecules in the sheep. *Vet.Immunol.Immunopathol.* **52**, 265-270.

Rhind, S. M., Dutia, B. M., Howard, C. J., and Hopkins, J. (1996a). Discrimination of two subsets of CD1 molecules in the sheep. *Vet.Immunol.Immunopathol.* **52**, 265-270.

Rincon, M., Anguita, J., Nakamura, T., Fikrig, E., and Flavell, R. A. (1997). Interleukin (IL)-6 directs the differentiation of IL-4-producing CD4+ T cells. *J.Exp.Med.* **185**, 461-469.

Rissoan, M. C., Soumelis, V., Kadowaki, N., Grouard, G., Briere, F., de Waal, M. R., and Liu, Y. J. (1999). Reciprocal control of T helper cell and dendritic cell differentiation. *Science* **283**, 1183-1186.

Rivier, A., Chanez, P., Pene, J., Michel, F. B., Godard, P., Dugas, B., and Bousquet, J. (1994). Modulation of phenotypic and functional properties of normal human mononuclear phagocytes by granulocyte-macrophage colony-stimulating factor. *Int.Arch.Allergy Immunol.* **104**, 27-32.

Roake, J. A., Rao, A. S., Morris, P. J., Larsen, C. P., Hankins, D. F., and Austyn, J. M. (1995). Dendritic cell loss from nonlymphoid tissues after systemic administration of lipopolysaccharide, tumor necrosis factor, and interleukin 1. *J.Exp.Med.* **181**, 2237-2247.

Romani, N., Gruner, S., Brang, D., Kampgen, E., Lenz, A., Trockenbacher, B., Konwalinka, G., Fritsch, P. O., Steinman, R. M., and Schuler, G. (1994). Proliferating dendritic cell progenitors in human blood. *J.Exp.Med.* **180**, 83-93.

Romani, N., Koide, S., Crowley, M., Witmer-Pack, M., Livingstone, A. M., Fathman, C. G., Inaba, K., and Steinman, R. M. (1989). Presentation of exogenous protein antigens by dendritic cells to T cell clones. Intact protein is presented best by immature, epidermal Langerhans cells. *J.Exp.Med.* **169**, 1169-1178.

Ruco, L. P., Uccini, S., and Baroni, C. D. (1989). The Langerhans' cells. *Allergy* **44 Suppl 9**, 27-30.

Rush, C., Mitchell, T., and Garside, P. (2002). Efficient priming of CD4+ and CD8+ T cells by DNA vaccination depends on appropriate targeting of sufficient levels of immunologically relevant antigen to appropriate processing pathways. *J.Immunol.* **169**, 4951-4960.

Sakai, T., Horii, T., Hisaeda, H., Zhang, M., Ishii, K., Nakano, Y., Maekawa, Y., Izumi, K., Nitta, Y., Miyazaki, J., and Himeno, K. (1999). DNA immunization with Plasmodium falciparum serine repeat antigen: regulation of humoral immune response by coinoculation of cytokine expression plasmid. *Parasitol.Int.* **48**, 27-33.

Salgado, C. G., Nakamura, K., Sugaya, M., Tada, Y., Asahina, A., Fukuda, S., Koyama, Y., Irie, S., and Tamaki, K. (1999). Differential effects of cytokines and immunosuppressive drugs on CD40, B7-1, and B7-2 expression on purified epidermal Langerhans cells1. *J.Invest Dermatol.* **113**, 1021-1027.

Sallusto, F., Cella, M., Danieli, C., and Lanzavecchia, A. (1995). Dendritic cells use macropinocytosis and the mannose receptor to concentrate macromolecules in the major histocompatibility complex class II compartment: downregulation by cytokines and bacterial products. *J.Exp.Med.* **182**, 389-400.

Sallusto, F. and Lanzavecchia, A. (1994). Efficient presentation of soluble antigen by cultured human dendritic cells is maintained by granulocyte/macrophage colony-stimulating factor plus interleukin 4 and downregulated by tumor necrosis factor alpha. *J.Exp.Med.* **179**, 1109-1118.

Sambrook, J., Fritsch, E. F., and Maniatis, T. (1989). "Molecular Cloning: A Laboratory manual." Cold Spring Harbor Laboratory Press, Cold Spring Harbor, N.Y.

Santiago-Schwarz, F., Belilos, E., Diamond, B., and Carsons, S. E. (1992). TNF in combination with GM-CSF enhances the differentiation of neonatal cord blood stem cells into dendritic cells and macrophages. *J.Leukoc.Biol.* **52**, 274-281.

Santin, A. D., Hermonat, P. L., Ravaggi, A., Chiriva-Internati, M., Cannon, M. J., Hiserodt, J. C., Pecorelli, S., and Parham, G. P. (1999). Expression of surface antigens during the differentiation of human dendritic cells vs macrophages from blood monocytes in vitro. *Immunobiology* **200**, 187-204.

Sasaki, S., Takeshita, F., Xin, K. Q., Ishii, N., and Okuda, K. (2003). Adjuvant formulations and delivery systems for DNA vaccines. *Methods* **31**, 243-254.

Sato, S., Sugiyama, M., Yamamoto, M., Watanabe, Y., Kawai, T., Takeda, K., and Akira, S. (2003). Toll/IL-1 receptor domain-containing adaptor inducing IFN-beta (TRIF) associates with TNF receptor-associated factor 6 and TANK-binding kinase 1, and activates two distinct transcription factors, NF-kappa B and IFN-regulatory factor-3, in the Toll-like receptor signaling. *J.Immunol.* **171**, 4304-4310.

Sato, Y., Roman, M., Tighe, H., Lee, D., Corr, M., Nguyen, M. D., Silverman, G. J., Lotz, M., Carson, D. A., and Raz, E. (1996). Immunostimulatory DNA sequences necessary for effective intradermal gene immunization. *Science* **273**, 352-354.

Saunders, D., Lucas, K., Ismaili, J., Wu, L., Maraskovsky, E., Dunn, A., and Shortman, K. (1996). Dendritic cell development in culture from thymic precursor cells in the absence of granulocyte/macrophage colony-stimulating factor. *J.Exp.Med.* **184**, 2185-2196.

Sauter, B., Albert, M. L., Francisco, L., Larsson, M., Somersan, S., and Bhardwaj, N. (2000). Consequences of cell death: exposure to necrotic tumor cells, but not primary tissue cells or apoptotic cells, induces the maturation of immunostimulatory dendritic cells. *J.Exp.Med.* **191**, 423-434.

Scarozza, A. M., Ramsingh, A. I., Wicher, V., and Wicher, K. (1998). Spontaneous cytokine gene expression in normal guinea pig blood and tissues. *Cytokine* **10**, 851-859.

Scheerlinck, J. P., Casey, G., McWaters, P., Kelly, J., Woollard, D., Lightowlers, M. W., Tennent, J. M., and Chaplin, P. J. (2001). The immune response to a DNA vaccine can be modulated by co-delivery of cytokine genes using a DNA prime-protein boost strategy. *Vaccine* **19**, 4053-4060.

Scheerlinck, J. P., Karlis, J., Tjelle, T. E., Presidente, P. J., Mathiesen, I., and Newton, S. E. (2004). In vivo electroporation improves immune responses to DNA vaccination in sheep. *Vaccine* **22**, 1820-1825.

Schlecht, G., Leclerc, C., and Dadaglio, G. (2001). Induction of CTL and nonpolarized Th cell responses by CD8alpha(+) and CD8alpha(-) dendritic cells. *J.Immunol.* **167**, 4215-4221.

Schnurr, M., Then, F., Galambos, P., Scholz, C., Siegmund, B., Endres, S., and Eigler, A. (2000). Extracellular ATP and TNF-alpha synergize in the activation and maturation of human dendritic cells. *J.Immunol.* **165**, 4704-4709.

Schoenhaut, D. S., Chua, A. O., Wolitzky, A. G., Quinn, P. M., Dwyer, C. M., McComas, W., Familletti, P. C., Gately, M. K., and Gubler, U. (1992). Cloning and expression of murine IL-12. *J.Immunol.* **148**, 3433-3440.

Schreiber, S., Kilgus, O., Payer, E., Kutil, R., Elbe, A., Mueller, C., and Stingl, G. (1992). Cytokine pattern of Langerhans cells isolated from murine epidermal cell cultures. *J.Immunol.* **149**, 3524-3534.

Schuler, G. and Steinman, R. M. (1985). Murine epidermal Langerhans cells mature into potent immunostimulatory dendritic cells in vitro. *J.Exp.Med.* **161**, 526-546.

Seder, R. A., Gazzinelli, R., Sher, A., and Paul, W. E. (1993). Interleukin 12 acts directly on CD4+ T cells to enhance priming for interferon gamma production and diminishes interleukin 4 inhibition of such priming. *Proc.Natl.Acad.Sci.U.S.A* **90**, 10188-10192.

Seiffert, M., Cant, C., Chen, Z., Rappold, I., Brugger, W., Kanz, L., Brown, E. J., Ullrich, A., and Buhring, H. J. (1999). Human signal-regulatory protein is expressed on normal, but not on subsets of leukemic myeloid cells and mediates cellular adhesion involving its counterreceptor CD47. *Blood* **94**, 3633-3643.

Selvaraj, P., Plunkett, M. L., Dustin, M., Sanders, M. E., Shaw, S., and Springer, T. A. (1987). The T lymphocyte glycoprotein CD2 binds the cell surface ligand LFA-3. *Nature* **326**, 400-403.

Shen, Z., Reznikoff, G., Dranoff, G., and Rock, K. L. (1997). Cloned dendritic cells can present exogenous antigens on both MHC class I and class II molecules. *J.Immunol.* **158**, 2723-2730.

Shi, Y., Evans, J. E., and Rock, K. L. (2003). Molecular identification of a danger signal that alerts the immune system to dying cells. *Nature* **425**, 516-521.

Siegal, F. P., Kadowaki, N., Shodell, M., Fitzgerald-Bocarsly, P. A., Shah, K., Ho, S., Antonenko, S., and Liu, Y. J. (1999). The nature of the principal type 1 interferon-producing cells in human blood. *Science* **284**, 1835-1837.

Silberberg-Sinakin, I., Thorbecke, G. J., Baer, R. L., Rosenthal, S. A., and Berezowsky, V. (1976). Antigen-bearing langerhans cells in skin, dermal lymphatics and in lymph nodes. *Cell Immunol.* **25**, 137-151.

Sims, J. E. (2002). IL-1 and IL-18 receptors, and their extended family. *Curr.Opin.Immunol.* **14**, 117-122.

Sin, J. I., Kim, J. J., Boyer, J. D., Ciccarelli, R. B., Higgins, T. J., and Weiner, D. B. (1999). In vivo modulation of vaccine-induced immune responses toward a Th1 phenotype increases potency and vaccine effectiveness in a herpes simplex virus type 2 mouse model. *J.Virol.* **73**, 501-509.

Sin, J. I., Kim, J. J., Ugen, K. E., Ciccarelli, R. B., Higgins, T. J., and Weiner, D. B. (1998). Enhancement of protective humoral (Th2) and cell-mediated (Th1) immune responses against herpes simplex virus-2 through co-delivery of granulocyte-macrophage colony-stimulating factor expression cassettes. *Eur.J.Immunol.* **28**, 3530-3540.

Singh-Jasuja, H., Scherer, H. U., Hilf, N., Arnold-Schild, D., Rammensee, H. G., Toes, R. E., and Schild, H. (2000). The heat shock protein gp96 induces maturation of dendritic cells and down-regulation of its receptor. *Eur.J.Immunol.* **30**, 2211-2215.

Smith, J. B., McIntosh, G. H., and Morris, B. (1970). The traffic of cells through tissues: a study of peripheral lymph in sheep. *J.Anat.* **107**, 87-100.

Smith, P. D., Lamerson, C. L., Wong, H. L., Wahl, L. M., and Wahl, S. M. (1990). Granulocyte-macrophage colony-stimulating factor stimulates human monocyte accessory cell function. *J.Immunol.* **144**, 3829-3834.

Smith, R. E., Patel, V., Seatter, S. D., Deehan, M. R., Brown, M. H., Brooke, G. P., Goodridge, H. S., Howard, C. J., Rigley, K. P., Harnett, W., and Harnett, M. M. (2003). A novel MyD-1 (SIRP-1alpha) signaling pathway that inhibits LPS-induced TNFalpha production by monocytes. *Blood* **102**, 2532-2540.

Song, P. I., Park, Y. M., Abraham, T., Harten, B., Zivony, A., Neparidze, N., Armstrong, C. A., and Ansel, J. C. (2002). Human keratinocytes express functional CD14 and toll-like receptor 4. *J.Invest Dermatol.* **119**, 424-432.

Spies, B., Hochrein, H., Vabulas, M., Huster, K., Busch, D. H., Schmitz, F., Heit, A., and Wagner, H. (2003). Vaccination with plasmid DNA activates dendritic cells via Toll-like receptor 9 (TLR9) but functions in TLR9-deficient mice. *J.Immunol.* **171**, 5908-5912.

Stan, A. C., Casares, S., Brumeanu, T. D., Klinman, D. M., and Bona, C. A. (2001). CpG motifs of DNA vaccines induce the expression of chemokines and MHC class II molecules on myocytes. *Eur.J.Immunol.* **31**, 301-310.

Steinman, R. M. (1991). The dendritic cell system and its role in immunogenicity. *Annu.Rev.Immunol.* **9**, 271-296.

Steinman, R. M., Lustig, D. S., and Cohn, Z. A. (1974). Identification of a novel cell type in peripheral lymphoid organs of mice. 3. Functional properties in vivo. *J.Exp.Med.* **139**, 1431-1445.

Steinman, R. M. and Nussenzweig, M. C. (2002). Avoiding horror autotoxicus: the importance of dendritic cells in peripheral T cell tolerance. *Proc.Natl.Acad.Sci.U.S.A* **99**, 351-358.

Stephens, S. A., Brownlie, J., Charleston, B., and Howard, C. J. (2003). Differences in cytokine synthesis by the sub-populations of dendritic cells from afferent lymph. *Immunology* **110**, 48-57.

Stevens, T. L., Bossie, A., Sanders, V. M., Fernandez-Botran, R., Coffman, R. L., Mosmann, T. R., and Vitetta, E. S. (1988). Regulation of antibody isotype secretion by subsets of antigen-specific helper T cells. *Nature* **334**, 255-258.

Stockwin, L. H., McGonagle, D., Martin, I. G., and Blair, G. E. (2000). Dendritic cells: immunological sentinels with a central role in health and disease. *Immunol.Cell Biol.* **78**, 91-102.

Stoll, S., Jonuleit, H., Schmitt, E., Muller, G., Yamauchi, H., Kurimoto, M., Knop, J., and Enk, A. H. (1998). Production of functional IL-18 by different subtypes of murine and human dendritic cells (DC): DC-derived IL-18 enhances IL-12-dependent Th1 development. *Eur.J.Immunol.* **28**, 3231-3239.

Stoll, S., Muller, G., Kurimoto, M., Saloga, J., Tanimoto, T., Yamauchi, H., Okamura, H., Knop, J., and Enk, A. H. (1997). Production of IL-18 (IFN-gamma-inducing factor) messenger RNA and functional protein by murine keratinocytes. *J.Immunol.* **159**, 298-302.

Storozynsky, E., Woodward, J. G., Frelinger, J. G., and Lord, E. M. (1999). Interleukin-3 and granulocyte-macrophage colony-stimulating factor enhance the generation and function of dendritic cells. *Immunology* **97**, 138-149.

Suemoto, Y., Ando, O., Kurimoto, M., Horikawa, T., and Ichihashi, M. (1998). IL-12 promotes the accessory cell function of epidermal Langerhans cells. *J.Dermatol.Sci.* **18**, 98-108.

Sun, X., Hodge, L. M., Jones, H. P., Tabor, L., and Simecka, J. W. (2002). Co-expression of granulocyte-macrophage colony-stimulating factor with antigen enhances humoral and tumor immunity after DNA vaccination. *Vaccine* **20**, 1466-1474.

Svanholm, C., Bandholtz, L., Castanos-Velez, E., Wigzell, H., and Rottenberg, M. E. (2000). Protective DNA immunization against Chlamydia pneumoniae. *Scand.J.Immunol.* **51**, 345-353.

Tada, Y., Asahina, A., Nakamura, K., Tomura, M., Fujiwara, H., and Tamaki, K. (2000). Granulocyte/macrophage colony-stimulating factor inhibits IL-12 production of mouse Langerhans cells. *J.Immunol.* **164**, 5113-5119.

Tailleux, L., Schwartz, O., Herrmann, J. L., Pivert, E., Jackson, M., Amara, A., Legres, L., Dreher, D., Nicod, L. P., Gluckman, J. C., Lagrange, P. H., Gicquel, B., and Neyrolles, O. (2003). DC-SIGN is the major Mycobacterium tuberculosis receptor on human dendritic cells. *J.Exp.Med.* **197**, 121-127.

Takahara, K., Omatsu, Y., Yashima, Y., Maeda, Y., Tanaka, S., Iyoda, T., Clausen, B. E., Matsubara, K., Letterio, J., Steinman, R. M., Matsuda, Y., Inaba, K., and Clusen, B. (2002). Identification and expression of mouse Langerin (CD207) in dendritic cells. *Int.Immunol.* **14**, 433-444.

Takeda, K., Kaisho, T., and Akira, S. (2003). Toll-like receptors. *Annu.Rev.Immunol.* **21**, 335-376.

Takeuchi, O., Hoshino, K., Kawai, T., Sanjo, H., Takada, H., Ogawa, T., Takeda, K., and Akira, S. (1999). Differential roles of TLR2 and TLR4 in recognition of gram-negative and gram-positive bacterial cell wall components. *Immunity.* **11**, 443-451.

Tang, A., Amagai, M., Granger, L. G., Stanley, J. R., and Udey, M. C. (1993). Adhesion of epidermal Langerhans cells to keratinocytes mediated by E-cadherin. *Nature* **361**, 82-85.

Tang, D. C., DeVit, M., and Johnston, S. A. (1992). Genetic immunization is a simple method for eliciting an immune response. *Nature* **356**, 152-154.

Thery, C., Regnault, A., Garin, J., Wolfers, J., Zitvogel, L., Ricciardi-Castagnoli, P., Raposo, G., and Amigorena, S. (1999). Molecular characterization of dendritic cell-derived exosomes. Selective accumulation of the heat shock protein hsc73. *J.Cell Biol.* **147**, 599-610.

Timares, L., Takashima, A., and Johnston, S. A. (1998). Quantitative analysis of the immunopotency of genetically transfected dendritic cells. *Proc.Natl.Acad.Sci.U.S.A* **95**, 13147-13152.

Torres, C. A., Iwasaki, A., Barber, B. H., and Robinson, H. L. (1997). Differential dependence on target site tissue for gene gun and intramuscular DNA immunizations. *J.Immunol.* **158**, 4529-4532.

Townsend, W. L., Gorrell, M. D., and Mayer, R. (1997). Langerhans cells in the development of skin cancer: a qualitative and quantitative comparison of cell markers in normal, acanthotic and neoplastic ovine skin. *Pathology* **29**, 42-50.

Traver, D., Akashi, K., Manz, M., Merad, M., Miyamoto, T., Engleman, E. G., and Weissman, I. L. (2000). Development of CD8alpha-positive dendritic cells from a common myeloid progenitor. *Science* **290**, 2152-2154.

Tschachler, E., Schuler, G., Hutterer, J., Leibl, H., Wolff, K., and Stingl, G. (1983). Expression of Thy-1 antigen by murine epidermal cells. *J.Invest Dermatol.* **81**, 282-285.

Turner, J. G., Tan, J., Crucian, B. E., Sullivan, D. M., Ballester, O. F., Dalton, W. S., Yang, N. S., Burkholder, J. K., and Yu, H. (1998). Broadened clinical utility of gene gun-mediated, granulocyte-macrophage colony stimulating factor cDNA based tumor cell vaccines as demonstrated with a mouse myeloma model. *Hum.Gene Ther.* **9**, 1121-1130.

Ulmer, J. B., Deck, R. R., DeWitt, C. M., Donnhly, J. I., and Liu, M. A. (1996). Generation of MHC class I-restricted cytotoxic T lymphocytes by expression of a viral protein in muscle cells: antigen presentation by non-muscle cells. *Immunology* **89**, 59-67.

Ulmer, J. B., Donnelly, J. J., Parker, S. E., Rhodes, G. H., Felgner, P. L., Dwarki, V. J., Gromkowski, S. H., Deck, R. R., DeWitt, C. M., and Friedman, A. (1993). Heterologous protection against influenza by injection of DNA encoding a viral protein. *Science* **259**, 1745-1749.

Valladeau, J., Clair-Moninot, V., Dezutter-Dambuyant, C., Pin, J. J., Kissenpfennig, A., Mattei, M. G., Ait-Yahia, S., Bates, E. E., Malissen, B., Koch, F., Fossiez, F., Romani, N., Lebecque, S., and Saeland, S. (2002). Identification of mouse langerin/CD207 in Langerhans cells and some dendritic cells of lymphoid tissues. *J.Immunol.* **168**, 782-792.

Valladeau, J., Dezutter-Dambuyant, C., and Saeland, S. (2003). Langerin/CD207 sheds light on formation of birbeck granules and their possible function in Langerhans cells. *Immunol.Res.* **28**, 93-107.

Valladeau, J., Duvert-Frances, V., Pin, J. J., Dezutter-Dambuyant, C., Vincent, C., Massacrier, C., Vincent, J., Yoneda, K., Banchereau, J., Caux, C., Davoust, J., and Saeland, S. (1999). The monoclonal antibody DCGM4 recognizes Langerin, a protein specific of Langerhans cells, and is rapidly internalized from the cell surface. *Eur.J.Immunol.* **29**, 2695-2704.

Valladeau, J., Ravel, O., Dezutter-Dambuyant, C., Moore, K., Kleijmeer, M., Liu, Y., Duvert-Frances, V., Vincent, C., Schmitt, D., Davoust, J., Caux, C., Lebecque, S., and Saeland, S. (2000). Langerin, a novel C-type lectin specific to Langerhans cells, is an endocytic receptor that induces the formation of Birbeck granules. *Immunity.* **12**, 71-81.

Van Der, L. N., de Leij, L. F., and ten Duis, H. J. (2001). Immunohistopathological appearance of three different types of injury in human skin. *Inflamm.Res.* **50**, 350-356.

Vely, F. and Vivier, E. (1997). Conservation of structural features reveals the existence of a large family of inhibitory cell surface receptors and noninhibitory/activatory counterparts. *J.Immunol.* **159**, 2075-2077.

Vermaelen, K. Y., Carro-Muino, I., Lambrecht, B. N., and Pauwels, R. A. (2001). Specific migratory dendritic cells rapidly transport antigen from the airways to the thoracic lymph nodes. *J.Exp.Med.* **193**, 51-60.

Vernon-Wilson, E. F., Kee, W. J., Willis, A. C., Barclay, A. N., Simmons, D. L., and Brown, M. H. (2000). CD47 is a ligand for rat macrophage membrane signal regulatory protein SIRP (OX41) and human SIRPalpha 1. *Eur.J.Immunol.* **30**, 2130-2137.

Voisine, C., Hubert, F. X., Trinite, B., Heslan, M., and Josien, R. (2002). Two phenotypically distinct subsets of spleen dendritic cells in rats exhibit different cytokine production and T cell stimulatory activity. *J.Immunol.* **169**, 2284-2291.

Vremec, D., Lieschke, G. J., Dunn, A. R., Robb, L., Metcalf, D., and Shortman, K. (1997). The influence of granulocyte/macrophage colony-stimulating factor on dendritic cell levels in mouse lymphoid organs. *Eur.J.Immunol.* **27**, 40-44.

Vremec, D., Pooley, J., Hochrein, H., Wu, L., and Shortman, K. (2000). CD4 and CD8 expression by dendritic cell subtypes in mouse thymus and spleen. *J.Immunol.* **164**, 2978-2986.

Waclavicek, M., Majdic, O., Stulnig, T., Berger, M., Baumruker, T., Knapp, W., and Pickl, W. F. (1997). T cell stimulation via CD47: agonistic and antagonistic effects of CD47 monoclonal antibody 1/1A4. *J.Immunol.* **159**, 5345-5354.

Wang, B., Merva, M., Dang, K., Ugen, K. E., Boyer, J., Williams, W. V., and Weiner, D. B. (1994). DNA inoculation induces protective in vivo immune responses against cellular challenge with HIV-1 antigen-expressing cells. *AIDS Res.Hum.Retroviruses* **10 Suppl 2**, S35-S41.

Wang, R., Doolan, D. L., Le, T. P., Hedstrom, R. C., Coonan, K. M., Charoenvit, Y., Jones, T. R., Hobart, P., Margalith, M., Ng, J., Weiss, W. R., Sedegah, M., de Taisne, C., Norman, J. A., and Hoffman, S. L. (1998). Induction of antigen-specific cytotoxic T lymphocytes in humans by a malaria DNA vaccine. *Science* **282**, 476-480.

Wang, R., Epstein, J., Baraceros, F. M., Gorak, E. J., Charoenvit, Y., Carucci, D. J., Hedstrom, R. C., Rahardjo, N., Gay, T., Hobart, P., Stout, R., Jones, T. R., Richie, T. L., Parker, S. E., Doolan, D. L., Norman, J., and Hoffman, S. L. (2001). Induction of CD4(+) T cell-dependent CD8(+) type 1 responses in humans by a malaria DNA vaccine. *Proc.Natl.Acad.Sci.U.S.A* **98**, 10817-10822.

Warren, T. L. and Weiner, G. J. (2000). Uses of granulocyte-macrophage colony-stimulating factor in vaccine development. *Curr.Opin.Hematol.* **7**, 168-173.

Warringa, R. A., Koenderman, L., Kok, P. T., Kreukniet, J., and Bruijnzeel, P. L. (1991). Modulation and induction of eosinophil chemotaxis by granulocyte-macrophage colony-stimulating factor and interleukin-3. *Blood* **77**, 2694-2700.

Watkins, C., Lau, S., Thistlethwaite, R., Hopkins, J., and Harkiss, G. D. (1999). Analysis of reporter gene expression in ovine dermis and afferent lymph dendritic cells in vitro and in vivo. *Vet.Immunol.Immunopathol.* **72**, 125-133.

Watts, C. (1997). Immunology. Inside the gearbox of the dendritic cell. *Nature* **388**, 724-725.

Welsh, E. A. and Kripke, M. L. (1990). Murine Thy-1+ dendritic epidermal cells induce immunologic tolerance in vivo. *J.Immunol.* **144**, 883-891.

Werling, D., Hope, J. C., Howard, C. J., and Jungi, T. W. (2004). Differential production of cytokines, reactive oxygen and nitrogen by bovine macrophages and dendritic cells stimulated with Toll-like receptor agonists. *Immunology* **111**, 41-52.

Whitton, J. L., Rodriguez, F., Zhang, J., and Hassett, D. E. (1999). DNA immunization: mechanistic studies. *Vaccine* **17**, 1612-1619.

Williams, R. S., Johnston, S. A., Riedy, M., DeVit, M. J., McElligott, S. G., and Sanford, J. C. (1991). Introduction of foreign genes into tissues of living mice by DNA-coated microprojectiles. *Proc.Natl.Acad.Sci.U.S.A* **88**, 2726-2730.

Wilson, N. S., El Sukkari, D., Belz, G. T., Smith, C. M., Steptoe, R. J., Heath, W. R., Shortman, K., and Villadangos, J. A. (2003). Most lymphoid organ dendritic cell types are phenotypically and functionally immature. *Blood* **102**, 2187-2194.

Witmer-Pack, M. D., Olivier, W., Valinsky, J., Schuler, G., and Steinman, R. M. (1987). Granulocyte/macrophage colony-stimulating factor is essential for the viability and function of cultured murine epidermal Langerhans cells. *J.Exp.Med.* **166**, 1484-1498.

Wolff, J. A., Dowty, M. E., Jiao, S., Repetto, G., Berg, R. K., Ludtke, J. J., Williams, P., and Slautterback, D. B. (1992a). Expression of naked plasmids by cultured myotubes and entry of plasmids into T tubules and caveolae of mammalian skeletal muscle. *J.Cell Sci.* **103 (Pt 4)**, 1249-1259.

Wolff, J. A., Ludtke, J. J., Acsadi, G., Williams, P., and Jani, A. (1992b). Long-term persistence of plasmid DNA and foreign gene expression in mouse muscle. *Hum.Mol.Genet.* **1**, 363-369.

Wolff, J. A., Malone, R. W., Williams, P., Chong, W., Acsadi, G., Jani, A., and Felgner, P. L. (1990). Direct gene transfer into mouse muscle in vivo. *Science* **247**, 1465-1468.

Wolff, K. and Winkelmann, R. K. (1967). Quantitative studies on the Langerhans cell population of guinea pig epidermis. *J.Invest Dermatol.* **48**, 504-513.

Woodland, D. L. (2004). Jump-starting the immune system: prime-boosting comes of age. *Trends Immunol.* **25**, 98-104.

Xia, C. Q. and Kao, K. J. (2002). Heparin induces differentiation of CD1a+ dendritic cells from monocytes: phenotypic and functional characterization. *J.Immunol.* **168**, 1131-1138.

Xiang, Z. and Ertl, H. C. (1995). Manipulation of the immune response to a plasmid-encoded viral antigen by coinoculation with plasmids expressing cytokines. *Immunity.* **2**, 129-135.

Xiang, Z. Q., Spitalnik, S. L., Cheng, J., Erikson, J., Wojczyk, B., and Ertl, H. C. (1995). Immune responses to nucleic acid vaccines to rabies virus. *Virology* **209**, 569-579.

Yamashiro, S., Kamohara, H., Wang, J. M., Yang, D., Gong, W. H., and Yoshimura, T. (2001). Phenotypic and functional change of cytokine-activated neutrophils: inflammatory neutrophils are heterogeneous and enhance adaptive immune responses. *J.Leukoc.Biol.* **69**, 698-704.

Yang, R. B., Mark, M. R., Gray, A., Huang, A., Xie, M. H., Zhang, M., Goddard, A., Wood, W. I., Gurney, A. L., and Godowski, P. J. (1998). Toll-like receptor-2 mediates lipopolysaccharide-induced cellular signalling. *Nature* **395**, 284-288.

Yang, Z. Y., Kong, W. P., Huang, Y., Roberts, A., Murphy, B. R., Subbarao, K., and Nabel, G. J. (2004). A DNA vaccine induces SARS coronavirus neutralization and protective immunity in mice. *Nature* **428**, 561-564.

Yawalkar, N., Brand, C. U., and Braathen, L. R. (1996). IL-12 gene expression in human skin-derived CD1a+ dendritic lymph cells. *Arch.Dermatol.Res.* **288**, 79-84.

Yeh, K. Y., McAdam, A. J., Pulaski, B. A., Shastri, N., Frelinger, J. G., and Lord, E. M. (1998). IL-3 enhances both presentation of exogenous particulate antigen in association with class I major histocompatibility antigen and generation of primary tumor-specific cytolytic T lymphocytes. *J.Immunol.* **160**, 5773-5780.

Yirrell, D. L., Reid, H. W., Norval, M., Entrican, G., and Miller, H. R. (1991). Response of efferent lymph and popliteal lymph node to epidermal infection of sheep with orf virus. *Vet.Immunol.Immunopathol.* **28**, 219-235.

Yoshimura, A., Lien, E., Ingalls, R. R., Tuomanen, E., Dziarski, R., and Golenbock, D. (1999). Cutting edge: recognition of Gram-positive bacterial cell wall components by the innate immune system occurs via Toll-like receptor 2. *J.Immunol.* **163**, 1-5.

Zelickson, A. S. and Mottaz, J. H. (1968). Localization of gold chloride and adenosine triphosphatase in human Langerhans cells. *J.Invest Dermatol.* **51**, 365-372.

Zepter, K., Haffner, A., Soohoo, L. F., De Luca, D., Tang, H. P., Fisher, P., Chavinson, J., and Elmets, C. A. (1997). Induction of biologically active IL-1 beta-converting enzyme and mature IL-1 beta in human keratinocytes by inflammatory and immunologic stimuli. *J.Immunol.* **159**, 6203-6208.

Zhou, L. J. and Tedder, T. F. (1996). CD14+ blood monocytes can differentiate into functionally mature CD83+ dendritic cells. *Proc.Natl.Acad.Sci.U.S.A* **93**, 2588-2592.

Zhou, X., Zheng, L., Liu, L., Xiang, L., and Yuan, Z. (2003). T helper 2 immunity to hepatitis B surface antigen primed by gene-gun-mediated DNA vaccination can be shifted towards T helper 1 immunity by codelivery of CpG motif-containing oligodeoxynucleotides. *Scand.J.Immunol.* **58**, 350-357.

Zinkernagel, R. M. (2003). On natural and artificial vaccinations. *Annu.Rev.Immunol.* **21**, 515-546.

Appendix I Composition of solutions

15% acrylamide resolving gel

4.0ml of resolving gel buffer (1.5M Tris-HCl, pH 8.8, 0.4% SDS), 8ml of 30% acrylamide/Bis solution 29:1 (Biorad) 4ml of dH_20 and polymerised by adding 100µl of 10% ammonium persulphate and 10µl of TEMED.

4% acrylamide stacking gel

1.25ml stacking gel buffer (0.5M Tris-HCl, pH 6.8, 0.4% SDS), 0.8ml 30% acrylamide/Bis 29:1 solution, 4ml dH_2O. Add 25µl of 10% ammonium persulphate and 10µl TEMED, to polymerise.

Carbonate buffer

0.1M $Na_2CO_3.10H_2O$, 0.1M $NaHCO_3$, pH 9.6.

Double strength sample buffer

4% SDS, 20% glycerol, 0.01% Bromophenol Blue and 10% 2-ME in 124mM Tris-HCl, pH 6.8.

LB media

1% bacto-tryptone, 0.5% bacto-yeast extract and 0.5% sodium chloride, pH 7.0.

PBS

137mM NaCl, 27mM KCl, 8mM Na_2HPO_4, 15mM KH_2PO_4, pH 7.2.

10 × running buffer

25mM Tris, 190mM glycine, 0.1% SDS, pH 8.3.

SOC media

20g/l bacto-tryptone, 5g/l bacto-yeast, 0.5g/l NaCl, 2.5mM KCl, 25mM $MgCl_2$ and 50mM glucose).

TAE buffer (Tris-acetate-EDTA)

40 mM Tris, 0.114% glacial acetic acid, 1 mM EDTA

TBS (Tris-buffered saline)

0.05M Tris HCl, 0.15M NaCl, pH 7.2–7.6.

10x TE buffer (Tris-EDTA)

10mM Tris-Cl, pH 8.0, 1mM EDTA, pH 8.0.

Transfer buffer

48mM Tris, 39mM glycine, 0.037% (w/v) SDS, 20% methanol.

ZSF (Zinc Salts Fixative)

Tris-Ca acetate buffer (0.1M Tris –base, 0.05% Ca acetate, pH 7–7.4), 0.5% Zn chloride, 0.5% Zn acetate.

Appendix II Suppliers

Amersham Pharmacia Biotech	Little Chalfont, UK
Millipore	Watford, UK
Axis-Shield	Oslo, Norway
BDH	Poole, UK
BioGene	Kimbolton, UK
Bio-Rad	Hemel Hempstead, UK
BioWhittaker (Cambrex)	Nottingham, UK
Cambio	Cambridge, UK
Clontech	Basingstoke, UK
Dako(Cytomation)	Ely, UK
GraphPad Software	San Diego, California, USA
Invitrogen Life Technologies	Paisley, UK
Menzel-Glaser	Braunschweig, Germany
MWG biotech	Milton Keynes, UK
New England Biolabs	Hitchin, UK
Nalgene Nunc International	Rochester, NY, USA
Promega	Southhampton, UK
QIAGEN	Crawley, UK
Roche	Lewes, UK
Sigma-Genosys	Cambridge, UK
Surgipath	Peterborough, UK
ThermoHybaid	Ashford, UK
UltraViolet Products	Cambridge, UK
Vector Laboratories	Peterborough, UK
Zymed Laboratories Inc.	Cambridge, UK

Appendix III pGEM®-T Easy clones

Alignment of pGEM®-T Easy clones with GenBank sequences

Ovine TLR4 mRNA

Clone sequence

TGCAGGCGGCCGCGAATTCACTAGTGATTTTCACCTCTGCCTTCACTACAGGGACTTTATTCCTGGGGTGGCCATC
GCCGCCAATATCATCCAGGAAGGTTTCCACAAGAGCCGTAAGGTGATTGTCGTGGTGTCCCAGCACTTCATCCAGA
GCCGATGGTGTATCTTCGAGTACGAGATTGCCCAGACCTGGCAGTTTCTGAGCAGCCGTGCTGGCATCATCTTCAT
CGTCCTGCAGAAGCTGGAGAAGTCTCTCCTGCGGCAGCAGTTGAGAAGCTCATATCGCCTTCATGAACAGGAACAC
CTACCTGGAATGGGAAATCGAATTCCCGCGGCCGCCATGG

Aligned with bovine TLR4 mRNA (AY297043; 95% homology)

```
Clone:    29 tttcacctctgccttcactacagggactttattcctggggtggccatcgccgccaatatc
             ||||| ||||||||||||||||||||||||||||||||||||||||||||||||||||||
Bovine: 2132 tttcagctctgccttcactacagggactttattcctggggtggccatcgccgccaatatc

           89 atccaggaaggtttccacaagagccgtaaggtgattgtcgtggtgtcccagcacttcatc
              |||||||| |||||||||| |||||||||| ||||||||||||||||||||||||||
         2192 atccaggagggtttccacaaaagccgtaaggttattgtcgtggtgtcccagcacttcatc

          149 cagagccgatggtgtatcttcgagtacgagattgcccagacctggcagtttctgagcagc
              |||||||||||||||||||||||| ||||||||||||||||||||||||||||||||
         2252 cagagccgatggtgtatcttcgagtatgagattgcccagacctggcagtttctgagcagc

          209 cgtgctggcatcatcttcatcgtcctgcagaagctggagaagtctctcctgcggcagcag
              ||||||||||||||||||||||||||||||||||||||||||||||||||||||||||||
         2312 cgtgctggcatcatcttcatcgtcctgcagaagctggagaagtctctcctgcggcagcag

          269 ttgagaagctcatatcgccttcatgaacaggaacacctacctggaatggga
                | | ||||| |||||||||| ||| |||||||||||||||||| |||||
         2372 --gtggagctc-tatcgccttc-tgagcaggaacacctacctggagtggga
```

Aligned with human TLR4 mRNA (BC025294; 90% homology)

```
Clone:    29 tttcacctctgccttcactacagggactttattcctggggtggccatcgccgccaatatc
             ||||| |||||||||||||||| |||||||||| || |||||||| || ||||| |||
Human: 2024 tttcagctctgccttcactacagagactttattcccggtgtggccattgctgccaacatc

           89 atccaggaaggtttccacaagagccgtaaggtgattgtcgtggtgtcccagcacttcatc
              ||||| |||||||||| || ||||| |||||||||| ||||||||||||||||||||
         2084 atccatgaaggtttccataaaagccgaaaggtgattgttgtggtgtcccagcacttcatc

          149 cagagccgatggtgtatcttcgagtacgagattgcccagacctggcagtttctgagcagc
              |||||||| |||||||||| || || |||||||| ||||||||||||||||||||||||
         2144 cagagccgctggtgtatctttgaatatgagattgctcagacctggcagtttctgagcagt

          209 cgtgctggcatcatcttcatcgtcctgcagaagctggagaag
              |||||||| |||||||||| |||||||||| ||||||||
         2204 cgtgctggtatcatcttcattgtcctgcagaaggtggagaag
```

Ovine TLR9 mRNA

Clone sequence

GCGAATTCACTAGTGATTTGCTGTCCTACAACCACATTATCACCCTGGCACCCGAGGACCTGGCCAATCTGACTGC
CCTGCGTGTGCTTGGTGTGGGCGGGAACTGCCGCCGCTGCGACCACGCCCGCAACCCCTGCAGGGAGTGCCCAAAG
AACTTCCCCAAGCTGCACCCTGACACCTTCAGCCACCTGAGCCGCCTCGAAGGCCTGGTGTTGAAGGACAGTTCTC
TCTACAAACTAGAGAAAGATTGGTTCCGCAATCGAATTCCCGCGGCCGCCAT

Aligned with ovine TLR9 (NM_001011555; 98% homology)

```
Clone:  19  tgctgtcctacaaccacattatcaccctggcacccgaggacctggccaatctgactgccc
            ||||||||||||||||||| |||||||||||||||||||||||||||||||||||||||
Ovine: 765  tgctgtcctacaaccacatcatcaccctggcacccgaggacctggccaatctgactgccc

        79  tgcgtgtgcttggtgtgggcgggaactgccgccgctgcgaccacgcccgcaacccctgca
            |||||||||||| ||||||||||||||||||||||||||||||||||||||||||||||
       825  tgcgtgtgcttgatgtgggcgggaactgccgccgctgcgaccacgcccgcaacccctgca

       139  gggagtgcccaaagaacttccccaagctgcaccctgacaccttcagccacctgagccgcc
            ||||||||||||||||||||||||||||||||||||||||||||||||||||||||||||
       885  gggagtgcccaaagaacttccccaagctgcaccctgacaccttcagccacctgagccgcc

       199  tcgaaggcctggtgttgaaggacagttctctctacaaactagagaaagattggttccgc
            |||||||||||||||||||||||||||||||||||||||||||||||||| |||||||||
       945  tcgaaggcctggtgttgaaggacagttctctctacaaactagagaaagactggttccgc
```

Ovine CD207 (Langerin) mRNA

Sequence

GGGAATTCGATTGTCGTGGTGGACAACATCAGCTCCCTGAGTTCTGAGATCAAGAGGAACAGAGGTGCCCTGGTGG
CAGTGGGCTTTCAGGTCCGGATGGTGAATGCCAGCTTGGGCCGCATAAGCTCTCAGATCCGGAGGTTGGAAACAGG
CTTGAAGGAAGCCAGTGCGCAgctGCATGTGCTAACAAGTAGTTGGGAAGCAGTCGATGAGTTAAATGCCCAAATC
CCAGGGCTAAAACAAGATTTGGATAAAGCCAGTGCTTTAAATGCGAAGGTCCGGGAACTCCAGAGCGGTTTGGAGA
GTATCAGCAAATTCGCTTCAACAGCAAAATGACATTCTCCAGGTGGTTTCTCAAGGCTGGAAGTACTTCAGGGGGC
ACTTCTATTACTTTTCTCAAATCTCAAAGACCTGGTATAGTGCCAATCACTAGTGAATTCGCGGCCGCCTGCA

Aligned with bovine CD207 (predicted—XM_588243; 94% homology)

```
Clone:   19 gtggacaacatcagctccctgagttctgagatcaagaggaacagaggtgccctggtggca
            ||||||||||||||||||||||||||||||||||||||||||||||||||| ||||||||||
Bovine: 469 gtggacaacatcagctccctgagttctgagatcaagaggaacagaggtggcctggtggca

         79 gtgggctttcaggtccggatggtgaatgccagcttgggccgcataagctctcagatccgg
            || ||| |||||||||||||||||| |||||||||  |||||||| ||||||||||||
        529 gttggcattcaggtccggatggtgaacgccagcttggatcgcataagttctcagatccgg

        139 aggttggaaacaggcttgaaggaagccagtgcgcagctgcatgtgctaacaagtagttgg
            |||||||||||||||||||||||||||||||| |||||||| ||||||||||||||||||
        589 aggttggaaacaggcttgaaggaagccagtgcacagctgcaggtgctaacaagtagttgg
```

```
199 gaagcagtcgatgagttaaatgcccaaatcccagggctaaaacaagatttggataaagcc
    ||||||| ||||||||||||||||||||||| |||||||||||||||||||||||||||
649 aaagcagttgatgagttaaatgcccaaatcccagagctaaaacaagatttggataaagcc

259 agtgctttaaatgcgaaggtccgggaactccagagcggtttggagagtatcagcaaattc
    |||||||||||||| |||||||||||||||||||| ||||||||||||||||||||||
709 agtgctttaaatgcaaaggtccgggaactccagagtggtttggagagtatcagcaaatt-

319 gcttcaacagcaaaatgacattctccaggtggtttctcaaggctggaagtacttcagggg
    ||||||||||||||| |||||||||||||||||||| |||||||||||||||||| ||||
768 gcttcaacagcaaaaggacattctccaggtggtttcccaaggctggaagtacttcggggg

379 gcacttctattacttttctcaaatctcaaagacctggtatagtgcc
    |||||||||||||||||| ||||||| |||||||||| ||||||
828 gcacttctattacttttctaaaatctcgaagacctggtacagtgcc
```

Aligned with human CD207 (AJ242859; 85% homology)

```
Clone: 185 taacaagtagttgggaagcagtcgatgagttaaatgcccaaatcccagggctaaaacaag
           ||||||| |||||||||| ||||  |   |||||||||||||||||| | |||||   |
Human: 466 taacaagaagttgggaagaagtcagtaccttaaatgcccaaatcccagagttaaaaagtg

245 atttggataaagccagtgctttaaatgcgaaggtccgggaactccagagcggtttggaga
    ||||||| |||||||||||||||||| | ||| |||||| ||||||| || | |||||||
526 atttggagaaagccagtgctttaaatacaaagatccgggcactccagggcagcttggaga

305 gtatcagcaaattcgcttcaacagcaaaatgacattctccaggtggtttctcaaggctgg
     ||| ||||| || |||  |||  |||||||| ||||| ||||||||||||||||||||
586 atatgagcaagtt-gctcaaacgacaaaatgatattctacaggtggtttctcaaggctgg

365 aagtacttcagggggcacttctattacttttctcaaatctcaaagacctggtatagtgcc
    |||||||||| |||| |||||||||||||||||  ||  ||||||||||||||||||||
645 aagtacttcaaggggaacttctattacttttctctcattccaaagacctggtatagtgcc
```

Verification of quantitative RT-PCR standards

NB: pGEM®-T Easy sequences are highlighted in red; primer sequences are highlighted in green (see Table 2.11).

GAPDH: 99% identity with ovine GAPDH (AF030943)

GCGAATTCACTAGTGATTGGTGATGCTGGTGCTGAGTACGTGGTGGAGTCCACTGGGGTCTTCACTACCATGGAGA
AGGCTGGGGCTCACCTGAAGGGTGGCGCCAAGAGGGTCATCATCTCTGCACCTTCTGCTGACGCTCCCATGTTCGT
GATGGGCGTGAACCACGAGAAGTATAACAATACCCTCGAGATTGTCAGCAATGCCTCCTGCACCACCAACTGCTTG
GCCCCCCTGGCCAAGGTCATCCATGACCACTTTGGCATCGTGGAGGGACTTATGAAATCGAATTCCCGCGGCCGCC
ATGGC

IL-1β: 100% identity with ovine IL-1β (X54796.1)

GCGCGCCATGGCGGCCGCGGGAATTCGATTCCTTGGGTATCAGGGACAAGAATCTATACCTGTCTTGTGTGAAAAA
AGGTGATACACCGACCCTGCAGCTGGAGGAAGTAGACCCCAAAGTCTACCCCAAGAGGAATATGGAAAAGCGATTC
GTCTTCTACAAGACAGAAATCAAGAACACAGTTGAATTTGAGTCTGTCCTGTACCCTAACTGGTACATCAGCACTT
CTCAAATCGAAGAAAAGCCCGTCTTCCTGGGACGTTTTAGAGGTGGCCAGGATATAACTGACTTCAGAATGGAAAC
CCTCTCTCCCTAAAGAAAGCCATACGCAAATCACTAGTGAATTCGCGGCCGCCTGC

TNF-α: 98% identity with ovine TNF-α (X55152.1)

GCGAATTCACTAGTGATTGAATACCTGGACTATGCCGAGTCTGGGCAGGTCTACTTTGGGATCATCGCCCTGTGAG
GGCGCAGGACATGCATCCTCTCCCACCTCAGTTACCTTATTATTTACTCCTTCAGACCCTCCTCATCCCCTTCTGG
TTTAGAAAGGGAATTAGGGGCTCAGGGCTGGGCTCCAAGCGTCCAACTTCAAACAACAGCTGCACTTAGAAATTAG
GGATGTAGGGAAGTGAGGAATCGAATTCCCGCGGCCGCCATGGCGGCGCGGAGCATGCGACGTCGGGCCCAATTCG
CCCTATAGTGAGTCGTATTACAATTCACTGGCCGTCGTTTTACAACGTCGTGACTGGGAAAACCCTGGCGTTACCC
AACTTAATCGCCTTGCAGCACA

IL-18: 98 % identity with ovine IL-18 (AJ401033.1)

CCGCGAATTCACTAGTGATTTGAACAGTCAGAATCAGGCATATCCTCAAAGACAGGTTGATTTCCCTGGCTAATGA
AGAGAACTTGGTCGTTCAAATTTCGTATGACTGAGAGCTTAGGTTCAAGCTTGCCAAAGTGATCTGATTCCAGGTC
TTCGCCATTTTCAGCTACAAAATAAAGTGTATTGTTAATAAATTTCATTTCCACAAAGCTGATGCAATTGTCTTCT
ACTGGTTCTGCAGCCATCTTTATGCCTGTGCTCAATCGAATTCCCGCGGCCGCCATGGCGGCGGAGCATGCGACG

IL-12p40: 98% identity with ovine IL-12p40 (AF209435.1)

CCGCCGCCATGGCGGCCGCGGGAATTCGATTTCAGACCAGAGCAGTGAGGTCCTGGGCTCTGGCAAAACCTTGACC
ATCCAAGTCAAAGAGTTTGGAGATGCTGGGNAGTACACCTGTCACAAAGGAGGCGAGGTTCTGAGTCGTTCACTCC
TCCTGCTGCACAAAAAGGAAGATGGAATTTGGTCCACTGATATTTTAAAGGATCAGAAAGAACCCAAAGCTAAGAG
TTTTTTAAAATGTGAGGCAAATGATTATTCTGGACACTTCACCTGCAATCACTAGTGAATTCGCGG

IL-10 (100% identity with ovine IL-10 (OAINLE10)

TGCAGGCGGCCGCGAATTCACTAGTGATTACCGCCTTGCTCTTGTTTTCGCAGGGCAGAAAGCGATGACAGCGCCG
CAGCCGCAGCCGGAGGGTCTTCAGCTTCTCCCCCAGCGAGTTCACGTGCTCCTTGATGTCAGGCCCATGGTTCTCA
GCCTGTGGCATCACCTCCTCCAGGTAAAACTGGATCATTTCCGACAAGGCTTGGCAACCCAGGTAACCCTTAAAGT
CATCCAGCAGAGACTGGGTCAACAGAATCGAATTCCCGCGGCCGCCATGGCG

IL-3: 98% identity with ovine IL-3 (Z18897.1)

(Original primers used, Table 2.11)

ATATGGTCGACCTGCAGGCGGCCGCGAATTCACTAGTGATTTGAAGTCTGAAGCCCAGTTCCCTCTCTGAAGCCTC
AGATCATCAGTGACAACAAACTGTCCTAAATTTCTTCGATGTTTCTCACATGGTCCAGGCCTGGAAGAATTAATTT
TCTCCTGTGGAGCCAGATGAATCGTTAATTATTTAACTCCTGATATGTGTGGCCCCCATTTGTCCTTTTGGGATTA
TGTTCTCATTTTTAATCTATTGAGACTTATTTATTTATGTATGTATTTATTTATTACCTTGTGCAAATGTGAAGGG
TATTTATTTTAGCAGGGGAGTCATGTTCTGCTCCTTCTGGACAAAACTTAAGATGGGGACTTGGGAATAATCGAAT
TCCCGCGGCCGCCATGGCGG